

Shengzhao Long
Balbir S. Dhillon *Editors*

Man-Machine- Environment System Engineering

Proceedings of the 22nd International
Conference on MMESE



Lecture Notes in Electrical Engineering

Volume 941

Series Editors

Leopoldo Angrisani, Department of Electrical and Information Technologies Engineering, University of Napoli Federico II, Naples, Italy

Marco Arteaga, Departament de Control y Robótica, Universidad Nacional Autónoma de México, Coyoacán, Mexico

Bijaya Ketan Panigrahi, Electrical Engineering, Indian Institute of Technology Delhi, New Delhi, Delhi, India

Samarjit Chakraborty, Fakultät für Elektrotechnik und Informationstechnik, TU München, Munich, Germany

Jiming Chen, Zhejiang University, Hangzhou, Zhejiang, China

Shanben Chen, Materials Science and Engineering, Shanghai Jiao Tong University, Shanghai, China

Tan Kay Chen, Department of Electrical and Computer Engineering, National University of Singapore, Singapore, Singapore

Rüdiger Dillmann, Humanoids and Intelligent Systems Laboratory, Karlsruhe Institute for Technology, Karlsruhe, Germany

Haibin Duan, Beijing University of Aeronautics and Astronautics, Beijing, China

Gianluigi Ferrari, Università di Parma, Parma, Italy

Manuel Ferre, Centre for Automation and Robotics CAR (UPM-CSIC), Universidad Politécnica de Madrid, Madrid, Spain

Sandra Hirche, Department of Electrical Engineering and Information Science, Technische Universität München, Munich, Germany

Faryar Jabbari, Department of Mechanical and Aerospace Engineering, University of California, Irvine, CA, USA

Limin Jia, State Key Laboratory of Rail Traffic Control and Safety, Beijing Jiaotong University, Beijing, China

Janusz Kacprzyk, Systems Research Institute, Polish Academy of Sciences, Warsaw, Poland

Alaa Khamis, German University in Egypt El Tagamoa El Khames, New Cairo City, Egypt

Torsten Kroeger, Stanford University, Stanford, CA, USA

Yong Li, Hunan University, Changsha, Hunan, China

Qilian Liang, Department of Electrical Engineering, University of Texas at Arlington, Arlington, TX, USA

Ferran Martín, Departament d'Enginyeria Electrònica, Universitat Autònoma de Barcelona, Bellaterra, Barcelona, Spain

Tan Cher Ming, College of Engineering, Nanyang Technological University, Singapore, Singapore

Wolfgang Minker, Institute of Information Technology, University of Ulm, Ulm, Germany

Pradeep Misra, Department of Electrical Engineering, Wright State University, Dayton, OH, USA

Sebastian Möller, Quality and Usability Laboratory, TU Berlin, Berlin, Germany

Subhas Mukhopadhyay, School of Engineering & Advanced Technology, Massey University, Palmerston North, Manawatu-Wanganui, New Zealand

Cun-Zheng Ning, Electrical Engineering, Arizona State University, Tempe, AZ, USA

Toyoaki Nishida, Graduate School of Informatics, Kyoto University, Kyoto, Japan

Luca Oneto, Department of Informatics, Bioengineering., Robotics, University of Genova, Genova, Genova, Italy

Federica Pascucci, Dipartimento di Ingegneria, Università degli Studi "Roma Tre", Rome, Italy

Yong Qin, State Key Laboratory of Rail Traffic Control and Safety, Beijing Jiaotong University, Beijing, China

Gan Woon Seng, School of Electrical & Electronic Engineering, Nanyang Technological University, Singapore, Singapore

Joachim Speidel, Institute of Telecommunications, Universität Stuttgart, Stuttgart, Germany

Germano Veiga, Campus da FEUP, INESC Porto, Porto, Portugal

Haitao Wu, Academy of Opto-electronics, Chinese Academy of Sciences, Beijing, China

Walter Zamboni, DIEM - Università degli studi di Salerno, Fisciano, Salerno, Italy

Junjie James Zhang, Charlotte, NC, USA

The book series *Lecture Notes in Electrical Engineering* (LNEE) publishes the latest developments in Electrical Engineering - quickly, informally and in high quality. While original research reported in proceedings and monographs has traditionally formed the core of LNEE, we also encourage authors to submit books devoted to supporting student education and professional training in the various fields and applications areas of electrical engineering. The series cover classical and emerging topics concerning:

- Communication Engineering, Information Theory and Networks
- Electronics Engineering and Microelectronics
- Signal, Image and Speech Processing
- Wireless and Mobile Communication
- Circuits and Systems
- Energy Systems, Power Electronics and Electrical Machines
- Electro-optical Engineering
- Instrumentation Engineering
- Avionics Engineering
- Control Systems
- Internet-of-Things and Cybersecurity
- Biomedical Devices, MEMS and NEMS

For general information about this book series, comments or suggestions, please contact leontina.dicecco@springer.com.

To submit a proposal or request further information, please contact the Publishing Editor in your country:

China

Jasmine Dou, Editor (jasmine.dou@springer.com)

India, Japan, Rest of Asia

Swati Meherishi, Editorial Director (Swati.Meherishi@springer.com)

Southeast Asia, Australia, New Zealand

Ramesh Nath Premnath, Editor (ramesh.premnath@springernature.com)

USA, Canada:

Michael Luby, Senior Editor (michael.luby@springer.com)

All other Countries:

Leontina Di Cecco, Senior Editor (leontina.dicecco@springer.com)

**** This series is indexed by EI Compendex and Scopus databases. ****

More information about this series at <https://link.springer.com/bookseries/7818>

Shengzhao Long · Balbir S. Dhillon
Editors

Man-Machine-Environment System Engineering

Proceedings of the 22nd International
Conference on MMESE



 Springer

The Springer logo, which consists of a stylized chess knight piece on a pedestal, followed by the word "Springer" in a serif font.

Editors

Shengzhao Long
Astronaut Center of China
Beijing, China

Balbir S. Dhillon
Department of Mechanical Engineering
University of Ottawa
Ottawa, ON, Canada

ISSN 1876-1100

ISSN 1876-1119 (electronic)

Lecture Notes in Electrical Engineering

ISBN 978-981-19-4785-8

ISBN 978-981-19-4786-5 (eBook)

<https://doi.org/10.1007/978-981-19-4786-5>

© The Editor(s) (if applicable) and The Author(s), under exclusive license to Springer Nature Singapore Pte Ltd. 2023, corrected publication 2023

This work is subject to copyright. All rights are solely and exclusively licensed by the Publisher, whether the whole or part of the material is concerned, specifically the rights of translation, reprinting, reuse of illustrations, recitation, broadcasting, reproduction on microfilms or in any other physical way, and transmission or information storage and retrieval, electronic adaptation, computer software, or by similar or dissimilar methodology now known or hereafter developed.

The use of general descriptive names, registered names, trademarks, service marks, etc. in this publication does not imply, even in the absence of a specific statement, that such names are exempt from the relevant protective laws and regulations and therefore free for general use.

The publisher, the authors, and the editors are safe to assume that the advice and information in this book are believed to be true and accurate at the date of publication. Neither the publisher nor the authors or the editors give a warranty, expressed or implied, with respect to the material contained herein or for any errors or omissions that may have been made. The publisher remains neutral with regard to jurisdictional claims in published maps and institutional affiliations.

This Springer imprint is published by the registered company Springer Nature Singapore Pte Ltd. The registered company address is: 152 Beach Road, #21-01/04 Gateway East, Singapore 189721, Singapore



Grandness Scientist Xuesen Qian's Sky-high Estimation for the Man-Machine-Environment System Engineering, Pointed out: "You are Creating This Very Important Modern Science and Technology in China!"

龙升照同志:

我收到您主编的《人机环境系统工程研究进展(第一卷)》, 翻阅了之后, 感到非常高兴, 1985年秋提出的一个想法, 现在8年之后已赫然成书, 500多页的巨卷! 而且研究范围已大大超出原来航天, 内容涉及航空、航天、舰艇、兵器、电子、能源、交通、电力、煤炭、冶金、体育、康复、管理……等领域! 你们是在社会主义中国开创了这门重要现代科学技术!

此致

敬礼!

钱学森

1993.10.22



Grandness Scientist Xuesen Qian's Congratulatory Letter to the 20th Anniversary Commemorative Conference of MMESE Foundation, Pointed out: "Hope you can do even more to make prosper development in the theory and application of MMESE, and make positive contribution to the progress of science and technology in China, and even in the whole world!"

龙升照同志:

你的来信已收到。欣悉人-机-环境系统工程创立 20 周年纪念大会暨第五届全国人-机-环境系统工程学术会议即将召开, 我向你们表示最热烈的祝贺!

20 年来, 你们在人-机-环境系统工程这一新兴科学领域进行了积极的开拓和探索, 并取得了非常可喜的成绩, 我感到由衷的高兴。

希望你们今后再接再厉, 大力推动人-机-环境系统工程理论及应用的蓬勃发展, 为中国乃至世界科学技术的进步作出积极贡献!

祝

工作顺利!

钱学森
2001年6月26日

Preface

In 1981, under the directing of the great scientist Xuesen Qian, an integrated frontier science—Man-Machine-Environment System Engineering (MMESE)—came into being in China. Xuesen Qian gave high praise to this emerging science. In the letter to Shengzhao Long, he pointed out, **“You are creating this very important modern science and technology in China!”** in October 22, 1993.

In the congratulation letter to the commemoration meeting of 20th anniversary of establishing the Man-Machine-Environment System Engineering, the great scientist Xuesen Qian stated, “You have made active development and exploration in this new emerging science of MMESE, and obtained encouraging achievements. I am sincerely pleased and hope you can do even more to make prosper development in the theory and application of MMESE, and **make positive contribution to the progress of science and technology in China, and even in the whole world**” in June 26, 2001.

October 22, which is the day that the great scientist Xuesen Qian gave high praise to MMESE, was determined to be Foundation Commemoration Day of MMESE by the 2nd conference of the 5th MMESE Committee on October 22, 2010. On this very special day, the great scientist Xuesen Qian pointed out in the letter to Shengzhao Long, **“You are creating this very important modern science and technology in China!”**

The 22nd International Conference on MMESE will be held in Beijing, China, on October 21–23 of this year; hence, we will dedicate *Man-Machine-Environment System Engineering: The Proceedings of the 22nd International Conference on MMESE* to our readers.

Man-Machine-Environment System Engineering: Proceedings of The 22nd International Conference on MMESE is the academic showcases of The 22nd International Conference on MMESE held by the Beijing KeCui Man-Machine-Environment System Engineering Technology Research Academy in Beijing, China. The *Man-Machine-Environment System Engineering: Proceedings of the 22nd International Conference on MMESE* consisted of 100 more excellent papers selected from more than 600 papers. Due to limitations on space, some excellent papers have been left out, we feel deeply sorry for that. Crudeness in

contents and possible incorrectness are inevitable due to the somewhat pressing editing time and we hope you kindly point them out promptly, and your valuable comments and suggestions are also welcomed.

Man-Machine-Environment System Engineering: Proceedings: The 22nd International Conference on MMESE will be published by Springer-Verlag, German. Springer-Verlag is also responsible for the related matters of index to EI, so that the world can know the research quality and development trend of MMESE theory and application. Therefore, the publication of *Man-Machine-Environment System Engineering: Proceedings of the 22nd International Conference on MMESE* will greatly promote the vigorous development of MMESE in the world and realize the grand object of **“making positive contribution to the progress of science and technology in China, and even in the whole world”** proposed by Xuesen Qian.

We would like to express our sincere thanks to Springer-Verlag, German, for their full support and help of during the publishing process.

July 2022

Shengzhao Long

A handwritten signature in black ink that reads "Shengzhao Long". The signature is written in a cursive, flowing style with some loops and flourishes.

Organization

Program and Technical Committee Information

General Chairman

Shengzhao Long Astronaut Research and Training Center
of China, China

Program Committee Chairman

Balbir S. Dhillon University of Ottawa, Canada

Technical Committee Chairman

Enrong Mao College of Engineering, China Agricultural
University, China

Program and Technical Committee Members

Yanping Chen University of Management and Technology,
USA

Hongfeng Gao University of California, USA

Michael Greenspan Queen's University, Canada

Birsen Donmez University of Toronto, Canada

Xiangshi Ren Kochi University of Technology, Japan

Kinhuat Low Nanyang Technological University, Singapore

Baiqiao Huang System Engineering Research Institute of China
State Shipbuilding Corporation, China

Baoqing Xia Weapon Industrial Hygiene Research Institute,
China

Chenming Li The Quartermaster Research Institute of
Engineering and Technology, China

Fang Xie China North Vehicle Research Institute, China

Guangtao Ma Haoting Liu	Shenyang Jianzhu University, China University of Science and Technology Beijing, China
Hongjun Xue Lijing Wang	Northwestern Polytechnical University, China Beijing University of Aeronautics and Astronautics, China
Long Ye Senior Engineer	Beijing Jiaotong University, China Qichao Zhao, Beijing King Far Technology Co., Ltd., China
Qing Liu Weijun Chen Xiaochao Guo Yongqing Hou Yanqi Wang	Jinggangshan University, China Shanghai Maritime University, China Institute of Aviation Medicine, Air Force, China China Academy of Space Technology, China Weapon Industrial Hygiene Research Institute, China
Yinying Huang Yuhong Shen	Agricultural Bank of China, China The Quartermaster Research Institute of Engineering and Technology, China

Contents

Research on the Man Character

Research on Cognitive Theory Model of Man-Machine Combination Pilot Based on Information Processing	3
Siyu Chen, Hongjun Xue, Xiaoyan Zhang, Jue Qu, and Sina Dang	
Study on Subspace Alignment EEG Classification for Cross Session Visual Tasks	10
Hongquan Qu, Mengyu Zhang, and Liping Pang	
Mental Workload Classification Method Based on Transfer Component Analysis with Cross-Session EEG Data	17
Hongquan Qu, Hanwen Dong, and Liping Pang	
Development of Competency Model for Test Pilots Selection and Training	24
Yanyan Wang, Huifeng Ren, Xiaochao Guo, Yu Bai, Yu Duan, Zhengtao Cao, Duanqin Xiong, and Qingfeng Liu	
Experimental Research on Team Dynamic Function Allocation Strategy Optimization	30
Chenyuan Yang, Liping Pang, Xin Wang, Ye Deng, and Yuan Liu	
Eye Movement Characteristics During Rifle Aiming	37
Jie Cao, Yaping Wang, Sheng Guo, and Cancan Hu	
Research on User's Subjective Preference of Taohuawu New Year Painting Based on CycleGAN	44
Funan Dai, Zhengqing Jiang, Yiao Fang, and Xin Guan	
Personalized HRIR Based on PointNet Network Using Anthropometric Parameters	54
Dongdong Lu, Jun Zhang, Haiyang Gao, and Chuang Liu	

Effects of 15 days -6° Head-Down Bed Rest Simulated Weightlessness on the Judgment of Motion Direction 60
Tianxin Cheng, Duming Wang, Yu Tian, Zhen Yuan, and Lian Wang

Passenger Car’ Sitting Posture Prediction Research 67
Lipeng Qin, Peiwen Zuo, and Hui Lv

Psychological Adjustment of High Intensity Physical Training 73
Yu Luo, Qiaoyang Zheng, Hu Wang, Xia Chen, Shu Jiang, Mingze Li, Hao Li, and Mengxi Li

Research on Audience Cognition of Audio-Visual Interactive Art from the Perspective of Mental Model 77
Yijie Zhang, Zhengqing Jiang, and Haiyun Zheng

Comparative Study on the Reachability Distance Measurement Method: Difference Between the Real Environment and Mixed Reality Simulation 84
Wei Xiong, Zhi Liang, and Xiaoqing Yu

The Effect of Face Mask and Approach Pattern on Interpersonal Distance in COVID-19 Pandemic Using VR Technology 92
Wei Xiong, Congyi Wang, and Xiaoqing Yu

Investigation and Research on Occupational Mental Health Status of Grassroots Firefighters 99
Yanqiu Sun, Zhenfang Chen, Ao Zhang, Jingqi Gao, Jianwu Chen, Bin Yang, Yin Jiang, and Jia Wang

Study on the Relationship Between Emotional Regulation Self-efficacy and Fatigue in the Sedentary Population 107
Xiangpeng Pan

Depth Perception and Distance Assessment Under Night Vision Goggles and Their Influence Factor 115
Shan Chen, Dawei Tian, Fei Yu, Qinglin Zhou, Jian Du, Qingsheng Xiang, and Zengming Li

Understanding Driver Preferences for Secondary Tasks in Highly Autonomous Vehicles 126
Qingkun Li, Zhenyuan Wang, Wenjun Wang, and Quan Yuan

Classification of Mental Load of Special Vehicle Crew Based on Convolutional Neural Network 134
Fang Xie, Mingyang Guo, Xiaoping Jin, Sijuan Zheng, and Zhongliang Wei

Prevalence of Musculoskeletal Symptoms Among Construction Workers 140
Xinye Hong and Yuchi Lee

Establishment and Verification of Flight Fatigue Model Induced by Simulated Aircraft Driving 146
 Wei Jiang, Zhenling Chen, Haishan Xu, Tiebing Liu, Lili Li, and Xianfa Xu

Comparative Study on Inducing Effect of Two Kinds of Shape Flash in Pilot Selection by EEG Detection 153
 Yongsheng Chen and Dawei Tian

Application of Multi-motive Grid for Acceptance Test in the Pilots 159
 Yan Zhang, Yang Liao, Yishuang Zhang, Jian Du, and Liu Yang

Evaluation of Different Salmonella and Escherichia Coli Antibodies Based on ELISA 164
 Yan Gao, Yanan Huang, Shuxin Du, Weifeng Xia, and Fengfeng Mo

Study of the Intensity of Feedback of Vibration Information from Different Parts of the Human Body 170
 Jianyi Zhang, Shan Du, Haochen Dong, Wei Li, Haolin Sui, and Xinyang Zhao

Research on Psychological Service Needs of Paratroopers Based on Stress Events 177
 Yang Liao, Chuang Xu, Yiwen Hu, Xin Liu, Yuyang Zhu, Yan Zhang, Yishuang Zhang, Miao Jin, and Liu Yang

Design of Psychological Measurement and Archives Management System Based on WLAN 184
 Yishuang Zhang, Dongxue Chen, Yan Zhang, Yang Liao, Jian Du, Rong Lin, Duanqin Xiong, and Liu Yang

Research on the Machine Character

Mechanical Analysis of the Structure of a Large-Scale Pipeline System Detecting Robot 195
 Siyi Xiang, Xinyue Ma, Duzhong Feng, Yangguang Li, Shengyao Zheng, Dengchao Liang, and Bo Zhu

Design Point of Civil Aircraft Precooler Based on a Dimensionless Coefficient Method 203
 Zhiyong Min, Xiaodan Huang, Yi Cao, Huayan Liu, and Xuhan Zhang

Research on Application of Stepper Motor in Cabin Pressure Regulation System 210
 Ying Wang, Zhendeng Xing, Quanyi Zheng, and Guoyuan Zhang

Analysis and Design of the Shopping Trolley for Elderly People Based on Ergonomics 218
 Yaxuan Song, Ding Ding, Runsen Wang, and Hanzheng Di

Design and Development of Human Motion Capture System	226
Yuhong Shen, Chenming Li, Xiyu Bi, and Huilin Wei	
Human–Machine Analysis and Design of the Handrail System in Changzhou Subway	234
Min Qu, Xinying He, Yilin Ou, and Danning Hao	
An Improved Force-Directed Automatic Layout Method for Undirected Compound Graphs	242
Junyao Liu, Zhongnan Wang, Jiamin Yu, Haitian Liu, and Tong Li	
Improved Design of Multimedia Podium Under the New Teaching Method	250
Jiarong Zhang and Zihang Chen	
The Transmutation of the Traditional Instrument Performance Under the Visual Threshold of Science Technology Art	257
Yaru Zhu and Zhengqing Jiang	
Design of Manned On-Orbit Maintenance Interface for Space Station	265
Zhihai Li, Haocheng Zhou, Wei Zhang, and Xiangjun He	
Time Series Prediction Model of Spacecraft Health Management System Based on Wavenet Convolutional Neural Network	272
Ping Zhang, Xinyu Xiang, Jieren Cao, Chunjian Zhu, Qiang Yuan, Renping Li, Lijing Wang, and Ke Li	
Deep Reinforcement Learning Algorithm and Simulation Verification Analysis for Automatic Control of Unmanned Vehicles	279
Yonghong Chen, Yuxiang Zhang, Jiaao Chen, Junyu Zhao, Ke Li, and Lijing Wang	
Autonomous Vehicles Based on Gesture Recognition Control Using CNN and CPM Model	287
Xiulin Zhang, Chong Zhen, Quxiao Lei, Yifeng Wang, Jiaao Chen, Weiyi Jin, Ke Li, and Lijing Wang	
Research on Simulation Model System Integration and Interconnection Methods	295
Yan Hao, Jun Zhen, Ying Qu, and YaFei Zhang	
Detection of VOCs in E. Coli Based on Gas Chromatography-Mass Spectrometry	302
Handong Yao, Shuang Nie, Shuxin Du, Qianqian Ni, Xun Liu, and Fengfeng Mo	
Design Suggestion of Epidemic Prevention System for Shared Car Based on Scenario and Data	309
Zhouce Huang and Quan Yuan	

Prediction Model of Accident Vehicle Speed Based on Artificial Intelligence Decision Tree Algorithm 317
 Wei Ji, Tiantong Yang, Quan Yuan, Gang Cheng, and Shengnan Yu

Control Design to Underwater Robotic Arm 325
 Jiahong She, Shang Huan, Shaoli Xie, Deli Zhang, Liangliang Han, and Jian Yang

Research on Development of Vehicular High Power Microwave Weapons 336
 Bing Qian, Wei Yu, Heyuan Hao, and Haoran Zhu

The Near-Infrared Forearm Vessel Image Segmentation and Application Using Level Set 343
 Haoting Liu, Yajie Li, and Yuan Wang

Evaluation of CCGA Solder Pillar Grinding Effect Based on End-Face Imaging Analysis 349
 Mengmeng Wang, Haoting Liu, and Shaohua Yang

Near-Infrared Vascular Image Enhancement Using Deep Convolutional Neural Network 356
 Yajie Li, Haoting Liu, and Yuan Wang

Research on the Environment Character

The Development and Suggests of Planetary Protection 365
 Lantao Zhang

Research on Calculation Method of Aircraft Cabin Inner Wall Temperature Based on Parameter Sensitivity Analysis 370
 Yi Cao

Study on the Noise Control Technology in the Batching Room of a Dairy Production Enterprise 376
 Zhenfang Chen, Jianwu Chen, Qing Zhang, Bin Yang, and Yanqiu Sun

Study on the Environmental Characteristics of UAV Swarm Anti-swarm 384
 Zeliang Jiao, Qian Liu, Yanyan Ding, Hongyan Ou, Jiantao Liu, Hongyi Li, and Weixin Liu

Research on the Comprehensive Evaluation of Environmental Comfort in Deep-Sea Confined Space Based on Entropy Weight Method 389
 Chuan Wang, Juan Wang, Ziyang Wang, and Zhibo Lu

Applicability Analysis of Adaptive Power and Thermal Management System 397
 Junhao Zhang, A. Rong, Liping Pang, and Xiaodong Cao

New Detection Technology for Food Pesticide Contamination 404
Handong Yao, Dawei Tian, Fengfeng Mo, and Shuang Nie

Noise Hazard Analysis and Sound Insulation Research of a Semiconductor Manufacturer 411
Zhenfang Chen, Jianwu Chen, Xiaotong Chen, Yanqiu Shun, Bin Yang, and Weijiang Liu

Acoustic Target Recognition Based on MFCC and SVM 418
Kai Ding, Shoujun Zheng, Xiaogang Qi, Shan Huang, and Haoting Liu

Research on the Man-Machine Relationship

Description Strategy Selection in Collaborative Spatial Tasks 427
Ying Zhu, Duming Wang, Guangshan Liao, Liang Liu, Yunfei Chen, Lizhi Wang, Hanjun Yang, Wenhao Zhan, and Yu Tian

Research on Human-Robot Cooperative Target Recognition for Spatial Sampling Task 434
Shuqi Xue, Guangshan Liao, Lifeng Tan, Yu Tian, Yuan Wu, Yan Fu, Zhixian Zhang, and Chunhui Wang

Interface Design of a Health APP Based on the Mentality of the Elderly 442
Yanhui Xue and Jilei Yuan

Flight Deck Layout Design of a SSBJ 450
Guiqing Liu and Zheng Yang

Research on Man-Machine Interface Layout Method of Intelligent Command Cabin Based on GA-AA 457
Aiguo Lu, Bo Dong, Xiaoye Tong, and Wen Li

Research on the Recognition and Decision-Making of Carrier-Based Aircraft Interception and Landing Based on Visual Information 464
Xi Wan and Wen Li

Research on the Man-Environment Relationship

Research on the Adaptability Drills of Special Forces in Swimming Across Low Temperature Seawater 473
Chunlai Wang

Impact of Continuous Night Shifts on Crew Performance in 9-day Isolated Environment Shift Experiments 479
Ze Zheng Qiu, Liang Guo, Chenyuan Yang, and Liping Pang

Modeling of Human Cold Stress in Low Temperature Environment 485
Yuhong Shen, Chenming Li, Ting Zou, and Huilin Wei

Study on Prediction Model of Human Heat Stress in High Temperature Environment 494
 Chenming Li, Yuhong Shen, Ruoshi Xu, and Huilin Wei

Thermal Comfort Assessment of Occupants in Special Vehicle Cabin 503
 Sijuan Zheng, Feina Shi, Fang Xie, Qiufang Wang, and Zhongliang Wei

Research on the Selection of Cognitive Status Test Items and Indicators for Workers in Confined Spaces 509
 Chuan Wang, Ting Wang, Yi Chen, Xiaojun Wang, and Ziyang Wang

Research on the Evaluation of Abnormal Cognitive Status of Workers in Confined Spaces 517
 Chuan Wang, Qianxiang Zhou, Xiaojun Wang, and Ziyang Wang

Research on the Machine-Environment Relationship

Analysis on Loitering Attack Missile Application in Nagorno-Karabakh Conflict 527
 Lingpeng Kong, Heyuan Hao, and Lin Liu

Research on UAV Swarm Operations 533
 Lingpeng Kong, Zaochen Liu, Li Pang, and Ke Zhang

Analysis on the Operation of Bionic UAV in Tropical Mountain and Jungle 539
 Jiwen Sun, Heyuan Hao, Jianfeng Li, Junlong Guo, and Tao Li

Energy System Simulation for Low-Altitude Solar-Powered UAVs 544
 Dapeng Zhou, Yang Zhang, Ke Li, Bin Zhao, Meixian Wang, Ning Wang, and Lijing Wang

Research on the Configuration of Radar Jamming Force in Air Defense Operation 552
 Xilian Tan, He Wu, Yanyan Ding, and Yujin Wang

The Research on Optimal Design of Drawing Die for Non-circular Long Parts in Processing Environment 558
 Wobo Zhang, Jianguo Shi, and Huichao Liu

Research on the Overall Performance of Man-Machine-Environment System

Correlation Analysis of Traffic Accident Severity of the Heavy Trucks Based on Logistic Model 567
 Rufen Jiang, Xuejun Niu, and Huairui Zhang

Thoughts on Strengthening the Management of Dangerous Sources in Air Defense Force Training 574
 Lie Wang, Zhenguo Mei, Chunxin Wang, Kun Cao, and Weifei Wu

Prominent Problems and Management Countermeasures of Military Safety Work 579
 Kun Cao, Zhenguo Mei, Yanjiao Wang, Weifei Wu, and Peng Gong

Safety Risk Prevention and Control in Army Training: Model and Strategy 584
 Zhenguo Mei, Qian Shen, Weifei Wu, Kun Cao, and Peng Gong

Discussion on the Control of Major Hazard Sources in Unit Training 590
 Weifei Wu, Zhenguo Mei, and Kun Cao

Risk Assessment in Air Defense Forces Unit Training 595
 Qian Shen, Zhenguo Mei, Xuechen Yao, and Weifei Wu

A Framework of Aircraft Error-Prevention Verification Based on Routine Maintenance During Flight Test 600
 Yuqi Zhang, Feimin Li, and Hongjiao Wu

Study on Quantitative Evaluation Method of Aviation Equipment Error-Prevention 609
 Yuqi Zhang, Tao Ma, and Bao Lv

Improvement of Work Efficiency of Intelligent Manufacturing Operator 4.0 from the Perspective of HCPS 617
 Chaoan Lai and Ruobing Zhao

Research on the Mechanism of Intelligent Operations Command 626
 Haimin Hu, Weixin Liu, Hao Liu, Lei Tang, Hongyan Ou, and Junfei Wang

Research on Operational Effectiveness Evaluation of a Certain Type of Equipment 632
 Hongyan Ou, Qian Liu, Di Wu, Junfei Wang, Shuxin Wang, and Weixin Liu

An Analysis of the U.S. Red Flag Military Exercises 638
 Weixin Liu, Hao Jiang, Hongyan Ou, Shuxin Wang, and Kang Yu

Demand Analysis of Air Defense Unit Training Evaluation System 644
 Hao Liu, Yanyan Ding, Haimin Hu, Hongyan Ou, Weixin Liu, and Junfei Wang

Application of Grey AHP in Occupational Health Risk Assessment of Maintenance Operation in Xi'an Subway 650
 Miao Zhang, Jianwu Chen, Zhenfang Chen, Hong Yang, and Yan Wang

Theory and Application Research

Human Factors Design for Space Station 661
Wei Zhang, Yongqing Hou, Jian Jin, and Bing Wu

Man-Machine-Environment System Engineering in System of Systems Content 668
Baiqiao Huang, Peng Zhang, and Kunfu Wang

Man-Machine-Environment System Engineering Based Mine Ventilation System Safety Analysis Method Study 675
Hanqin Su and Baiqiao Huang

Design of Artificial Intelligence Monitoring and Early Warning System in Safety Manufacturing Based on Man-Machine-Environment System Engineering 684
Peng Zhang, Baiqiao Huang, Kunfu Wang, Wei Feng, and Jun Zhen

Application of Man-Machine-Environment System Engineering in Yacht Driving Simulator 691
Kunfu Wang, Li Guo, Wei Feng, Peng Zhang, and Baiqiao Huang

Emergency Search and Rescue Command Simulation Equipment Based on Man-Machine-Environment System Engineering 697
Ruolin Xing, Jun Zhen, Yan Hao, and Yafei Zhang

Perceptual Evaluation on the Man-Machine-Environment System of Music Library 703
Kunzhu Zhang, Haoyu Yang, and Quan Yuan

Research on Man-Machine-Environment Design of Stratospheric Airships 710
Jing Lv, Yuanping Zhang, Qian Wang, and Heng Gao

Hand Operation Ergonomics Study and Design of CCGA Grinding Process 719
Haoting Liu, Jianyue Ge, Yuan Wang, Shengjie Wang, Pengrong Lin, Shaohua Yang, and Duming Wang

Correction to: Prediction Model of Accident Vehicle Speed Based on Artificial Intelligence Decision Tree Algorithm C1
Wei Ji, Tiantong Yang, Quan Yuan, Gang Cheng, and Shengnan Yu

Author Index 727

Biography of Editor in Chief

Professor Shengzhao Long is the founder of the Man-Machine-Environment System Engineering (MMESE), the chairman of the Man-Machine-Environment System Engineering (MMESE) Committee of China, the chairman of the Beijing KeCui Academy of Man-Machine-Environment System Engineering (MMESE), and the former director of Ergonomics Lab of Astronaut Research and Training Center of China. In October 1992, he is honored by the National Government Specific Allowance.

In 1981, directing under famous Scientist Xuesen Qian, he founded MMESE theory; in 1982, proposed and developed human fuzzy control model using fuzzy mathematics; from August 1986 to August 1987, conducted research in Man-Machine System as a visiting scholar at Tufts University, Massachusetts, USA; in 1993, organized Man-Machine-Environment System Engineering (MMESE) Committee of China; published “Foundation of theory and application of Man-Machine-Environment System Engineering” (2004) and “Man-Machine-Environment System Engineering” (1987); and edited “Proceedings of the 1st–21st Conference on Man-Machine-Environment System Engineering” (1993–2021).

(E-mail: shzhlong@sina.com)

Dr. Balbir S. Dhillon is a professor of Engineering Management in the Department of Mechanical Engineering at the University of Ottawa, Canada. He has served as a chairman/director of Mechanical Engineering Department/Engineering Management Program for over 10 years at the same institution. He has published over 345 (i.e., 201 journal + 144 conference proceedings) articles on reliability, safety, engineering management, etc. He is or has been on the editorial boards of nine international scientific journals. In addition, Dr. Dhillon has written 34 books on various aspects of reliability, design, safety, quality, and engineering management published by Wiley (1981), Van Nostrand (1982), Butterworth (1983), Marcel Dekker (1984), Pergamon (1986), etc. His books are being used in over 85

countries, and many of them are translated into languages such as German, Russian, and Chinese. He has served as the general chairman of two international conferences on reliability and quality control held in Los Angeles and Paris in 1987.

Prof. Dhillon has served as a consultant to various organizations and bodies and has many years of experience in the industrial sector. At the University of Ottawa, he has been teaching reliability, quality, engineering management, design, and related areas for over 29 years, and he has also lectured in over 50 countries, including keynote addresses at various international scientific conferences held in North America, Europe, Asia, and Africa. In March 2004, Dr. Dhillon was a distinguished speaker at the Conf./Workshop on Surgical Errors (sponsored by White House Health and Safety Committee and Pentagon), held at the Capitol Hill (One Constitution Avenue, Washington, D.C.).

Professor Dhillon attended the University of Wales where he received a BS in electrical and electronic engineering and an MS in mechanical engineering. He received a Ph.D. in industrial engineering from the University of Windsor.

(E-mail: dhillon@genie.uottawa.ca)

Research on the Man Character



Research on Cognitive Theory Model of Man-Machine Combination Pilot Based on Information Processing

Siyu Chen¹, Hongjun Xue¹(✉), Xiaoyan Zhang¹, Jue Qu^{1,2}, and Sina Dang²

¹ Northwestern Polytechnical University, Xi'an 710072, China
xuehj@nwpu.edu.cn

² Air Force Engineering University, Xi'an 710051, China

Abstract. The cockpit design of information integration have changed the role of pilot. The role of Pilot in flight changes from the operator to the monitor of flight data, which put forward higher requirements for the pilot's information processing ability. Pilots will receive a lot of information and they must make decisions in a short time. Due to the need to process a large amount of information under the time pressure, the cognitive load of pilots is increasing and the work performance is decreasing, which would affect flight safety. Thus, this paper have analyzed the characteristics of information acquisition and processing from the perspective of pilot and cockpit. And then, the information processing framework based on pilot cognitive characteristics has been established. Finally the pilot cognitive theoretical model and Man-machine combination precision cognitive system model was proposed. The model considered both human and aircraft information interaction, quantified the cognitive load of pilots from the perspective of information processing ability.

Keywords: Pilot cognition model · Cognitive behavior modelling · Pilot information processing · Cockpit

1 Introduction

With the development of engineering technology and airworthiness technology, the reliability of aircraft mechanical system is increasing, and the safety and reliability of aircraft equipment have been greatly improved during flight mission. The number of serious aviation accidents caused by the damage of aircraft structure, components and system equipment is decreasing year by year. At the same time, with the improvement of aircraft automatic control system and the realization of information integration cockpit design, the human-aircraft system in flight mission is becoming more and more complex, and the flight environment poses challenges to the pilot's response and decision-making in emergency situations. With the application of artificial intelligence technology, the role of the pilot has changed from the operator to the monitor, but the cockpit design of information integration also makes the pilot need to process a large amount of real-time data at the same time, which puts forward high requirements for the pilot's cognition and decision-making ability [1].

Modern cognitive theory has absorbed the research achievements of system theory, information theory, cybernetics and computer science in the development process, and put forward the information processing model of human cognition, which regards human cognition as a process of information acquisition and processing. From the perspective of information processing, the cognitive mechanism and theory of man-machine combination can be classified into two categories: human cognitive characteristics and human-machine interaction cognitive characteristics.

In the operating environment, people are often processed under high cognitive load and state of emergency. For the research on cognitive characteristics of people under pressure and state of emergency. Sun [2] studied the hazard perception model of automobile drivers based on KAP theory. The cognitive structure equation of human danger perception is constructed, and the stress state is described objectively by combining demographic indicators such as driver age and gender, driving experience, visual search mode, traffic constraint cognition, risk attitude and other factors. Wu [3] through the study of complex information task error in the cognitive mechanism of interface. The integrated use of cognitive psychology, design science, experimental psychology, human factors engineering, and related theory and method of cognitive neuroscience and error source is put forward from the failure of tasks - factor to solve the complex information task interface design optimization problem. By establishing a mathematical model of misjudgment and misoperation in emergency situations, Huang [4] demonstrated the deficiencies and defects of the operator's cognitive behavior model in the existing human-machine system, and studied how to further optimize the human cognitive model after considering misprocessing.

The cognitive process research of specific display layout design is also the key issue of commander's human-computer interaction. By combining the memory mechanism of Chinese characters with long-term memory in working memory theory and intelligent methods such as point set topology, Liang [5] made an intelligent design for the cognitive processes such as character formation, literacy and character memorization and realized the mathematical explanation of the coding process. Wang [6] studied the design of digital interface information display, such as sensory perception, memory system, thinking and decision-making, and complete the action transmission of human machine. The core of HMI research is the coordination problem of human-machine relationship in a specific environment. Through excellent human-machine interface design, the effectiveness, efficiency, safety and comfort mechanism of human-machine interaction can be effectively solved.

The cognitive process of specific task types is an important application of human cognition. Liu [7] optimized the interface design of typical monitoring tasks in terms of visibility, cognition and experience by studying the information processing and storage methods of human brain. Shao [8] obtained the information display layout of pilot panel under warning and alarm tasks by analysing the coding rules of flight images and combining the cognitive theory of visual perception. Wu [9] studied the cognitive error mechanism for complex information tasks, providing theoretical improvements for subsequent cognitive optimization and interface optimization design. Li [10] solved the tasks related to the cognitive model of miners' safety behavior through intelligent technology, providing a method guidance from a cognitive perspective for monitoring

and patrol operations. The situation where the operator is overwhelmed and overburdened with information. The key of man-machine combination interaction is the display and processing method of all kinds of information which appears in normal man-machine interaction. The most important characteristic of complex human-machine combination interaction system is the information coupling of perception, decision and execution. The most important problem is to distinguish the machine-assisted human tasks from human tasks, and to solve and implement different task domains, that is, to analysis the characteristics of human and machine in the system, in order to determine the influencing factors of function allocation.

2 Study on Cognitive Mechanism Based on Cognitive Characteristics of Pilots

2.1 Research on Cognitive Mechanism

The aircraft display and control system displays the task information, parameter information, auxiliary decision information, statistical summary information and status display information to the pilot by displaying layers, numbers, icons, images, texts, text tables and dialog boxes on the interface. Pilots use sensory processing to store information received by their senses in the form of visual or sound representations. Selective attention decision and control information is further strengthened and processed into short-term memory. Perception is produced by processing in the brain. Short-term memory is transformed into working memory and long-term memory through perceptual processing. At the same time, relevant experiences are extracted from long-term memory as working memory for perceptual processing. The pilot makes decisions through thinking and reasoning, and then gives instructions to the display control system, which feeds back new information to the pilot. The specific pilot cognitive mechanism is shown in Fig. 1.

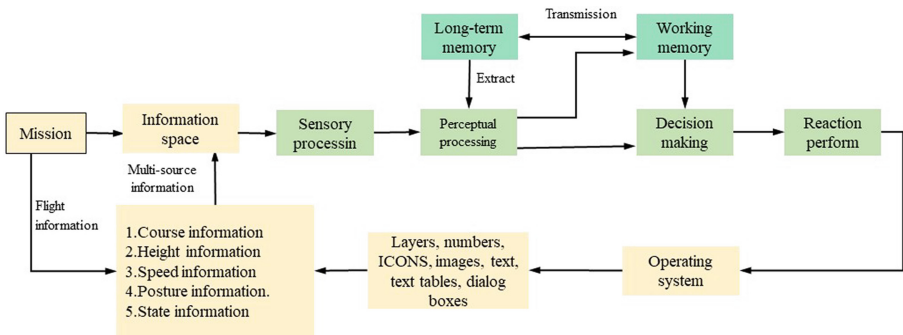


Fig. 1. Cognitive mechanism based on pilot characteristics

2.2 Core Cognitive Theory of Enhanced Cognition

Based on the cognitive mechanism and the different cognitive characteristics, man and machine are combined for cognition in the aspects of cognitive acquisition, analysis,

decision-making and action. The core cognitive theory of enhancing cognition is shown in Fig. 2.

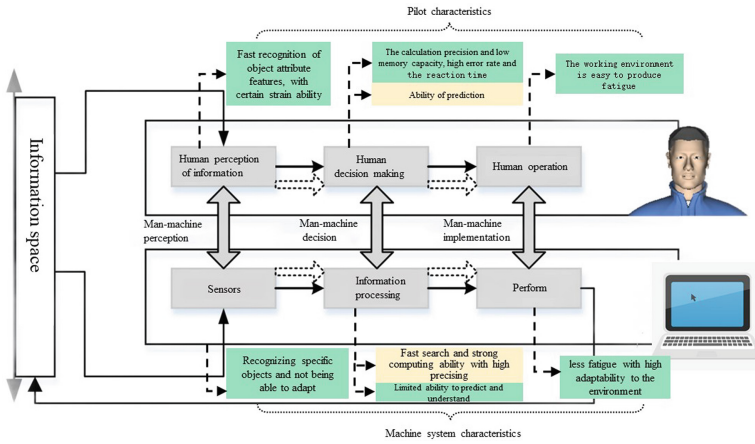


Fig. 2. Human computer combination cognitive enhancement

2.3 Natural, Efficient and Accurate Man-Machine Combination Cognition Mechanism

On the basis of man-machine combination cognition and machine system of multi-source information processing, machine system is disturbed to the environment monitoring and feedback processing. personal factors, experience of reasoning decision-making, and other functions, the influence of the adaptive algorithm based on pilot cognitive mechanism, the study of natural, efficient and accurate the man-machine combination of cognitive mechanism are shown in Fig. 3.

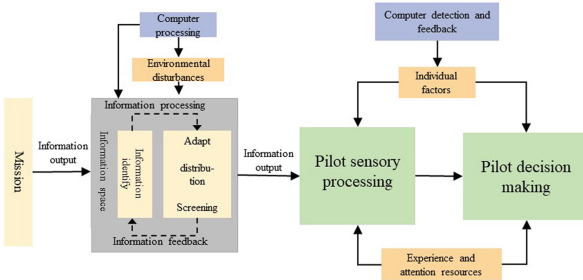


Fig. 3. Machine processing, monitoring and feedback

3 Human-Machine Combination Precision Cognitive Framework

3.1 Human-Machine Combination Precision Cognitive Framework

Based on the pilot’s cognitive mechanism, the pilot’s information processing model is constructed. The cognitive mechanism and information processing model, the cognitive framework of pilots are established. The human-machine combination precise cognitive framework is established by combining the machine system information processing rule base. The specific cognitive framework is shown in Fig. 4.

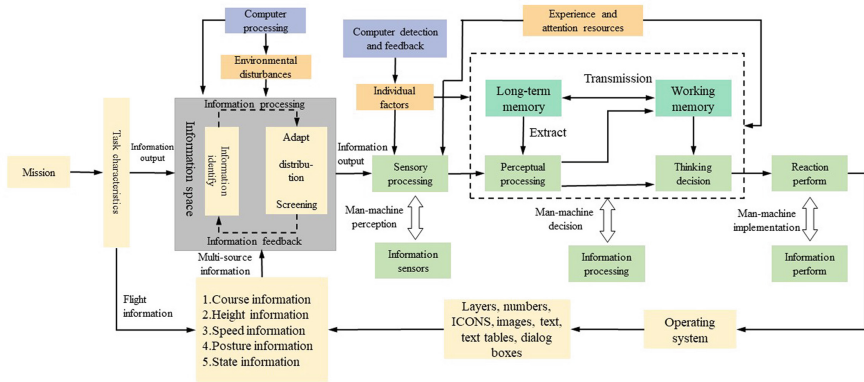


Fig. 4. Man-machine combination precision cognitive framework

3.2 Model Construction, Simulation and Effectiveness Evaluation of Human-Machine Combination Precision Cognition System

The man-machine combination precision cognition system model uses Matlab and Simulink as development tools. Based on intelligent control theory and man-machine combination precision cognition framework, neural network, machine learning and ATA module are adopted to screen and predict the information required for pilot’s cognition. Monitor and feedback the physiological, psychological, micro-expression and other indicators of human body are used to establish the human-machine integrated cognitive system model. The simulation system is consisted of development environment and operation environment. The development environment includes the establishment of information knowledge base, the determination of neural network structure, the selection of training samples, neural network learning and training of samples. The operating environment is used to control the controlled object, including human-machine perception information input, information synthesis and task allocation, inference machine, neural network, knowledge discovery, knowledge base adjustment, human-machine combination intelligent voting processing. Finally, the effectiveness evaluation system of simulation results is embedded in the simulation platform to evaluate the efficiency of the model, as shown in Fig. 5.

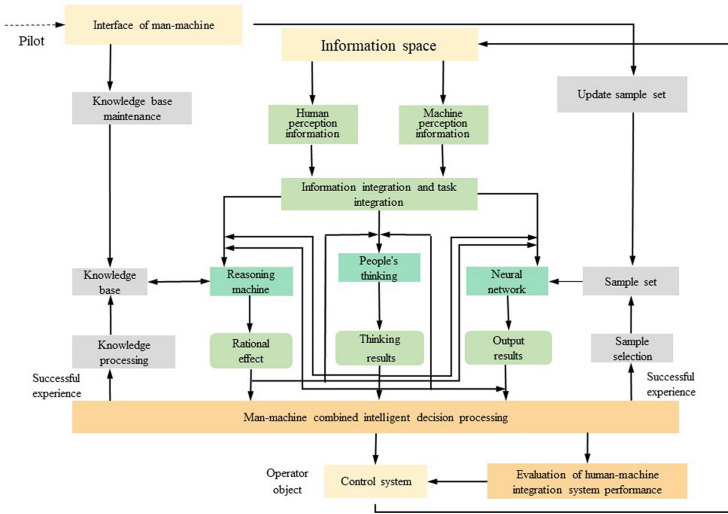


Fig. 5. Man-machine combination precision cognitive system model

4 Conclusion

This paper pay attention to the study of the pilot’s information processing capability during the mission. Based on the theory of pilot model and the framework of intelligent control system, this paper proposed Man-machine combination precision cognitive system model. At first, the task information and environmental information that can affect human-machine cognition process under specific task scenarios are selected to construct information space. Based on this information space, the characteristics of machine information acquisition and processing has been studied, which providing theoretical basis for the necessity of man-machine combination cognition research. Combined with the information processing of the machine, the cognitive mechanism model could describe the cognitive ability of the operator in the task. Then the efficient man-machine combination precision cognition mechanism is studied. The paper constructs a cognitive framework based on the cognitive mechanism of pilot. By studying the human-computer combination cognitive process and machine-aided information acquisition, expression, processing and decision transmission, an efficient human-computer combination accurate cognitive model is constructed. The monitoring and extraction of physiological data, the simulation of cognitive model and efficiency evaluation are realized on the experimental platform.

References

1. Chen, H., Cui, L., Ren, B., et al.: Monte Carlo method for sensitivity analysis of aviation unsafe incidents under uncertain conditions. *J. Beijing Univ. Aeronaut. Astronaut.* **324**(02), 177–184 (2020)
2. Sun, J.: Research on visual cognition mechanism of drivers’ danger perception. Chang’an University (2019)

3. Wu, X.: Study on error cognition mechanism of complex information task interface. Southeast University (2016)
4. Huang, S., Zhang, L., Li, X., et al.: Mathematical model of misjudgment and misoperation in emergency. *Hum. Ergon.* **6**(4), 4 (2000)
5. Liang, T., You, P., Qiu, Z., et al.: *J. South China Univ. Technol. Nat. Sci. Edn.* **36**(5), 4 (2008)
6. Wang, H.: Research on digital interface information design and evaluation method based on cognitive mechanism. Southeast University (2015)
7. Liu, R.: Design and evaluation of ship monitoring system software interface based on cognitive mechanism. Harbin Engineering University (2016)
8. Shao, J.: Research on information coding method of helmet display interface based on visual cognition Theory. Southeast University (2016)
9. Wu, X.: Research on error cognitive mechanism of complex information task interface. Southeast University (2016)
10. Li, J., Wang, J.: Research on key technologies of early warning, monitoring and emergency response of coal mine safety accidents. *J. Taiyuan Univ. Technol.* **40**(2), 4–10 (2009)



Study on Subspace Alignment EEG Classification for Cross Session Visual Tasks

Hongquan Qu¹, Mengyu Zhang¹, and Liping Pang²(✉)

¹ North China University of Technology, Beijing, China

² Beijing University of Aeronautics and Astronautics, Beijing, China
pangliping@buaa.edu.cn

Abstract. Mental workload (MW) is closely related to work efficiency. It is of great significance to obtain MW from electroencephalogram (EEG) signals. Due to the characteristics of random nonstationarity, EEG signals in different time sessions are quite different. This results in the poor generalization ability and low accuracy of the model when task generated EEG signals are used to identify MW. To solve the above problems, this paper proposes a MW classification method based on EEG cross-session subspace alignment. The labeled EEG signals with known MW and the unlabeled EEG signals to be identified are obtained. By learning a linear mapping, the source subspace base vector is aligned with the target subspace base vector, which solves the problem of different marginal distribution of EEG signals in the same space in different sessions. Through experiments, compared with the existing methods, this method can obtain better classification results.

Keywords: Mental workload · EEG · Cross-session · SVM

1 Introduction

The MW is closely related to the operator's professional knowledge, personality, task type and physiological variables [1]. Excessive MW can lead to rapid fatigue, distraction, and reduced efficiency, which result in errors in analysis and decision-making tasks. But too low MW can lead to waste of human resources [2].

The existing main methods of MW measurement include subjective measurement, performance measurement and psychophysiological measurement [3]. EEG refers to the recording of the electrical activity originated by brain [4]. Most EEG research methods divide EEG signals into four rhythms according to frequency band, including Alpha, Beta, Theta, Delta [5], and some studies have shown that the energy information in EEG is an important feature that can be used for classification [6].

EEG signals are non-stationary [7], the signals will change greatly due to the physiological changes of operators, environmental changes, and instrument changes [8]. When the distribution of data changes, most statistical models need to be rebuilt from scratch using newly collected training data. It is expensive or impossible to recollect the needed training data and rebuild the models [9].

Therefore, this paper proposes a MW classification method based on EEG Cross-Session Subspace Alignment (CSSA), which can build a personalized model for the mental load of new sessions, make full use of the existing session data, and improve the classification accuracy.

2 Experiments and Data Preprocess

2.1 Experiments

A 32-channel Neuroscan Neuamps (Synamps2, Scan4.3, EI Paso, USA) system is shown in Fig. 1, which can record all EEG signals. M1 and M2 are the reference electrodes of the system, which are located at the mastoid position behind the left and right ears respectively. EEG raw data is digitized at 1024 samples per second. Band-pass filter settings were 0.1–200 Hz [10].

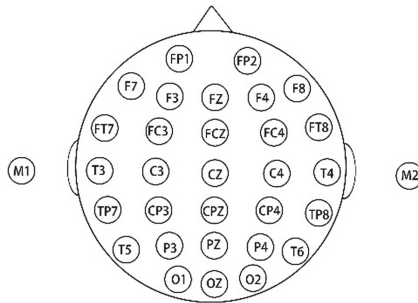


Fig. 1. Channel location

EEG signals were collected from 13 subjects in Beihang University (aged between 22 and 25 years, with 2 females and 11 males). The Multi Attribute Task Battery (MATB-II, National Aeronautics and Space Administration (NASA), USA) was used as the platform of experiment. Its task interface is shown in Fig. 2. The four regions correspond to some visual and operational missions respectively. During the experiment, two levels of MW were set, and they are low mental workload (LMW) and high mental workload (HMW).

The difficulty of the experimental task is defined by the occurrence frequency of the four sub-tasks. In the LMW task, 1 task occurred in 1 min, and in the HMW task, 24 tasks occurred in 1 min.

2.2 Data Preprocess

The average values of M1 and M2 were used as the reference of data processing. The 30-channel EEG signals were filtered with 1–30 Hz finite impulse response (FIR) band-pass filter, and the filter order was 3300.

To ensure the reliability of data analysis, the EEG signals of 10 participants (sub1~sub10, aged between 22 and 25 years, with 2 females and 8 males) were selected to analyze according to the selection criteria of high performance and less artifacts [11].

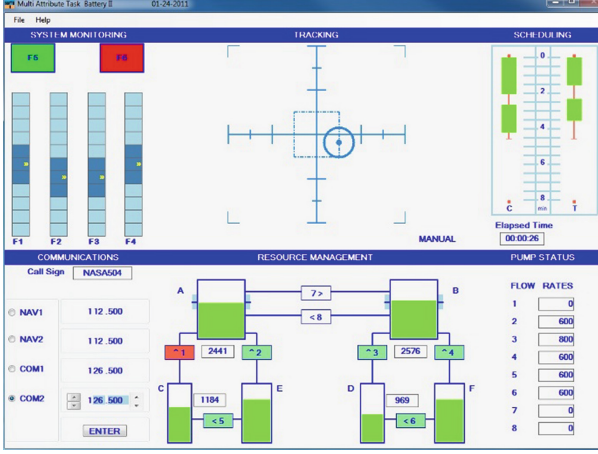


Fig. 2. MATB-II tasks

The power spectral density (PSD) at different frequencies is often used to extract the features of EEG signals in the frequency domain [12]. Fourier transform in Formula (2.1) was performed on each data segment to obtain $F_s(n)$.

$$F_s(n) = \sum_{n=0}^{N-1} S e^{-\frac{2\pi j}{N} n} \quad (2.1)$$

where S is the ICs of a group of EEG signals and is the Fourier transform of the signal. N is the number of signal samples. The value of n is 0 to $N - 1$.

The corresponding PSD of EEG ICs was calculated with Formula (2.2).

$$p_s(n) = \frac{F_s(n)F_s^*(n)}{N} \quad (2.2)$$

where $p_s(n)$ is PSD of EEG ICs; $F_s^*(n)$ is the conjugate of $F_s(n)$. N is the length of signal.

3 Classification for Cross Session Visual Tasks

3.1 Classification Method Based on CSSA

The method is divided into two parts. The first part is data preprocessing, which includes obtaining the independent components of EEG through ICA and extracting the energy features of ICs. The second part is domain adaptation, which includes subspace and dimension reduction features obtained with PCA algorithm, transfer features obtained with SA and MW classifier construction.

Before obtaining the EEG signals of the new session, we have obtained the EEG signals identified from session 1 to session N . We preprocess the known data separately and take the energy characteristics of EEG signals in each SA as a source domain. We

do the same preprocessing to the unlabeled new session EEG signals and take the energy characteristics of the new session EEG signals as the target domain. The we aligned the subspace between the source domain and the target domain by SA method, the transfer domains were the training sample to construct the classification model.

3.2 SA Method

Let $X \in x$ be the EEG recorded of a sample (X, y) , where $x = RC \times D$, where C is the number of channels, D is the number of samples of time series, in this paper, $C = 30$, $D = 300$. $Y \in Y$ represent the corresponding MW label. Let $P(X)$ be the marginal probability distribution of X , and $P(Y|X)$ be the conditional probability distribution. We represent the source domain as X_{Si} , where $X_{Si} = x_{Si, 1}, y_{Si, 1}, \dots, x_{Si, j}, y_{Si, j}, \dots, (x_{Si, D}, y_{Si, D})$, $i = 1, 2, \dots, N$, $j = 1, 2, \dots, D$. Similarly, the target domain is represented as X_T , where $X_T = x_{T, 1}, y_{T, 1}, \dots, x_{T, j}, y_{T, j}, \dots, (x_{T, D}, y_{T, D})$, $j = 1, 2, \dots, D$. Where $(X_{Si}, X_T) \in X$ is the normalized relative power spectral density. Although both source domain data and target domain data are in d -dimensional space, their marginal distributions are different, while their conditional distributions are almost the same. We assume $P(X_S) \neq P(X_T)$, but $P(Y|X_S) = P(Y|X_T)$, which means there are differences between different domains. The purpose of domain adaptation is to make $P(\phi(X_S)) = P(X_T)$ with a linear mapping ϕ .

According to PCA theory, we find the eigenvectors corresponding to the l largest eigenvalues in each domain. These eigenvectors are defined as source domain subspace and target domain subspace, which are represented as Z_S and Z_T respectively. Assuming that there is a linear relationship between Z_S and Z_T , we can find a linear mapping to align the source subspace with the target subspace. We use the transformation matrix S from Z_S to Z_T to align the basis vectors. The matrix S transforms the source subspace coordinate system into the target subspace coordinate system by aligning the source and target basis vectors. The transformation matrix S is achieved by minimizing the following Bregman matrix divergence:

$$F(S) = \min \|Z_S S - Z_T\|_F^2 \quad (3.1)$$

where $\|\cdot\|_F^2$ is the F-norm. Because of the orthogonality of the F-norm, the above formula can be rewritten as:

$$\min \|Z_S^T Z_S S - Z_S^T Z_T\|_F^2 = \min \|S - Z_S^T Z_T\|_F^2 \quad (3.2)$$

It can be seen from the above formula that when $S^* = Z_S^T Z_T$, the minimum value of the above formula is obtained. For the coordinate system of the source domain, it can be written as:

$$X_a = Z_S Z_S^T Z_T \quad (3.3)$$

By calculating Formula (3.4), we can get the representation of the source domain and the target domain in the new coordinate system after subspace alignment. Currently, the target domain and the source domain have the most similar marginal distribution.

$$\begin{aligned} G &= X_S X_a \\ H &= X_T Z_T \end{aligned} \quad (3.4)$$

4 Results of Classification Method Comparison

4.1 Comparison of Mental Workload Classification Using CSSA and not Using CSSA

MW Classification accuracy using CSSA and not using CSSA will be compared in this section. The former presented in this paper is named as Method 1, In method 2, the energy features of EEG ICs are used, PCA method is directly used to reduce the dimension of data instead of domain adaptation method. SVM classifier is used to obtain the MW classification results.

Through the experiment, EEG signals of 10 subjects lasting for one week were obtained and preprocessed. In this section, Session 0 represent the first day, and the data of this session is only used as training data. From the second day to the seventh day. Sessions 1 to 6 represent the second to seventh days. From the second day, the preprocessed energy features of the previous day are used as the training set, and the features of the day are used as the test set to construct the classification model.

The comparison of classification accuracy of the two methods is shown in Fig. 3. For the same time and data, the accuracy of Method 1 ranged from 73.3% to 88.1%, and the average classification accuracy was 80.2%. The accuracy of Method 2 ranged from 50.2% to 63.3%, and the average classification accuracy was 52.9%. Compared with method 2, the accuracy of method 1 is improved by 23% to 31.5%, with an average of 27.3% .

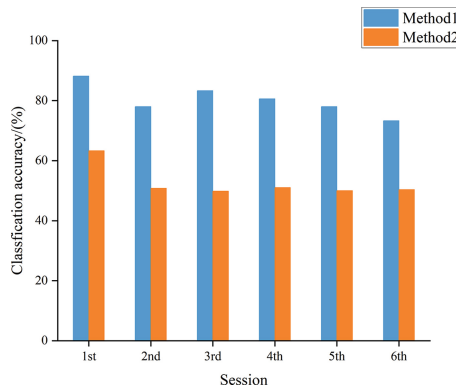


Fig. 3. Classification accuracy comparison of Method 1 and Method 2

4.2 Comparison of Mental Workload Classification Using CSSA and TCA

MW Classification accuracy using CSSA and using TCA will be compared in this section. The same experiment as in Sect. 4.1 was completed.

The EEG signals were preprocessed in the same way, in the domain adaptation part, the accuracy of SVM classifier constructed by the proposed method and TCA method is compared. The comparison of classification accuracy of the two methods is shown in Fig. 4.

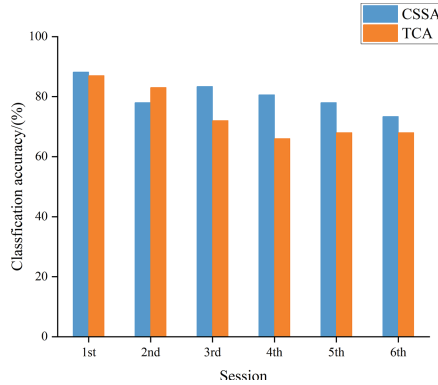


Fig. 4. Classification accuracy comparison of CSSA and TCA

- (1) The accuracy of CSSA is between 73.3% and 88.2%, and the average accuracy is 80.2%.
- (2) The accuracy of TCA is between 66% and 87%, and the average accuracy is 74%.

The average classification accuracy of CSSA is higher than that of TCA, this is because the TCA method only uses the shared features in the two domains. The difference is that CSSA uses the relevant features of the two domains. On the other hand, the stability of CSSA method is better than TCA method. This is different from TCA method in dealing with the original data, CSSA method processes its subspace, which makes the algorithm more robust. Therefore, we choose CSSA method as the method of cross time MW classification.

5 Conclusion

In this study, we propose a MW classification method based on EEG cross-session subspace alignment, it includes filtering EEG signals, obtaining ICs by ICA method, extracting energy features, obtaining subspace according to PCA theory, aligning the source subspace base vector with the target subspace coordinate system base vector by learning a linear mapping.

The conclusions are as follows:

Compared with Method 2, the classification accuracy of the proposed CSSA method is improved from 52.9% to 80.2%. Compared with other domain adaptive methods, the proposed CSSA method has 6% improvement in classification accuracy compared with TCA method and can introduce multi-source domain to further improve the classification accuracy.

Compliance with Ethical Standards. The study was approved by the Logistics Department for Civilian Ethics Committee of North China University of Technology.

All subjects who participated in the experiment were provided with and signed an informed consent form.

All relevant ethical safeguards have been met with regard to subject protection.

References

1. Hao, G.U., Zhong, Y.: Mental workload assessment based on EEG and a hybrid ensemble classifier. *Softw. Guide* **18**, 1–4 (2019)
2. Salomao, T., Alberto, L.: Operator functional state modelling and adaptive control of automation in human-machine systems (2016)
3. Thea, R.: Dual frequency head maps: a new method for indexing mental workload continuously during execution of cognitive tasks. *Front. Physiol.* **8**, 1019 (2017)
4. Zhang, J., Cao, X., Wang, X., et al.: Physiological responses to elevated carbon dioxide concentration and mental workload during performing MATB tasks. *Build. Environ.* **195**, 107752 (2021)
5. Abhang, P.A., Gawali, B.W., Mehrotra, S.C.: Technological basics of EEG recording and operation of apparatus. In: *Introduction to EEG- and Speech-Based Emotion Recognition* (2016)
6. Fasil, O.K., Rajesh, R.: Time-domain exponential energy for epileptic EEG signal classification. *Neurosci. Lett.* **694**, 1–8 (2018)
7. Von Wegner, F., Tagliazucchi, E., Laufs, H.: Information-theoretical analysis of resting state EEG microstate sequences - non-Markovianity, non-stationarity and periodicities. *Neuroimage* **158**, 99–111 (2017)
8. Pan, S.J., Yang, Q.: A survey on transfer learning. *IEEE Trans. Knowl. Data Eng.* **22**(10), 1345–1359 (2010)
9. Zanini, P., Congedo, M., Jutten, C., et al.: Transfer learning: a riemannian geometry framework with applications to brain-computer interfaces. *IEEE Trans. Biomed. Eng.* **1** (2017)
10. Xu, G., Jing, W., Zhang, Q., et al.: A spike detection method in EEG based on improved morphological filter - ScienceDirect. *Comput. Biol. Med.* **37**, 1647–1652 (2007)
11. Croft, R.J., Barry, R.J.: Removal of ocular artifact from the EEG: a review. *Neurophysiol. Clin./Clin. Neurophysiol.* **30**, 5–19 (2000)
12. Huang, X., Li, Q., Xie, D., et al.: Study on the characteristics of EEG power spectral density in suspension Moxibustion at Dubi (ST 35) of different states. *World Chin. Med.* (2019)



Mental Workload Classification Method Based on Transfer Component Analysis with Cross-Session EEG Data

Hongquan Qu¹, Hanwen Dong¹, and Liping Pang²(✉)

¹ School of Information Science, Technology of North China University, Beijing 100144, China
qhghpd@ncut.edu.cn, donghanwen@mail.ncut.edu.cn

² School of Aeronautic Science and Engineering of Beihang University, Beijing 100191, China
pangliping@buaa.edu.cn

Abstract. Due to the non-stationary randomness of the EEG signals, which results in a trained classifier with very low generalization ability. In order to improve the cross-session classification accuracy of Mental Workload (MW), a domain adaptive classification method is studied based on Transfer Component Analysis (TCA) using EEG Independent Components (ICs) in this paper. First step is to transform the EEG data in source and target domains in a same way. The TCA algorithm is used to build the transformation ϕ in order to minimize their Maximum Mean Discrepancy (MMD) distance between the source domain and the target domain. Second step is to train a MW classifier using the SVM and the transformed EEG data in the source domain. The target domain data are used for test. The presented method is compared with Subspace Alignment (SA). EEG data in the source and target domains are measured 24 h apart. A-distance is calculated to reveal the distribution difference between the transformed source and the target domains. The results show that the classification accuracy of the proposed method can be improved by 15.11% compared with SA. The A-distance of TCA is significantly lower than that of SA.

Keywords: EEG · Classification of mental workload · Independent Component Analysis (ICA) · Transfer Component Analysis (TCA) · Subspace Alignment (SA)

1 Introduction

Mental workload has been defined as the portion of an individual's mental capacity which is actually required by task demands [6]. With the rapid development of machine learning, more researchers used the algorithm [9] to explore the correspondence between EEG features and MW levels. A large number of traditional machine learning models have been adopted, including the Support Vector Machine (SVM) [5, 12], the Linear Discriminant Analysis (LDA) [4], the Extreme Learning Machine (ELM) [15] and so on. With the deepening of research, researchers further discovered that the non-stationarity of

EEG data with time [8, 10]. The non-stationarity of EEG results in data not to conform the assumptions of traditional machine learning, namely the training data and test data should observe the same distribution. Therefore, in order to solve the negative impact caused by the nonstationarity of EEG signals, we propose Mental Workload Classification Method Based on TCA.

2 Experiment and Feature Extraction Methods

2.1 Experiment

8 graduate students were selected as subjects (sub01–sub08), including 6 males and 2 females. All subjects are between 22–25 years old. The experiment time was set in the morning. We obtained the EEG signals of the subjects for 6 consecutive days.

The brain electrode distribution adopted a 32 standard lead system. The system used M1 and M2 electrodes as a common reference, which was located at the position of the human mastoid. The data sampling rate was 1024 Hz. The experimental platform was the multi-attribute task battery (MATB-II, National Aeronautics and Space Administration (NASA), USA) [7]. By adjusting the frequency of each subtask, the subjects can achieve low MW or high MW.

2.2 Feature Extraction Based on ICs

Independent Component Analysis (ICA) [2] originated from blind source separation study is often used to separate mixed speech signals and obtain their ICs. The power spectral density (PSD) at different frequencies is often used to extract the features of EEG signals in the frequency domain. According to the EEG signal frequency band distribution, it can be divided into four frequency bands: δ (1–4 Hz), θ (4–8 Hz), α (8–14 Hz) and β (14–30 Hz).

In order to reveal the MW changes in details, the ICs of EEG signals are divided into data segments with 2 s time interval before extracting the features. The middle 5-min EEG data of each MW are used. There are 600s EEG data and they are divided into 300 data segments.

3 Methodology

In order to assure the normalization performance of classifier cross different sessions, a MW classification method based on TCA [13] is presented in this section. It mainly composes of two steps:

Step 1: EEG feature extraction based on ICA as shown in Fig. 1.

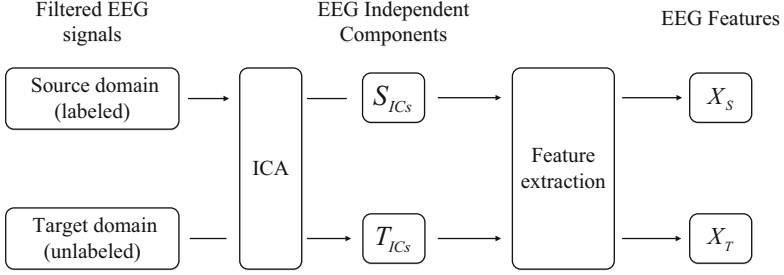


Fig. 1. EEG feature extraction based on ICA

The 30-channel mixed EEG signals were filtered with 1 Hz high-pass filter and 35 Hz low-pass filter, respectively.

The filtered EEG signal is separated by the ICA algorithm to obtain EEG ICs. In this paper, we set the data in the source domain after ICA as S_{ICs} , and the data in the target domain after ICA as T_{ICs} .

With the feature extraction method in Sect. 2.2, there are 300 EEG segments for each MW experiment. The number of EEG segments is 600 for two MW experiments. Each segment has 30 EEG ICs, and each EEG ICs can extract four relative energy features of $E_{s,\delta}^*$, $E_{s,\theta}^*$, $E_{s,\alpha}^*$ and $E_{s,\beta}^*$, so 120-dimensional energy features are obtained finally. In this paper, the feature in the source domain is F_s , and the feature of the target domain is F_T . Step 2: Cross-session MW classifier based on TCA as shown in Fig. 2.

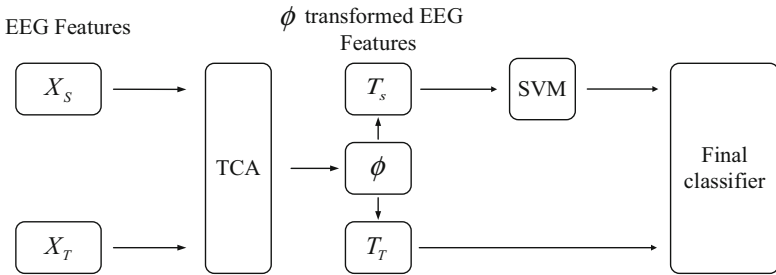


Fig. 2. Cross-session MW classifier based on TCA

In this step, the EEG data in source and target domains are transformed in a same way. The TCA is used to build the transformation ϕ in order to minimize their MMD distance between the source domain and the target domain. This step can ensure the marginal distribution becomes similar for the EEG data in the source and target domains. In this way, X_S and X_T are transformed by the same ϕ , and then $T_S = \phi(X_S)$ and $T_T = \phi(X_T)$ are obtained, respectively. Then a SVM classifier [11] is trained using the transformed EEG data in the source domain. The SVM classifier uses linear kernel function, grid search and cross-validation to find the optimal parameters in order to get the final classifier. This classifier will be used to predict the transformed target domain data.

4 Results and Comparisons

In this paper, we obtain the 6-day characteristic data of each subject. Choose the 6th day as the target domain, and 1–5 days as the source domain respectively, and send them to our proposed method for MW classification. We will give the average classification accuracy of 8 subjects per day.

In order to prove the effectiveness of the transform learning, we compared the classification accuracy of the source domain and the target domain without TCA operation, TCA operation and SA operation, as shown in Fig. 3.

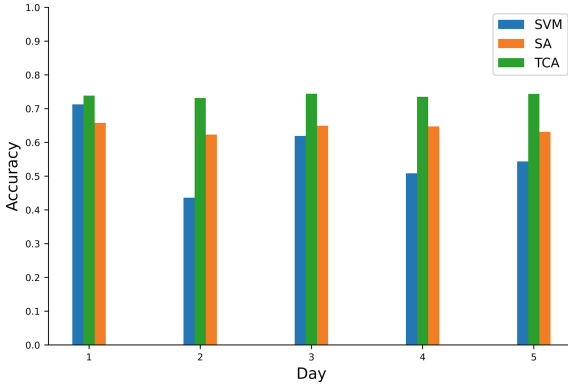


Fig. 3. Comparison of classification accuracy with TCA, without TCA and SA

From Fig. 3, we can observe that:

1. The MW classification accuracy using the TCA algorithm is between 0.7313–0.7440, and the average accuracy is 0.7384.
2. The MW classification accuracy of without TCA algorithm is between 0.4360–0.7125, and the average accuracy is 0.5638.
3. The accuracy range of SA is between 0.6229 and 0.6577, and its average accuracy is 0.6415.

In the MW classification, the accuracy of the classifier is improved by 30.97% when using the TCA algorithm and not using the TCA algorithm. It shows that the linear classifier that has not been trained in the source domain of the TCA algorithm has poor generalization ability. The minimum classification accuracy of TCA is 17.40% higher than the minimum classification accuracy of SA. The highest classification accuracy of TCA is 13.12% higher than the highest classification accuracy of SA. The average accuracy of MW classification using TCA is improved by 15.11% compared to using SA.

In order to show the effectiveness of our proposed network, we compare it with the SA [1] method of subspace learning. In addition A-distance [14] is used to reveal the distribution difference between the transformed source and the target domains. But it

is difficult to directly calculate its exact value, and an approximate method to estimate A-distance is used in this paper [3]. The A distance between the source domain and the target domain after SA and TCA transformations is compared in Fig. 4.

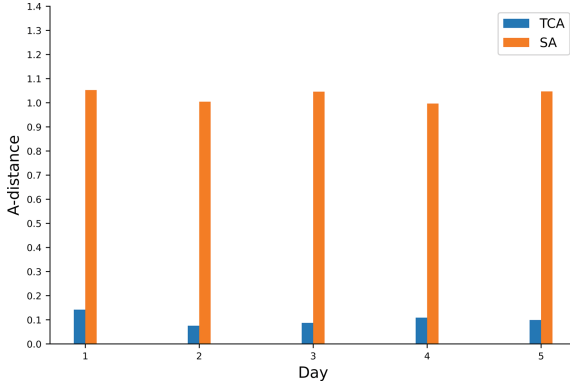


Fig. 4. Comparison of A-distance with TCA and SA.

From Fig. 4, we can observe that:

1. The A-distance of TCA is between 0.0033 and 0.3933, and its average A-distance is 0.1025.
2. The A-distance of SA is between 0.3400 and 1.6533, and its average A-distance is 1.0291.

The A-distance of the source domain and target domain after SA transformation is significantly larger than the A-distance after TCA transformation. This shows that TCA can better reduce the distribution difference between the source domain and the target domain compared with SA. This explains why the average classification accuracy of TCA is better than the one of SA.

5 Conclusions

In this study, we propose a mental workload classification method based on TCA for classify cross-session EEG data to realize cross-session recognition of EEG. It tries to provide a possible and effective solution to overcome poor generalization of cross-session MW classifiers caused by the non-stationarity of EEG. Its classification performance is compared with the traditional SVM MW classifier and the SA-based cross-session MW classifier. Some conclusions are drawn from our study as follows:

1. In the MW classification of 6 days EEG data of the same subject, the classification accuracy of the TCA classifier can be improved by 30.97% compared with the classifier without using the TCA algorithm. The generalization ability of the presented classifier has been greatly improved.

2. The classification accuracy of the TCA classifier can be improved by 15.11% compared with the classifier with SA algorithm. The TCA algorithm is a better choice than the SA algorithm for cross-session MW recognition.
3. In this paper, the A-distance is introduced to reveal the distribution difference between the transformed source and target domains. Results show that the A-distance of the same source domain and target domain after the TCA is significantly smaller than the one after the SA transformation. This can support that the proposed method might be better to reduce the distribution difference between the source domain and the target domain compared to the SA method.

References

1. Fernando, B., Habrard, A., Sebban, M., Tuytelaars, T.: Subspace alignment for domain adaptation. [arXiv:1409.5241](https://arxiv.org/abs/1409.5241), pp. 1–20 (2014)
2. Bigan, C., Woolfson, M.: Independent component extraction methods in biosignal processing. In: The 26th Annual International Conference of the IEEE Engineering in Medicine and Biology Society, pp. 511–513 (2004). <https://doi.org/10.1109/IEMBS.2004.1403206>
3. Chen, Z.: Geographic entity relationship extraction based on domain adaptive transfer learning. M.S. thesis, Wuhan University of Technology, Wuhan, China (2019)
4. Rajaguru, H., Prabhakar, S.K.: Optimization of fuzzy outputs for classification of epilepsy from EEG signals using linear discriminant analysis. In: 2017 International conference of Electronics, Communication and Aerospace Technology (ICECA), pp. 598–602 (2017). <https://doi.org/10.1109/ICECA.2017.8203607>
5. Gu, H., Yin, Z., Zhang, J.: EEG based mental workload assessment via a hybrid classifier of extreme learning machine and support vector machine. In: 2019 Chinese Control Conference (CCC), pp. 8398–8403 (2019). <https://doi.org/10.23919/ChiCC.2019.8865496>
6. Albuquerque, I., et al.: On the analysis of EEG features for mental workload assessment during physical activity. In: 2018 IEEE International Conference on Systems, Man, and Cybernetics (SMC), pp. 538–543 (2018). <https://doi.org/10.1109/SMC.2018.00101>
7. Linch, J.P.: Price Code A, and Price Code A National Aeronautics and Space Administration (NASA). Springer, Berlin/Heidelberg (2011)
8. Sadatnejad, K., Roc, A., Pillette, L., Appriou, A., Monseigne, T., Lotte, F.: Channel selection over Riemannian manifold with non-stationarity consideration for brain-computer interface applications. In: ICASSP 2020 - 2020 IEEE International Conference on Acoustics, Speech and Signal Processing (ICASSP), pp. 1364–1368 (2020). <https://doi.org/10.1109/ICASSP40776.2020.9053101>
9. Lemm, S., Benjamin, B., Thorsten, D., Klaus-Robert, M.: Introduction to machine learning for brain imaging. *Neuroimage* **56**, 387–399 (2011)
10. Hasib, M.M., Nayak, T., Huang, Y.: A hierarchical LSTM model with attention for modeling EEG non-stationarity for human decision prediction. In: 2018 IEEE EMBS International Conference on Biomedical & Health Informatics (BHI), pp. 104–107 (2018). <https://doi.org/10.1109/BHI.2018.8333380>
11. Sani, M.M., Norhazman, H., Omar, H.A., Zaini, N., Ghani, S.A.: Support vector machine for classification of stress subjects using EEG signals. In: 2014 IEEE Conference on Systems, Process and Control (ICSPC 2014), pp. 127–131 (2014). <https://doi.org/10.1109/SPC.2014.7086243>

12. Rathipriya, N., Deepajothi, S., Rajendran, T.: Classification of motor imagery ecog signals using support vector machine for brain computer interface. In: 2013 Fifth International Conference on Advanced Computing (ICoAC), pp. 63–66 (2013). <https://doi.org/10.1109/ICoAC.2013.6921928>
13. Pan, S.J., Tsang, I.W., Kwok, J.T., Yang, Q.: Domain adaptation via transfer component analysis. *IEEE Trans. Neural Netw.* **22**(2), 199–210 (2011). <https://doi.org/10.1109/TNN.2010.2091281>
14. Ben-David, S., Blitzer, J., Crammer, K., Pereira, F.: Analysis of representations for domain adaptation. In: NIPS, pp. 137–144 (2007)
15. Peng, Y., Zhu, J., Zheng, W., Lu, B.: EEG-based emotion recognition with manifold regularized extreme learning machine. In: 2014 36th Annual International Conference of the IEEE Engineering in Medicine and Biology Society, pp. 974–977 (2014). <https://doi.org/10.1109/EMBC.2014.6943755>



Development of Competency Model for Test Pilots Selection and Training

Yanyan Wang¹, Huifeng Ren², Xiaochao Guo¹, Yu Bai¹, Yu Duan¹, Zhengtao Cao¹,
Duanqin Xiong¹, and Qingfeng Liu¹(✉)

¹ AirForce Medical Center, FMMU, PLA, Beijing 100142, China
littleponds@163.com

² Special Section, 92493 Hospital of PLA, Huludao 125110, China

Abstract. Objective: To explore the competency model of test pilots, and to provide theoretical basis for psychological selection and post matching. **Methods:** On the basis of reviewing more than 200 relevant research papers, technical reports and reviews, 2130 evaluation indexes describing pilots' psychological attributes were collected. According to the job requirement of test pilots, 108 items were selected by three aviation psychologists which were used to develop the questionnaire of test pilots' psychological quality. All items were constructed as four dimensions including "knowledge", "skill", "ability" and "others". Then 30 test pilot experts were asked to complete the questionnaire, the multigrade fuzzy set (MFS) evaluation technique was used to determine the competency model of test pilot. **Results:** ① A total of 24 indexes were included in the competency model of test pilots. ② Dedication and flight procedure were identified as the most important indexes of test pilots (MFS value > 0.704); Eight indexes were identified as important indexes for evaluating test pilots (0.704 > MFS value > 0.599) and 14 relatively important indexes (MFS < 0.599). ③ The Hierarchical competency model which concluded 4 dimensions and 3 levels was developed based on the importance and specificity of 24 indexes. **Conclusion:** This study provides theoretical basis and technical support for the establishment of competency evaluation model of test pilots which would be used in psychological selection and training of test pilots.

Keywords: Test pilot · Competency model · Delphi method · Multistgrade fuzzy set · Selection

1 Introduction

Test pilot is defined as a pilot who specializes in putting new or experimental airplanes through maneuvers designed to test them (as for strength) by producing strains in excess of normal [1]. Otto Lilienthal's famous saying [2], to design a flying machine is nothing, to build it is not much, to test it is everything, shows that test pilots play an extremely important role in flight test and aircraft development.

As a special group in pilots, there are independent requirements for the psychological quality of test pilots [3], and American test pilot schools have established enrollment requirements and Comprehensive Candidate Evaluation Program [4, 5]. The latest

test pilot selection system and comprehensive evaluation procedures were developed to evaluate the professional skills, engagement, test flight ability and test flight environment adaptability of candidate pilots, replacing the Pilot Candidate Selection Method (PCSM) which included three components, Air Force Officer Qualifying Test, Test of Basic Aviation Skills and previous flying experience [6].

With the development of new aviation weapons and equipment, the demand for high-level test pilots is also increasing. Liu studied the the mental attributes of aged test pilots in order to maximum professional span and suggested routine aptitude test which would benefit the need for test pilot and aviation safety [7]. However, there is no clear standard for test pilot selection and relevant studies are rare in China. Therefore, it is necessary to establish competency model for test pilots base on flight test tasks so as to provide a theoretical basis for the psychological selection and posttraining of test pilots.

2 Methods

2.1 Subjects

There are 30 active flight test pilot experts (flight level: Level I or above) with rich flight test experience, aged 40 ± 6.53 yrs participated the survey and completed the questionnaire. Admission requirements were that the severic time must more than 10 years and 1500 h or Instructor Pilot in a major aircraft system.

2.2 Survey Tool and Methods

On the basis of reviewing more than 200 relevant research papers, technical reports and reviews, 2130 evaluation indexes describing pilots' psychological attributes were collected. According to the job requirement of test pilots, 108 indexes were selected by three aviation psychologists using Delphi method [8]. Each index consists of a word or phrase representing a psychological quality term and a clause to determine the defintion. The questionnaire of test pilots' psychological quality with 108 items was developed for the importance evaluation of each psychological quality using five levels scale according to the five level positive importance estimation fuzzy set model [9, 10]. The five levels were commonly, a little important, important, more important, very important. All items were constructed as four dimensions including "knowledge", "skill", "ability" and "non ability factors". In order to ensure the credibility of the results, psychologists were required to self rate the degree of familiarity with the field, with a full score of 10 and the admission criteria of ≥ 8 .

Flight test experts are invited to complete the questionnaire by rating the importance of psychological quality for an excellent test pilot.

2.3 Statistical Analysis

All data were expressed as Mean and statistically analyzed on SPSS statistical software package of version 20.0. An alpha-level of 0.05 was used as threshold for significance.

3 Results

Among the 30 subjects actually surveyed, 30 copies were recovered and 30 copies were effective, with an effective rate of 100%.

3.1 Sequency of Importance of Evaluation Items of Competency for Test Pilots

According to the principle of fuzzy set evaluation [10], the indexes with the value of fuzzy set (MFS) less than 0.477 are deleted. A total of 24 relevant qualities were included in the model after 84 items with the value of fuzzy set (MFS) less than 0.477 were deleted. Then 24 items were classified as three levels according to MFS value: items with MFS value > 0.704 is “very important”, MFS value < 0.599 is “more important”, and MFS value between 0.704 and 0.599 is “important”. Dedication and flight procedure were identified as the most important indexes of test pilots (MFS value > 0.704); Eight indexes, including aircraft system, emergency coping ability, judgment and decision-making, were identified as important indexes for evaluating test pilots (0.704 > MFS value > 0.599); Analytic ability, verbal understanding and expression, and sense of responsibility were 14 relatively important indexes (MFS < 0.599) Table 1.

Table 1. Sequency of importance of evaluation items of competency for test pilots (n = 30)

Qualities	MFS score	Qualities	MFS score	Qualities	MFS score
Dedication	0.815	Judgement and decision making	0.630	Operation and control	0.519
Flight program	0.778	Self-control	0.593	Independent	0.519
Aircraft system	0.704	Stress resistance	0.593	Verbal understanding and expression	0.481
Flight control system	0.704	Responsibility	0.593	Coperation	0.481
Honest	0.667	Aerodynamics	0.556	Emotion stability	0.481
Rigorous	0.630	Analytic ability	0.556	Firmness	0.481
Aircraft performance	0.630	Self-confidence	0.556		
Engine theory	0.630	Flight mechanics	0.519		
Emergency coping ability	0.630	Finding and coping disorder	0.519		

3.2 Establishment of Competency Evaluation Model for Test Pilots

The Hierarchical competency model which concluded 4 dimensions and 3 levels was developed based on the importance and specificity of 24 indexes. (Fig. 1). The four

dimensions are “knowledge”, “ability”, “skill” and “other factors”. Among them, “knowledge” includes 7 evaluation indexes, “ability” includes 3 evaluation indexes, “skill” includes 6 evaluation indexes, “other factors” includes 10 evaluation indexes. The first level just concludes two indexes, Dedication for other factors and Flight program for Knowledge. There is no first level indexe for Skill and Ability dimensions.

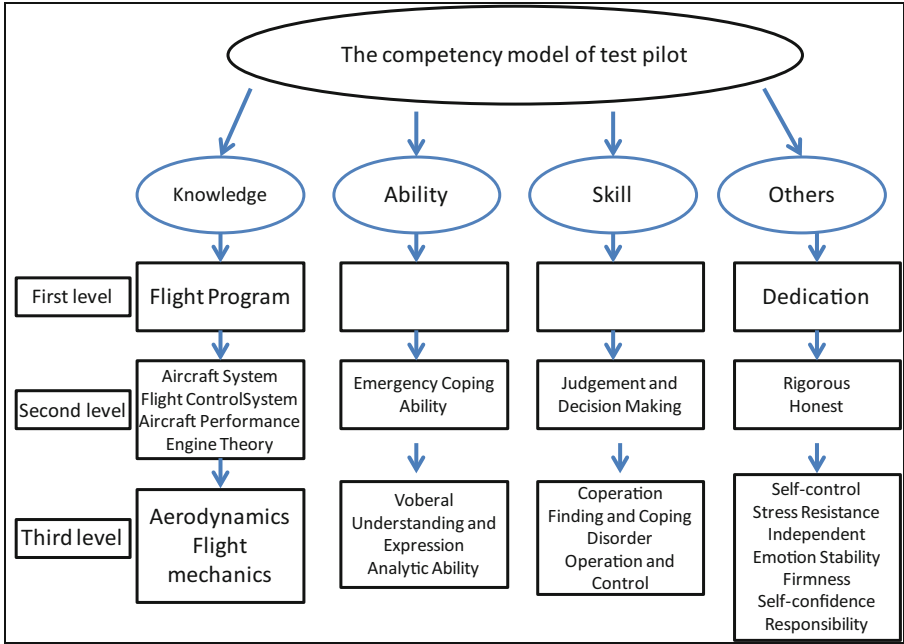


Fig. 1. The competency model of test pilots

4 Discussion

Competency refers to core traits and individual potential that distinguish the excellent person from the general ones in a job or organization [11]. A good competency model can predict their work performance [12, 13]. Competency models are widely accepted in many countries in recent decades since David Mc Clelland made his famous remark in the year 1973: Testing for Competence Rather than Intelligence. However, the competence concept was driven from many selection practices including AirForce selection.

Competency model of pilots see competence in terms of knowledge, abilities, skills, and other factors such as motivation, traits, self-concept, attitude or values [14]. Then it links two common misunderstandings of competence, one approach is to link it exclusively to task performances and another is to define competence as the generic attributes.

However test pilots are special pilots. In the past three decades, aircraft handling qualities and automation have improved rapidly which lead to great change in flight and

mission. Long missions at medium altitudes and operation of precision weapon system supplanted searching targets with eyes in low altitudes. Pilots are system operators other than pilots. As a result traditional stick-and-rudder control skills and flight envelope awareness are being less important. But test pilots still require these skills because they may fly a developmental aircraft with an unguaranteed automation or lower handling qualities [15]. At the same time, test pilots must make a diagnosis on the potential design problems of the test aircraft and put forward the the proposal for improvement of the handling qualities. In order to accomplish these tasks, they must not only know how to operate, but also understand how and why does the increasingly complex systems work [16]. In addition, they must handle emergency conditions when the aircraft equipment goes down or the flight environment becomes worsen. To sum up, the skills necessary for an operational pilot and the skills necessary for a test pilot become increasingly different since the job requirements become different. Some countries have establish.

In the research results, “dedication” and “flight procedure” are identified as the most important indicators to evaluate test pilots, and among the 24 evaluation indicators included in the test pilot competency model, 7 indicators belong to the category of “knowledge”. We should emphasize the importance of “knowledge” in both test pilots selection and training, because requirement of aviation theoretical knowledge is more relevant for test pilots than civil aviation pilots and military pilots. As mentioned above, the flight test mission determines that the test pilot should not only be able to complete various flight test subjects, but also verify whether the aircraft meets the design indicators and use needs through personal experience. Only in this way can they find the design defects in flight quality and man-machine interface, and put forward the direction of improving the design. The evaluation indexes of test pilots in the research results are compared with the results of Miao Danmin et al. [17] on the competency of young pilots. Knowledge isn’t been included in the Model of young pilots competency. Test pilot competency stresses emergency handling ability more than typical pilots which mostly due to the great differences between test pilots and military pilots in completing tasks and performing duties. Especially for new aircraft test flights, emergencies occur from time to time, so test pilots must keenly monitor and judge the aircraft response in the process of flight test, find the abnormal phenomena of the aircraft or system in time, and deal with them timely and correctly. In addition, in terms of other factors, test pilots emphasize “honest”. The opinions of test pilots have a significant legal and economic impact on the labor achievements of tens of millions of people, and once “dishonesty” may bring irreparable losses.

In the past century, a large number of experimental verification studies have been carried out on the predictive validity of pilot competency. Hunter and Burke (1994) [18] and martinussen (1996) [19] analyzed the predictive validity of various ability characteristics of pilot selection system through meta-analysis method. The comprehensive results show that in the predictive validity of KASO, the prediction of ability factor is better, while the prediction of personality is lower. Limited by the number of investigators, the competency evaluation model of test pilots established in this study only provides a theoretical basis for the selection, evaluation and training of test pilots, and needs to be further verified.

Compliance with Ethical Standards. The study was approved by the Logistics Department for Civilian Ethics Committee of AirForce Medical Center, FMMU, PLA.

All subjects who participated in the experiment were provided with and signed an informed consent form.

All relevant ethical safeguards have been met with regard to subject protection.

References

1. Test pilot. Merriam-Webster.com Dictionary, Merriam-Webster. <https://www.merriam-webster.com/dictionary/test%20pilot>. Accessed 14 Feb 2022
2. Brooke, M.: Trials and Errors. History Press (2015)
3. Test pilot school. <http://en.wikipedia.org/wiki/Test-pilot.2013-9-28>
4. U.S.AirForce, test pilot school, AF Instruction 99-107, D RAFT ed., vol. 10 (2009)
5. U.S.AirForce, test pilot school, Comprehensive Candidate Evaluation Program, Operating Instruction 99-2, Draft ed., vol. 10 (2009)
6. Carretta, T.R.: Pilot candidate selection method. *Aviat. Psychol. Appl. Hum. Factors* **1**(1), 3–8 (2011). <https://doi.org/10.1027/2192-0923/a00002>
7. Liu, Q., et al.: Study on mental attributes of aged test pilots. In: Long, S., Dhillon, B.S. (eds.) *MMESE 2017. LNEE*, vol. 456, pp. 77–83. Springer, Singapore (2018). https://doi.org/10.1007/978-981-10-6232-2_10
8. Osborne, J., Collins, S., Ratcliffe, M., et al.: What “ideas-about-science” school is taught in school science? A delphi Study of the Expert Community. *J. Res. Sci. Teach.* **40**, 692–720 (2003)
9. Dey, P.K.: Integrated project evaluation and selection using multiple attribute decision-making technique. *Int. J. Prod. Econ.* **103**(1), 90–103 (2006)
10. Danmin, M.: The fuzzy set model of multistage evaluation degree of positivity importance and it use. *J. Psychol. Sci.* **20**(6), 551–552 (1997)
11. Spencer, J., Spencer, S.M.: *Competence at Work: Models for Superior Performance*, pp. 25–28. Wiley, New York (1993)
12. Schmidt, F.L., Hunter, J.E.: The validity and utility of selection methods in personal psychology: practical and theoretical implications of 85 years of research findings. *Psychol. Bull.* **124**(2), 262–274 (1998)
13. Shippmann, J.S., Ash, R.A., Battista, M., et al.: The practice of competency modeling. *Pers. Psychol.* **53**(3), 703–740 (2000)
14. Carretta, T.R.: Pilot candidate selection method: still an effective predictor of us air force pilot training performance. *Aviat. Psychol. Appl. Hum. Factors* **1**(1), 3–8 (2011)
15. Cooper, G.E., Harper, R.J.: The use of pilot rating in the evaluation of aircraft handling qualities. *Epigenet. Off. J. DNA Methylation Soc.* (1969). NASA Ames Technical Report: NASA-TN-D-5153
16. Gray, W.: USAF test pilot selection for the next generation. In: *U.S. Air Force T&E Days 2010* (2010)
17. Dan-min, M.I.A.O., Zhengxue, L.U.O., Xufeng, L.I.U., et al.: The competency model of young pilots. *Chin. J. Aerosp. Med.* **15**(1), 30–34 (2004)
18. Hunter, D.R., Burke, E.F.: Predicting aircraft pilot-training success: a meta-analysis of published research. *Int. J. Aviat. Psychol.* **4**, 297–313 (1994)
19. Martinussen, M.: Psychological measures as predictors of pilot performance: a meta-analysis. *Int. J. Aviat. Psychol.* **6**, 1–20 (1996)



Experimental Research on Team Dynamic Function Allocation Strategy Optimization

Chenyuan Yang¹, Liping Pang^{1(✉)}, Xin Wang², Ye Deng², and Yuan Liu²

¹ School of Aeronautical Science and Engineering, Beijing University of Aeronautics and Astronautics, Beijing 100191, China
pangliping@buaa.edu.cn

² Marine Human Factors Engineering Lab, China Institute of Marine Technology and Economy, Beijing 100081, China

Abstract. This paper mainly focused on the dynamic function allocation strategy proposed by the team, and carries out relevant experimental research. The underwater vehicle consists of three workstations, including Operating Officer (OO), Vehicle Officer (VO) and Leader, was designed and built. Twelve healthy male college-age students were recruited to investigate the effects of two allocation strategies on their mental workload and task performance. Although the result showed that the improvement of Operating Officer's task performance was less at human-machine allocation strategies than at human-human allocation strategies, the Vehicle Officer's task performance decreased significantly at human-human allocation strategies. Hence, human-machine collaboration strategy is still the primary scheme at dynamic function allocation based on the convenience of intelligent systems. If the mental workload level and job performance level of Operating Officer are underperforming after the human-machine allocation strategy is completed, part of the Operating Officer's fault task processing function is assigned to Vehicle Officer.

Keywords: Function · Allocation strategy · Team · Underwater vehicle

1 Introduction

Automation and intelligent systems are widespread in the field of transportation, factory manufacturing, nuclear power plants, aerospace, navigation and other fields by the continuous development and progress of industrial level [1, 2]. Automation can improve system performance without increasing manpower demand by delegating routine tasks to automated assistive equipment. The use of automated monitoring assistive equipment can not only improve security, but also increase the productivity of the system to reduce the total cost of the system [3].

However, in the design and functional allocation of automated systems, ignoring human factors can bring many challenges, such as loss of situational awareness, unbalanced workloads, vigilance and skill degradation, which can lead to disastrous results [4]. Therefore, Fitts proposed the concept of man-machine functional allocation, which

refers to the process of assigning functions or tasks in a system to a person or machine [5]. The primary purpose of dynamic function allocation is to keep operator situational awareness and load levels at acceptable levels. According to the Yerkes-Dodson law, it keeps the worker's cognitive load at a moderate level, i.e., optimal performance [6].

The emergence of automation and intelligent systems has replaced the work of operators and reduced the need for human resources. As time goes on, a lot of new jobs have come up. The nature of human work has shifted from manual to primarily cognitive tasks such as monitoring, diagnosing and solving problems. Even in advanced human-machine systems, humans are still one of the most influential actors. It is worth noting that the failure of human-machine partnership in recent years is mostly caused by human factors, such as loss of professional knowledge, excessive reliance on automation and complacency, people's trust in machines, etc. Then, human-centered human-machine system should be guaranteed in human-machine design [7].

In recent years, people-oriented system development methods have been developed [8]. Task analysis is an important part of many human-centered development methods. In task analysis, what computers and humans do should be distinguished [9]. The 1951 Fitts list marked the beginning of the distribution of man-machine functions. Fitts lists (or variants of them) are still the most widely used feature allocation technique, although they have been questioned and criticized by some scholars [10]. Therefore, in order to ensure rational task allocation, Fitts list is main basis in the allocation strategy of this study.

At present, most literatures about man-machine function assignment mainly involve single-person positions, but this paper mainly focuses on the dynamic function allocation strategy proposed by the team, and carries out relevant experimental research.

2 Methods

2.1 Task Scenario

This paper designed and built the underwater vehicle, which consists of three workstations, including Operating Officer (OO), Vehicle Officer (VO) and Leader. Three participants in the experiment work together in their respective positions to complete the tasks prescribed by the simulator. Figure 1 show the task interface diagrams of all positions. The key responsibilities of each position are shown in Table 1.

2.2 Allocation Strategy

It can be known that the workload of operators is high, while the workload of navigators is low through the actual field investigation. Human and machine have different advantages according to the Fitts list. The machine can respond quickly to find the fault, but the personnel are good at judgment processing. Then, based on the difference in the ability of machines and personnel, there are two allocation strategies when adjusting the task amount of each position for the purpose of the balance of cognitive load of team members. One is human-machine function allocation: the Operating Officer's search function for fault task is assigned to the machine; the other is human-human function allocation: the Operating Officer's processing function for fault task is assigned to the Vehicle Officer. Table 2 show the detail description of team function allocation strategy.

Table 1. Team position and responsibility description

Character	Duty description
Operating Officer (OO)	Check the internal parameters of the ship to ensure the normal operation of the cabin and balance the change of the water quantity in the ship
Vehicle Officer (VO)	Monitors changes in the ship’s course, speed and depth
Leader	The commanding decision-maker of the entire cabin gives instructions to other station personnel

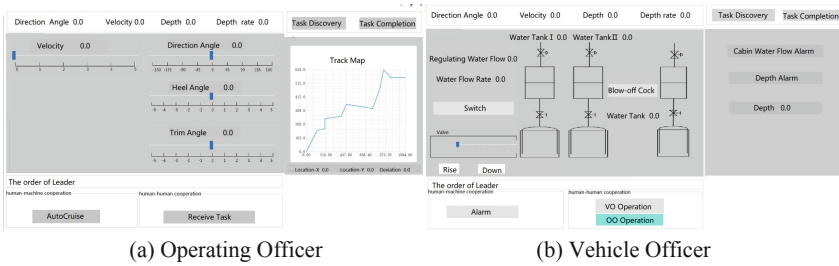


Fig. 1. The interface chart of the underwater vehicle system

Table 2. The detail description of team function allocation strategy

Allocation strategy		Describe
The human-machine function allocation	Strategy0-1 (S0-1)	The initial state
	Strategy1-1 (S1-1)	The part of the Operating Officer’s search function for fault task is assigned to the machine
	Strategy1-2 (S1-2)	The whole of the Operating Officer’s search function for fault task is assigned to the machine
The human-human function allocation	Strategy0-2 (S0-2)	The initial state
	Strategy2-1 (S2-1)	The part of the Operating Officer’s processing function for fault task is assigned to the Vehicle Officer
	Strategy2-2 (S2-2)	The whole of the Operating Officer’s processing function for fault task is assigned to the Vehicle Officer

2.3 Participants

Twelve male students (age 23.250 ± 2.314 years) with good science and engineering background were recruited for this experiment. The subjects were healthy, right-handed and had normal or corrected visual acuity. Before and during the experiment, the subjects had adequate sleep and a good mental state, and did not drink stimulant substances such as caffeine and alcohol, and did not take any drugs. Participants received sufficient training before the experiment proper starts. Since the experiment ended, each participant accepted a monetary reward.

2.4 Study Design

Six team of twelve Subjects were divided into two groups: there were three teams in each group. Each team was exposed to two strategies every day. One group of teams tested the human-machine collaboration strategies at 9:0–11:00, and the human-human collaboration strategies were tested at 15:00–17:00. The other group of teams did the opposite. In addition, every allocation strategy with three different workloads were performed in the order designed by the Latin square method.

2.5 Experimental Procedure

The test under each allocation strategy lasted for more than seventy minutes. There were 5 min for preparation before the formal experiment. And then the 1 h was used for test. The formal test includes resting test, the team tasks with three workloads and filling in the NASA-TLX scale. The experimental scene were displayed in Fig. 2.



Fig. 2. Experimental scene of the formal test

2.6 Statistical Analysis

Generalized additive mixed effect model (GAMM) analyses were performed using the open-source statistical package R version 3.6.1 (R Project for Statistical Computing, Vienna, Austria) to test the fixed effect estimates of potential influencing factors on human task performance and NASA-TLX, treating the subject as a random effect.

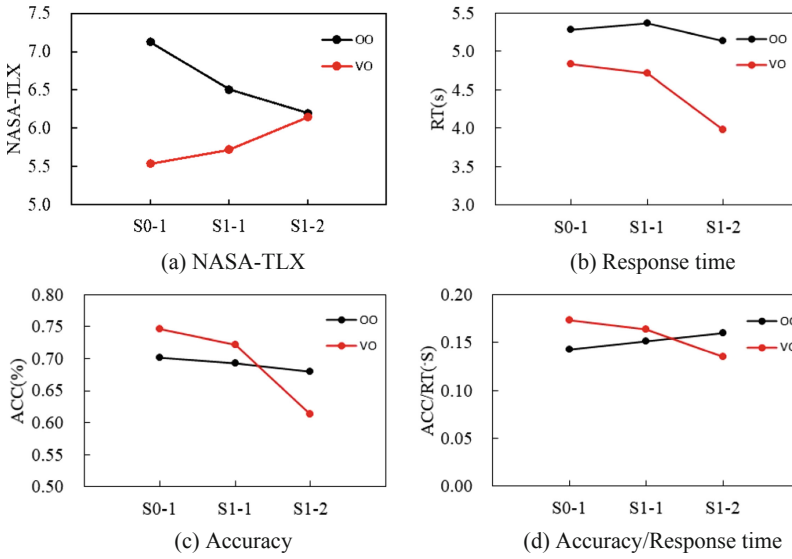


Fig. 3. The mental workload and task performance of team in the human-machine function allocation strategies

3 Result

3.1 The Human-Machine Function Allocation

As shown in Fig. 3(a), the mental workload of Operating Officer gradually decreases along with the increase of workload assigned to machines. Meanwhile, the Operating Officer’s performance improved, in Fig. 3(b), (c) and (d). Vehicle Officer’s workload did not change. Then, the mental workload and performance of Vehicle Officer remained unchanged.

3.2 The Human-Human Function Allocation

Figure 4(a) showed that along with the increase of the Operating Officer’s workload assigned to Vehicle Officer, the Operating Officer’s mental workload decreased significantly, however, the Vehicle Officer’s mental workload increased significantly. The variation of the Operating Officer’s performance was different with the Operating Officer’s mental workload. The response time and accuracy of Operating Officer at S2-1 were better than at S0-2 and S2-2, as shown in Fig. 4(b) and (c). Nevertheless, the variation of the Vehicle Officer’s performance decreased significantly along with the increase of workload.

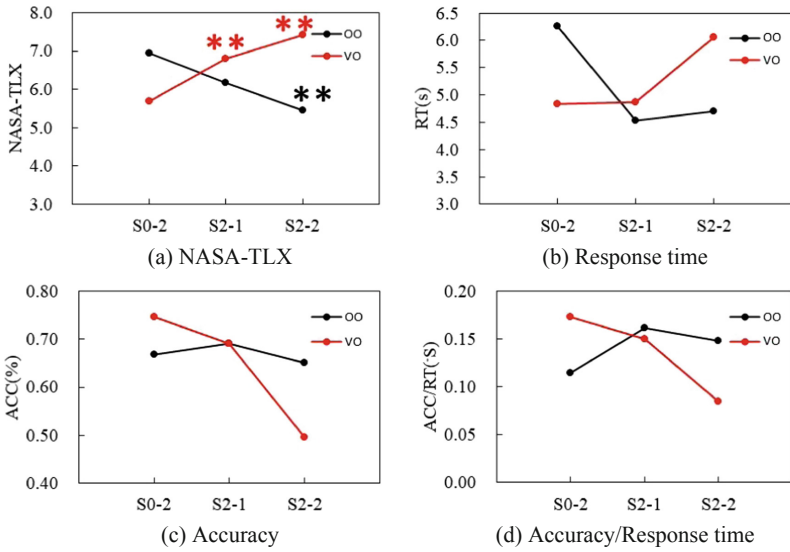


Fig. 4. The mental workload and task performance of team in the human-human function allocation strategies

4 Conclusion

Human-machine collaboration strategy could improve Operating Officer's mental workload and job performance appropriately, but not significantly, which may be related to the small quantity of participants in this experiment. Although there is a significant improvement about Operating Officer's mental workload and job performance at human-human collaboration strategy, the Operating Officer's mental workload and job performance could be optimal, only when the workload was kept at a moderate level, which was proposed by the previous researches, and the performance was the best at moderate mental workload [11]. Meanwhile, the overmuch workloads lead to increase Vehicle Officer's mental workload and decrease Vehicle Officer's mental workload performance, significantly. Therefore, in order to guarantee that the overall mental workload and job performance of the team are optimal, part of the Operating Officer's workload should be allocated to Vehicle Officer.

In summary, Human-machine collaboration strategy is still the primary scheme at dynamic function allocation based on the convenience of intelligent systems. If the mental workload level and job performance level of Operating Officer are underperforming after the human-machine allocation strategy is completed, part of the Operating Officer's fault task processing function is assigned to Vehicle Officer.

Compliance with Ethical Standards. The study was approved by the Logistics Department for Civilian Ethics Committee of School of Aeronautical Science and engineering, Beijing University of Aeronautics and Astronautics.

All subjects who participated in the experiment were provided with and signed an informed consent form.

All relevant ethical safeguards have been met with regard to subject protection.

References

1. Valente, A., Carpanzano, E., Nassehi, A., Newman, S.T.: A STEP compliant knowledge based schema to support shop-floor adaptive automation in dynamic manufacturing environments. *CIRP Ann. - Manuf. Technol.* **59**(1), 441–444 (2010)
2. Parasuraman, R., Sheridan, T.B., Wickens, C.D.: Situation awareness, mental workload, and trust in automation: viable, empirically supported cognitive engineering constructs. *J. Cogn. Eng. Decis. Making.* **2**(2), 140–160 (2008)
3. Rouse, W.B.: Human-computer interaction in the control of dynamic systems. *ACM Comput. Surv.* **13**(1), 71–99 (1981)
4. Hogenboom, S., Rokseth, B., Vinnem, J.E., Utne, I.B.: Human reliability and the impact of control function allocation in the design of dynamic positioning systems. *Reliabil. Eng. Syst. Saf.* **194**(C), 106340 (2019)
5. Fitts, P.M.: Human engineering for an effective air-navigation and traffic-control system. National Research Council, Division of Anthropology and Psychology, Committee on Aviation Psychology (1951)
6. Johnson, A.W., Oman, C.M., Sheridan, T.B., Duda, K.R.: Dynamic task allocation in operational systems: issues, gaps, and recommendations, pp. 1–15. *IEEE* (2014)
7. Hoc, J.M.: From human - machine interaction to human - machine cooperation. *Ergonomics* **43**(7), 833–843 (2000)
8. Iivari, J., Iivari, N.: Varieties of user-centredness: an analysis of four systems development methods. *Inf. Syst. J.* **21**(2), 125–153 (2011)
9. Zhang, P., Carey, J., Te'eni, D., Tremaine, M.: Incorporating HCI development into SDLC: a methodology. *Commun. AIS* **15**(29), 512–543 (2005)
10. Winter, J.C.F., Dodou, D.: Why the Fitts list has persisted throughout the history of function allocation. *Cogn. Technol. Work.* **16**(1), 1–11 (2014)
11. Rueb, J., Vidulich, M., Hassoun, J.: Establishing workload acceptability: an evaluation of a proposed Kc-135 cockpit redesign. In: *Proceedings of the Human Factors and Ergonomics Society Annual Meeting*, pp. 17–21 (1992)



Eye Movement Characteristics During Rifle Aiming

Jie Cao¹, Yaping Wang¹(✉), Sheng Guo², and Cancan Hu¹

¹ School of Mechanical Engineering, Nanjing University of Science and Technology, Nanjing 210094, China
zykdou@163.com

² No. 208 Research Institute of China Ordnance Industries, Beijing 102202, China

Abstract. Objective. The purpose was to explore the eye movement characteristics during rifle aiming at different target holes and baselines. Methods. The eye movement characteristics were measured by the eye tracker. The proportion of saccades behavior and the range of eye movement were the analysis indicators. Statistical analysis with Pearson's correlation coefficient was performed. Conclusion. The proportion of saccade behavior and the range of eye movement decreased with the increase of the diameter of the target hole. Decreased significantly by 60%–80% and 50%–80% respectively when the diameter of the target hole was 1 mm–3 mm. The proportion of saccades behavior and the eye movement range decreased with the increase of the aiming baseline lengths decreased significantly by 40%–65% and 40%–70% respectively when the aiming baseline lengths was 200 mm–300 mm. The eye movement range was more suitable as an indicator for evaluating aiming efficiency from the correlation analysis. Application. This study reveals the eye movement characteristics during rifle aiming, which provides approaches for rifle design and structural optimization. It also provides a basis for the evaluation of rifle aiming efficiency.

Keywords: Rifle aiming · Proportion of saccade duration · Eye movement range · Aiming efficiency

1 Introduction

The aiming stage is an important stage during rifle shooting. It is generally believed that the conscious or unconscious saccade behavior of human beings can better reflect the cognitive processing of the brain. The tiny saccade behavior during maintaining gaze reflects the autonomous choice for environmental information and the difficult process of aiming and centering. HADDAH [1] (1973) demonstrates that eye movement characteristics would be affected by light and shade through experiments. Shepherd [2] (1986) points out that it is impossible to carry out eye movements without corresponding attentional shifts by study. Fogarty [3] et al. (1989) study the blinking behavior in the cognitive process. They find that the blink latency can be used as a tool to assess the level of complexity of this processing under different task requirements. Hoffman [4]

(1995) points out that visuospatial attention is an important mechanism for spontaneous saccades. Unema [5] (2005) points out the variation of gaze characteristics and eye movement range with time. Liao y.g. [6] (2015) studies the reverse saccades of shooting athletes and college students without shooting experience during shooting. They find that the professional group has stronger self-conscious control and cognitive inhibition, but has longer saccade latency. Chen Cai s.l. [7] (2017) study the aiming process of different target hole diameters and baseline lengths of different rifles, and initially revealed the eye movement law of the aiming process. Jia b.j. [8] (2020) conducts the attentional stability of shooters. The results show that cognitive processing task difficulty had a significant impact on behavioral indicators and eye movement indicators.

At present, the research on the rifle aiming process mainly focuses on exploring the eye movement characteristics of different levels shooters [4], and the eye movement laws under different difficulty gaze tasks [6]. The literature [5] analyzes the eye movement characteristics of different rifles. The variables can't been controlled due to the different quality, shape and center of gravity position of rifles. It cannot reflect the influence of parameters on eye movement behavior. In this paper, a customized firearms was used for testing to remaining the quality and structural parameters of the rifle. The influences of target hole diameters and baseline lengths on eye movement characteristics are obtained. It provides approaches for ifle design and structural optimization and a basis for the evaluation of rifle aiming efficiency.

2 Methods

2.1 Subjects

Three shooters with shooting experience participated the test. All participants were right-handed with binocular corrected visual acuity was 5.0 ± 0.2 . Participants were in good physical condition prior to the test. The test was carried out outdoors with the required light intensity for the test. The ambient temperature is 18–24 °C.

Trial participants were informed about the objectives procedure.

2.2 Test Firearms

The test rifle is a customized firearm. The rear sight device with different diameters can be replaced. The position of the rear sight relative to the front sight (baseline length) can be adjusted. The diameter of the sight hole is 1 mm, 2 mm, 3 mm and 4 mm; baseline lengths are to be selected as 350 mm, 300 mm, 250 mm and 200 mm . The test gun is shown in Fig. 1.

2.3 Apparatus and Test Indicators

Tobii Pro Glasses3, as shown in Fig. 2. The sampling rate was 1000 Hz. The proportion of saccade duration and the range of eye movement were the analysis indicators. The data processing adopts the speed threshold recognition (I-VT) gaze classification algorithm, here, it was the fixation behavior when the eye movement speed is less than $30^\circ/s$, it is



Fig. 1. Test gun

the saccade behavior when the eye movement speed is greater than $30^{\circ}/s$. Considering that the complete aiming processing time was short, the minimum fixation duration was 60 ms. The eye movement range is the product of the horizontal and vertical pixel ranges of the subject's gaze point in the screen coordinate system.



Fig. 2. Eye tracker

2.4 Measures and Procedures

The test trial procedure was as follows:

- (1) A simulated 25-m shooting aiming target was set at a distance of 5 m from the subject, as shown in Fig. 3.
- (2) After the shooter was familiar with the environment and grasps the basic steps of the test, shooter with gun ready to aim, as shown in Fig. 4(a).
- (3) When the test recorder speaks the “prepare” password, the shooter started raising the gun to aim, after a short while, the test recorder speaks the “start” password and collected the eye movement data, as shown in Fig. 4(b).
- (4) After aiming, the shooter pulls the trigger, the test recorder stops recording and speaks the “end” password, the shooter completes the aiming and enters the ready state of holding the gun.
- (5) Each shooter tested each program 10 times, and took a short rest (1 min) after each test to prevent eye and arm fatigue from affecting the test results. 3 subjects completed the above experimental process in turn.

3 Results

3.1 Effect of Target Hole Diameter on Eye Movement Characteristics

When the baseline length was 380 mm, the proportion of saccades behavior and the range of eye movement with different target hole diameters were obtained. The eye



Fig. 3. Simulated 25 m target



Fig. 4. (a) Shooter pre-aimed; (b) Shooter aiming.

movement data of the three shooters were analyzed for consistency, the invalid data was eliminated and the average value was processed, the Pearson correlation analysis was used to carry out the correlation analysis of the influence of the target hole diameter on the eye movement characteristics. The results are shown in Tables 1 and 2.

Table 1. The proportion of saccade behavior under different target hole diameters

Sub. no.	1 mm	2 mm	3 mm	4 mm	r	P
1	0.105 ± 0.061	0.050 ± 0.027	0.037 ± 0.021	0.030 ± 0.024	-0.903	0.097
2	0.304 ± 0.081	0.206 ± 0.053	0.125 ± 0.060	0.058 ± 0.033	-0.996**	0.004
3	0.136 ± 0.035	0.075 ± 0.024	0.032 ± 0.018	0.002 ± 0.004	-0.988*	0.012

Table 2. Eye movement range under different diameters of target holes

Sub. no.	1 mm	2 mm	3 mm	4 mm	r	P
1	4373 ± 2172	3397 ± 1511	1968 ± 1043	1719 ± 849	-0.971*	0.029
2	9420 ± 2235	7389 ± 2026	4071 ± 1868	1467 ± 1114	-0.996**	0.004
3	5909 ± 1564	4730 ± 671	1424 ± 497	758 ± 51	-0.967*	0.033

Note: ** at the 0.01 level (two-tailed), the correlation is extremely significant; * at the 0.05 level (two-tailed), the correlation is significant. 0.8–1.0 strong correlation; 0.6–0.8 strong correlation; 0.4–0.6 moderate correlation; 0.2–0.4 weak correlation; 0–0.2 no related.

The changing trends of the eye movements of the three shooters are shown in Figs. 5 and 6.

As the diameter of the target hole increases, the proportion of saccade behavior and the range of eye movement both show a downward trend. The proportion of saccade behavior decreases less gradually when the diameter of the target hole was 1 mm–4 mm. From 1 mm to 3 mm, it decreased by 64.8%, 58.9%, and 76.5% respectively, This is due to the small target hole has a small amount of light, which makes the target observed by the shooter blurred through the target hole. At this time, shooters take more attention to locate the target, resulting in increased saccade behavior in shooters. The trend of eye movement changed gradually less after more than 3 mm, the proportion of saccade

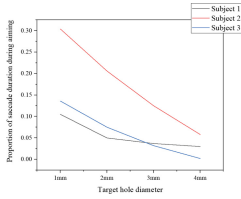


Fig. 5. Trend of saccade behavior

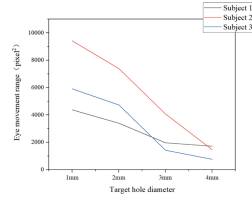


Fig. 6. Trend of eye movement range

decreased by 6.7%, 22.0%, and 22.1% respectively. Eye movement range also showed the same changes, which decreased significantly from 1 mm to 3 mm, by 55%, 56.8%, and 76.0% respectively. The eye movement range decreased less after 3 mm, it decreased by 5.7%, 27.6% and 11.3% respectively. To sum up, both eye movement characteristics are significantly reduced when the diameter of the target hole was 1 mm–3 mm. The aiming efficiency and eye movement stability increase when the diameter of the target hole is greater than 3 mm, but the larger target hole will cause a lower aiming accuracy, so 3 mm target hole is the better choice. It can be seen in the correlation analysis that the diameter of the target hole has a significant correlation with the proportion of the saccade behavior except for subject 1. The diameter of the target hole was significantly correlated with the eye movement range of the three shooters.

3.2 The Effect of Baseline Length on Eye Movement Characteristics

The eye movement data at different baseline lengths were obtained under the diameter of the 3 mm target hole, and a correlation analysis similar to 3.1 was performed, The results are shown in Tables 3 and 4.

Table 3. The proportion of saccade behavior under different baseline lengths

Sub. no.	200 mm	250 mm	300 mm	350 mm	r	P
1	0.131 ± 0.056	0.093 ± 0.045	0.050 ± 0.019	0.045 ± 0.014	-0.962*	0.038
2	0.693 ± 0.074	0.690 ± 0.093	0.388 ± 0.144	0.372 ± 0.143	-0.907	0.093
3	0.251 ± 0.067	0.221 ± 0.029	0.094 ± 0.031	0.086 ± 0.049	-0.942	0.058

Table 4. Eye movement range at different baseline lengths

Sub. no.	200 mm	250 mm	300 mm	350 mm	r	P
1	3988 ± 1391	3245 ± 1465	2197 ± 579	2055 ± 868	-0.967*	0.033
2	30420 ± 11132	25733 ± 8375	8402 ± 3368	5328 ± 2135	-0.960*	0.04
3	9947 ± 3474	7355 ± 3341	2873 ± 642	2089 ± 780	-0.971*	0.029

The changing trends of the eye movements of the three shooters are shown in Figs. 7 and 8.

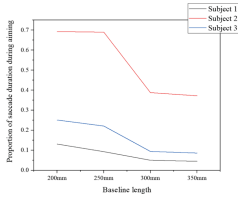


Fig. 7. Trend of saccade behavior

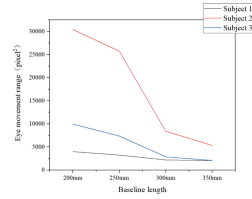


Fig. 8. Trend of eye movement range

As the baseline length was longer, all three shooters showed a downward trend in both eye movement behaviors. The proportion of saccades behavior of the three subjects did not decrease significantly when the baseline length was 200 mm–250 mm, but decreased significantly from 250 mm to 300 mm, decreasing by 32.8%, 43.6%, and 50.6%, respectively; the proportion of saccades behavior in the three subjects decreased by a small margin when the baseline length was 300 mm–350 mm, decreasing by 3.8%, 2.3%, and 3.2%, respectively. The eye movement range of the three shooters was significantly reduced by 44.9%, 72.4%, and 71.1%, respectively when the baseline length was 200 mm–300 mm. The eye movement range of the three shooters decreased slightly when the baseline length was 300 mm–350 mm, decreasing by 3.6%, 10.1%, and 7.9%, respectively. This is because the fovea of the human eye is likely to form a line of sight with the sight, and in the process of continuing to extend the line of sight to a distant target, the line of sight is prone to deviation, and this deviation will gradually decrease with the increase of the baseline length. However, a longer baseline will make the design of firearms difficult, so the baseline length of firearms should be selected between 300 mm and 350 mm under the premise of taking into account aiming efficiency, eye movement stability and firearm size requirements.

It can be seen that the baseline length has no significant correlation with the proportion of saccades behavior except for subject 1 in the correlation analysis, the baseline length has a significant correlation with the eye movement range of the three subjects.

4 Conclusion

The purpose is to explore the influence of the structural parameters of the firearm sighting device on the eye movement characteristics of the shooter. The conclusions are as follows:

- (1) As the diameter of the target hole increases, the proportion of saccade behavior decreases, the eye movement range gradually decreases as well, which indicates the improvement of eye movement stability. However, when aiming with a larger hole, the confirmation of the center position of the target hole is prone to larger errors, resulting in lower shooting accuracy. Therefore, the 3 mm target hole was selected under the premise of taking into account the aiming efficiency, stability and accuracy.
- (2) As the baseline length was longer, both the range of eye movements and the proportion of saccades behavior decrease, the aiming efficiency of the shooter increases. However, an excessively long baseline will bring higher requirements on firearm design, so it is recommended that the baseline length be 300 mm–350 mm.

- (3) Since the diameter of the target hole and the baseline length are significantly correlated with the range of eye movement, the range of eye movement is more suitable as an index to evaluate aiming efficiency than the proportion of saccades behavior.

Compliance with Ethical Standards. The study was approved by the Logistics Department for Civilian Ethics Committee of Nanjing University of Science and Technology.

All subjects who participated in the experiment were provided with and signed an informed consent form.

All relevant ethical safeguards have been met with regard to subject protection.

References

1. Haddad, G.M., Steinman, R.M.: The smallest voluntary saccade: implications for fixation. *Vision. Res.* **13**(6), 1075-1086 (1973)
2. Shepherd, M., Findlay, J.M., Hockey, R.J.: The relationship between eye movements and spatial attention. *Q. J. Exp. Psychol.* **38**(3), 475-491 (1986)
3. Fogarty, C., Stern, J.A.: Eye movements and blinks: their relationship to higher cognitive processes. *Int. J. Psychophysiol.* **8**(1), 35-42 (1989)
4. Hoffman, J.E., Subramaniam, B.: The role of visual attention in saccadic eye movements. *Percept. Psychophys.* **57**(6), 787-795 (1995)
5. Unema, P.J.A., Pannasch, S., Joos, M., et al.: Time course of information processing during scene perception: the relationship between saccade amplitude and fixation duration. *Vis. Cogn.* **12**(3), 473-494 (2005)
6. Liao, Y., Yang, R., Wang, Q.: Research on the reverse saccade of shooting athletes. *J. Tianjin Inst. Phys. Edu.* **30**(04), 312-316 (2015)
7. Chen, C.: Ergonomics research of individual soldier system based on vision and accessibility. Nanjing University of Science and Technology (2017)
8. Jia, B., Liao, Y.: Eye movement research on attention stability of shooters. *Ind. Technol. Forum* **19**(05), 71-73 (2020)



Research on User's Subjective Preference of Taohuawu New Year Painting Based on CycleGAN

Funan Dai, Zhengqing Jiang^(✉), Yiao Fang, and Xin Guan

East China University of Science and Technology, Shanghai 200030, China
jzq20000@126.com

Abstract. Objective. Exploring a feasible method for studying users' subjective preferences of image samples based on style transfer; exploring contemporary young people's subjective preference for different styles in the historical development of Taohuawu New Year painting. **Methods.** A detailed review of the development and style evolution of Taohuawu New Year painting. CycleGAN (Cycle Generative Adversarial Networks) was used to transfer the two artistic styles of Changmen Kusu Prints and Taohuawu woodblock New Year paintings to the typical representative pictures of Taohuawu New Year pictures, and to conduct user preference experiments on the images of the two styles. **Results.** The images of Changmen Kusu Prints style had higher user preference. **Conclusions.** CycleGAN can be effectively applied to the study of users' subjective preference for images; Changmen Kusu Prints is more favored by contemporary young people in terms of quality, style and subject matter, and it is necessary to focus on its inheritance and development.

Keywords: CycleGAN · Taohuawu New Year painting · User preference · Style transfer

1 Introduction

Intangible Cultural Heritage is an important spiritual wealth for the survival and development of a country and a nation. Our country is rich in Intangible Cultural Heritage resources, and as a descendant of Yan and Huang, we have an inescapable responsibility for the inheritance of national culture [1]. Suzhou Taohuawu New Year painting has a long history and are widely circulated among the masses for its fine workmanship and rich decorative effect [2]. Suzhou Taohuawu New Year painting has left many works of different themes and styles after hundreds of years of development, but its development in modern is in trouble. The primary problem is that it does not understand the preferences of contemporary young people and cannot form a wide spread among them. Therefore, it is necessary to understand the style preferences of contemporary young people on New Year paintings from the perspective of user preferences.

1.1 Research Status

Taohuawu New Year paintings were once very popular, and scholars' research on them has never stopped. The first is to systematically study Taohuawu New Year paintings from a broad perspective. Liu et al. [3] used the method of "cultural translation" to extract and design the cultural IP of Taohuawu New Year Woodblock paintings, and finally completed the design of Taohuawu New Year Woodblock paintings digital cultural creation. In addition, Zhang [4] used virtual reality technology to digitally display Taohuawu New Year Woodblock paintings. From the iconographic research of Taohuawu New Year paintings, Zhao et al. [5] interprets the multi-layered cultural images of Taohuawu New Year paintings and applies them to clothing design. Wang et al. [6] extracted the modeling elements of Taohuawu New Year paintings and applied them to modern interior design.

With the advent of the experience era, the research on users' subjective preferences has become the focus, how to collect users' subjective data in a timely manner in real situations, there is no systematic method [7]. Specifically for media research samples such as pictures and videos, there are generally two existing user subjective preference experimental methods. One is the selection of carousel pictures, which is simple to operate, but the physical and psychological burden of the participants will be relatively large when the number of samples is large, and the time cost and labor cost are relatively high. The other is to use equipment such as eye-tracking devices for objective statistics, some eye-tracking devices are head-mounted, although they can more accurately reflect the user's attention on an image. However, the price is high and the samples collected are relatively limited, which not only has a certain impact on the user's psychology, but also makes the operation relatively difficult [8].

Summarizing the above research, it can be found that most of the research on Taohuawu New Year paintings is to select a small number of samples, extract image features and apply them to other design fields, without clearly distinguishing their historical development period and different styles. This kind of research on user's subjective preference for pictures mostly chooses the way of carousel pictures, and the number of samples will greatly affect the experimental results. Therefore, it is necessary to make a clear distinction between the historical development periods and different styles of Taohuawu New Year paintings. At the same time, CycleGAN can be used to train the different styles of New Year paintings, and use the typical representative of Taohuawu New Year paintings themes as content images to style transfer. Which can largely avoid the above problems in the process of researching user preferences, and obtain more accurate experimental results.

1.2 Research Content and Process

As shown in Fig. 1, Taohuawu New Year paintings have gone through periods of development such as origin, prosperity, and transformation, and during these centuries of development, numerous works with different themes and styles have appeared. In conclusion, this art would consist of two major periods. In the first period, from the Early Qing Dynasty to the Taiping Heavenly Kingdom period, which is academically called the

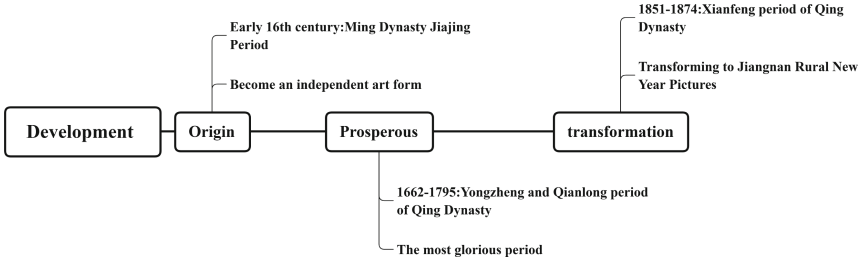


Fig. 1. The development period of Taohuawu New Year painting

Changmen Kusu Prints, which also belongs to the category of Taohuawu New Year paintings. After the Taiping Heavenly Kingdom, it was the Taohuawu New Year Woodblock paintings. These two periods saw a major change in the style of New Year paintings, a detailed comparison of which is shown in Table 1.

Table 1. Comparison of the two periods of Taohuawu New Year pictures

	Changmen Kusu prints	Taohuawu New Year woodblock painting
Period	Early Qing Dynasty-Taiping Heavenly Kingdom	Taiping Heavenly Kingdom-Now
Time background	Social stability, economic development, cultural prosperity	Social turmoil, people’s livelihood
Artistic features	The work is magnificent, pays attention to perspective and light and shadow, finely portrayed, and has an elegant style	The style is festive and warm, bright and simple, with strong contrast
Subject matter	Mainly depicting urban life and civic life	Demonstrate rural life and customs

The Changmen Kusu Prints and the Taohuawu New Year Woodblock painting became two styles of samples for the study.

The research process is shown in Fig. 2.

Firstly, collected samples of two major periods of New Year paintings through literature research and field investigation, and screened the obtained samples. Secondly, processed the screened image samples for style training, formed two major New Year painting style libraries. Thirdly, selected content images for style transfer and conducted user preference experiments. Lastly, analyzed the experimental results.

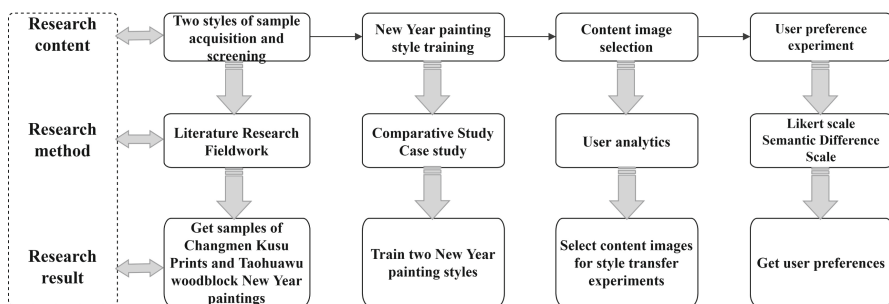


Fig. 2. Research flow figure

2 Materials and Methods

2.1 Sample Acquisition and Screening

Through literature research, field investigation, expert interviews, etc. Obtained a total of 350 samples from Shanghai Library, Suzhou Taohuawu New Year Woodblock Paintings Society, Taohuawu New Year Woodblock Paintings Museum and other places, and screened the collected samples to remove duplicates and resolutions. After the lower sample, there are 338 remaining samples, including 128 samples of Changmen Kusu Prints and 210 samples of Taohuawu New Year Woodblock paintings.

2.2 Style Training Experiment

2.2.1 Select Content Image

This experiment required the selection of content images for the style transfer of the two styles trained. According to research and observation, most of the Taohuawu New Year paintings show folklore, historical stories, operas, ladies and flowers, etc. Therefore, this paper conducted a photo search with the keywords “Suzhou + five main themes” and obtained 25 sample pictures. 20 experimenters in the field of design and culture were invited to select 5 samples (one for each of the 5 main themes) that best matched the impression of Taohuawu New Year paintings as content images according to their subjective impressions. The final selected content images are shown in Fig. 3.



Fig. 3. Content image selection

2.2.2 Training Model Selection

The implementation of this experiment mainly relies on the image style transfer technology in the computer field. The current mainstream image style transfer technology based on deep learning can be roughly divided into two types, one is CNN (convolutional neural network), and the other is through CycleGAN. CNN consists of a series of convolutional matrix operation layers and is widely used in image analysis and object recognition. CycleGAN can capture features from one image set [9] and can transfer these features to other image sets, enabling domain-to-domain image transformation.

Firstly, the effect of the two technical models is compared through the pre-experiment. The pre-experiment selects the Changmen Kusu Prints as the experimental sample for the control experiment. The comparison results are shown in Fig. 4.

As shown in Fig. 4, in terms of content retention, CycleGAN can retain more details than CNN, and a lot of details in the images processed by CNN are lost, and only part of the edges are enhanced. In terms of style retention, the style features retained by CycleGAN technology are also more obvious and vivid. For a comprehensive comparison, we use CycleGAN technology to conduct the following experiments.



Fig. 4. Comparison of CycleGAN and CNN

2.2.3 Training Process

The resolution of the sample images screened in Sect. 2.1 is processed to $256 * 256$, and the main body of the content should be ensured to the greatest extent possible during the processing. The final training sample picture is shown in Fig. 5 (only the part is shown).

The experiment was carried out using a cloud server, the server was a Linux system, the CPU model was Intel Xeon Gold 5218, the GPU model was Tesla T4, and the video memory was 16G. The software platform used in the experiment is PyCharm Professional 2021.3.1, which is connected to the cloud server through PyCharm, and the programming language used is Python 3.8. First, the two styles of generators are trained separately for 200 epochs, and then the trained generator is used to generate style images.

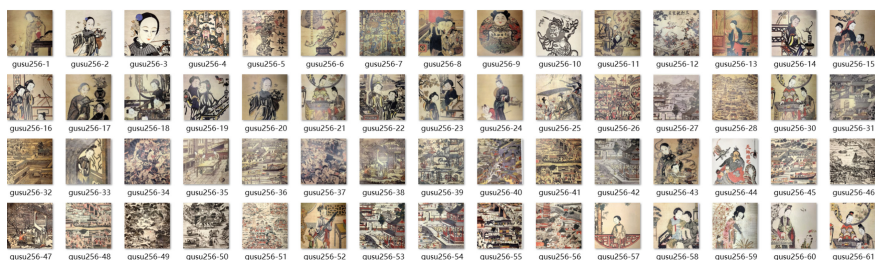


Fig. 5. Training sample display (part)

Finally, five images of each style are obtained, with a resolution of 1024×1024 , and the numbers are as follows shown in Fig. 6.



Fig. 6. User preference experiment image

2.3 User Preference Experiment

In order to accurately measure the user's preference for the two styles of Changmen Kusu Prints and Taohuawu New Year Woodblock paintings, authoritative image evaluation standards are needed. At present, most of the academic research on image evaluation is based on the three-layer theory proposed by German art historian Erwin Panofsky. The three-layer theory refers to pre-iconography, iconography, and iconology, and perfected and optimized on this theoretical basis [10]. In 2015, Huang [11] proposed a three-layer theory of image topic description on the basis of Panofsky's theory, including the visual characteristics of images, the meaning and interpretation of images, and the functions of images. Among them, the visual features of an image are mainly the evaluation of visual elements such as color, shape, and form, and the meaning and interpretation of an image is to reflect the meaning of the image. The image function mainly emphasizes the emotional and psychological impact of the image on the viewer.

Since this study uses the same content images for style transfer, excluding the meaning and explanatory factors of the images, the preference study for image style will be

conducted from two dimensions, the visual characteristics of images and the emotional and psychological effects of images on viewers.

The first is the visual characteristics of the image, excluding the influence of the same visual factors (shape, color, line, etc.) brought by the same content image, and comprehensively evaluates from the two aspects of color and texture. With the help of literature research related to design and iconography, vocabulary describing the color and texture of Taohuawu New Year paintings is collected and filtered to obtain nine subdimensions for evaluation. The style image color dimensions were evaluated as: harmonious and unified, real and imaginary, soft, rich and crystal clear; the style image texture dimensions were evaluated as: uniform, gorgeous, clear and rich in texture. The experimenters gave a score of 1–5 based on their subjective feelings about the style images of New Year paintings, and the collected data were used to analyze the preference survey for the visual characteristics of style images.

The second is the experiment on the influence of style images on users’ emotions and psychology. Using semantic analysis method and desktop research to collect 56 adjectives with user perception descriptions of Taohuawu New Year paintings from the Internet, Taohuawu New Year painting books and papers. Preliminary screening was carried out by eliminating the same words and synonyms, and 36 primary semantic words were selected; through interviews with relevant staff and research enthusiasts, the words were further screened, and finally 9 groups of adjective phrases with opposite semantic expressions were selected. The final choice of words must have the following characteristics.

Firstly, they can better reflect the psychological or emotional feelings of the Taohuawu New Year painting style. Secondly, there are clear and opposite emotional semantics between phrases. According to the emotional and psychological influence words corresponding to the above samples, the corresponding Richter seven-level scale was established, and the user’s subjective preference survey questionnaire was made. The final semantic difference scale is shown in Table 2.

Table 2. Semantic Difference Scale

Semantics (negative)	Score							Semantics (positive)
Detached	−3	−2	−1	0	1	2	3	Complete
Discord	−3	−2	−1	0	1	2	3	Harmonious
Ugly	−3	−2	−1	0	1	2	3	Beautiful
Old	−3	−2	−1	0	1	2	3	Novel
Boring	−3	−2	−1	0	1	2	3	Interesting
Vulgar	−3	−2	−1	0	1	2	3	Elegant
Ordinary	−3	−2	−1	0	1	2	3	Unique
Rough	−3	−2	−1	0	1	2	3	Exquisite
Worthless	−3	−2	−1	0	1	2	3	Valuable

The procedure of the experiment is that the experimenter watches the experimental samples, and comprehensively judges the two styles from the two dimensions of the visual characteristics of the image and the impact of the image on the user's emotion and psychology.

In this experiment, the user is completely based on subjective ideas, without any human interference.

3 Results

The purpose of this research is to investigate users' preferences for the two styles of Changmen Kusu Prints and Taohuawu New Year Woodblock paintings. A total of 100 online questionnaires were sent out, of which 30 participants were postgraduates in the field of design and culture, college teachers and Taohuawu related practitioners, while the rest of the questionnaires were sent to people aged 16–30 in different cities, with different educational backgrounds and different occupations.

Before the data analysis, the reliability and validity of the questionnaire need to be analyzed to ensure that the data obtained from the questionnaire has analyzable value. After testing, the reliability and validity of this scale questionnaire are good, and the data obtained have analytical value. The collected samples were tested by paired sample T test in SPSS, and the final results are shown in Table 3.

Table 3. Statistical table of user preference experiment results (use shorthand for sample names)

Dependent variable	Mean (SD)		
	Changmen	Taohuawu	<i>p</i>
Image visual features	3.40 (.12)	2.91 (.18)	0.042
The impact of images on users' emotions and psychology	1.01 (.35)	0.29 (.42)	0.032

As shown in Table 3, in terms of the visual characteristics of the images, there is a significant difference between the Changmen Kusu Prints and the Taohuawu New Year Woodblock paintings ($p < 0.05$), and the average value of the Changmen Kusu Prints of 3.40 is greater than that of the Taohuawu New Year Woodblock paintings 2.92, therefore, the visual features of Changmen Kusu Prints are more popular with contemporary young people; there are also significant differences between the two styles in the impact of images on users' emotions and psychology ($p < 0.05$), and Changmen's scored higher than the Taohuawu.

Based on the above results, the user preference of Changmen Kusu Prints is higher than that of Taohuawu New Year Woodblock paintings. That is to say, Changmen Kusu Prints style are more popular among contemporary young people. Next, analyze the reasons for this result by analyzing specific image samples.

Figure 7 shows the representative samples of the Changmen Kusu Prints and Taohuawu New Year Woodblock paintings. First of all, in terms of craftsmanship, the Changmen Kusu Prints is very exquisite, and the engraving and multi-color overprinting techniques are extremely high. Therefore, its works are more exquisite, in line with the quality of life pursued by contemporary young people.

Secondly, in terms of style, the Changmen Kusu Prints is not so full of New Year's flavor, its vivid charm and elegant style, and thus more in line with the hobbies and aesthetic needs of contemporary young people.

In addition, in terms of subject matter, the Changmen Kusu Prints mostly depicts urban life and civic life, and is basically a depiction of actual scenes, which is closer to the life of contemporary young people; while Taohuawu New Year Woodblock paintings focus on gods and Buddhas, which are in line with modern times. On the whole, there are traces of the Changmen Kusu Prints gaining a higher user preference.

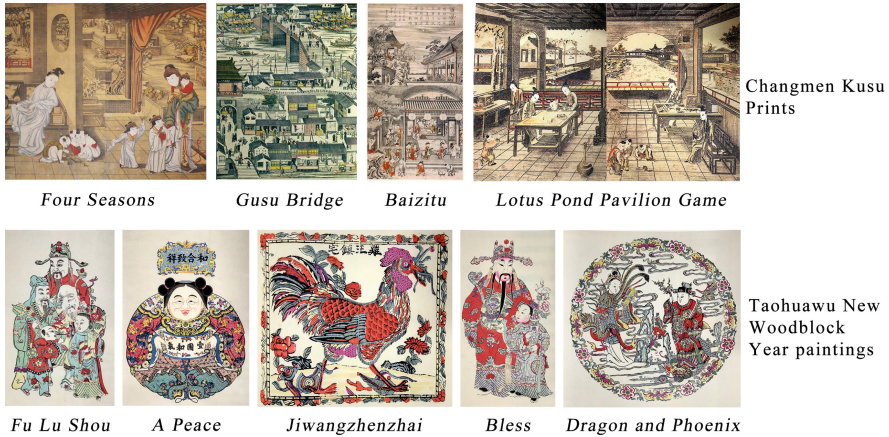


Fig. 7. Two styles of New Year pictures

4 Discussion

Through a detailed review of the historical period and style evolution of Taohuawu New Year paintings, the Taohuawu New Year pictures are divided into two artistic styles: Changmen Kusu Prints and Taohuawu New Year Woodblock paintings. CycleGAN was used to train two styles of New Year paintings samples for adversarial generation and transfer their styles to typical representative images of the Taohuawu New Year painting's theme for user preference experiments, finally concluding that the Changmen Kusu Prints are more popular among young people, and arguing the reasons for this result from various aspects.

The conclusions drawn are helpful for the targeted inheritance and development of the styles that users prefer. This experimental research is only the first step, and the follow-up research will in-depth explore the reasons for the style preference, and

explore the contemporary development path of Changmen Kusu Prints from the aspects of technology, materials, media, etc., so as to bring this classic art to the public and rejuvenate it.

References

1. Zhang, A.: Exploration on visual design and translation of intangible cultural heritage. *Packag. Eng.* **39**(20), 121–125 (2018)
2. Zhou, X.: Discussion on the strategy of inheritance and development of suzhou taohuawu new year paintings. *Popular Lit. Art* **63**(10), 49 (2019)
3. Liu, Y., Yin, J.: Digital cultural and creative design of Taohuawu woodblock New Year pictures based on cultural translation. *Packag. Eng.* **43**(10), 326–334 (2022)
4. Zhang, Z.: Research on digital art reproduction and interactive experience design of Taohuawu woodcut new year pictures. Master's thesis, Nanjing University of Aeronautics and Astronautics (2018)
5. Zhao, Y., Xu, Y., Zhang, Y.: The application of Taohuawu woodcut new year pictures cultural image in clothing design. *J. Wuhan Text. Univ.* **32**(03), 33–36 (2019)
6. Wang, Z., Deng, L.: The application of modeling elements of Taohuawu woodblock New Year pictures in modern interior design. *Packag. Eng.* **42**(04), 285–291 (2021)
7. Mu, S., Liu, Z., Su, G.: Research on the subjective data collection method of instant on-site users. *Packag. Eng.* **42**(14), 155–163 (2021)
8. Ma, X.: Research on image retrieval algorithms based on deep neural networks. Master's thesis, Soochow University (2018)
9. Zhao, X., Li, D.: Game image generation in traditional Chinese painting style based on CycleGAN. *Electron. Test* **28**(24), 53–56 (2021)
10. Guo, J., Song, N., Wang, X.: Evaluation of the semantic description method of digital images of Dunhuang frescoes from the perspective of users. *Libr. Inf. Knowl.* **36**(03), 66–77 (2018)
11. Huang, X., Dagobert, S., Judith, L.: Modeling and analyzing the topicality of art images. *J. Assoc. Inf. Sci. Technol.* **66**(8), 1616–1644 (2015)



Personalized HRIR Based on PointNet Network Using Anthropometric Parameters

Dongdong Lu^(✉), Jun Zhang, Haiyang Gao, and Chuang Liu

Beijing Institute of Spacecraft Environment Engineering, Beijing 100094, China
1157835731@qq.com

Abstract. A novel deep neural network model was proposed to reconstruct the head-related impulse response (HRIR) by using three dimensional anthropometric parameters. Aiming at the point physiological parameters in the HRTF database of Chinese pilots', this paper adopts a Point-Net network composed of three convolutional layers and two hidden layers. The convolutional layer is used to extract the features of physiological parameters, and the hidden layer is used to generate hrir. The spectral distortion (SD) is adopt to quantify the difference between the measured and the reconstructed HRTF. Consequently, the proposed method performs better than the deep-neural-network based model.

Keywords: Head related impulse response (HRIR) · Personalization · PointNet

1 Introduction

Vision and hearing are two important ways for people to perceive the environment, which cooperate with each other to enable people to make accurate judgments on the environment. Compared with the visual system [1], which can only capture the target of limited orientation, the hearing system can capture all-round audio information in three-dimensional space thereby reducing the visual load. Based on this characteristic of the auditory system, researchers hope to use the auditory system to enhance the subject's perception of the environment, especially in a complex environment.

Recently, with the substantial improvement of software and hardware capabilities, virtual reality and augmented reality technologies are rapidly integrating into people's lives. Virtual hearing, one of the important components of virtual reality, has also developed rapidly.

The head-related transfer function (HRTF) describes the comprehensive filtering effect of the head, torso and auricle on the sound source in the free-field situation. Listeners gain a sense of space based on the Inter-aural level difference and the inter-aural time difference. Due to the different physiological structure of the listener's, there are certain differences in auditory perception. Studies have shown that the virtual sound synthesized by personalized HRTF can effectively enhance the listener's auditory perception.

So far a various methods have been proposed for HRTF personalization, including measurement, database matching, theoretical calculation, and numerical fitting [2]. Among them, the numerical fitting method from physiological parameters to HRTF has

received the most attention. To date, which anthropometric parameters are decisive for HRTF remains an open question.

Meanwhile, some researchers are trying to introduce deep learning methods into HRTF personalization. Different from database matching and numerical fitting, neural networks only need to consider the input and the output, rather than the relationship between the input and the output.

Chun [3] introduced a deep neural network (DNN) model to HRTF personalization which directly establish the connection between the physiological parameters and the head related impulse response (HRIR), in which 37-dimensional physiological parameters was select as the input, passing through multiple fully connected layers, and finally outputs HRIR.

Lee [3] combined convolutional neural network (CNN) and DNN network to form a new network, which used CNN network to process the ear physiological parameters, and selected DNN network to process the head and torso, and then the outputs of the two sub-networks are combined as input to obtain the HRIR.

In this paper, the Point-Net network is used to realize the direct regression from physiological parameters to HRTF, in which the three-dimensional physiological parameters of the pilots' are used as input, and the HRTFs as output.

2 Chinese Pilots' HRTF Database

The database used in this paper is the of Chinese pilots' HRTF database [4], which contains the HRTFs of 63 subjects in 723 different directions.

In this paper, we choose the three-dimensional physiological parameters in the database for research. In this paper, we choose the three-dimensional physiological parameters in the database for research. The physiological parameters are given in the form of points, with a total of 93 points. These 93 feature points would be sure to include the feature points of the head, ear, and torso.

3 PointNet Network

Qi proposed the PointNet network in 2017 for the characteristics of point cloud data. This network enables point cloud data to be directly applied in deep learning.

The PointNet network directly took the point set as input, and each point was composed of its coordinates and additional features such as color, normal, etc.

The PointNet network shows in Fig. 1, consists of three parts: a max-pooling layer that aggregates information from all points as a symmetric function; a combined local and global structure; and two joint alignments for aligning input points and point features.

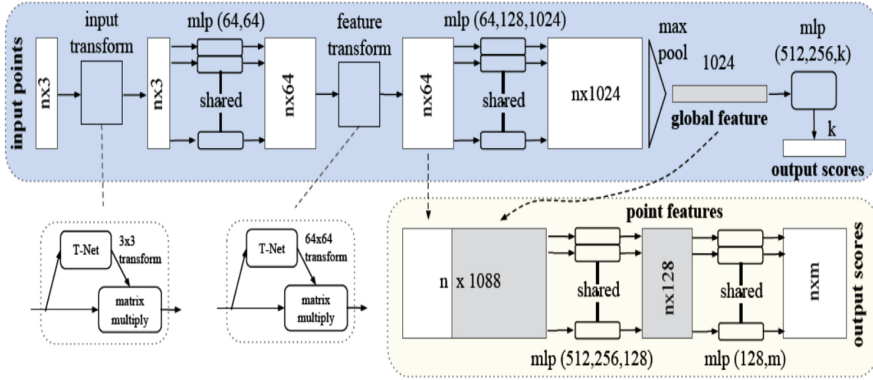


Fig. 1. The structure of PointNet network

3.1 Neural Network Architecture

There exist three strategies to keep the model invariant to the input permutation: (1) sorting the input in canonical order; (2) training the RBM with the input as a sequence, but augmenting the training data with various combinations; (3) integrating the information of each point with a simple symmetric function.

For the proposed model, the input is point cloud data. Unlike the PointNet network in, this network does not apply input transport to perform matrix transformation, which is related to the type of input data. In this paper, the input data is sorted in a specific order, (no matter for training data or for test data), therefore, the network proposed in this paper does not require input transport.

Figure 2 shows the structure of the proposed model which takes the human physiological parameters of 93×3 as the input feature and HRIR as the output.

The proposed model took anthropometric data as input. Firstly, normalizes the anthropometric parameters, and three convolutional layers is followed. For these three convolutions, the filters are different, 64, 128, and 1024 in turn, but the filter kernel and activation function are the same, 1 and sigmoid, respectively. Then there is a max pooling layer and an expansion layer. The max pooling and expansion layers convert the input point cloud data into one-dimensional data, followed by two hidden layers. The hidden layer has different node numbers of 256 and 512 respectively, while the activation functions are both sigmoid.

The network can only be trained for a single angle, and the left ear HRIR and right ear HRIR are trained separately.

3.2 Supervised Learning

In order to achieve rapid model convergence, Xavier initialization technology is used to process the weights of all layers, and all deviations are set to 0. At the same time, in order to quantify the difference of the measured and the estimated target, for the cost function we select the mean square error (MSE). An adaptive matrix is used to optimize the back-propagation algorithm, with the decay rate and the learning rate of 0.9 and 0.01, respectively. Finally, the dropout technique is used to avoid overfitting of the model.

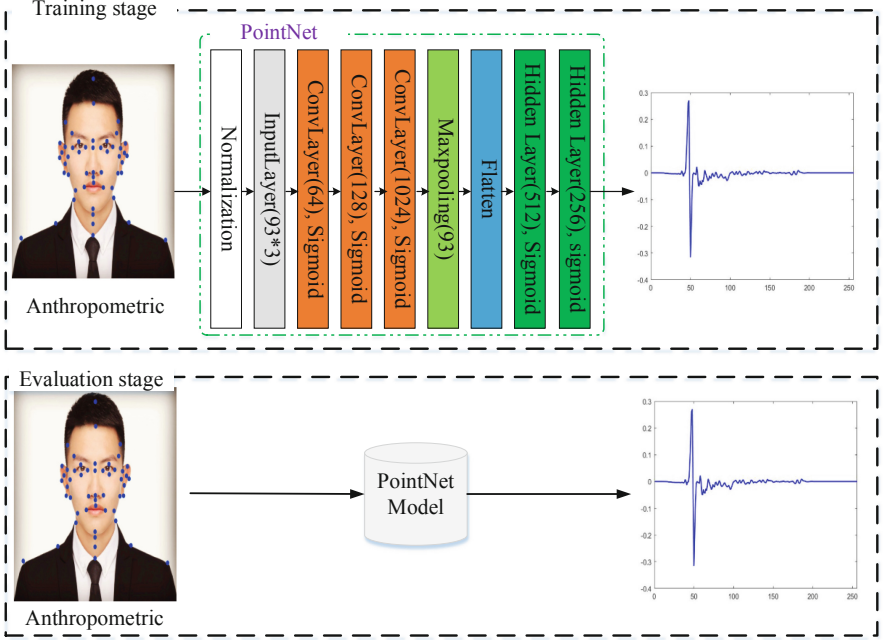


Fig. 2. Network block diagram of HRIR estimation method based on point cloud physiological parameters (some physiological parameters are marked on the anthropometric map)

4 Performance and Evaluation

In HRTF related studies, the spectral distortion (SD) is usually employed to calculate the discrepancy of the reference HRTF $H(f_k)$ and the estimated HRTF $\hat{H}(f_k)$. The smaller of the SD, the higher the similarity of the two HER. It should be noted that SD is aimed at a single ear.

The SD is defined by Eq. (4.1):

$$SD^{(d)}(H, \hat{H}) = 20 \sqrt{\frac{1}{N} \sum_{n=1}^N (\log_{10} \|H^{(d)}(n)\| - \log_{10} \|\hat{H}^{(d)}(n)\|)^2} \quad (4.1)$$

where, the unit of SD is decibel, and N is the frequency bin. $H(f_k)$ and $\hat{H}(f_k)$ denote the measured HRTF and the evaluate HRTF, respectively. f is the frequency in kHz.

Table 1. The impact of Dropout parameters on proposed model

Dropout parameter	0.5	0.6	0.7	0.8	0.9	0.95
Training error	0.0077	0.0088	0.0108	0.0135	0.0260	0.0644
Test error	0.0058	0.0063	0.0053	0.0050	0.0067	0.0133
Validation SD/dB	2.50	2.68	2.44	2.45	3.04	5.01

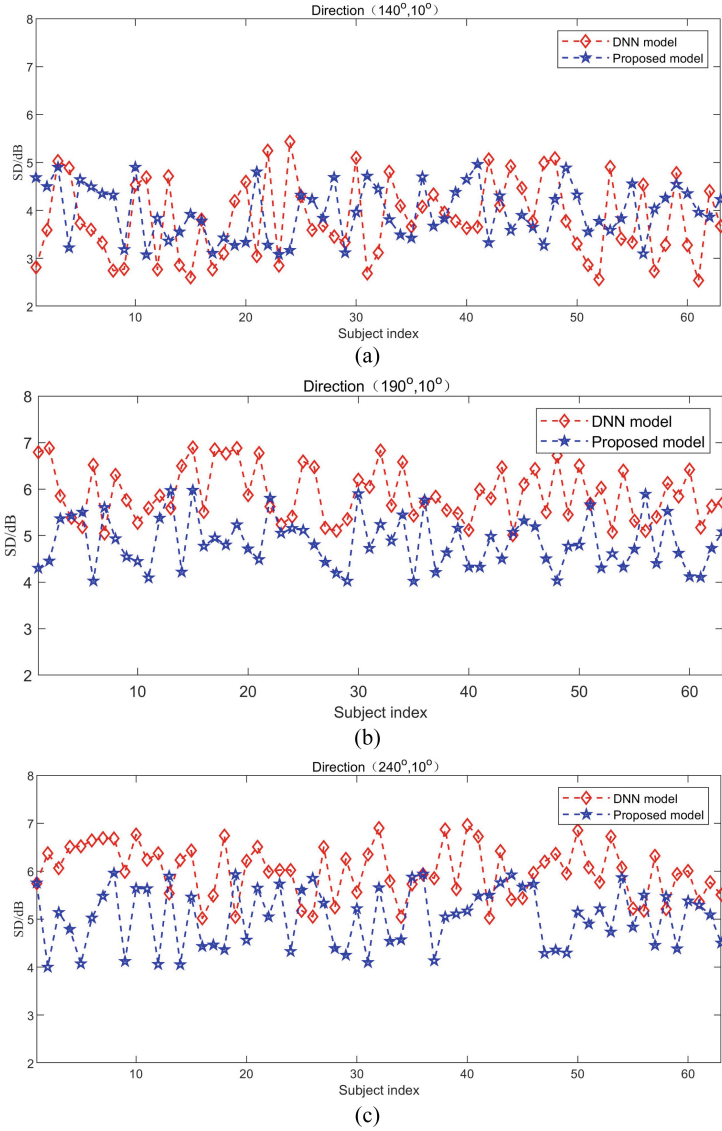


Fig. 3. The SDs of the proposed method and the DNN method at orientation (140°, 10°), (190°, 10°) and (240°, 10°)

In Table 1, with the increase of the Dropout parameter, the training error is increasing, while the test error has a tendency to increase after decreasing. This reflects that the proposed model has a certain degree of over-fitting. It can be seen from the validation set that when the Dropout is between 0.5 and 0.8, the SD of the validation set is maintained at a low level. When the Dropout is 0.90 and 0.95, the validation The set SD has an obvious increasing trend, which to a certain extent indicates that the network is over-fitting. Therefore, in this paper we set the dropout parameter of the proposed model equal to 0.7 to prevent over-fitting.

Figure 3 showed the SD of 63 subjects at direction $(140^\circ, 10^\circ)$, $(190^\circ, 10^\circ)$ and $(240^\circ, 10^\circ)$, and the frequency band ranged from 0 to 22.05 kHz. It can be seen from the figure that for the direction $(140^\circ, 10^\circ)$ there is no significant difference in SD between the two methods. For the direction $(190^\circ, 10^\circ)$ and $(240^\circ, 10^\circ)$ the minimum SD of the proposed model was smaller than the minimum SD of DNN [3] model, and the fluctuates of the proposed model is smaller, which indicates that the proposed model can better approximate the measured HRTF.

5 Conclusion

In this paper, we proposed a deep learning model to obtain a personalized HRTF, based on the PointNet network, and the PointNet network is modified according to the characteristics of the pilot HRTF data. For the proposed model, the physiological parameters of human point cloud are used as input, and HRIR is output. According to the characteristics of physiological parameters, the CNN network is used to extract more dimensional features. Compared with the DNN model, the SD of the test HRTF obtained by applying the PointNet network is greatly reduced, and the SD is less than 5.7 dB.

References

1. Cohen, M., Wenzel, E.M.: The design of multi-dimensional sound interfaces, pp. 291–346. Oxford University Press, Inc., New York (1995)
2. Hu, H.M.: Research on key technologies in the realization of virtual auditory space. Southeast University, Nanjing (2008)
3. Lee, G.W., Kim, H.K.: Personalized HRTF modeling based on deep neural network using anthropometric measurements and images of the ear. *Appl. Sci.* **8**(11), 2180 (2018)
4. Guo, X.C., Xiong, D.Q., Wang, Y.Y., et al.: HRTF database of Chinese male pilots. In: Proceedings of the 16th International Conference on MMESE, Xi'an, China, 3–11 October 2016



Effects of 15 days -6° Head-Down Bed Rest Simulated Weightlessness on the Judgment of Motion Direction

Tianxin Cheng¹, Duming Wang¹(✉), Yu Tian², Zhen Yuan¹, and Lian Wang³

¹ Department of Psychology, Zhejiang Sci-Tech University, Hangzhou 310018, China
wduming@163.com

² National Key Laboratory of Human Factors Engineering, Astronaut Center of China, Haidian District, Beijing 100094, China

³ School of Mechanical Engineering, University of Science and Technology Beijing, Beijing 100083, China

Abstract. To explore the effect of long-term simulated weightlessness on the judgment of motion direction, the -6° head-down bed rest (HDBR) was used to simulate the effect of long-term weightlessness, and the judgment task of motion direction was performed on the four main directions: upward, downward, leftward, and rightward. Twenty-five males were tested on the 2nd, 8th, and 13th days of the -6° HDBR position, as well as pre-test and post-tests in the supine position. The results show that the upward direction judgment deviation was minimal over time, while the downward direction judgment deviation decreased substantially in the first test of HDBR compared to the pre-test, narrowing the judgment gap between the downward and upward direction. Long-term simulated weightlessness had a great influence on the judgment of downward direction in the initial stage, which showed better performance, and the performance tends to be stable along time increased.

Keywords: Head-down bed · Simulated weightlessness · Motion direction judgment

1 Introduction

The ability to perceive motion direction is critical to an individual's survival. The performance of various space activities, such as hand-controlled interactive docking, teleoperation of space manipulator, and cognitive operation tasks, is influenced by motion direction perception function [1]. An oblique effect in direction perception has been discovered in previous research, which shows that people judge horizontal and vertical directions more accurately than diagonal directions, and this effect has been supported in a variety of tasks [2, 3]. The horizontal effect was reported by Pilz et al. [4], who discovered that judgment performance was better in the horizontal direction than in the cardinal direction in their study. This form of direct variation is caused by gravity's influence. We are more familiar with environmental structures that are parallel or vertical to

the direction of gravity in our daily lives [5, 6], resulting in the associated perceptual direction effect.

Microgravity can cause complex changes in vestibular organs and sensorimotor systems [7, 8], thus affecting various perceptual and operational performance, such as the ability to avoid collision prediction and different motion control performance. Therefore, it is necessary to investigate the effect of weightlessness on perception to avoid the corresponding risks.

-6° HDBR is considered to be the most effective method to simulate physiological effects under weightlessness [9]. Wang et al. [10] used the occlusion paradigm to discuss the judgment of motion direction and found that the judgment deviation of upward direction increased significantly under the condition of simulated weightlessness for a short time, while the impact on other directions was small. The space station is built to enable astronauts to live weightless for long periods, it's an environment where both the person and the space can move with six degrees of freedom, they'll have different position relations with each other, which induce higher requirements on the orientation discrimination ability of astronauts [11]. Furthermore, prolonged HDBR posture causes cephalad fluid shift, bone and muscle loss, weakened metabolism, and decreased sensory stimulation [12]. Therefore, it is of great significance to study the characteristic rules of motion direction judgment in a long-term weightlessness environment.

In this work, we continue to explore the influence of long-term simulated weightlessness on the judgment of motion direction by using the occlusion paradigm which is closer to the space mission. Three tests were carried out under the HDBR posture for 15 days, and two tests before and after in supine position.

2 Method

2.1 Subject

Twenty-five males aged from 24–35 ($M = 28.2$, $SD = 2.8$) voluntarily participated in this study, all of them were right-handed, and have no special medical history through relevant physical examinations. All volunteers signed in the informed consent form and fully understand the content of the experiment.

2.2 Instruments

As shown in Fig. 1 and Fig. 2, the bed rest study was conducted on a standard intelligent recumbent laboratory bed. The bed can be adjusted. The stimulus presentation displayer is a DELL 23-in. Computer Monitor S2319HS with a 1920 * 1080 resolution and a 60 Hz refresh rate. The display is 60 cm from the bed surface. The mouse used for the operation was Logitech's MK235 placed on the bed. Bose noise-canceling headphones were worn during the experiment to prevent noise. The temperature in the experimental room was kept at 25 °C.

The bed rest period was 15 days. During the bed rest period, the volunteers maintained a -6° HDBR position in bed and could turn left and right along the body axis. The rest of the physiological activities, such as eating, defecation, washing, and rest, were all performed on the bed. The subjects were tested on the 2nd (BR2), 8th (BR8), and 13th (BR13) of the HDBR, as well as 6 days ($-BR6$) before and 4 days (BR+4) after.



Fig. 1. Intelligent experimental bed



Fig. 2. Experimental scenario

2.3 Tasks and Procedures

The experimental software was programmed by C#. The task interface is shown in Fig. 3. The black area in the ring is the occlusion area, and the black solid point in the center is the target. The visible distance is 350 px, the occlusion distance is 150 px, the diameter of the target is 40 px, and the movement speed of the target is $4^\circ/s$. The target is visible for 1.45 s. The experimental procedure is shown in Fig. 4. The target's black dot is initially located in the middle of the ring for 500 ms, then moves at a uniform speed from the center to the outside. When it enters the occlusion zone, the target vanishes and is replaced by a blue boundary around the outer ring.

Subjects try to predict where the dot will end up if the previous motion trajectory is followed, and then click the corresponding place with the mouse. The red dot appears after clicking, representing the end of a trial. Finally, the deviation of the individuals' judgment angles was measured using the absolute value of the difference between the judgment angle and the actual angle.

As shown in Fig. 4, the movement direction includes four main directions: upward, downward, leftward and rightward, and seven different movement directions are set for each main direction: $-15^\circ, -10^\circ, -5^\circ, 0^\circ, 5^\circ, 10^\circ, 15^\circ$, the negative value is the counterclockwise direction of the main direction. The subjects had to complete 56 trials in total, which were presented in random order, with two trials at each angle. Four different trials were practiced before the formal experiment. The practice phase presents straight-line feedback, and the formal experiment does not provide feedback.

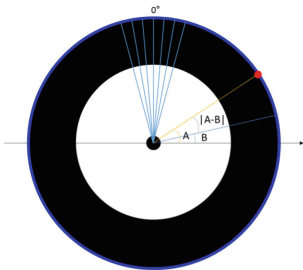


Fig. 3. Testing interface

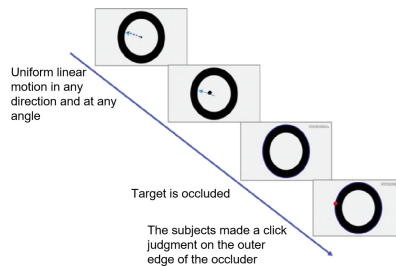


Fig. 4. The experimental process

3 Result

The judgment deviation values were statistically analyzed after the extreme values were eliminated according to the “ $\pm 3S$ ” principle. The mean values of the judgment deviation are shown in Fig. 5.

The result of RMANOVA of 5×4 show that the main effect of direction is significant ($F_{(3,72)} = 9.21, p = 0.00, \eta_p^2 = 0.714$), the further simple effect shows that upward motion judgment deviation is significantly smaller than the downward motion judgment deviation ($p = 0.007$), the leftward direction ($p = 0.006$), and the rightward direction ($p = 0.00$). The main effect of time is not significant ($F_{(4,96)} = 0.853, p = 0.495$).

There is a significant interaction between time condition and motion direction ($F_{(12,288)} = 2.651, p = 0.002, \eta_p^2 = 0.839$). The pre-test (BR-6) reveals that the upward direction’s judgment deviation is significantly lower than the downward direction’s ($p = 0.006$), leftward direction’s ($p = 0.026$), and rightward direction ($p = 0.003$). The upward direction’s judgment deviation is much smaller than the downward direction’s ($p = 0.01$) on the first HDBR test (BR2). The upward direction’s judgment deviation is much smaller than the leftward direction’s ($p = 0.005$) on the second HDBR test (BR8). On the second HDBR test (BR13), the upward direction’s judgment deviation is smaller than the left-ward ($p = 0.005$) and right-ward ($p = 0.009$) directions. On the post-test (BR+4), the upward direction’s judgment deviation is significantly lower than the downward ($p = 0.001$), leftward ($p = 0.03$), and rightward ($p = 0.00$) directions. Between the pretest and the first head down test (BR2) ($p = 0.08$), as well as between the pretest and the third head down test (BR13) ($p = 0.055$), the downward direction judgment was marginally significant, details are shown in Fig. 6.

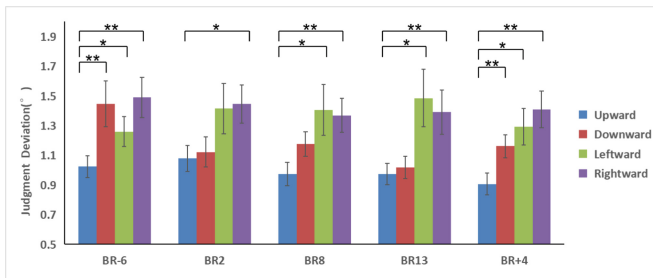


Fig. 5. Mean value of judgment deviation in different directions of HDBR tests. $**p < 0.01, *p < 0.05$. Error bar: standard error.

4 Discussion

In this study, we want to discuss the influence of long-term simulated weightlessness on the judgment of motion direction. The subjects performed three tests in a -6° HDBR posture in 15 days, as well as pre-test and post-tests.

The results showed that the judgment deviation of the upward movement direction was the smallest in each test, which was consistent with the research results of Wang

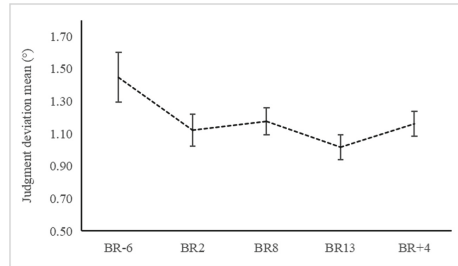


Fig. 6. The mean values of the judgment deviation for the downward direction. Error bar: standard error

et al. [10]. The study by Naito et al. found a similar effect, in the random-dot motion paradigm, the upward direction was more easily identified at low-speed conditions. For this result, the author considered the human visual orientation selection related to the motion advantage, the upward direction was used as the forward direction, so it had more familiarity advantage [13].

The judgment deviation of the downward direction decreases sharply in the first HDBR test, while the changes in the other three directions are not obvious, indicating that the downward direction is greatly affected by the head-down position. Furthermore, the difference in judgment performance between the upward and downward directions was narrowed, and the judgment deviation between the two directions was not significant during the entire HDBR posture. Claassen [14] has found, when gravity cues were reduced, the difference in discrimination sensitivity for upward and downward directions decreased, while it has little influence on the judgment of left and right directions. In the field of motor control [15], the effects of weightlessness are also concentrated in the vertical direction, showing a reduction in asymmetry perception between upward and downward motion. The main reasons can be summarized as follows: Because of gravity, upward and downward saccade gains are asymmetric, with upward saccade gains smaller downward. When the body is tilted at a -6° HDBR posture, the downward eye movement frequency is minimized, resulting in more precise tracking of downward eye movement [16]. In addition, when the body is tilted, the downward direction, as the direction of gravity, conflicts with the direction of gravity perceived by the vestibular organs, which the motion law is inconsistent with the natural dynamics, the visual area in the brain will be activated [17], and the perception of motion will rely more on the information provided by the vision and less on the prior knowledge of gravity.

In addition, Wang et al. [10] employed the -6° HDBR position for 3 min to simulate the short-term effect of weightlessness in a previous study. This is inconsistent with the findings in this paper that better downward judgment performance leads to a narrower gap between upward and downward judgments. With the prolonging of the HDBR duration, the judgment of the downward direction first decreased and then increased, but there was no obvious significant effect. It is speculated that the HDBR posture within 3 min caused the body fluid to move rapidly to the head, so the deviation of direction judgment of upward increase is the negative result of vestibular and visual disturbances under postural changes. Previous studies concluded that cognitive function and motor system

performance improved in weightlessness, which was mainly due to the adaptation and self-regulation of the human body to the weightless environment [18]. Therefore, in the long-term condition, the subjects gradually adapted to the state of weightlessness, and the negative impact of gravity on motion perception was weakened.

The effect of 3 min and 15 days of head down on the perception of motion direction shows that the impact of head down on motion direction judgment is dynamic. As time goes on, the human body gradually adapts to weightlessness, and the overall performance is that the performance of motion direction judgment improves. This also shows that it is meaningful to explore the short-term and long-term weightlessness state.

5 Conclusion

- (1) The upward direction judgment deviation is the smallest under the occlusion paradigm. This phenomenon occurs in a variety of postures (supine, HDBR) and simulated weightlessness durations.
- (2) Under the condition of long-term -6° HDBR simulating weightlessness, the downward direction is greatly affected, which is manifested as a decrease in judgment bias, thereby narrowing the perceived gap between the upward and downward directions during the simulated weightlessness. As the simulated weightlessness time is prolonged, the performance tends to be stable.

Acknowledgment. This work is supported by Space Medical Experiment Project “Research on the Effects of Long-term In-orbit flight on Astronauts’ Space Cognitive Ability (No. HYZHXM03001)”, the Foundation of The Key Laboratory of Human Factors Engineering (No. 614222204020617), and the Natural Science Foundation of Zhejiang Province (No. LQ19C090008).

Compliance with Ethical Standards. The study was approved by the Logistics Department for Civilian Ethics Committee of Zhejiang Sci-Tech University. All subjects who participated in the experiment were provided with and signed an informed consent form. All relevant ethical safeguards have been met with regard to subject protection.

References

1. Wang, C.H.: Design and development of astronaut modeling and simulation system. Doctoral dissertation, Tianjin University (2017)
2. Gentaz, E., Hatwell, Y.: The haptic ‘oblique effect in children’s and adults’ perception of orientation. *Perception* **24**(6), 631–646 (1995)
3. Wong, W., Price, N.S.C.: Testing neuronal accounts of anisotropic motion perception with computational modeling. *PLoS ONE* **9**(11), e113061 (2014)
4. Pilz, K.S., Papadaki, D.: An advantage for horizontal motion direction discrimination. *Vision Res.* **158**, 164–172 (2019)
5. Senot, P., Zago, M., Lacquaniti, F., McIntyre, J.: Anticipating the effects of gravity when intercepting moving objects: differentiating up and down based on nonvisual cues. *J. Neurophysiol.* **94**(6), 4471–4480 (2005)

6. Séac'h, L., Brec'hed, A., Senot, P., McIntyre, J.: Egocentric and allocentric reference frames for catching a falling object. *Exp. Brain Res.* **201**(4), 653–662 (2010)
7. Manzey, D., Lorenz, B.: Mental performance during short-term and long-term spaceflight. *Brain Res. Rev.* **28**(1–2), 215–221 (1998)
8. Sandal, G.M., Leon, G.R., Palinkas, L.: Human challenges in polar and space environments. *Rev. Environ. Sci. Bio/Technol.* **5**(2–3), 281–296 (2006)
9. Watenpaugh, D.E.: Analogs of microgravity: head-down tilt and water immersion. *J. Appl. Physiol.* **120**(8), 904–914 (2016). <https://doi.org/10.1152/jappphysiol.00986.2015>
10. Wang, D., Han, Q., Tian, Y.: The influence of short-time head-down tilt simulated weightlessness on performance of motion direction judgment. In: Long, S., Dhillon, B.S. (eds.) *Man-Machine-Environment System Engineering: Proceedings of the 18th International Conference on MMESE*, pp. 425–432. Springer, Singapore (2019). https://doi.org/10.1007/978-981-13-2481-9_49
11. Cheng, S.G., Wang, C.H., Chen, X.P., et al.: Study on the variation characteristics of human operational ability in long term space flight. *Aerosp. Med. Med. Eng.* **28**(1), 1–10 (2015)
12. Taibbi, G., Cromwell, R.L., Zanello, S.B., et al.: Ocular outcomes comparison between 14-and 70-day head-down-tilt bed rest. *Invest. Ophthalmol. Vis. Sci.* **57**(2), 495–501 (2016)
13. Naito, T., Sato, H., Osaka, N.: Direction anisotropy of human motion perception depends on stimulus speed. *Vision Res.* **50**(18), 1862–1866 (2010). <https://doi.org/10.1016/j.visres.2010.06.007>
14. Claassen, J., Bardins, S., Spiegel, R., Strupp, M., Kalla, R.: Gravity matters: Motion perceptions modified by direction and body position. *Brain Cogn.* **106**, 72–77 (2016). <https://doi.org/10.1016/j.bandc.2016.05.003>
15. Gaveau, J., Berret, B., Angelaki, D.E., Papaxanthis, C.: Direction-dependent arm kinematics reveal optimal integration of gravity cues. *Elife* **5**, e16394 (2016)
16. Pierrot-Deseilligny, C.: Effect of gravity on vertical eye position. *Ann. N. Y. Acad. Sci.* **1164**(1), 155–165 (2009). <https://doi.org/10.1111/j.1749-6632.2009.03864.x>
17. Miller, W.L., et al.: Vestibular nuclei and cerebellum put visual gravitational motion in context. *J. Neurophysiol.* **99**(4), 1969–1982 (2008). <https://doi.org/10.1152/jn.00889.2007>
18. Strangman, G.E., Sipes, W., Beven, G.: Human cognitive performance in spaceflight and analogue environments. *Aviat. Space Environ. Med.* **85**(10), 1033–1048 (2014). <https://doi.org/10.3357/ASEM.3961.2014>



Passenger Car' Sitting Posture Prediction Research

Lipeng Qin^(✉), Peiwen Zuo, and Hui Lv

China Auto Information Technology Co., Ltd., Tianjin, China
632410058@qq.com

Abstract. Sitting posture as the input of the design of Automobile seat face, makes a huge effect on the overall seat comfort. The current software for sitting posture calculation is based on the SAE manikin and European driving habits for sitting, which is much different from the Chinese one. This paper firstly analyzes the key factors that affect the driving posture, and defines the input of the prediction model, and then predict the position of eye points and H point in different vehicles for different drivers, with the step-wise regression method. A inverse kinematic method is applied to solve the posture of torso, upper limbs and lower limbs to obtain the overall sitting posture. Finally, the accuracy of the model is verified by a comparison between the measured data and the predicted one.

Keywords: Sitting posture · Influencing factors · Stepwise regression · Inverse kinematics · Model optimization

1 Introduction

Driving posture definition is the key for automotive seat design. After the interior layout is finished, the digital human model is used to define the driving angles, based on which, the supporting forces of the seat cushion and back are designed, and the seat foam then can be designed. Therefore, the accurate posture definition is crucial to the overall seat comfort.

The sitting posture is not only influenced by the anthropometry, but also is directly related with the driving habits in different countries [1]. A significant difference between the Chinese anthropometry and the European and American ones exists, which leads to a big discrepancy also, therefore, it is necessary to establish the driving posture prediction model based on the Chinese anthropometry.

This paper builds the sitting posture prediction model based the Chinese anthropometry, using stepwise regression and inverse kinematics methods [2–4], and realizes the purpose that predict sitting postures of different drivers in different seats, which also could provide automobile engineers the posture defining and checking tools.

2 Experimental Scheme

The stratified sampling is used to recruit 1800 drivers from 6 cities of China, in which female subjects are 1/3 of the male ones, and their ages are in uniform distribution among 20–60.

There are 3 passenger cars for measuring, which are coded as A, B and C. Every subject’s sitting postures in 3 cars are measured respectively, in order to research on the posture difference among drivers in different cars, as Fig. 1(a) shows [5].

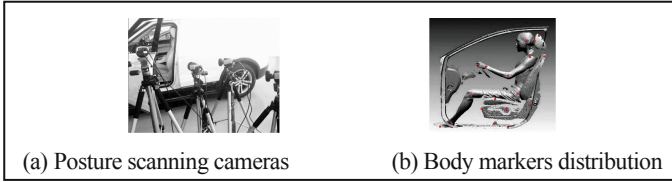


Fig. 1. Posture scanning facility and body markers

The subjects enter the car’s driving position after their bodies are marked with reflective makers, just as Fig. 2(b) shows. They are guided to adjust seat to the most comfortable status in their mind, after that, subjects’ sitting postures are measured and recorded, as Table 1 shows.

Table 1. Sitting posture angles list

A1	A2	A3	A4	A5	A6	A7	A8	A9
Torso angle	Hip angle	Knee angle	Ankle angle	Upper arm angle	Elbow angle	Wrist angle	Heel angle	Thigh angle

3 Posture Influencing Factors

This paper explores impact from gender and vehicle to sitting postures using repeated measures ANOVA. The Bonferroni correction is adopted to make multiple comparisons among different factors to investigate the simple main effect if interaction effect exists between the two factors. Effects are considered as “significant” when $p < 0.05$.

The stepwise regression model is used to explore the relationships between the postural data and the age and anthropometric measurements. Define the entry and removal of using probability of F as 0.05 and 0.1 respectively. The analysis finds that gender and vehicle both have a significant effect on the posture [5].

The stepwise regression analysis between the posture angles and anthropometry and gender needs to standardize all three types data, and results are demonstrated as Table 2.

Table 2. Stepwise regression results

Vehicle	Factors	Postural angles								
		A1	A2	A3	A4	A5	A6	A7	A8	A9
A	AGE	0	-0.082	0.072	0	0	0	0	0	0.043
	Stature	0	-0.535	0	-0.133	0	0	0	0	0.614
	WEI	-0.205	-0.116	0	0.105	0.134	0	-0.085	0.023	0
	SH	0.065	0.133	0.063	0	0.127	0.26	-0.117	0	-0.213
	TRH	0	0	-0.252	0	0	-0.06	0.104	0	0
	SAH	0	0.086	0	0	0	0.102	-0.132	0	0
	ATO	0	0	0	0	0	0	0	0	0
B	AGE	0	0	0	0.055	0	0	-0.054	0	0
	Stature	0.287	-0.259	0	0	0	0.211	0	0	0.543
	WEI	-0.296	-0.142	0.097	0	0.147	0	-0.107	0	-0.07
	SH	0	0	0	0	0	0	0	0	0
	TRH	-0.139	-0.117	-0.256	0	0	-0.149	0	0	0
	SAH	0	0.089	0.066	0	0.088	0.242	-0.13	0.105	-0.112
	ATO	0	0	0	0	0	-0.08	0	0	0.075
C	AGE	0	0	0	0	0	0	0	0.105	0
	Stature	-0.019	-0.401	0	-0.221	0	0	0	0	0.539
	WEI	-0.284	-0.134	0.075	0	0.167	0	-0.071	-0.148	-0.07
	SH	0	0	0	0	0	0	0	0	0
	TRH	0	0	-0.114	0	0	0	0	0	0
	SAH	0	0.109	0	0.114	0.071	0.142	-0.113	0	-0.133
	ATO	0	0	-0.097	0	0	0	0	0	0

The anthropometric measurements include: stature, weight (WEI), sitting height (SST), trochanter height (TRH), sitting acromion height (SAH), acromion to olecranon length (ATO).

Table 2 tells that Stature, WEI, SH, SAH and also vehicle are the main factors influencing postural angles, which are selected as the inputs to the prediction model.

4 Posture Prediction Model

Driver's anthropometry, seat parameters and vehicle layout make effects on the postures, which are taken as input to the model, as Fig. 2 shows.

Simplification is done to the prediction model to reduce the calculation complexity. The three-dimensional human model is simplified as the two-dimensional one, considering that sitting posture mainly indicates the joint angles. Also, it is deemed that normal driving posture is sagittally symmetric, and hands are assumed to be continuous with the forearms, and foot posture is neglected. The coordinate is simplified as x-z plane without y axis, as only the two-dimensional driving posture is concerned.

The eye and H point location regression equations are as Table 3 shows.

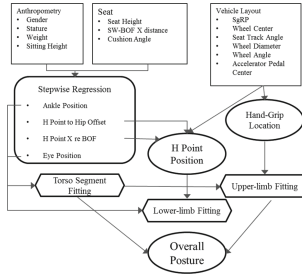


Fig. 2. Posture prediction model schematic diagram [1]

Table 3. Posture regression equation

Variables	Stature	Sitting height	H30	SW-BOFX	Cushion angle	Adjusted R ²	RMSE
Hip X re BOF	0.4701	-429.8	-0.173	0.4511	-1.04	0.67	36.3
Hip-to-eye angle	0.00638		115.73	0.0188	0.11	0.21	4.4
Eye X re BOF	0.5758	913.4	-0.1514	0.5847		0.71	51.1
Eye Z re AHP	0.3134	615.7	1.04	0.0288		0.79	22.3
Eye X re hip	0.1177	1350.2		0.155	1.22	0.31	37.9
Eye Z re hip	0.3324	665.4		-0.0221		0.57	25.7
Ankle X re BOF	0.06	458.1	0.175	0.147	1.5	0.28	20.3
Ankle Y re A pedal	-0.047					0.11	25.4
Ankle Z re AHP	0.0341		0.1312		0.47	0.21	18.4
Knee angle	-0.0066	57.3	-0.0341	0.0785	-0.61	0.34	10.2
Head angle	0.00922	141.5				0.04	12.3
Neck angle	-0.01214		0.0114			0.05	11.2
Thorax angle	0.01214	46.1		0.00998		0.04	8.2
Abdomen angle	0.011	190.5		0.0314		0.11	8.5
Pelvis angle	0.0112	101.2		0.0181	0.41	0.05	11.4

The upper extremity and lower limb fitting are calculated using inverse kinematic method after the hip and eye locations are obtained. This paper solve the inverse kinematic with MATLAB Robotics toolbox.

The postural data of a female subject and a male subject are collected respectively to verify the model accuracy. The measured and predicted results are shown in Table 4.

Table 4. Comparison of measured and predicted results

Posture	Subject					
	Male			Female		
	Measured	Predicted	Error	Measured	Predicted	Error
Torso angle	23.755	22.566	5.01%	18.8326	19.411	3.07%
Hip angle	101.254	106.78	5.46%	95.6201	104.36	9.14%
Knee angle	113.33	112.554	0.68%	109.09	110.22	1.04%
Forearm angle	19.4491	22.563	16.01%	56.4071	61.47	8.98%
Elbow angle	108.362	112.45	3.77%	143.651	147.225	2.49%
Thigh angle	12.2552	13.41	9.42%	11.0793	12.177	9.91%

The comparison results show that all the posture prediction error are all below 10% except for the male forearm posture.

5 Conclusion

It is found that driver's characteristics, vehicle design make a significant effect on the sitting posture. Take the identified effect factors as inputs to the model to predict eye, hip location, upper and lower limb fitting.

A comparison concludes that the model could predict Chinese driver's sitting postures well except the male forearm's error exceeds 10%.

The study was approved by the Logistics Department for Civilian Ethics Committee of China.

All subjects who participated in the experiment were provided with and signed an informed consent form.

All relevant ethical safeguards have been met with regard to subject protection.

Compliance with Ethical Standards. The study was approved by the Logistics Department for Civilian Ethics Committee of China Auto Information Technology Co., Ltd.

All subjects who participated in the experiment were provided with and signed an informed consent form.

All relevant ethical safeguards have been met with regard to subject protection.

References

1. Reed, M.P., et al.: Comparison of methods for predicting automobile driver posture. In: Digital Human Modeling for Design and Engineering Conference and Exposition, Dearborn, Michigan (2000)
2. Beck, D.J., Chaffin, D.B.: Evaluation of inverse kinematic models for posture prediction. In: Proceedings of the International Conference on Computer Aided Ergonomics and Safety - CAES 1992, May 18–20, pp. 329 (1992)
3. Zhang, X., Chaffin, D.B.: Task effects on three-dimensional dynamic postures during seated reaching movements: an analysis method and illustration. In: Proceedings of the 1996 40th Annual Meeting of the Human Factors and Ergonomics Society, Philadelphia, PA, Part1, vol. 1, pp. 594–598 (1996)
4. Faraway, J.J., Zhang, X.D., Chaffin, D.B.: Rectifying postures reconstructed from joint angles to meet constraints. *J. Biomech.* **32**, 733–736 (1999)
5. You, J., Qin, L., Zuo, P., Wang, X., Zhang, C.: Chinese drivers' preferred posture for sedans' seat ergonomic design. In: Long, S., Dhillon, B.S. (eds.) MMESE 2020. LNEE, vol. 645, pp. 23–32. Springer, Singapore (2020). https://doi.org/10.1007/978-981-15-6978-4_3



Psychological Adjustment of High Intensity Physical Training

Yu Luo¹, Qiaoyang Zheng², Hu Wang¹, Xia Chen¹, Shu Jiang¹, Mingze Li¹, Hao Li¹,
and Mengxi Li¹ (✉)

¹ Artillery and Air Defense Forces Academy (Zhengzhou Campus), Zhengzhou 450052, China
386809659@qq.com

² HeNan Open University, Zhengzhou 450000, China

Abstract. Mental preparation before high-intensity physical training can make individuals in high spirits, strengthen the correlation between ideology and biological reaction. It serves useful purposes in whole training process. This paper is based on the perspective of practice, attempt to explore the significance and application of the adjustment of the high-intensity physical training center from three aspects: the psychological preparation before the high-intensity physical training, the main methods of psychological adjustment in the high-intensity physical training and the application suggestions of psychological adjustment in the high-intensity physical training. This paper makes a preliminary discussion on the role of psychological factors in high-intensity physical training, it aims to provide psychological support and help for high-intensity physical training.

Keywords: High-intensity · Physical training · Psychological adjustment

1 Mental Preparation Before High-Intensity Physical Training

Mental preparation before training mainly includes two aspects: physical and mental preparation and behavioral process before training.

1.1 Physical and Mental Preparation

Participants arrive at the training site while simultaneously meaning their all activities should be served to training, all internal and external disturbances that may have a negative impact on the training effect should be excluded. In order to stimulate the potential and ensure the training quality to the greatest extent, the effect making preparation before training exerts on the training results is massive in scale. Prepared investment will make the training effect of participants get twice the result with half the effort, while a large amount of unprepared training is a waste of time. Accordingly, the undergoing training undergraduates have to do enough preparation on spirit and mood so that promoting high-intensity physical training can achieve better results.

1.2 Behavioural Process Before High-Intensity Physical Training

For the sake of ensure that the trained undergraduates have a good mental and emotional state, and put in the effort safely and quickly in the least time, behavioral process before training also plays a crucial role, including: (1) set up good surroundings; (2) Check the safety of training equipment/venue; (3) arrange/look for suitable companion; (4) Clear training objectives; (5) do psychological awakening.

2 Main Methods of Psychological Adjustment in High-Intensity Physical Training

During training, the pain and fatigue of the participants can be considered to be the most challenging part of high-intensity strength training. Mood can also affect the ability to tolerate pain and fatigue, this is as well as one of the most important psychological characteristics of the success of high-intensity physical training. At present, the commonly used emotion regulation methods in training mainly include: (1) imagine adjustment: let the participants experience the physical feeling and emotional state of their past success before or during training, it will significantly enhance the participants' confidence and effectively improve the training results; (2) expression adjustment: consciously change the expression and posture to adjust mood; (3) activity intervention: with increasing of muscles movement, there are more impulses from muscles to brain, and the excitement level of the brain is high, so the mood will rise; (4) music rousing: research reveal that music can make people feel excited, calm and balanced, so by playing music with different rhythms in training can maintain in good condition; (5) respiratory control: When someone get nervous, breathe will be fast and shallow. Due to fast breathing, the body inhales a lot of oxygen and exhales a lot of carbon dioxide. Excessive exhalation of carbon dioxide will cause the carbon dioxide in the blood flow to lose balance, thus the central nervous system will quickly make an inhibitory protective response; (6) hint adjustment: hint phenomenon is to be widely used in daily life no matter what effects are positive or negative, it can affect the psychological activity state of participants by language, gestures, expressions or other signals; (7) catharsis adjustment: Timely and fully vent their suffering, sadness, grievance and regret in an appropriate way to control their emotions. Moreover, odor regulation, diet regulation, transfer regulation and intensification regulation are also common psychological adjustment methods in sports psychology.

3 Suggestions on the Application of Psychological Adjustment in High-Intensity Physical Training

A variety of psychological skill combinations are mainly used in sports psychology, such as breathing regulation skills, muscle relaxation skills, self venting and suggestion skills which can help reduce the anxiety of participants, improve the psychological endurance of participants in high-intensity physical training, and then improve the training quality.

3.1 Respiratory Regulation Skills

When the participants are nervous, they breathe fast and shallow, and the concentration of carbon dioxide in the blood is reduced and unbalanced. Over time, the central nervous system quickly makes a consistent protective response. At this time, the tension can be eliminated by deepening or slowing down the breathing rate. When the participants are depressed, they can practice with regular inhalation and strong exhalation to improve their emotional excitement.

3.2 Implying Skill

Implying has a wide range of functions in daily life, which can be generally divided into autosuggestion and others suggestion. Before training, coaches and participants should try to use positive language to analyze the difficulties and problems that may be encountered in physical training and establish confidence; In the training, the coach should not only use positive words to enlighten the participants, but also suggest the participants to hint themselves by meditation, such as 'I can defeat it' 'I am awesome', it exerts a subtle influence on the trainees.

3.3 Self-venting

During the training, participants need to overcome their physical limits to achieve certain results. Boring and repetitive exercise is likely to increase the anxiety of participants, such as easy to lose their temper. In the meanwhile, it is suggested that when trainees are nervous, stamp their feet, relax their arms, or shout a few times to venting tension, so as to achieve the purpose of stabilizing their mind.

3.4 Muscle Relaxation Skills

High intensity physical training is prone to muscle soreness, muscle swelling and hardening. Besides relaxing, Adjusting the sore muscles with low intensity and small range movements, shaking and kneading muscles are viable patterns to achieve the purpose of active relaxation. If the emotion is too tense, use some action exercises with low intensity, large range, slow speed and rhythm to reduce the excitement of the emotion and eliminate the excessive tension.

Furthermore, Let the participants clearly and repeatedly imagine the movement skills and movement situations in their minds, such as 20 m rapid round-trip running, in-situ weight-bearing swing and so on, and repeatedly present the movement situations and movement skills in their minds. This can not only make the participants perceive the possible physical feeling and emotional state in the training in advance, but also help the participants enhance their self-confidence and understanding of motor skills, in order to improve their ability of emotional control and finally improve their training results.

4 Epilogue

This paper makes a preliminary discussion on the role of psychological factors in high-intensity physical training, and introduces the role of psychology in high-intensity physical training from three aspects: psychological preparation before high-intensity physical training, main methods of psychological adjustment in high-intensity physical training and suggestions on the application of psychological adjustment in high-intensity physical training. Although the author summarizes and considers the matters of high-intensity psychological adjustment, due to the limited academic level and conditions, there are also many problems, such as insufficient theoretical application and insufficient empirical research, which need to be further studied and step forward in the future.

References

1. Whiumarsh, B.: *Mind & Muscle*. Human Kinetics, Champaign (2001)
2. Davis, J.M., Bailey, S.P.: Possible mechanisms of central nervous system fatigue during exercise. *Med. Sci. Sports Exerc.* **29**, 45–57 (1997)
3. Chen, N.: Research on the correlation between the level of psychological stress and the changes of blood biochemical indexes of outstanding participants in physical fitness projects at different stages of competition. *J. PLA Sports* (4), 34–37 (2000)
4. Feng, Y.: Psychological and cognitive intervention effect of high-load training evaluation of outstanding trainees. *Sports Sci.* (12), 43–45 (2005)
5. Tao, Y.: Discussion on the application of psychological training to the students majoring in speed skating in colleges and universities to restore physical fitness. *Ice Snow Sports* (2), 42–43 (2002)
6. Wang, Z.: The effect of psychological and behavioral training on recruits' physical fitness test scores. *PLA Med. J.* (7), 604–605 (2003)



Research on Audience Cognition of Audio-Visual Interactive Art from the Perspective of Mental Model

Yijie Zhang, Zhengqing Jiang^(✉), and Haiyun Zheng

East China University of Science and Technology, Shanghai 200030, China
645356875@qq.com

Abstract. Objective Media art with the intervention of computer development has greatly increased the audience's participation, and has to become one of the factors that artists consider in the creative process. In this paper, semi-structured interviews are conducted with highly involved audiences in this field through metaphor extraction technology, and constructs are extracted to establish a cognitive map of the audience, in an attempt to explore the influencing factors of audience participation. The research finds that when the audience participates in the audio-visual interactive art with subjective initiative, they generally have interaction and connection with the works, in the whole process of audience acceptance, "emotional experience" has the highest influence on whether audience participates in the work. Moreover, it has a progressive influence from the instinctive, behavioral and reflective layers of audience experience.

Keywords: Mental model · Metaphor extraction technology · Consensus map · Audience cognition · Audio-visual interactive art

1 Introduction

Audio-visual interactive art is a new media art form that explores the real-time interactive relationship between sound and visual elements by means of digital media technology [1]. According to the different presentation media, the audio-visual interactive art usually has two presentation modes: screen and device interaction. The core of its art is to make the information transmission nonlinear and multidimensional. Through multi sensory stimulation, the audience can truly "touch" the story that the artist wants to express [2]. The experience, interaction and randomness of audio-visual interaction make the audience change from passive viewing to active participation in the space created by artists. In the whole process of artistic activities, the audience is no longer just a receiver, but also a creator and a part of artistic works.

2 The Transformation of Audience Identity

In terms of time development, the intervention of science and technology divides the field of art into “Traditional Art” and “Media Art” [3]. With the continuous expansion of the audience’s artistic vision, the aesthetic requirements for artistic works are increasing day by day. Collingwood pointed out the new era of new trend: “artists are not like they are used to, there are many signs that they, than in the past, than 30 years ago even more willing to see the audience as collaborators”, artists gradually hope the audience to interact with their work [4]. The transformation of media art to audience identity also stems from the gradual improvement of audience psychology in this period, which prompted many art researchers to focus on artist creation on the art recipient—audience, believing that the audience is an essential part of art activities [5].

For the first time in “The Theory of Acceptance of Aesthetics and Acceptance”, Hollab proposed that the integrity of art can only be reflected in the audience participation and the aesthetic dialogue of the works of art [6]. Roy Ascott, in his book, *The Future is the Now: Art, Technology, and Consciousness*, believes that in interactive art, “... , the audience is responsible for the extension of the meaning of art. In the symbolic world he faced, he became a decision-maker with a very important role and significance in the whole activities of artistic aesthetics [7]”. Sartre also stressed: “Only for the audience, there is art; only through the audience, there is art [8]”. The audio-visual interactive art is the same as the video interactive installation art. The experience and dynamic characteristics in the audio-visual interactive art [1] emphasize audience participation more than other media art works. Therefore, it is essential and necessary to study the audience [9]. Therefore, this paper explores the feelings of the audience participating in the audio-visual interactive art from the perspective of audience experience, tries to provide a new dimension for the creation of the audio-visual interactive art from the perspective of audience cognition, and provides corresponding audience data for the exhibition planners of this type of art.

3 Exploration and Implementation of Audience Cognitive Process Based on Mental Model

3.1 Study Methods

Audience’s participation, interactive behavior and experience of interactive art of sound and painting are psychological activities. Without appropriate scientific research methods, it will be difficult to understand the connection between audience and interactive art of sound and painting and to excavate audience’s existing cognition.

Zaltman’s metaphor extraction technique was proposed by Professor Zaltman of Harvard Business School in 1990 to make tacit knowledge explicit through the combination of words and texts. By means of semi-structured interview and metaphor extraction, good research results can be obtained [7].

3.2 Study Process

Through the related literature reading and finishing found that metaphor extraction method has not directly used in art audiences cognitive domain, but due to its advantages of above mentioned and the nature of the great interactive art, this paper studies the problem is suitable for ZMET metaphor extraction technology to dig the great interactive audience subconscious feelings and expectations of this new art form. In the complete ZMET proposed by Zalmant, this method has 10 steps. In this study, the main objective is to extract the cognitive elements and formation reasons of the audience. In order to avoid the fatigue and duration resistance of the conversation, the process is simplified as follows by sorting out the key points of the study. There are five steps: sampling of respondents, in-depth interview, item construct extraction, compilation of common construct and consensus map construction.

3.3 Study Results—Cognitive Map Under Construct Extraction

At the end of the depth interview, and through the interview the data recording, word picture image analysis and integration of the narrative text by Nvivo12 qualitative analysis software for the extraction of high frequency words, composition, cuts, to get each respondents personal construct hierarchy, and narrative text matching output based on the personal construct mental map and based on common construct the consensus of the figure. Personal constructs can be divided into three types according to different levels: initial constructs, connective constructs, and final structure constructs. Personal initial construct can be summarized as the object or object of perception of the interactive art form of sound and painting, Connective constructs refer to the experience result and cognitive association under the perceptual object evoked by the emotion or situation evoked by initial constructs. The final structure idea is the further thinking and cognition of the interactive art form of sound and painting.

According to the principle of Zalmant's construct extraction, the constructs mentioned by 1/3 of the interviewees and the relationships between the constructs mentioned by 1/4 of the interviewees will be included in the final consensus graph. There were 8 respondents in this study, and 153 constructs were finally obtained through classification and induction. Finally, 16 original constructs, 26 associated constructs and 14 final constructs were included in the consensus map.

Finally, in order to verify the reliability and validity of experimental studies, the study calculated the coverage rate of eight respondents and found that the average coverage rate of eight respondents was 68.95%, basically meeting the requirements of the coverage rate of constructs. After testing the credibility of the experiment, the climbing method [10] was used to disintegrate and analyze the cognition of 8 interviewees about the art symbols of the interactive art of sound and painting, and draw a consensus map based on their common cognitive understanding of the research subject according to Zaltman's principle. The consensus map is simplified through the chain method of target means, as shown in Fig. 1.

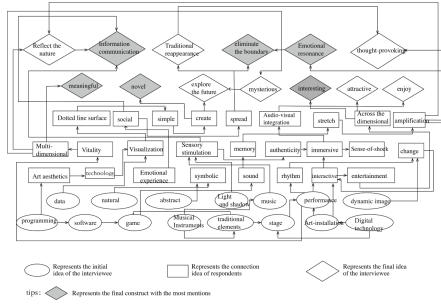


Fig. 1. Construct consensus map of audience cognition in the audio-visual interactive art

After classifying the data, the consensus map of the audience for the cognitive process of audio and painting interactive art is obtained, After the consensus map and the respondents were finally confirmed again, According to the principle of 1/3 and 1/4 of metaphor extraction technology [11] and the frequency mentioned, the final construct of the audience’s cognitive process is selected. Audiences’ existing cognition of the interaction of sound and painting mainly revolves around “information communication”, “novel”, “emotional resonance”, “interesting”, “boundary elimination” and “meaningful”, which are derived from the five related constructs of “sensory stimulation”, “emotional experience”, “memory association”, “interactive experience” and “technology”. Due to their initial construct itself is a more concrete things referred to, and connect the construct is usually cited on microscopic mood changes and their own feelings on memory, in the whole cognitive process, “connective constructs” are the most uncertain, will become the audience in the process of cognitive factors that affect the degree of willingness to participate in great interaction.

4 Analysis of Influencing Factors of Audience Cognition

According to the selection principle of metaphor extraction in the consensus map, the factors influencing the audience participation experience of audio-visual interactive art are finally selected: sensory stimulation, memory association, emotional experience, interactive experience and technology. In order to clarify the influence of these factors, the evaluation system of weighted analysis method is adopted here, and the importance comparison score of each indicator is weighted. Moreover, this experiment is a small sample with a fixed number of experiment participants. Questionnaire at the same time set up five points Likert scale as a benchmark for design, respectively installed on both ends of the poles as “Very much in line with my ideas” and “Not in line with my ideas”, corresponding to the number of “1, 2, 3, 4, 5” is used to numerically quantify, and with “S1, S2, S3” and so on corresponding to each other, the higher the score shows the audience for this level of care, the more obvious. Data sources mainly focus on 8 interviewees who participated in metaphorical extraction technology interview. The collected data are analyzed in SPSS for the proportion of each factor at each level of 5. In the process of data processing, innovation expectation is taken as the main factor for quantitative processing and replaced by A. The selected constructs as sub-factors are

replaced by A1, A2 and A3 (and so on), as shown in Table 2. Finally, the importance score of principal factor A is $S = S1 * 1 + S2 * 2 + S3 * 3 + S4 * 4 + S5 * 5$. Finally, the quantized value are compared and analyzed (Table 1).

Table 1. Influencing factors of innovation expectation of audience participation

Level of factor	Sub-index
An innovation expectations	A1 Sensory stimulates A2 memory with an associative (memory) A3 emotional experience A4 Interactive experience (interactive) A5 technology development (technology)

Table 2. Weight analysis of influencing factors of audience participation innovation expectation

	S 1	S 2	S 3	S 4	S 5	Average value	Standard deviation
A 1	0/8	0/8	1/8	2/8	5/8	4.5	1.17
A 2	0/8	1/8	2/8	3/8	2/8	3.75	0.57
A 3	0/8	0/8	0/8	3/8	5/8	4.6	1.24
A 4	0/8	0/8	2/8	2/8	4/8	4.25	0.92
A 5	0/8	0/8	2/8	4/8	2/8	4	0.76

After sorting out the questionnaire data of 8 interviewees, the weighted average was calculated, and the standard deviation of each factor was calculated by using mathematical tools to easily judge the stability of data. Through data sorting Table 2, in the five factors S value in the calculation of the influence degree of the highest is A3 (emotional experience) is looking forward to innovation under the perspective of the main influence factors, and the rest of the four component factors from big to small, respectively according to degree of A1 (sensory stimulation), A4 (interactive experience), A5 (technology), A2 (memory).

Through experiments and data, it is found that emotional experience becomes the main factor of audience experience in the process of audience participation in the experience of audio-visual interactive art, followed by sensory stimulation, interactive experience, technology and memory association. The emotional experience proposed here refers to the emotions and feelings acquired by the audience during artistic activities with a certain work. Combined with Donald’s research on emotional experience, general emotional experience can be divided into three types: instinctive layer, behavioral layer and reflective layer.

These three situations are combined with audio-visual interactive art works for creative analysis, we can find the instinct layer as the foundation layer. In the audio-visual interactive art, the closest thing is the overall visual design and overall impression of the work; And The behavior layer is based on the instinct layer, and the artist delivers the

experience to the audience through the aesthetic expression and interactive logic of the artwork, to analysis behavior layer to get the audience to participate in the process of some feedback to find the aesthetic needs of audience and aesthetic expectation; emotional experience at the reflective level is the highest level, which usually occurs in the process of understanding and participating in the work after the connection between the audience and the work. The audience will generally extract useful information and internalize it according to their own experience. At this time, if the artist consciously carries out some design. The stimulation and guidance of the story attempt on the audience's long-term memory will strengthen the audience's memory of the work.

5 Conclusion

The combination of multi-sensory stimuli in the works also shows the change and improvement of the aesthetic needs of the audience, and the audience also gets an artistic experience different from that of the past. Meanwhile, the audience also plays an important role in the art. The research focuses on the audience and tries to carry out a new dimension of research, providing a new perspective for the research of the audio-visual interactive art. It is found that the audience, as the art receiver in the interactive art of sound and painting, will be one of the potential influencing factors for the artist to conceive the interactive logic. When the audience actively participates in the audio-visual interactive art, they will generally have interaction and connection with the work. In the whole process of audience acceptance, the "emotional experience" in the relevant construct has the highest influence on whether the audience participates in the work. Among them, the emotional experience in the audio and painting interactive works can affect the audience's overall experience and memory of the work from the instinctive level, the behavioral level and the reflective level respectively.

Finally, it should be noted that in the process of extracting audience cognition, this study tries to use metaphor extraction technology to improve the validity of the interview of the original pure qualitative research, and obtains a good conclusion in the actual operation. Among them, the limitation and insufficiency is that the average educational background of the interviewees is relatively high and relatively single. However, the interviewees' qualifications originally set by metaphor extraction method are those who have a deep understanding of the research topic and can describe their own ideas. In previous studies, monotonous demographic structure of interviewees also appeared. In the following studies, conclusions of other types of studies can be combined to verify each other, thus effectively explaining people's cognition of the interactive art of sound and painting.

Compliance with Ethical Standards. The study was approved by the Logistics Department for Civilian Ethics Committee of East China University of Science and Technology.

All subjects who participated in the experiment were provided with and signed an informed consent form.

All relevant ethical safeguards have been met with regard to subject protection.

References

1. Zheng, H.: Research on contemporary audiovisual art creation from the perspective of mental model. Master's thesis, East China University of Science and Technology (2021)
2. Wang, Z.: Creating Chinese cultural memory with science and technology art. *Design* (12), 76–81 (2020)
3. Hu, Z., Liu, J.: What is media art. *Mod. Commun.* (1), 72–76 (2014)
4. Collingwood: *Principles of Art*. China Social Sciences Press, Beijing (1985)
5. Chu, C.: Uncontrollable group subjectivity – analysis of new media art audience. *Popular Lit. Art* (21), 202–203 (2012)
6. Holab, R.C.: *Reception Aesthetics and Reception Theory*, p. 437. People's Publishing House, Liaoning (1987)
7. Iser, W.G.: *The Act of Reading: A Theory of Aesthetic Response*. The Johns Hopkins University Press, Baltimore (1980)
8. Sartre, J.P.: *Collected Works of Sartre*. People's Literature Publishing House, Beijing (2000)
9. Bahkin, M.M.: *The Formal Method in Literature and Art*. China Federation of Literary and art Circles Publishing Corporation, Beijing (1992)
10. An, X., Cao, Y., Jiao, X., Ming, D.: *J. Electron. Measur. Instrum.* **31**(07), 983–993 (2017)
11. Zaltman, G., Coulter, R.H.: Seeing the voice of customer: metaphorbased advertising research. *J. Advert. Res.* **35**(4), 35–51 (1995)



Comparative Study on the Reachability Distance Measurement Method: Difference Between the Real Environment and Mixed Reality Simulation

Wei Xiong¹, Zhi Liang¹, and Xiaoqing Yu²(✉)

¹ School of Design, South China University of Technology, Panyu Street, Guangzhou 510640, China

² School of Mechanical and Aerospace Engineering, Nanyang Technological University, Nanyang Avenue, Singapore 639798, Singapore
xiaoqing003@e.ntu.edu.sg

Abstract. The study aimed to analyze the feasibility of Mixed-Reality (MR) in measuring reachability distance and to compare it with the real environment method. The effect of participants' gender was also taken into consideration. Thirty-six subjects were recruited in this study. Subjects were asked to provide the reachability distance they perceived when they faced the confederate in both real environment and MR environment. Two-way ANOVA was used to clarify the relationship between the independent variables (participants' gender and measurement method) and the dependent variable (reachability distance). The intraclass correlation coefficient was used to indicate the reliability of these two measurement methods. The experiment results showed that the distance measured in the MR environment was consistent with that collected in the real environment, and the MR simulation method showed higher reliability. For the gender effect, the reachability distance of male subjects was larger than that of female subjects. In addition, there was no significant interaction effect between gender and measurement method. The findings of this study validated the reliability of the MR simulation method when collecting reachability distance and proposed that MR technology was a promising tool in conducting psychological experiments and studying human behaviors.

Keywords: Mixed reality · Reachability distance · HoloLens2 · Comparative evaluation

1 Introduction

In the neuro-cognitive field, the space around people is called peripersonal space (PPS), in which individuals can reach out and interact with other people and objects around themselves [1–3]. As the range is seen as the first barrier between people and the outside world, individuals feel safe from being violated by others outside of that space

[4]. Besides, PPS is of great importance for the individual in predicting and detecting interactions [5].

The “reachability distance measurement” is a typical method to measure the size of peripersonal space [3, 6]. Subjects are required to estimate the reachability distance to the confederate when they interact with the confederate in a real environment and the distance was measured by the experimenter [6]. Previous studies indicated that the reachability distance people perceived can be modulated by many factors of confederate such as the facial expression, eye gaze, among others. It is hard to control these variables at a constant level by the real environment measurement method, and the expression has a great influence on the experimental results [7–9].

Virtual reality technology has been widely used in psychological experiments, which can easily simulate different social interaction scenes and virtual characters to save space and labor costs [10]. Although the results of Bailenson et al. [11] have demonstrated the feasibility of virtual reality technology in studying the interpersonal distance. The previous experiment showed that there are still differences between the virtual reality simulation and real environments in collecting the reachability distance [10]. Moreover, the study of Lee et al. [12] pointed out that both the reachability distance and comfort distance measured by virtual reality simulation was larger than that measured by the real environment method.

At the same time, mixed reality (MR) technology has become a noteworthy evaluation method. Previous studies applied MR and VR technology in the field of surgical simulation and medical training, and the results proved the superiority of the technique in authenticity and immersion through comparative experiments [13, 14]. MR technology can well mix the holographic model with the real environment, which helps the experimenter control unrelated variables such as confederation’s facial expression and ambient light during the experimental procedure. Yu and Lee [12, 15] analyzed the influence of virtual reality on human comfort distance and reachability distance with the help of VR technology. To the best of our knowledge, however, there is little research on the difference between MR environment and real environment in measuring reachability distance. Therefore, this study aims to evaluate the difference between these two measurement environments and compare the reliability of the two methods.

2 Method

2.1 Subjects

This study recruited 36 university students (18 male) aged between 19 and 27. The subjects had normal vision. The average height and the average arm length of male subjects were 177.11 cm and 73.95 cm, respectively; the average height and the average arm length of female subjects were 164.11 cm and 68.38 cm, respectively. All the subjects didn’t know the purpose of the experiment before the experiment and each of them made an informed registration.

2.2 Experimental Setting

The experiment was conducted in an empty room (5.8 m * 8.0 m). The facilities and lighting inside the room were always consistent. There was a 4 m yellow guideline on the ground to guide the subjects to walk along. The experiment recruited a 178 cm tall confederate who had a general appearance of Chinese and always maintains a neutral expression.

The experimental scene was developed by Unity 3D (Unity, Unity, California, United States) and was released to a pair of MR glasses (HoloLens2, Microsoft, Redmond, United States). Subjects wearing hololens2 could see a holographic model of confederate standing in a fixed position. Subjects were allowed to walk around in the room freely. The glasses have a 2K resolution screen and 60 Hz refresh rate, with a FOV of 43° horizontally and 29° longitudinally [16]. Since the interaction of the device can be conducted entirely by gesture and voice, the subjects didn't need to hold any other accessories.

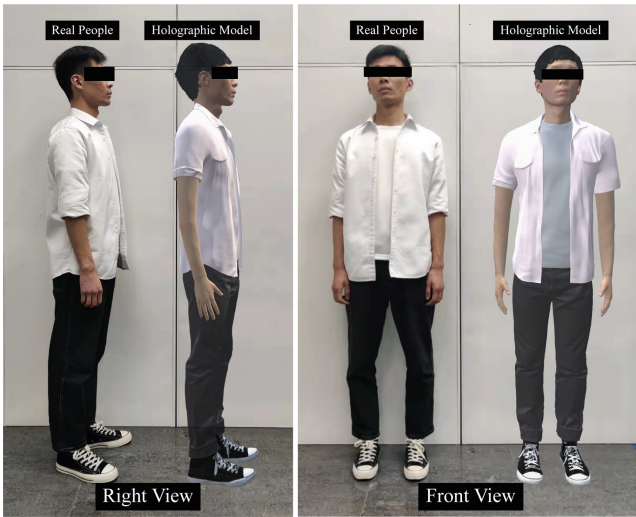


Fig. 1. The side view and front view of the holographic model and real person in this study

To control the confederate unchanged and enhance the immersion of subjects, as shown in Fig. 1, the holographic model of confederate was scanned by a 3D scanner (Reeyee Pro 2x, Reeyee, Nanjing, China) and then reconstructed in a three-dimensional modeling software (Maya, Autodesk, California, United States) to ensure that the holographic model is close to reality. The standing position, clothing, and hairstyle of the confederate in the real environment and the virtual environment were always the same.

2.3 Procedure

The experiment was divided into two stages: real environment and MR environment. Before the experiment, the subject was required to fill out the informed consent form and complete the basic information survey. The experimenter introduced the experimental process orally to each participant. A marked point was attached to the toe cap of the subjects to increase the measurement precision.

For the real environment measurement method, at the beginning of the experiment, the confederate should stand in the middle of the guideline naturally, align his feet with the ground marker, and keep his feet 15 cm apart. The subjects were asked to approach the confederate from a distance of 3 m at a speed of 0.5 m per second until they felt they could touch the confederate with their hands. After the subjects stopped and identified the position, the distance from the ground mark to the tip of the subject's shoe was measured using a laser rangefinder. During each trial, subjects were asked to see the chin of the confederate to reduce the effect of eye gazing [17]. Before the formal measurement, the subjects need to complete two pre-tests to become familiar with the experimental process.

As for the MR simulation measurement method, the experimenter helped the subjects wear the MR glasses comfortably. After confirming that the hologram was in the right position, the subjects were allowed to walk around the room for about five minutes to familiarize themselves with the environment. The measurement method, experimental details, and the movement of the subjects in the experiment are consistent with those in the real environment.

Each trial was repeated twice, a 5-min break was provided to each subject between two stages to avoid fatigue. Before each stage of the experiment, the laser rangefinder was calibrated to avoid measurement errors. The order of the two stages was randomly assigned and counterbalanced. Each trial took about 30 s, and each subject took about 20 min in total.

2.4 Statistical Analysis

SPSS 25.0 was used to analyze the data with a significance level of 0.05. According to S-W Test, the experimental data presented normal distribution. and the data passed the Levene Test. Descriptive statistics show the preliminary relationship between different dependent variables clearly. Two-way ANOVA was used to further analyze the effects of gender and experimental method on the reachability distance. Besides, the reliability and repeatability of MR and real measurement method were evaluated by intraclass correlation coefficient (ICC) analysis.

3 Results

The reachability distance of male and female subjects measured by the two methods was shown in Fig. 2, results showed that the reachability distance of female subjects ($M = 63.07$ cm, $SD = 8.45$ cm) was smaller than that of male subjects ($M = 70.53$ cm, $SD = 9.11$ cm). For both males and females, the data from MR and the real environment were very close.

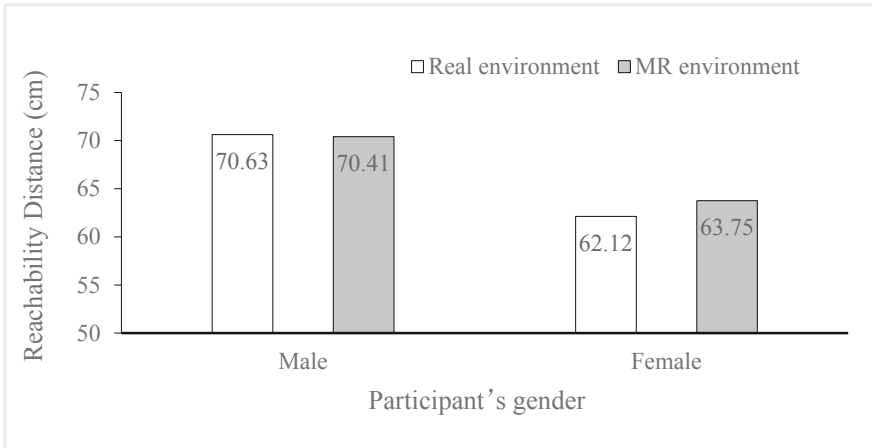


Fig. 2. Reachability distance of male and female participants in two methods

In further two-way ANOVA analysis as shown in Table 1, the effect of participants' gender on the reachability distance was significant ($F = 15.643, p < 0.001, \eta^2 = 0.201$). There was no significant difference between the real and MR method in measuring the reachability distance ($F = 0.134, p = 0.715$). In addition, there was no significant interaction between gender and measurement methods.

Table 1. Two-way ANOVA results on reachability distance (cm)

Terms	F	df	p-value	η^2
Participant's gender	15.643	1	0.000	0.201
Method	0.134	1	0.715	0.002
Participant's gender*method	0.232	1	0.632	0.004

Table 2 showed the ICCs of two different methods under twice replicate measurements. The data indicated that both methods had high reliability and repeatability, the repeatability of MR simulation measurement ($ICC = 0.96$) was slightly higher than that of the real method ($ICC = 0.95$).

Table 2. Intraclass correlation coefficient (ICCs) results of two measurement methods

Method	ICC
Real environment	0.95
Mixed reality simulation	0.96

4 Discussion

The data analysis showed that the reachability distance of female subjects was smaller than that of male subjects, which was consistent with findings of Iachini et al. [17, 18]. The main reason for the difference was that the arm length of male subjects ($M = 73.95$ cm, $SD = 2.51$ cm) was larger than that of female subjects ($M = 68.38$ cm, $SD = 4.09$ cm).

From the analysis, we could know that as two methods, MR and real measurement showed same results in measuring the reachability distance, which means there was no difference in distance perception between the real person and the holographic model for the subjects. This finding indicated that MR technology is an effective tool for measuring reachability distance.

In a real-world environment, it's hard to control the posture of the confederate and remain the environment always the same. Previous research showed that experiment in a virtual reality environment needs a lot of work to build virtual scenes, and such visual effects were still difficult to be close to the real environment [10]. MR techniques can address both issues simultaneously, saving effort and better controlling for irrelevant variables.

The ICC levels of both measurement and real-world measurement were very high (both above 0.95), which showed that the overall design of the experiment and the two measurement methods both had sufficient reliability and repeatability. The ICC data of the MR measurement method was slightly higher than that of the real measurement method, possibly because the expression, posture, and eyes of the holographic model were more stable than those of the real person. Moreover, based on the observations in the MR measurement methods section, subjects would intentionally bypass or attempt to touch the holographic model in the scene, which also demonstrated that the experimental environment could give subjects a sufficient sense of authenticity and immersion. This finding was consistent with the post-experimental interview results.

Overall, there was no difference between the reachability distance measured by MR techniques and the real environment. Both MR and real environmental measurement methods collected highly consistent results for both male and female subjects. Besides, the MR simulation measurement method had slightly higher reliability than real environment measurement.

5 Conclusion

The homogeneity of the results in collecting reachability distance between two methods showed that the different methods don't affect the reachability distance, the MR technique can be used as a good alternative to the real measurement method. In the field of psychology, MR simulation can give subjects an environment with sufficient feelings of authenticity. The current experiment mainly focuses on the reachability distance in front of the confederate, and it is worth investigating whether the reachability distance in the lateral and back direction remains the same under different environment methods. In addition, the subjects for this experiment were all recruited from universities with high acceptance of the new technology, which needs to be extended to a wider age range

for future studies. This study verified the feasibility of MR technology in psychological experiments and provided a theoretical basis for other researchers to choose appropriate experimental methods for their experiments. With the advancement of mixed reality technology, experiments assisted by MR will show higher reliability, and MR will be applied in a wider scenario.

Compliance with Ethical Standards. The study was approved by the Logistics Department for Civilian Ethics Committee of South China University of Technology.

All subjects who participated in the experiment were provided with and signed an informed consent form.

All relevant ethical safeguards have been met with regard to subject protection.

References

1. Colby, C.L.: Action-oriented spatial reference frames in cortex. *Neuron* **20**(1), 15–24 (1998)
2. Grefkes, C., Fink, G.R.: The functional organization of the intraparietal sulcus in humans and monkeys. *J. Anat.* **207**(1), 3–17 (2005)
3. Ruggiero, G., Ruotolo, F., Orti, R., Rauso, B., Iachini, T.: Egocentric metric representations in peripersonal space: a bridge between motor resources and spatial memory. *Br. J. Psychol.* **112**(2), 433–454 (2021)
4. de Vignemont, F., Iannetti, G.D.: How many peripersonal spaces? *Neuropsychologia* **70**, 327–334 (2015)
5. Serino, A., Canzoneri, E., Avenanti, A.: Fronto-parietal areas necessary for a multisensory representation of peripersonal space in humans: an rTMS study. *J. Cogn. Neurosci.* **23**(10), 2956–2967 (2011)
6. Ferri, F., Tajadura-Jiménez, A., Väljamäe, A., Vastano, R., Costantini, M.: Emotion-inducing approaching sounds shape the boundaries of multisensory peripersonal space. *Neuropsychologia* **70**, 468–475 (2015)
7. Uzzell, D., Horne, N.: The influence of biological sex, sexuality and gender role on interpersonal distance. *Br. J. Soc. Psychol.* **45**(3), 579–597 (2006)
8. Yu, X., Xiong, W., Lee, Y.-C.: An investigation into interpersonal and peripersonal spaces of Chinese people for different directions and genders. *Front. Psychol.* **11**, 981 (2020)
9. Adams, L., Zuckerman, D.: The effect of lighting conditions on personal space requirements. *J. Gen. Psychol.* **118**(4), 335–340 (1991)
10. Xiong, W., Yu, X., Lee, Y.-C.: The difference in measuring reachability distance between using virtual reality technology and manual measurement. In: 2020 IEEE 7th International Conference on Industrial Engineering and Applications (ICIEA), pp. 390–393. IEEE (2020)
11. Bailenson, J.N., Blascovich, J., Beall, A.C., Loomis, J.M.: Interpersonal distance in immersive virtual environments. *Pers. Soc. Psychol. Bull.* **29**(7), 819–833 (2003)
12. Lee, Y.-C., Yu, X., Xiong, W.: A comparative evaluation of the four measurement methods for comfort and reachability distance perceptions. *Behav. Res. Methods* 1–12 (2021)
13. Cardan, R., Covington, E.L., Popple, R.: A holographic augmented reality guidance system for patient alignment: a feasibility study. *Cureus* **13**(4), e14695 (2021)
14. Mao, R.Q., Lan, L., Kay, J., Lohre, R., Ayeni, O.R., Goel, D.P.: Immersive virtual reality for surgical training: a systematic review. *J. Surg. Res.* **268**, 40–58 (2021)
15. Yu, X., Lee, Y.-C.: Investigating the comfort distance of Chinese in eight directions. In: Long, S., Dhillon, B.S. (eds.) *MMESE 2019. LNEE*, vol. 576, pp. 461–468. Springer, Singapore (2020). https://doi.org/10.1007/978-981-13-8779-1_53

16. HoloLens 2—Overview, Features, and Specs—Microsoft HoloLens [Internet]. <https://www.microsoft.com/en-us/hololens/hardware>. Accessed 20 Feb 2022
17. Iachini, T., Coello, Y., Frassinetti, F., Ruggiero, G.: Body space in social interactions: a comparison of reaching and comfort distance in immersive virtual reality. *PLoS ONE* **9**(11), e111511 (2014)
18. Iachini, T., Coello, Y., Frassinetti, F., Senese, V.P., Galante, F., Ruggiero, G.: Peripersonal and interpersonal space in virtual and real environments: effects of gender and age. *J. Environ. Psychol.* **45**, 154–164 (2016)



The Effect of Face Mask and Approach Pattern on Interpersonal Distance in COVID-19 Pandemic Using VR Technology

Wei Xiong¹, Congyi Wang¹, and Xiaoqing Yu²(✉)

¹ School of Design, South China University of Technology, Guangzhou 510640, China

² School of Mechanical and Aerospace Engineering, Nanyang Technological University, Singapore 639798, Singapore

xiaoqing003@e.ntu.edu.sg

Abstract. In the COVID-19 pandemic, control measures including wearing masks, ensuring hand hygiene, and maintaining a physical distance of at least 1 m were recommended to prevent the spread of virus. The purpose of this study was to investigate the influence of face mask, approach pattern and participants' gender on interpersonal distance in the pandemic environment. Virtual reality (VR) technology was applied to build the experimental environment. This study recruited 31 participants including 17 males and 14 females, who were asked to interact with virtual confederates with and without a face mask. The interpersonal distance was recorded when participants actively walk towards the virtual confederate or approached passively by the confederate. Three-way ANOVA results showed that face mask and approach pattern had significant effects on interpersonal distance. The distance when facing the confederate with a face mask was significantly closer than without a face mask. Moreover, participants preferred a significantly larger distance in the passive pattern than in the active pattern. The participants' gender showed no significant effect on interpersonal distance and no interaction effects were found. The findings in this study helped to further investigate the nature of interpersonal distance and contributed to a better understanding of the human behaviors in the pandemic environment.

Keywords: COVID-19 pandemic · Interpersonal distance · Virtual reality · Face masks · Approach pattern

1 Introduction

The COVID-19 pandemic is still spreading around the whole world and poses a threat to global health. In order to reduce the risk of virus transmission [1], World Health Organization (WHO) recommended that people have to maintain a certain physical distance and wear face masks in public places, which changed people's lifestyle and social behavior. Interpersonal distance was defined by social psychology as the safety buffer maintained by individuals between themselves and others [2–4]. Interpersonal distance will expand when people feel uncomfortable or dangerous and decrease when

people feel safe and comfortable. Ruggiero et al. [5] and Cartaud et al. [6] found that interpersonal distance increased when people saw an angry facial expression than a happy one. Another study found that interpersonal distance increased when people heard an aggressive conversation than a neutral one [7]. After the outbreak of the pandemic, whether the interpersonal distance changed in the background of the epidemic needs to be studied, and the impact of wearing masks and active and passive needs to be further studied.

There were four common measurement methods to collect interpersonal distance, including real measurement, virtual reality simulation, video method, and paper and pen test [8, 9]. Yu et al. [10] measured the interpersonal distance in eight directions in the real environment. However, the real environment measurement may increase the face-to-face interaction between people and increase the risk of infection in the epidemic. The questionnaire method was used in the study of Wang et al. [11], which showed that interpersonal distance would be reduced when participants faced confederate who wore face masks, but this method could not enable participants to experience the feelings of true interaction. However, VR technology allows participants to immerse in the virtual environment and interact with the virtual confederate, which can bring the true feelings in the social activities. One of the main advantages of VR simulation is its immersion and interactivity. Besides, VR simulation can fully control the experimental variables. For example, the characteristics and behaviors of virtual confederates such as walking speed, eye gaze, facial expressions, etc. [12], can be controlled by researchers. In addition, communication between participants and researchers can be decreased to reduce the risk of infection in the epidemic.

Therefore, the purpose of this study was to further explore the interpersonal distance in the epidemic and evaluate the effects of wearing masks, approach pattern and gender of participants on the interpersonal distance in the background of the epidemic. The findings of this paper contribute to further study the nature of interpersonal distance and help to better understand the human behaviors in the epidemic.

2 Method

2.1 Participants

Thirty-one college students (14 females) ageing 19 to 27 years old ($M = 21.6$, $SD = 2.17$) were recruited. Each participant had a normal or corrected vision, and no cognitive impairment or any other disease was found according to their self-reporting. Besides, all participants were not familiar with the virtual confederate and were not aware of the purpose of the experiment.

2.2 Experimental Environment

The experiment was carried out in a $6 * 8 * 4 \text{ m}^3$ laboratory with no obstacles. The experimental VR device was Oculus Quest2 which equipped with an LCD display. The VR headset has a single-eye resolution of $1832 * 1920$ and supports the refresh rate of 90 Hz, which could realize controller-free gesture tracking. Unity software was used

to simulate the virtual environment scenes and build the confederate model. Wearing VR glasses, participants will see an open square with three buildings on the left and a playground on the right. There was a yellow line on the ground to guide participants towards the front. A virtual confederate with a height of 175 cm who was standing 4 m in front of the participants. The virtual confederate wore a white shirt and black jeans. During the experiment, there were two conditions: one confederate wearing a face mask and the other did not wear a face mask. The virtual environment was shown in Fig. 1.

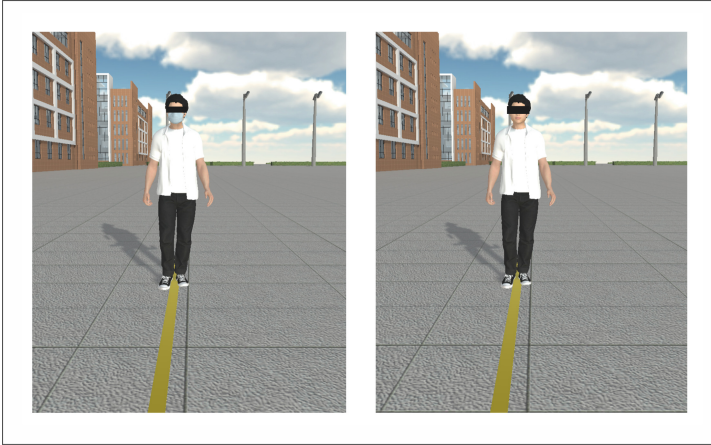


Fig. 1. Virtual reality experimental environment and virtual confederate with or without a face mask.

2.3 Procedure

Before the formal experiment, experimenter helped participants wear the VR device and the physical environment around them was isolated. Accordingly, participants can familiarize themselves with the virtual environment under the guidance of the experimenter including watching and walking freely in the virtual lab for about 2 min. Two trails were provided to participants to be familiar with the experimental procedure before the formal experiment. In active pattern, participants were required to approach the virtual character actively. When participants felt uncomfortable due to the proximity they stopped and pressed the button on handle to affirm the position, then the distance between the middle of virtual confederate and the participant was calculated and saved automatically. In the passive pattern in which the virtual character walked towards the participant at the speed of 0.5 m/s, when the participants felt uncomfortable, the virtual character can be stopped by pressing the handle similarly. Once the handle was pressed during the experiment, the distance between the participant and the virtual character will be automatically recorded.

The experiment was conducted in two approach patterns and two face mask states. The experiment sequence was random and balanced, and a 2-min break between every two experiments was offered for participants to have a rest. Each trail was repeated

twice, and a total of 8 measurements were required for each participant. During the formal experiment, as shown in Fig. 2, participants conducted the experiment according to oral instructions of experimenter.



Fig. 2. The experiment procedure: the participant is walking towards the confederate in VR environment

2.4 Statistical Analysis

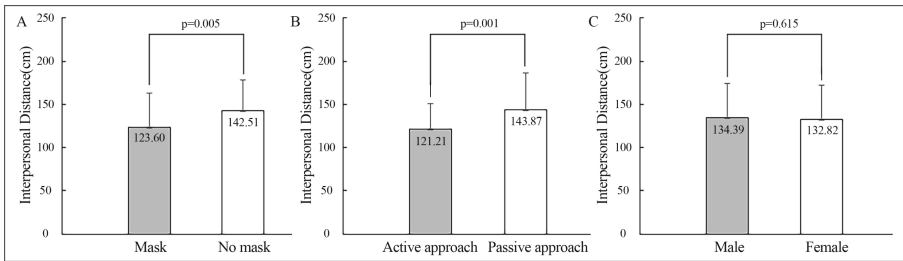
Each experiment trail was repeated twice, and the average was calculated and used for the analysis of variance (ANOVA). In the study, data were analyzed using SPSS 25.0, and a three-way ANOVA was performed to clarify the relationship between independent variables (mask wearing, approach pattern and participants' gender) and dependent variables (interpersonal distance).

3 Results

As shown in Table 1, results of ANOVA showed that face mask had a significant effect on interpersonal distance ($F = 7.924$, $p = 0.006$, $\eta_p^2 = 0.062$). In Fig. 3, the interpersonal distance of participants when facing the virtual confederate with face mask ($M = 123.60$ cm, $SD = 39.03$ cm) was significantly smaller than that of facing the virtual confederate without face mask ($M = 142.51$ cm, $SD = 36.12$ cm). The approach pattern had a significant influence on interpersonal distance ($F = 10.947$, $p = 0.001$, $\eta_p^2 = 0.084$). When participants approached the virtual confederate actively ($M = 121.21$ cm, $SD = 29.78$ cm), the interpersonal distance was significantly smaller than that when participants were approached by the virtual confederate passively ($M = 143.87$ cm, $SD = 42.94$ cm). In contrast, gender had no significant effect on interpersonal distance ($F = 0.255$, $p = 0.615$, $\eta_p^2 = 0.002$), and no significant interaction effects were found.

Table 1. Three-way ANOVA results of face mask, approach pattern and gender

Terms	F	df	p-value	η_p^2
Face mask	8.273	1	0.005	0.068
Approach pattern	10.928	1	0.001	0.088
Gender	0.255	1	0.615	0.002
Face mask* Approach pattern	0.000	1	1.000	0.000
Face mask* Gender	1.728	1	0.191	0.015
Approach pattern* Gender	0.004	1	0.950	0.000
Face mask* Approach pattern* Gender	0.199	1	0.657	0.002

**Fig. 3.** The interpersonal distance under each main effect including face mask (A), approach pattern (B) and gender (C).

4 Discussion

The results showed that face mask and approach pattern had a significant effect on the interpersonal distance. Participants showed a larger interpersonal distance when they faced a confederate without a face mask than with a face mask, which was consistent with the research results of Wang et al. [11] and Lee et al. [13]. They compared the interpersonal distance of participants facing confederate with and without masks by using online survey. The reason of this phenomenon might be that people felt more dangerous and uncomfortable when they faced a confederate not wearing a face mask. Lisi et al. [14] found a reduction in the interpersonal distance when participants faced mask wearers who tested negative for COVID-19. Importantly, even when COVID-19 test results were unknown or positive, the interpersonal distance from a member wearing a face mask remained shorter. It could be seen that in the context of the epidemic, to some extent, wearing face mask enhanced a sense of security and shortens the social distance between people.

Participants preferred a greater distance when they were approached passively than the case when they actively approached the confederate. This finding was consistent with that of Iachini et al. [15, 16]. When participants were unable to move, they kept a greater

distance, which reflected that controlling the virtual confederate in the passive approach could increase the sense of security. These results further supported the finding that the conditions of motion proximity play a key role in spatial regulation [5]. In the passive approach, a sense of invasion and uncomfortable feeling was generated, leading to a larger interpersonal distance. Different from the results of Lee et al. [13] who adopted the online survey method, which had no real sense of experience. Participants had no chance to feel the sense of pressure when the virtual confederates approached. While using VR technology measurement, participants were immersed in the real experience of passive pressure. Similarly, the results of Lee et al. [12] showed that the comfort distance and reachability distance measured in the VR environment were basically consistent with those measured in the real environment, which indicated that VR technology can simulate the real environment.

The gender of the participants had no significant effect on the interpersonal distance of the virtual confederates. Yu et al. [10] explored interpersonal distance in eight directions, and the gender of participants showed no significant difference, which was in accordance with the results of this study. Therefore, gender differences in the perception of interpersonal distance were not significant, both male and female participants showed a similar interpersonal distance to virtual confederate.

5 Conclusion

To sum up, the effects of face mask, approach pattern and participants' gender on interpersonal distance in the COVID 19 pandemic were explored in this study. VR technology was used to simulate the experimental scenes and build the virtual confederate. Participants preferred larger interpersonal distance when they faced a virtual confederate with no face mask than with a face mask due to the feelings of insecurity and invasion. People were not allowed to move their body in the passive pattern, leading to a larger interpersonal distance than in the active case. However, participants' gender showed no significant effects, and no significant interaction term was found. The current study further investigates the interpersonal distance and individuals' social behaviors in the pandemic context, which contribute to the deeper understanding of the motor nature of this psychological cognitive distance. Based on the constrictions of experiment conditions, there are still some shortcomings in this study. The participants recruited were all college students with a relatively young age. In the future studies, the age group of participants will be expanded, and the impact of other anti-epidemic measures on interpersonal distance can be further discussed.

Compliance with Ethical Standards. The study was approved by the Logistics Department for Civilian Ethics Committee of South China University of Technology.

All subjects who participated in the experiment were provided with and signed an informed consent form.

All relevant ethical safeguards have been met with regard to subject protection.

References

1. Leung, N.H.L., et al.: Respiratory virus shedding in exhaled breath and efficacy of face masks. *Nat Med.* **26**(5), 676–680 (2020)
2. Hall, E.T., Hall, E.T.: *The Hidden Dimension*, vol. 609. Anchor (1966)
3. Sommer, R.: *Personal space. The behavioral basis of design* (1969)
4. Hayduk, L.A.: Personal space: where we now stand. *Psychol. Bull.* **94**(2), 293 (1983)
5. Ruggiero, G., Frassinetti, F., Coello, Y., Rapuano, M., di Cola, A.S., Iachini, T.: The effect of facial expressions on peripersonal and interpersonal spaces. *Psychol. Res.* **81**(6), 1232–1240 (2016). <https://doi.org/10.1007/s00426-016-0806-x>
6. Cartaud, A., Ott, L., Iachini, T., Honoré, J., Coello, Y.: The influence of facial expression at perceptual threshold on electrodermal activity and social comfort distance. *Psychophysiology* **57**(9), e13600 (2020)
7. Vagnoni, E., Lewis, J., Tajadura-Jiménez, A., Cardini, F.: Listening to a conversation with aggressive content expands the interpersonal space. *PLoS ONE* **13**(3), e0192753 (2018)
8. Gessaroli, E., Santelli, E., di Pellegrino, G., Frassinetti, F.: Personal space regulation in childhood autism spectrum disorders. *PLoS ONE* **8**(9), e74959 (2013)
9. Bailenson, J.N., Blascovich, J., Beall, A.C., Loomis, J.M.: Interpersonal distance in immersive virtual environments. *Pers. Soc. Psychol. Bull.* **29**(7), 819–833 (2003)
10. Yu, X., Lee, Y.-C.: Investigating the comfort distance of Chinese in eight directions. In: Long, S., Dhillon, B.S. (eds.) *MMESE 2019. LNEE*, vol. 576, pp. 461–468. Springer, Singapore (2020). https://doi.org/10.1007/978-981-13-8779-1_53
11. Wang, M., Lee, Y.-C.: Investigating the effects of face mask and gender on interpersonal distance judgments. In: Long, S., Dhillon, B.S. (eds.) *MMESE 2021. LNEE*, vol. 800, pp. 40–45. Springer, Singapore (2022). https://doi.org/10.1007/978-981-16-5963-8_4
12. Lee, Y.-C., Yu, X., Xiong, W.: A comparative evaluation of the four measurement methods for comfort and reachability distance perceptions. *Behav. Res. Methods* 1–12 (2021)
13. Lee, Y.-C., Chen, Y.-L.: Influence of wearing surgical mask on interpersonal space perception between mainland Chinese and Taiwanese people. *Front. Psychol.* **12**, 692404 (2021)
14. Lisi, M.P., Scattolin, M., Fusaro, M., Aglioti, S.M.: A Bayesian approach to reveal the key role of mask wearing in modulating interpersonal distance during the COVID-19 outbreak (2020)
15. Iachini, T., Coello, Y., Frassinetti, F., Ruggiero, G.: Body space in social interactions: a comparison of reaching and comfort distance in immersive virtual reality. *PLoS ONE* **9**(11), e111511 (2014)
16. Iachini, T., Coello, Y., Frassinetti, F., Senese, V.P., Galante, F., Ruggiero, G.: Peripersonal and interpersonal space in virtual and real environments: effects of gender and age. *J. Environ. Psychol.* **45**, 154–164 (2016)



Investigation and Research on Occupational Mental Health Status of Grassroots Firefighters

Yanqiu Sun^{1,2}, Zhenfang Chen^{1,2}✉, Ao Zhang³, Jingqi Gao³, Jianwu Chen^{1,2},
Bin Yang^{1,2}, Yin Jiang^{1,2}, and Jia Wang^{1,2}

¹ China Academy of Safety Science and Technology, Beijing 100012, China
czf1c7922@126.com

² NHC Key Laboratory for Engineering Control of Dust Hazard, Beijing 100012, China

³ China University of Geosciences (Beijing), Beijing 100083, China

Abstract. In order to investigate and research the occupational mental health status of grassroots fire rescue personnel. This paper adopted the random sampling method. Descriptive statistics, t-test, chi-square test, non-parametric test and other methods were used to statistically analyze the data from the mental health scale for grassroots fire rescue personnel using SPSS 24.0 software. The results show that age, military age, political affiliation, educational level and marital status have a significant effect on the occupational mental health of grassroots firefighters, but each factor affects in different dimensions, Nationality, gender and the only child or not have no significant effect on firefighters' occupational mental health.

Keywords: Mental health · Depression · Anxiety · SCL-90 · Grassroots firefighters

1 Research Purpose

Firefighters are recognized as one of the most complex and dangerous occupations in the world, they belong to the national comprehensive fire rescue team, including full time fire brigade, voluntary fire brigade and other forms of fire protection organization [1]. With the rapid development of social economy, the mission and responsibilities of firefighters have also changed significantly. Which has changed from the fire fighting and rescue, combat readiness and business training to carry out the fire fighting and rescue, business training, emergency rescue, social rescue and other related works, the tasks are increasing. With the change of responsibilities and the increase of tasks, firefighters are exposing to hazardous substances and harsh environment more and more frequently in the course of performing the task [2, 3]. The particularity of occupation determines that the firefighters must have good psychological quality, and the adaptability to emergency, difficult, dangerous and heavy fire fighting and rescue, emergency rescue, emergency disposal and so on. Firefighters should not only have certain professional fire knowledge, rich practical experience, excellent technical and tactical measures, but also have

good psychological quality. The fire occupation characteristics of high risk and high load determine that the inducements of psychological problems of firefighters increase greatly [4]. Therefore, psychological factors have become another important factor of occupational hazards for firefighters, mainly manifested in emotional tension, irritability and anxiety, mental depression, emotional loss of control, psychological balance, personality paranoid, highly fear and so on. Healthy professional psychology can promote firefighters to form a good and positive attitude, which can improve work efficiency, work efficiency satisfaction and happiness index.

This study evaluated the occupational mental health status of grassroots fire rescue personnel by investigating and researching on the occupational mental health status of grassroots firefighters, which provided basic data for the following up study of occupational mental health of firefighters, and provided reference for relevant departments to carry out targeted occupational mental health work.

2 Research Object and Method

2.1 Survey Object

Nationwide grassroots fire rescue personnel were selected as the study subjects. A random sampling method was used to investigate the occupational mental health status of firefighters. 146 questionnaires were received, of which 143 were valid, with an efficiency rate of 97.95%. All the subjects were informed and agreed to participate in this survey.

2.2 Research Tool

Based on the comparative analysis study results of common occupational mental health scales, the SCL-90 was selected for the development of an occupational mental health scale of grassroots firefighters. The evaluation scale consisted of demographic information and symptom self-assessment scale. The demographic information covers 8 factors including gender, age, military age, ethnicity, political affiliation, education level, marital status, and the only child or not [5–7]. The symptom self-assessment scale consists of 10 dimensions of somatization, obsessive-compulsive symptoms, interpersonal sensitivity, depression, anxiety, hostility, phobic anxiety, paranoia, psychoticism, and eating and sleeping.

2.3 Statistical Analysis

Descriptive statistics, t-test, chi-square test, non-parametric test and other methods were used to statistically analyze the data from the mental health scale for grassroots fire rescue personnel using SPSS 24.0 software.

3 Study Conclusions

3.1 Demographic Factors Frequency Statistical Results

Of the 143 valid questionnaires, 130 (90.9%) were male and 13 (9.1%) were female. The oldest age was 61 years old, 1 person; the youngest was 18 years old, 1 person; the average age was 28 years old, the median was 26 years old, and the plural was 22 years old (12 people, 8.4%). The largest military age is 25 years, 1 person; the smallest is 0 years, 49 people; the average military age is 3.9 years, the median is 2 years, the plural is 0 years, 49 people, accounting for 34.3%. The Han nationality includes 135 people, accounting for 94.4%; minority 8 people, accounting for 5.6%. In terms of political appearance, 45 people are members of the CPC, accounting for 31.5%; 21 people are members of the League, accounting for 14.7%; 73 people are masses, accounting for 51.0%; 4 people are others, accounting for 2.8%. In education level, there were 12 people in junior high school or below, accounting for 8.4%; 45 people in high school, accounting for 31.5%; 60 people in college, accounting for 42.0%; 17 people in bachelor's degree, accounting for 11.9%; 4 people in master's degree, accounting for 2.8%; 5 people in doctoral degree, accounting for 3.5%. In terms of household type, there were 47 urban households, accounting for 32.9%; 96 rural households, accounting for 67.1%. Besides, 58 people were married, accounting for 40.6%; 85 people were unmarried, accounting for 59.4%. Another 39 people were only children, accounting for 27.3%; 104 people were not only children, accounting for 72.7%.

3.2 Impact Analysis Results Based on Ethnicity

The subjects were Levene's chi-square test and independent samples t-test by Han Chinese and ethnic minorities separately. The results of Levene's chi-square test showed that all ten dimensions were chi-square among different ethnic groups ($P > 0.05$), thus the results of t-test were chosen when the variances were equal. The mean and t-test analysis results of the 10 dimensions among different ethnic groups are shown in Table 1, which indicate that there is no significant difference in the mean values of the 10 dimensions between different ethnicity groups ($P > 0.05$), that no significant effect of ethnicity on firefighters' occupational mental health exists.

Table 1. The mean and t-test analysis results of the 10 dimensions among the Han Chinese and ethnic minorities

Dimensions	Han Chinese (N = 135)	Ethnic Minorities (N = 8)	t	P
Somatization	1.29 ± 0.47	1.16 ± 0.23	0.823	0.412
Obsessive-compulsive	1.36 ± 0.50	1.33 ± 0.51	0.192	0.848
Interpersonal sensitivity	1.28 ± 0.50	1.26 ± 0.47	0.092	0.927
Depression	1.26 ± 0.48	1.23 ± 0.42	0.179	0.858
Anxiety	1.20 ± 0.46	1.23 ± 0.56	-0.121	0.904
Hostility	1.22 ± 0.44	1.25 ± 0.46	-0.171	0.864
Photic anxiety	1.11 ± 0.30	1.11 ± 0.20	0.027	0.978
Paranoia	1.22 ± 0.48	1.23 ± 0.58	-0.067	0.947
Psychoticism	1.19 ± 0.42	1.10 ± 0.28	0.629	0.530
Eating and sleeping	1.32 ± 0.52	1.20 ± 0.40	0.668	0.505

3.3 Impact Analysis Results Based on Age

The subjects' age was divided into five age groups of 17–20, 21–25, 26–30, 31–35 years old and 35 years and above. The Levene's chi-square test was conducted first for the 10 dimensions of each age group, and the results are shown in Table 2.

Table 2. The chi-square test of 10 dimensions among different age groups.

Dimensions	Levene's statistics	df_1	df_2	Sig.
Somatization	6.803	4	138	0.000
Obsessive-compulsive	3.565	4	138	0.008
Interpersonal sensitivity	7.956	4	138	0.000
Depression	4.179	4	138	0.003
Anxiety	7.522	4	138	0.000
Hostility	4.126	4	138	0.003
Photic anxiety	5.345	4	138	0.000
Paranoia	11.474	4	138	0.000
Psychoticism	5.469	4	138	0.000
Eating and sleeping	3.308	4	138	0.013

It is evident from the table that the variance of each dimension in all age groups is not chi-square ($P < 0.05$), which means the 10 dimensions have significant differences in different age groups. Using the Kruskal-Wallis method, a nonparametric test was performed and the results are shown in Table 3.

Table 3. The nonparametric test of 10 dimensions

Dimensions	χ^2	<i>df</i>	Asymptotic significance
Somatization	7.227	4	0.124
Obsessive-compulsive	21.950	4	0.000
Interpersonal sensitivity	14.292	4	0.006
Depression	18.852	4	0.001
Anxiety	16.748	4	0.002
Hostility	21.563	4	0.000
Photic anxiety	13.067	4	0.011
Paranoia	19.762	4	0.001
Psychoticism	15.998	4	0.003
Eating and sleeping	13.506	4	0.009

The LDS two-by-two comparison and nonparametric pairwise comparison analysis, combined with the mean values of the 10 dimensions, yielded the mean values and significance levels of each dimension score as shown in Table 4. In general, with increasing age, the scores of all dimensions, except the Somatization, also gradually increased, and the scores of all dimensions for fire rescue personnel over 35 years old were higher than those of the rest of the age group, and it can be concluded that age has a significant effect on the mental health of firefighters.

Table 4. The mean values and significance levels of 10 dimensions among different age groups

Dimensions	17–20 years old (N = 8)	21–25 years old (N = 57)	26–30 years old (N = 40)	31–35 years old (N = 21)	35 and above (N = 17)	Sig.
Somatization	1.08 ± 0.13	1.21 ± 0.37	1.28 ± 0.42	1.34 ± 0.41	1.58 ± 0.79	0.124
Obsessive-compulsive	1.13 ± 0.15	1.24 ± 0.36	1.31 ± 0.49	1.44 ± 0.47	1.88 ± 0.73	0.000
Interpersonal sensitivity	1.06 ± 0.84	1.18 ± 0.35	1.26 ± 0.45	1.27 ± 0.43	1.78 ± 0.84	0.006
Depression	1.04 ± 0.04	1.19 ± 0.38	1.20 ± 0.43	1.30 ± 0.42	1.69 ± 0.78	0.001
Anxiety	1.04 ± 0.05	1.13 ± 0.32	1.16 ± 0.35	1.14 ± 0.48	1.61 ± 0.87	0.002
Hostility	1.08 ± 0.13	1.16 ± 0.41	1.15 ± 0.31	1.25 ± 0.36	1.64 ± 0.74	0.000
Photic anxiety	1.00 ± 0.00	1.06 ± 0.15	1.13 ± 0.38	1.11 ± 0.24	1.29 ± 0.45	0.011
Paranoia	1.02 ± 0.06	1.15 ± 0.40	1.14 ± 0.25	1.23 ± 0.43	1.72 ± 0.93	0.001
Psychoticism	1.03 ± 0.05	1.15 ± 0.40	1.15 ± 0.32	1.15 ± 0.25	1.54 ± 0.66	0.003
Eating and sleeping	1.11 ± 0.17	1.22 ± 0.44	1.26 ± 0.52	1.38 ± 0.47	1.76 ± 0.63	0.009

3.4 Impact Analysis Results Based on the Others Demographic Factors

3.4.1 Impact Analysis Results Based on Gender

The research results show that there is no significant difference in 10 dimensions between different gender groups ($P > 0.05$). It can be concluded that gender has no significant effect on firefighters' mental health.

3.4.2 Impact Analysis Results Based on Military Age

The subjects' military age was divided into six groups of 1 year and below, 2–3, 4–6, 7–9, 10–12 and 12 years and above. The research results show that there were significant differences in the five dimensions of sensitivity, depression, hostility, paranoia, eating and sleeping between different military age groups ($P < 0.05$), firefighters with more than 10 years of military age scored higher in the mean values of five dimensions than other military age groups. It can be concluded that military age has a significant effect on firefighters' mental health.

3.4.3 Impact Analysis Results Based on Political Affiliation

Political affiliation mainly includes CPC members, league members, the masses and the others four categories. The research results show that there were significant differences in the two dimensions of anxiety, paranoia between different political affiliation groups ($P < 0.05$), the others scored higher in the mean values of two dimensions than other political affiliation groups. It can be concluded that political affiliation has a significant effect on firefighters' mental health.

3.4.4 Impact Analysis Results Based on Education Level

The educational level was divided into junior high school and below, senior high school, junior college, undergraduate, master and doctor six groups. The research results show that there were significant differences in the three dimensions of obsessive-compulsive symptoms, phobic anxiety and paranoia between different education level groups ($P < 0.05$), undergraduate scored higher in the mean values of obsessive-compulsive symptoms, paranoia two dimensions than other education level groups, master scored higher in the mean values of obsessive-compulsive symptoms, phobic anxiety two dimensions than other education level groups. It can be concluded that education level has a significant effect on firefighters' mental health.

3.4.5 Impact Analysis Results Based on Marital Status

The subjects were divided into married and non-married groups. The research results show that there were significant differences in the seven dimensions of obsessive-compulsive symptoms, interpersonal sensitivity, depression, hostility, phobic anxiety, paranoia, eating and sleeping between different marital status groups ($P < 0.05$), married scored higher in the mean values of seven dimensions than other marital status groups. It can be concluded that marital status has a significant effect on firefighters' mental health.

3.4.6 Impact Analysis Results Based on the Only Child or Not

The subjects were divided into the only child and non-only child groups. The research results show that there is no significant difference in 10 dimensions between the only child group and non-only child groups ($P > 0.05$). It can be concluded that the only child or not has no significant effect on firefighters' mental health.

4 Conclusions

This paper draws the following conclusions through research and analysis:

- (1) Nationality, gender and the only child or not have no significant effect on firefighters' occupational mental health.
- (2) Age, military age, political affiliation, educational level and marital status have a significant effect on the occupational mental health of grassroots firefighters, but each factor affects in different dimensions.

5 Discussions

The data in this study are all filled in subjectively by the subjects, and the amount of data has certain limitations. Firefighters occupational mental health has distinct occupational characteristics, Therefore, for the factors which have significant impact on the research conclusion, managers and firefighters should improve their own protection awareness, strengthen the learning of occupational mental protection knowledge, actively carry out occupational mental training, introduce mental intervention mechanism, reduce the impact of tasks on firefighters' mental health.

Acknowledgement. This work is supported by the fundamental research funds for China Academy of Safety Science and Technology (No. 2022JBKY02).

Compliance with Ethical Standards. The study was approved by the Logistics Department for Civilian Ethics Committee of China Academy of Safety Science and Technology.

All subjects who participated in the experiment were provided with and signed an informed consent form.

All relevant ethical safeguards have been met with regard to subject protection.

References

1. Zhu, X., Zhao, C., et al.: Occupational hazards to fighters and their prevention and control methods. *China Occup. Med.* (05), 421–423 (2008)
2. Fan, X., Yan, G., et al.: Present status and strategies of cultivating firefighters in China. *Chin. J. Disaster Med.* **2**(05), 245–248 (2014)

3. Chen, H.: Occupational mental health status and countermeasures of employees in China. In: China Occupational Safety and Health Association. Summary of the 25th Cross-Straits and Hong Kong, Macao Occupational Safety and Health Academic Research Association and China Occupational Safety and Health Association Academic Annual Meeting and Science and Technology Awards Conference. China Occupational Safety and Health Association, China Occupational Safety and Health Association, vol. 2 (2017)
4. Du, Y., Zhao, G., et al.: An investigation of the mental health of Chinese firefighter. *J. Armed Police Acad.* **27**(02), 72–74 (2011)
5. Guan, Z., et al.: Comparative analysis research of occupational mental health assessment scale. In: Long, S., Dhillon, B.S. (eds.) *MMESE 2021*. *LNEE*, vol. 800, pp. 148–154. Springer, Singapore (2022). https://doi.org/10.1007/978-981-16-5963-8_21
6. Chen, J., et al.: *Basic Principles and Applications of Occupational Ergonomics*. Emergency Management Press, Beijing (2020)
7. Song, Y., Fang, J., Sun, L.: Development status of mental health assessment and systematic study of psychological strength assessment (MSA). *Psychol. Sci. J.* **5**, 1195–1197 (2008)



Study on the Relationship Between Emotional Regulation Self-efficacy and Fatigue in the Sedentary Population

Xiangpeng Pan^(✉)

East China University of Science and Technology, Shanghai 200237, China

Abstract. Objective: To study the relationship between mood and fatigue among sedentary people in college students, and to provide appropriate psychological and physical counseling and help. **Methods:** Through reliability and validity analysis of the self-efficacy scale (POS, NEG) and fatigue scale-14 (F-14) and by statistics. The correlation and regression analysis of POS (HAP, GLO) and NEG (ANG, DES, and COM) and the three factors of the fatigue scale (physical fatigue, mental fatigue, and fatigue) were conducted. **Results:** Both positive and negative emotions positively promoted fatigue, and negative effects between GLO in HAP and mental fatigue. **Conclusions:** Emotion can not effectively improve the problem of sedentary fatigue, in sedentary state, can slow down mental fatigue. University student Finch replacement should appropriately reduce sedentary time, reduce physical and psychological damage.

Keywords: Self-efficacy scale · Fatigue scale-14 · Sedentary · Correlation and regression analysis · Mood

1 Introduction

With the development of society, the sedentary behavior in daily life, work and study becomes more and more common. Studies have shown that those who sit in the same environment for a long time, namely the sedentary state, and the most obvious group in the sedentary state is mainly teenagers and college students, so sitting for a long time has become a health problem endangering young college students. Sedentary people body long fixed posture easy to the body, especially the lower limbs and brain blood circulation, cervical spondylosis, lumbar disc herniation, obesity and other diseases incidence increased [1], especially college students face social pressure, peer pressure and more and more serious, make college students have to sit for a long time, this state, due to the change of college students emotional instability and easy to produce mental health disease, whether will increase the physical and psychological fatigue. This paper aims to study the relationship between emotional self-efficacy and fatigue in the sedentary college students, so as to provide appropriate psychological and physical counselling and assistance to the sedentary college students in the future.

2 Materials and Methods

2.1 Object of Study

This topic is the relationship between emotional regulation self-efficacy scale of mood and sedentary fatigue, so the subject group had better have most people once or now often need to be in a sedentary state, and college students is a good case, in the long-term environment, in order to complete learning tasks will produce sedentary problems. In this experiment, college students on campus were taken as an example. A random sampling method of 205 students from a university in Shanghai were selected to participate in the inquiry study. A total of 201 valid questionnaires were obtained, including 105 boys and 96 girls. Since the sedentary population in this experiment, the questionnaire was divided into 151 sedentary people (sitting in the same environment for a long time) and 50 non-sedentary people (sitting for less than 2 h in the same environment for a long time).

2.2 Research Tools and Methods

2.2.1 Self-efficacy Scale

Self-efficacy scale the emotion regulation self-efficacy scale was compiled after a Caprara preliminary study of emotion regulation self-efficacy, this version of the scale. It contains two subscales: the sense of ability to express positive emotions (5 questions) and the sense of ability to manage the negative Guangxu (9 questions). The scale adopts the five-point scoring method. As the study progressed, Caprara et al. [2] revised the scale to identified three types of emotional self-regulation efficacy, expressing positive emotional self-efficacy (POS, 4 topics), managing anger/anger self-efficacy (ANG, 4 topics), and managing frustration/painful emotional self-efficacy (DES, 4 topics), and fit ANG and DES into a primary factor-managing negative emotional self-efficacy. On this basis, Yujie Wang et al. [3] further modified research found that people's emotions through self-reflection, the mood can be positive or negative, will express positive emotions of self-efficacy (POS) as a primary factor is divided into two secondary factors are respectively, express happiness/excitement self-efficacy (HAP, 3 topics) and self-efficacy in expressing pride (GLO, 3 topics), the efficacy of emotions expressing negative emotions (NEG, 4 topics) as the primary factors is divided into three secondary factors: self-efficacy of managing anger/anger (ANG, 4 topics), and self-efficacy of managing cursing/painful emotions (DES) and self-efficacy in managing guilt/shame emotions (COM, 3 topics), with a scale consisting of 17 items, using a 5-point scoring method, as shown in Table 1.

2.2.1.1 Project Description

According to the project analysis results, the correlation coefficient between the 17 measured items and the total questionnaire score was between 0.729 and 0.849, which all reached significant levels.

2.2.1.2 Reliability Analysis

After removing the sedentary population, the total questionnaire was 0.962, 0.832 for HAP, 0.792 for GLO, 0.861 for ANG, 0.823 for DES, and 0.857 for COM. Since the

Table 1. The scoring criteria for the mood regulation self-efficacy scale

The primary factor	Secondary factor	Clauses and subclauses
Express a positive emotional self-efficacy (POS)	Express pleasure/excitement of emotional self-efficacy (HAP)	A1 A2 A3
	Self-efficacy that expresses pride (GLO)	A4 A5 A6
Managing Negative Emotional Self-efficacy (NEG)	Self-efficacy in managing anger/anger (ANG)	A7 A8 A9 A10
	Self-efficacy in managing curse/distress emotions (DES)	A11 A12 A13 A14
	Self-efficacy in managing guilt/shame emotions (COM)	A15 A16 A17

Cronbach α coefficient of each part meets the condition of Cronbach $\alpha > 0.7$, the answer of the attitude scale question is reliable and highly reliable.

2.2.1.3 Validity Analysis

The validity study is used to analyze whether the research term is reasonable and meaningful. The validity analysis uses comprehensive analysis through KMO value, degree, variance interpretation rate value, to verify the validity level of the data. The validity analysis of the questionnaire using SPSS 26.0 showed that the common value of all study items is higher than 0.4, indicating that the study item information can be valid Extraction; KMO value of 0.968, greater than 0.6 indicates that the data can be effectively extracted; the variance interpretation value of one factor is 62.489% and 59.574% $> 50\%$ after rotation, meaning that the information of the study item can be effectively extracted; moreover, the χ^2 value is 1929.209 for Bartlett spherical test, DOF df is 94 and $P < 0.001$, indicating that the questionnaire results are suitable for factor analysis. The 17 items in the questionnaire can be explained by five factors, visible in Table 2, the absolute value of standardized load system corresponding to each topic and factor is greater than 0.6 and $P < 0.001$ showed significant, implying a good correspondence. Factor I is named expression happiness/excitement self-efficacy (HAP), expression happiness/excitement self-efficacy (GLO), factor III is named self-efficacy (ANG) for managing anger/anger, self-efficacy (DES), and self-efficacy (COM) for managing guilt/shame. In terms of model fit, visible from Table 3, the chi-square degrees of freedom are less than 3 than χ^2/df , RMSEA less than 0.10, RMR less than 0.05, and fit measures such as CFI, NFI and NNFI are all greater than 0.90, indicating good model fit.

2.2.2 Questionnaire Analysis of the Fatigue Measurement Scale

2.2.2.1 Fatigue Measurement Scale

The Fatigue Scale-14 (Fatigue Scale-14, FS-14) was compiled in 1992 by many British experts, including Chalder. Fatigue as subjective the feeling of, has been a difficult one to define with describing the symptoms of [4]. The FS-14 scale was used to determine

Table 2. Exploratory factor analysis of emotion regulation self-efficacy questionnaire (n = 151)

Items	HAP	GLO	ANG	DES	COM	Common degree	Characteristic root	Interpretation rate
A1	0.5748					0.743		
A2	0.5778					0.751		
A3	0.5794					0.755	2.250	74.99%
A4		0.5632				0.674		
A5		0.5891				0.738		
A6		0.5795				0.714	2.126	70.86%
A7			0.5074			0.727		
A8			0.5035			0.716		
A9			0.5091			0.732		
A10			0.4795			0.649	2.824	70.60%
A11				0.5040		0.665		
A12				0.5277		0.729		
A13				0.4824		0.609		
A14				0.4845		0.614	2.617	65.42%
A15					0.5799	0.785		
A16					0.5914	0.816		
A17					0.5604	0.733	2.334	77.79%

Table 3. Fitting analysis of the questionnaire model of the emotional regulation self-efficacy scale (n = 151)

	χ^2	df	p	χ^2/df	GFI	RMSEA	RMR	CFI	NFI	NNF I
Standard	–	–	>0.05	<3	>0.9	<0.1	<0.05	>0.9	>0.9	>0.9
Numeric value	114.051	94	0.078	1.213	0.901	0.000	0.046	0.989	0.939	0.985

the severity of fatigue symptoms, assess clinical efficacy, and by screening fatigue cases in epidemiological studies. The Fatigue Scale-14 consists of 14 entries used to assess fatigue in subjects. According to the compliance of the content with the actual situation of the subject, answer “yes” or “No” except articles 10, 13 and 14, reverse score of “Yes”, “0” and “No”, and the other 11 entries are positive score. The 14 entries reflect the severity of fatigue from different angles and have divided them into two categories. One reflects physical fatigue (Physical Fatigue), including 8 entries 1 to 8, with a highest score of 8 points; one reflects mental fatigue (Mental Fatigue), including 6 entries 9th to 14, with a highest score of 6. The total score of fatigue is the sum of physical fatigue and

mental fatigue. The total score is 14 points, and the higher the score is, the more severe the fatigue is. The Cronbach α coefficient of the total fatigue score in this study was 0.928, half-reliability was 0.916, somatic fatigue 0.888 and 0.896, and mental fatigue 0.954 and half-reliability 0.960.

2.2.2.2 Statistical Analysis

Because the research content of this article is the relationship between mood and sedentary fatigue, it is necessary to select the sedentary people through the questionnaire. Through consulting previous studies, we can see that sitting in the same environment for a long time is a sedentary state. This paper counted the feedback information on the fatigue scale-14 and the emotional regulation self-efficacy scale to facilitate the further study of the relationship between the two. Non-sedentary student population emerged as a control group.

3 Results

3.1 Characteristics of Emotional Regulation Self-efficacy Table and Fatigue in Sedentary People

Through the questionnaire analysis of the two scales, the relationship between the two scales, as shown in Table 4, each factor in the self-efficacy scale showed a significant positive correlation with somatic fatigue, and a significant negative correlation with mental fatigue (both $P < 0.05$).

Table 4. Correlation coefficient of emotional regulation self-efficacy and fatigue in sedentary people ($n = 151$)

Items	HAP	GLO	ANG	DES	COM
Body fatigue	0.875**	0.881**	0.922**	0.885**	0.903**
Mental fatigue	-0.186*	-0.229**	-0.208*	-0.190*	-0.206*
Fatigue	0.849**	0.845**	0.892**	0.858**	0.874**

Note: * $p < 0.05$ ** $p < 0.01$

3.2 Regression Analysis of Emotional Regulation Self-efficacy on Fatigue in Sedentary People

By using the three influence factors of fatigue as dependent variables (physical fatigue, mental fatigue, fatigue) the three influence factors of fatigue were analyzed by the various influence factors of self-efficacy (HAP, GLO, ANG, DES and COM) as predictive variables. The results showed that GLO, ANG, DES, and COM efficiently predicted fatigue, with an R^2 value of 0.855. In terms of various factors of fatigue, HAP, GLO, ANG, DES, and COM significantly predicted somatic fatigue, with R^2 of 0.855; GLO negatively predicted mental fatigue, and R^2 of 0.053. Of the three fatigue factors, the most GLO was introduced (three times), the least HAP (1 time), and the rest was all twice. Specific data are shown in Table 5.

Table 5. Multiple progressive regression analysis of mood regulation self-efficacy in sedentary people

	β					R^2	F	P
	HAP	GLO	ANG	DES	COM			
Body fatigue	0.116	0.196	0.238	0.115	0.180	0.918	325.88	0.00**
Mental fatigue		0.053				0.053	8.279	0.00**
Fatigue		0.161	0.254	0.144	0.205	0.855	215.007	0.00**

Note: * $p < 0.05$ ** $p < 0.01$

3.3 Comparison Between Sedentary and Non-sedentary Populations in Mood-Regulated Self-efficacy and Fatigue

According to multiple gradual regression analysis, the three factors (ANG, DNS, COM) and GLO in B positive emotions (POS) all have high effects on fatigue, indicating that positive and negative emotions play an important role in the regulation of fatigue in sedentary people. To test whether this effect was only present in sedentary populations, further while comparing previously classified non-sedentary populations with sedentary populations. Since HAP factors in positive mood (POS) were less introduced into the multiple stepwise regression analysis, they were not included in the subsequent studies. The top 27% were ranked by ranking the individual minor items in GLO, ANG, DES, and COM they were divided into low groups, dividing the latter 27% into high groups, with an independent sample t-test.

Sedentary and non-sedentary populations have differences in the regulation of self-efficacy. The non-sedentary groups had lower middle and low self-efficacy (GLO) divisions than sedentary ones and higher ones in high groups than sedentary ones, That is, non-sedentary people have significantly higher efficacy (POS) than sedentary people ($P < 0.01$); Sedentary people express self-efficacy (ANG) in managing anger/anger, curse/distress (DES), self-efficacy (COM in managing guilt/shame), In addition to the individual data for A 7, A 11, Almost low and high groups were higher than non-sedentary groups, That is, sedentary people have a significantly higher efficacy (NEG) level of expressing negative emotions than in non-sedentary people ($P < 0.01$). Therefore, sedentary people express more negative emotions than non-sedentary people. In non-sedentary people are more inclined to express positive emotions. In general, fatigue regulation for non-sedentary people, is not both positive and negative emotions work, more positive mood.

4 Discussion

This paper mainly studied the relationship between emotion and sedentary fatigue on the basis of the modified emotional regulation self-efficacy scale and combined with the fatigue scale-14. The results of this study show that both POS and NEG produce positive predictions of physical fatigue and fatigue. For mental fatigue, GLO in POS, the self-efficacy of expressing pride, produces negative predictions of their PO, and

mainly express positive emotions in non-sedentary people, so there will be no joint effect between POS and NEG [5].

Correlation analysis showed that, there were positive associations between five factor scores for sedentary self-efficacy and physical fatigue and fatigue scores. So the positive emotions don't slow down the fatigue state, And negative emotions don't increase fatigue, either, It is the result of the two working together, The greater the change in the mood, The longer the feeling of sedentary fatigue also is, And this emotional change can be changed either from positive to negative emotions or from negative to positive emotions, that is, fatigue in sedentary people will not change the fatigue state because of changes in negative or positive emotions. The negative correlation between the five factor scores of self-efficacy and mental fatigue scores in sedentary people exists, indicating that the greater the mood changes, the smaller the mental fatigue.

The regression analysis showed that, with the exception of HAP, in the equations predicting the somatic fatigue and fatigue, GLO in POS and ANG, DES and COM in NEG can positively predict the somatic fatigue and fatigue. Visible positive emotions and negative emotions will increase sedentary people body fatigue and fatigue, which means that no matter what mood into the sedentary state or in the sedentary state how the mood changes, body fatigue and fatigue will increase, and not because of the positive or negative and slow down fatigue, this requires us to reduce sedentary state or sedentary time, avoid fatigue continues to increase. In addition, studies have shown that fatigue caused by [1] sedentary behavior is easy to insufficient blood supply to the brain, causing visual fatigue, inattention and other phenomena, which will lead to sedentary people often in negative states such as depression and depression, affecting the efficiency of work and learning. For mental fatigue, but only the factor GLO in the POS enables a negative prediction of mental fatigue. The other four factors did not significantly predict fatigue there. It can be seen that GLO (expressing self-efficacy of pride) can effectively reduce mental fatigue in sedentary people. To some extent, GLO can improve the thinking ability and sensitivity of the brain and help solve more difficult problems. Therefore, sedentary people, especially for continuous brain use, should pay attention to the management of extreme emotions, and can maintain positive emotions in a sedentary state, but GLO can also positively predict physical fatigue And fatigue, so also reduce your time spent while being sedentary. Studies have also confirmed that both positive and negative emotions do not occur in non-sedentary people, who tend to express positive emotions during study or work.

Compliance with Ethical Standards. The study was approved by the Logistics Department for Civilian Ethics Committee of East China University of Science and Technology.

All subjects who participated in the experiment were provided with and signed an informed consent form.

All relevant ethical safeguards have been met with regard to subject protection.

References

1. Peiqi, G., Jianshe, L., Yaodong, G.: Progress in studying the impact of sedentary posture on human health. *Zhejiang Sports Sci.* (05), 98–101 (2017)

2. Caprara, G.V., Di Giunta, L., Eisenberg, N., Gerbino, M., et al.: Assessing regulatory emotional self-efficacy in three countries. *Psychol. Assess.* (3), 227–237 (2008)
3. Yujie, W., Dou, K., Liu, Y.: Revision of the emotional regulation self-efficacy scale. *J. Guangzhou Univ. (Soc. Sci. Ed.)* (01), 45–50 (2013)
4. Yuzhen, L., Wei, W., et al.: Fatigue scale-14 reliability and validity tests in automotive assembly workers. *Ind. Hyg. Occup. Dis.* (5), 346–350 (2016)
5. Kai, D., Yangang, N., Yujie, W., Jianbin, L.: Relationship between self-efficacy and mental health. *Sch. Health China* (10), 1195–2119 (2012)



Depth Perception and Distance Assessment Under Night Vision Goggles and Their Influence Factor

Shan Chen¹, Dawei Tian¹, Fei Yu¹, Qinglin Zhou¹, Jian Du¹, Qingsheng Xiang², and Zengming Li²(✉)

¹ Air Force Medical Center, Fourth Military Medical University, Beijing 100142, China

² Rocket Army Medical Center, PLA, Beijing 100088, China

421065535@qq.com

Abstract. Objective: To review the research progress of depth perception and distance assessment under night vision goggles in foreign and domestic countries, and to understand the influence of night vision goggles on depth perception and distance assessment. **Method:** 35 references and reports in related fields at home and abroad were cited. **Result:** This paper studies the influence of night vision goggles on depth perception or distance assessment, and focuses on the internal factors of night vision goggles leading to depth perception problems, such as narrow field of vision, resolution, image noise, instrument myopia, spectral sensitivity effect and binocular vision, as well as some external factors, such as contrast, illumination observation condition and the interaction between various factors. Finally, depth perception training is briefly summarized. **Conclusions:** Due to the influence of the working environment of night vision goggles and the limitation of the special structure of night vision goggles, night vision goggles reduce ability of airmen to judge the depth perception and distance. The accuracy of judgment can be improved through the depth perception training under night vision goggles.

Keywords: Depth perception · Stereo vision · Distance assessment · Night vision goggles

1 Introduction

Depth perception, also known as “stereo perception” or “distance perception”, is the perception of three-dimensional objects or the distance of different objects. The retina can only receive stimuli in two-dimensional space, and its response to three-dimensional space is mainly realized by binocular vision [1]. The monocular cues for depth perception include relative size, interspersed, line perspective, aerial perspective, monocular parallax, brightness and shadow, and eye accommodation; binocular cues include binocular convergence and stereoscopic parallax. Binocular convergence is only valid for objects within 6 ft, while stereo disparity is the primary binocular cue for judging depth perception of distant objects. Stereoscopic parallax occurs when the image of the retina of the

right eye is different from the image of the left eye when viewing an object in space. Theoretically, the basic stimulus condition for stereo parallax is the difference in the angle of convergence between the binocular line of sight (a) that converges at a fixed target point and the binocular line of sight (b) that converges at another target point, resulting in the retinal Parallax is the cause of stereoscopic vision. It has been shown that depth perception is effective within 452.63 m [2, 3].

Over the past few decades, growing reliance on night vision of aviation personnel has led to the development of various night imaging devices, especially night vision goggles, which are widely used in night helicopter operations. Helicopter accident data, however, shows increasing incidence of accidents due to airmen error when using night vision goggles, where night vision goggle-related accidents are often associated with extremely poor ambient lighting and contrast and the imaging limitation of night vision goggles [4]. Studies have found that compare with daytime viewing conditions, night vision goggles reduce the ability of airmen to perceive depth and distance assessment [5–7].

2 The Effect of Night Vision Goggles on Depth Perception and Distance Assessment

With the development and application of night vision goggles, the depth perception problem caused by night vision goggles has also attracted widespread attention from aviation personnel in various countries. Wiley [8] conducted an experiment to assess depth perception through night vision goggles. Relative depth thresholds for various conditions were tested at 6 m using the Howard-Dorman apparatus. The instrument brightness was set to 7 fL ($1 \text{ fL} = 3.426 \text{ cd/m}^2$) under unaided conditions; under all night vision goggle viewing conditions, the instrument brightness was set to 0.012 fL. The test conditions are: monocular, binocular, monocular AN/PVS-5, binocular AN/PVS-5, binocular AN/PVS-7A and binocular AN/PVS-7B. The results showed significant differences between the unassisted binocular condition and all other conditions. In addition to laboratory studies, the researchers also conducted numerous field experiments. Foyle and Kaiser [9] studied the problem of depth perception using night vision goggles AN/AVS-6 at 20–200 ft ($1 \text{ ft} = 0.3048 \text{ m}$). The subjects were asked to observe the target at 20–100 ft and to estimate the absolute distance under different conditions. The test conditions are daytime, daytime visual field 40° nighttime and nighttime visual field 40° . The findings showed that daytime measurements were more accurate than nighttime measurements. Half of the subjects (airmen of helicopter with night vision goggle flying experience) underestimated distance, and the other half overestimated distance. Wiley and Holly [10] studied depth perception under night vision goggles. The first part is laboratory measurements. Relative depth thresholds were measured in the laboratory using a modified Howard-Dorman apparatus, where subjects could adjust the variable lever remotely. Four test conditions: binocular (6.70 fL), monocular (6.70 fL), night vision goggles binocular (0.012 fL), and night vision goggles monocular (0.012 fL), and the depth threshold of 6 subjects was measured at a viewing distance of 6 m. The naked eye binocular depth threshold is significantly better than the other three test conditions, but the observation conditions of night vision goggles have no significant

effect on the depth threshold. The second part is the field test. Subjects see huge white targets at distances of 200, 500, 1000, 1500 and 2000 ft from the helicopter. Relative depth thresholds obtained by binocular night vision goggles and daytime binocular and monocular observations under full moon conditions. Only at 2000 ft the monocular and binocular depth thresholds were significantly different. The depth threshold for night vision goggles differed significantly from the monocular depth threshold at all distances except 200 ft, and the depth threshold for night vision goggles differed significantly from the binocular threshold at all distances except 200 and 500 ft. The results of the study show that the distance assessment of night vision goggles is significantly weaker than that of the naked eye during the daytime. Hadani [11] pointed out in the research report that the nearby objects are closer than the actual distance when wearing night vision goggles. However, Brickner [12] shows that the objects are farther than the actual distance.

All the above studies have shown that, compared with naked eye vision, night vision goggles can lead to a decrease in relative depth discrimination [8–13]. Under certain conditions, depth perception under night vision goggles may approximate uncorrected monocular vision [10, 14]. In addition, night vision goggles may degrade the estimation of the slope, which is essential during landing [12].

3 Factors Related to Night Vision Goggles Affecting Depth Perception

3.1 Internal Factors of Night Vision Goggles Leading to Depth Perception Problems

Many laboratory and field experimental studies have proved that night vision goggles have many limitations in the visual environment. The differences between under night vision goggles and naked eye vision include monochrome image, decline in resolution and contrast, narrow field of vision, dynamic noise and so on. Kaiser and Foyle [15] proposed that the static illusion when wearing night vision goggles is mostly caused by the wrong assessment of the height above the terrain, that is, the depth problem. The limitations of night vision goggles that lead to depth perception problems can be summarized as narrow visual field, resolution and image noise, instrument myopia, spectral sensitivity effect and binocular vision.

3.1.1 Narrow Field of Vision

The range of direct field of vision is about 90° in the vertical direction and 190° in the horizontal direction [16], and night vision goggles usually provide only 30° to 40° field of vision [12, 14, 17]. Therefore, night vision goggles provide less than 25% of the horizontal field of view and are basically tubular. The reduction of visual field area is positively correlated with the decline of depth perception. The smaller the visual field is, the more obvious the decline of depth perception is. The narrow field of vision makes the observer unable to see the whole environment at a glance. The scene must be scanned through a variety of perspectives to integrate the information from different perspectives into a coherent perception of the world [18]. In the case of naked eyes, the airmen can

effectively scan the whole environment through eye and head movement. However, the field of vision of night vision goggles is limited and more head movement scanning is required. Usually, the whole scene can be seen only in the same area covered by eye movement, resulting in increased airmen fatigue [12] and slow response time [14], which interferes with the ability of airmen to integrate views. If there is not enough head compensation movement, the peripheral visual field will be reduced, and the airmen will lose the peripheral clues that produce stereo vision and help to judge the distance, resulting in the wrong judgment of the height and distance of the target and increasing the possibility of collision with adjacent objects. For example, the helicopter pilot must judge whether the helicopter rotor blades can cross the obstacle or landing area, and whether the landing area is wide enough for the aircraft to land safely. If the pilot wears night vision goggles, the limited field of vision may lead to the relative extension of the time to find obstacles, and there is the possibility of potential flight accidents.

3.1.2 Resolution and Image Noise

Compared with daytime vision, the working environment and internal structure of night vision goggles determine the low resolution, brightness and contrast of night vision goggle images [12]. The reason may be the loss of texture gradient and image noise caused by improper adjustment of night vision goggles and reduced resolution. That is, the image under the night vision goggles is more blurred and lower resolution than the image under normal conditions. The signal-to-noise ratio of night vision goggles has a significant impact on vision. With the decrease of illumination, the gain of goggles increases, resulting in more electronic noise and lower signal-to-noise ratio. When the illumination level is the lowest, the signal-to-noise ratio has the greatest impact on vision [19]. Under the best visibility conditions, the Snellen vision of night vision goggles ANIPVS-5 can reach 20/50, and the Snellen vision of night vision goggles ANIPVS-6 can reach 20/40, but this situation is not common [14]. For example, under full moon illumination, the resolution of night vision goggles may be only 8 cycles per degree or less, which is about 20/70 of Snellen's vision [10]. The reduction of resolution under night vision goggles and image noise may lead to poor discrimination of objects in depth and poor observation ability of high spatial frequency objects (such as wires) [20–22].

3.1.3 The Phenomenon of “Instrument Myopia”

When observing the outside scene through the night vision goggles, the night vision goggles can project the outside image to the optical infinity, so that the outside scene can be clearly imaged under the night vision goggles. Despite this, the observer still tries to focus his eyes on a closer distance when wearing night vision goggles, resulting in the observed external image being closer than the actual distance, making the distance assessment wrong, that is, the phenomenon of instrument myopia. A study has shown that 29% of aviation personnel in the United States have experienced instrument myopia [23].

3.1.4 Spectral Sensitivity Effect

The wavelength range of the image intensifier tube of night vision goggles is about 560–1000 nm, so night vision goggles are more sensitive to red light and near-infrared light, and have a strong image enhancement effect [24]. When aviation personnel look at the red light on another aircraft through night vision goggles, they will feel that the brightness of the red light under the night vision goggles is stronger than the actual brightness, so that the aviation personnel have the illusion that the distance between the planes is closer than the actual distance. Night vision goggles have weaker enhancement to other short-wave light. When aviation personnel look at short-wave light through night-vision goggles, they feel that the short-wave light is weaker than the actual light, resulting in the feeling that the light is far away from themselves [23].

3.1.5 Binocular Vision

According to the technical requirements of night vision goggles, its two optical axes must be completely parallel, but sometimes there will still be different degrees of deflection. If both optical axes are deflected inward, a convergence phenomenon will be formed, and the position of the image perceived by the retina will be closer than the actual position, which will cause the wearer of the night vision goggles to underestimate the distance and size of the target. If it is deflected outward, radiation will occur, visual fatigue will occur, and the judgment of the target distance will be affected. Additionally, limitations in the design of photocathodes, microchannel plates, and phosphor screens can also lead to some type of overload that increases errors in image display, reduces resolution, and affects depth perception.

3.2 External Factors of Night Vision Goggles Causing Depth Perception Problems

In addition to the intrinsic factors of night vision goggles, the depth perception problem caused by night vision goggles also includes some external factors, such as contrast, illumination, observation conditions and the interaction between various factors. The following discussion will focus on the factors that have a greater impact on depth perception.

3.2.1 Motion Perspective

The size and shape of objects imaged on the retina are important factors in judging depth perception. Normally, when the head or eye moves with the object being observed, the retinal image also moves relatively. When a pilot wears night vision goggles to conduct flight search and observe moving targets at night, because the image of the external scene is not directly projected on the retina, but on the night vision goggles screen, the moving speed of the screen image is often higher than the retina expects normal speed. Depending on the moving speed of the target, the imaging position and size of the target image on the retina of the human eye will also change accordingly, which may lead to errors in distance judgment [25].

3.2.2 Contrast

The importance of contrast to depth perception has not been widely recognized by society [25, 27, 28]. Ogle and Weil [26] studied the differences in depth perception under different contrasts. The results of the study showed that when subjects viewed stereoscopic objects with varying brightness through the filter, different contrast levels had no significant effect on stereoscopic vision. However, some scholars have found the opposite. Richards and Foley [27] determined the effect of brightness and contrast on stereoscopic vision with 2 rods that can be changed in the horizontal direction. The angular spacing of the rods is $1/2^\circ$, 1° , 2° and 4° , each with different brightness and contrast. The findings show that for smaller angular spacing ($1/2^\circ$), the depth threshold decreases with decreasing brightness and contrast. However, fairly low brightness or contrast can actually increase the depth threshold for large angular distances. Halpern and Blake [28] experimentally examined the effect of contrast on depth perception. The luminance distribution of the study target was matched to the tenth derivative (D10) of the Gaussian function. The advantage of these targets is limited spatial frequency (previous researchers have used targets with complex spatial frequencies). Depth threshold is measured at 6 contrast levels. The results show that the increase in contrast greatly increases the depth perception threshold. Armentrout [3] studies have shown that an important factor in contrast affecting depth perception is the difference between daylight and night vision goggle conditions. Under daylight conditions, depth perception error increases in a relatively linear fashion as contrast decreases. Under the condition of night vision goggles, the effect of contrast on depth perception is not significant, but there are certain differences. As the contrast decreases, the depth perception error increases, with the largest increase in error when the contrast is reduced from 53% to 25%. Low contrast (<50%) reduces stereo acuity in both daylight and night vision goggle conditions. Scene contrast <50% under night vision goggles may reduce depth perception to a greater extent than under normal viewing conditions. Considering the environment in which night vision goggles are used, this is a very important finding. Tjernstrom [29] confirmed that most scenes where helicopter pilots fly with night vision goggles rarely exceed 50% contrast.

Most vision studies demonstrate that vision is better in high-contrast conditions than in low-contrast conditions. The reason may be that higher contrast allows better eye fixation on a given target, while at the same time achieving better depth perception due to the more precise viewing angle of each eye.

3.2.3 Illuminance

The effect of resolution on depth perception varies with illuminance. Some of the loss of stereoscopic acuity caused by night vision goggles can be attributed to the limited night vision goggle resolution compared to daylight resolution. Studies have shown that, depending on the night vision goggle system, the illuminance is 0.004 8–0.002 4 fc (1 fc = 10.764 lx) night vision goggles have the highest resolution, and the depth perception is relatively stable, but the resolution will be at both ends of the illumination range. drop [3]. The reason for this may be that the resolution decreases when the illuminance exceeds 0.004 8 fc or more. When the illuminance is lower than 0.002 4 fc, the decrease of the

signal-to-noise ratio mainly leads to the decrease of the illuminance. As the illumination decreases, the brightness gain of the night vision goggles increases, the generated electronic noise increases, the signal-to-noise ratio decreases, and the resolution decreases with the decrease of the signal-to-noise ratio. Therefore, it is necessary to improve the signal-to-noise ratio under low lighting conditions [3].

3.2.4 Halo Phenomenon

In the case of high illumination, because the illumination exceeds the range that can be processed by the image intensifier of the night vision goggles, the image will appear obvious “fading” phenomenon, that is, the halo phenomenon. Even if the observer cannot detect it, the interference to the human eye caused by the phenomenon of “halos” and “halos” caused by bright light and reflections can reduce the visibility of the road conditions ahead, making the pilot’s perception of the width and distance of the objects ahead drop, thereby taking the wrong action. As the illuminance increases, the effects of “halo” and “halo” phenomena and other influencing factors on depth perception may become larger and larger. The effective way to solve this problem now is to coat the microchannel plate with an ion barrier film and set up a fast, automatic switching power supply, which can significantly reduce the halo phenomenon.

3.2.5 Observation Conditions

Observation conditions have significantly different effects on depth perception. Wiley [8] believes that the loss of depth perception under naked eye conditions at night is related to the reduction of the resolution of the environment at night. Reduced resolution may be a major factor in the overall loss of depth perception. The binocular night vision goggle condition was significantly different from the naked eye condition at night, with a more pronounced decrease in depth perception under binocular night vision goggles, possibly because some factors in night vision goggles interfere with depth perception [8, 10]. Studies have shown that when night vision goggles have reached a relatively high resolution (40 LP/mm), the degree of depth perception decline when wearing night vision goggles exceeds 100% [3]. The author believes that the loss of depth perception may involve other factors, the most important of which may be the noise in the night vision goggle image. Image noise may reduce stereoscopic acuity when using night vision goggles. It has also been suggested that the loss of monocular cues may reduce depth perception [8], but there is no evidence to support this argument, as no significant difference was found between monocular vision conditions and monocular night vision goggles.

3.2.6 Interaction of Illumination and Observation Conditions

The interaction of illumination and viewing conditions may be the key to the reduction of depth perception by night vision goggles. Studies have shown that the effect of illumination on depth perception when using night vision goggles is different from that under naked eye conditions during the day [3]. Daytime light had relatively little effect on depth perception, and there was little tendency for light to reduce depth

perception. Under night vision goggles, illuminance has a very large effect on depth perception. The error in depth perception is relatively constant under full moon and half moon lighting conditions, and significantly higher than under 1/10-month conditions. In 1/100 month (starlight) conditions, the depth perception error is significantly lower than in 1/2 month conditions. Visible night vision goggles have the best depth perception between starlight and half-moon, where depth perception is likely to be reduced both above and below this illumination level, and depth perception is worst under full and half-moon conditions. This is very important for the use of night vision goggles when the scene illumination exceeds 0.012 fc (half moon). Armentrout [3] observations show that halo and halo effects are more pronounced and image fading is more pronounced at the two highest illumination levels compared to the lower two illumination levels. Pilots who use night vision goggles in actual flight operations also noted that January/April to January/February is usually the pilot's favorite flying environment. The interaction of illuminance and viewing conditions is also very important that even the lowest daylight illumination is significantly better than depth perception under all night vision goggles. Because the scene brightness under 0.79 fc daylight conditions is roughly equivalent to the scene brightness displayed by night vision goggles (about 1 cd/m²). Since the brightness is nearly equal, but depth perception is different, this rules out the possibility that low brightness levels of night vision goggle displays have a significant effect on depth perception.

3.2.7 Night Vision Goggles Assessment

The adjustment of night vision goggles mainly includes the adjustment of interpupillary distance, diopter, and focal length. Pilots mainly obtain clear images through focusing and diopter. If the refraction adjustment of the image intensifier tube is improper (such as too high, too low or unbalanced) or the interpupillary distance adjustment is not appropriate, the image quality will be affected, and the image will be dark, blurred and interfered, etc., which will cause night vision goggles wearers. Visual fatigue, symptoms such as headache, diplopia and dizziness, leading to misjudgment of distance.

4 Depth Perception Training Under Night Vision Goggles

The depth perception problem caused by night vision goggles has received extensive attention. The most important factor to overcome depth perception is training. Therefore, some researchers have tried to improve the error of distance estimation when wearing night vision goggles through training [30–32]. Gibson and Bergman [33] demonstrated that rectified training with distance estimation improves absolute distance estimates with a 19% reduction in error after training and subjects are able to correlate distance cues such as perspective and texture gradient changes with distance changes. Gibson [34] studied distance estimation training with night vision goggles to determine whether training improves depth perception. The experimental group was trained by the grading method, and was given a scale to help researchers make judgments, while the control group was not given a scale. Then the absolute distance is estimated for the experimental group and the control group. The results show that both the absolute error and variability of distance estimates in the training group are better than those in the control group.

In 1994, Reising [35] selected 8 male pilots to use night vision goggles AN/AVS-6 at 20 to 140 ft for absolute distance estimation. The experiment includes a test area and a training area. For pilots, especially helicopter pilots, incorrect distance estimation is an extremely serious problem when wearing night vision goggles. Because pilots often need to estimate their distance to objects and the distance between two objects during the hover and landing phases of flight. Thirteen numbered targets, all white isosceles triangles 40 ft high and 27 ft wide, were placed around the test area. A target was placed every 10 ft within a range of 20 to 140 ft from the subject. The distance estimation included the distances between 12 subjects-targets and 12 target-targets, and the distances between each subject-target and target-target are equal and correspond one-to-one. Subjects performed 2 distance estimates for each 24 distance intervals in random order. After pre-training, bring subjects to the training area and inform subjects of training requirements, including spacing between field targets. Eleven targets were placed within a distance known to subjects in the training area, and the training distance included a total of 42 (21 subject-target and 21 target-target). Subjects viewed the target vertically from the viewing area (positions "A-G") to each marker. At location A, tell the subject to be 20 ft from target 1, 46 ft from target 8, 62 ft from target 3, and between target 1 and target 8 is 32 ft, 74 ft between targets 1 and 9, and 53 ft between targets 3 and 9. The subject then moved to position B for another 6 distance checks. Inform subjects to study distance intervals for pilots to perform distance calibration under night vision goggles. The training lasted approximately 10 min, after which the subjects were brought back to the testing area for post-training evaluation. The results of the study show that both the absolute error (46.1% drop) and variability (31% to 15% drop) are significantly reduced after training, however at critical distances of 40–60 ft (a typical range for helicopter rotor blade lengths) the error is still as high as 8 ft. These study show that the error of depth perception after training is significantly reduced, and the accuracy of distance estimation is also significantly improved. However, the control conditions of the above studies are not very strict. And there are still many problems to be solved about training, such as the accuracy of training, the duration of training, and different training methods required in different operating environments.

Pilots need to have basic skills of depth and distance assessment. And accurate distance estimation is an important task for most pilots, especially for helicopter pilots. Decreased depth perception may adversely affect low-altitude flying, landings, and formation flying. Only with a sufficient understanding of the depth perception under night vision goggles can improve the pilot's accuracy of depth and distance estimation and reduce flight accidents.

Acknowledgements. This work is supported by National Military Standard, China (No. BKJ18B033). Chen Shan and Dawei Tian contributed equally to this work as co-first author of the paper.

References

1. Kang, L.: The influence of field-dependent cognitive style and stimulus color on depth perception. Nanjing Normal University, Nanjing (2020)

2. Wang, G.: *Binocular Vision. 3 Version*, pp. 11–22. People's Medical Publishing House, Beijing (2020)
3. Armentrout, J.J.: An investigation of stereopsis with AN/AVS-6 night vision goggles at varying levels of illuminance and contrast. Virginia Polytechnic Institute and State University, Blacksburg, Virginia (1993)
4. Smith, L.L., Fedor, O.H.: The basics of human error analysis—where to place the blame. In: *Proceedings of the Human Factors Society Annual Meeting*, vol. 28, no. 2, pp.188–191 (1984). <https://doi.org/10.1177/154193128402800222>
5. Knight, K.K., Apsey, D.A., Jackson, W.G., et al.: A comparison of stereopsis with ANVIS and F4949 night vision goggles. *Aviat. Space Environ. Med.* **69**(2), 99–103 (1998)
6. Delucia, P.R., Task, H.L.: Depth and collision judgment using night vision goggles. *Int. J. Aviat. Psychol.* **5**(4), 371–386 (1995). https://doi.org/10.1207/s15327108ijap0504_3
7. Donohue-Perry, M.M., Task, H.L., Dixon, S.A.: Visual acuity versus field of view and light level for night vision goggles. *Proc. SPIE Int. Sco. Opt. Eng.* **2218**(1), 71–81 (1994). <https://doi.org/10.1117/12.177350>
8. Wiley, R.W.: AD-A211 522 Visual acuity and stereopsis with night vision goggles. U.S. Army Aeromedical Research Laboratory, Fort Rucker, pp. 1–24 (1989)
9. Foyle, D.C., Kaiser, M.K.: Airmen distance estimation with unaided vision, night-vision goggles, and infrared imagery, pp. 314–317. *SID International Symposium Digest of Technical Papers*, Moffett Field (1991)
10. Wiley, R.W., Holly, F.F.: AL 36362 Vision with the AN/PVS-5 night vision goggles. AGARD, Neuilly-Sur-Seine (1976)
11. Hadani, I.: Corneal lens goggles and visual space perception. *Appl. Opt.* **30**(28), 4136–4147 (1991). <https://doi.org/10.1364/AO.30.004136>
12. Brickner, M.S.: NASA-TM-101039 Helicopter flights with night-vision goggles-human factors aspects, pp. 1–34. NASA Ames Research Center, Moffett Field (1989)
13. Sheehy, J.B., Wilkinson, M.: Depth perception after prolonged usage of night vision goggles. *Aviat. Space Environ. Med.* **60**(6), 573–579 (1989)
14. Verona, R.W., Rash, C.E.: Human factors and safety considerations of night vision systems flight. *Proc. SPIE* **1117**, 2–12 (1989). <https://doi.org/10.1117/12.960916>
15. Kaiser, M.K., Foyle, D.C.: Human factors issues in the use of night vision devices. In: *Proceedings of the Human Factors Society 35th Annual Meeting*, vol. 35, no. 20, pp. 1502–1506 (1991)
16. Proctor, R.W., Trisha, V.Z.: *Human Factors in Simple and Complex Systems*, pp. 433–465. Allyn and Bacon, Boston (2008)
17. Isbell, W., Estrera, J.P.: Wide-field-of-view (WFOV) night vision goggle. *Proc. SPIE* **5079**, 203–211 (2003)
18. Shao, Z.: *Cognitive Psychology*, pp. 77–119. China Light Industry Press, Beijing (2017)
19. Riegler, J.T., Whitely, J.D., Task, H.L., et al.: AL-TR-1991–0011 The effect of signal-to-noise ratio on visual acuity through night vision ogles, pp. 1–21. Armstrong Laboratory, Wright-Patterson AFB, OH (1991)
20. Donderi, D.C.: Visual acuity, color vision, and visual search performance at sea. *Hum. Factors* **36**(1), 129–144 (1994). <https://doi.org/10.1177/001872089403600108>
21. Uttal, W.R., Baruch, T., Allen, L.: Psychophysical foundations of a model of amplified night vision in target detection tasks. *Hum. Factors* **36**(3), 488–502 (1994). <https://doi.org/10.1177/001872089403600306>
22. Elkind, J.I., Card, S.K., Hochberg, J., et al.: *Human Performance Models for Computer-Aided Engineering*, pp. 310–324. National Academy of Science, Washington, DC (1989)
23. Wang, S.: *Night Flight and Vision*, pp. 99–111. People's Military Medical Press, Beijing (2010)

24. Biggs, K., Burris, M., Stanley, M.: *The Complete Guide to Night Vision*, pp. 33–63. CreateSpace Independent Publishing Platform, San Bernardino (2014)
25. He, S., Hiroshi, F.J., Yuji, I., et al.: The influence of different cues in three-dimensional space on object depth perception. *Acta Opt. Sinica* **39**(10), 377–383 (2019)
26. Ogle, K.N., Weil, M.P.: Stereoscopic vision and the duration of the stimulus. *AMA Arch Ophthalmol.* **59**(1), 4–17 (1958). <https://doi.org/10.1001/archophth.1958.00940020028002>
27. Richards, W., Foley, J.M.: Effects of luminance and contrast on processing large disparities. *J. Opt. Soc. Am.* **64**(12), 1703–1705 (1974). <https://doi.org/10.1364/josa.64.001703>
28. Halpern, D.L., Blake, R.R.: How contrast affect stereoacuity. *Perception* **17**(4), 483–495 (1988). <https://doi.org/10.1068/p170483>
29. Tjernstrom, L.: Night vision goggles resolution performance at low contrast levels. In: *SPIE Infrared Technology XVIII*, vol. 1762, pp. 206–210 (1992). <https://doi.org/10.1117/12.138962>
30. Niall, K.K., Reising, J.D., Martin, E.L., et al.: AL/HR-TR-1998–0148 Distance estimation with night vision goggles: a direct feedback training method, pp. 1–28. Armstrong Laboratory, Wright-Patterson AFB, OH (1997)
31. Reising, J.D.: AL/HR-TR-1994-0138 Distance estimation training with night vision goggles under low illumination. University of Dayton Research Institute, Mesa (1995)
32. Niall, K.K., Reising, J.D., Martin, E.L.: Distance estimation with night vision goggles: a little feedback goes a long way. *Hum. Factors* **41**(3), 495–506 (1999). <https://doi.org/10.1518/001872099779611012>
33. Gibson, E.J., Bergman, R.: The effect of training on absolute estimation of distance over the ground. *J. Exp. Psychol.* **48**(6), 473–482 (1954). <https://doi.org/10.1037/h0055007>
34. Gibson, E.J., Bergman, R., Purdy, J.: The effect of prior training with a scale of distance on absolute and relative judgments of distance over ground. *J. Exp. Psychol.* **50**(2), 97–105 (1955). <https://doi.org/10.1037/h0048518>
35. Reising, J.D.: AL/HR-TR-1994-0090 Distance estimation training with night vision goggles: a preliminary study. University of Dayton Research Institute, Mesa (1994)



Understanding Driver Preferences for Secondary Tasks in Highly Autonomous Vehicles

Qingkun Li, Zhenyuan Wang, Wenjun Wang^(✉), and Quan Yuan

State Key Laboratory of Automotive Safety and Energy, School of Vehicle and Mobility,
Tsinghua University, Beijing 100084, China
wangxiaowenjun@tsinghua.edu.cn

Abstract. Highly autonomous vehicles are expected to free human drivers from continuous driving tasks. Therefore, for highly autonomous vehicles, the secondary tasks that human drivers tend to involve in are significantly different from conventional vehicles. Understanding driver preferences for secondary tasks in highly autonomous vehicles is beneficial to improve the acceptance of the vehicles. This study adopted an online questionnaire to investigate and understand human drivers' preferences for secondary tasks in highly autonomous vehicles in China. Moreover, drivers' understanding of different secondary tasks was collected and analyzed. Further, we compared and examined the differences in the secondary subtask preferences of drivers with different individual characteristics (e.g., driving experience, motion sickness, and attitudes towards autonomous driving). This study contributes to providing the basis for the studies on driving safety analysis for highly autonomous vehicles.

Keywords: Highly autonomous vehicles · Secondary tasks · User Preferences · Individual differences

1 Introduction

Autonomous vehicles have attracted considerable attention in recent years [1]. However, fully autonomous vehicles are not yet available due to technical and policy limitations [2]. Therefore, highly autonomous vehicles (i.e., the vehicles under the Level 3 and Level 4 automation) are a necessary transition from conventional vehicles to fully autonomous vehicles and are more likely to be realized shortly [3]. On the one hand, for highly autonomous vehicles, human drivers are still mandatory. On the other hand, the drivers are not required to constantly observe the traffic environment and vehicle operations in highly autonomous vehicles. This indicates that for highly autonomous vehicles, the secondary tasks (also known as non-driving-related activities) that human drivers may involve in are significantly different from conventional vehicles. For instance, human drivers can sleep or wear make-up under highly autonomous driving [4]. However, the human driver in a highly autonomous vehicle remains responsible for driving safety and

needs to take over the vehicle when a take-over request is delivered [5]. Hence, investigating and understanding driver preferences for secondary tasks in highly autonomous vehicles contributes to providing the basis for the studies on human drivers' take-over performance under different secondary tasks and improving the acceptance of highly autonomous vehicles.

Secondary tasks can be divided into standardized secondary tasks and naturalistic secondary tasks. Standardized secondary tasks (e.g., the N-back task) allow a more exact task difficulty and workload assessment. In contrast, naturalistic secondary tasks are more relevant to realistic situations and hold more ecological validity [6]. In recent related studies, naturalistic secondary tasks have been more widely adopted to examine the impact of driver states on the take-over performance and driving safety [7].

Existing studies have investigated the driver preferences for different types of naturalistic secondary tasks in autonomous vehicles employing online surveys or structured interviews [8, 9]. However, these studies usually lack the distinction between fully autonomous driving and highly autonomous driving, which might negatively affect the validity of the findings. Moreover, existing studies have not provided an adequate comparative analysis of driver preferences across different groups (i.e., the drivers with different individual characteristics). In addition, there is a lack of studies that analyze drivers' understanding of different secondary subtasks. Hence, this study aims to 1) investigate and understand human drivers' preferences for secondary tasks in highly autonomous vehicles in China, 2) compare the differences in the secondary subtask preferences of drivers with different individual characteristics, and 3) analyze drivers' understanding of different secondary subtasks.

2 Questionnaire Design

There are four main parts of the questionnaire adopted in this study, including the individual characteristics statistics section, the understanding of different secondary subtasks section, drivers' preferences for secondary tasks section, and the section used to collect other information.

The individual characteristics statistics section is adopted to collect the basic demographic statistics (e.g., age, gender, and education), driving experience (e.g., driving years, annual driving mileage, and traffic accident), and additional ride-related characteristics (e.g., motion sickness and the attitudes towards autonomous driving). Drivers' subjective perception of the risk level of different secondary tasks (i.e., the subjective degree to which different secondary tasks affect driving safety) is obtained in the understanding of different secondary subtasks section. In the drivers' preferences for secondary tasks section, respondents' preferences for the 17 secondary tasks (see Table 1) under Level 3, Level 4, and Level 5 autonomous driving are acquired. The last section is to obtain other information not relevant to this study, so the last section is not analyzed in this study.

Table 1. The 17 secondary tasks in this study.

Number	Secondary task
1	Sleeping
2	Playing video games on a smartphone
3	Reading
4	Using a computer for entertainment or work
5	Making up
6	Typing and chatting on a smartphone
7	Watching videos on a smartphone
8	Using an iPad for entertainment or work
9	Attending an online meeting
10	Watching videos with onboard devices
11	Making a call
12	Drinking water or eating
13	Smoking
14	Enjoying the scenery outside windows
15	Talking to the passengers
16	Using onboard navigation system
17	Listening to music

In the second section, the respondents are asked to subjectively rate the danger of the 17 secondary tasks via a four-point Likert scale. In the third section, three multi-choice scales are provided to obtain respondents' preferences for secondary tasks under the three levels of autonomous driving.

3 Respondents

There are 367 Chinese respondents recruited to complete the online questionnaire in the present study. The investigation was carried out in September 2021, and all the respondents were remunerated, regardless of whether he/she provided a valid sample. Based on the validity check, 153 invalid samples were excluded, indicating that there were 214 valid samples for analysis.

The respondents' ages ranged from 18 to 61 years (mean = 30.13, SD = 6.28). The gender ratio was relatively balanced, with 101 female and 113 male respondents. The respondents' occupations varied, including doctors, sellers, teachers, college students, etc. According to the self-report, 188 respondents held a valid driving license, and 100 of them had experience in driving autonomous vehicles. One respondent had a doctoral degree, 17 respondents had a master's degree, 171 respondents had a bachelor's degree, and 25 respondents were below undergraduate.

Moreover, 91 respondents reported they had never experienced motion sickness, whereas 123 respondents claimed to have experienced it. Ninety-two respondents expressed a supportive attitude towards highly autonomous vehicles, while 92 respondents were skeptical about highly autonomous vehicles.

4 Results

Descriptive statistics were gathered on respondents’ preferences on secondary tasks under highly autonomous driving (Level 3 and Level 4) and fully autonomous driving (Level 5) [10]. The statistical significance level was set at 0.05 in the present study.

4.1 Drivers’ Subjective Perception on the Risk Level of Different Secondary Tasks

In this study, the respondents are asked to subjectively rate the danger of the 17 secondary tasks via a four-point Likert scale from ‘not dangerous at all’ (1) to ‘very dangerous’ (4). As shown in Fig. 1, sleeping was recognized as the most dangerous secondary task, whereas the respondents considered listening to music to have the most negligible impact on driving safety.

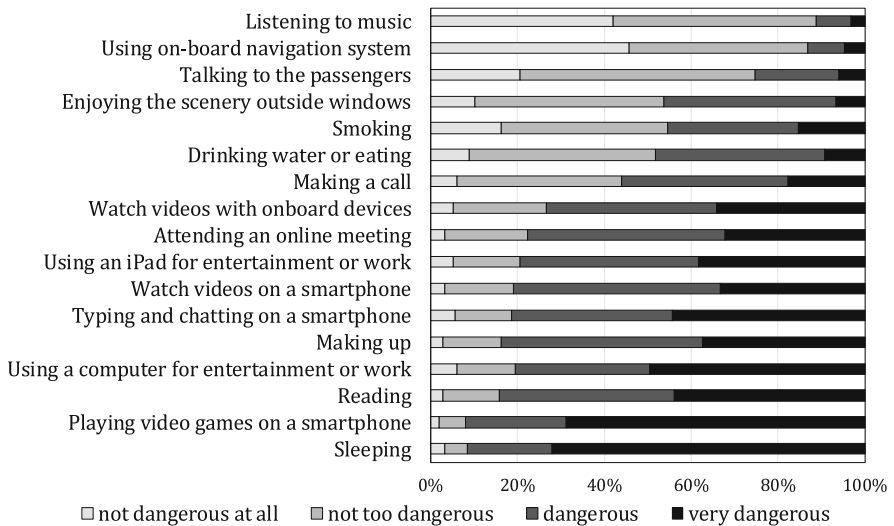


Fig. 1. Drivers’ subjective perception on the risk level of different secondary tasks

The results indicated that the subjectively perceived risk of secondary tasks was related to the number of resources occupied by the secondary tasks and the degree of resistance to the driver's ability to regain control authority. Listening to music only takes up auditory resource and part of the cognitive resource, and auditory resources are less influential on driving safety than visual and motor resources. Hence, the driver can quickly switch from listening to music to driving with full concentration (i.e., a fast regaining the control authority). The subjectively perceived risk is higher for secondary tasks taking up visual, auditory, and cognitive resources (e.g., watching videos with onboard devices and attending an online meeting). In addition, playing video games on a smartphone, which occupies visual, auditory, cognitive, and motor resources is considered the second most dangerous secondary task.

Although sleeping does not seem to occupy much visual, auditory, cognitive, and motor resources, the amount of these resources available to human drivers is significantly reduced when they are sleeping. During sleeping, the driver's situational awareness is at a deficient level and therefore takes a long time for the driver to regain control.

4.2 Driver Preferences for Secondary Tasks in Highly Autonomous Vehicles and Fully Autonomous Vehicles

Three multi-choice scales were adopted to obtain respondents' preferences for secondary tasks under Level 3, Level 4, and Level 5 autonomous driving. The drivers' preferences for the different secondary tasks can be obtained by calculating the percentage of each selected secondary task selected.

As shown in Fig. 2, as the level of automation increases, the frequency of possible engagement increases for almost all the secondary tasks, especially for dangerous secondary tasks such as sleeping and playing video games on a smartphone. The results also indicated that compared with fully autonomous vehicles, drivers were more likely to be in-the-loop rather than engage in various secondary tasks more frequently in highly autonomous vehicles. On the contrary, for the secondary tasks that have less impact on driving safety (e.g., listening to music and enjoying the scenery outside windows), the frequency of possible involvement does not increase with the level of automation increasing.

In general, respondents were more likely to participate in the secondary tasks that have less impact on drivers' ability to regain control of the autonomous vehicles, regardless of the level of automation. Moreover, the secondary tasks related to lifestyle habits, such as smoking in this study, had a low preference among drivers, even when they were considered to have a minor impact on driving safety.

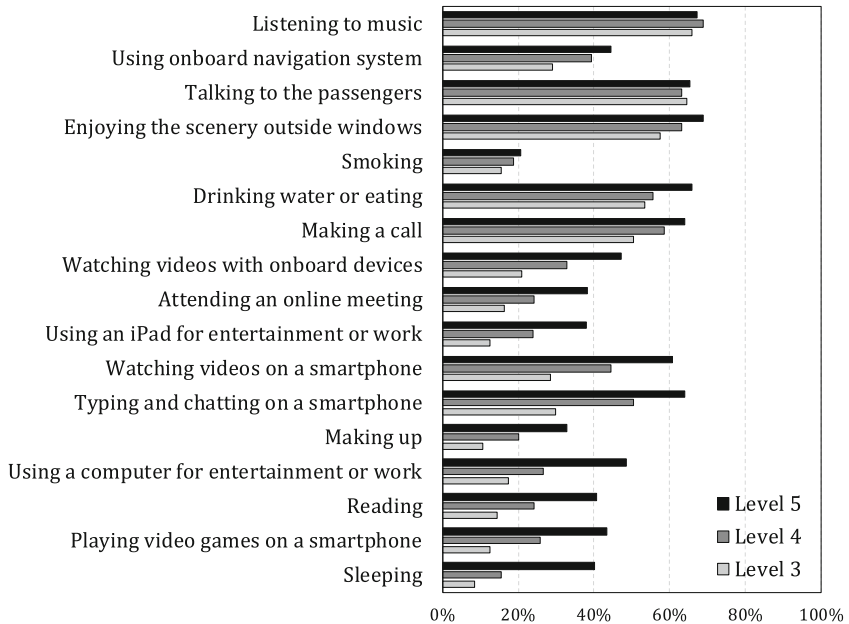


Fig. 2. Drivers' preferences for the different secondary tasks under Level 3, Level 4, and Level 5 autonomous driving

4.3 Individual Characteristics and Driver Preferences for Secondary Tasks in Highly Autonomous Vehicles

According to existing studies [11, 12], several individual characteristics such as driving experience, motion sickness, gender, and the attitudes towards autonomous driving significantly affect the user need and the subjectively perceived safety of autonomous vehicles. Hence, it is necessary to examine their effect on drivers' preferences for secondary tasks in highly autonomous vehicles. Note that in the following, the analysis for highly autonomous vehicles indicates the average of the analyses for Level 3 and Level 4 autonomous vehicles.

The results showed that for the respondents with a driving license, the driving years did not significantly affect the preference for any secondary tasks in highly autonomous vehicles (i.e., $p > 0.05$ for all the secondary tasks). Further, based on self-reported driving experience, the respondents were divided into two groups: the drivers with experience in driving autonomous vehicles and the drivers without experience in driving autonomous vehicles. The results indicated that the drivers with experience in driving autonomous vehicles tended to engage in less for all the secondary tasks. A possible explanation is that they know more about the limitations of autonomous driving systems based on the instructions and practical experience, which makes them become more cautious when using the systems. In addition, the accident experience did not show any significant effect on the preference on the secondary tasks ($p > 0.05$ for all the secondary tasks).

The respondents with motion sickness experience were reported to engage more in enjoying the scenery outside windows ($p < 0.001$), sleeping ($p = 0.013$), and talking to

the passengers ($p = 0.043$), but more unwilling to be involved in using a computer for entertainment or work ($p < 0.001$), reading ($p = 0.038$) and using onboard navigation system ($p = 0.035$). The results indicated that the motion sickness had a considerable impact on drivers' preference for the secondary tasks. Hence, it is promising to improve the user experience and acceptance by easing the motion sickness.

According to the results, female drivers are significantly more inclined to engage in listening to music ($p = 0.019$), enjoying the scenery outside windows ($p = 0.022$) and making up ($p = 0.009$), but less likely to participate in reading ($p = 0.027$), using a computer for entertainment or work ($p = 0.041$) and smoking ($p = 0.011$) than male drivers. The results indicated that except for habits-related secondary tasks (i.e., making up and smoking), male drivers were more likely to engage in more dangerous secondary tasks, indicating that male drivers might trust the autonomous driving systems more.

5 Conclusion

This study analyzed drivers' understanding of different secondary subtasks, investigated human drivers' preferences for secondary tasks in highly autonomous vehicles, and compared the differences in the secondary subtask preferences of drivers with different individual characteristics. The results indicated that the preference for engagement increases for almost all the secondary tasks as the level of automation increases. Moreover, gender, motion sickness, and the experience in driving autonomous vehicles significantly affect drivers' preference for secondary tasks in highly autonomous vehicles, whereas there is no noticeable effect of driving years. This study contributes to providing the basis for the research on driving safety analysis for highly autonomous vehicles.

Acknowledgement. This work is supported by Tsinghua University-Toyota Joint Research Center for AI Technology of Automated Vehicle under Grant TTAD2021-05, and the National Natural Science Foundation of China under Grant 51965055 and 52072214.

Compliance with Ethical Standards. The study was approved by the Logistics Department for Civilian Ethics Committee of Tsinghua University.

All subjects who participated in the experiment were provided with and signed an online informed consent form.

All relevant ethical safeguards have been met with regard to subject protection.

References

1. Li, Q., et al.: An adaptive time budget adjustment strategy based on a take-over performance model for passive fatigue. *IEEE Trans. Hum.-Mach. Syst.* (2021). <https://doi.org/10.1109/THMS.2021.3121665>
2. Choi, D., Sato, T., Ando, T., Abe, T., Akamatsu, M., Kitazaki, S.: Effects of cognitive and visual loads on driving performance after take-over request (TOR) in automated driving. *Appl. Ergon.* **85**, 103074 (2020)
3. Wan, J., Wu, C.: The effects of lead time of take-over request and nondriving tasks on taking-over control of automated vehicles. *IEEE Trans. Hum.-Mach. Syst.* **48**(6), 582–591 (2018)

4. Hecht, T., Darlagiannis, E., Bengler, K.: Non-driving related activities in automated driving – an online survey investigating user needs. In: Ahram, T., Karwowski, W., Pickl, S., Taiar, R. (eds.) IHSED 2019. AISC, vol. 1026, pp. 182–188. Springer, Cham (2020). https://doi.org/10.1007/978-3-030-27928-8_28
5. Zeeb, K., Buchner, A., Schrauf, M.: What determines the take-over time? An integrated model approach of driver take-over after automated driving. *Accid. Anal. Prev.* **78**, 212–221 (2015)
6. Li, Q., et al.: Drivers' visual-distracted take-over performance model and its application on adaptive adjustment of time budget. *Accid. Anal. Prev.* **154**, 106099 (2021)
7. McDonald, A.D., et al.: Toward computational simulations of behavior during automated driving takeovers: a review of the empirical and modeling literatures. *Hum. Factors* **61**(4), 642–688 (2019)
8. Wilson, C., Gyi, D., Morris, A., Bateman, R., Tanaka, H.: Non-driving related tasks and journey types for future autonomous vehicle owners. *Transp. Res. Part F: Traffic Psychol. Behav.* **85**, 150–160 (2022)
9. Ataya, A., Kim, W., Elsharkawy, A., Kim, S.: How to interact with a fully autonomous vehicle: naturalistic ways for drivers to intervene in the vehicle system while performing non-driving related tasks. *Sensors* **21**(6), 2206 (2021)
10. Taxonomy SAE: Definitions for terms related to driving automation systems for on-road motor vehicles. *SAE Stand. J.* **3016**, 2016 (2016)
11. Dam, A., Jeon, M.: A review of motion sickness in automated vehicles. In: 13th International Conference on Automotive User Interfaces and Interactive Vehicular Applications, pp. 39–48, September 2021
12. Dettmann, A., et al.: Comfort or not? Automated driving style and user characteristics causing human discomfort in automated driving. *Int. J. Hum.-Comput. Interact.* **37**(4), 331–339 (2021). <https://doi.org/10.1080/10447318.2020.1860518>



Classification of Mental Load of Special Vehicle Crew Based on Convolutional Neural Network

Fang Xie¹, Mingyang Guo², Xiaoping Jin², Sijuan Zheng¹(✉), and Zhongliang Wei¹

¹ China North Vehicle Research Institute, Huaishuling No. 4 Court, Fengtai District, Beijing 100072, China
Christie_xie@163.com

² College of Engineering, China Agricultural University, Beijing 100083, China

Abstract. Detecting the mental load state of special vehicle crew is of great significance to monitor the driving state of crew and improve the comprehensive combat effectiveness of crew. Based on the virtual simulation system of crew task of a special vehicle, 12 subjects were selected to carry out the brain load experiment of special vehicle commander for the new task of special vehicle commander. The experimental results show that adding sub tasks to typical combat tasks has higher scores on Subjective scales and lower accuracy of typical combat tasks than only completing typical combat tasks; Compared with the attack and report stage, the search stage has higher scores of Subjective scales and absolute power of theta band, alpha band and beta band. A feasible model of deep learning network based on EEG to detect the mental load of special vehicle passengers is established. The deep learning network model is based on THE RESNET convolutional neural network. The results show that the deep learning model can effectively extract the characteristics of EEG and realize the classification of crew mental load.

Keywords: Special vehicles · Mental fatigue · EEG · CNN · Classification recognition

1 Introduction

With the in-depth application and integration of automation, informatization, intelligence and other technologies in the man-machine system of special vehicle cabin, the operational accident rate caused by vehicle performance is significantly reduced [1]. However, special vehicle tasks are highly random, large amount of real-time information interaction, multiple dimensions of function and information display, and complex operation behaviors [2]. Therefore, drivers need high cognitive ability in information processing. Studies have shown that long-term task execution will produce task time effect [3], which refers to the cognitive decline caused by long-term task execution, resulting in distraction and fatigue of the operator, so that the optimal execution strategy cannot be adopted in time [4]. Therefore, a long time mission will affect the ability of the special vehicle crew to deal with emergency situations and endanger the safety and war situation of the crew. Therefore, timely detection and reduction of mental fatigue

of special vehicle occupants can improve their operational performance. The mental fatigue state of drivers can be accurately judged by analyzing mental load level. A common method for analyzing the level of mental load is to perform feature analysis based on EEG signals [5], which can provide accurate information about the driver's mental state. Binias et al. [6] used the EEG data of F3, F4, F7, and F8 to calculate the power spectrum, and found that during the pilot mission, with the increase of mission time, the Theta band power spectrum increased. Dehais et al. [7] used two tasks with high and low cognitive fatigue levels and found that when the cognitive fatigue level was higher, the task error rate was higher, and the theta band and alpha band of the two fatigue levels were significantly different, using sLDA classifier classified the EEG features with an average accuracy of 76.9%. Wu et al. [8] used a Deep Shrinking Sparse Autoencoder Neural Network (DCSAEN) network to classify the power spectral ratios of experimentally relevant electrode point data with an average accuracy of 81.5%. Bashivan et al. [9] proposed a method to identify EEG data features based on convolutional neural networks, and classified the subjects into four workload states, with an average accuracy of 91.1%.

However, the current fatigue classification technology based on EEG data is mostly used in the field of flight, and the relevant theoretical research and experimental data support in the field of special vehicles is very limited. Considering the high mental load burden of special vehicle operation tasks on the crew, the virtual simulation system of the special vehicle crew task is used to conduct research on the changes of the commander's mental load level under different cognitive fatigue level tasks for the new operation task of the special vehicle commander, and based on the CNN neural network, the experimental data is classified into the fatigue level of the driver.

2 Method

2.1 Subjects

A total of 12 adult males were recruited as subjects, aged 20–30 years (mean = 22.56 years). All subjects received adequate training, were familiar with the experimental procedures and operating steps, and voluntarily signed a written informed consent. All subjects were in good physical condition, right-handed, with normal or corrected-to-normal vision, normal hearing, and no history of neurological disease. And before the experiment, the subjects were required to ensure adequate sleep (6–8 h), avoid alcohol and coffee, and participated in the EEG experiment for the first time.

2.2 Measuring Equipment

The experiment relies on the virtual simulation experiment system of a certain special vehicle crew task, which can realize the whole process and operation of a typical combat mission, and can realize the collection of crew task performance data.

The brain products were used to measure the EEG signal in the experiment. According to the international 10–20 system, a 32-electrode acquisition cap was used, and the bilateral mastoids were used as the reference electrode position. The EEG data sampling frequency was 500 Hz, use medical conductive paste to reduce the impedance, so that the impedance of each electrode point is reduced to below 5k ohms.

2.3 Experimental Design

The experiment was designed to induce different fatigue states of the captain by designing two experimental paradigms. Each experiment lasted at least three hours, and after completing each task, the subjects would be asked how difficult it was to complete the task and fill in the NASA-TLX scale.

Control paradigm: The subject needs to complete a typical combat mission with the help of the crew mission virtual simulation experiment system, that is, the subject plays the role of the commander and searches for the enemy vehicle target through the peripheral mirror. Vehicles, fire first to the enemy, complete the attack on the enemy and report the completion of the mission to the command. A complete combat mission process can be divided into two phases: search and strike reporting, as shown in Fig. 1.

Subtask paradigm: The experimental design subtasks include visual subtasks and cognitive subtasks. Among them, the visual sub-task adopts the arrow task, which mainly induces the change of the subject's fatigue state by occupying the subject's visual resources while completing the combat task; At the same time, the cognitive resources of the subjects were occupied to induce the changes of the subjects' fatigue state.

2.4 Experimental Process

During the experiment, the subjects were required to complete the corresponding subtasks while completing the typical combat tasks. Among them, the arrow task means that the subjects need to monitor the arrow screen while performing the combat task, and answer the displayed 4×4 arrow matrix picture as quickly as possible. There are several upward arrows, and then the results are spoken orally, and the experimenter Record. The arrow task appears once in 5–30 s. The mental arithmetic task means that the subjects need to add and subtract the two-digit numbers mentioned by the experimenter when they perform combat tasks, and quickly obtain the answer through mental arithmetic and express it orally, and the experimenter records the results.

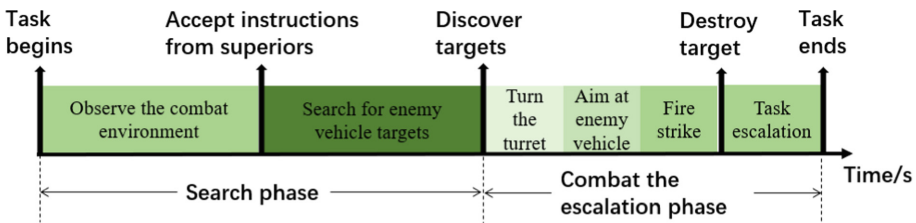


Fig. 1. Schematic diagram of the division of combat missions

The subjects were randomly sorted and the experiments were carried out one by one. Each subject needs to complete three sets of experiments. After each experiment, the subjects rest for 15–30 min and fill in the NASA-TLX subjective evaluation scale.

3 Data Collection

Subjective scales, physiological measures and job performance measures were comprehensively used as the evaluation methods of members' mental load. Evaluation indicators include subjective evaluation data, EEG indicator data and task performance data.

3.1 Subjective Evaluation Data

The study used the NASA-TLX scale for subjective evaluation. The NASA-TLX scale evaluates one's own mental load level from six dimensions, including mental needs, physical needs, time needs, effort, performance evaluation, and frustration.

3.2 EEG Index Data

The EEG data was collected using the BrainProducts EEG instrument. Under normal circumstances, EEG signals will be interfered by various noises during the acquisition process, including blinking artifacts, eye movement artifacts, EMG interference, power frequency interference, and baseline drift. It has a great impact on the analysis and processing of EEG signals. In order to eliminate the influence of various interferences on the EEG signal, firstly, the EEG signal was subjected to a 0.1 Hz high-pass filter and a 40 Hz low-pass filter, and then the independent component analysis (ICA) algorithm was used to distinguish the independent components of the EEG signal, and Remove impurities such as blinking, eye movement, head movement, ECG and power frequency interference in the EEG signal. The data collected for each experiment was divided into 5s segments of data, which contained 4s of data repetitions, so that the order information could be preserved in the data while completely separating the experimental data.

Since the CNN model performs best when used to recognize images, the processed EEG data is converted into image form. First, the power spectral density of each frequency band is calculated based on the wavelet transform (WT) [10], where the frequency of theta band is 4–8 Hz, which often occurs when adults are sleepy; Quiet and closed eyes often appear in the alpha band. It is generally believed that the alpha band is the main manifestation of the brain's wakefulness; the frequency of the beta band is 13–20 Hz. The beta band is the main performance of the brain when it is nervous and excited. Therefore, three bands of theta band, alpha band, and beta band are selected as the distinguishing bands. By calibrating the absolute power peaks of different frequency bands by a unified standard, an EEG image of size 32×32 characterized by energy is drawn as the input of the CNN model.

3.3 Task Performance Data

The virtual simulation experiment system of an special vehicle crew mission used in the experiment includes a data acquisition module. During the experiment, the system can automatically record the subjects' performance data including the time to destroy the enemy, the time to search, and the correct rate of operation.

4 Results and Discussion

4.1 Task Performance Data Analysis

Mission performance includes the time taken to complete typical combat tasks and the accuracy of typical combat tasks. The results of the duration of typical combat missions are shown in Fig. 2. The results of variance analysis showed that the secondary task had no significant effect on the duration of typical combat tasks ($p = 0.332 > 0.05$). For the accuracy rate indicators of typical combat tasks, the average accuracy rate of the control group is $(96.15\% \pm 3.85\%)$, the average accuracy rate of the visual sub-task group is $(92.31\% \pm 7.69\%)$, the average accuracy rate of the cognitive sub-task group is $(84.62\% \pm 15.38\%)$, and the average accuracy rate of the control group task is obvious. higher than the sub-task group.

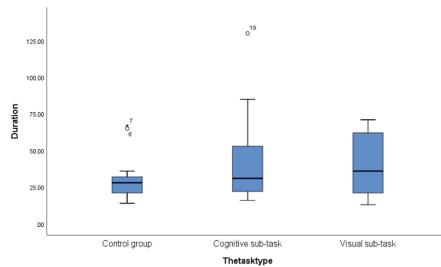


Fig. 2. Time duration results of typical combat missions under different experimental conditions

4.2 Experimental Results

Taking into account the effects of task stages and subtasks on the mental load state of the subjects, this study divided the subjects' mental load into two states of high mental load and low mental load. The mental load status corresponding to each stage and subtask is shown in Table 1.

Table 1. Corresponding task settings under different mental load levels

Task phases	Secondary task type	Mental load state
Search phase	Control	High
	Visual sub-task	High
	Cognitive sub-task	High
Search strike reporting phase	Control	Low
	Visual sub-task	High
	Cognitive sub-task	High

5 Conclusion

This paper investigates the possibility of classifying the fatigue level of special vehicle captains based on EEG data and the proposed classification method based on CNN neural network. The EEG data of the special vehicle commander was obtained from the virtual simulation environment of the simulated special vehicle occupant mission, and the classification of the fatigue level was realized. For the mental load of the special vehicle commander caused by different mission stages, the absolute power indicators of the NASA-TLX scale, theta band, alpha band, and beta band showed good sensitivity. This paper focuses on the classification of EEG data. In order to increase the convenience, efficiency and versatility of the classification system, other physiological data can be added to establish a comprehensive network. In addition, further research can be done in the direction of establishing a better deep learning framework and transmission model.

Compliance with Ethical Standards. The study was approved by the Logistics Department for Civilian Ethics Committee of China North Vehicle Research Institute.

All subjects who participated in the experiment were provided with and signed an informed consent form.

All relevant ethical safeguards have been met with regard to subject protection.

References

1. Guo, S., et al.: The influence of intelligent design and information processing channel complexity on the mental load of armored vehicle crew. *J. Ordnance Eng.* **42**(02), 234–241 (2021)
2. Fu, B., et al.: Design and development of ergonomic test platform for armored vehicle information system. *J. Ordnance Eng.* **40**(07), 1537–1545 (2019)
3. Qi, P., et al.: Neural mechanisms of mental fatigue revisited: new insights from the brain connectome. *Engineering (Beijing, China)* **5**(2), 276–286 (2019)
4. Han, M., et al.: Research progress of pilot mental fatigue assessment based on EEG. *Manned Spaceflight* **27**(05), 639–645 (2021)
5. Ping, S.: Research on Brain Load Identification Based on EEG Independent Component Features, p. 60. North China University of Technology (2021)
6. Binias, B., et al.: Evaluation of alertness and mental fatigue among participants of simulated flight sessions. *IEEE* (2016)
7. Dehais, F., et al.: Monitoring pilot's mental workload using ERPs and spectral power with a six-dry-electrode EEG system in real flight conditions. *Sensors* **19**(6), 1324 (2019)
8. Wu, E.Q., et al.: Detecting fatigue status of pilots based on deep learning network using EEG signals. *IEEE Trans. Cogn. Dev. Syst.* **13**(3), 575–585 (2021)
9. Bashivan, P., et al.: Learning representations from EEG with deep recurrent-convolutional neural networks. In: International Conference on Learning Representations, ICLR, San Juan, Puerto Rico (2016)
10. Zhao, J., et al.: EEG time-frequency analysis based on Morlet wavelet transform. *Chin. J. Med. Phys.* (01), pp. 56–59+11 (2006)



Prevalence of Musculoskeletal Symptoms Among Construction Workers

Xinye Hong¹ and Yuchi Lee²(✉)

¹ South China University of Technology, Guangzhou 510006, China

² College of Management and Design, Ming Chi University of Technology, New Taipei
City 243303, Taiwan

Yclee@mail.mcut.edu.tw

Abstract. To investigate the prevalence of musculoskeletal discomfort in construction workers, a cross-sectional study was conducted on 100 randomly selected subjects. Data were collected using the Nordic Musculoskeletal Questionnaire (NMQ) through semi-structured interviews. The results showed that the prevalence of musculoskeletal discomfort among construction workers was 61%, with the highest prevalence in the neck (28%), followed by the shoulder (23%), lower back (15%), and elbow (14%). The workstations with the highest prevalence were decorators (91.3%), followed by ironworkers (68.4%), bricklayers (58.3%), concreters (50.0%), and laborers (40.6%). The findings of this study indicate that construction workers have a high prevalence of musculoskeletal symptoms and that the highest affected body regions vary across workstations. Thus, it is important to conduct further investigations to examine specific associated factors to develop interventions strategies to improve occupational health.

Keywords: Prevalence · Musculoskeletal disorders symptoms · Construction workers · Nordic Musculoskeletal Questionnaire

1 Introduction

Construction industry is regarded as one of the most dangerous industries due to high casualty rate [1]. Researches show that the risk of injury and death in construction industry is about five times [2] higher than in other profession and that the direct and indirect costs of fatal and non-fatal injuries in construction industry exceed 10 billion dollars [3]. This is related to the chemical and physical hazards faced by construction sites in construction industry. However, the negative impact of construction industry on the health of workers cannot be ignored in addition to these hazards. Among them, musculoskeletal disorders (MSDs) are the most common occupational hazard in construction industry.

MSDs are caused by injury or disorder of tendons, muscles, joints, ligaments, nerves and bones [4]. MSDs in the construction industry are caused by construction workers in the working conditions such as repetitive exertion, dangerous posture, heavy lifting and body vibration. In addition, psychological and population-related factors also cause MSDs of construction workers [5]. The sickness rate of MSDs in construction industry

around the world is generally high, ranging from 30% to 84.7% [6]. It shows that there is some differences in the results of different regions. The concerns about occupational safety of construction workers in China have been improved, but MSDs as cumulative hazards haven't been appreciated, and the MSDs assessment and research have been scarce. Therefore, this study is aimed at investigating the demographic and work-related factors of workers of different occupations in the China's construction industry, and assessing the prevalence of MSDs.

2 Method

This study adopted the cross-sectional study method, and collecting data by asking respondents to fill in self-report questionnaires. The systematic random sampling method was used in the investigation of 100 construction workers. Through analyzing questionnaire data, the descriptive statistics was used to determine the prevalence and distribution of MSDs.

2.1 Study Site and Sample

This study was carried out in March 2020 at many large construction sites in Guangzhou, Guangdong Province. Before the study, the workers with at least one year of experience in construction industry were considered, and the personnel with the history of injury, musculoskeletal disorders and pregnant women were excluded. In Guangzhou, a random sample of 100 workers from several large construction sites participated in this study. Before the survey, all participants were informed, and the research scheme was approved by the ethics committee. Construction workers were divided into the following five categories, including ironworkers, concreters, bricklayers, decorators (including plasterers, carpenters, plumbers) and labourers (including measurers, elevator drivers, handymen) in this study.

2.2 Questionnaire Design

Before sending out the employee questionnaires, the expert panel consisting of three ergonomics specialists and two construction industry professionals conducted preliminary interview and site observation, and designing a structured self-report questionnaire for construction workers to investigate the musculoskeletal disorders related to the work. The questionnaire covered the demographic information of construction workers, such as gender, age, height, weight, exercise, etc. At the same time, there were a series of questions related to work-related characteristic, such as work experience, daily working hours, workstations, etc. In addition, construction workers were required to use the modified Nordic Musculoskeletal Questionnaire (NMQ) to determine work-related musculoskeletal symptoms they have experienced in the past 12 months. Then the frequency and strength of musculoskeletal symptoms in the main parts of body (neck, shoulder, upper back, elbow, wrist, lower back, thigh/knee, ankle/foot) were determined. Deakin et al. indicated that the questionnaire had the reliability of 77% to 100% and the validity of 80% to 100% [7]. Researches show that the questionnaire has been translated and adjusted to adapt to different cultures and countries, with good results, including in China [8].

2.3 Data Analysis

SPSS 26.0 software (IBM Corporation, Armonk, NY, USA) was used in data input. The distribution of the demographic and work-related factors was shown by the descriptive statistical method of average value, standard deviation (SD), frequency, and percentage. In construction workers, the prevalence of MSDs symptoms was listed as a percentage. The prevalence of MSDs symptoms by body part was the percentage of respondents.

3 Results

3.1 Basic Characteristics of Participants

The characteristics of participants are shown in Table 1. 100 construction workers participated in this study, including 19 ironworkers, 14 concreters, 12 bricklayers, 23 decorators and 32 labourers. Respondents had an average age of 39.2 (8.8) years old and ranged from 20 to 57 years old, including 87 males and 13 females. Respondents had an average height of 167.9 (5.9) cm and an average weight of 63.7 (8.5) kg. Respondents had an average BMI of 22.5(2.3) kg/m², and most of the respondents had a BMI in the normal scope. Most workers (68%) did not conduct physical exercise on a daily basis. The average working experience in construction was 9.1 (6.4) years, and the average working time was 8.5 (1.1) hours every day.

Table 1. General information about the study participants (N = 100)

Study variables	Value	Study variables	Value
Gender (% sample)		Exercise (% sample)	
Male	87	No	68
Female	13	Yes	32
Age (years)		Job tenure (years)	
Mean (SD)	39.2 (8.8)	Mean (SD)	9.1 (6.4)
Range	20–57	Range	1.0–25.0
Height (cm)		Daily working time (h)	
Mean (SD)	167.9 (5.9)	Mean (SD)	8.5 (1.1)
Range	152–181	Range	6–12
Weight (kg)		Workstations (% sample)	
Mean (SD)	63.7 (8.5)	Ironworkers	19
Range	46–88	Concreters	14
BMI (kg/m ²)		Bricklayers	12
Mean (SD)	22.5 (2.3)	Decorators	23
Range	17.4–28.4	Labourers	32

3.2 Prevalence of Musculoskeletal Symptoms in Workers

The prevalence of work-related musculoskeletal symptoms in various parts of the body in construction workers is shown in Table 2. Generally speaking, the self-reported prevalence of musculoskeletal symptoms in construction workers was 61% in the last 12 months. The body part with the highest prevalence was the neck (28%), and followed by shoulders (23%), lower back (15%), elbow (14%), upper back (13%), thigh/knee (13%), hand/wrist (9%) and foot/ankle (8%). The post with the highest prevalence was decorators (91.3%), and followed by ironworkers (68.4%), bricklayers (58.3%), concreters (50.0%) and labourers (40.6%).

When different body parts were linked with workers' jobs, the result showed that the ironworkers had the highest prevalence in neck and shoulder (36.8%), and followed by elbow (26.3%). Similarly, concreters had the highest prevalence in neck, shoulders, thighs and knees (28.6%). Bricklayers had the highest prevalence in the lower back (25.0%), and followed by neck and shoulders (16.7%). Decorator MSDs symptoms were most common in the neck (39.1%), and followed by shoulders (30.4%) and lower back (26.1%). Similarly, labourers had the highest prevalence in the neck (18.8%), and followed by shoulders and upper back (9.4%).

Table 2. The prevalence of MSDs symptoms in different body regions of construction workers

Body parts	Any station (%, n = 100)	Ironworkers (%, n = 19)	Concreters (%, n = 14)	Bricklayers (%, n = 12)	Decorators (%, n = 23)	Labourers (%, n = 32)
Neck	28	36.8	28.6	16.7	39.1	18.8
Shoulders	23	36.8	28.6	16.7	30.4	9.4
Upper back	13	15.8	21.4	0.0	17.4	9.4
Elbows	14	26.3	14.3	8.3	17.4	6.3
Hand /wrists	9	10.5	21.4	8.3	13.0	0.0
Lower back	15	5.3	21.4	25.0	26.1	6.3
Thighs/knees	13	10.5	28.6	8.3	21.7	3.1
Ankles/feet	8	5.2	21.4	8.3	8.7	3.1
Any region	61	68.4	50.0	58.3	91.3	40.6

4 Discussion

This study is aimed at determining the prevalence and location of musculoskeletal symptoms in construction workers. The research result shows that about 61% construction workers reported musculoskeletal discomfort in at least one body part in the last 12 months. The result in the current study is higher than Lette's investigation result

(43.9%) in Southeastern Ethiopia for MSDs symptoms in construction workers [9]. At the same time, the result of this study is lower than that of Bodhare et al. for construction workers in Karimnagar (77%) [10]. The differences may be caused by working conditions, the relevant country culture, social management, etc.

In addition, the research results show that construction workers have higher MSDs symptoms in the neck (28%) and shoulder (23%), which may be related to long-time work, awkward posture, working at height of construction workers in construction industry. However, the previous research results show that the lower back is the part with the highest prevalence [11] in construction industry, which is different from the results of this study. At present, a large number of equipment and instrument are adopted, reducing manual handling work. The previous research results show that carrying materials by hands are required in construction industry, which is an important factor of lower back MSDs in construction workers [12].

Decorators (91.3%) have the highest prevalence in this study. The workers in construction industry had the highest prevalence [13] in previous studies, while labourers had the lowest prevalence (40.6%) in this study. This may be caused by the differences in work content. The labourers in this study mainly worked on supporting work, while the workers in the previous study mainly worked on lifting, carrying, pushing and pulling large amounts of construction materials.

Research results show that the body parts of workers in different workstations of construction industry have differences in the highest prevalence. In addition to shoulders and neck, decorators and bricklayers have the highest prevalence in the lower back, ironworkers in the elbow, concreters in the thigh/knee, and labourers in the upper back. This may be related to the differences in work contents of workers in different workstations. For example, the decorators working on floor, high position or corner, are forced to maintain awkward positions that can put pressure on back, resulting in fatigue and muscle damage; bricklayers often bend down to pick up bricks and mortar and put them on the wall, which can require bending and twisting frequently, resulting in fatigue and the increased risk of lower back diseases.

Some limitations in this study need to be improved. For example, the sample volume of the study is limited, and the collected data and information are limited. In the future study, physical, psychological and work-related factors shall be considered to further understand the influencing factors.

5 Conclusion

In the cross-sectional study, we have investigated the epidemic conditions of MSDs in construction workers. The prevalence of MSDs in workers was generally higher (61%). There were differences in the prevalence of workers in different workstations. Neck, shoulder, lower back and elbows were the most affected area of body. The body parts with the highest prevalence were different in different workstations. This research results can be used to improve the work environment in construction industry. It is recommended to further investigate specific influencing factors and formulate intervention strategies to improve occupational health.

References

1. Jo, B.W., Lee, Y.S., Kim, J.H., Khan, R.M.A.: Trend analysis of construction industrial accidents in Korea from 2011 to 2015. *Sustainability* **9**, 1297 (2017)
2. Khosravi, Y., Asilian-Mahabadi, H., Hajizadeh, E., Hassanzadeh-Rangi, N., Bastani, H., Behzadan, A.H.: Factors influencing unsafe behaviors and accidents on construction sites: a review. *Int. J. Occup. Saf. Ergon.* **20**, 111–125 (2014)
3. Gittleman, J.L., et al.: [Case Study] CityCenter and cosmopolitan construction projects, Las Vegas, Nevada: lessons learned from the use of multiple sources and mixed methods in a safety needs assessment. *J. Saf. Res. Elsevier* **41**, 263–281 (2010)
4. Da Costa, B.R., Vieira, E.R.: Risk factors for work-related musculoskeletal disorders: a systematic review of recent longitudinal studies. *Am. J. Ind. Med.* **53**, 285–323 (2010)
5. Chakraborty, T., Das, S.K., Pathak, V., Mukhopadhyay, S.: Occupational stress, musculoskeletal disorders and other factors affecting the quality of life in Indian construction workers. *Int. J. Constr. Manag.* **18**, 144–150 (2018). <https://doi.org/10.1080/15623599.2017.1294281>
6. Meseret, M., Ehetie, T., Hailey, G., Regasa, Z., Biruk, K.: Occupational injury and associated factors among construction workers in Ethiopia: a systematic and meta-analysis. *Arch. Environ. Occup. Health* **77**(4), 328–337 (2022)
7. Deakin, J.M., Stevenson, J.M., Vail, G.R., Nelson, J.M.: The use of the Nordic Questionnaire in an industrial setting: a case study. *Appl. Ergon.* **25**, 182–185 (1994)
8. López-Aragón, L., López-Liria, R., Callejón-Ferre, Á.-J., Gómez-Galán, M.: Applications of the standardized nordic questionnaire : a review. *Sustainability* **9**, 1514 (2017)
9. Lette, A., Hussen, A., Kumbi, M., Nuriye, S., Lamore, Y.: Musculoskeletal pain and associated factors among construction construction workers in Southeastern Ethiopia. *Int. J. Ind. Ergon.* **3** (2019)
10. Bodhare, T., Valsangkar, S., Bele, S.: An epidemiological study of work-related musculoskeletal disorders among construction workers in Karimnagar Andhra Pradesh. *Indian J. Community Med.* **36**, 304–307 (2011)
11. Yi, W., Chan, A.: Health profile of construction workers in Hong Kong. *Int. J. Environ. Res. Public Health* **13**, 1232 (2016)
12. Anwer, S., Li, H., Antwi-afari, M.F., Wong, A.Y.L.: Associations between physical or psychosocial risk factors and work-related musculoskeletal disorders in construction workers based on literature in the last 20 years: a systematic review. *Int. J. Ind. Ergon.* **83**, 103113 (2021)
13. Khan, S.C., Ullah, S., Darain, H., Rahman, M.U.: Prevalence of work-related musculoskeletal disorders among construction workers in Hayatabad Peshawar KP Pakistan. *Rehman J. Heal Sci.* **1**, 17–20 (2019)



Establishment and Verification of Flight Fatigue Model Induced by Simulated Aircraft Driving

Wei Jiang¹, Zhenling Chen¹, Haishan Xu¹, Tiebing Liu¹, Lili Li¹, and Xianfa Xu^{1,2}(✉)

¹ Institute of Civil Aviation Medicine, Civil Aviation Medicine Center of Civil Aviation Administration of China, Beijing 100123, China
xuxianfa2012@163.com

² Civil Aviation General Hospital, Beijing 100123, China

Abstract. On the basis of work analysis for airline pilot, joystick operating and instruments monitoring are extracted as the two core tasks, to build a simulation of the aircraft driving induced flight fatigue model. The model including the computerized simulation of dual task operation module, system management module and eye video monitoring module. In the validation study, 15 volunteers were recruited, their scores on the Stanford sleepiness scale (SSS) and their percentage of eyelid closure (PERCLOSE) in the task was recorded for 5 min were collected before and after the fatigue induced task for 3 h. The validity of the model was verified by comparing the subjective and objective fatigue indexes before and after the fatigue induced task. the score of SSS was increased, and the fatigue closure time of eyelid closure was significantly prolonged, all reaching the statistically significant level ($P < 0.01$). The simulation of aircraft dual task model can effectively induce flight fatigue and provide a tool for flight fatigue research.

Keywords: Flight fatigue · Flight simulation · Percentage of eyelid closure

1 Introduction

Flight fatigue is a serious threat to aviation safety. Many flight accidents and accident symptoms are directly or indirectly related to flight fatigue. Pilots' psychological fatigue is not only one of the main hidden dangers of flight safety, but also the main academic difficult problems perplexing the aviation industry. A large number of studies on flight fatigue have been carried out over the past decade, both military aviation and civil aviation [1–3].

The establishment of flight fatigue model based on simulated aircraft driving is of great significance to understand the physiological and psychological mechanisms related to the generation and elimination of flight fatigue. The simulated driving model induced fatigue has been widely used and played an important role in the research of road driving fatigue [4, 5]. However, there are great differences between aviation driving and road driving. Aviation driving operation is more complex and more difficult. The number of instrument panels faced by pilots in the aircraft cockpit is much higher than that of vehicle driving, and many instrument displays are much more complex, which requires

higher attention span of instrument monitoring. Because of the huge differences in the above, the research on flight fatigue, can't be carried out by using road vehicle driving simulator.

At present, all kinds of large aircraft have corresponding cockpit simulators, and the cockpit of simulators is completely consistent with the cockpit of real aircraft, and can also set flight tasks and flight environment. However, due to its high price and few domestic purchases, it is mainly used for pilot training and assessment. Therefore, there is an urgent need to develop a simple and easy civil aircraft simulation driving system to meet the needs of flight fatigue research.

2 Design of Flight Fatigue Model Induced by Simulation

In order to meet the research needs of flight fatigue, the flight fatigue model induced by simulated aircraft driving should have the following three functions: firstly, the function of simulating aircraft driving; secondly, system setting and management functions; thirdly, the function of monitoring and recording whether the subject has fatigue. Therefore, in this model designs three modules corresponding to the above three functions.

2.1 Design of Simulated Aircraft Driving Module

Based on the work analysis of the civil aviation airline pilots, the core indexes are extracted, the computerized interface for simulating civil aviation flight is established, and the dual task for operation and monitoring is adopted [6]. As shown in the top picture of Fig. 1, flight fatigue is induced by simulating continuous dual task. One of the task is to control the "aircraft" for maintaining a balance flight state through the joystick by pushing, pulling, left changing, and right changing. The dynamic picture is used to simulate the aircraft state of motion, which is updated every 50 ms, based on the random interference of sinusoidal variation. The difficulty level is set by self-adaption method. The higher the difficulty level grow, the greater the deviation for the subjects to control. At the same time, the deviation of the control lever operation of the subject shall be recorded. Another task for dual-task is the instrument monitoring task, which monitors the corresponding dynamic instrument status through the six corresponding positions of the keypad. When an instrument warning light turns red, it is an emergency and requires accurate response. When an instrument indicator turns yellow, requires alarm, but can't respond. Record the reaction time, number of correct reactions, number of missed reactions and number of wrong reactions after the red warning light appears in the process of instrument monitoring.

2.2 Design of System Setting Management Module

In the system setting and management module, the roles of personnel participating in fatigue research are set, including administrator, examiner and subject. The roles of administrator and examiner are assumed by researchers. Subjects refer to volunteers recruited by the project of flight fatigue research.

Different role has different tasks and management permissions. The administrator has the highest management permission and is the only global role. Its permissions include setting program schedule, organization management, examiner management and report download. The administrator can view and download the report data of all institutions in all sessions. The role and tasks of the examiner include subject management, examination room management and examination management in which includes organizing examination, invigilating examination, dynamically adding new subjects, data summary and analysis and report download. The examiner only can view and download the data report and original data of examination activities under his management. The subject role is the tested role, whose task is to take an online examination and operate the dashboard and joystick.

2.3 Design of Video Monitoring Module

In the research of driving fatigue for many years, researchers have tried to monitor and evaluate driver fatigue by using subjective scale, EEG algorithm, head position measurement, blink monitoring, PERCLOS (percentage of eyelid closure). The study on comparing these methods show that PERCLOS method is the most reliable [7]. It can infer the occlusion state of the pupil through the image processing of the video output from the pupil module, and calculate the value of eyelid closure for fatigue judgment [8]. Therefore, we decided to use PERCLOS method to monitor and evaluate the fatigue induced by subjects in simulated aircraft driving.

The video monitoring and recording module of the subject face, especially the eyes, is constructed in our model, as shown in the lower left of Fig. 1. The camera is placed in front of the subject, parallel to the eye position of the acquisition device. The HD camera



Fig. 1. Operation of the model for inducing flight fatigue by simulated aircraft driving

is used and supported by a tripod to ensure the stability of the camera. When the subject starts the simulation dual task, it starts to record and collect the blink information. The examiner should make corrections during the examination, as shown in the lower right of Fig. 1. Then use the visual analysis software to process the video image, record and analyze the eyelid closure value of each blink, and output the PERCLOS value of each specified period.

3 Validation of Model Induced Flight Fatigue

3.1 Method

3.1.1 Volunteers

15 volunteers were recruited as subjects to carry out the fatigue inducing task of simulating aircraft driving operation for a total of 3 h, aged 30–45 years, in good health, with sufficient sleep 1–2 days before the experiment, and coffee and tea drinks are prohibited.

3.1.2 Test Tools

Stanford Sleepiness Scale

Stanford Sleepiness Scale (SSS) is a subjective fatigue perception scale commonly used in fatigue research. It adopts 7-point hierarchical evaluation, corresponding to 7 descriptions of fatigue state respectively [9, 10]. The degree of fatigue continues to improve. The content of the scale is concise, clear and easy to understand, which is convenient for testers to report themselves.

Eyelid Closure

PERCLOS refers to the percentage of eyelid closure time in the whole blink time during each blink. P80 is often used to define fatigue standard in PERCLOS fatigue research [9]. P80 refers to the situation that the above value is greater than or equal to 80%, that is, the eyelid closing time is greater than or equal to 80% in a blink process, which is considered to be a blink process of fatigue. Referring to the methods of relevant research, [8] if there is I times eye closure in the continuous sampling period T , and the time when the pupil of the I eye closure is covered by the eyelid for 80% is T_i , the PERCLOS value can be calculated by Formula 1.1

$$\text{PERCLOS} = \frac{\sum_{i=1}^n t_i}{T} \quad (1.1)$$

In this study, in order to verify fatigue, the PERCLOS testing time are in the beginning 5 min which after 20 min practice for mastering and familiar with task and the last 5 min of 3-h fatigue simulation task.

3.1.3 Experimental Procedure

The experimenter act as the administrator to set the program list. In this experiment, based on the pre-study, we set the task difficulty as 65 levels (the task difficulty range is 1–100 levels), set the double task introduction and practice time for 10 min, and then

after 2 min rest., start the formal 3 h dual-task simulation. In order to prevent muscle pain or stiffness caused by long-term continuous operation, we set 1.5 min of rest after every 20 min of continuous operation for muscle relaxation.

The examiner arranged the subjects to participate in the simulated flight fatigue operation, introduced the model and experimental requirements, and filled in the informed consent form. Then examiner teach the subjects to learn to perform dual task operation and supervise the operation process. The subjects sit in front of the computer, their faces, including their eyes, are facing the HD camera, and their eye movement is recorded in the whole process for PERCLOS analysis. The flight fatigue model system automatically collects the real-time experimental data. The eye movement of subjects was recorded in the whole process with high-definition camera, and PERCLOS analysis was calculated with computer program.

Before and after the simulated driving task, the subjects were investigated with the Stanford Sleepiness Scale, and the results were recorded by examiner.

3.1.4 Data Analysis

SPSS was used to input and sort out the scale values and PERCLOS values before and after the task. The paired sample t-test method was used to analyze and investigate the differences between before and after the continued dual-task. $P < 0.05$ was statistically significant.

3.2 Results

3.2.1 Results of Stanford Sleepiness Scale

The statistical analysis results of the sleepiness scale of 15 volunteers are shown in Table 1. After 3 h simulated flight fatigue task, the fatigue degree of the subjective reports of all volunteers has increased, three volunteers has increased from grade 1 to grade 2, five volunteers has increased from grade 2 to grade 3, six volunteers has increased from grade 1 to grade 3, and one volunteer has increased from grade 2 to grade 4. The results of paired t-test showed that the difference before and after the task reached a statistically significant level, $t(14) = 11.00$, $P < 0.01$.

3.2.2 PERCLOS Results

The PERCLOS values of 18 volunteers in the 5 min before the simulated task and the 5 min after the 3-h simulated task are shown in Table 1. The last 5 min PERCLOS value after the 3-h simulated task of all volunteers increased by different ranges. The average number of PERCLOS after fatigue induced task was 18.32. According to the fatigue standard of PERCLOS greater than 15%, [9] the volunteers induced different degrees of fatigue after 3 h of simulated task. The results of paired t-test showed that the difference before and after the 3 h simulated flight fatigue task reached a statistically significant level, $t(14) = 3.92$, $P < 0.01$.

Table 1. The change of SSS and PERCLOS between the pre-task and post-task

Index	Pre-Task	Post-Task	T Value	P Value
Score of SSS	1.40 ± 0.51	2.87 ± 0.52	11.00	0.000
PERCLOS (%)	0.37 ± 0.35	18.32 ± 17.63	3.92	0.001

4 Discussion

The research of flight fatigue has become an important topic in field of aviation human factors. The establishment of flight fatigue model induced by simulated aircraft driving is of great significance to the research of flight fatigue and the protection of aviation safety. There are many ways to induce flight fatigue, “sleep deprivation model” and “cognitive task model” are the mainly methods. “Sleep deprivation model” often induces fatigue by limiting people’s sleep time and sleep quality, mostly passively; “Cognitive task model” induces people’s mental fatigue through continuous cognitive activities, and emphasizes people’s active participation [11]. Therefore, compared with the “sleep deprivation model”, the “cognitive task model” is more in accord with the cognitive activities of flight. Based on the work analysis of pilots in civil aviation, our study establishes a dual task cognitive model with operation and monitoring as the core task.

In this study, the induced flight fatigue model was preliminarily verified. After completing the 3-h fatigue inducing task, the subjective reported fatigue degree of all volunteers increased by 1 to 2 scores. At the same time, this model adopts the objective index based on eyelid closure, by comparing the PERCLOS (p80) data after and before the induced fatigue task, the results showed that the eye closure time was prolonged and the PERCLOS index increased after the fatigue task. Therefore, both subjective and objective indicators verify that the model successfully induces mental fatigue through continuous dual task.

At the other hand, this model can flexibly set the task difficulty and task time in the form of program list. Two single tasks of operation and monitoring and dual tasks can be selected. The difficulty level of each cognitive task can also be adjusted to change the cognitive load and investigate the impact of different workload intensity on flight fatigue. In future research, this model can be used to further study the mechanism of flight fatigue, so as to provide basic data for flight fatigue risk control and aviation safety.

5 Conclusion

Based on the work analysis of the pilots in civil aviation, this study establishes a computer interface simulation aircraft driving induced flight fatigue model, which has the function of simulating aircraft driving, as well as the function of system setting and management, monitor and evaluation flight fatigue through eyelid closure. After preliminary verification, the subjective fatigue report and the objective index of eyelid closure show that the model is effective and can successfully induce flight fatigue. This model can provide basic research platform and technical support for fatigue research in the future.

Acknowledgement. This work is supported by the National Natural Science Foundation of China, No. u1333132 and Major science and technology projects of Civil Aviation Administration of China, No. mhrd20140101.

Compliance with Ethical Standards. The study was approved by the Logistics Department for Civilian Ethics Committee of civil aviation medicine center of CAAC.

All subjects who participated in the experiment were provided with and signed an informed consent form.

All relevant ethical safeguards have been met with regard to subject protection.

References

1. Ling, L., Zhang, Y.: Current status and future direction of mental fatigue research in civil aviation pilots. *Space Med. Med. Eng.* **28**(01), 74–78 (2015)
2. Reis, C., Mestre, C., Canho, H.: Prevalence of fatigue in a group of airline pilots. *Aviation Space Environ. Med.* **84**(8), 828–833 (2013)
3. Jiang, W.D., Xia, C.M., Zhang, Y., et al.: Static fatigue analysis of upper trapezius muscle based on factual dimension of mechanomyography. *Space Med. Med. Eng.* **32**(03), 259–264 (2019)
4. Zhao, S.F., Xu, G.H.: Study on fatigue driving based on driver model parameter identification. *China Saf. Sci. J.* **20**(9), 38–44 (2010)
5. Liu, P., Jiang, C.H., Xiong, J., et al.: Detection of human eye status in the study of driving fatigue. In: Chinese Biomedical Engineering Academic Conference 2007, Shanxi, Xian (2007)
6. Jiang, W., Feng, T.Z., Pan, J.: Development and psychometric analysis of cognitive aptitude battery for Chinese AB-INITIO pilots in civil aviation. *J. Prev. Med. Chin. PLA* **32**(2), 122–124 (2014)
7. Dinges, D.F., Grace, R.: PERCLOS: a valid psychophysiological measure of alertness as assessed by psychomotor vigilance. Federal Highway Administration Publication No. FHWA-MCRT-98-006 (1998)
8. Guo, B.Y., Fang, W.N.: Fatigue detection using eye tracking system. *Space Med. Med. Eng.* **17**(4), 256–260 (2004)
9. David, F.D., Richard, G.: PERCLOS: a valid psychophysiological measure of alertness as assessed by psychomotor vigilance. Federal Highway Administration Publication No. FHWA-MCRT-98-006 (1998)
10. Liu, J., Liu, X., Wang, X.Y., et al.: Effects of prolonged driving on driving safety under real road condition. *China Saf. Sci. J.* **21**(03), 9–15 (2011)
11. Pilcher, J.J., Band, D., Odle-Dusseau, H.N., et al.: Human performance under sustained operations and acute sleep deprivation conditions: toward a model of controlled attention. *Aviat. Space Environ. Med.* **78**(1), B15–24 (2007)



Comparative Study on Inducing Effect of Two Kinds of Shape Flash in Pilot Selection by EEG Detection

Yongsheng Chen^(✉) and Dawei Tian

Air Force Medical Center, PLA, Beijing 100142, China
chenyongsheng65@sina.com, tiandawei@163.com

Abstract. Objective To compare the differences of two types of EEG flash evoked effect in pilot selection, and to provide evidence for optimizing the effect of EEG pilot selection. **Methods** A total of 500 high school students aged 17 to 20 were selected to participate in the Air Force pilot selection in 2020 to 2021. Two kinds of flash (arc and round plate) were used for flash evoked selection respectively. There were 250 people in the arc shaped lamp group and 250 people in the round plate shaped lamp group, and the selection effect and difference of the two kinds of different shaped flash lamp were compared. **Results** In the arc-shaped group, 238 patients (95.2%) had normal EEG photic driving response. There were 12 patients (4.8%) with abnormal EEG, including 6 patients (2.4%) with abnormal photic driving, 2 patients (0.8%) with multiple reaction, 3 patients (1.2%) with fractional reaction, and 1 patient (0.4%) with abnormal EEG wave. There were 237 (94.8%) normal EEG photic driving in the round plate lamp group. There were 13 patients (5.2%) with abnormal EEG, including 5 patients (0.2%) with abnormal photic driving, 3 patients (1.2%) with multiple reaction, 3 patients (1.2%) with fractional reaction, and 2 patients (0.8%) with abnormal EEG wave. There was no significant difference between the eliminate rates ($X^2 = 0.890$, $P = 1.000$). The elimination rate of arc shaped lamp group was 4.8%, and that of round plate shaped lamp group was 5.2%, there was no significant difference between them ($X^2 = 0.042$, $P = 0.837$). **Conclusion** The evoked effect of two kinds of shaped flash is basically the same.

Keywords: Flash · Appearance · Flash evoked selection · Electroencephalogram (EEG) · Pilot selection · High school student

1 Introduction

Intermittent photic stimulative induction (IPSI) is one of the key procedures for pilot selection (including closing eye, open-closing eye, hyperventilation, photic driving in EEG examination). The purpose is to screen for “photosensitive epilepsy” [1]. Arc shaped flash is specially designed for pilot selection, but is bulky and not easy to carry. Demand for mobile selection, designed the round plate shaped flash, size relatively smaller than that of arc shaped flash, luminosity decreased, to prevent decrease of evoked effect due

to smaller size, luminosity decline, it is necessary to compared with arc shaped flash to round plate shaped flash in order to provide the accuracy and effectiveness for pilot selection.

2 Objects and Methods

2.1 Objects and Group

500 male high school graduates, aged 17 to 20 years old, with an average age of 18 ± 2.4 years old, were selected to participate in the recruitment selection in 2020–2021. They were healthy and had no history of neuro-psychiatric diseases or drug use. All of them passed the primary and comprehensive examination of the Air Force pilot selection. Five hundred people were divided into two groups, 250 in each group.

2.2 Methods

2.2.1 Equipment

(1) Arc Shaped Flash Lamp

The shell of the flash lamp is curved, including an Angle of radian of 127° , the luminous surface circumference of 50 cm, transparent plexiglass, built-in 3 rows of 27 light-emitting diodes, the total brightness $>20 \text{ cd/m}^2$ [2]. Placed 30 cm in front of the eyes during EEG examination.

(2) Round Plate Shaped Flashlight

The flashlight is a round plate shell, the diameter of the luminous surface is 15 cm, which is transparent plexiglass, and 11 leds are evenly distributed in it. The total brightness is less than 15 cd/m^2 , and it is placed 15 cm in front of the eyes during EEG examination. Both types of flash use the same evoked frequency, flash stimulation time and interval time (8 Hz, 10 Hz, 13 Hz, 15 Hz; The flash stimulation time 5 s and interval time 5 s) appearance shown in Fig. 1 and Fig. 2.



Fig. 1. Arc shaped flash



Fig. 2. Round plate shaped flash

2.2.2 Examine Procedure

The use of flash lights during the EEG examination was conducted in stages, one during the pilot selection in 2020 and the other during the pilot selection in 2021.

2.2.3 The Selection Criteria

Based on the electroencephalogram standard in the physical examination method of flight cadets recruited by the PLA Air Force, and the EEG shall be identified as normal or abnormal [1, 3–5].

2.3 Statistic Analysis

Detection rate and elimination rate were calculated according to the normal and abnormal number of IPSI and eliminated number in the two groups, and X^2 test between multiple rates was performed. 0.05 means the difference is statistically significant, and the data is expressed as %.

3 Results

3.1 Comparison of IPSI Number of Two Types of Flash

In arc shaped flash group, 238 people (95.2%) had normal photic driving reaction. There were 12 students with abnormal reaction, accounting for 4.8%, including 6 patients with photic driving reaction, accounting for 2.4%, 2 students with multiple reaction, accounting for 0.8%, 3 students with fractional reaction, accounting for 1.2%, and 1 person with abnormal brain wave, accounting for 0.4%. In round plate shaped flash group, 237 people (94.8%) had normal photic driving reaction. The number of abnormal reactions was 13 (5.2%), among which 5 (0.2%) had photic driving reactions, 3 (1.2%) had multiple reactions, 3 (1.2%) had fractional reactions, and 2 (0.8%) had abnormal brainwaves, as shown in Table 1.

Table 1. Comparison of IPSI number of two types of flash (n = 500, %)

Equipment	EEG index													
	Normal						Abnormal							
	Photic driving	%	Multiple reaction	%	Decimal reaction	%	Photic driving	%	Multiple reaction	%	Decimal reaction	%	Abnormal brain wave	%
Arc flash group (250)	238	95.2	0	0	0	0	6	2.4	2	0.8	3	1.2	1	0.4
Round plate flash group (250)	237	94.8	0	0	0	0	5	0.2	3	1.2	3	1.2	2	0.8

3.2 Comparison of IPSI Inspection Effect of Two Kinds of Flash

IPSI detection rates of the two types of flash lamps are shown in Table 2.

Table 2. Comparison of IPSI efficiency between two types of flash (n = 500, %)

Equipment	EEG index				
	Normal	Abnormal			
	Photic driving	Photic driving	Multiple reaction	Decimal reaction	Abnormal brain wave
Arc flash group (250)	95.2a	2.4a	0.8a	1.2a	0.4a
Round plate flash group (250)	94.8a	0.2a	1.2a	1.2a	0.8a
χ^2			0.089		
P			1.000		

Note: A indicates that there is no significant difference among indexes in each column, $P > 0.05$.

3.3 Comparison of IPSI Elimination Rates of Two Kinds of Flash

The elimination rates of the two types of flash are shown in Table 3.

Table 3. Comparison of IPSI elimination rates of two flash (n = 500, %)

	Normal EEG	Abnormal EEG
Arc flash group (250)	238 (95.2)	12 (4.8)
Round plate flash group (250)	237 (94.8)	13 (5.2)
χ^2	0.042	
P	0.837	

4 Discussion

4.1 The Differences Between the Two Types of Flash

Arc shaped flash is specially designed for EEG pilot selection and is large in size. Three rows of 21 leds are installed inside the lamp, and the flash brightness exceeds 30 cd/m^2 , using a folding stents. The diameter of the round plate shaped flash is only 15 cm, which is much smaller than the volume of the arc shaped flash. Only 9 leds are set in the lamp body, and the flash brightness is 15 cd/m^2 . For easy carrying, it uses a flexible snakeskin tube holder, and the overall weight is much lighter than the arc shaped flash. Because of the reduction of the lamp body, the luminance decreases correspondingly, and the brightness drops by more than half compared with the arc shaped lamp, which is the only shortcoming compared with the arc shaped flash lamp.

4.2 The Use Effect of the Two Types of Flash is the Same

In the normal EEG evoked by flash light, 95.2% (238/250) and 94.8% (237/250) were evoked by arc shaped flash light and round plate shaped flash, respectively. It shows that the two kinds of flash successfully induced more than 90% of the students' photic driving effect, and the overall inspection effect of the flash is good. Multiple response, fractional response and abnormal brainwave indexes are the specific manifestations of IPSI. In the abnormal EEG evoked by arc shaped flash, the detection rates of photic driving response, multiple response, fractional response and abnormal brainwave were 2.4%, 0.8%, 1.2% and 0.4%, respectively. The detection rates of multiple reaction, fractional reaction and abnormal brainwave in round plate flash lamp were 0.2%, 1.2%, 1.2% and 0.8%, respectively. There was no significant difference ($X^2 = 0.890$, $P = 1.000$), indicating that although the brightness of the round plate shaped flash was lower than that of the arc shaped flash, it was still able to distinguish the difference of abnormal EEG.

The IPSI effect depends on the frequency, duration, time interval, luminance of the lamp body and the induced distance (the horizontal distance between the lamp body and the eye) [4–9]. In this study, IPSI stimulation frequencies selected by pilot selection of Air Forec are used for the two types of flash lamps in accordance with the regulations: 8 Hz, 10 Hz, 13 Hz, 15 Hz; The duration of the stimulus was 5 s, and the interval was 5 s. Therefore, the only possible factors affecting the induction effect were flash brightness and stimulus distance. However, the results showed that there was no significant difference in EEG elimination induced by the two types of flash ($X^2 = 0.042$, $P = 0.837$), which might compensate for the difference caused by the reduced brightness of the round plate shaped flash by shortening the distance between the flash and the eye. The horizontal distance between the flashlight and the eye is 20–30 cm (horizontal distance), which is the conventional distance for clinical EEG examination. In this study, the round plate shaped flashlight was placed 15 cm in front of the eyes to obtain the inducing effect compared with the conventional 30 cm, indicating that the horizontal distance of the round plate shaped flashlight is feasible under the current design parameters.

Compliance with Ethical Standards. The study was approved by the Logistics Department for Civilian Ethics Committee of Air Force Medical Center, PLA.

All subjects who participated in the experiment were provided with and signed an informed consent form.

All relevant ethical safeguards have been met with regard to subject protection.

References

1. Chen, Y., Zhu, L., Liu, X., et al.: Study on electroencephalogram flash induction technique and identification index in medical examination. *Chin. J. Aerosp. Med.* **28**(2), 97–101 (2017)
2. Chen, Y., Jia, H.: Development of portable electroencephalogram testing kit. *Med. Equip.* **36**(12), 43–48 (2015)
3. Rosenow, F., Klein, K.M., Hamer, H.M.: Non-invasive EEG evaluation in epilepsy diagnosis. *Expert Rev. Neurother.* **15**(4), 425–444 (2015)

4. Gao, X., Guo, D., Feng, Y.: Study on the improvement of EEG positive rate by rhythmic flash stimulation-analysis of 109 cases of clinical EEG flash stimulation. *J. Brain Neurol. Dis.* **2**(1), 23–24 (1994)
5. Ebersole, J.S., Pedley, T.A.: *Modern Clinical Electroencephalography*. Expert Group of Chinese Anti-Epilepsy Association, trans., pp. 120–240. People’s Medical Publishing House, Beijing (2009)
6. Koutroumanidis, M., Tsirka, V., Panayiotopoulos, C.: Adult-onset photosensitivity: clinical significance and epilepsy syndromes including idiopathic (possibly genetic) photosensitive occipital epilepsy. *Epilepsy Dis.* **17**(3), 275–286 (2015)
7. Kasteleijn-Nolst Trenité, D., Rubboli, G., Hirsch, E., et al.: Methodology of photic stimulation revisited: updated European algorithm for visual stimulation in the EEG laboratory. *Epilepsia* **53**(1), 16–24 (2021)
8. Chen, X., Sha, F., Jiang, W.: Photosensitivity and EEG analysis of intermittent flash stimulation in children with epilepsy. *J. Clin. Neurol.* **32**(1), 29–32 (2019)
9. Su, Q., Gan, W.: Clinical analysis of video electroencephalogram in children with intermittent flash stimulation positive epilepsy. *Med. Rev.* **26**(17), 3532–3536 (2020)



Application of Multi-motive Grid for Acceptance Test in the Pilots

Yan Zhang, Yang Liao, Yishuang Zhang, Jian Du, and Liu Yang^(✉)

Air Force Medical Center, Air Force Medical University of PLA, Beijing 100142, China
yangliuhenry@aliyun.com

Abstract. *Objective:* To study the applicability of Multi-motive Grid for Acceptance (MMG) in the pilots. *Methods:* 43 pilots completed the MMG, and the internal correlation, differentiation and reliability of the scale were tested according to their results. *Results:* The cronbach's alpha of three kinds of motivation and six kinds of motivation tendency measured by the scale ranged from 0.800 to 0.931, and the guttman split-half ranged from 0.710 to 0.899. The degree of differentiation ranged from 0.66 to 0.74. The internal correlation between the approach and avoidance direction of each motivation is consistent with the previous research results. *Conclusion:* This scale can be used as a measuring tool to evaluate pilot motivation.

Keywords: Pilot · Achievement motivation · Affinity motivation · Power motivation

1 Introduction

Motivation stimulates individual psychological energy and guides individuals to important tasks and goals. Pilots with stronger internal motivation can obtain more comprehensive flying experience [1]. A comparative study on flight training effectiveness and motivation shows that motivation can predict flight training effectiveness and the possibility of training flight cadets in aviation university [2]. Therefore, motivation measurement plays an important role in pilot psychological evaluation. There are two traditional forms of motivation measurement in psychometric field: self-reported questionnaire and thematic apperception test. For example, the Aeromedical Consult Service (ACS) of the Us Air Force Aviation Medical College developed a Pilot Motivation Scale and Determination Scale in order to better investigate the pilot motivation and determination. Declarative statements can be used to ask subjects directly what their goals are or what they would choose to do in a specific situation. However, the questionnaire method has some disadvantages such as poor task camouflage and social acceptability bias. Thematic apperception tests can explore individual motivations through individual imagination or free association (projection), and reveal potential tendencies that individuals are unwilling or unable to recognize [3]. However, its measurement and interpretation are relatively complicated and difficult to be used in the pilot evaluation. Multi-motive Grid for Acceptance (MMG) is a new method to measure implicit motivation developed in recent years.

It combines the characteristics of thematic apperception test and self-reported questionnaire, which can not only measure the conscious and unconscious motivation tendency of individual self-concept, but also facilitate the implementation of the test and the interpretation of results. This study will preliminarily explore the feasibility of this scale in the pilots.

2 Object and Method

2.1 Object

There were 43 pilots, all male, aged from 28 to 47.

2.2 Method

2.2.1 Assessment Tools

The MMG contains 14 images, all of which are taken from the fuzzy contour map of thematic apperception test. A series of statements are attached to each image to describe the thoughts or feelings that people may have under this image situation [3]. MMG uses grid technology to design pictures (i) and statements (j) into $i \times j$ matrix or grid, which is composed of six motivational tendencies: Hope of success (HS), Fear of failure (FF), Hope of Power (HP), Fear of power (FP), Hope of affiliation (HA), and Fear of reject. These can be calculated as three motivations: achievement motivation, affinity motivation, and power motivation [4].

2.2.2 Statics Analysis

SPSS18.0 was used to analyze the reliability and differentiation of each subscale, and the internal correlation between each subscale was calculated.

3 Result

3.1 Reliability Analysis

The results are shown in Table 1. The cronbach's alpha was between 0.800–0.931, and the guttman split-half was between 0.710–0.899.

Table 1. Cronbach's alpha and Guttman split-half of MMG ($n = 43$)

Dimension	Cronbach's alpha	Guttman split-half
HS	0.853	0.710
FF	0.908	0.892
HA	0.831	0.853
FR	0.914	0.899
HP	0.931	0.894
FP	0.876	0.750
Achievement motivation	0.800	0.736
Affinity motivation	0.843	0.837
Power motivation	0.925	0.859

3.2 Discrimination Analysis

The discrimination of subscales is analyzed as shown in Table 2. The discrimination of related dimensions of each scale ranged from 0.66 to 0.74, all of which were greater than 0.4.

Table 2. Discrimination of subscales ($n = 43$)

Dimension	Discrimination
Achievement motivation	0.67
Affinity motivation	0.74
Power motivation	0.66

3.3 Internal Correlation Analysis

As shown in Table 3, all negative correlations occurred between the direction of approach and avoidance. There was a significant negative correlation between HS and FF in achievement motivation ($r = -0.348, p < 0.05$), and a low correlation between HA and FR in affinity motivation ($r = -0.222, p > 0.05$), although the latter was not a negative correlation. However, there was a positive correlation between the two tendencies of power motivation ($r = 0.316, p < 0.05$), which was consistent with the application of this scale in Chinese college students [5].

Table 3. Correlation analysis between dimensions of MMG ($n = 43$)

	HS	FF	HA	FR	HP
HS	1				
FF	-0.348*	1			
HA	0.585**	-0.042	1		
FR	-0.454**	0.732**	-0.222	1	
HP	0.162	0.478**	0.308*	0.426**	1
FP	-0.554**	0.697**	-0.213	0.740**	0.316*

* $P < 0.05$, ** $P < 0.01$

4 Discussion

Motivation is the inner driving force of flight psychological activities, and it is the relatively stable and lasting trait as well as effective power that motivate pilots to achieve flight success. At present, the most studied and applied motivations are achievement motivation, power motivation and affinity motivation [4], and scholars have realized the important position of these three motivations in selecting, motivating and developing employees. However, as for self-reported questionnaire and thematic apperception test, there are many measures of achievement motivation, but few measures of power motivation and affinity motivation [6]. Therefore, MMG is a supplement and improvement to the traditional questionnaire and projection test, which combines the advantages of both tests, reduces the surface validity of the test, and facilitates the implementation and interpretation.

The results of this study show that the MMG has good reliability and discrimination ability when applied to pilot population. In the internal relationship of each motivation tendency, except the two tendencies of power motivation are positively correlated, the two tendencies of achievement motivation and affinity motivation are negatively correlated. This may be due to cultural differences, where Asian countries tend to shy away from reporting sensitive traits and behaviors such as power-seeking. However, some foreign studies have found that the correlation between the two tendencies of power motivation is 0.11 [5, 7, 8], suggesting that MMG also has good construct validity when used in pilot groups. The current results support existing theories and research hypotheses.

From the demand of pilot group for the three motivations, the high risk and high challenge of flying career make pilots have to make great efforts to deal with the problems of increasing flight load and changing driving mode. Sufficient achievement motivation is an important factor to support them to achieve success in training and complete various tasks successfully. At the same time, due to the requirements of network information sharing, more team actions make pilots pay more attention to team cooperation than before, and strong affinity motivation helps to form team cohesion. In joint missions, pilots need to change their focus from flight control to task management and provide guidance, instruction and intangible strength encouragement to team members at any time. This motivation characteristic required by the intention of leadership role is power

motivation. Therefore, achievement motivation, affinity motivation and power motivation are important factors affecting the psychological effectiveness of pilots, and can be used to reflect the psychological traits related to flight performance.

5 Conclusion

In conclusion, this study verified the applicability of MMG in the pilots, suggesting that the scale can be used as a measurement tool to measure achievement motivation, affinity motivation and power motivation simultaneously, providing a new method to evaluate excellent traits of pilots.

Acknowledgement. This work is supported by the Foundation Strengthening Program Technical Area Fund, No. 2020-JCJQ-JJ-370.

Compliance with Ethical Standards. The study was approved by the Logistics Department for Civilian Ethics Committee of Air Force Medical Center. All subjects who participated in the experiment were provided with and signed an informed consent form. All relevant ethical safeguards have been met with regard to subject protection.

References

1. Marshburn, T.H.: Why they fly: an expectancy-based analysis of the factors that motivate commissioned Army aviators to gain flying experience. Fort Leavenworth (KS): U.S. Army Command and General Staff College (2007)
2. Forsman, J.W.: The creation and validation of a pilot selection system for a Midwestern university aviation department. Minnesota State University, Mankato (MN) (2012)
3. Sokolowski, K., Schmalt, H.D., Langens, T.A., et al.: Assessing achievement, affiliation, and power motives all at once: the multi motive grid (MMG). *J. Pers. Assess.* **74**(1), 126–145 (2000)
4. Can, J., Min-qiang, Z., Li, W., et al.: Revised report on the Chinese version of the multiple motivational grid test (MMG-S). *Stud. Psychol. Behav.* **8**(1), 49–53 (2010)
5. Lu-fang, L.: Research on the reliability and effectiveness of multi-motivation grid technology. Liaoning Normal University, Liaoning (2009)
6. Li-ping, Y.: Social motivation and its relationship with well-being. *Soc. Psychol. Res.* (4), 18–25 (1997)
7. Schmalt, H.D.: Power motivation and the perception of control. In: Halisch, F., Kuhl, J. (eds.) *Motivation, Intention, and Volition*. Springer, Berlin, Heidelberg (1987). https://doi.org/10.1007/978-3-642-70967-8_9
8. Schmalt, H.D.: Assessing the achievement motive using the grid technique. *J. Res. Pers.* **33**(2), 109–130 (1999)



Evaluation of Different Salmonella and Escherichia Coli Antibodies Based on ELISA

Yan Gao¹, Yanan Huang², Shuxin Du¹, Weifeng Xia¹, and Fengfeng Mo²(✉)

¹ School of Engineering, Huzhou University, Huzhou 313000, China

² Department of Naval Nutrition and Food Hygiene, Naval Medical University, Shanghai 200433, China
mo.feng.feng@smmu.edu.cn

Abstract. With the development of food hygiene industry, food safety has gradually become a major problem threatening human life and health. Food bacterial infection and food poisoning are the most widespread phenomena in foodborne diseases. The specific detection of foodborne pathogens is one of the effective measures to prevent foodborne diseases. At present, the commercial antibodies against foodborne pathogens are also common in the market, nevertheless, the specificity of these antibodies in the market has not been systematically evaluated. In order to better comprehend the application effect of commercial antibodies in the market, we choose Salmonella antibodies and Escherichia coli antibodies in the market as examples and evaluate the specificity of the six antibodies by enzyme-linked immunosorbent assay (ELISA), so as to find the best Salmonella antibody and Escherichia coli antibody by evaluating the experimental data.

Keywords: Food safety · Salmonella · Escherichia coli · Antibody · Specificity

1 Introduction

Salmonella and Escherichia coli are common foodborne pathogens that cause serious harm to human body, and they are the most common pathogenic microorganisms causing diarrhea [1]. Therefore, the detection and precaution of food pollution caused by Salmonella and Escherichia coli play an important role in food safety. With the development of biomedicine, microbial detection technologies emerge in endlessly. Among them, fast detection and excellent performance are the focus of technical research. The use of bacterial antibodies has been a very mature method among a variety of detection methods, such as agglutination reaction, serological identification and enzyme-linked immunosorbent assay (ELISA) and so on. With a more particular knowledge of the COVID-19 strain, COVID-19 antibody detection is being widely used to control the spread of the virus. Enzyme linked immunosorbent assay (ELISA) is common in the process of using antibodies to specially detect bacteria. Which is mainly based on the solid phase of antigen or antibody and its enzyme labeling. The antigen or antibody is connected with an enzyme and form an enzyme labeled antigen or antibody. Such

enzyme labeled antigen or antibody retains both its immune activity and enzyme activity [2]. During detection, the sample to be tested reacts with the antigen or antibody on the surface of the solid-phase carrier and then form an immune complex. Generally, the immune complex formed on the solid-phase carrier is separated from other substances in the solution through multiple washing, and then the enzyme labeled antigen or antibody is added and combined on the solid-phase carrier through reaction. At this time, the amount of enzyme on the solid-phase is in a certain proportion to the amount of the tested substance. After adding the substrate of the enzyme reaction, the substrate and the enzyme have a color reaction, and the amount of the obtained product is directly related to the amount of the tested substance in the sample, so it can be analyzed qualitatively or quantitatively according to the color depth [3].

The conventional bacterial antibody preparation methods on the market mainly include serum technology and hybridoma technology. Serum technology includes antigen preparation, animal immunization, antiserum preparation and specific antibody purification. Hybridoma technology is mainly to immunize mice with antigen, obtain splenocytes from super immune donors, then fuse with myeloma cells with genetic markers and adapted to tissue culture, then determine the ability of hybrid cells to secrete antibodies, and finally clone and build a single cell [4]. Most of the antibodies prepared by serum technology are polyclonal antibodies. Polyclonal antibodies have poor homogeneity and weak specificity. They are prone to cross reaction when used in immunological detection [5]. Most monoclonal antibodies prepared by hybridoma technology are mouse derived. The prepared antibodies target a certain antigenic determinant, and the antigenic valence often cannot form a network precipitation with the antigen [6]. In order to effectively evaluate the detection effect of bacterial antibodies in the domestic market, we selected a series of Salmonella and Escherichia coli antibody products in the market and test their specificity, so as to screen the antibodies with the best performance.

2 Materials and Methods

2.1 Experimental Materials

Salmonella typhimurium (CCTCC AB 204062), Escherichia coli (CCTCC AB 93154), Escherichia coli BL21 (CCTCC AB 204033), Staphylococcus aureus (CCTCC AB 91093) and Extraintestinal Escherichia coli (CCTCC AB 2013345) were purchased in the Chinese typical culture collection center. Salmonella monoclonal antibody (SM-Mab-01)/Salmonella antibody 1, Escherichia coli O157 monoclonal antibody (EC-Mab-01)/Escherichia coli antibody 1 were purchased from Shanghai Huiyun Biotechnology Co., Ltd. Salmonella antibody 2, Escherichia coli antibody 2, Escherichia coli antibody 3 and Escherichia coli antibody 4 were donated to Shanghai University of technology. ELISA chromogenic solution, ELISA termination solution, secondary antibody (A0216), 1xPBS solution, purchased from Shanghai Beyotime Biotechnology Co., Ltd. 96 well plate, purchased from Sangong Bioengineering (Shanghai) Co., Ltd.

2.2 Specific Detection of Salmonella Antibody

Take Salmonella typhimurium, Escherichia coli, Escherichia coli BL21, Staphylococcus aureus and parenteral Escherichia coli with a concentration of about 10^9 cfu/mL,

the antibody concentration is 25 ug/mL, and the control is PBS. ELISA experimental conditions: antigen incubation plate for 1 h, blocking for 1 h, primary antibody hole for 1 h, secondary antibody for 1 h, color development for 10 min and termination for 5 min.

The specific steps are as follows: The different bacteria in PBS solution were directly coated on the plate, arranged in vertical rows, 100 μ L per well, placed at 37 °C for 1 h, washed with PBST four times, and dried by shaking. 5% skim milk powder solution was prepared with 1 \times PBS, and the plate was sealed with 200 μ L per well. After 1 h at 37 °C, the plate was washed with PBST four times and dried by shaking. The antibody was diluted to 25 ug/mL, and placed in a horizontal row according to the type of antibody, adding 100 μ L to each well. After incubation at 37 °C for 1 h, the plate was washed with PBST four times and dried by shaking. Add secondary antibody 100 μ L (1:250) to each well, incubate at 37 °C for 1 h, wash the plate with PBST for five times, and dry by shaking. Add 100 μ L ELISA color buffer to each well, and react at 37 °C for 10 min away from light. On the basis of the previous step, 100 μ L per well ELISA stop solution was added to stop the reaction. 5 min later, the absorbance value of each well at 450 nm was measured with a microplate reader.

2.3 Specific Detection of Escherichia Coli Antibody

Take Salmonella typhimurium, Escherichia coli, Escherichia coli BL21, Staphylococcus aureus and parenteral Escherichia coli with a concentration of about 10^9 cfu/mL. The blank group is PBS and the antibody concentration is 40 ug/mL. ELISA experimental conditions: antigen incubation plate for 1 h, blocking for 1 h, primary antibody for 1 h, secondary antibody for 1 h, color development for 10 min and termination for 5 min.

The specific steps are as follows: The processed PBS bacteria were directly coated on the plate, arranged in vertical rows with 100 uL in each hole, placed at 37 °C for 1 h, washed with PBST four times, and dried by shaking. 5% skim milk powder solution was prepared with 1 \times PBS, and the plate was sealed with 200 uL per well. After culturing at 37 °C for 1h, the plate was washed with PBST four times and dried by shaking. The antibody was diluted to 40 ug/mL and placed in a horizontal row according to the type of antibodies. The diluted antibodies were added into each well with 100 uL, and the rest as above.

3 Results and Discussion

3.1 Specificity Test of Salmonella Antibody

In different Salmonella antibody specificity test experiments, 25 ug/mL Salmonella antibody and 10^9 cfu/mL Salmonella typhimurium, Staphylococcus aureus, Escherichia coli, Escherichia coli BL21 and extraintestinal Escherichia coli were selected to detect the specificity of Salmonella antibody by ELISA. The experiment was repeated three times.

The specificity results of Salmonella antibody 1 are shown in Fig. 1A. According to Fig. 1A, the absorbances of 450 nm are ranked from low to high. The response signals

of Salmonella antibody 1 and Staphylococcus aureus, Escherichia coli BL21, parenteral Escherichia coli, Escherichia coli and Salmonella typhimurium gradually increase. Salmonella antibody 1 shows high-binding rate to Escherichia coli and Salmonella typhimurium, and the lowest-binding rate to Staphylococcus aureus. It can be seen that Salmonella antibody 1 does exhibit relatively high binding rate to Salmonella typhimurium, but the specificity is not good enough.

The specificity of Salmonella antibody 2 is shown in Fig. 1B. It can be seen from the figure that its binding to Salmonella typhimurium and Escherichia coli is similar to that of Salmonella antibody 1. In terms of specificity, the performance of the two antibodies is similar. The results showed that Salmonella antibody 1 and Salmonella antibody 2 had poor specificity for Salmonella typhimurium.

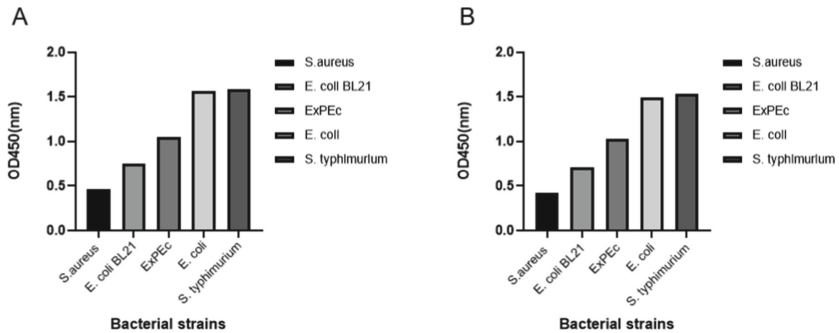


Fig. 1. Salmonella antibody specificity test. **A** Test results of specific reaction between Salmonella antibody 1 and different bacteria. **B** Test results of specific reaction between Salmonella antibody 2 and different bacteria.

3.2 Specificity Test of Escherichia Coli Antibody

In this E. coli antibody specificity test experiment, the four antibodies were diluted to make the concentration at 40 ug/mL, and the Salmonella typhimurium, Staphylococcus aureus, E. coli, E. coli BL21 and parenteral E. coli with the concentration at 10^9 cfu/mL were tested. The experiment was repeated for three times and the average value was counted.

The specificity of E. coli antibody 1 is shown in Fig. 2A. The binding rate of E. coli antibody 1 to E. coli and Salmonella typhimurium is very high, and even reach the highest from Fig. 2A. The reaction signal to Staphylococcus aureus is relatively low, and the reaction signal to the other three E. coli is lower than Staphylococcus aureus. The specificity of E. coli antibody 2, E. coli antibody 3 and E. coli antibody 4 is shown in Fig. 2B, Fig. 2C and Fig. 2D, respectively. The specificity of E. coli antibody 2, E. coli antibody 3 and E. coli antibody 4 to the test bacteria is similar with high binding rate to Salmonella typhimurium, with low binding rate to other bacteria. The results showed that the specificity of E. coli antibody 2, E. coli antibody 3 and E. coli antibody 4 to E. coli was not obvious.

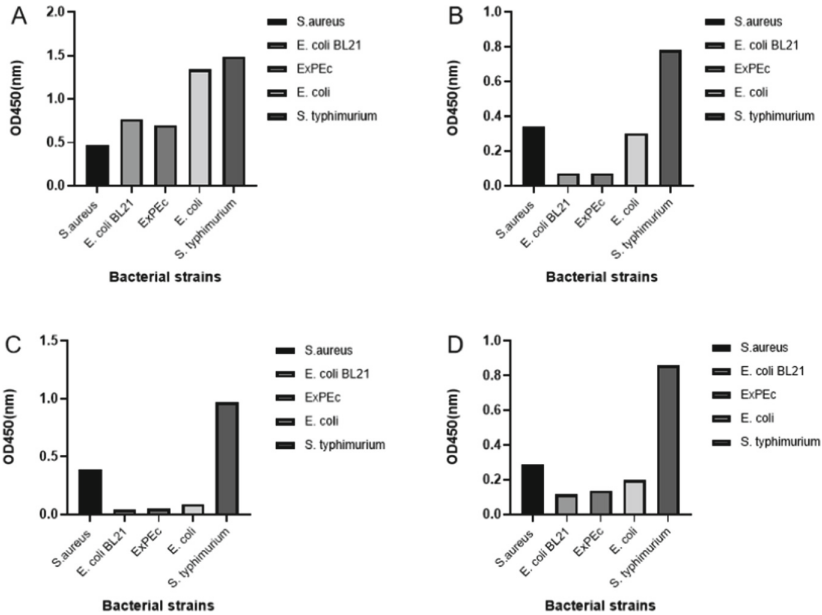


Fig. 2. Escherichia coli specificity test. **A** Test results of specific reaction between Escherichia coli antibody 1 and different bacteria. **B** Test results of specific reaction between Escherichia coli antibody 2 and different bacteria. **C** Test results of specific reaction between Escherichia coli antibody 3 and different bacteria. **D** Test results of specific reaction between Escherichia coli antibody 4 and different bacteria.

4 Discussion and Porspect

Through the specificity evaluation of six Salmonella antibodies and Escherichia coli antibodies on the market, we found that their specificities were not good enough. Relevant research results showed that many surface proteins of Salmonella were very similar to those of Escherichia coli [7]. The data showed that the structural similarity of some proteins in the two bacteria was even more than 50% [8]. The high similarity of this protein structure may lead to the high recognition of Salmonella antibody to E. coli and E. coli antibody to Salmonella typhimurium. Therefore, if we can screen out the differential surface proteins between Salmonella and Escherichia coli and find that there is a relatively unique surface protein on its surface, which does not exist in other bacteria. After identifying differentiated surface proteins, specific proteins on the surfaces of Salmonella and Escherichia coli need to be expressed in order to screen out specific phages [9]. We can further prepare antibodies against food-borne pathogens that are more specific than the market by phage display technology. It can improve the specificity and sensitivity of foodborne pathogenic bacteria detection, lay a foundation for the rapid detection of foodborne pathogenic bacteria, and effectively prevent the health hazards brought by foodborne diseases.

Acknowledgements. This work is supported by the Military Biosafety Research Project (grant number: A3702022004). Yan Gao and Yanan Huang contributed equally to this work.

References

1. Teplitski, M., Barak, J.D., Schneider, K.R.: Human enteric pathogens in produce: un-answered ecological questions with direct implications for food safety. *Curr. Opin. Biotechnol.* **20**, 166–171 (2009). <https://doi.org/10.1016/j.copbio.2009.03.002>
2. Sharma, A., Gautam, S., Bandyopadhyay, N.: Enzyme immunoassays:overview. *Encyclopedia Food Microbiol* 680–687 (2014). <https://doi.org/10.1016/B978-0-12-384730-0.00099-9>
3. Wardley, R.C., Elzein, E., Wilkinson, J.: A solid-phase enzyme linked immunosorbent assay for the detection of African swine fever virus antigen and antibody. *J. Hyg.* **83**, 363–369 (1979). <https://doi.org/10.2307/3862540>
4. Hisanori, I., Yagami, H., et al.: Monoclonal antibodies based on hybridoma technology. *Pharm. Patent Anal.* (2013). <https://doi.org/10.4155/ppa.13.2>
5. Candlish, A.A.G., Smith, J.E., Stimson, W.H.: Monoclonal antibody technology for mycotoxins. *Biotechnol. Adv.* 401–418 (1989). [https://doi.org/10.1016/0734-9750\(89\)90182-1](https://doi.org/10.1016/0734-9750(89)90182-1)
6. Moraes, J., Hamaguchi, B., Braggion, C., et al.: Hybridoma technology: is it still useful? (2021). <https://doi.org/10.1016/j.crimmu.2021.03.002>
7. Wong, R.M.Y., et al.: Sample sequencing of a Salmonella typhimurium LT2 lambda library: comparison to the Escherichia coli K12 genome. *FEMS Microbiol. Lett.* (2) (2010). <https://doi.org/10.1111/j.1574-6968.1999.tb13533.x>
8. UniProt: the universal protein knowledgebase in 2021 (2020) The UniProt Consortium. <https://www.uniprot.org/uniprot/A5JP12>
9. Miersch, S., Sidhu, S.S.: Synthetic antibodies: concepts, potential and practical considerations. *Methods* **57**, 486–498 (2012). <https://doi.org/10.1016/j.ymeth.2012.06.012>



Study of the Intensity of Feedback of Vibration Information from Different Parts of the Human Body

Jianyi Zhang¹(✉), Shan Du¹, Haochen Dong², Wei Li¹, Haolin Sui¹,
and Xinyang Zhao¹

¹ School of Mechanical Power Engineering, Harbin University of Science and Technology,
Harbin 150080, Heilongjiang, China

jianyi990925@126.com

² University of Washington, Seattle 98105, USA

Abstract. The physiological feedback data and subjective evaluation results of the subjects' human bodies at different positions and different vibration intensities were obtained by designing human vibrotactile experiments using personal questionnaire methods and electrical skin data. Statistical and variance tests were used to compare and analyse the subjects' comfort at different position intensities. The author's research explores the subjects' subjective feelings and electrical skin responses in different vibration intensities on different human body parts to provide a physiological basis for natural human-computer interaction research and haptic feedback device development.

Keywords: Human-Machine Interaction · Surface electrodermal signal · Vibrotactile · Spss · Human perception characteristics

1 Introduction

The long-established single mode of information transformation has led to over-reliance on people's visual channels, overloading the visual information, and more bi-directional haptic interaction systems. With the development of wearable devices and virtual reality technologies, the impact of haptic channels on the human body is progressively being appreciated [1].

Tactile sensation has a wide range of applications inside the human body. Over 98% of human skin covers the tactile receptors [2] and is characterized by direct and rapid feedback. Twelve locations on the human body were selected by Karuei et al. [3], 15 locations by Dim et al. [4] Meier et al. [5] selected three areas, and their studies covered multiple parts of the human body such as earlobes, arms, wrists, fingers, neck, back, waist, thighs, and feet. According to their conclusion, the wrist, foot, and earlobe are more sensitive than other body parts, which can effectively identify the vibrations.

Electrodermal activity measurement is an objective physiological measurement that is commonly used as a physiological psychometric indicator in psychology. Neurophysiological responses have an extremely close relationship with the change in emotions

[6]. Therefore, Electrodermal signals can objectively evaluate the state of the human body and have broad-ranging applications in affective computing [7]. Skin conductance was linearly correlated with levels of emotional arousal [8].

Previous studies have investigated the properties and advantages of human part vibrotactile sensation from the perspective of haptic perception. Nevertheless, only a few studies analyzed the subjective perceptions combined with physiological data. This study proposes a method to perform haptic perception experiments on various human body parts using a human vibrotactile expression device in laboratory settings to figure out the advantages and disadvantages of feedback locations for multiple body parts.

2 Experimental Design

2.1 Experimental Purpose

This study aims to find correlations between human locations' subjective and physiological perceptions in response to stimuli from various vibration intensities. The purpose is to determine whether the differences in the subjective perception of stimuli from different vibration intensities correspond to different physiological responses, i.e., changes in the skin's electrical activity.

2.2 Experimental Equipment and Subject Selection

There were 24 subjects, 12 males and 12 females, aged between 22 and 28 years old, recruited at the Harbin University of Technology by publishing a recruitment letter for the experiment. Researchers explained to the subjects the experiment's procedure and how to fill in the subjective evaluation form of the intensity of the tactile signals after the experiment. For each part of the experiment, the device consists of a control module with the function of receiving commands and a vibration motor module. When different switches were pressed, the processor would receive different signals and produce a corresponding vibration stimulus. The specific experimental equipment is shown in Fig. 1.

Researchers used a wearable surface electrodermal measurement system for testing in this experiment. The ErgoLAB human-computer environment synchronization cloud platform recorded electrodermal signals and analyzed data between each subject. The wearable surface electrodermal measurement system was appropriately calibrated and placed on the middle and index fingers. To maintain the accuracy of the data, the experiment required subjects to keep stationary during the entire process.

2.3 Pre-experiments

Different parameters of the vibration signal deliver different perceptual effects [1]. By adjusting the vibration module's voltage (0 to 5 v), the vibration intensity can be well controlled. The experimental vibration duration for this experiment was one second. Ten subjects, five of each sex, were selected for the pre-experiment. The vibration stimuli were delivered to the subjects from 0 V to 5 V by order with 0.5 V intervals of increasing intensities. The four vibration intensities of Strength I (2.5 V), Strength II (3.0 V), Strength III (3.5 V), and Strength IV (4.0 V) were used as experimental data.

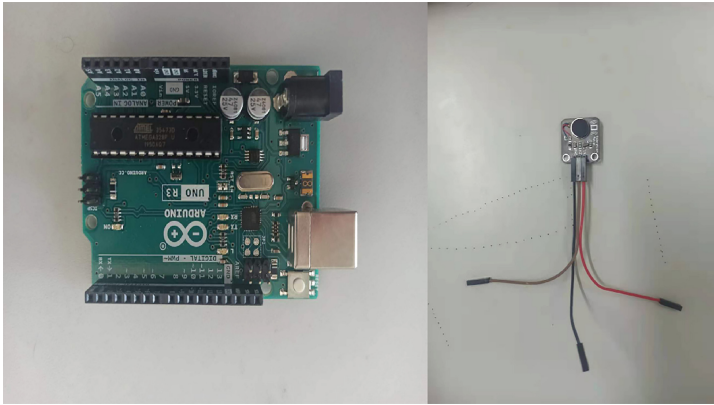


Fig. 1. Arduino controller with a vibration module

2.4 Experimental Design of Perceived Comfort with Different Vibration Intensities

Barghout and other researchers [9] found that people can perceive mechanical vibrations effectively and that the epidermis at joints is more sensitive to vibrations than other non-joints parts. Thus, four jointed body features, neck, wrist, fingers, and waist, were selected for the experiment. Before the experiment, a dermatographic device, see Fig. 2.



Fig. 2. Wearing a dermatographic device.

Four different vibration intensities were tested in one group, and each subject was required to perform four sets of experiments in selected areas. A questionnaire is used to record the subject's comfort level based on their subjective evaluation during the investigation. In each group, the researcher pressed a switch with different intensity control signals in sequence with a 5-s interval so that the subject had sufficient time to offer feedback. At the end of each experiment, a 1-min pause was required before continuing with the subsequent experiments—such decisions provided each subject to

fill in the subjective questionnaire and take a break. After all the experiments, evaluation forms were collected and analysed using SPSS.

3 Research Results

3.1 Subjective Evaluation Results

At the end of the experiment, the mean rating box plots for the subjects were plotted using vibration intensity as the horizontal coordinate and subjective comfort as the vertical coordinate, see Fig. 3.

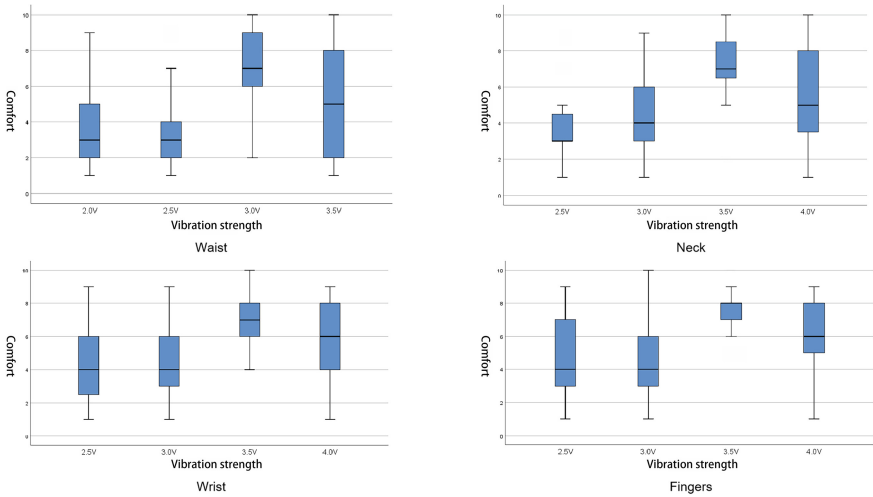


Fig. 3. Scoring box chart

According to the graph above, the variation in the ratings of the neck and waist was more widely distributed, and the mean and median ratings of these parts were generally lower than those of the wrist and fingers, which suggests that the neck and waist were typically less comfortable and unstable for the subjects. The wrist is a suitable site for perceiving vibrotactile signals. The issues can detect the occurrence of signs and experience greater comfort when different vibration intensities are applied to the skin surface. The standard deviation of Strength III (3.5 V) was 1.1169, which was the lowest among the four signals, indicating that the overall rating of Strength III (3.5 V) fluctuated more steadily among the four intensities.

3.2 Electrical Skin Reaction

The level of tension in the electrical activity of the skin, known as skin conductance level (SCL), varies slowly and slightly on a time scale of tens of seconds to minutes, and can vary significantly for each individual [10].

Due to the individual variability of the subjects, it is necessary to pre-process the electrodermal data and perform statistics on the electrodermal results of the subjects, using the rate of change of electrodermal for statistics and analysis, i.e., the rate of change of electrodermal = (measured value – baseline value)/baseline value. Figure 4 shows the study of the baseline electrodermal level data of the experimenter. The average baseline tare level figure is 7.77.

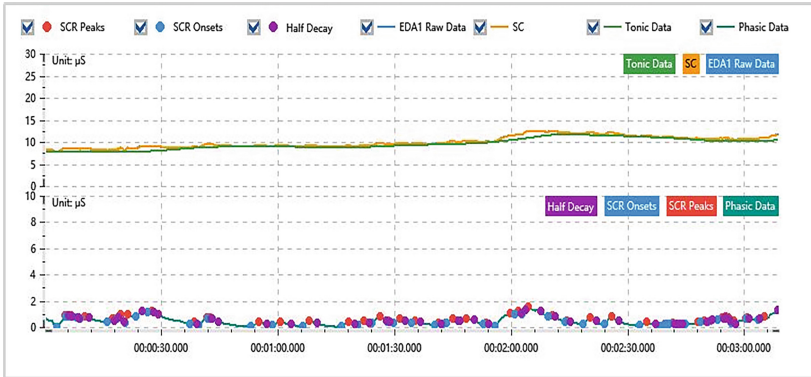


Fig. 4. Benchmark skin electrical level data analysis graph

Table 1 gives the mean change in the rate of change of the electrodermal level on the rate of change of the electrodermal at different vibration intensities. From the table, it can be seen that the mean rate of change of piezoelectricity increases with the increase of vibration intensity, and the vibration intensity has a significant effect on the piezoelectricity level.

Table 1. Average skin electrical rate of change

	Strength I	Strength II	Strength III	Strength IV
Neck	0.405175405	0.427054597	0.790177655	0.847490211
Waist	0.429825699	0.582165584	1.006427006	1.179536107
Wrists	0.30341484	0.320422084	0.530948026	0.551079979
Fingers	0.318960054	0.321437916	0.52177762	0.527812894

A one-way repeated ANOVA was performed on the dermatographic results to investigate whether there was significance in the subjects’ dermatographic data for repeated measurements of different intensities. The one-way ANOVA significance was 0.031, indicating that the subjects had statistically significant differences in the data on the rate of change of dermatography at different intensities. The results suggest that electrodermal levels can be used to estimate the degree of perception of subjects at different vibration intensities.

4 Research Analysis and Discussion

This study used experiments to compare the intensity of vibration in different locations of the human body in order to get subjective evaluations of tactile feedback. Furthermore, the study quantified the connection between vibration intensity and dermal electrical activity through skin conductance data in four experiments. These experiments and reports prove that effective vibration can improve the emotional experience of the subjects and give more acceptable tactile communication.

The electrodermal results regarding intensity revealed the significant differences in the physiological feedback of the subjects corresponding to the subjective questionnaire, that is, the higher the intensity, the greater the fluctuation in electrodermal feedback. The emotions such as nervous, happy, and frightening were much higher than other emotions.

The experimentally obtained human vibrotactile data can be functionally matched to navigation tasks based on the manipulation-display compatibility principle, providing an important alternative information transfer pathway for many people with visual impairments [11]. These findings contribute to the understanding of human haptic perceptual properties and how body position and vibration intensity affect haptic feedback behaviour in different ways, providing a physiological basis for natural human-computer interaction research and haptic feedback device development.

Acknowledgement. This work is supported by the Human Factors Study on the Design of Intelligent Guiding Devices for the Blind, No. 201901024027.

Compliance with Ethical Standards. The study was approved by the Logistics Department for Civilian Ethics Committee of Harbin University of Science and Technology.

All subjects who participated in the experiment were provided with and signed an informed consent form.

All relevant ethical safeguards have been met with regard to subject protection.

References

1. Liu, Y., Tang, W.-Y.: Research on vibratory stimulation-based haptic human-computer interaction in wearable devices. *Theatre House* **16**(16), 218–219 (2018)
2. Ravikanth, D., Mishra, M., Hariharan, P.: Review on Hapticstechnology and its modeling, rendering and future applications ontecture identification. In: 2015 International Conference on Man andMachine Interfacing (MAMI), no. 1. Bhubaneswar (2015)
3. Karuei, I., MacLean, K.E., Foley-Fisher, Z., et al.: Detecting vibrations across the body in mobile contexts. In: Proceedings of the SIGCHI Conference on Human Factors in Computing Systems, BC, Canada, pp. 3267–3276 (2011)
4. Dim, N.K., Ren, X.: Investigation of suitable body parts for wearable vibration feedback in walking navigation. *Int. J. Hum. Comput. Stud.* **97**, 34–44 (2017)
5. Meier, A., Matthies, D.J.C., Urban, B., et al.: Exploring vibrotactile feedback on the body and foot for the purpose of pedestrian navigation. In: Proceedings of the 2nd International Workshop on Sensor-based Activity Recognition and Interaction, pp. 1–11 (2015)
6. Li, F., Zhu, Z., Bai, X.: Validity and time course of emotion evoked by happy and sad movie clips. *Psychol. Behav. Res.* **7**(01), 32–38 (2009)

7. Ji, X., Li, H., Lu, Z., Wang, Z., Chai, X.: Research on the electrodermal activity during walking and running. In: 2019 4th International Conference on Control and Robotics Engineering (ICCRE), pp. 179–183 (2019). <https://doi.org/10.1109/ICCRE.2019.8724244>
8. Houlihan, M.: *Electrodermal Activity*, 2nd edn., Wolfram Boucsein. *Personality and Individual Differences*, vol. 53, no. 5. Springer, New York (2012). <https://doi.org/10.1007/978-1-4614-1126-0>
9. Barghout, A., Cha, J., El Saddik, A., et al.: Spatial resolution of vibrotactile perception on the human forearm when exploiting funneling illusion. In: *Haptic Audio-Visual Environments and Games, HAVE 2009, IEEE International Workshop*, pp. 19–23 (2009)
10. Distefano, N., Leonardi, S., Pulvirenti, G., Romano, R., Boer, E., Wooldridge, E.: Mining of the association rules between driver electrodermal activity and speed variation in different road intersections. *IATSS Res.* **46**(2), 200–213 (2022). ISSN 0386-1112
11. Maeno, T., Kobayashi, K., Yamazaki, N.: Relationship between the structure of human finger tissue and the location of tactile receptors. *Bull. JSME Int.* **41**(1), 94–100 (1998)



Research on Psychological Service Needs of Paratroopers Based on Stress Events

Yang Liao¹, Chuang Xu², Yiwen Hu¹, Xin Liu¹, Yuyang Zhu¹, Yan Zhang¹,
Yishuang Zhang¹, Miao Jin¹, and Liu Yang¹(✉)

¹ Air Force Medical Center, Air Force Medical University, Beijing 100142, China
yangliuhenry@aliyun.com

² Department of Teaching and Research, Paratrooper Training Base, Guilin 541003, China

Abstract. Understanding the main stress events faced by paratroopers and the use of coping styles is helpful to clarify the needs of psychological services. In this study, 86 paratroopers were selected as the research objects by stratified sampling method. The frequency and impact of stress events, frequency and effect of coping styles in paratroopers were investigated by Likert five point scales. The results showed that paratroopers in different positions had significant differences only in the stress event of workplace interpersonal conflict. The influence of workplace interpersonal conflict on the psychological state of officers is significantly higher than that of sergeants and soldiers. Officers and sergeants prefer to use exercise and breathing relaxation to deal with stress events, while soldiers prefer to play video games to deal with stress events. The results of this study indicate that the types of stress events and preferred coping styles of paratroopers in each position are different. In psychological service, psychologist need to choose targeted measures based on their characteristics in order to effectively maintain mental health and operational efficiency.

Keywords: Paratroopers · Stress events · Coping style

1 Introduction

Paratroopers often face multiple stresses, such as combat stress, special occupational stress, military operation environment stress and life event stress, which not only restrict their operation efficiency, but also increase the difficulty and risk of administrative management [1, 2]. At present, the promotion of paratroopers' operation efficiency lacks effective targeted technology and equipment support. Relying solely on the limited psychological professional team could not meet the increasingly diversified psychological service needs of paratroopers.

This study investigates the current situation and needs of paratroopers' psychological services through Likert five point scales, and combs the occurrence frequency and impact of stress events, the use of coping styles and effects on psychological state of paratroopers. The results may help to understand the current needs of paratroopers' psychological service, and provide basis for the subsequent improvement of paratroopers' psychological service mode.

2 Method

2.1 Participants

86 paratroopers, all male, were selected by stratified sampling. The age range was 18–41 years old. The details were shown as below (Table 1).

Table 1. Demographic variable of the participants

Demographic variables	Category	Number	Percentage (%)
Positions	Officers	16	18.60
	Sergeants	38	44.19
	Soldiers	32	37.21
Educational level	Undergraduate	28	32.56
	Junior college	40	46.51
	High school and below	18	20.93
History of psychological counseling	Yes	8	9.30
	No	78	90.70
Willingness to seek psychological services	Yes	11	12.79
	No	75	87.21

2.2 Tools

Likert five point scales was used to investigate the needs of psychological services in paratroopers. According to the previous literatures, we listed 11 stress events that may affect the psychological state of paratroopers in the questionnaire, involving three aspects: training, family and career development. Based on the grade score of each stress event, the occurrence frequency of the stress events (Grade 5 score, 1-very few, 2-relatively few, 3-medium, 4-relatively many, 5-very many) and the degree of influence on the psychological state (Grade 5 score, 1-basically no influence, 2-small influence, 3-medium influence, 4-great influence, 5-very great influence) was collected. In addition, based on the participants' use frequency and effect scores of 11 coping styles, we can understand the main ways to solve the current paratroopers' psychological problems. The use frequency of coping styles were ranked in 5-level score (1-very few, 2-relatively few, 3-medium, 4-relatively many, 5-very many), and the effect of coping styles were also ranked in 5-level score (1-basically no effect, 2-A little effect, 3-medium effect, 4-good effect, 5-very good effect).

2.3 Statistics

Statistical package for the social sciences (SPSS 20.0) was used for statistic, and the significant level was 0.05.

3 Results

3.1 The Occurrence Frequency of Stress Events and the Degree of Influence on the Psychological State of Paratroopers

According to the occurrence frequency score of stress events in subjective feeling, there are significant differences among paratroopers of different positions in five stress events: initial parachute jumping training ($F = 7.821, P < 0.01$), daily parachute jumping training ($F = 16.269, P < 0.01$), training in different places ($F = 5.462, P < 0.01$), death of relatives ($F = 7.427, P < 0.01$) and difficulty in completing tasks ($F = 4.063, P < 0.05$). The occurrence frequency of the first parachute jumping training event in soldiers was significantly higher than that in officers ($P < 0.05$) and sergeants ($P < 0.01$). The occurrence frequency of daily parachute jumping training event in soldiers was significantly higher than that in officers ($P < 0.01$) and sergeants ($P < 0.01$). The occurrence frequency of three stress events in officers, namely, training in different places ($P < 0.01$), death of relatives ($P < 0.01$) and difficulty in completing work tasks ($P < 0.05$), were significantly higher than that in soldiers.

From the perspective of different positions, the stress events with high occurrence frequency in officers are difficulty in completing tasks, not promoted and training in different places. The stress events with high occurrence frequency in Sergeants are difficulty in completing tasks, not promoted and separation of spouses. The stress events

Table 2. Comparison of occurrence frequency scores of stress events among paratroopers in different positions

Types of stress event	Occurrence frequency of stress events			<i>F</i>	<i>P</i>
	Officers	Sergeants	Soldiers		
Initial skydiving training	1.50 ± 1.03 ^b	1.34 ± 0.67 ^c	2.25 ± 1.25 ^{bc}	7.821	0.001
Daily skydiving training	1.81 ± 0.75 ^b	1.42 ± 0.79 ^c	2.84 ± 1.39 ^{bc}	16.269	0.001
Cross day and night training	2.00 ± 0.97	1.47 ± 0.80	1.91 ± 0.93	3.010	0.055
Training in different places	2.06 ± 1.06 ^b	1.61 ± 0.97	1.22 ± 0.49 ^b	5.462	0.006
Illness or injure on oneself	1.56 ± 0.51	1.50 ± 0.60	1.38 ± 0.55	0.705	0.497
Death of relatives	1.69 ± 0.79 ^b	1.32 ± 0.57	1.06 ± 0.25 ^b	7.427	0.001
Separation of spouses	1.94 ± 1.57	1.66 ± 1.28	1.31 ± 1.03	1.453	0.240
Conflict with family members	1.44 ± 0.51	1.42 ± 0.92	1.22 ± 0.42	0.883	0.417
Not promoted	2.06 ± 0.77	1.66 ± 1.02	1.44 ± 0.80	2.569	0.083
Workplace interpersonal conflict	1.56 ± 0.73	1.50 ± 0.73	1.53 ± 0.62	0.050	0.951
Difficulty in completing tasks	2.25 ± 0.78 ^b	1.79 ± 0.81	1.59 ± 0.67 ^b	4.063	0.021

Note: a indicates that there is a significant difference in scores between officers and sergeants, b indicates that there is a significant difference in scores between officers and soldiers, c indicates that there is a significant difference in scores between sergeants and soldiers, and the meaning of these symbols in the rest tables are the same as this table.

with high frequency in soldiers are daily skydiving training, initial skydiving training and cross day and night training (Table 2).

According to the score of the impact of stress events on psychological state, there was significant difference only in the stress event of workplace interpersonal conflict among paratroopers of different positions ($F = 5.934$, $P < 0.01$). The impact of workplace interpersonal conflict on the psychological state of officers was significantly higher than that of sergeants ($P < 0.05$) and soldiers ($P < 0.01$).

From the perspective of different positions, officers think that the stress events that have a greater impact on the psychological state are the death of relatives, conflict with family members and separation of spouses. Sergeants think that the stress events that have a greater impact on the psychological state are the death of relatives, conflict with family members and difficulty in completing tasks. Soldiers think that the stress events that have a greater impact on the psychological state are the death of relatives, conflict with family members and separation of spouses (Table 3).

Table 3. Comparison of impact of stress events among paratroopers in different positions

Types of stress event	Impact of stress events			<i>F</i>	<i>P</i>
	Officers	Sergeants	Soldiers		
Initial skydiving training	2.19 ± 1.05	1.58 ± 0.79	1.69 ± 0.93	2.664	0.076
Daily skydiving training	1.69 ± 0.70	1.47 ± 0.76	1.41 ± 0.71	0.798	0.454
Cross day and night training	1.94 ± 0.77	1.61 ± 0.86	1.75 ± 0.92	0.860	0.427
Training in different places	1.75 ± 0.93	1.50 ± 0.76	1.44 ± 0.72	0.888	0.415
Illness or injure on oneself	2.38 ± 0.96	2.08 ± 1.08	2.09 ± 1.09	0.487	0.616
Death of relatives	3.63 ± 1.09	3.03 ± 1.37	3.28 ± 1.61	1.032	0.361
Separation of spouses	2.88 ± 1.09	2.03 ± 1.20	2.50 ± 1.46	2.763	0.069
Conflict with family members	2.94 ± 1.06	2.26 ± 1.06	2.53 ± 1.41	1.799	0.172
Not promoted	2.63 ± 1.09	2.13 ± 0.99	2.06 ± 1.01	1.773	0.176
Workplace interpersonal conflict	2.75 ± 0.93 ^{ab}	1.95 ± 0.90 ^a	1.84 ± 0.88 ^b	5.934	0.004
Difficulty in completing tasks	2.69 ± 0.95	2.21 ± 0.88	2.09 ± 1.00	2.233	0.114

3.2 Main Ways of Paratroopers Coping with Stress Events and Their Effects

According to the frequency scores of paratroopers' use of various coping styles, different positions of paratroopers have significant differences in the frequency of seeking help from psychological experts ($F = 3.212$, $P < 0.05$), going to psychological clinic ($F = 4.630$, $P < 0.05$), travel ($F = 3.927$, $P < 0.05$), sharing with relatives and friends ($F = 7.640$, $P < 0.01$) and fade impact over time ($F = 3.458$, $P < 0.05$). Among these, the frequency of soldiers' use of going to the psychological clinic was significantly higher than that of sergeants ($P < 0.05$), the frequency of officers' use of travel was significantly

higher than that of sergeants ($P < 0.05$) and soldiers ($P < 0.05$), the frequency of soldiers' use of sharing with relatives and friends was significantly higher than that of sergeants ($P < 0.01$), and the frequency of officers' use of fade impact over time was significantly higher than that of sergeants ($P < 0.05$).

From the perspective of different positions, the coping styles used more frequently by officers in response to stress events are exercise, breathing relaxation and fade impact over time. The coping styles used more frequently by sergeants in response to stress events are exercise, playing video games and breathing relaxation. The coping styles used more frequently by soldiers in response to stress events are exercise, sharing with relatives and friends and playing video games (Table 4).

Table 4. Comparison of frequency of coping styles used by paratroopers in different positions

Coping styles	Frequency of coping styles			<i>F</i>	<i>P</i>
	Officers	Sergeants	Soldiers		
Seek help from a psychologist	1.06 ± 0.25	1.08 ± 0.36	1.34 ± 0.65	3.212	0.045
Go to psychological clinic	1.13 ± 0.34	1.03 ± 0.16 ^c	1.34 ± 0.65 ^c	4.630	0.012
Adjust with relaxation equipment	2.06 ± 1.18	2.05 ± 1.27	2.19 ± 1.23	0.114	0.892
Breathing relaxation	3.06 ± 1.44	2.53 ± 1.35	2.88 ± 1.16	1.175	0.314
Meditation	2.44 ± 1.21	2.05 ± 1.11	1.94 ± 0.88	1.232	0.297
Exercises	3.63 ± 1.09	3.45 ± 1.27	3.66 ± 1.18	0.292	0.748
Play video games	2.75 ± 1.34	2.71 ± 1.35	3.06 ± 1.19	0.701	0.499
Write a diary	2.06 ± 1.29	1.47 ± 0.73	1.97 ± 1.20	2.771	0.068
Travel	2.69 ± 1.25 ^{ab}	1.82 ± 1.21 ^a	1.78 ± 1.00 ^b	3.927	0.023
Sharing with relatives and friends	2.63 ± 1.20	2.16 ± 1.00 ^c	3.13 ± 0.98 ^c	7.640	0.001
Fade impact over time	2.94 ± 1.29 ^a	2.05 ± 1.14 ^a	2.19 ± 1.09	3.458	0.036

According to the effect scores of paratroopers using different coping styles, there were significant differences among different positions in the effects of using three coping styles: seeking the help of psychologist ($F = 5.577$, $P < 0.01$), going to the psychological clinic ($F = 6.615$, $P < 0.01$) and sharing with relatives and friends ($F = 3.815$, $P < 0.05$). Among these, the effect of using the coping style of seeking the help of psychologist in soldiers is significantly better than that in sergeants ($P < 0.05$). The effect of using the coping style of going to the psychological clinic among soldiers is significantly better than that in sergeants ($P < 0.05$). The effect of using the coping style of sharing with relatives and friends in soldiers is significantly better than that in sergeants ($P < 0.01$).

From the perspective of different positions, the coping styles with better effect in response to stress events among officers are exercise, sharing with relatives and friends, and travel. The coping styles with better effect in response to stress events among sergeants are exercise, playing video games and breathing relaxation. The coping styles with better effect in response to stress events among soldiers are travel, exercise and sharing with relatives and friends (Table 5).

Table 5. Comparison of effect of coping styles used by paratroopers in different positions

Coping styles	Effect of coping styles			<i>F</i>	<i>P</i>
	Officers	Sergeants	Soldiers		
Seek help from a psychologist	2.69 ± 1.35	1.84 ± 1.22 ^c	2.81 ± 1.33 ^c	5.577	0.005
Go to psychological clinic	2.63 ± 1.31	1.87 ± 1.12 ^c	2.88 ± 1.21 ^c	6.615	0.002
Adjust with relaxation equipment	2.88 ± 1.20	2.34 ± 1.15	2.97 ± 1.18	2.789	0.067
Breathing relaxation	3.00 ± 1.10	2.84 ± 1.13	2.81 ± 1.18	0.153	0.858
Meditation	2.56 ± 1.03	2.05 ± 1.01	2.16 ± 1.22	1.233	0.297
Exercises	3.56 ± 0.73	3.58 ± 1.15	3.47 ± 1.14	0.096	0.908
Play video games	2.81 ± 0.83	2.84 ± 1.24	3.13 ± 1.16	0.655	0.522
Write a diary	2.50 ± 1.21	1.87 ± 1.04	2.31 ± 1.26	2.171	0.121
Travel	3.19 ± 1.33	2.82 ± 1.52	3.50 ± 1.30	2.067	0.133
Sharing with relatives and friends	3.31 ± 0.87	2.61 ± 1.24 ^c	3.31 ± 1.23 ^c	3.815	0.026
Fade impact over time	2.44 ± 1.09	2.11 ± 1.06	1.88 ± 1.07	1.491	0.231

4 Discussion

Over the past two decades, previous researches on the psychological state of paratroopers mainly focused on parachute jumping, the main psychological stressor of military operations. Most of them used psychological scales or physiological and biochemical monitoring methods to evaluate the stress response of parachute jumping, mainly focused on the induced negative emotions such as anxiety and fear [3, 4]. From the survey results of the current study, among the stress events related to military operation, parachute jumping and cross day and night training have a great impact on the psychological state of paratroopers, which is similar to the previous research results [5]. From the perspective of all types of stress events, the high occurrence frequency of stress events faced by paratroopers is mainly some frustration events in the workplace, such as difficult work tasks, not promoted and so on. In terms of the impact on the psychological state, family related stress events have a great impact on the psychological state of paratroopers, mainly reflected in the change or loss of intimate relationships. This suggests that in the psychological service, psychologists should pay attention to the psychological impact of workplace stress events on paratroopers, especially the group of officers. They feel higher stress in the workplace than other groups. Psychologists need to take specific measures to help them relieve the pressure at work. In daily management, psychologists should pay attention to the personnel with family changes, and give sufficient social support in time when the intimate relationship deteriorates or loses, so as to avoid the adverse impact of such stress events on their psychological state.

From the results of the investigation on the coping styles of stress events, paratroopers with different positions all prefer use exercises to relieve pressure. This self-regulation method is not restricted by external environmental factors and is more suitable for military personnel [6, 7]. It is worth noting that young sergeants and soldiers in paratroopers

are more likely to use playing video games to cope with pressure, which reflects the preference differences between paratroopers of different ages. Previous studies have shown that moderate playing video games can help relieve stress, improve mood, and promote mental health [8, 9]. This result suggests that when guiding paratroopers to deal with stress events, psychologist should take the characteristics of subdivided groups in consideration and guide them to use coping styles which are more likely been accepted by them.

5 Conclusion

The results of the current study indicate that the types of stress events and preferred coping styles of paratroopers in each position are different. In psychological service, psychologist need to choose targeted measures based on their characteristics in order to effectively maintain mental health and operational efficiency.

Acknowledgements. This work is supported by the Efficiency improvement plan, No. 2020JSTS13.

Compliance with Ethical Standards. The study was approved by the Logistics Department for Civilian Ethics Committee of Air Force Medical Center.

All subjects who participated in the experiment were provided with and signed an informed consent form.

All relevant ethical safeguards have been met with regard to subject protection.

References

1. Sundin, J., Jones, N., Greenberg, N., et al.: Mental health among commando, airborne and other UK infantry personnel. *Occup. Med.* **60**(7), 552–559 (2010)
2. Dollah, S.N., Abd Majid, R., Abd Rahim, M., et al.: Stress and temporomandibular disorders among Malaysian armed forces paratroopers. *Malays. J. Psychiatry* **28**(1), 63–72 (2019)
3. Messina, G., Valenzano, A., Moscatelli, F., et al.: Effects of emotional stress on neuroendocrine and autonomic functions in skydiving. *J. Psychiatry* **18**, 1–7 (2015)
4. Lewis, G.F., Hourani, L., Tueller, S., et al.: Relaxation training assisted by heart rate variability biofeedback: Implication for a military predeployment stress inoculation protocol. *Psychophysiology* **52**(9), 1167–1174 (2015)
5. Clemente-Suárez, V.J., Robles-Pérez, J.J., Fernández-Lucas, J.: Psycho-physiological response in an automatic parachute jump. *J. Sport Sci.* **35**(19), 1872–1878 (2017)
6. Simpson, R.J., Kunz, H., Agha, N., et al.: Exercise and the regulation of immune functions. *Prog. Mol. Biol. Transl.* **135**, 355–380 (2015)
7. Caddick, N., Smith, B.: Exercise is medicine for mental health in military veterans: a qualitative commentary. *Qual. Res. Sport Exerc.* **10**(4), 429–440 (2018)
8. Villani, D., Carissoli, C., Triberti, S., et al.: Videogames for emotion regulation: a systematic review. *Games Health J.* **7**(2), 85–99 (2018)
9. Halbrook, Y.J., O'Donnell, A.T., Msetfi, R.M.: When and how video games can be good: a review of the positive effects of video games on well-being. *Perspect. Psychol. Sci.* **14**(6), 1096–1104 (2019)



Design of Psychological Measurement and Archives Management System Based on WLAN

Yishuang Zhang¹, Dongxue Chen², Yan Zhang¹, Yang Liao¹, Jian Du¹, Rong Lin¹, Duanqin Xiong¹, and Liu Yang¹ (✉)

¹ Air Force Medical Center, Fourth Military Medical University, Beijing 100142, China
yangliuhenry@aliyun.com

² Psychology Future (Beijing) Technology Co. Ltd., Beijing 100142, China

Abstract. *Objective.* To develop a system based on WLAN for psychological measurement and archives management system. *Methods.* The system is based on B/s and WLAN architecture, and realizes data acquisition through self-organizing LAN. Users can use their own mobile phone as the evaluation terminal, access the LAN through WiFi, log in to the system and do some work. All collected evaluation information and other data are summarized and saved in the server database. System hardware equipment includes server, gateway, switch, base station, Poe power supply module, etc. The software is mainly divided into manager and user system. The administrator can log in to the manager, bind the evaluated scale information for the user role, analyze the psychological data, and manage the user authority, psychological archives and so on. The participants can register and log in to the client to test the corresponding scale and view the evaluation results. *Results.* Experiments showed that the system was reliable and anti jamming. *Conclusion.* The system has good portability, a wide range of one-time measurement, and does not need to maintain the evaluation terminal, reducing the measurement cost. At the same time, the system has powerful functions of data statistics and Archives management. It is suitable for large-scale psychological survey and special personnel selection. It can establish and manage psychological files for the army.

Keywords: Psychometric questionnaire test · WLAN · Psychological archives

1 Technical Background

The combat capability of the army depends on the overall quality of the soldiers. The psychological quality of the soldiers is the core component of the overall quality of the soldiers, and the mental health of the soldiers is the basis of the excellent psychological quality of the soldiers. Therefore, the mental health level of soldiers is closely related to the overall combat capability of the Army [1]. As an effective method to quickly and comprehensively understand the mental health level of officers and soldiers, psychological measurement is receiving more and more attention in our army [2, 3].

The psychological evaluation means of our army has experienced four stages of development. The first stage is dominated by pencil and paper test. The process includes answering questions, data entry, calculating test results, etc. this test method is time-consuming and laborious, and is prone to entry errors. With the development of computer technology and computer network technology, psychological measurement has entered the second stage. The subjects answer questions by networking computers, and there is no need to manually enter the test results, that greatly improves the test efficiency [4]. Because this evaluation method needs to rely on computer network, it is not suitable for large-scale measurement of grass-roots forces, nor for the rapid evaluation link in the psychological crisis intervention of military personnel. In order to improve the evaluation efficiency, Hu Wendong and others developed the evaluation system based on infrared data transmission [5] in 2004, and further improved the data transmission method [6]. The participants can view the evaluation questions through PPT and answer with handheld equipment, which is no longer dependent on the computer network environment. The equipment is relatively small and flexible, and support a large number of participants in the test at the same time. However, because the test questions need to be played uniformly, it is difficult for individuals to adjust the answer time according to their own needs. In recent years, the development of wireless data transmission technology and intelligent handheld terminals provides a new solution for psychometric, and portable psychological evaluation system is becoming the mainstream. The evaluation system is composed of a server and handheld terminals. The participants conduct autonomous psychological tests through the handheld terminal, and the test results are automatically uploaded to the server and being calculated. However, there are still some problems in this kind of system, such as maintenance and charging of the terminals, obvious decline in performance with the service life, and limited personnel for one-time measurement, which need to be improved.

In view of the above problems, this paper will introduce a design scheme of psychological measurement and file management system based on WLAN. users can use their mobile phone as the evaluation terminal and access the LAN through wireless AP for evaluation. On the premise of meeting the requirements of data confidentiality, this system can evaluate 500 people at a time without special maintenance of terminal equipment. The system also has the function of archives management, which realizes the classification, hierarchical query and comparative analysis of personnel psychological archives in different units and departments.

2 Overall Design

2.1 Design Mode

In view of the above problems, the system adopts the design mode of ui-dal-sql server, and other functions are added, deleted, modified and queried by calling “stored procedure” by program.

2.2 System Structure

In order to ensure the safety of the data, the system is based on B/s and WLAN architecture, and realizes data acquisition through self-organizing LAN. Users can use their

own mobile phone as the evaluation terminal, access the LAN through WiFi, log in to the system and do some work. All collected evaluation information and other data are summarized and saved in the server database.

2.3 Function Design

With the goal of providing an all-in-one management, the system was divided into two basic functional sections: the management side and the client side. The specific structure was shown in Table 1.

Table 1. Functional architecture of psychological measurement and archives management system

	Classification	Specific module and functional requirements
Manager system	Basic information management	Organization management: realize the classified management of different units, and support different organizations to carry out psychological evaluation and archives management on demand
		Role management: realize hierarchical management of permissions for different user roles
		Corner data import: supports batch import of user data by formwork
		Permission management: support role permission assignment and set different permissions for different levels of roles
	Information investigation management	Questionnaire management: users can independently set the contents of questionnaires
		Questionnaire binding: it supports individualization personalized questionnaires for different institutions and roles
	Scale management	Scale platform: includes commonly used psychological scales such as MMPI, SCL-90, EPQ, evaluation algorithms and evaluation norms, and supports users to revise them independently
		Scale setting: in order to facilitate the search and use of the scale, the scale is classified according to the categories of mental health, personality, emotion, etc

(continued)

Table 1. (continued)

	Classification	Specific module and functional requirements
		Scale binding: supports assigning different evaluation tasks to different institutions and roles
	Archives administration	Psychological evaluation archives: support different roles to view and customize the psychological evaluation archives within the scope of permission
		Information investigation archives: support different roles to view and customize the information investigation archives within the scope of permission
		Comprehensive information archives: support different roles to view and customize the comprehensive information archives within the scope of permission
	Data analysis	psychological measurement Data statistics: supports batch export of evaluation analysis reports, original records and evaluation results
		Exception data statistics: supports automatic filtering, alert and batch export of exception data
		Comprehensive statistics: supports data filtering and batch export under user-defined conditions
User system	Account management	Account management: support users to register, log in and manage passwords according to the regulations of the administrator
	Information investigation	Participate in information investigation: support users to participate in information investigation according to the contents specified by the administrator

(continued)

Table 1. (continued)

	Classification	Specific module and functional requirements
	Psychological measurement	Participate in psychological measurement: support users to participate in psychological measurement according to the contents specified by the administrator
	Report viewing	Report viewing: users can view evaluation reports and alerts within their permissions

3 Hardware Composition

According to the requirements of system testing environment and functional architecture design, the system shall include basic hardware equipment such as server, gateway, switch and APs. Among them, the server is responsible for data processing and storage; The gateway is responsible for repackaging, sorting and translating all kinds of data information received, and provides filtering and security functions; The switch is responsible for networking multiple AP; AP can deploy WLAN in indoor/outdoor environment to meet the wireless application requirements within its coverage. At the same time, considering the insufficient deployment scope of AC power supply in outdoor collective measurement environment, POE power supply module should also be configured to use network cable to supply power to AP, so that the AP is not limited by AC power deployment location. Figure 1 is the schematic diagram of system hardware connection.

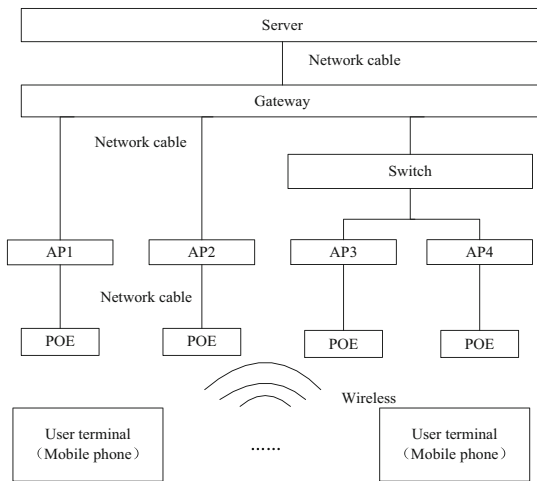


Fig. 1. The schematic diagram of system hardware connection

4 System Software Design

The system is mainly divided into manager and user system. Users enter the existing account and password into the system through the unified login interface, and the system automatically judges the user role. The administrator enters the background management system, and the general user enters the foreground user system. The manager binds information for users, roles and institutions, and users can conduct psychological measurement at the user system. The specific process is shown in Fig. 2.

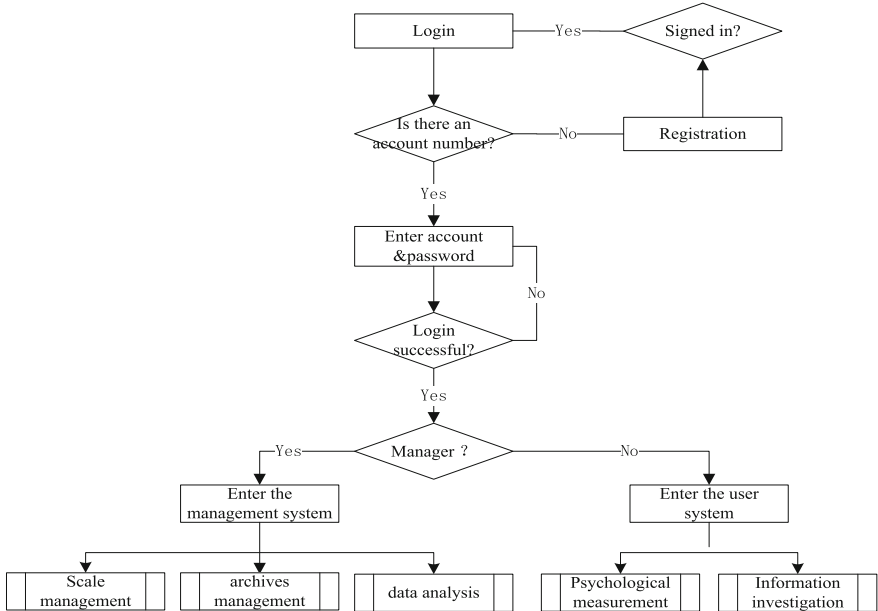


Fig. 2. Program flow chart

4.1 Manager System Design

According to the basic function design, the management end mainly includes six functional modules: basic information management, information investigation management, psychological scale management, psychological archives management, psychological data analysis and exception data management, which are mainly realized through three processes: scale management, archives management and data analysis. The specific process is shown in Fig. 3.

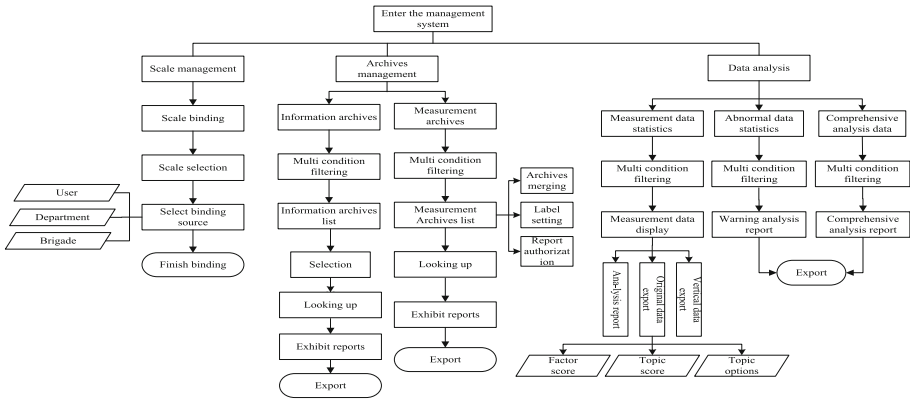


Fig. 3. Flow chart of management system

4.2 User System Design

Before the psychological measurement, the system detects whether the user has completed the information investigation questionnaire. If not, the information investigation questionnaire needs to be completed first. In the measurement interface, the user could answer the scale questions. After the measurement was completed and submitted, the current test report would be generated. users could export the report to the document. The specific process was shown in Fig. 4.

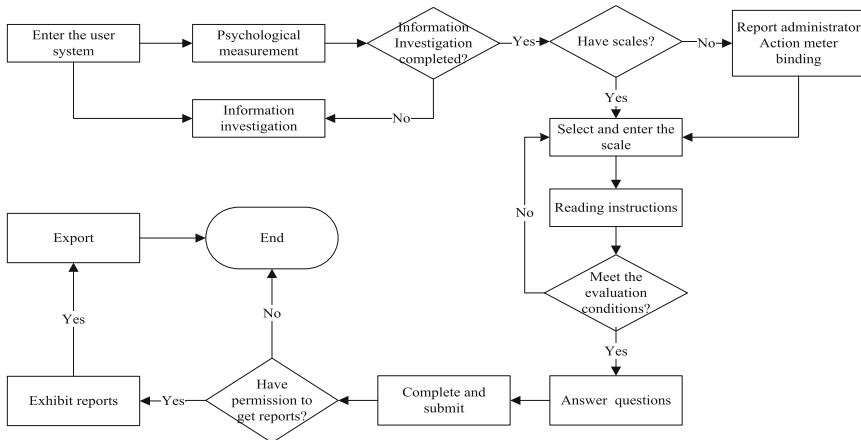


Fig. 4. Flow chart of user system

5 Results and Conclusions

The system was tested in an auditorium that can accommodate 1000 people in order to test the reliability. The system server, gateway and switch are placed at the rostrum

of the auditorium. The auditorium area is divided into four area with the vertical and horizontal axis of symmetry as the boundary. Four APs are arranged in the middle of each block and powered by POE power supply module. The tester logged in to the manager system on the server and set role permissions and evaluation tasks; 8 subjects were divided into 4 groups, located at any position in 4 areas, used mobile phones to access WLAN, completed psychological measurement and, and checked whether the report was displayed normally according to the tester permission allocation condition. In order to check the data transmission and storage, all subjects were required to select A-B-C-D in turn, conducted 20 groups in total, and then checked the database. The test shows that the system runs smoothly and the received data is 100% correct. The research team also applied the system to conduct psychological tests on two military units with about 2500 and 1200 people, established the psychological archives of soldiers, and will continue to apply the system to manage the psychological archives in future work.

This study designs a psychological measurement and archives management System suitable for large-scale psychological measurement, psychological ability selection test, psychological measurement data storage and management of military personnel. Based on the original single soldier handheld psychological evaluation equipment, the system uses the user's mobile phone as the measurement terminal, which greatly reduces the system quality and improves the portable performance. Through the practical application in psychological measurement, psychological archives establishment and management, it is proved that the system has good performance in stability and anti-interference. It is especially suitable for large-scale psychological measurement and special personnel selection. It is a favorable tool to do a good job in military mental health work.

Acknowledgements. This work was supported by National MS Project, No. BKJ21B011.

Compliance with Ethical Standards. The study was approved by the Logistics Department for Civilian Ethics Committee of Air Force Medical Center, PLA.

All subjects who participated in the experiment were provided with and signed an informed consent form.

All relevant ethical safeguards have been met with regard to subject protection.

References

1. Xinfu, Y., Qian, Z., Shushan, C.: Changes in mental health of members of the Chinese army (1990–2007): a cross-temporal meta-analysis. *Acta Psychol. Sin.* **44**(2), 226–236 (2012)
2. Lei, X., Juan, J., Jia, W., et al.: Comparative study of Chinese and foreign military mental health. *China J. Health Psychol.* **25**(8), 7 (2017)
3. Quan, G.: Studies and design on the expert system of psychological consultation and web test for soldiers. National University of Defense Technology (2004)
4. Wendong, H., Tao, W., Xiaojing, L., et al.: Development of group psychological measurement multimedia system. *J. Fourth Mil. Med. Univ.* **20**(3), 225–227 (1999)
5. Zhihong, W., Wendong, H., Xiaojing, L.: Design of infrared multi machine response system. *Chin. Med. Equip. J.* **27**(9), 197–198 (2006)
6. Tao, W., Zhihong, W., Wendong, H., et al.: Development of psychometric system based on wireless communication technology. *Chin. Med. Equip. J.* **30**(12), 5–7 (2009)

Research on the Machine Character



Mechanical Analysis of the Structure of a Large-Scale Pipeline System Detecting Robot

Siyi Xiang^(✉), Xinyue Ma, Duzhong Feng, Yangguang Li, Shengyao Zheng, Dengchao Liang, and Bo Zhu

Hohai University, Changzhou 213000, China
1487750189@qq.com

Abstract. As an important tool for material transportation, the inner wall of the pipeline of large ocean going freighter is corroded all year round, which not only affects the normal work, but also endangers the safety of life and property. The existing maintenance technology is difficult to meet the complex needs of industry and life. In order to regularly inspect and repair the inner wall of the pipeline, a parallel robot structure that can adapt to the pipeline environment of cargo ships is designed. In order to realize and optimize the normal work of the pipeline robot, it is necessary to carry out mechanical analysis on the key parts and assembly parts of the robot, so as to be efficient. To complete this check accurately, with the help of computer finite element analysis software.

Keywords: Pipeline robot · Finite element analysis · Modal analysis

1 Introduction

Pipeline system is an important material conveying tool. With the development of modern industry, it has become an indispensable part of industry and human life [1]. In industrial and domestic use, due to force majeure, natural disasters and their own defects, the pipeline is likely to have a series of problems such as leakage, corrosion, leakage and aging [2], which seriously affects the work of the pipeline and brings great hidden dangers to the safety of life and property. In order to avoid the above problems in the pipeline system, the inner wall of the pipeline must be inspected and maintained regularly. At present, the widely used methods include disassembly inspection [3], acoustic inspection [4], electromagnetic inspection, pressure inspection [5] and endoscopy. These methods are inefficient, high cost, and easy to leave a dead corner that is difficult to detect. Therefore, pipeline robot has important practical significance for the development of industry. A detection robot for cargo ship pipeline is analyzed by ANSYS tool. UPFs, UIDL, TCL and other languages of ANSYS provide users with a good secondary development environment [6, 7].

2 Detecting Robot System Architecture

The front and rear parts of the pipeline robot are connected by a steering mechanism in the middle. The front part assumes the role of driving, and both the front and rear parts have the function of reducing diameter. The overall model of the robot is shown in Fig. 1.

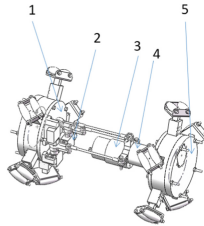


Fig. 1. The overall model of the robot. 1-rear unit; 2-steering gear; 3-drive motor; 4-conductive slip ring; 5-front unit

The physical prototype of the robot is shown in Fig. 2. The finite element analysis flow of pipeline system detection robot is shown in Fig. 3.

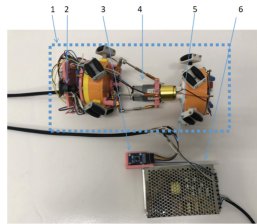


Fig. 2. The physical prototype of the pipeline detection robot. 1-Robot body; 2-camera module; 3-control handle; 4-DC drive motor; 5-aviation cable; 6-power

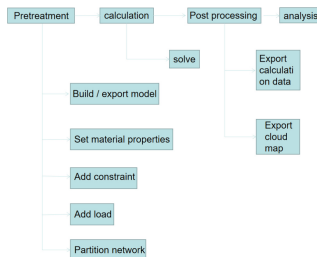


Fig. 3. Flow chart of finite element analysis

3 Statics Analysis of the Platform on the Parallel Mechanism

According to the designed robot structure, the load is mainly concentrated on the part of the parallel mechanism responsible for steering, and the upper platform connection where the three branches of the parallel mechanism are combined is the most stressed. At the same time, in the design plan, the upper platform is also used to fix the DC motor, which is the core part of the robot. Therefore, static analysis is required for this part to verify the reliability of its structure.

First, the part is modeled by the 3D modeling software Solidworks2018, as shown in Fig. 4. After the model is built, save it as a x_t format and then import it into ANSYS workbench.

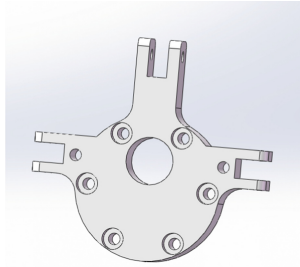


Fig. 4. Three-dimensional model of the platform on the parallel mechanism

Select the static analysis module in the workbench project and define the material properties. Because the part is subject to large forces and torques, and is located in the key part of the robot, it is processed and manufactured by aluminum alloy. Aluminum alloy has excellent mechanical properties and good corrosion resistance; and compared with structural steel, aluminum alloy has a lower density, which is beneficial to reduce the load of the robot. The material parameters of aluminum alloy are shown in Table 1.

Table 1. Aluminum alloy material parameter table

Young's modulus	Density	Poisson's ratio
68×10^3 MPa	2.70 g/cm ³	0.33

Constraints and loads are added to the part according to the design plan. The front and back sides of the part bear the torque generated by the weight of the robot at both ends, and the three cantilever beams bear the tension of each branch chain of the parallel mechanism and the pre-tightening force of the assembly screws. Refer to the mechanical design manual, where the screw assembly adopts 3.6-level strength and the pre-tightening force is 630 N. One side of this part is matched with the front half of the robot. The rollers of the front half of the diameter reducing mechanism are supported on

the inner wall of the pipe, which can be considered as a fixed constraint; the other side is equipped with a motor, which is subjected to torque. The magnitude of the torque is:

$$M = GL = 0.1 \text{ N} \cdot \text{m} \tag{3.1}$$

In the meshing step, the tetrahedron provided by ANSYS can adapt to parts with irregular shape, so it can be meshed automatically with this shape.

According to the above analysis results, constraints and loads are added in ANSYS and the mesh is divided. After calculation, the stress cloud diagram and strain cloud diagram are derived, as shown in Fig. 5.

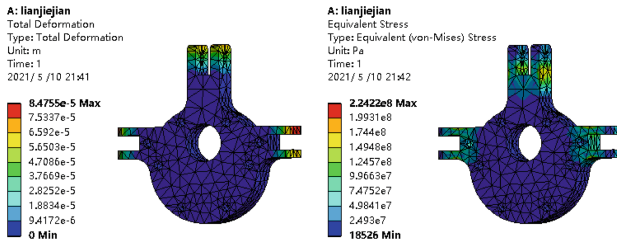


Fig. 5. Cloud diagram of strain (left) and stress (right) of upper platform of parallel mechanism

It can be seen from the above two figures that the maximum equivalent stress that the part bears is approximately approximately 218.8 MPa, and the tensile strength of the aluminum alloy is 263 MPa, and the yield strength is 229 MPa less than these two values, indicating that the strength of the part can meet the design plan. need. The total deformation value 1.947×10^{-5} m is very small relative to the structural size of the part, will not affect the accuracy of the parallel mechanism, and meet the design requirements.

4 Transient Dynamic Analysis of the Transmission Gear of the Reducing Mechanism

The diameter-reducing mechanism of the pipeline detection robot uses the output gear of the stepping motor to mesh with the large gear to transmit torque, which in turn drives the rotation of the plane thread to realize the radial expansion and contraction of the claw. Among them, the plane thread processing is more difficult, so 3D is selected. Make it by printing. Commonly used 3D printing consumables are PLA, ABS, and epoxy resin. Considering that the surface of the flat thread should be as smooth as possible, if there are burrs or unevenness, it may be impossible to rotate. Therefore, the resin with the smoothest and smoothest surface is selected as the printing consumable. However, the mechanical properties of resin parts are poor, so it is necessary to check whether they meet the design requirements. In particular, it is necessary to pay attention to the frequent operation of the reducing mechanism of the robot at the curved pipe, so the impact between the internal and external gears must be checked.

After assembling the two parts in Solidworks2018, import them into the transient dynamics solution module of ANSYS workbench, define structural steel and epoxy resin

and add them to the properties of the two parts. The relevant parameters are shown in Table 2.

Table 2. Material parameter table

Material name	Young's modulus	Density	Poisson's ratio
Structural steel	2×10^5 MPa	7.85 g/cm ³	0.3
Epoxy resin	2.4×10^4 MPa	1.117 g/cm ³	0.38

The constraints of the external gear are rotation constraints and the plane constraints of the slip ring; according to the selected stepper motor model, add the corresponding torque to the internal gear:

$$M = 0.1764 \text{ N} \cdot \text{m} \quad (4.1)$$

Different from the static analysis, the transient dynamic analysis object here is an assembly, and a contact plane needs to be added. Because it is a transient process, it is not necessary to set all tooth surfaces as contact surfaces, and 10 surfaces are selected at the assembly parts of internal and external gears to be defined as contact surfaces; In principle, the contact type should be Coulomb friction model. However, due to the large difference in the dimensions of internal and external gears here, the selection of rough surface contact type is more conducive to the convergence of calculation results, that is, there is only normal phase motion and no tangential motion on the two contact surfaces. The contact surface is shown in Fig. 6.

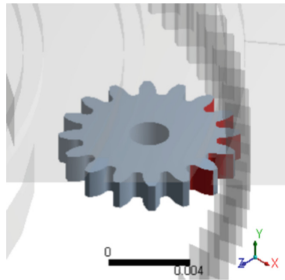


Fig. 6. Gear mating contact surface

For finite element analysis, gears are very irregular parts, which often lead to calculation failure. In order to help the finite element calculation to more easily converge, the transient process is divided into several sub-steps, and the minimum number of sub-steps is set to 25. The maximum is 100 steps, and the large deformation switch is turned off at the same time, and the mesh type to be divided is selected as tetrahedron. In addition, due to the large difference in the structural size of the internal and external gears, the

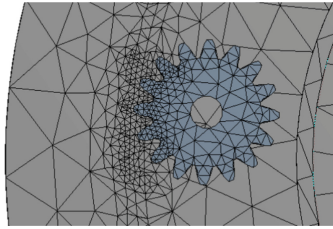


Fig. 7. Local refinement of the grid

mesh must be refined at the pinion, especially near the contact surface of the two gears, otherwise large errors will occur. The local mesh is refined as shown in the Fig. 7 shown.

To solve the assembly part, ANSYS used 95 steps to complete the analysis and derive the Strain diagram and stress diagram, as shown in Fig. 8.

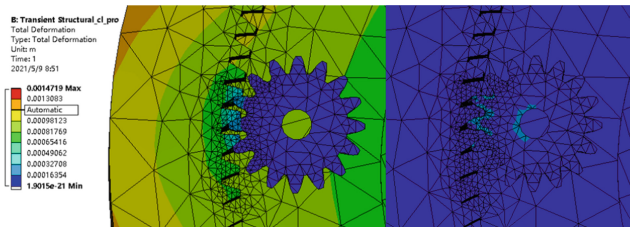


Fig. 8. Gear meshing strain and stress diagram

Among them, the stress of gear meshing is mainly analyzed, and the maximum stress value during the transient motion is derived from ANSYS, as shown in Fig. 9.

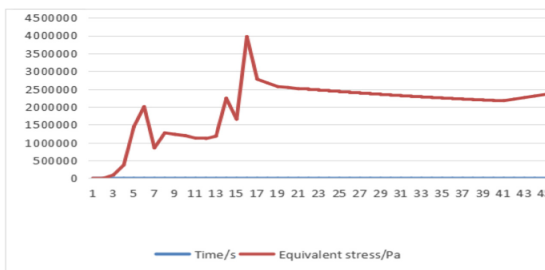


Fig. 9. Maximum stress during transient motion

Draw the above values into a line graph, as shown in Fig. 10, you can find that there are three obvious peaks. These three peaks are due to the gap between the two gears. When the internal gear starts to rotate, the three pairs of teeth in contact with the external gear will generate three impact loads at different time points. The working state of the motor is constantly stopping and starting, and impacts will occur frequently.

The maximum impact stress is 3.97 MPa that the allowable stress of various commonly used epoxy resin 3D printing consumables is generally 20 MPa above, which meets the design index requirements.

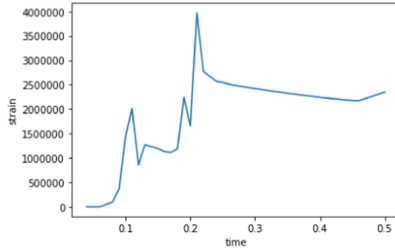


Fig. 10. Time - equivalent stress diagram

5 Modal Analysis of the Robot Body

In order to avoid resonance caused by the vibration of the motor during the movement of the robot, the robot body needs to be modal analysis to prevent the robot from being out of balance or leaving small parts in the pipeline. Modal analysis is a method of analyzing the dynamic characteristics of a mechanism. The modal reflects the natural vibration characteristics of the designed mechanism. Each order of modal corresponds to a specific natural frequency. The finite element analysis can quickly calculate the overall robot Natural frequency of vibration.

Import the 3D model assembly of the robot into ANSYS and generate it as a whole for easy solution. Here first choose to find the frequency from 1 to 20, and draw the solution result into a histogram, as shown in Fig. 11.

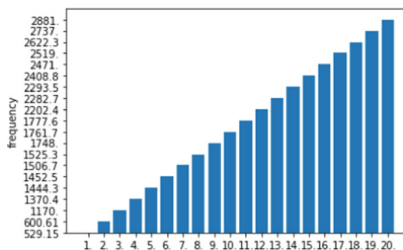


Fig. 11. Modal analysis 1–20 order frequency

The selected DC drive motor speed is 22 r/min, converted to frequency:

$$F = 22/60 = 0.37 \text{ Hz} \tag{5.1}$$

Therefore, the vibration of the DC motor will not cause resonance. Similarly, when controlling the rotation of the stepping motor of the reducing mechanism, the rotation frequency cannot be made the same as the frequency obtained by the modal analysis.

6 Conclusion

Based on the designed robot body structure, combined with its specific working conditions, a finite element analysis model was established using ANSYS workbench, and a key part, an important assembly part and the entire robot body were analyzed statically and transiently respectively. Dynamic analysis and modal analysis. The rationality of the design scheme is verified, and a basis is provided for the setting of the rotation frequency of the motor.

Acknowledgements. This work is supported by the **2018 national innovation training program for College Students**, No. **201910294104z**.

References

1. Qu, G.: Accelerating the development of the natural gas industry is one of the core tasks of my country's energy structure adjustment. *Sino-Foreign Energy* **16**(1), 2–7 (2011)
2. Li, L., Zhang, T., Gao, H., et al.: Research on the development of pipeline robots. *Mach. Manuf.* **58**(10), 5–7 (2020)
3. Chen, W.: Research on Low-Cost Pipeline Inspection Robot System. Chang'an University, Xi'an (2018)
4. Chen, S.: Research on Structural Design and Dynamic Characteristics of Ship Pipeline Inspection Robot. Shenyang University of Technology, Shenyang (2019)
5. Li, Z., Ding, L., Lu, M.: A drainage device for the air compressor tank. China, Utility Model Patent. CN208687360U, 02 April 2019
6. Li, G., Chen, W.: Research on the structural strength of the gearbox of a rotary drilling rig based on ANSYS. *Mech. Des.* **38**(S2), 155–159 (2021). <https://doi.org/10.13841/j.cnki.jxsj.2021.s2.032>
7. Kovalov, A., Otrosh, Y., Chernenko, O., Zhuravskij, M., Anszczak, M.: Modeling of non-stationary heating of steel plates with fire-protective coatings in Ansys under the conditions of hydrocarbon fire temperature mode. *Mater. Sci. Forum* **6266** (2021)



Design Point of Civil Aircraft Precooler Based on a Dimensionless Coefficient Method

Zhiyong Min^(✉), Xiaodan Huang, Yi Cao, Huayan Liu, and Xuhan Zhang

Shanghai Aircraft Design and Research Institute, Shanghai 201210, China
minzhiyong@comac.cc

Abstract. Pneumatic system is the hub of many aircraft air consumer systems, which provide the air source after preliminary temperature and pressure regulation for cabin pressurization, air conditioning, anti-ice, fuel inerting. Precooler is the core component of pneumatic system to adjust temperature. So it is a key issue to confirm the design point in thousands of operating conditions, so that the design can cover the maximum heat load to satisfy the downstream system requirement. In this paper, a simple and efficient method combined with heat exchange and engineering experience is proposed, which calculating the dimensionless coefficient of heat transfer intensity directly only by engine and environment parameters. Meanwhile, evaluating the heat transfer intensity of precooler on different operation condition by a verified model of a civil aircraft type in service to demonstrate the reliability of this method is presented in the paper.

Keywords: Pneumatic system · Dimensionless coefficient method · Design point · Precooler

1 Introduction

Pneumatic system is a crucial guarantee of the environment control system to keep the safety of flight and passenger health, which provide preliminary regulated air of appropriate temperature and pressure to downstream subsystems. Precooler is the key of temperature regulation. By means of transferring the heat from hot air imported from engine compressor to the cold air, the outlet temperature of pneumatic system will be adjusted to an accepted temperature, usually be 232 °C in experience.

The traditional way to define the design point of the precooler is totally based on engineering experience. The design point is usually chosen when aircraft operating on ground idle condition on a hot day due to the high bleed temperature and low mass flow in cold side are both serve to the heat exchange. The experienced method is partially satisfied the requirement when the similar performance system has been already verified on the other aircraft type. But it will lead to more design iteration on a new type of aircraft with particular system requirement of downstream systems, because too much operation condition is beyond consideration. In recent decades, some targeted study has been focus on this issue. Huang [1] and Chen [2] developed a steady model respectively to estimate the outlet temperature of the precooler. The model solved the problem on

neglect of whole flight envelope condition, but each case need to iterate the flow and differential pressure of fan air valve for several times is in low efficiency, as well as this method need to estimate the efficiency of heat exchanger in experienced method. Besides, the other research put more focus on simulation and control logic of pneumatic system. Mathieu [3] developed some components model of pneumatic system, as well as Linares [4] developed the whole dynamic model of CS300 environmental control system. These research built the models, which were helpful to study the system performance, dynamic response and control logic, but do no good to the component design. Pollok and Casella [5] studied several control strategies aim to improve the performance when the bleed air system is often prone to limit cycle oscillations.

Considering the importance of precooler design, the research is devoted to finding out an efficient and convenient way to solve it. And the method is applied on a pneumatic system of a type of aircraft in service to confirm the design point. As well as, a dynamic model in that type of pneumatic system is built to evaluate the heat transfer performance of each flight cases to verify that the design case chosen by the method proposed in the paper is most sever of all.

2 Method

The dimensionless coefficient method is developed below. Considering the heat exchange in precooler is steady and adiabatic, the heat transfer of cold side and hot side can be calculated by Eq. 1 and Eq. 2 [6] respectively:

$$Q_h = \dot{m}_h \cdot C_p \cdot (T_{bleed} - T_{target}) \quad (1)$$

$$Q_c = \dot{m}_c \cdot C_p \cdot \Delta T_c \quad (2)$$

where \dot{m}_h and \dot{m}_c are mass flow rate of air in cold side and hot side. C_p is the specific heat of air. T is air temperature.

Before designing, the mass flow rate and the outlet temperature are both unknown, so the heat transfer in Eq. 2 can not be solved directly. Therefore, the potential energy of temperature difference in the cold side can be approximately replaced by the deviation of the cold side inlet temperature and outlet target temperature of the hot side. Generally, the larger the deviation of temperature, the lower the cold side flow rate required in the situation of the same heat transfer. The relationship between flow rate and pressure difference of the whole cold side flow channel can be approximately regarded in Eq. 3:

$$\dot{m}_c \propto f(P_{fan} - P_{amb}) \quad (3)$$

where P_{fan} and P_{amb} represent the pressure of engine fan and ambient.

Ideally, the ratio of heat transfer between the hot and cold sides is 1 when neglecting the energy dissipation. Ignoring the change of physical property parameters caused by temperature, the heat transfer intensity factor (HF) can be defined as the ratio of heat transfer between the hot and cold sides, and the relationship is as follows in Eq. 4:

$$HF = \frac{\dot{m}_h \cdot (T_{bleed} - T_{target})}{(P_{fan} - P_{amb}) \cdot (T_{target} - T_{fan})} \quad (4)$$

Based on the above equation, the higher the dimensionless factor HF is, the higher heat transfer performance requirement of precooler is required.

3 System Model

In order to verify the accuracy and reliability of the dimensionless coefficient method proposed in this paper, a dynamic model of pneumatic system will be established following for proving that the design point of the precooler based on the dimensionless coefficient method can cover all the heat transfer demand of the system among flight envelope.

3.1 Hypothesis

All the components model of this type of pneumatic system are developed by following assumptions and hypothesis:

1. All components are adiabatic.
2. All models are lumped parameter models.
3. Air is regarded as an ideal gas.
4. Simplifying the dynamic response of components, due to it does no effect on the steady performance. So the response of temperature sensor and heat exchanger are regarded as one order inertia. The response of pneumatic valve with torque motor is regarded as simple time delay.

3.2 Formulation

3.2.1 Valve

The mass flow rate of the butterfly valve is calculated by Chester-Smith formulation [7] by Eq. 5:

$$\dot{m} = \frac{K_{cs} C A P_u N}{\sqrt{T_u}} \quad (5)$$

where A is flow area of valve, C is discharge coefficient and N is restriction factor. K_{cs} is a constant equal to 0.53 in imperial units. P_u and $\sqrt{T_u}$ in the above equation are all in total form.

The flow area can be calculated related to valve angle by Eq. 6:

$$A = \frac{\pi D^2}{4} (1 - \cos(\alpha)) \quad (6)$$

where D is valve diameter and α is valve angle.

3.2.2 Precooler

The outlet temperature of the precooler hot side can be calculated by Eq. 7:

$$T_{ho} = T_{hi} - \varepsilon_h(T_{hi} - T_{ci}) \quad (7)$$

where ε_h is the heat transfer efficiency.

The outlet temperature of the precooler cold side can be calculated by Eq. 8:

$$T_{co} = T_{ci} + \frac{\dot{m}_h C_{p,h}(T_{hi} - T_{ho})}{\dot{m}_c C_{p,c}} \quad (8)$$

3.2.3 Duct

The pressure loss of the duct can be calculated by Eq. 9:

$$\sigma \Delta P = \alpha \dot{m}^\beta \quad (9)$$

where ΔP is pressure difference. $\sigma = \frac{\rho}{\rho_0}$, ρ_0 is the density of air on standard condition. α and β are fitted by CFD simulation or experiment.

3.2.4 Temperature Mixture

The mixture of temperature can be calculated by Eq. 10:

$$T_o = \frac{\sum_1^n (\dot{m}_{i,j} T_{i,j})}{\dot{m}_o} \quad (10)$$

3.2.5 Rate of Pressure Change

The rate of pressure change in control volume is key to the conservation of mass, which can be calculated by Eq. 11:

$$\frac{dP}{dt} = \frac{\gamma RT}{V} \left(\sum_1^n \dot{m}_{i,j} - \sum_1^m \dot{m}_{o,j} \right) \quad (11)$$

where $\gamma = \frac{C_p}{C_v} = 1.4$. R is the gas constant which equals to 287 J/kg · K. V is the volume.

3.2.6 Downstream System Characteristic

In order to make sure the formulation conservative, the downstream characteristic of pneumatic system is simplified in an orifice. The parameters of the orifice should be calibrated by the flight test data. The orifice can be calculated by Eq. 12:

$$\dot{m} = \frac{K_o A p_u}{\sqrt{T_u}} \frac{2\gamma g \left(\phi^{\frac{2}{\gamma}} - \phi^{\frac{1+\gamma}{\gamma}} \right)^{0.5}}{(\gamma - 1)R} \quad (12)$$

where $\phi = \frac{p_d}{p_u}$, when $\frac{p_d}{p_u} > 0.5283$. And $\phi = 0.5283$, when $\frac{p_d}{p_u} \leq 0.5283$.

4 Discussion

4.1 Design Point

Confirming the design point of precooler based on the engine data of a civil aircraft in service by the dimensionless coefficient method. And the engine data is preliminarily screened in the following conditions:

1. Layout in all economy and the bleed configuration is in 1B2P mode.
2. Flight conditions: Take off, Holding, Cruise, Descent.
3. Target temperature of the precooler hot side outlet is 232 °C.
4. Ambient temperature is chosen in hot day.

777 cases have been calculated in total, and the result of design point is shown in the Table 1.

Table 1. The design point of precooler

Altitude (ft)	Mach	Ambient pressure (psi)	Ambient temperature (K)	Fan pressure (psi)	Fan temperature (K)
5000	0.3	12.23	303.24	14.20	318.78
IP pressure (psi)	IP temperature (K)	HP pressure (psi)	HP temperature (K)	HF	
48.59	497.95	175.33	724.56	3.01	

4.2 Verification

The dynamic model is built by Simulink in method of chapter 3. When each cases solving, the pneumatic system is operated in different configuration, pressure and temperature target. So the simple PID algorithm is designed for valve control by the classical control theory. The model is calibrated and the error of the cold side flow rate does not exceed 6.6% compared to the flight test data.

All the system parameters are calculated automatically by programming a script. The result shows all the outlet temperature can be controlled to 232 °C, so that the design of precooler met the requirement. Mass flow rate, volume flow rate, the heat transfer of precooler and HF factor are chosen to evaluate the heat transfer intensity. The sever conditions evaluated by these indexes are show in Table 2. We need to discuss that the design point we found is the most sever condition of these.

Table 2. The most severe conditions of precooler

Case 2106					
Altitude (ft)	Mach	Ambient pressure (psi)	Ambient temperature (K)	Fan pressure (psi)	Fan temperature (K)
5000	0.3	12.23	303.24	14.20	318.78
IP pressure (psi)	IP temperature (K)	HP pressure (psi)	HP temperature (K)	Mass flow rate of cold side (kg/s)	Volume flow rate of cold side (m ³ /s)
48.59	497.95	175.33	724.56	1.9	1.78
Heat transfer (kJ)	Outlet temperature (K)	HF			
518.27	505	3.01			
Case 2116					
Altitude (ft)	Mach	Ambient pressure (psi)	Ambient temperature (K)	Fan pressure (psi)	Fan temperature (K)
5000	0.35	12.23	303.09	14.91	323.38
IP pressure (psi)	IP temperature (K)	HP pressure (psi)	HP temperature (K)	Mass flow rate of cold side (kg/s)	Volume flow rate of cold side (m ³ /s)
57.81	519.20	214.61	757.40	2.22	1.99
Heat transfer (kJ)	Outlet temperature (K)	HF			
597.99	505	2.60			
Case 17622					
Altitude (ft)	Mach	Ambient pressure (psi)	Ambient temperature (K)	Fan pressure (psi)	Fan temperature (K)
41000	0.73	231.92	303.24	5.59	293.41
IP pressure (psi)	IP temperature (K)	HP pressure (psi)	HP temperature (K)	Mass flow rate of cold side (kg/s)	Volume flow rate of cold side (m ³ /s)
35.19	531.13	159.75	826.63	1.78	3.87
Heat transfer (kJ)	Outlet temperature (K)	HF			
608.60	505	2.03			

Compared with Case 2116 and Case 17622, the heat transfer of the precooler is close to each other, as well as, the cold side heat transfer efficiency of Case 2116 is lower, which is 0.58 and 0.60 respectively. So it can be concluded that Case 2116 is more severe. Taking flow performance into account at the same time, the mass flow of the cold side required by Case 2116 is greater, but the total pressure is lower, so the flow performance requirement is more severe too.

Compared with Case 2106 and Case 2116, the environmental parameters and flow demand of pneumatic system are the same. The heat transfer is lower, because of the bleed

temperature of Case 2106 is lower due to the engine thrust cause by passenger attendance. Compared with the precooler efficiency at the same time, it is found that Case 2106 is much lower than Case 2116, which are 0.54 and 0.58 respectively, indicating that the heat transfer performance of Case 2106 is more severe. Meanwhile, flow performance is taken into the consideration. The cold side mass flow rate in Case 2116 is 1.16 times that of Case 2106. It can be considered commonly that the flow is approximately proportional to the pressure difference and inversely proportional to the square root of the temperature. Under the circumstances that the inlet air temperature is closed, the total head of cold side in Case 2116 is 1.36 times that of Case 2106. It can be proved that the flow performance of Case 2106 is also more severe.

So it can be concluded that Case 2106 is the most severe case of precooler when it operates in 777 cases among the flight envelope.

5 Conclusions

A dimensionless coefficient method is proposed in this paper based on basic principle of heat transfer and engineering experience. This method can confirm the design point of precooler efficiently by only using engine and environment data. By screening the data of a civil aircraft in service, we found the design point.

A dynamic model of pneumatic system is built for verifying the method in that type of civil aircraft data. Heat transfer, HF factor, mass flow rate and volume flow rate of cold side have been calculated for all flight cases to evaluated the working intensity of precooler. By analyzing the data, we found that the case chosen by HF factor was suitable for designing the precooler because it takes both transfer intensity and flow performance into consideration, as well as, it can cover all other severe cases. So we can confirm that the method proposed in this paper is reasonable and can be applied in engineering design.

References

1. Huang, X., Wang, R.: Calculation of temperature regulation performance of civil aircraft air intake system. *Sci. Technol. Inf.* **20**, 2 (2011). (in Chinese)
2. Chen, B.: Selection and analysis of design points for civil aircraft precooler. *Sci. Technol. Vis.* **8**, 2 (2017). (in Chinese)
3. Mathieu, K.: *Simulation of Components from the Environmental Control System* (2006)
4. Linares, D.P.: *Modeling and Simulation of an Aircraft Environmental Control System* (2016)
5. Pollok, A., Casella, F.: Comparison of control strategies for aircraft bleed-air systems. *IFAC-PapersOnLine* **50**(1), 14194–14199 (2017)
6. Yang, S., Tao, W.: *Heat Transfer*, 4th edn. Higher Education Press (2006)
7. Smith, C.W.: Calculations of flow of air and diatomic gases. *J. Aeronaut. Sci.* **13** (2015)



Research on Application of Stepper Motor in Cabin Pressure Regulation System

Ying Wang^{1,2(✉)}, Zhendeng Xing², Quanyi Zheng², and Guoyuan Zhang²

¹ School of Aeronautic Science and Engineering, Beijing University, Beijing 100191, China
wangying20080910@126.com

² Xinxiang Aviation Industry (Group) Co., Ltd., Xinxiang 453049, China

Abstract. In order to realize the control of the small and high reliability cabin exhaust valve, adapt to the application of intelligent manufacturing technology, the paper studies high-performance stepper motor drive, solve the problem of the stepper motor step-out, vibration, heating, improves the ability of the stepper motor, and reduces the use of the device and improves the economy. According to the characteristics of two-phase hybrid stepper motor, Frequency Modulation (FM) of two phases is designed. On the other hand, aiming at the heating problem of stepper motor, poor controllability, optimization of stepper motor acceleration, deceleration dynamic characteristics, reduced jitter when starting and stopping, and reduced excess adjustment of the motor by using the sigmoid function as the basis. The experimental results show that, based on the soft breakdown stepper motor drive of Frequency Modulation (FM) technology has better performance than the traditional open-loop control method, the acceleration can reach 60 rpm/ms or more (28 V). During the stepper motor acceleration and deceleration, the starting current decreases by the excess 50%, and the continuous running current is not much than the 0.3 A, 0–10°/s speed change in 100 ms, which can satisfy the different type stepper motor control of the 0–10 mNm torque and strengthens the loading ability.

Keywords: Stepper motor · FM · Micro-stepping · S shape acceleration-deceleration curve · Outflow valve

1 Introduction

The cabin pressure controller system (CPCS) adjusts the opening or speed of the exhaust valve in real time according to the pressure system. With the development of brushless DC technology, the actuator of cabin pressure regulation system at home and abroad tends to adopt brushless DC motor drive scheme. The scheme is equipped with rotary transformer and HALL sensor to collect angle and speed. Domestic CPCS execution parts are not product adopts stepper motor, some models abroad and domestic inlet CPCS is still using stepper motor, mainly because of the airborne equipment size and weight limit, for civilian airliners economy into consideration, and the advantages of pulse stepper motor driver, etc., so that it is still has a huge advantage. Compared with

DC motor scheme, the weight and size of stepper motor can be reduced by more than 20% and 30% under the same control requirements. However, it has some problems [1] such as high noise, speed limit, heating and step-out, which bring great challenges to engineering application and increase the complexity of control.

Stepper motor has the advantages of economy, high torque, simple structure, locked-rotor will not damage the motor [1–4], etc. There are many researches on stepper motors at home and abroad, and many solutions are given for common problems, but most of them are solved for specific problems, without considering the comprehensive and applicability of practical engineering applications, such as Limited resources, how to better optimize motor control. In this paper, the driving control of the actuator of CPCS was studied. In view of the requirements of miniaturization, high reliability, and applicability, and component selection, the soft subdivision driving control based on S-curve was studied.

At present, stepper motor subdivision drive technology has been mature application [5], the current from 0 to the maximum to form a few intermediate states, and further improve the operation stability. However, there are some limitations in device selection and cost. In this paper, the subdivision drive adopts a two-stage soft subdivision strategy, which can reduce the induced electromotive force (EMF) during the commutation through PWM, reducing the motor current. Considering the torque-frequency characteristics of stepper motor, in the low-frequency region, the electromagnetic torque decreases slowly, while in the high-frequency region, the torque-frequency curve drops sharply [6] and the electromagnetic torque decreases rapidly. Sigmoid function is used as the basis of acceleration-decelerate control strategy to optimize the dynamic characteristics of [7], which ensures that stepper motor runs without losing step, and gives full play to the inherent characteristics to shorten the acceleration-decelerate time.

2 Based on S-Shaped Acceleration-Decelerate Curve Control Strategy

The dynamic equation of the stepper motor is:

$$T_M - T_L = J \frac{d\omega}{dt} + B\omega \quad (2.1)$$

To solve the differential equation:

$$\omega = \frac{(T_M - T_L)}{B} \left(1 - e^{-t \frac{B}{J}}\right) \quad (2.2)$$

According to Eq. (2.2), an exponential acceleration curve can be obtained (Fig. 1), which is consistent with torque-speed characteristic. But in practical application, stepper motor is overcome by load torque, and the inertia torque on the shaft, if the acceleration is large when startup, it is possible to overcome the load that is heavier than the continuous operation, which can be lost or volatile [8]. The linear acceleration curve is combined with the sigmoid function, which is translated by translation and scaling operation (Fig. 1).

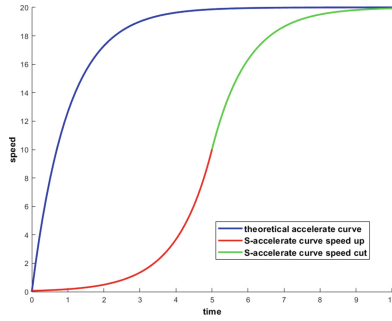


Fig. 1. Stepper motor acceleration curve

The formula of S-type acceleration curve is:

$$\begin{cases} v = \frac{v_{cmd}}{2} e^{A(t-\frac{T}{2})}, & t < \frac{T}{2} \\ v = \frac{v_{cmd}}{2} \left(1 - e^{-A(t-\frac{T}{2})} \right) + \frac{v_{cmd}}{2}, & t \geq \frac{T}{2} \end{cases} \quad (2.3)$$

where, A is acceleration-decelerate factor, T is acceleration-decelerate time, and v_{cmd} is the target speed.

3 Software Design

3.1 Acceleration-Decelerate Curve Optimization Design

The acceleration-decelerate curve optimization design of stepper motor can reduce the acceleration-decelerate time and optimize the motor dynamic performance. In order to meet the change of the initial position in acceleration-decelerate curve, searching acceleration initial position strategy is added (Fig. 2).

- (1) When the speed instruction received is updated, it need to look again the position, ensure that the acceleration point falls within the acceleration interval, and search the initial position of acceleration:

$$\begin{cases} p = j, & \text{if } v_{cmd} * N_j \geq v, \text{ forward} \\ p = n, & \text{reversal} \end{cases} \quad (3.1)$$

$j \in [1, \dots, n]$, N_j is the value of the j acceleration point in the acceleration curve. The current target speed is accelerated from this position to the received speed instruction position.

- (2) In embedded system, the calculation of exponential function is complicated, Taylor formula is adopted to approximate expression, and the calculation formula of acceleration-decelerate step target value is obtained:

$$\begin{cases} v_{object} = v_{cmd} * [N_k + (k - \text{floor}(k)) * dN_k], & k < n \\ v_{object} = v_{cmd}, & k \geq n \end{cases} \quad (3.2)$$

where, $k = p * c$, c is acceleration-decelerate coefficient. $k, p \in [j, \dots n]$, If the motor accelerates, p add 1; Motor decelerates, p minus 1, until 0. N_k, dN_k Obtained by Eq. (3.2).

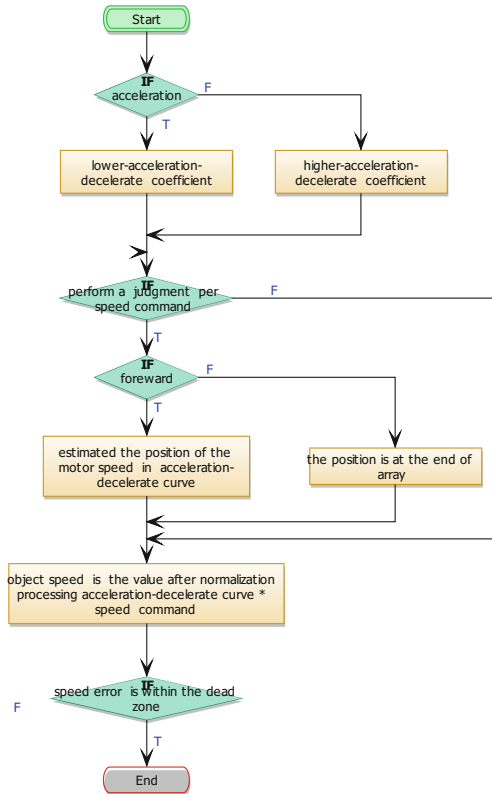


Fig. 2. Software implementation process

3.2 Subdivision Drive Design Based on FM Technology

In this paper, the stepper motor (see Table 1) is involved. When the size and weight meet the requirements of the pressure regulation system, the continuous running current and peak current exceed 14% in series mode and 50% in parallel mode. Therefore, the subdivision technology is studied to reduce the current on the premise of meeting the rotor torque.

When the power supply is constant, it is assumed that the charging time of the stator winding is T_c us and the minimum driving pulse frequency is $1/T_c$ kHz. If the pulse period is less than $1/T_c$ kHz, the stator winding cannot obtain enough energy to generate a torque to drive the rotor, so that the rotor cannot keep up with the stator rotating magnetic field speed, and each step falls behind the balance position that should be reached, resulting step-out.

Constant Angle subdivision will maintain the same size, to ensure the same synthesis torque, to achieve stable motor operation. The disadvantage is that when the load changes, the motor may be step-out, because the torque is insufficient or too large. Using FM subdivision technology, is according to the change of the load. Under different angular acceleration conditions, the constant current is the target value, and the PWM carrier frequency is changed to ensure that the large load change is met, the motor heating is reduced as far as possible, and the reliability of motor operation is improved. Figure 3 shows the change of PWM duty cycle under the condition of current change.

$$f_m = \frac{d_i - 20}{u_i} \tag{3.3}$$

$$f_k = \min(f_m - \lambda, f_c) \tag{3.4}$$

where, $\lambda \in (i, \dots n), i \in (1, \dots n)$, According to the table, the duty cycle corresponding to the target acceleration a_i is d_i , the original carrier frequency is f_m , and the target carrier frequency is $f_c = d_i/u_i$.

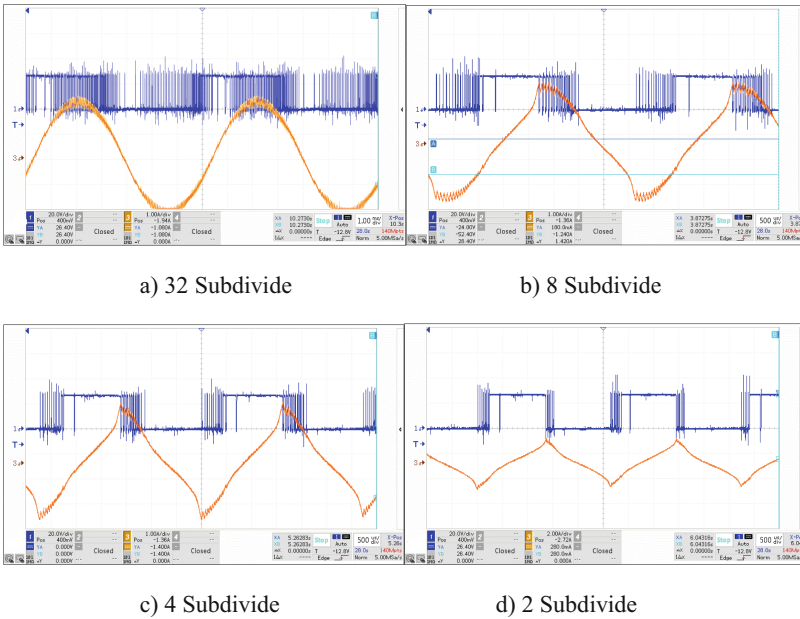


Fig. 3. FM Subdivided driving technology

4 Experimental Results

Speed instruction range is $-10-10^\circ/s$, resolution ratio: 0.00122. It is required that $0-10^\circ/s$ speed changes within the range of 100 ms. The encoder has 1024 pulses in each

circle, and the corresponding angular resolution is 0.088° . Each turn, the index channel output an index pulse, used to calculate the motor speed.

The motor was selected for test, and the maximum speed was 2000 rpm. Its specific parameters were shown in Table 1, and the torque-frequency characteristic curve of the motor was shown in Fig. 4.

Table 1. Stepper motor parameter

Type	Two-phase hybrid	Phase current/A	In series 0.47 In parallel 0.94
Power source/V	28	Peak phase current/A	In series 0.91 In parallel 1.81
Stator winding charging time/us	30	Phase inductance/mH	36
Holding torque/mNm	62	Step angle/ $^\circ$	3.6

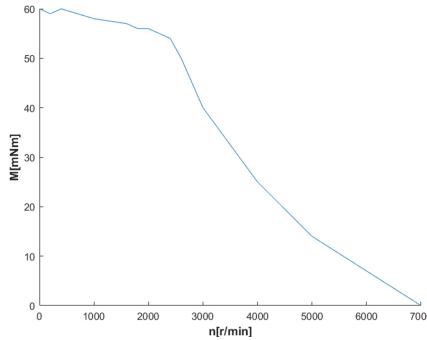


Fig. 4. Torque-frequency characteristic curve of stepper motor

Test the current changes of the motor under different duty ratios (Table 2), through the summarize of the current under different duty ratios, select the appropriate soft subdivision point, to control the current.

Table 2. The current under different duty ratios

Duty	Speed current/A			
	2 $^\circ$ /s	5 $^\circ$ /s	8 $^\circ$ /s	10 $^\circ$ /s
100%	0.842	0.271	0.199	0.182
70%	0.300	0.200	0.162	0.152
50%	0.150	0.139	—	—
30%	0.119	—	—	—

The acceleration curves of $10^\circ/s$ and $5^\circ/s$ were analyzed respectively in Fig. 5 and Fig. 6. Figure 7 shows the frequency change corresponding to the acceleration curve.

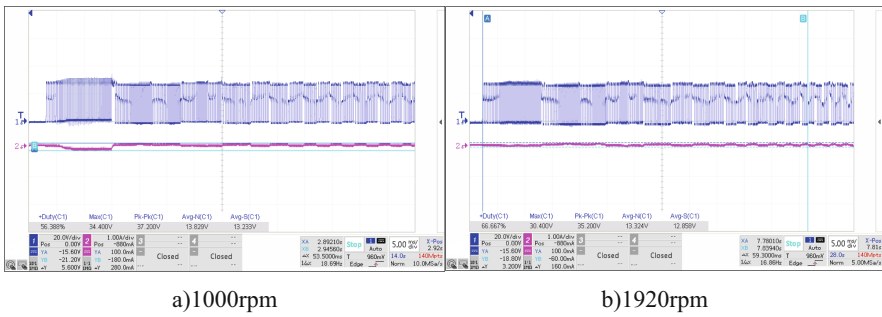


Fig. 5. Acceleration-decelerate curve and current waveform with no-load

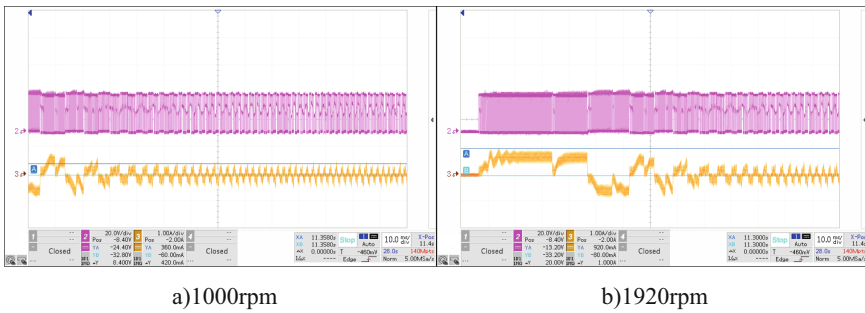


Fig. 6. Acceleration-decelerate curve and current waveform with loading conditions

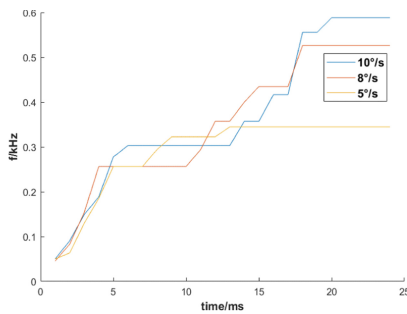


Fig. 7. The change in frequency that acceleration curve

- (1) It can be seen from the test results that loading situation, the speed ranges from 0 to 1920 rpm, the acceleration time is about 78.6 ms, and the time from 0 to

1000 rpm is about 40 ms. The deceleration time is about 76 ms and 38 ms respectively. The deceleration time is shortened compared with the acceleration time, mainly because of the change of friction of mechanical structure. The acceleration-decelerate coefficients can be set separately to adjust the consistency of positive and negative rotation. When the motor is unloaded, 0 to 1920 rpm, the acceleration time is 30 ms. With the increase of load, the motor reduces the growth time to improve the acceleration kinetic energy, to adapt to the load change.

- (2) From the current changes at different speeds, when the speed is small, the current is large. The reason is that input power is constant, low speed, large torque, large current. High speed induction current, small torque. When carrying, the peak current of 5°/s is not more than 0.8 A, and the normal operating current is about 0.2 A, less than 25% of the rated current of the motor, the power will run for a long time without heating. At 10°/s, the peak current is no more than 0.15 A under no-load, and the operating current is about 0.15 A.

5 Conclusion

Through test, the soft segmentation algorithm based on S curve can well meet the demand of cabin pressure control actuators, However, considering the complexity of the CPCS in practical application, still need constant attention, such as reliability and stability, as a further research direction.

References

1. Colombo, R., Bianchi, M.: Sensor-less estimation of frictions and moment of inertia of a stepper motor in a machining device. In: Electronics, Control, Measurement, Signals and Their Application to Mechatronics, pp. 1–5. IEEE (2017)
2. Vasylenko, O.V., Zhavzharov, I.L.: Model of a stepper motor for studying of automated positioning systems in ECAD (1), 31–38 (2017)
3. Ionica, I., Modreanu, M., Morega, A., et al.: Design and modeling of a PM stepper motor from the perspective of differentially flat systems. In: Control Conference. IEEE (2015)
4. Sun, Z.: Design and Implementation of High Performance Closed-loop Drive System for Stepper Motor Under Nonlinear Load. Zhejiang University (2019)
5. Gaan, D.R., Kumar, M., Sudhakar, S.: Real time precise position tracking with stepper motor using frequency modulation based micro stepping. IEEE Trans. Ind. Appl. 1 (2017)
6. Feng, Q., Deng, X., et al. Electromechanical rotation control. Huazhong University of Science & Technology Press (2011)
7. Chen, Z., Huang, F.: Research on S-curve control of stepper motor **10**(5), 640–645 (2019)
8. Lin, H.: Research on the Control System of Stepper Motor in Automatic Handheld Syringe. Zhejiang University (2018)



Analysis and Design of the Shopping Trolley for Elderly People Based on Ergonomics

Yaxuan Song^(✉), Ding Ding, Runsen Wang, and Hanzheng Di

Hohai University, Changzhou 213000, Jiangsu, China
1961710108@hhu.edu.cn

Abstract. Shopping trolley enjoys great popularity among the elderly products market, and it can bring certain convenience to the elderly. However, after the research about the actual using experience of them, it is found out that the current design can hardly meet users' needs with the unreasonable structure and unsuitable size, being incompatible with the machine and environment led to a poor level of satisfaction. Based on ergonomics, this paper carried out systematic analysis mainly focused on the handle part and wheel part. Besides, according to the trouble found in the investigation, we made a improved design with more practical features, improved folding and braking function and more matched color choice, which aims to better the experience of using shopping carts for the elderly and enable them to play a helpful role in other life scenarios.

Keywords: Young elderly · Ergonomics · Shopping trolley

1 Research Purpose

The purpose of this paper is to redesign the shopping trolley, so that they can meet the elderly people's physical conditions and real life needs, making shopping a more convenient thing for them.

2 User Research and Analysis

According to the definition of the World Health Organization, people aged 65–74 are called young aged [1].

Considering the physical health status, mentality and behavioral characteristics of them, the elderly between 65 to 74 years old can still take care of themselves with the ability of self-care and self-reliance. Although their physical conditions have declined to a certain extent, they still pursue new things in their hearts and are eager to establish a link with our society. So we choose the elderly people of 65–74 years old as our targeted users and summarize their characteristics as the following table (Table 1).

Table 1. Target users' characteristics

Characteristics	Conditions
Physical function	They are easy to fatigue with low endurance, agility and flexibility
Sensory function	They are troubled with passivation of sensation and poor eyesight and hearing
Psychological function	They suffered memory loss and imagination decline
Paranoia and sensitivity	Due to the decline of physical function, it becomes inconvenient and sensitive for them to participate in some social activities
Negative attitude	Because the degradation of bodily function, they may resist new products to a certain extent

3 Design Based on Ergonomics

We summarize the the data as the main design references in terms of GB10000–88 *Chinese Adult Body Size* [2] (Table 2).

Meanwhile, it is worth considering the decrease of the height of the elderly due to the aging of the lumbar intervertebral disc, water loss and the compression of the lumbar intervertebral disc caused by standing for a long time [3].

So specific and appropriate corrections of the data should be made in the following design calculation considering the actual situation.

Table 2. Body size percentage (unit: mm)

Measurement items	Male			Female		
	P ₅	P ₅₀	P ₉₅	P ₅	P ₅₀	P ₉₅
Height	1588	1683	1776	1486	1572	1661
Elbow height	956	1026	1097	900	961	1025
Shoulder width	346	376	404	320	350	378
Hand width	76	82	89	70	76	82
Hand length	170	183	196	159	171	184

3.1 The Handle Part

Height: The height of the trolley is determined by the height of the handle, which is based on the elbow height. In order to ensure that 95% of people can use it, P₉₅ of that of the male should be used as the upper limit of the design parameter, while P₅ of that of the female as the lower limit. However, considering factors such as the decrease in height of the elderly and the hunchback in the actual situation, the P₅₀ of male is finally selected as the upper limit correction value.

According to Body size percentage (Table 2), the two limit values are 1026 mm and 900 mm respectively.

Besides, the most comfortable height for human body is 76 mm below the height of the human elbow.

So, based on the above analysis, the *minimum length* is:

$$900 - 76 = 824 \text{ mm} \quad (1.1)$$

The minimum length is:

$$1026 - 76 = 950 \text{ mm} \quad (1.2)$$

Diameter: As the data depends on the size of the hand, a comprehensive consideration [4] was made with the hand length in Table 1 and the formula (1.3).

$$L = \pi \cdot D \quad (1.3)$$

As a result, the suitable range is 30 mm to 40 mm. Therefore, we decided the width of the large end was 40 mm while the small end was 30 mm (Fig. 1).



Fig. 1. Diagram of the diameter

The way the handle is stressed:

The scenario when elderly people walking up the stairs is shown in Fig. 2.

It is easy to see that the elderly have to bend down to adapt to the height of the trolley in the right (Fig. 2). Since bending will cause discomfort and damage to the waist of the elderly, we choose the left style (Fig. 2) in our design project which can save effort when going upstairs. At the same time, it diversified the usage of shopping cart as it can be pushed or pulled by changing the position.

3.2 Improved Foldability

Inspired by the field research, although most of the existing trolleys have a folding function, there is no fixed connection between the folding rack and the trolley frame. The two needed to be manually fixed to ensure that the rack does not fall back (Fig. 3).

Therefore, it is considered to add a snap connection to fix the position. The details are shown in Fig. 4. Therefore, it can help reduce the pressure on the hands when folding the stack up, which makes pulling large goods such as big cartons filled with drinks more convenient and labor-saving.

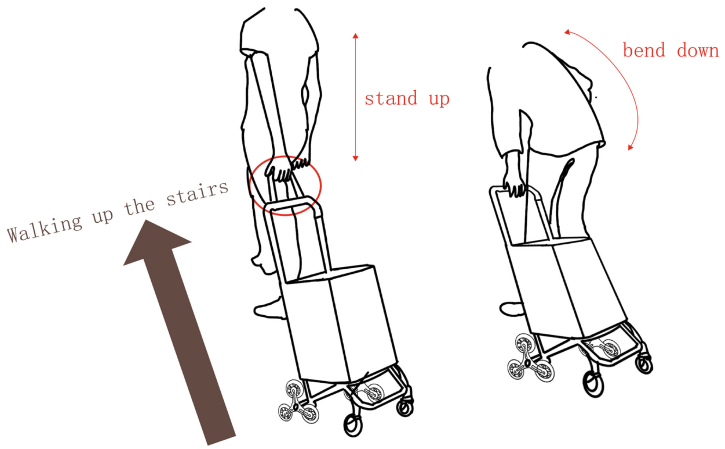


Fig. 2. Different postures with two handle styles when going upstairs

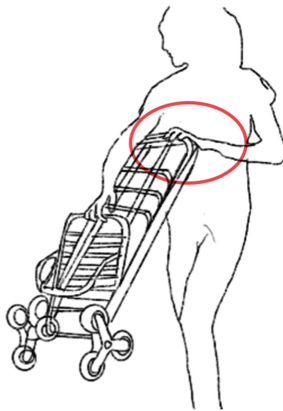


Fig. 3. Diagram of the existing shopping trolley after folding

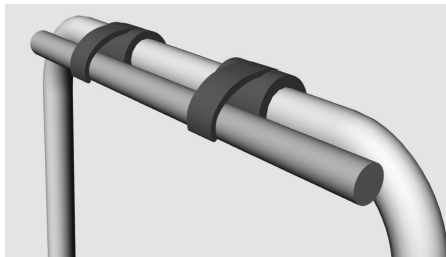


Fig. 4. Diagram of the fixing mechanism

3.3 Item Storage

Thinking about the needs of the elderly especially outside the market or shopping malls, a phenomenon deserved to be mentioned is that the elderly in the park usually need to temporarily put aside their bottles, handbags and other items before exercising. Nowadays, they mostly choose to put them on the public chairs or simply on the ground, showing the lack of infrastructure for this need.

In order to cater to such demand, we add an item storage bag based on the shape of the conventional trolley, as shown in Fig. 5.

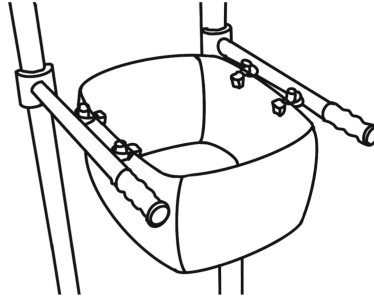


Fig. 5. Diagram of the added item storage space

3.4 Wheel Part

We carried out another improvement of our design (Fig. 6) regarding the wear resistance, slip resistance and height adaptability of the triangular stair climbing type, which is the most popular wheel type at the present market.

In order to improve the wear resistance of the wheels, the front wheel is made of solid wear-resistant rubber material, and the rear wheel is made of PU outsourcing material. In terms of anti-skid running of wheels, the anti-skid property of solid rubber material is better than that of ordinary plastic, so rubber material is used.

In addition, the texture roughness of the surface will also deepen. According to the national standard, the height of the steps of public stairs is 160–170 mm. The common cement base stairs in the home are based on this standard, and the a comparatively comfortable height is about 160 mm. However, according to the actual situation, the height of some triangular wheels on the market is less than 16 cm. Therefore, we make the overall height of the triangular stair climbing wheel get higher to 160 mm, as shown in Fig. 6.

3.5 Crutch Placement

Considering the target group of the shopping trolley, not every elderly person needs a crutch placement part. So the crutch placement part is designed as a detachable buckle structure.

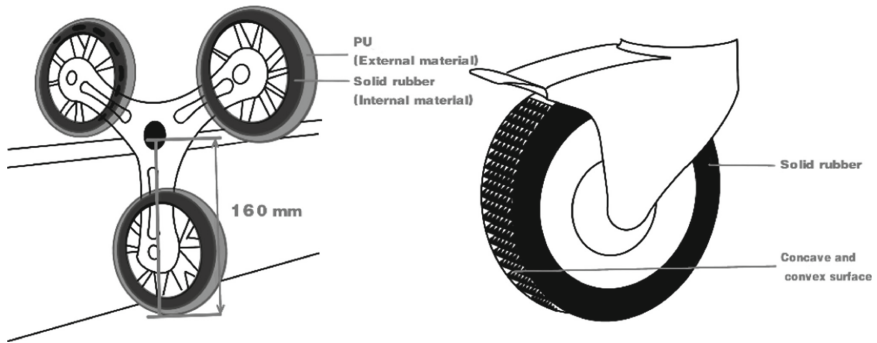


Fig. 6. Schematic diagram of wheel improvement

Since the size of the tie rod is 30 mm, the inner diameter of the joint part of the buckle and the tie rod is 28–30 mm. The upper diameter of the crutches is approximately 18–24 mm. The average value of the joint between the buckle and the crutches is 21 mm, as shown in Fig. 7.

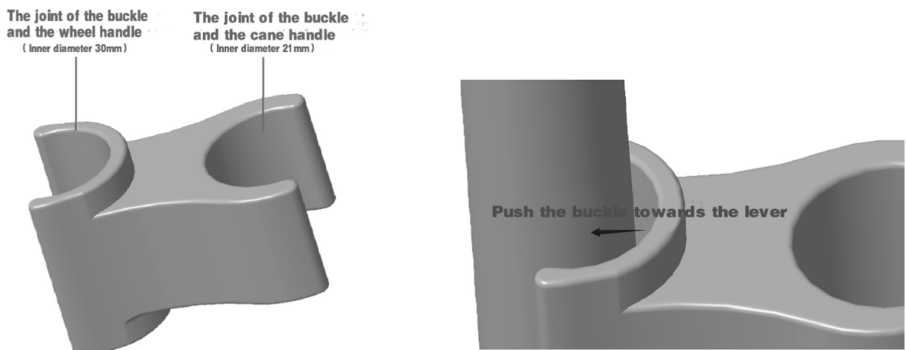


Fig. 7. Cane placement clip design

3.6 Brake Part

As for the problem that the body of the trolley tilted when brake the cart by foot from the front, we transformed the foot brake to hand brake control.

Considering the factors that continuous decline of bone density in the legs, muscle contraction, and the lack of alertness of joints [5], the brake control device of the brake will be placed to the hand, which is more convenient for the elderly to control the speed of the cart when walk on a landslide. This way, there is no need to go to the front of the trolley to control, which will improve the efficiency and safety (Fig. 8).

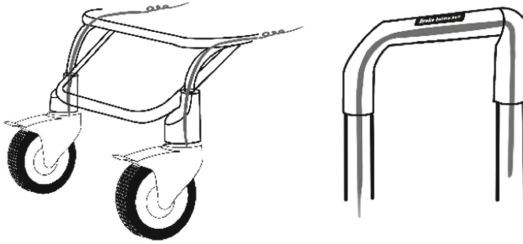


Fig. 8. Brake improvement diagram

3.7 Color Matching

According to the survey, the elderly are more inclined to colors with higher brightness and lower saturation, while warm colors have a more soothing effect on the psychology of them. In the specific function indication area, we need to change the single, dull, dim cool color system. Through bright colors, the visual attention of the elderly is attracted, which is conducive to memorizing operation and identifying information for the elderly. Besides, the bright color can also enhance the personalization and fashion sense of the product.

4 Design Outcome

As a result of our integrated design process, we developed the final product in three different colors (Fig. 9).

It meets the requirements of ergonomics and can effectively better elderly people's using experience by the optimization of structure and function.



Fig. 9. Display of different color schemes

References

1. World Health Organization integrated care for older people. In: Aging and Health (2015). <https://www.who.int/>. Accessed 6 Jan 2022
2. State Technical Supervision Bureau GB/T 10000-1988. In: Human dimensions of Chinese adults (1988). <http://www.gb688.cn/bzgk/gb/newGbInfo?hcno=A78583489235BF9BF9EE253E74DC76B9>. Accessed 6 Jan 2022
3. Luo, L., Liu, X.: Comprehensive optimization design of product size based on the principle of ergonomics. Microelectronics and Computers (2006)
4. Ding, Y.L.: Ergonomics. Beijing Institute of Technology Press, China (2011)
5. Hu, H., Li, X.: Body measurements of the elderly in Beijing. Ergonomics (2006). <https://doi.org/10.3969/j.issn.1006-8309.2006.01.013>.



Design and Development of Human Motion Capture System

Yuhong Shen, Chenming Li, Xiyu Bi, and Huilin Wei^(✉)

Institute of Quartermaster Engineering Technology, Beijing, China
154491268@qq.com

Abstract. In this work, a human motion capture system was designed to explore the influence of special equipment on the movement of human joints. In the system, 12 motion capture cameras were used to make the system equipment and configuration. The motion targets were designed according to the motion range and structural characteristics of different body segments. The motion measurement model was designed by using neural network algorithm, and the test software was developed. The test results suggested that the human motion capture system meets the static and dynamic multi-joint angle capture test requirements. It can realize the static detection of human activity and measure the range of motion of shoulder, elbow, wrist, finger, head and neck, waist, hip, knee, ankle and other joints in sagittal plane, coronal plane and horizontal plane, and the motion posture detection accuracy is up to 0.2° .

Keywords: Human motion capture system · Motion measurement model · Neural network algorithm · Human joints movement

1 Introduction

Human motion state monitoring mainly explores the testing technology of human activity under the condition of special equipment, which is mainly related to the measurement technology of the maximum range of human activity of various parts of the human body under static conditions and the statistics of human activity under dynamic conditions. Based on the photoelectric measurement technology, the research of human motion state monitoring adopts optoelectronic imaging equipment to detect, track, measure and estimate human targets in order to achieve the purpose of human activity detection under the condition of special equipment.

The content of static detection of human body under the condition of special equipment includes: measuring the range of motion parameters of human shoulder, elbow, wrist, finger, head and neck, waist, hip, knee, ankle and other joints in sagittal plane, coronal plane and horizontal plane, to obtain the maximum range of movement of each part of the human body [1, 2].

The dynamic detection of human activity under the condition of special equipment involves identifying and tracking the key points of the human body in the image space [3, 4]. Specifically, it obtains the spatial position of human joints through computer vision measurement technology, measures the changes of human movement angle and amplitude, obtains the dynamic statistics of human body, and estimates the influence of equipment on the overall movement of human body.

2 System Architecture Design and Development

The overall architecture design of human motion capture system roughly includes management layer and equipment layer. In the management layer, the high-performance workstation completes the management of the system, the software and hardware settings of the system, the calibration of the human vision system, the acquisition and processing of image data, and the estimation of the static range of motion and dynamic motion of the human body [5, 6]. In the equipment layer, the system is a photoelectric sensing device with the motion capture camera as the core. It arranges 12 motion capture cameras to collect distributed images in the test site, and cooperates with the human body target device to obtain the position and attitude information of various parts of the human body in real time, and then transmits it to the workstation through the network switch for processing and analysis.

2.1 System Equipment and Configuration

The system integrates multiple motion capture cameras and related accessories to achieve large space positioning. The system captures the special marked points (active/passive Marker points) fixed on the human body, interactive equipment and rigid body at the shooting rate of hundreds of frames per second (180FPS/240FPS/360FPS), and constructs the human bone information or three-dimensional position information of the marked points in real time and accurately, providing users with real-time and accurate acquisition of human motion data and rigid body position data. The system has flexible construction environment, sub-millimeter (0.1 mm) positioning accuracy and real-time six-degree-of-freedom data acquisition ability. The system equipment is shown in Table 1.

Table 1. Hardware System Device Table

NO	Name	Model	Specification	Number
1	Camera	PX13W	Resolution: 1280 × 1024 Frame rate: 30–240 FPS (adjustable)	6
2	Camera	PX22	Resolution: 2048 × 1088 Frame rate: 30–360 FPS (adjustable)	6
3	Calibration tool	CS-200	L-shaped calibration right angle	1
4	Calibration tool	CW-500	T- shaped calibration rod	1
5	Data switch	GS752TPP	Industrial-grade GigE interface data switch, with data synchronization and PoE + power supply functions, including 10G acquisition network card	1
6	Cable	LY-C6-EC3000	Category 6 dedicated RJ45 Gigabit Ethernet cable	13
7	Marked point	LY-MKR140M4–10	Dedicated full body motion capture markers	100
8	Installation tool	KB-0	Installation tool kit, including head, power clamp, custom heavy duty bracket	12

2.2 Camera Setup Layout

In order to fully obtain and track human movements in a large space environment, the installation positions of 12 cameras are calculated accurately. Taking into account the field of view and accuracy factors of the system, the following camera architecture layout is adopted. That is, six cameras are arranged in the north-south direction, two in the east-west direction, and one camera in each of the four corners to maximize the camera's field of view (Fig. 1).

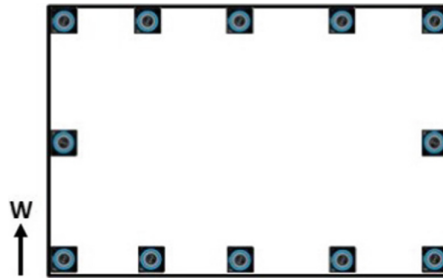


Fig. 1. Schematic layout of the camera

In order to determine the coverage of the three-dimensional visual field of the camera, Solidworks is used. According to the internal and external parameters of the camera, the coverage of the field of view in three-dimensional space is calculated. The simulation results imply that the designed camera layout scheme satisfies the requirements of the application scene (Fig. 2).

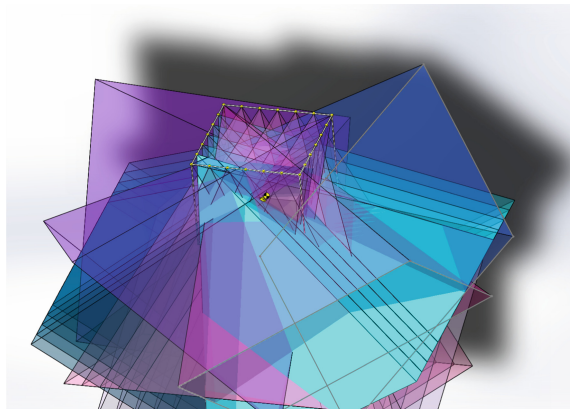


Fig. 2. Solidworks simulated camera field of view space coverage

3 Human Target Design

Anthropometric measurements include shoulder movements, elbow movements, wrist movements, finger joint movements, head and neck movements, waist movements, hip movements, knee joint movements and ankle movements. According to the test, targets are required to be placed in all parts of the human body movement. The system is required to measure the range of motion and motion state of human joint angle by detecting the position and posture of the target.

The target is designed as follows: the base of the preset mounting hole is fastened to the head, chest, back, upper arm, forearm, hand, thigh, calf and foot by bandage and gluing. On the mounting holes of each base, the reflective ball target is fixed at the end of the connector through rigid connectors and studs. Each pedestal contains at least three target spheres as a rigid body coordinate system. Each rigid body coordinate system can be distinguished by the angle of the mounting hole on the base and the length of the connector to realize the measurement and tracking of each moving part of the human body.

4 Dynamic Motion Capture and Analysis Methods

The dynamic motion capture and analysis adopts the detection scheme based on the target, and then estimates the detection of the amount of human motion by obtaining the three-dimensional coordinates of the key points with the target. When the target points are attached to the main joints of the human body, the corresponding joint position can be detected through the target detection and target detection algorithm, and then the spatial position of the joint can be obtained by the method of three-dimensional modeling. After obtaining the three-dimensional coordinates of the main nodes of the human body, a multi-layer feed forward neural network model is designed, which inputs the coordinate vector sequence of the main nodes of the human body, and outputs the estimated value of the total activity of the human body. The training of the neural network can use the standard human movement as the input and the estimation of the amount of human motion under the guidance of expert knowledge as the output for iterative optimization and learning. At the same time, it assists the human body 3D modeling method to visually display the human motion.

The estimation of the dynamic movement of the human body, through the discrete target motion of the main parts of the human body to estimate the overall motion of the human body, which is a non-linear regression problem. Considering the modeling problem of this kind of typical nonlinear system, the neural network model is used for fitting. The implementation of the exercise estimation model is as follows:

- 1) Collect 14 main joint angle sequence data in the process of dynamic motion of the human body, and perform preprocessing operations such as filtering and erroneous data elimination on the data to improve data quality.
- 2) Carry on the signal amplitude-frequency analysis to the data processed by the filter. Considering that the main joints of the body move periodically in the process of walking and running, accordingly, the joint angle sequence is also a periodic signal. Extract the amplitude-frequency feature of the signal.
- 3) Utilize the signal amplitude, frequency, signal mean variance and other data as the feature quantity to observe the dynamic motion of the human body to form the eigenvector space.

- 4) Design the neural network model as a multi-layer feed forward network. The input layer consists of 42 neurons, corresponding to the eigenvector space, 60 neurons in the hidden layer and 1 neuron in the output layer.
- 5) Neural network model identification. It refers to the estimation and scoring of the amount of human movement in each group according to the three-dimensional coordinates of the target point, which is based on several sets of human dynamic motion process data. The project team uses the subjects to perform the given standard actions, and the system collects multiple groups of data. After scoring and judging manually according to the amplitude of the action, several groups of input and output data are formed to identify the neural network model.

Before measuring the action, paste the target as shown in the following picture (in which the purple point can be pasted arbitrarily under the condition of ensuring the relative position with the surrounding white point), and establish a digital human body in the software (Fig. 3).

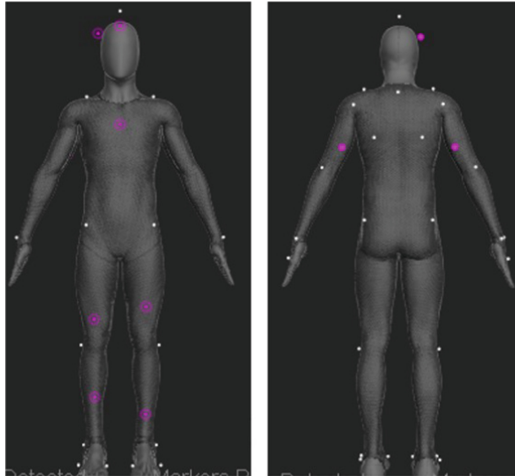


Fig. 3. Schematic diagram of target layout for human body dynamic motion detection

5 Dynamic Motion Capture and Analysis Experiment

Dynamic measurement includes the measurement of nine joint angles of head, left forearm, left forearm, right forearm, left thigh, left calf, right thigh and right calf. When measuring, it selects the corresponding test item, clicks “start Collection” and then does the specified action as required. Joint information is automatically saved in the measurement. After the end of the action, it clicks “finish collecting” to obtain the joint angle information of the action (Fig. 4).

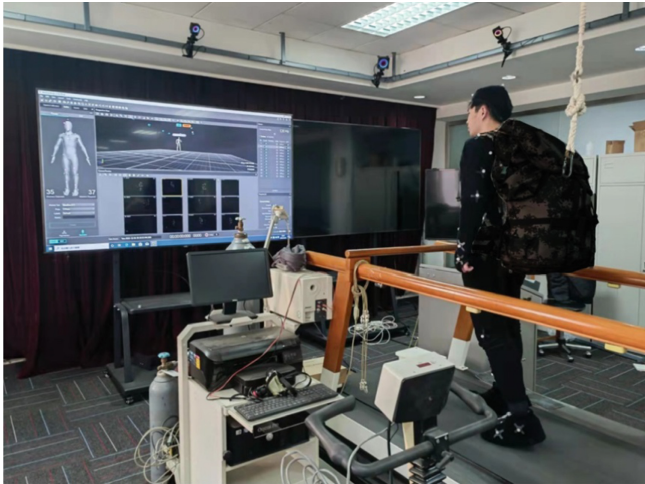


Fig. 4. Dynamic motion capture and analysis experiment

The test results are shown in Table 2.

Table 2. The amount of main joint movement of the human body in the walking/running state

Body parts	Left shoulder	Left elbow	Right shoulder	Right elbow	Left knee	Left ankle	Right knee	Right ankle	Amount of exercise
Walk	40.72	20.10	42.14	15.27	161.9	131.5	156.1	171.1	78.69
Run	53.38	33.04	65.81	26.69	158.6	123.6	144.4	158.2	95.96

According to the application test and functional verification, the developed system can realize the static detection of human activity and measure the range of motion of shoulder, elbow, wrist, finger, head and neck, waist, hip, knee, ankle and other joints in sagittal plane, coronal plane and horizontal plane. The system realizes the dynamic detection of human activity, identifies and tracks the key points of the human body in the image space; obtains the depth image of the human body through the computer vision measurement technology, and then realizes the three-dimensional reconstruction of the dynamic human body. the spatial position of the joint is obtained, and the accuracy of motion posture detection is 0.2°; extracts and tracks 14 key nodes (head, drive dry, shoulder joint, elbow joint, knee joint, hip joint, hand, foot), and the processing speed is 30 frames per second; and measures the changes of human movement angle, amplitude, etc., and obtains the dynamic statistics of human body.

Compliance with Ethical Standards. The study was approved by the Logistics Department for Civilian Ethics Committee of IQET, AMS.

All subjects who participated in the experiment were provided with and signed an informed consent form.

All relevant ethical safeguards have been met with regard to subject protection.

References

1. Sy, L.W., Lovell, N.H., Redmond, S.J.: Estimating lower body kinematics using a lie group constrained extended kalman filter and reduced IMU count (2021)
2. Rempe, D., Birdal, T., Hertzmann, A., Yang, J., Sridhar, S., Guibas, L.J.: Humor: 3d human motion model for robust pose estimation (2021)
3. Shafaei, A., Little, J.J.: Real-time human motion capture with multiple depth cameras (2016)
4. Fern'Ndez-Baena, A., Susin, A., Lligadas, X.: Biomechanical validation of upper-body and lower-body joint movements of kinect motion capture data for rehabilitation treatments. In: International Conference on Intelligent Networking & Collaborative Systems. IEEE (2012)
5. Das, S., Trutoiu, L., Murai, A., Alcindor, D., Hodgins, J.: Quantitative measurement of motor symptoms in parkinson's disease: a study with full-body motion capture data. In: Conference Proceedings: Annual International Conference of the IEEE Engineering in Medicine and Biology Society. IEEE Engineering in Medicine and Biology Society Conference 2011, pp. 6789-6792 (2011)
6. Lee, J., Ha, I.: Real-time motion capture for a human body using accelerometers. *Robotica* **19**(6), 601–610 (2011)



Human–Machine Analysis and Design of the Handrail System in Changzhou Subway

Min Qu^(✉), Xinying He, Yilin Ou, and Danning Hao

Hohai University, Jiangsu, China
2217476349@qq.com

Abstract. At present, the subway is one of the major modes of transportation for people. The subway's handrail system is the greater factor that affects people's travel experience. In addition to the basic grip function, people have higher requirements for the design of the handrail system. This paper mainly focuses on the human-machine analysis and design of the Changzhou subway handrail system. By analyzing the current design of Changzhou Metro Line 1 handrail system with the online and field research, the problems are identified and the improvement directions are summarized. Eventually, a reasonable improvement plan is proposed based on Changzhou's cultural characteristics and additional functions of the handrails, which improves the rationality, aesthetics and functionality of the handrail system in Changzhou subway.

Keywords: Ergonomics · Subway handrails · Improved design

1 Introduction

The subway car is responsible for the important function of carrying passengers, so it has high requirements for safety and comfort. Therefore, it is essential to set up safety handrails [5]. The handrail system of subway includes three types of handrails: the hanging ring, the vertical pole and the horizontal pole. Many scholars have studied different aspects of metro handrail systems. The evolution of the handrails in the subway in terms of connection structure and materials is described in detail by Yanling Lu et al. [7]; Shengwei Xin et al. [6] conduct a specific study on the design and key dimensions of the handrails in the B-type subway vehicles. Jun Xiao et al. [2] propose a localized solution for the center height of the public transportation handrail system in the southwest region. Feng Wei [1] and others follow the national standards and combine with the human-machine design principles to calculate and demonstrate that the highest comfort rating is obtained when the height of the ring is 1710 mm and the height of the crossbar is 1860 mm.

This paper analyses the Changzhou Metro Line 1 handrail system from the perspectives of size, material, safety, layout, function, and appearance, uncovers the problems and summarizes the directions for improvement. The purpose of this study is to improve the rationality, aesthetics and functionality of the handrail system in Changzhou subway cars.

2 Research on the Handrail System in Changzhou Subway Cars

2.1 The Composition of the Changzhou Subway Handrail System

All domestic subway models are divided into three categories: A-type cars, B-type cars and C-type cars. The model of Changzhou Metro Line 1 is B-type. The model size and parameters are shown in Table 1.

Table 1. Subway carriage specifications

Properties	B-vehicle
Length of subway car	19 m
Width of subway car	2.8 m
Number of doors per carriage	8

The space of the handrail system of Changzhou Metro Line 1 is drawn based on the photos of the layout of the handrail system taken in the field study. (Fig. 1).

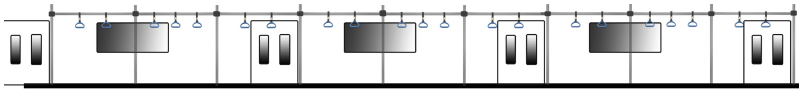


Fig. 1. Spatial arrangement of the handrail system of Changzhou metro line 1

The characteristics of the handrail system in one car of Changzhou subway are shown in Fig. 2.

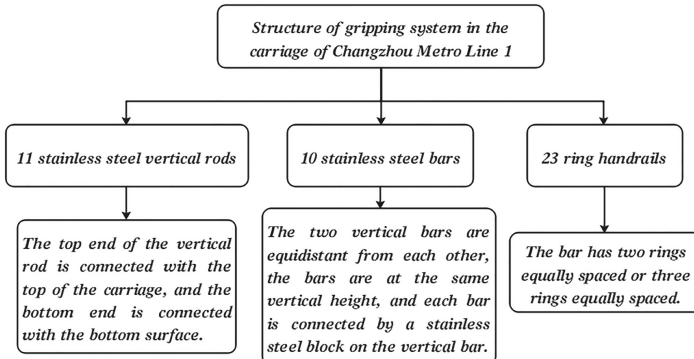


Fig. 2. Composition characteristics of the handrail system in One Car of Changzhou metro line 1

2.2 Dimensions of the Changzhou Metro Line 1 Handrail System

Through field measurements, three handrail layouts are drawn and dimensioned in order to visualize the measured data. The arrangement of the rings on the crossbar is divided into two cases, one with two handrail rings equally spaced on the crossbar and one with three rings equally spaced on the crossbar (Fig. 3).

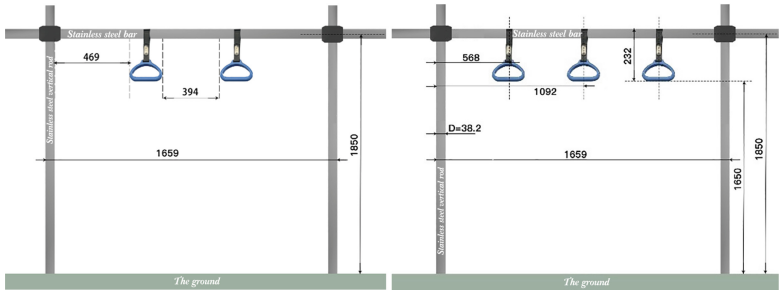


Fig. 3. Distribution of the handrail rings

At present, there are two forms of handrail rings for Changzhou Metro Line 1, one is the ordinary handrail type and the other is the billboard implantation type. The dimensional data diagram is shown in Fig. 4.

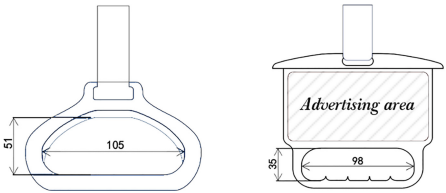


Fig. 4. Two types of handrail ring inner diameter size

2.3 Material Analysis of Handrails of Changzhou Metro Line 1

Both handrail rings have wavy depressions in the handrail part, in line with the reasonable man-machine relationship when the knuckles handrail, but with some differences in materials.

- The fixed part of the ordinary handrail ring is made of stainless steel, the connecting part is a strip made of polyester, and the handrail part is made of plastic. Overall, the shape is relatively simple.
- Billboard implantable rings are fixed by plastic pieces, the connecting part is a strip made of polyester, the handrail part is plastic, and the middle part has a plastic plate for placing advertising messages
- The horizontal and vertical rods are made of stainless steel, and the surface treatment process is brushed metal, which has the advantages of scratch resistance.

2.4 Existing Problems of Changzhou Metro Line 1 Handrails System

- *Size problems*

- (1) Non-adjustable height.
- (2) When the carriage is crowded, the single vertical bar design makes some passengers keep their body balance.
- (3) The inner diameter size of the ring makes it uncomfortable to handrail.

- *Material problems*

- (1) Stainless steel is cold to the touch.
- (2) Polyester material with low tensile strength is easy to break.

- *Safety problems*

- (1) The rings are prone to swaying arbitrarily with the swaying of the body. When the vehicle is in motion with any form of accelerated motion such as bumping and swaying, it can lead to passenger vertigo [9].
- (2) The plastic material causes slipping problems when it encounters sweat.

- *Layout problems*

Passengers prefer to stand in a position that is not coordinated with the distribution of the handholding system, which can easily cause local crowding problems.

- *Functional problems*

Only considering the grasp function. The function is too single.

- *Appearance problems*

No warning effect of colour. The current design has no urban characteristics and recognition in the shape.

3 Analysis of Human-Machine Problems in Handrail Systems

An armrest that is more accessible to the general public needs theoretical support from ergonomics. We will develop the ergonomic problem from five aspects, including body size, color, material, stability and layout.

3.1 Body Size Analysis

The use of improperly designed handrail tools that do not take into account the physiological characteristics of the human hand can lead to a variety of upper limb disorders and even systemic injuries.

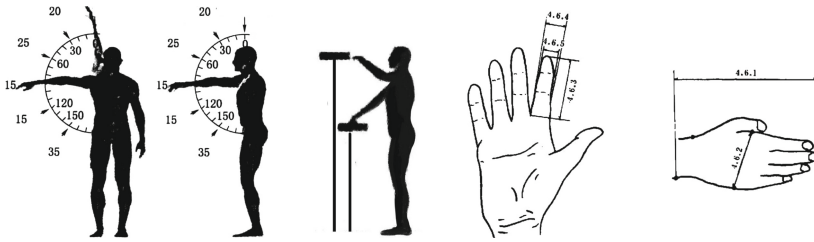


Fig. 5. Schematic diagram of the human-organ system in the handrail system

- *Anatomical factors*

The spreader ring and armrest should be used in such a way that the posture and body position of the passengers are in line with the force application characteristics of the hand and arm as far as possible [8].

- *Functional height of the hand in the standing position*

Referring to the large size design principle, combined with the height adjustment function to meet the comfortable use of more people. It was determined that the height of the ring was designed to be adjustable between 1650 mm and 1750 mm after the calculation.

- *The method of determining the surface by using the height as the base*

The ratio associated with the design of the crossbar is 7/6 between the height of a shelf that can hold something at will and the human body. Also, the relevant literature proves that a crossbar height of 1850 mm can meet most people's requirements [1]. Generally, the crossbar height was established as 1850 mm.

- *The comfortable adjustment range for shoulder joint*

The person grasps the vertical bar by swinging the upper limb forward, which involves the design reference of the comfortable adjustment range of the shoulder joint and the height of the shelf to facilitate the use (Fig. 5). A comprehensive calculation of the vertical bar wrapped in a comfortable material set within the range of 563.63 to 1503.42 mm.

- *Width and thickness of the palm of the hand*

The inner width at the handrail of the ring is set to 100 mm and the inner height to 33 mm, which is convenient for fast and accurate handrail. For the cross-sectional diameter of the horizontal or vertical bar, the reference value was set between 32 and 38 mm during the design [5].

3.2 Color Analysis

Taking into account the color of the handrail system, which should be a warning and reminder to the passengers, and the coordination of the overall color of the interior of Changzhou Metro Line 1, the blue complementary color orange is used as the main color to achieve the effect of the finishing touch.

Table 2. The meaning of common colors in graphic symbols

Color of graphic symbols	Meaning
Red	Stop, Prohibited, highly dangerous
Orange	Security measures, warnings
Blue	Calm and comfortable

3.3 Material Analysis

In response to the problem of sweaty handrail, consider attaching non-slip rubber to the ring puller or making itself into a non-slip panel. In addition, the comfort of the rubber pull ring also improved. Also, consider replacing the handle without grooves and easy to clean to avoid the viruses. For the cold problem caused by the stainless steel in winter, consider covering the handrail with cotton material.

3.4 Stability Analysis

Consider adding restraint to the handrail of the ring and its fixation to reduce wobble. Also, replace the handrail with a waterproof and sweat-absorbent material to improve slippage caused by hand sweat residue. Replace the material with a stronger tensile stiffness to avoid the connection from breaking.

3.5 Layout Analysis

The layout of the handrail system needs to consider the guidance of the standing position of passengers to maximize the efficiency of the train ride.

The door area is an important place for subway passengers to enter and exit, and vertical bars are usually set up here instead of horizontal bars. From the questionnaire, passengers are more willing to stand on both sides of the carriage when there is just no seat, so the addition of horizontal poles and rings can be considered here. Also, the handrail points can be increased by adding single and dichotomous uprights in other areas of the B carriage except for the door area [4] (Fig. 6).

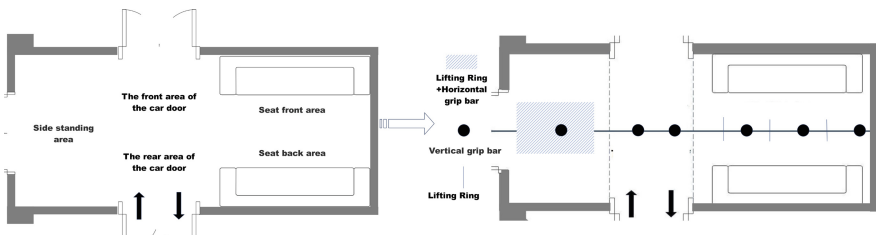


Fig. 6. Layout improvement figure of handholding system

4 Improved Design for Changzhou Metro Line 1

Combining the historical and cultural characteristics of “Changzhou - Dragon City”, the dragon was extracted as the element, and the structure was simplified on this basis, following the principle of simplicity and highlighting cultural characteristics [3]. The creation process of the special hanging ring is shown in Fig. 7.

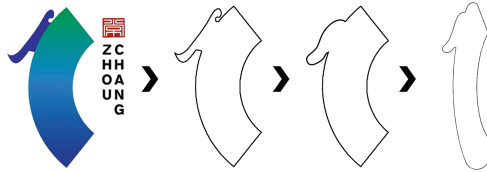


Fig. 7. The creation process of Changzhou Longcheng hanging ring shape

Combined with the above discussion, orange is used as the primary color. The modified solution takes advantage of the rubber protective cover to improve the comfort of handrail; the vertical bar is designed with six handrail positions, which are functionally partitioned by color and material to maximize the handrail space of the vertical bar. This design not only maintains the cultural characteristics of Changzhou but also improves the efficiency and comfort of the use of the handrail system. The details are shown in Fig. 8.

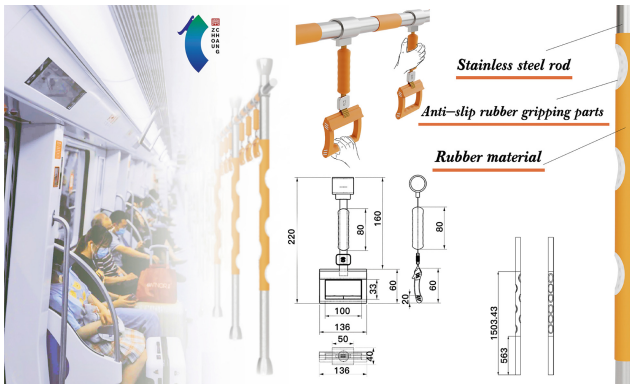


Fig. 8. Illustration of the program description

5 Conclusion

This paper focuses on a theoretical basis, through multifaceted research and data analysis, to propose improvements to the human-machine problems in the Changzhou subway handrail system. The study combines the cultural characteristics and additional functions

of the city to improve the design to enhance the rationality, aesthetics and functionality of the Changzhou subway carriage handrail system.

Acknowledgements. The paper is the stage result of “Ergonomics Course Project”, and has been guided by Prof. Canqun He.

Compliance with Ethical Standards. The study was approved by the Logistics Department for Civilian Ethics Committee of Hohai University.

All subjects who participated in the experiment were provided with and signed an informed consent form.

All relevant ethical safeguards have been met with regard to subject protection.

References

1. Feng, W.E.I., Bochu, X.U., Jinyi, Z.H.I., Shiyu, D.O.N.G.: Human-machine functional design of subway passenger room equipment. *Southwest Jiaotong Univ.* **53**(04), 865–872 (2018)
2. Xiao, J., Luo, W., Yuan, S.: Ergonomic design of bus handrails in Southwest China. *Mach. Manufact. Autom.* **40**(02), 33–34+66 (2011). <https://doi.org/10.19344/j.cnki.issn1671-5276.2011.02.012>
3. Zhang, K.: The First Prize of Changzhou City Image Publicity Phrase and Logo Online Collection Activity. [EB/OL]. <https://ishare.ifeng.com/cs/7z44DAEvO53>
4. Jiang, L., Lu, X., He, S.: Quiet Current status and optimization of the design of in-vehicle support system of subway. *Design* **33**(10), 110–112 (2020)
5. Sun, L., Wang, L.: Ergonomics analysis of subway vehicle interior design. *J. Dalian Jiaotong Univ.* **31**(02), 15–19 (2010). <https://doi.org/10.13291/j.cnki.djdxac.2010.02.010>
6. Xing, S.: Design of handrails in passenger compartment of B-type aluminum alloy subway car. *Sci. Technol. Outlook* **22**, 176 (2014)
7. Lu, Y., Liu, H., Meng, L.: Standardized design of vehicle interior handrails of Wuhan rail transit line 1 phase 2 project. *Electric Locomotives Urban Rail Veh.* **33**(03), 25–2641 (2010). <https://doi.org/10.16212/j.cnki.1672-1187.2010.03.007>
8. Ding, Y.: *Ergonomics*. Beijing University of Technology Publishing, Beijing (2011)
9. Li, Z.: Human factors analysis of train seat placement angle and motion sickness. *Art Des. (Theory)* **03**, 162–164 (2008). <https://doi.org/10.16824/j.cnki.issn10082832.2008.03.058>



An Improved Force-Directed Automatic Layout Method for Undirected Compound Graphs

Junyao Liu, Zhongnan Wang, Jiamin Yu, Haitian Liu, and Tong Li^(✉)

Beijing University of Technology, 100 Pingleyuan, Beijing, China
litong@bjut.edu.cn

Abstract. In software engineering, the undirected compound graph serves as a medium for human-machine communication, translating human intent into machine language to efficiently deliver and demonstrate people's demands by utilizing its outstanding analysis capability. Still, the industrial adoption of goal models is hindered by the scalable data and the massive manual workload it incurs. Overt problems, including the uncertainty of iteration direction and the difficulty of controlling the number of edge crossings, remain unsolved. We introduce the method of graph folding, which continuously collapse indecisive nodes to reduce the data scale and remain the basic structure of the original graph simultaneously to provide a possible solution to this dire state. The folding method confirms the direction of the iterations and considerably reduces its number, which greatly improves the efficiency of the man-machine communication. We repeatedly operate adjustment and expansion of the graph to ensure the optimal solution, and the results are promising.

Keywords: Automatic layout · Graph collapsing · Iteration direction

1 Introduction

The force-directed algorithm is widely used in graph drawing, and it is particularly suitable for laying out undirected graphs [2]. Researchers have made great efforts to promote its broad utilization. In 1991, Fruchterman, Thomas M. J, et al. proposed graph drawing by force-directed placement [1]. In 2014, L. Wang, X. Wang, et al. put forward the concept of reducing the number of nodes to provide a better layout solution with fewer crossings and overlaps [2]. In 2019, Z. Xu and P. Zhang improved the algorithm by introducing the PageRank method, which overcomes the shortcomings that the traditional force-directed algorithm is unavailable to show the importance of nodes [5]. In 2020, Y. L. Wang and A. M. Grubb presented FLAAG, a domain-specific variant of a generic algorithm for undirected compound graphs, and introduced a set of heuristics to evaluate its effectiveness [4]. However, trivial but overt problems are yet to solve. Limitations, including the ambiguous iterative direction and the unpredictable edge crossings, still act as crucial barriers.

The overriding aim of this paper is to resolve the issues listed above. The second chapter illustrates the model and rationale of the force-directed algorithm, providing

basic formulas that are fundamental to the design of layout function. The third chapter puts forward the basic logic and detailed descriptions of main functions and pseudocodes. Using the method of node combination, this paper provides a generic solution to the iteration direction and, to the greatest extent, reduces the edge crossings for large-scale graphs.

2 The Model of Force-Directed Algorithm

The force-directed algorithm is a classic layout algorithm for graphs simulating the physical system. The model is established by assuming edges as springs and nodes as repelling objects [3]. As shown in Fig. 1, when operating the algorithm, repulsion force will separate compact node sets and push nodes away from each other while edges do the opposite. The graph will ultimately come to equilibrium after iterations.

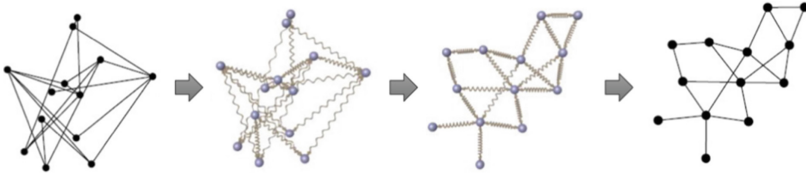


Fig. 1. The spring analogy [3]

We use the FR (Fruchterman and Reingold) layout algorithm to calculate the positions of each node and edge. Note that forces are modelled based on the optimal distance between vertices, which is calculated as below:

$$k = C * \sqrt{\frac{area}{number\ of\ nodes}} \tag{1}$$

As shown in Eq. 1, k represents the radius of the empty area around a node, while the constant C is found experimentally. In this way, nodes can be distributed uniformly in a canvas. Subsequently, we define f_a and f_r for attractive and repulsive forces, respectively, and they are calculated when the distance between two nodes is given. The formulas are shown as below:

$$f_a(d) = \frac{d^2}{k} \tag{2}$$

$$f_r(d) = -\frac{k^2}{d} \tag{3}$$

Our automatic layout approach has considered each edge’s weight in the graph, which is denoted as EW . We are concerned that the edges with higher weight indicate that the nodes linked to will be arranged closer. Thus, we improve the formula for attractive forces as:

$$f_a(d) = EW * \frac{d^2}{k} \tag{4}$$

As illustrated above, our improved FR algorithm will be iteratively applied to calculate the position of each node.

3 Optimization for Force-Directed Algorithm

This chapter illustrates the primary process and the main functions of our optimized force-directed algorithm. Graph folding is the pre-processing step, which compresses the original graph to a suitable scale, thus facilitating the subsequent steps. The automatic layout section includes the calculate-display and expansion function, which achieves a high-quality layout by iteratively crossing the above two processes. The application of the algorithm we put forward in this chapter can break through the limitations of the traditional force-directed algorithm to a certain extent.

3.1 Graph Folding

Large-scale graphs are widely applied in industrial development with high frequency. However, standard iterative algorithms turn out to be slow and unavailable (i.e. often fall into local optimal) when facing thousands of vertices and nodes [2]. Thus, the overriding aim of folding graphs is to minimize the data amount to improve the efficiency and effectiveness of the automatic layout process.

The main idea of graph folding is to merge nodes with minor importance into the one linked directly with them. We do so only to eliminate indecisive nodes so that the processed graph can still capture the basic structure of the original one. The collapsing process has the following four steps:

- Step 1 Read and store the graph data.
- Step 2 Calculate the importance of each node.
- Step 3 Estimate and generate the optimal outcome of the graph folding.
- Step 4 Fold and update the graph.

A single-time simplification operation is not enough for complex graphs to optimize their automatic layout results significantly. In order to generate satisfying outcomes and reduce edge-crossings, the number of nodes needs to be decreased by orders of magnitude. Thus, intrinsic graphs usually require repeated operations.

Each collapsing operation can only process a single node rather than all the available nodes with the same degree at the same time. We denote a set of collapsing operations performed on nodes of the same degree as a layer, which is presented as a subsequence. Every single operation within the layer is queued in order. As shown in Fig. 2, layers form the collapsing sequence, while every single operation is arranged in the subsequence corresponding to the layer it belongs.

We propose two functions as follows to realize the simplification process.

INITIALIZATION Function. The INITIALIZATION function reads and stores the information of the graph, including the connection relationship between nodes and their indexes, the pre-processing degree, and the type of nodes.

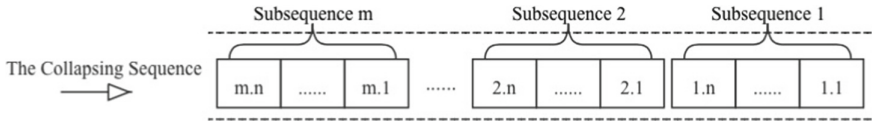


Fig. 2. The collapsing sequence

COLLAPSE Function. The COLLAPSE function (see Function 1) first determines whether the graph is available to be collapsed. After estimating the graph’s validity, all the nodes are traversed to find the collapsing objectives and record their information. The collapsing objectives consist of two nodes: the one with the slightest degree among all nodes (*node_mindg*) and the highest among nodes adjacent to the former (*node_clps*). The function folds the node with the least degree into the one with the highest. Simultaneously, information, including degree, weight, and connection relationship, are transferred to the combined node (Table 1).

Table 1. The pseudocode of the collapse function.

Function 1 Collapse	
1:	function COLLAPSE (<i>nodeSet</i> , <i>edgeSet</i>)
2:	while <i>nodenum</i> > 5 do
3:	for <i>nodemindg</i> ∈ <i>nodeSet</i> do ▷ nodes that have minimum degree
4:	if <i>nodeclps.degree</i> ≥ <i>othernodes.degree</i> then ▷ adjacent node
5:	<i>nodeclps.weight</i> = <i>nodeclps.weight</i> + <i>nodemindg.weight</i>
6:	<i>nodemindg.weight</i> = 0
7:	MIGRATECONNECTIONRELATIONSHIPS (<i>nodemindg</i> , <i>nodeclps</i>)
8:	SAVECHANGES (<i>nodemindg</i> , <i>nodeclps</i>)
9:	<i>nodenum</i> = <i>nodenum</i> - 1
10:	end if
11:	end for
12:	end while
13:	end function

3.2 Automatic Layout

In order to reduce labor costs and improve layout efficiency, the application of automatic layout algorithms on undirected compound graphs is of outstanding importance. As mentioned previously, the force-directed algorithm can effectively layout graphs with small volumes, which is especially appropriate to process graphs after folding. We apply our improved force-directed algorithm to automatically adjust nodes and edges.

When laying out graphs with a considerable data scale folded for several turns, the graph should be adjusted multiple times following the sequence of its collapsing operations. This means that the graph will be alternatively adjusted and expanded until

the original graph is completely laid out. Thus, the whole automatic layout process repeatedly operates the following 4 steps:

- Step 1 Calculate the attraction and repulsion force of a node.
- Step 2 Calculate the target coordinate and re-orientate the node.
- Step 3 Expand a single node.
- Step 4 Get the next objective according to the collapsing sequence.

According to the 4 steps listed above, the automatic layout process can be segmented into two sections: adjustment and expansion.

3.2.1 Adjustment

The adjustment of nodes uses the improved FR method with the optimized formula for attraction force, which is based on the magnetic spring model we addressed previously. The adjustment process redistributes the position of nodes and edges only by manipulating the coordinates.

We propose the *Adjust* function below to distribute the position of nodes and edges after a single-time layout.

ADJUST Function. The ADJUST function (see Function 2) reads in the data of a node and determines its validity before adjusting. Adjust function only operates on available nodes. Subsequently, the function calculates the attraction and repulsion force between the node and the other ones, and adds up these two forces (*aForce*, *rForce*, both marked with positive or negative signs) to get the combined force. The function updates the node's position by adding the product of the combined forces and the constant coefficients to the original coordinates to update the node's position (Table 2).

Table 2. The pseudocode of the adjust function.

Function 2 Adjust	
1:	function ADJUST (<i>nodeSet</i> , <i>edgeSet</i> , C_N , C_M)
2:	for <i>node1</i> \in <i>nodeSet</i> do
3:	for <i>node2</i> \in <i>nodeSet</i> do \triangleright <i>node2</i> is adjacent to <i>node1</i>
4:	$aForce \leftarrow$ ATTRACTION (<i>node1</i> , <i>node2</i> , C_N)
5:	$rForce \leftarrow$ REPULSION (<i>node1</i> , <i>node2</i> , C_N)
6:	UPDATEFORCES (<i>node1</i> , $aForce$, $rForce$)
7:	end for
8:	end for
9:	for <i>node</i> \in <i>nodeSet</i> do
10:	$node.x = node.x + forceX * C_M$
11:	$node.y = node.y + forceY * C_M$
12:	end for
13:	end function

3.2.2 Expansion

Using the improved FR algorithm for a one-time automatic layout of an untreated graph is inefficient and tends to fall into local optimal rather than global ones. Implementing the “adjust-expand-adjust” method can gradually approach the global optimum for the graph and greatly reduce edge crossings. Therefore, the design of the *Expand* function is crucial for the automatic layout of undirected compound graphs.

As mentioned previously, to reduce the data scale, the graph folding process usually consists of multiple node collapsing operations. Thus, the unfolding process should also consist of multiple expansion operations to get the ultimate layout solution. We define that each expansion movement only unfolds one node abiding by order of the collapsing sequence to ensure effectiveness.

We propose the *Expand* function below to recover the graph’s original node-set and connection relationships. The function is called repeatedly until the number of nodes and edges is the same as the original graph.

EXPAND Function. The EXPAND Function (see Function 3) operates the recovery of the relationships inside the graph. The function first determines the target operation node based on the collapsing sequence generated in the graph folding stage, then reads the information of that node. Then, the two nodes (the node with the minor degree when folding and the node it merged into) are spread out with the position of the merged node as the center (Table 3).

Table 3. The pseudocode of the expand function.

Function 3 Expand	
1:	function EXPAND (<i>nodeSet</i> , <i>edgeSet</i>)
2:	<i>nodemindg</i> , <i>nodeclps</i> \leftarrow LOADCHANGES (<i>nodemindg</i> , <i>nodeclps</i>)
3:	MIGRATECONNECTIONRELATIONSHIPS (<i>nodemindg</i> , <i>nodeclps</i>)
4:	<i>nodemindg.x</i> = <i>average.x</i> + <i>nodeclps.weight</i>
5:	<i>nodemindg.y</i> = <i>average.y</i> + <i>nodeclps.weight</i>
6:	<i>nodeclps.x</i> = <i>average.x</i> + <i>nodemindg.weight</i>
7:	<i>nodeclps.y</i> = <i>average.y</i> + <i>nodemindg.weight</i>
8:	end function

3.3 The Customized Force-Directed Layout Algorithm

In this paper, we propose an optimization of the force-directed automatic layout algorithm so that its effectiveness is not only limited to small-scale graphs but can also process graphs with large data volumes through compression and recovery.

With the use of functions illustrated above, including *Initialization*, *Collapse*, *Adjust*, and *Expand*, our customized force-directed layout algorithm is presented as below (Table 4).

Table 4. The pseudocode of the customized force-directed layout algorithm.

Algorithm A Customized Force-directed Layout Algorithm	
Require: Model $G = \langle V, E \rangle$	
Constants C_N, C_M	\triangleright constants for Nodes and Moves
Ensure: Final Graph Layout Information	
1: $(nodeSet, edgeSet) \leftarrow$ INITIALIZATION (G)	
2: COLLAPSE ($nodeSet, edgeSet$)	
3: while $Change > 0$ do	
4: ADJUST ($nodeSet, edgeSet, C_M$)	
5: EXPAND ($nodeSet, edgeSet$)	
6: end while	
7: ADJUST ($nodeSet, edgeSet, C_M$)	
8: return ($nodeSet, edgeSet$)	

4 Conclusion

In this paper, we have made significant progress in improving the human-computer communication efficiency by optimizing the stability and operating time of the automatic layout algorithm for undirected compound graphs. By introducing the graph collapsing and expansion method, we compressed the data scale of a graph. The simplification-recovery process generates two positive outcomes: edge crossings reduction and layout efficiency improvement.

To adapt the FR automatic layout algorithm's property, which can be well performed to reduce edge crossings only on small-scale graphs, we proposed the graph folding method. The implementation of the collapsing process provides a suitable process environment for the FR algorithm. By gradually laying out local areas, edge crossings can be limited to acceptable.

We clarified the iteration condition and determined its direction to be along the collapsing sequence of the graph. This eliminates the randomness and uncertainty of the iteration process, which enables the automatic layout algorithm to avoid redundant and invalid iterations. The experimental outcomes indicate that this improvement reduces layout computation time by orders of magnitude. This means that the delay between human operation and the computer's calculation time has been significantly reduced to the range that humans cannot perceive, enabling human-machine interaction to be completed rapidly and user-oriented. Our overriding aim of this paper is to propose a generic, basic layout algorithm for undirected compound graphs. With the application of collapsing method and improvement of the FR algorithm, the testing outcome turns out to be promising. To match the practical needs of graph drawing more closely, we will extend our algorithm to accommodate nest relationships in future work.

References

1. Fruchterman, T.M.J., Reingold, E.M.: Graph Drawing by Force-Directed Placement. *Softw.-Prac. Experience* **21**(11), 1129–1164 (1991). (Wiley)

2. Wang, L., Wang, X., Wang, Q., Xu, M.: Research on force-directed algorithm optimization methods. In: Proceedings of 2014 International Conference on e-Education, e-Business and Information Management (ICEEIM 2014), pp. 23–27 (2014)
3. Id, M.S.: Social Network Visualization. Master's thesis, School of Computer Science and Engineering, Royal Institute of Technology, Sweden (2008)
4. Wang, Y.L., Grubb, A.M.: Towards a general solution for layout of visual goal models with actors. In: 2020 IEEE 28th International Requirements Engineering Conference (RE), pp. 352–357 (2020). <https://doi.org/10.1109/RE48521.2020.00047>
5. Xu, Z., Zhang, P.: An Improved force-directed algorithm based on PageRank. In: 2019 IEEE 4th Advanced Information Technology, Electronic and Automation Control Conference (IAEAC), pp. 2507–2510 (2019). <https://doi.org/10.1109/IAEAC47372.2019.8997830>



Improved Design of Multimedia Podium Under the New Teaching Method

Jiarong Zhang^(✉) and Zihang Chen

Hohai University, Changzhou 213000, Jiangsu, China
x593756110@163.com

Abstract. With the development of science and technology and the improvement of education level, the existing multimedia platform can no longer meet the new teaching methods that emerge as the times require, and there are various problems. The article analyzes these problems and proposes an improved scheme of multimedia podium under a new teaching method. We use the principles of ergonomics to improve the design of the overall size of the podium, the size of each part and the layout of each functional unit. At the same time, considering the needs of teachers in the new teaching method, we creatively propose a detachable teaching tablet and an integrated seat the design of the chair improves teachers' teaching experience and teaching efficiency.

Keywords: Multimedia podium · Ergonomics · Integrated seat

1 Introduction

Multimedia teaching has already become a teaching mode in the new era, but with the continuous improvement of education level, most of the multimedia podiums can no longer meet the new teaching methods that came into being incompatibility and other issues. These problems greatly affect the teaching efficiency of teachers and the efficiency of students' listening. Therefore, designing a multimedia podium that meets the needs of new teaching methods can not only meet the needs of the times, improve classroom efficiency, but also promote the development of education.

2 Market Research and Analysis

2.1 Conclusions from the Relevant Literature

Before carrying out the improved design, we searched for relevant literature [1, 2], and learned that there are currently three types of multimedia lecterns on the market: left and right horizontal push type, clamshell type, and flip up and push back type, none of which can satisfy the need for a new teaching mode. The existing problems are as follows:

1. The functional division is unreasonable, and the primary and secondary are not clear enough.
2. The teaching platform lacks linkage with other teaching auxiliary facilities.
3. The use of materials is not humane enough, and the colors are relatively single.

2.2 User Research

Through on-the-spot investigation and questionnaire survey, we obtained the size data of the multimedia platform and user feedback, and concluded the following problems:

1. Height size and display screen adjustment problem: The fixed design of the height of the podium and the display screen angle cannot meet the needs of users of different heights.
2. Function button identification problem: The function buttons of the multimedia platform are difficult to identify.
3. Teaching interaction problems: Teachers' activity space is limited to the front of the podium, and there is a lack of close interaction with students.
4. Teachers' teaching experience: Some teachers have the need to sit and teach.

After analyzing the above survey results, we put forward an improvement plan for the multimedia podium under the new teaching method.

3 Key Points of Design

1. The main part of the podium is designed with reasonable man-machine size.
2. Optimize the layout of the countertop and improve the operation efficiency.
3. Combine with new teaching aids.
4. Add additional equipment to improve the teacher experience.
5. Pay attention to the appearance design of the product.

4 Design Based on Ergonomics

Based on the previous survey results and the proposed design points, we use the relevant principles of ergonomics to improve the design of the main part of the multimedia platform.

4.1 Determine the Type of Product

The multimedia lectern mainly plays the role of assisting teachers in teaching and meeting the needs of most people. At the same time, the multimedia lectern belongs to the category of general industrial products, so it is defined as a type III product, and in the selection of percentiles, P_{50} is used as the basis for product size design.

4.2 Main Size Calculation

4.2.1 Determine the Height of the Podium

Through observation and research, most teachers are used to teaching in a standing position. When working in a standing position, the height of the multimedia platform should be 60% of the user's height or the table top should be about 50–100 mm lower

than the elbow height [3]. We use the table top to be 50 mm lower than the elbow height as the design basis. Refer to GB10000–88 Chinese adult body size [4] (Table 1), we calculate as follows:

The size for man is:

$$1024 - 50 = 974 \text{ mm} \quad (1)$$

The size for woman is:

$$960 - 50 = 910 \text{ mm} \quad (2)$$

Taking the average of the two is:

$$974 + 910 \div 2 = 942 \text{ mm} \quad (3)$$

Referring to the correct amount of dress and decoration in *Ergonomics* [5], it is necessary to correct the shoe height by 25–38 mm, here is 38 mm, and the final height of the podium is 980 mm.

Table 1. Standing body size (50th percentile)

Measurement items	Age group	
	18–60 years old (male)	18–60 years old (female)
Eye height	1568	1454
Shoulder height	1367	1271
Elbow height	1024	960
Hand function height	741	704
Perineal height	790	732
Tibial height	444	410

4.2.2 Determine the Length and Width of the Countertop

Referring to the schematic diagram of the comfortable operating range for both hands (Fig. 1) in *Ergonomics* [5], the length of the main functional area of the countertop should not exceed 1500 mm.

The size data of the main equipment is shown in Table 2. The following is the calculation of the distance between each equipment through the hand-eye coordination area (Fig. 2):

The angle of the monitor can be adjusted. According to the survey results, under normal circumstances, the angle between the monitor and the table is about 40° , and the horizontal width of the monitor is:

$$268.1 \times \cos 40^\circ = 205.4 \text{ mm} \quad (4)$$

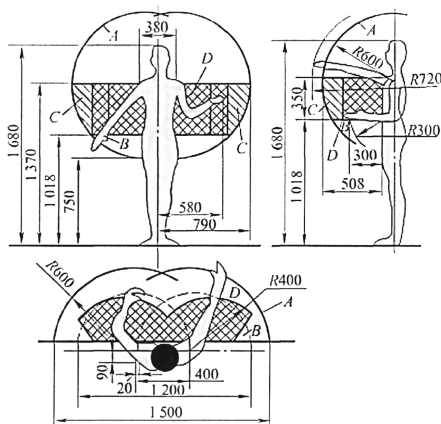


Fig. 1. Schematic diagram of the comfortable operating range of both hands

The combined platform width of the monitor and keyboard and mouse is:

$$205.4 + 170 = 375.4 \text{ mm} \quad (5)$$

To keep the top edge of the display in the comfort zone, the distance is:

$$535 - 375.4 = 159.6 \text{ mm, integrated into } 160 \text{ mm} \quad (6)$$

In order to ensure that the two platforms do not interfere with each other when they run up and down, the distance between the two platforms is set to 80 mm, and the distance between the platform where the keyboard and mouse is placed is 80 mm from the edge of the table.

The total length of the platform on which the monitor is placed and the length of the control panel is:

$$560 + 200 = 760 \text{ mm} \quad (7)$$

Obviously, the platform is in the hand-eye coordination area. For the convenience of use, the distance between the platform and the control panel is set to 20 mm.

The work area is mainly used for laptops carried by teachers, and its length is 360 mm, so the length of the work area can be set to 470 mm, and the gap for placing the folding hidden door needs to be 60 mm.

Combining the above data and considering the margins of each functional area, the size of the podium table top is finally determined to be 1400 * 880 mm, and the edge of the work surface is 730 mm from the front edge of the table.

4.2.3 Determine the Size of the One-Piece Seat

The one-piece chair we designed mainly provides teachers with a sitting-stand alternating working posture to relieve the fatigue of long-term standing teaching.

Table 2. Main equipment size

Equipment	Size (mm)
Keyboard	440 * 140
Mouse pad	200 * 150
Keyboard and mouse platform	680 * 170
Monitor	476.6 * 268.1
Monitor platform	560 * 350
Control panel	200 * 120

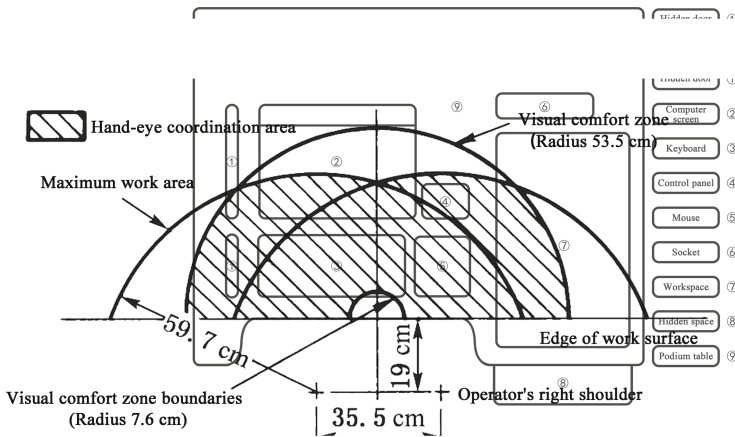


Fig. 2. Hand-eye coordination areas in countertop layouts

Referring to the human body horizontal dimension (Table 3) in *Ergonomics* [5], the length dimension of the seat is based on the maximum shoulder width of the human body horizontal dimension, and we take the P₉₅ percentile of the male's maximum shoulder width as the reference value, which is 469 mm, so the length of the seat should be ≥ 469 mm, which is 470 mm here. As shown in Fig. 3, according to the prototype of the office seat [5], the width of the seat is 435 mm, the height of the seat surface from the ground is 395 mm, the inclination angle of the seat surface is 4°, the height of the seat back is 400 mm, and the height of the lumbar support from the seat surface is 235 mm.

Table 3. Horizontal size of the human body (95th percentile)

Measurement item	Age group	
	18–60 years old (male)	18–60 years old (female)
Chest width	315	299
Chest thickness	245	239
Shoulder width	403	377
Maximum shoulder width	469	438
Hip width	334	346

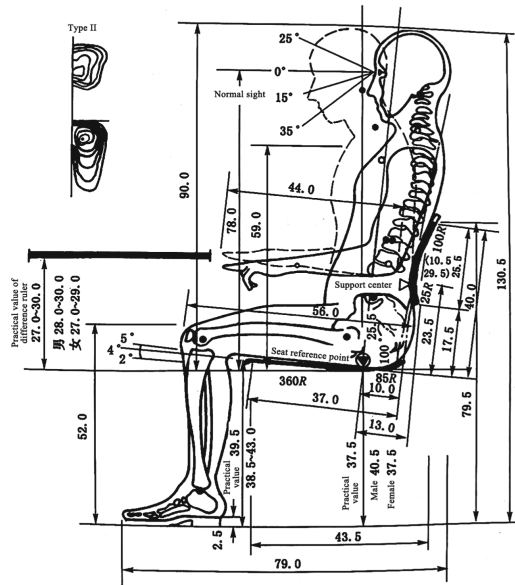


Fig. 3. Office chair prototype

5 Innovative Design

In order to meet the needs of new teaching methods, we have also carried out innovative design in function.

1. Folding Hidden Door

In order to improve the space utilization efficiency, we designed a folding hidden door. When the podium is not in use, the hidden door is closed and level with the podium surface, making the overall appearance more tidy; when the podium is in use, the hidden door is opened and folded and retracted, and the platform of the monitor and mouse and keyboard is raised.

2. Auxiliary Teaching Tablet

In order to liberate teachers from the front of the podium, we propose a detachable teaching tablet, which is combined with a multimedia podium. Teachers can easily remove the tablet, step off the podium, and use it to perform PPT page changes and other operations. This allows teachers to communicate closely with students.

6 Final Scheme

Through the detailed design of the dimensions of each part of the podium, we have obtained a multimedia podium design scheme in line with ergonomic principles. At the same time, we have proposed more functions on the basis of the traditional multimedia platform to improve the teaching efficiency and user experience of teachers. The following are the renderings (Fig. 4):

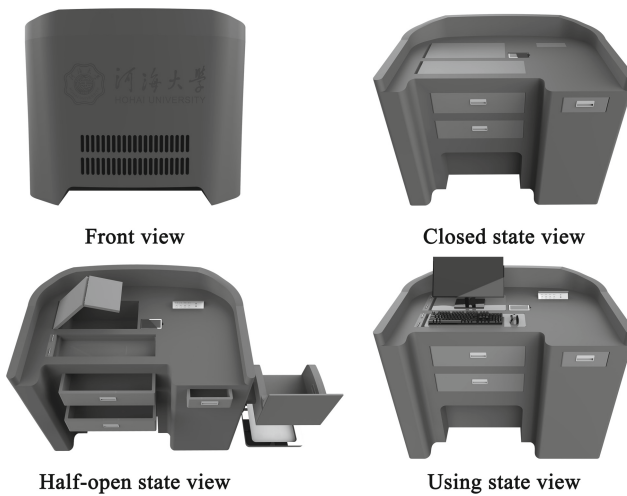


Fig. 4. Complete solution display

References

1. Xuejing, C., Xiaoli, J.: Application of humanized design concept in multimedia podium design. *Art Des. (Theory)* **2**(11), 93–95 (2019). <https://doi.org/10.16824/j.cnki.issn10082832.2019.11.030>
2. Li, Y., Jiang, L., Zhang, X., Li, Z.: Research on natural interaction design of multimedia podium. *Ergonomics* **21**(05), 57–61 (2015). <https://doi.org/10.13837/j.issn.1006-8309.2015.05.0012>
3. Lu, W.: Research and Optimization Design of Multimedia Podium in Colleges and Universities. Southwest Jiaotong University (2013)
4. State Technical Supervision Bureau GB/T 10000-1988. In: Chinese adult body size (1988). <http://www.gb688.cn/bzgk/gb/newGbInfo?hcno=A78583489235BF9BF9EE253E74DC76B9>. Accessed 7 Jan 2022
5. Yulan, D.: Ergonomics. Beijing Institute of Technology Press (2011)



The Transmutation of the Traditional Instrument Performance Under the Visual Threshold of Science Technology Art

Yaru Zhu and Zhengqing Jiang^(✉)

East China University of Science and Technology, Shanghai 200030, China
jzq20000@126.com

Abstract. The Performing forms of traditional instruments can be summed up as “Performer - Instrument - Performance venue - Audience” such a field. With the development of science and technology, the performance in the form of traditional instrument audiovisual and experience are changed. Starting from the visual stimulus, auditory stimulus, Interactive stimulus three aspects, this paper sorts out the changes made by traditional Musical Instruments to performance, venues and instruments. The research finds that the traditional musical instrument performance has changed into a kind of artistic expression under the Science Technology Art, and has produced a qualitative difference with the traditional musical instrument performance. Performance is characterized by high behavioral participation, high interactive immersion experience and high technological content.

Keywords: Chinese traditional instrument · Audience Experience and Engagement · Science Technology Art

1 The Development of Traditional Musical Instrument Performance

Traditional musical performance is an important part of the artistic spectrum. In the traditional performance mode, the performance form is relatively simple, the song and dance music trinity, the audience is relatively narrow, the general performance space for stage, theater, and other indoor small music venues, instrumentally players sit on the stage, sometimes improvisational arrangements. Under the influence of today’s rapidly developing technology and art, this traditional performance mode has gradually changed. In any music instrument playing scenario, the main body want to pass information to the object, or instrument players want to music or music expression and the significance of emotional and other information to the audience, must include the following four points: instrument players, Musical Instruments, the audience and the Performance venue, the four constituted a complete ring domain (Fig. 1).

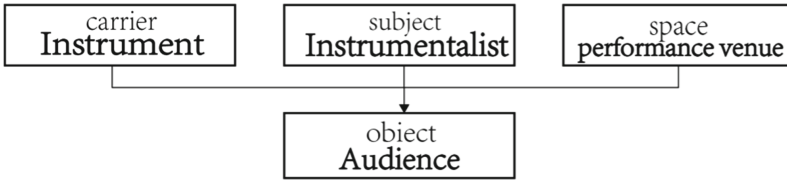


Fig. 1. Traditional performance field schema

David Berlo, an American scholar, analyzed the process of information transmission, and put forward the “S-M-C-R” (source-message-channel-receiver) transmission process model based on the transmission model proposed by Shannon-Weaver. In the information transmission field of traditional musical instrument performance, “S” in SMCR mode means “Source”, which is the starting point of information transmission. Factors affecting the transmission process and effect include emotion, culture and knowledge. M means Message. The main factor affecting the propagation process and effect is music. “C” means “Channel”, which includes auditory Channel, visual Channel and tactile Channel in musical instrument performance. “R” stands for “Receiver”, the Receiver of information, or the audience of the performance (Fig. 2).

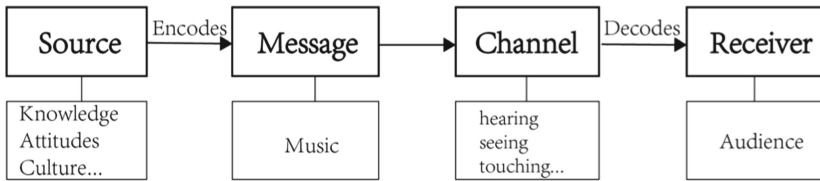


Fig. 2. “S-M-C-R” model and the performance in the field of traditional musical instruments

With the development of time and technology, the form of channel has gradually changed. In fact, since ancient times there have been changes to the dress of the stage performers to allow the audience to increase the enjoyment of the visual passage. In addition to enhancing the visual attraction on the performers, the modern society also adds visual stimulation on the performance ground. In “Listening to the Qin” painted by Zhao Ji in the Northern Song Dynasty, the venue is selected under the green pines to increase the visual artistic atmosphere. Hyundai adds visual effect by playing video on a screen in the background of the performer. In the past decade, with the development of science and technology and art, audiences are not satisfied with the status quo, and gradually begin to pursue the innovation of visual channel, auditory channel, tactile channel and interactive channel to get more enjoyment (Fig. 3).



Fig. 3. “Listening to the Qin” painted by Zhao Ji in the Northern Song Dynasty & The performance of “12 Girls Band”

2 Evolution of Traditional Musical Instrument Performance Under the Influence of Science and Technology

With the change of The Times, in order to meet the audience’s needs for more experience and more sensory stimulation, especially under the influence of the current development of science and technology, many changes have taken place in traditional musical instrument performance.

2.1 Innovate Visual Channels for Performance Venues and Performers

First, there are many visual changes in the performance venues. Shanghai new media team “Fn media lab” as a new media art creation team and player, created “Ruan’s sound”, they made a series of changes to the arena, the light and shadow Mapping means of art, makes the player at the time of playing Musical Instruments light will change with the frequency jitter, Visually, it is more vivid and full to the audience (Fig. 4).

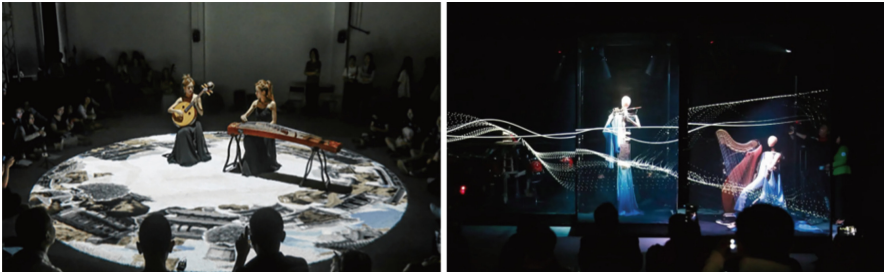


Fig. 4. “Ruan’s sound” crated by new media art team “Fn media lab” & “Mojia illusion” crated by Tsinghua team

In addition to the visual changes on the performance venue, there are also visual innovations on the performers. In 2019, The Tsinghua team created the first robot band with Chinese cultural characteristics -- Mojia. The harp robot “Kaiyang”, the bamboo flute robot “Yuheng” and konghou robot “Yaoguang” brought the robot musical stage play “Mojia Illusion”, which changed the performer from “human” to “non-human”, and the visual stimulation attracted a large number of audiences.

2.2 Innovate Auditory Channels for Musical Instruments

In addition to the innovative development of vision, the sound transformation and arrangement innovation of Musical Instruments are also in progress. The new media of Musical Instruments is one of the important research directions of music technological innovation and design. “Wang Meng + Yu Miao” is a group of new media band, as shown in Fig. 8. Wang Meng is mainly responsible for vision, Yu Miao is responsible for playing guzheng. Her main hardware is MIDI controller, and her software is mainly some interactive sequence software, such as: MAX/MSP, Jitter, Csound, Resolume Arena, AVES PureData, Kyma, etc., this kind of computer music emphasizes not the melodic pitch, rhythm and harmony in traditional instrumental music creation, but the overall timbre sound. Including sound density, sound phase, volume, brightness and so on [1]. This enables creators to break free from the shackles of stereotypes, dismantle their preconceived notions of “music” and explore more forms of musical expression (Fig. 5).



Fig. 5. The performance of “Wang Meng + Yu Miao”

2.3 Innovate Interactive Experience Channels for Audiences

After the audience’s hearing and vision are satisfied, interactive systems for audience participation in the performance are developed. “Harmony” created by artist Chen Junkai in 2016 makes use of new technologies to automate the performance of guzheng. He studied the shape, timbre and sound of Musical Instruments and sought breakthroughs in performance forms. He turns different traditional instruments into sound installations, with sensors in the center of the stage allowing the audience to dance to activate different components of the automated instruments. Artist Liu Yang creative lighting electric interactive device “Electric drum” line electric drum, traditional “drum”, and modern

art form “sound” and “light” combination. Who knock raised will have different music and lighting changes, can one side to experience the beauty of traditional lines drums, at the same time, can feel the modern electric lighting art audio and visual impact.

These interactive systems, through different sensors such as touch sensors, motion sensors, cameras and so on, provide real-time text or image feedback from the audience for the performer or generate real-time music based on the interaction of the audience. These interactive systems provide a wealth of ways for the audience to participate as a composer, as a conductor, as a performer, or as part of an audience. In addition, some systems put forward novel interactive ways, such as using mobile phones [2] or new hardware to invite the audience to participate in live music performances in real time and interact with the performers [3], or enable the audience to become players themselves or display rich visual feedback [4] (Fig. 6).

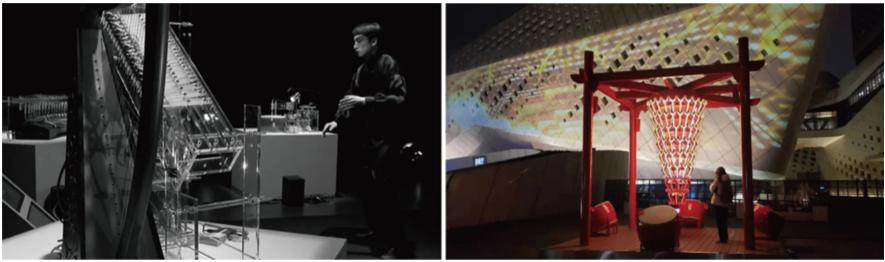


Fig. 6. “Harmony” crated by artist Chen Junkai & “Electric drum” crated by artist Liu Yang

3 The Intervention of Science and Technology Gave Birth to New Art Forms

With the addition of visual channel stimulation, auditory channel stimulation and now interactive stimulation channel, we gradually find that “Electric drum” or “Harmony” can no longer be called traditional musical instrument performance, and the current musical instrument performance has gradually evolved into a new art form. Because technology plays an important role in it, we can call it technological art performance (Fig. 7).

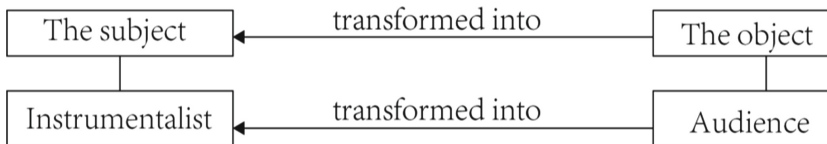


Fig. 7. Audience identity transformation

In the musical instrument performance of the technological art type, the subject changes from the performer to the audience. In the traditional instrument performance,

the protagonist is undoubtedly the music, and the performer presents the music to the audience through the instrument. However, with the development of The Times and the advent of experience economy, the subject of instrument performance has gradually changed from the only music to the parallel of music and audience experience. Audiences come to the performance site for the purpose of listening to music but also experience. In “Ruan’s sound”, “Wang Meng + Yu”, “Mojia illusion”, the audience’s desire to experience is gradually strengthened. In “Electric drum” or “Harmony”, the audience’s purpose has shifted from listening to music to experiencing. Since the main body of musical instrument performance has completely changed, it shows that the traditional performance form has completely changed. Whether the audience changes from the communication object to the subject in musical instrument performance becomes the dividing line between the traditional performance form and the performance form of technological art type.

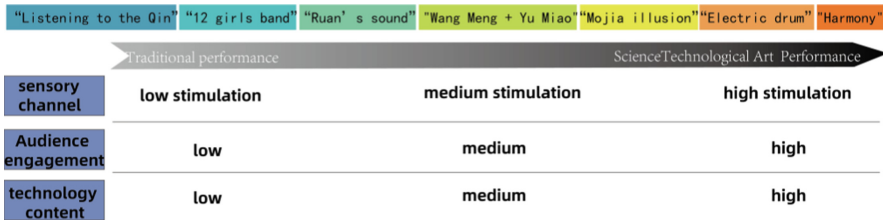


Fig. 8. Spectrum of the evolution from traditional performance to science technology art performance

Science Technology Art performance also has the following characteristics: performance has high behavioral participation, high interactive immersion experience, and high technological content, as shown in the spectrum in Fig. 8.

First of all, the audience’s behavioral participation has changed from low to high. The concept of “participation” is often mentioned in spectator studies in sports venues. Guo Chuanxin (2008), a Domestic scholar, believes that spectators’ involvement mainly includes two categories: cognitive and emotional category and behavioral category. On the one hand, the “participation” of music audience is the participation of action; The other aspect is cognitive and emotional involvement. In the traditional mode of playing, whether traditional Chinese instruments or western classical instruments, the audience is assumed to play a relatively passive role. They were asked to sit quietly, listen to pre-composed music, and only respond to the performers by applauding and attending the concert in the future [5]. On the one hand, most of the music played is made of high mountains and rivers, which is difficult for ordinary audiences to empathize with and lack cognitive and emotional “participation”. On the other hand, the player can only passively accept the information and cannot give their own feedback, so that the audience does not get enough participation, and there is no “participation” in action. In the works “Ruan’s sound”, although the audience can sitting beside the performer, has a certain action on participation. But the audience did not directly involved in the performance of the instrument, only the feeling on the vision more rich images of the subject and the object doesn’t change. So its nature is a form of traditional instruments. The audience has a high

degree of participation in “Harmony” and “Electric drum”. The audience becomes the performers themselves and directly participates in the performance. The audience is not only limited to the single identity of the recipient, but also the experienter and inspector of artistic products. From the perspective of economics, audiences are also participants and disseminators of artistic products, and they and artists jointly form the final value of artistic products [6]. Therefore, in this case, the performance form has undergone a qualitative change, from the traditional performance form to a new performance form with the participation of science and technology and art.

Secondly, the senses in musical performance change from low stimulation auditory and visual to high interactive immersion experience. In ancient times the performance, the audience heard is purely musical instruments sound, see is the same set. In the modern times, began to increase the effect on the vision, but also a relatively low frequency stimulation, until the “Ruan’s sound” is present, visual stimulus began to strengthen, and then to “Wang Meng + Yu Miao” show. There is not only visual high-frequency stimulation, but also auditory innovation, adding randomness and improvisation, no longer static performance, so that there is also auditory high-frequency stimulation. But so far, for the audience, it is only visual and auditory enhancement, the essence has not changed. Still only stays in the category of traditional musical instrument performance. Until “Harmoning” and “Electric Drumming”, these two works completely changed the audience’s senses. Apart from hearing and vision, they made the audience immerse themselves into the performance, which made the two works have an essential difference from the previous performances.

Finally, the involvement of science and technology in instrumental performance changes from low to high, which is also one of the important indicators different from traditional instrumental performance. In traditional performance forms, science and technology are less involved. At first, led screens were only used to play videos in the performance venue without any real-time or interactive effects. In “Ruan’s sound”, the artistic means of light Mapping was adopted to make the light and shadow change in real time with the vibration of the frequency when the performer played the instrument. As for “Wang Meng + Yu Miao” performance, in addition to visual software, auditory technology is also applied to MIDI controller and some interactive sequence software, such as MAX/MSP, Jitter, Csound, Resolume Arena, AVES PureData, Kyma, etc. To the “Voice of Mojia” this work, using robots and artificial intelligence technology means; When it comes to Harmoning, more technologies are used. In addition to visual and auditory interaction and somatosensory interaction, artistic and scientific transformation of installations is also required. It can be seen that in the change from traditional performance to technological art performance, the content and proportion of science and technology gradually increased, and finally turned into technological art.

4 Conclusion

China’s traditional Musical Instruments in the process of development by the influence of each era, there have been different changes. This technology in the present era, gradually began to merge both science and art, formed a new art form, traditional musical instrument performance as an art form has also been the impact of science and technology, changed the traditional mode of performance, into a new art form, we have

reason to call it - the science and technology under the art of the performing arts. New media never appear spontaneously and in isolation, they are gradually derived from the morphological changes of the old media. When newer forms emerge, older ones adapt and continue to evolve rather than die [7]. In this era of staying indoors, people still choose to listen to live music in theaters and other places, indicating that the experience brought by the audience's sense of presence is an advantage that will never be deprived of in instrument performance. Therefore, in the future development, traditional musical instrument performance and art performance under scientific and technological art will develop in parallel. Traditional musical instrument performance is responsible for inheritance, while artistic performance under scientific and technological art is responsible for innovation. Both of them jointly spread Chinese culture and music.

References

1. Wu, Y.: Research on music creation combining electronic music technology with instrumental performance. (Master's Thesis, Nanjing University of the Arts) (2016)
2. Weitzner, N., Freeman, J., Garrett, S., Chen Y.: Mass mobile-an audience participation framework. In: NIME 2012 Proceedings of the International Conference on New Interfaces for Musical Expression, pp. 92–95 (2012)
3. Freeman, J.: Large audience participation, technology, and orchestral performance. In: Proceedings of the 2005 International Computer Music Conference, pp. 757–760 (2005)
4. Gong Mood, Q.: Visualiser, Interactive Multimedia System for Live Music Performance (2014)
5. Pitts, S.E.: What makes an audience? investigating the roles and experiences of listeners at a chamber music festival. *Music Lett.* **86**, 257–269 (2005)
6. Han, X.F.: Research on the mechanism of value co-creation between music performing art institutions and audience participation. *Arts Management*, no. 04, pp. 75–81 (2019)
7. Ni, W.: Research on digital art communication form. (Master's Thesis, ShanDong University) (2009)



Design of Manned On-Orbit Maintenance Interface for Space Station

Zhihai Li^(✉), Haocheng Zhou, Wei Zhang, and Xiangjun He

Beijing Institute of Spacecraft System Engineering, China Academy of Space Technology,
Beijing 100094, China
haizi_up@163.com

Abstract. As a long-term vehicle and a complex system in orbit, the space station experiences a harsh space environment. In order to ensure that the space station can operate permanently and stably in the complex space environment, on-orbit maintenance has become an essential means. The long-term on-orbit presence of astronauts provides the necessary guarantee for the maintenance of equipment on the space station, and the equipment maintenance interface on the space station must also be designed considering Astronaut's ability and on-orbit environment must be considered during the design of the equipment maintenance interface on the space station. This paper analyzes the design characteristics of manned on-orbit maintenance interface from the perspective of man, machine and environment. And the methods of on-orbit maintenance interface design and ground verification were put forward. Finally, the effectiveness of maintenance interface design is verified by an on-orbit practice.

Keyword: Space station · Human · Maintenance interface

1 Introduction

The manned space station operates in orbit for a long time, and the system structure is extremely complex. A large number of equipment fail due to expiration of service life or random failure. As the space station has been in a harsh outer space environment for a long time, facing threats such as solar irradiation, atomic oxygen and space debris, the equipment will also fail due to debris impact or environmental erosion [1]. In order to ensure the long-term, safe and stable operation of the space station, on-orbit maintenance has become an essential means [2, 3].

Because people have subjective initiative, and the combination of human eyes and brain is superior to any automatic system, the long-term presence of astronauts on the space station provides necessary guarantee and great convenience for the on-orbit maintenance of products on the space station. Therefore, on-orbit maintenance has also become an important task for astronauts on orbit. The designed service life of Mir space station is 5 years, which is actually extended to 15 years through maintenance. Astronauts spend 75% of their time in maintenance [4, 5]. In order to ensure that astronauts can efficiently complete maintenance operations and the safety of the space station and astronauts

during the maintenance process, the maintenance interface of products on the space station must be specially designed according to the characteristics of the space station, astronauts and the space environment.

This paper expounds and analyzes The design characteristics of on-orbit maintenance interface was expounded and analyzed. Then the design and verification method of on-orbit maintenance interface were put forward. Finally the effectiveness of maintenance interface design was verified through an on-orbit example.

2 Characteristics of Manned Maintenance Interface Design for Space Station

The on orbit maintenance task of the space station takes the products on the space station as the maintenance object and the astronauts as the task implementation subject. At the same time, it is affected by the complex space environment. Therefore, the characteristics of the manned on orbit maintenance interface design of the space station were analyzed from the three aspects of man, machine and environment:

1. Astronauts have subjective initiative. Through the combination of eyes and brain, they can control the movement of limbs and complete various fine and complex operations. Therefore, during the design of maintenance interface, we should focus on visibility, accessibility and operability, and incorporate the astronauts' operation ability, accommodation space and visual feedback into the design elements of maintenance interface.
2. During the on orbit maintenance of products on the space station, the space station system is still working. Therefore, in the design of maintenance interface, it should be ensured that the equipment can be isolated from the space station system, and the safety of the space station platform will not be affected during the maintenance process.
3. The on-orbit maintenance of the space station is carried out in the space environment and has been affected by the space environment. In the design of maintenance interface, the operation ability of astronauts and the environmental tolerance of new products to be replaced under weightlessness and extravehicular vacuum environment should be considered.

3 On-Orbit Maintenance Interface Design

The maintenance interfaces of products on the space station mainly include power supply interface, information interface and maintenance operation interface. Therefore, based on the characteristics of on orbit maintenance interface design supported by Astronaut, the on-orbit maintenance interface design method was proposed mainly from the above three aspects.

3.1 Power Supply Interface Design

When astronauts repair the products, from the perspective of human factors, it is necessary to ensure the personal safety of astronauts during operation [6]. Considering the safety of the space station platform, it is necessary to ensure that other equipment of the platform will not be damaged and that the platform can operate normally. The products to be repaired are set to be powered off before maintenance. All products to be repaired on the space station are designed to be powered off independently. The power distribution mode of the space station is designed as a tree distributed topology. The power supply and distribution for the load is realized through the secondary bus, so as to prevent the astronauts from affecting the power supply safety of the primary bus when repairing the downstream load of the secondary bus. In order to ensure the normal operation of the space station during the maintenance of the distributor, the space station is designed with two power supply buses. The key products are powered by double buses. When the repaired distributor is powered off for maintenance, its downstream key load can be switched to another bus.

3.2 Information Interface Design

The equipment on the space station realizes information interaction and command control through information interface. On the one hand, the ground uplink command is sent to the space station, and the computer on the station sends commands to control the load; On the other hand, the state information of the load collected by the computer on the station is transmitted back to the ground through the measurement and control system for the ground monitoring personnel to judge the on orbit flight state of the space station. The space station adopts the information interface design of the combination of information bus and hard wire. Most of the information goes up and down through the information bus structure, and the key instructions and telemetry information are backed up by hard wire, so as to ensure the smooth operation of the space station during the maintenance of some equipment on the bus.

During the maintenance of space station products, the upstream and downstream equipment are not powered off. In order to prevent the impact of interface plug-in on the upstream and downstream equipment, information system isolation and interface circuit protection design are required. Both 1553B interface and analog telemetry interface support hot plug. For interfaces that do not support hot plug (such as RS422 interface [7]), separate relays are designed on relevant interfaces, and the interfaces that cannot be hot plug are powered off separately through instructions, so as to ensure the safety of platform equipment and astronauts.

3.3 Maintenance Operation Interface Design

The operation interface design of on-orbit maintenance supported by the astronauts was mainly considered from two aspects: human factors and space environment:

1. The astronauts' on orbit operation ability should be brought into full play to improve the astronauts' operation efficiency. Moreover, the operation safety of astronauts needs to be guaranteed.

2. The influence of weightlessness on the maintenance operation of the interface shall be considered. For Extravehicular maintenance, the influence of vacuum environment on astronauts' operation ability should also be considered.

Considering the above two aspects, the corresponding design methods were proposed for the common maintenance operation interfaces, including mechanical interface, electrical connector, and pipeline interface.

3.3.1 Mechanical Interface

The mechanical interface is mainly used to fasten the equipment to ensure the fixed installation of the equipment. Some equipment with grounding and heat conduction requirements also need to be mechanically fastened to ensure the reliable fit between the equipment and the mounting surface. Since the equipment needs to withstand the load of the rising section when launching with the cabin, the loading equipment generally adopts the method of fixed torque fastening with screws and gaskets to realize the fastening and installation of the equipment.

In order to avoid the floating objects caused by the floating away of the screw after disassembly under the condition of weight loss, the screw without pulling out is designed, which can not only meet the fastening requirements of the screw, but also the screw is still fixed on the product after disassembly. So it will not float out and form the surplus into the ventilation duct, which will bring risks to the platform (Fig. 1).



Fig. 1. The screws without pulling out

3.3.2 Electrical Connector

Electrical connectors are mainly used to realize the power supply and information transmission of products on the space station. The common electrical connectors on the space station are generally circular electrical connectors and rectangular electrical connectors.

The layout of the connectors of the repaired product shall consider the space for astronauts to hold their hands during unarmed operation, as shown in the figure below. The distance between the gripping surface of the plug end of the circular connector and the surrounding equipment and accessories shall not be less than 'L'. There are two

requirements for the distance between the grip surface of the plug end of the rectangular connector and the surrounding equipment and its accessories: The distance between both sides of the operation surface should be more than 'L1', and the distance between the front and back of the operation surface should be more than 'L2' (Fig. 2).

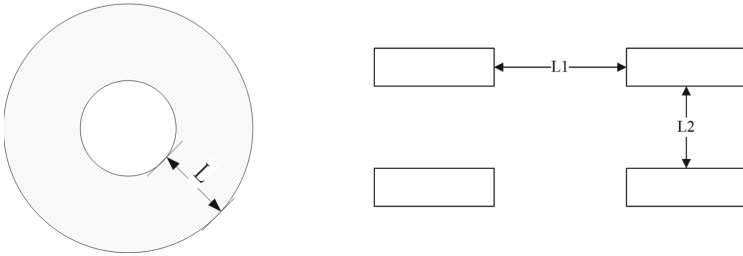


Fig. 2. The schematic diagram of operation space of electrical connector

3.3.3 Pipeline Interface

The pipeline interface on the space station is mainly used in the gas and liquid fluid circuit. During the maintenance of pipeline equipment in the fluid circuit, the pipeline interface needs to be disconnected and restored. Considering improving the operation efficiency of astronauts and reducing the operation difficulty, the pipeline interface is generally designed as cylindrical. In order to facilitate the alignment of astronauts, alignment marks are also designed on the pipeline joints.

Different pipeline interfaces are designed for two different pipelines: gas pipeline and liquid pipeline. The liquid interface is designed in the form of self sealing to prevent the outflow of working medium from damaging astronauts and platform equipment when astronauts disconnect the pipeline. If the working medium in the gas circuit interface is harmless to human body, such as nitrogen, oxygen, etc., the pipeline interface is designed as a non self sealing form. When the pipeline is disconnected, a small amount of gas can be directly discharged into the cabin.

4 Ground Verification Method

For the design of space station maintenance interface, the following two aspects of ground test verification methods are mainly studied.

1. Virtual simulation test

Using virtual simulation test technology, the design of maintenance interface for space station can be validated at the beginning of the project development. Through the design and development of three-dimensional digital simulation model, the evaluation system of on-orbit operation is established using on-orbit flight data. And based on ergonomic analysis software, a set of virtual simulation test evaluation system is integrated with motion capture, data glove and data helmet, which can support virtual and semi-physical operation simulation verification test.

2. Ground verification test

A set of ground simulation validation chamber system is established, in which the validation and evaluation of power supply information interface isolation, maintenance interface operability and other design can be carried out. For the validation of extravehicular operation in vacuum environment, an extravehicular operation simulation glove box was designed to validate the operability of extravehicular maintenance interface by simulating the glove status of extravehicular space suit in vacuum. For the operation verification under weightless environment, the neutral buoyant water tank is used to simulate the weightless environment and verify the whole process of extravehicular maintenance (Fig. 3).

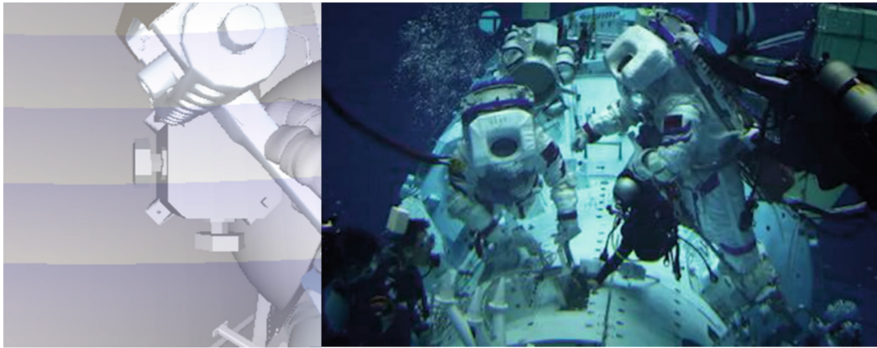


Fig. 3. Virtual simulation test and ground verification test

5 On-Orbit Maintenance Task Practice

China's space station was successfully launched into orbit on April 29, 2021. Up to now, the astronauts have completed 4 spacewalks and a number of in-flight maintenance and repair tasks, which fully validate the design of the maintenance interface for the space station. The extravehicular panoramic camera was taken as an example to introduce the on-orbit verification of its maintenance interface design.

The astronauts completed on-orbit disassembly and elevation of 3 panoramic cameras outside the space station through multiple spacewalks. The astronauts took maintenance tools and ancillary facilities out of the node cabin, one moved to the installation location of the panoramic camera with the help of a mechanical arm, and the other climbed to the installation point with the help of handrail on bulkhead. Before the repair operation started, the ground sent instructions to control the panoramic camera to power off. At the installation point, the astronauts completed the camera disassembly and lifting by plugging and unplugging the electrical connector and operating the power tools to disassemble and unscrew the screws. After the operation is completed, the ground sent instructions to power up the device. Before and after maintenance, the power supply and information interface design were verified, and other devices on the space station were

still working normally. The astronauts completed the insertion and removal of the electrical connector and the disassembly of the screw, and verified that the maintenance and operation design of the mechanical interface and electrical connector met the astronauts' operation requirements (Fig. 4).

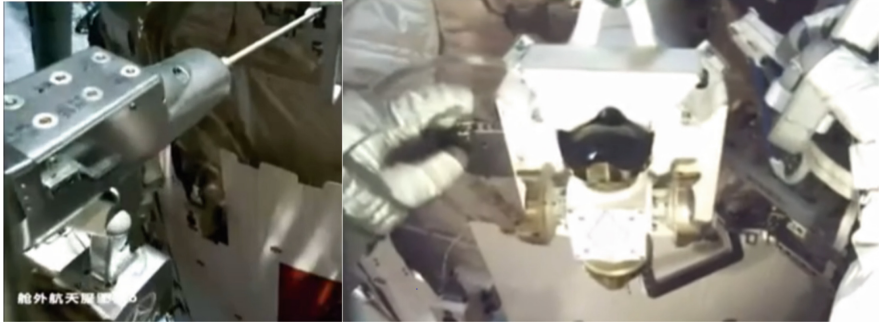


Fig. 4. On orbit operation of panoramic camera

6 Conclusion

Starting from the three aspects of man machine environment, the characteristics of on-orbit maintenance interface design supported by Astronauts was analyzed. And the design method of on-orbit maintenance interface was put forward from three aspects: power supply interface, information interface and maintenance operation interface. Then, the virtual policy and ground verification method were put forward. Finally, the effectiveness of maintenance interface design was verified by an on-orbit maintenance example, which can provide technical accumulation and ideas for the on-orbit maintenance interface design of manned spacecraft.

References

1. Xu, H.Q., Lü, C.: Space environment effect on the maintainability design of space system. *Aerosp. Shanghai* **20**(5), 38–41 (2003)
2. Wang, D.P., Tan, C.L., Zhang, B.N.: On-orbit maintainability system design for manned spacecraft. *Chin. Space Sci. Technol.* **30**(5), 16–21 (2010)
3. Wei, P.W.: Research of maintainability technology in manned spacecraft. *Spacecraft Eng.* **17**(6), 68–72 (2008)
4. Lv, C.: *Design Analysis and Verification of Maintainability*, pp. 6–12. National Defense Industry Press, Beijing (2012)
5. Wei, Z., Xia, Q.L.: Study on design and verification method of space station maintainability. *Manned Spaceflight*, **20**(2) (2014)
6. Nan, H.T., Liu, H.T., Wang, L.T.: Safety design of high voltage power supply for manned spacecraft. *Spacecraft Environ. Eng.* **30**(1), 94–97 (2013)
7. Chen, Y., Wang, M.D., LI, X.H.: Design of replaceable module plug-and-play interface based on FPGA. *J. Central South Univ.(Science and Technology)* (2013)



Time Series Prediction Model of Spacecraft Health Management System Based on Wavenet Convolutional Neural Network

Ping Zhang¹, Xinyu Xiang¹, Jieren Cao¹, Chunjian Zhu¹, Qiang Yuan², Renping Li², Lijing Wang³, and Ke Li³(✉)

¹ State Grid Zhejiang Electric Power CO., Ltd., Hangzhou Power Supply Company, 310000 Hangzhou, China

² Hangzhou Xuntong Software Co., Ltd., 310000 Hangzhou, China

³ School of Aeronautic Science and Engineering, Beihang University, Beijing 100191, China
like@buaa.edu.cn

Abstract. In this paper, we introduce the Time Series Prediction Model Based on Wavenet Convolutional Neural Network. This means can give early warning for the future working state and possible faults of spacecraft in advance. As the signal of spacecraft thermal control system belongs to one-dimensional time series, this topic proposes to use the time series model based on WaveNet convolution neural network to predict the time series signal of spacecraft thermal control system and interpret the prediction information. The experimental results show that the time series prediction model of WaveNet convolutional neural network has good effect in fault prediction in a certain range

Keywords: Fault diagnosis · Time series prediction · CNN · PHM

1 Introduction

Fault prediction is one of the core parts of spacecraft fault health management system. Through real-time signal acquisition equipment or system state characteristic data, the health monitoring and evaluation of spacecraft is carried out, that is, the future state of the spacecraft system is predicted [1–3]. This means can give early warning for the future working state and possible faults of spacecraft in advance. As the signal of spacecraft thermal control system itself belongs to one-dimensional time series, this topic proposes to use the time series model based on WaveNet convolution neural network to predict the time series signal of spacecraft thermal control system and interpret the prediction information, so as to realize the technical support of fault prediction of spacecraft system. Compared with the traditional long-term and short-term memory neural network (LSTM) model [4–6], this model reduces the problem of computational redundancy, improves the feature extraction ability of the network, and improves the operation efficiency of the network.

2 Wavenet Convolutional Neural Network

At first, WaveNet was proposed to serve the audio field, which can be applied to speech enhancement, audio generation, text-to-speech conversion, and other scenes. WaveNet convolutional neural network framework is a probabilistic autoregressive model [7–9], which predicts the current sample probability distribution through the previously generated samples. Now the model has obtained the best performance in the field of speech synthesis. In the WaveNet convolutional neural network model, firstly, the causal convolution is used to ensure that the model output will not disturb the data input order, and then the expanded convolution is used to expand the receptive field to avoid the reduction of receptive field caused by multi-layer causal convolution. Finally, the prediction results are given by activation function and normalized exponential function. The essence of the WaveNet model is to predict the subsequent time series by using the samples of the previous time series. Its formula is as follows:

$$p(x) = \prod_{t=1}^T p(x_t|x_1, \dots, x_{t-1}) \tag{1}$$

In the formula, time series $x = \{x_1, \dots, x_T\}$, p represents conditional probability.

2.1 Causal Convolution

The concept of causal convolution was first proposed by van den Oord [60] in the WaveNet paper in 2016. Its most important role is to avoid reconstructing the data sequence relationship and save training time. The essence of causal convolution is one-dimensional convolution, that is, the output of general convolution moves several time steps. For time series problems, it is mainly abstracted according to the previous sample $x_1 \dots x_t$ and $y_1 \dots y_{t-1}$ to predict y_t , so as to make the predicted value as close as possible to the real value (Fig. 1).

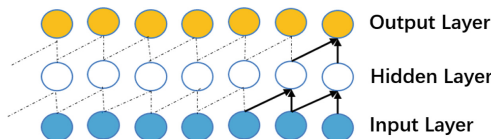


Fig. 1. Schematic diagram of causal convolution.

2.2 Dilation Convolution

Considering the accuracy of prediction, the longer the preamble time series that can be referenced, the more helpful it is to the accuracy of prediction generation because more reference factors can be introduced, but this will increase the number of convolution layers, resulting in the disappearance of gradient and the reduction of the receptive field. In order to avoid this situation, dilation convolution is introduced. The difference between dilation convolution and ordinary convolution lies in the dilation coefficient.

When the size of the convolution kernel is the same and the number of neural network parameters remains unchanged, the dilation coefficient can make the output layer, that is, the obtained characteristic layer, have a larger receptive field, as shown in Fig. 2. Comparing the figure with Fig. 2, it is found that when the original output element can only correspond to three input points, the introduction of dilation convolution can make an output element correspond to four input points (the dilation coefficient is 2), and the stacked dilation convolution can significantly correspond to a longer preamble time series, that is, it has a very large receptive field while retaining the input resolution and computational efficiency.

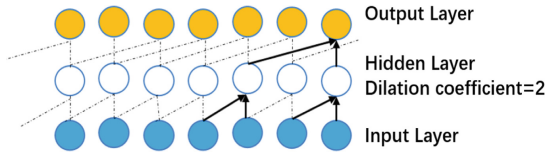


Fig. 2. Schematic diagram of dilation convolution.

2.3 Activation Function

The relu function was first proposed by Geoff Hinton [10, 11]. By setting all negative values in the matrix to zero and keeping the rest unchanged, the gradient disappearance problem is solved and the training speed is accelerated. It is a nonlinear activation function, which is now widely used in neural network learning. Its formula is as follows:

$$f(x) = \max(0, x) \tag{2}$$

In the formula, X represents the matrix, and Max represents the comparison of each number in matrix X with 0. When it is greater than 0, it remains unchanged; When less than 0, the corresponding position number in matrix X changes to 0.

3 Time Series Prediction Model Based on WaveNet Convolutional Neural Network

Aiming at the problem of signal prediction of spacecraft thermal control systems, this subject constructs the time series prediction model of WaveNet convolutional neural network and predicts the future time series by learning the sample points of the previous time series. The network model first defines the length of time series to be predicted, divides the time series in the data set, and divides it into two parts: historical time series and target prediction time series. Then, the data of the historical time series and the target prediction time series are smoothed to make them more subject to Gaussian distribution. Then, the prediction of time step 1 outside the current historical record is extracted from each iteration of the historical time series and then added to the previous historical record series. The whole prediction time series can be generated by setting the step

size of the prediction time series for several iterations. A priori guidance information is introduced into the training of time series prediction model of WaveNet convolutional neural network, and the model is forced to train with reference to the prior guidance information, so as to obtain the prediction sequence with set time step. Therefore, if you start from the history sequence and want to predict the first time step in the future, you can run the model on the history sequence and use the last time step of the output to correspond the time step to a time step other than the history sequence (Fig. 3).

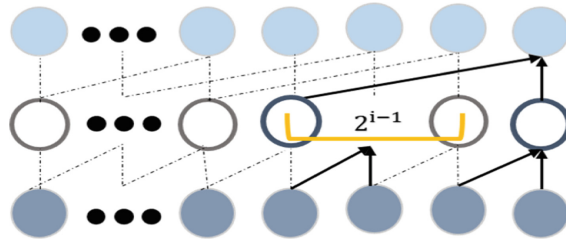


Fig. 3. Schematic diagram of causal and dilation convolution.

The time series prediction framework of WaveNet convolution neural network [12] is shown in Fig. 4. The input is a one-dimensional historical time series. Through the stacked causal dilation convolution layer module, the extracted effective time information is transmitted to the full connection layer, then sent to the random discard layer, and then sent to the full connection layer for regression judgment to judge the accurate prediction state of the next time point at that time, Continue to cycle this process, and finally get the target prediction time series. The model structure and number of parameters of the network are shown in Table 1.

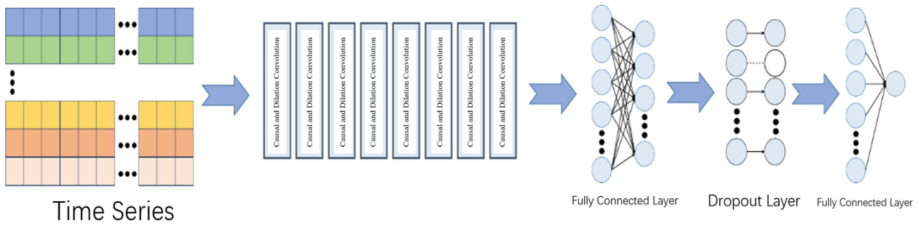


Fig. 4. Flow chart of time series prediction model of WaveNet convolutional neural network

Table 1. Parameter of time series prediction model structure of WaveNet convolutional neural network

Layer	Dilation coefficient	Output size	Number of coefficients
Input layer	/	1	0
DilationCausalConvLayer1	1	32	96
DilationCausalConvLayer2	2	32	2080
DilationCausalConvLayer3	4	32	2080
DilationCausalConvLayer4	8	32	2080
DilationCausalConvLayer5	16	32	2080
DilationCausalConvLayer6	32	32	2080
DilationCausalConvLayer7	64	32	2080
DilationCausalConvLayer8	128	32	2080
Fully connected layer	/	128	4224
Dropout layer	/	128	0
Fully connected layer	/	1	129

4 Experiment

4.1 Experiment Data

The experimental data adopts typical type 4 signals among 14 types of fault signals of spacecraft thermal control system. The schematic diagram of these four types of signals is shown in Fig. 5 below. The length of each type of signal is 1000. The training set and test set are divided. The training set is 80% of the number of each signal, and the remaining 20% is used as the test set. In the experiment, the length of the prediction time series is set to 60. In the training set, the time series with the length of 1–940 is taken as the historical time series and 940–1000 is taken as the test set. In the test process, the historical time series is used to continuously judge the next prediction point until the set length of the prediction time series is completed, Thus, a prediction and evaluation of the equipment condition of spacecraft thermal control system in the future is obtained.

4.2 Setting of Training Hyperparameters

In the time series prediction training of WaveNet convolutional neural network, Adam training method is adopted and the super parameters of Adam optimizer are optimized β_1 set to 0.9, super parameter β_2 is set to 0.999. In the process of experimental training, the batch training model is adopted. The size of each batch of training data is 1028. A total of 20 rounds of training are carried out. The random discarding probability in the random discarding layer is set to 0.2. The settings of training and super parameters involved in the model are shown in Table 2.

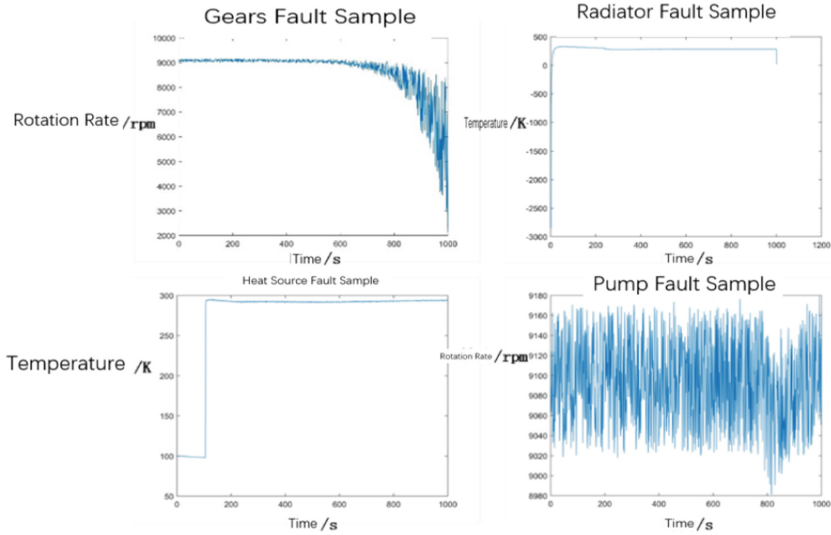


Fig. 5. Schematic diagram of some typical signals of spacecraft thermal control system

Table 2. Training process hyperparameter table of time series prediction model based on WaveNet convolutional neural network.

Hyperparameter	Value
<i>Learning rate lr</i>	0.001
<i>Adam optimizer hyperparameter β_1</i>	0.9
<i>Adam optimizer hyperparameter β_2</i>	0.999
<i>Batch size</i>	1028
<i>Epoch</i>	20
<i>Dropout prob</i>	0.2

5 Experiment Result

In order to intuitively and clearly analyze the time series prediction results of the WaveNet convolution neural network, the time series prediction results are visualized. After research and analysis, it is because the historical time series does not provide the burst characteristics of target prediction sequence learning, so it shows that the time series prediction model of WaveNet convolutional neural network has a limited range. Therefore, the algorithm can be applied to the life prediction of spacecraft thermal control system signals, and the available time of equipment can be obtained by predicting aging faults, which is of great engineering significance for fault prediction and health management (PHM) technology.

6 Conclusion

Firstly, this chapter introduces the background of the WaveNet convolution neural network and expounds on the principles of causal convolution and dilation convolution in detail. Then, aiming at the prediction problem of the one-dimensional time series data set of spacecraft thermal control system in this paper, a time series prediction model of WaveNet convolution neural network is proposed. The network framework module and network super parameter setting of the model are described and explained in detail, and the corresponding prediction experiments are carried out based on the model. The experimental results show that the time series prediction model of WaveNet convolutional neural network has good effect in fault prediction in a certain range.

Acknowledgements. This work are supported by the National grid Zhejiang Electric Power Corporation Technology Program (5211HZ19014S). Chinese National Natural Science Foundation (No. 61773039).

References

1. Xu, Z., Felix, X.Y., Shih-Fu, C., et al.: Deep transfer network: unsupervised domain adaptation (2015)
2. Zhou, J.T., Pan, S.J., Tsang, I.W.: A deep learning framework for hybrid heterogeneous transfer learning. *Artif. Intell.* **275**, 310–328 (2019)
3. Wen, L., Gao, L., Li, X.: A new deep transfer learning based on sparse auto-encoder for fault diagnosis. *IEEE Trans. Syst. Man. Cybern. Syst.* **49**(1), 1–9 (2017)
4. Zhang, Y., Li, K., Li, K., Liu, J., et al.: Intelligent Prediction Method for Updraft of UAV that is Based on LSTM Network. *IEEE Trans. Cogn. Dev. Syst.* 31 December 2020. <https://doi.org/10.1109/TCDS.2020.3048347>
5. Ghifary, W.M., Kleijn, B., Zhang, M., Balduzzi, D., Li, W.: Deep reconstruction-classification networks for unsupervised domain adaptation. In: Leibe, B., Matas, J., Sebe, N., Welling, M. (eds.) *Computer Vision – ECCV 2016: 14th European Conference, Amsterdam, The Netherlands, October 11–14, 2016, Proceedings, Part IV*, pp. 597–613. Springer International Publishing, Cham (2016). https://doi.org/10.1007/978-3-319-46493-0_36
6. Rethage, D., Pons, J., Serra, X.: A wavenet for speech denoising. In: *Icassp IEEE International Conference on Acoustics*. IEEE (2018)
7. Yaroslav, G., Victor, L.: Unsupervised domain adaptation by backpropagation (2014)
8. Sun, B., Saenko, K.: Deep CORAL: correlation alignment for deep domain adaptation. In: Hua, G., Jégou, H. (eds.) *Computer Vision – ECCV 2016 Workshops: Amsterdam, The Netherlands, October 8–10 and 15–16, 2016, Proceedings, Part III*, pp. 443–450. Springer International Publishing, Cham (2016). https://doi.org/10.1007/978-3-319-49409-8_35
9. Oord, A., Dieleman, S., Zen, H., et al.: WaveNet: a generative model for raw audio (2016)
10. Hinton, G.E., Salakhutdinov, R.R.: Reducing the dimensionality of data with neural networks. *Science* **313**(5786), 504–507 (2006)
11. Lan, W., Li, Q., Nan, Y., Wang, Q., Jia, S., Li, K.: The deep belief and self-organizing neural network as a semi-supervised classification method for hyperspectral data. *Appl. Sci.* **7**(12), 1212 (2017)
12. Bakar, A., Ke, L., Liu, H., Ziqi, X., Wen, D.: Design of low altitude long endurance solar-powered UAV using genetic algorithm. *Aerospace* **8**(8), 228 (2021)



Deep Reinforcement Learning Algorithm and Simulation Verification Analysis for Automatic Control of Unmanned Vehicles

Yonghong Chen¹, Yuxiang Zhang^{1,2}, Jiaao Chen², Junyu Zhao², Ke Li²(✉),
and Lijing Wang²

¹ Yangzhou Collaborative Innovation Research Institute Co., Ltd., Yangzhou, China

² School of Aeronautical Science and Engineering, Beihang University, Beijing, China

like@buaa.edu.cn

Abstract. This study conducted research mainly on the proven applicability of controlling the unmanned vehicle using a deep reinforcement learning algorithm and relative performance improvements. In specific, this study chose the AirSim platform developed by Microsoft as the simulation environment and conducted simulations mainly in the indoor parking lot Unreal 4 environment. In the simulations, the deep reinforcement learning method applied is Deep Q Networks for its effectiveness as well as simplicity. To improve the performance of the trained network, object detection methodology YOLO v3 is applied as the detection algorithm for the unmanned vehicle, and the network is improved using the output of object detection as its input to accelerate the training process. The implementation of the algorithms has efficiently proven the feasibility of using deep reinforcement learning agents for the unmanned vehicle in the project and the implementation of effective object detection.

Keywords: Deep reinforcement learning · YOLO · Simulation · Unmanned vehicles

1 Introduction

1.1 Background

Unmanned vehicle control is a sub-branch of autonomous driving, but as artificial intelligence, the term self-driving is often interpreted in a variety of ways. Unmanned vehicles, for example, are often used to describe specific technologies and applications including different levels of assisted driving, some of which require human collaboration, but the term unmanned represents 100% machine-controlled and does not include primary functions such as assisted driving.

Ideally, humans would like to see fully driverless cars replace existing human drivers, but in terms of the development of self-driving technology, there will be a transition period of 10 years or more in the future. To better differentiate between different levels of self-driving technology, SAE International released a six-tier classification system for self-driving in 2014 [1–4].

2 Methodology

2.1 Deep Reinforcement Learning (DRL)

2.1.1 Introduction

Reinforcement learning is a branch of machine learning, which is characterized by learning in interaction, compared to the classic supervised learning and unseeded learning problems of machine learning. The agent is more adaptable to the environment based on the rewards or penalties it receives in interactions with the environment. The paradigm of RL learning is very similar to the process by which we humans learn knowledge, and as a result, RL is seen as an important way to achieve universal AI [5].

Policy refers to the choice that Agent makes when it is in the state, defined as π , is the core of the Reinforcement Learning. The policy can be considered a mapping of action a after the agent perceives the environment. If the policy is stochastic, the policy selects actions based on the probability of each action $\pi(a|s)$, and if the policy is deterministic, the policy selects actions directly from the states. $a = \pi(s)$.

$$\text{Stochastic : } \sum_a \pi(a|s) = 1 \quad (1.1)$$

$$\text{Deterministic : } \pi: S \rightarrow A \quad (1.2)$$

Reward signal defines the goals that the agent is learning. Each time agent interacts with the environment, the environment returns to the reward, telling the agent if the action just happened is good or bad, which can be understood as a reward and punishment for the agent, as shown in the following image of the sequence flow of agent interaction with the environment. Note that Reward \neq Goal. That is, the goal of the agent is not the current maximum, but the average cumulative return is the largest. Reward Signal defines the immediate return value of an interaction. Value function, on the other hand, defines how good or bad the average return is in the long run. Model is a real-world simulation that models the response of the post-sample environment. In RL, methods that use model and planning are called model-free, and instead of model-and-error, the method of learning policy through try-and-error is called model-free [6].

2.1.2 Value-Based Learning

Value-Based Learning usually refers to learning the optimal value function $Q^*(s, a)$ (or action-value function, state value function). If we have the Q^* , the intelligence can make decisions based Q^* and choose the best action. Each time you observe a state s_t , enter it into the Q^* function and let the Q^* evaluate all actions, for example

$$Q^*(s_t, \text{Left}) = 273, \quad (1.3)$$

$$Q^*(s_t, \text{Right}) = -139, \quad (1.4)$$

$$Q^*(s_t, \text{Up}) = 195 \quad (1.5)$$

These Q values quantify how good each action is. The intelligence should act with the largest Q value, which is to move to the left. This action is expected to achieve an expected return of no more than 273 in the future, while the other two actions are expected to return no more than -139 and 195. Smart body decisions can be represented by this formula:

How to learn the Q* function? We need to use the states, actions, rewards collected by the intelligence, use them as training data, learn a table or a neural network, and use them to approximate Q*. The most famous method of value learning is Deep Q Network (DQN), which is detailed in the following sections [7-9].

2.1.3 Policy-Based Learning

Policy-Based Learning refers to the learning strategy function π (als). If we have a strategy function, we can use it directly to calculate the probability value of all actions, and then randomly select an action and execute it. Each time you observe a state st, enter it into π function and let the π evaluate all actions and get the probability value:

$$\pi_{Leftst} = 0.6 \tag{1.6}$$

$$\pi_{Rightst} = 0.1 \tag{1.7}$$

$$\pi_{Midst} = 0.3 \tag{1.8}$$

The intelligence does a random sample and then performs the selected action. All three actions are likely to be selected. How do I learn π strategy? Later sections of this book describe methods such as strategy gradients to learn π [10].

2.2 Deep Q Networks

2.2.1 DQN Algorithm

Q-Learning solves maze problems well, but its State Space and Action Space are small. In practice, most problems have a huge state space or action space. This results in insufficient memory size to establish a Q table according to Q-Learning and even increasing memory, the amount of data and the time it takes for Q tables to be established and accessed is a big problem.

To solve this problem, neural networks are used to represent Q functions, and the weight of each layer of the network is the corresponding value function. Simply put, we can take four frames of game images as State, output the Q value for each Action, if one wants to perform an update of the Q value, or select the corresponding Action with the highest Q value, we can immediately get the Q value for any action under that frame by simply entering a State and all its possible Action into the network. It is worth mentioning that the original input of DQN is a continuous 4 frames of the image, not only 1 frame screen is used to perceive the dynamics of the environment [11, 12].

The loss function of the DQN algorithm could be written as

$$Lw = Er + \gamma \max_{a'} Qs', a', w - Qs, a, w2 \tag{1.9}$$

2.2.2 Improvement

NIPS DQN uses the Explorer Replay Experience Pool based on the basic Deep Q-Learning algorithm. The correlation of the data samples is reduced by storing the trained data and then random sampling and therefore the performance could be improved. Next, one of the improvements nature DQN made was to add target Q Networks. That is, we use a dedicated target Q network when calculating target Q values, rather than using a pre-updated Q network directly. The purpose of this is to reduce the correlation between the target calculation and the current value.

$$Lw = Er + \gamma \max_{a'} Qs', a', w - Qs, a, w2 \tag{1.10}$$

As shown in the loss function formula above, the network that calculates the target Q value uses a w-, not a w. The original NIPS version of the DQN target Q network is dynamic changes, with the Q network update and change, which is not conducive to the calculation of the target Q value, resulting in the target Q value and the current Q value correlation greater. Therefore, it is proposed to use a single target Q network, from which just the delay is updated. That is, each time wait for training for a period before copying the parameter values of the current Q network to the target Q network.

In the case of Nature-DQN, there are three main extensions: Double-DQN, Selected Replay, and Dueling Network, all of which are covered one by one [13, 14].

The idea is modeled on Double Q-learning, where one Q network is used to select actions, and the other Q network is used to evaluate actions, alternate work, solve the upward-bias problem, specifically, there is a current network w used to select actions, and the action is used to evaluate the action is the older network of w-, the loss could be written as:

$$Lw = Er + \gamma Q(s', \operatorname{argmax}_{a'} Qs', a', w, w-) - Qs, a, w2 \tag{1.11}$$

Based on the priority replay mechanism, replay accelerates the training process, increases the sample in disguise, and is independent of the effects of the current training process.

$$Lw = Er + \gamma \max_{a'} Qs', a', w - -Qs, a, w2 \tag{1.12}$$

Breaking down Q (s, a) into V (s)– A (s, a), V(s) is not action-related, A(s, a) is action-related, is the relative good or bad of a relative s average return, is an advantage, solves the reward-bias problem.

$$Qs, a = Vs, v + A(s, a, w) \tag{1.13}$$

3 Results

3.1 YOLO

With the implementation of the YOLO algorithm [12], one could test its performance in object detection based on figures from the two UE4 scenes introduced above. In specific,

three figures are chosen to testify the result of the YOLO object detection algorithm as shown below.

The first figure is from the indoor parking lot environment, in which the agent unmanned vehicle is near its origin, and in the figure, there are two trucks as the obstacles of driving. The two trucks are detected as expected with the confidence of their classification with them showing 0.79 and 0.76. The detected blocks with the trucks in them are clearly around the borders of the trucks showing the accuracy of the YOLO algorithm in this parking lot scene. With the detected information of the trucks, the DQN [15] could use it as the input and therefore could improve its training speed as expected which is shown as Fig. 1.



Fig. 1. YOLO result in parking lot scene - 1

The second figure is from the mid-point from the origin to the destination in the parking lot scene. The main difference between the second figure with the first one is the size of the object. With the object in a larger area of the figure, the network for detection may have less confidence in its result. However, from the result of this figure, the only truck in the middle of the figure is shown with 0.73 confidence. Though comparing the result of the first figure, the detection's result has less confidence, the borders are still clear and the provided information of potential obstacles for the further training of DQN is still very effective which is shown as Fig. 2.



Fig. 2. YOLO result in parking lot scene - 2

3.2 DQN

The performance of the trained neural networks could be shown from the drawn rewards in the training. As introduced before, the reward is a function calculated based on the performance of the agent unmanned vehicle. Specifically, a larger reward indicates that the agent performs better in the scene. With the setting of the reward function, in this experiment, the reward has its maximum value of 500, and reaching the destination has a 150 bonus for the agent, which means that reward values larger than 350 could only be obtained by reaching the destination. Therefore, the evaluation of one trained model could be from the times that the networks reach the reward of 350. Another evaluation could be from the perspective of the training speed. That is, in the first episode the agent reaches the reward of 350 or reaches the destination which is shown as Fig. 3.

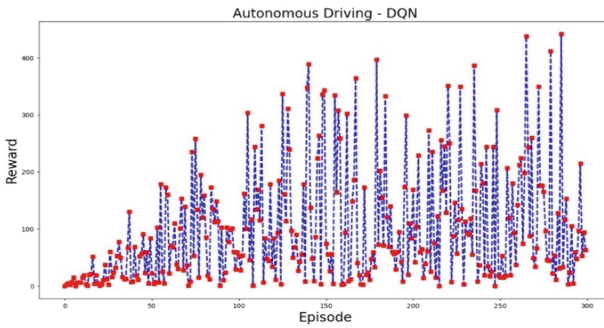


Fig. 3. Reward of DQN in 300 episodes

As shown in the figure above, that the reward increases gradually in the first 150 episodes with necessary low rewards showing that some directions might not be proper for the obstacle avoidance. The agent reaches its destination firstly in its 136's episode and the further training, the agent reaches its destination 11 times.

However, the agent doesn't have stable rewards after the 300 episodes. As could be seen from the figure, there are still multiple data points with rewards less than 200 after 250 episodes, which means the possibility that the unmanned vehicle agent not finishing the task still exists. The reason that the agent could not have stable performance is due to the policy helping the agent to find more possibilities. The random exploration not based on the detected Q-value network made the agent unstable. One potential improvement for the network could be limiting the exploration rate.

4 Conclusion

In specific, this study chose the AirSim platform developed by Microsoft as the simulation environment and conducted simulations mainly in the indoor parking lot Unreal 4 environment. In the simulations, the deep reinforcement learning method applied is Deep Q Networks for its effectiveness as well as simplicity. To improve the performance of the trained network, object detection methodology YOLO v3 is applied as the detection

algorithm for the unmanned vehicle, and the network is improved using the output of object detection as its input to accelerate the training process. With three experiments, putting the YOLO network before the input of DQN could greatly improve the training speed of the network. With the same set of 300-episodes experiments, DQN reaches its first apex reward after 130 episodes while the YOLO + DQN reaches its first apex only after 80 episodes. The YOLO + DQN also gains 30% more in average reward in the 300 episodes comparing with the DQN. It could be shown that one proper object detection could improve the average reward in the training of deep reinforcement learning algorithms in autonomous driving neural networks training.

Acknowledgements. This work are supported by the Chinese National Natural Science Foundation (No. 61773039), the Aeronautical Science Foundation of China (No. 2017ZDXX1043), and Aeronautical Science Foundation of China (No. 2018XXX).

References

1. Shende, V.: Analysis of research in consumer behavior of automobile passenger car customer. *Int. J. Sci. Res. Publ.* **4**(2), 1–8 (2014). <http://www.ijsrp.org/research-paper-0214/ijsrp-p2670.pdf>
2. Geiger, A., Lenz, P., Urtasun, R.: Are we ready for autonomous driving? the KITTI vision benchmark suite. In: *Proceedings of the IEEE Computer Society Conference on Computer Vision and Pattern Recognition 2012*, pp. 3354–3361 (2012). <https://doi.org/10.1109/CVPR.2012.6248074>
3. Paszke, A., et al.: PyTorch: an imperative style, high-performance deep learning library (2019). arXiv. <http://arxiv.org/abs/1912.01703>. Accessed 24 May 2021
4. CARSIM - Mechanical Simulation. <https://www.carsim.com/>. Accessed 07 Jun 2021
5. Li, Y.: Deep reinforcement learning: an overview (2017). <http://arxiv.org/abs/1701.07274>. Accessed 24 May 2021
6. Arulkumaran, K., Deisenroth, M.P., Brundage, M., Bharath, A.A.: Deep reinforcement learning: a brief survey. *IEEE Sig. Process. Mag.* **34**(6), 26–38 (2017). <https://doi.org/10.1109/MSP.2017.2743240>
7. Lv, L., Zhang, S., Ding, D., Wang, Y.: Path planning via an improved DQN-based learning policy. *IEEE Access* **7**, 67319–67330 (2019). <https://doi.org/10.1109/ACCESS.2019.2918703>
8. Zhang, Y., Li, K., Liu, J., et al.: Intelligent prediction method for updraft of UAV that is based on LSTM network. In: *IEEE Transactions on Cognitive and Developmental Systems*, 31 December 2020. <https://doi.org/10.1109/TCDS.2020.3048347>
9. Bakar, A., Ke, L., Liu, H.B., et al.: Design of low altitude long endurance solar-powered UAV using genetic algorithm. *Aerospace* **8**(8), 228 (2021)
10. Lillicrap, T.P., et al.: Continuous controlwith deep reinforcement learning (2016). <https://go.gi/J4PIAz>. Accessed 24 May 2021
11. Sewak, M.: Deep Q Network (DQN), Double DQN, and Dueling DQN. In: *Deep Reinforcement Learning*. Springer, Singapore, pp. 95–108 (2019). <https://doi.org/10.1007/978-981-13-8285-7>
12. Mnih, V., et al.: Human-level control through deep reinforcement learning. *Nature* **518**(7540), 529–533 (2015). <https://doi.org/10.1038/nature14236>

13. Carta, S., Ferreira, A., Podda, A.S., Recupero, D.R., Sanna, A.: Multi-DQN: an ensemble of deep Q-learning agents for stock market forecasting. *Expert Syst. Appl.* **164**, 113820 (2021). <https://doi.org/10.1016/j.eswa.2020.113820>
14. Gupta, L., Jain, R., Vaszkun, G.: Survey of important issues in UAV communication networks. *IEEE Commun. Surv. Tutorials* **18**(2), 1123–1152 (2016). <https://doi.org/10.1109/COMST.2015.2495297>
15. Tian, Y., Yang, G., Wang, Z., Wang, H., Li, E., Liang, Z.: Apple detection during different growth stages in orchards using the improved YOLO-V3 model. *Comput. Electron. Agric.* **157**, 417–426 (2019). <https://doi.org/10.1016/j.compag.2019.01.012>



Autonomous Vehicles Based on Gesture Recognition Control Using CNN and CPM Model

Xiulin Zhang^{1,2}, Chong Zhen¹, Quxiao Lei¹, Yifeng Wang¹, Jiaao Chen³, Weiyi Jin³,
Ke Li³(✉), and Lijing Wang³

¹ Avic Shenyang Aircraft Design and Research Institute, Shenyang, China

² Nanjing University of Aeronautics and Astronautics, Nanjing, China

³ School of Aeronautical Science and Engineering, Beihang University, Beijing, China

like@buaa.edu.cn

Abstract. In the autonomous motion control of unmanned equipment, in order to make the control more precise and efficient, in addition to the automatic operation of drones and unmanned vehicles, it is also necessary to introduce a certain amount of human-computer interaction. Therefore, in the control of unmanned equipment, it is very important to design a human-computer interaction program. In this paper, by analyzing the control requirements of unmanned equipment in specific cases and comparing with existing technologies, a gesture recognition program is established. The results show that it is feasible to control the movement of unmanned equipment through gesture recognition technology. Moreover, gesture control has the advantages of high accuracy, simplicity and efficiency, and can control multiple unmanned equipment in real time.

Keywords: Unmanned equipment control · Gesture recognition technology · Algorithm program · Verification on unmanned vehicle

1 Introduction

1.1 Introduction

Gesture detection is an old problem in the field of computer vision. Its purpose is to find the required target position in a given picture, and accurately mark the target through the box, that is, find the normalized coordinates of the upper left corner of the local gesture in the input image (a, b) and the normalized coordinates (c, d) of the lower right corner and output. There are many methods for traditional gesture detection algorithms. However, after the rise of deep learning, many gesture detection algorithms based on deep learning have surpassed traditional methods in all aspects and become the mainstream of the current academic world. Therefore, this article is based on deep learning methods. Gesture detection.

At present, the methods of gesture detection based on deep learning are mainly divided into two types based on candidate area + deep learning classification (two stage) and directly based on deep learning regression (one stage).

The potential detection result includes two aspects, one is the position of the gesture frame detected, and the other is the confidence of the detection. Therefore, the commonly used loss function is the weighted sum of model classification error and regression error:

$$L(x, c, l, g) = 1N L_{conf} \cdot c + \alpha L_{loc} x, l, g \tag{1.1}$$

$L(x, c, l, g)$ is the total loss function of the model, where c is the prediction confidence, l is the position of the prediction box, g is the position of the real box, α is the weight of the two, and N is the match to the object Number of preselected boxes.

The earliest gesture detection algorithm is implemented through a sliding window, which is a one-stage method. The execution step is to first classify the images in the taken window, and then use the non-maximum suppression (NMS) algorithm to extract the most suitable. The candidate frame is used as the final detection result. At the same time, in order to cope with the change of the target in the image scale, it is necessary to use multiple sliding windows of different sizes to identify sequentially. This method is computationally intensive and time-consuming.

Due to the many shortcomings of the sliding window model, a method of candidate region+deep learning classification appears. Among them, Girshick proposed the R-CNN algorithm framework in 2014 [1–5]. This framework is a two-stage framework. First, based on certain features of the image, such as texture, edge, color, etc., find the possible location of the target in the image, namely Candidate regions, and then identify and classify the candidate regions through the CNN structure. Compared with blind enumeration of sliding windows, this method reduces a lot of redundant calculations and maintains a higher recall rate under the premise of selecting fewer windows. The number of candidate regions can be determined according to the actual situation of the user. R-Extract 2000 candidate regions from each picture in CNN. In order to use the same classifier to classify the candidate regions, R-CNN adjusts the extracted candidate regions to the same resolution, then inputs all candidate regions to the pre-trained CNN for feature extraction, and finally inputs the extracted features to SVM classifier for classification. Figure 1 is a schematic diagram of the detection process of the R-CNN algorithm. Observation shows that the image after resolution adjustment will produce obvious deformation. At the same time, R-CNN separates the feature extraction part from the detection classification part, and the running speed is slow. The number of pre-selected regions in the classic R-CNN is defined as 2000. In actual use, it can be reset according to the actual situation of the user, including the complexity of the background and the lighting conditions.

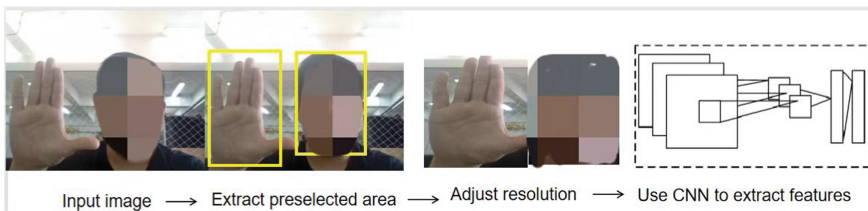


Fig. 1. Schematic diagram of R-CNN algorithm detection process

It can be seen from the above that R-CNN has two obvious shortcomings. First, the size of all the extracted candidate regions is adjusted, and the adjusted size has the same resolution. However, this deformation and stretching will limit the subsequent classifiers. Recognition accuracy, and convolution for each area separately, the speed is slow and the efficiency is too low. So later, He et al. proposed the Spatial Pyramid Pooling (SPP) algorithm in 2014, and designed a gesture detection network structure SPP-Net based on the SPP algorithm [6–9]. The framework guarantees different sizes of the SPP pooling layer. After the image is input to the network, the feature vector of uniform size can be obtained. Figure 2 shows the comparison of the detection process of SPP-net and R-CNN. The SPP pooling layer replaces the original convolutional pooling operation to normalize the original image. After the scaling operation is adjusted to the convolution pooling operation.

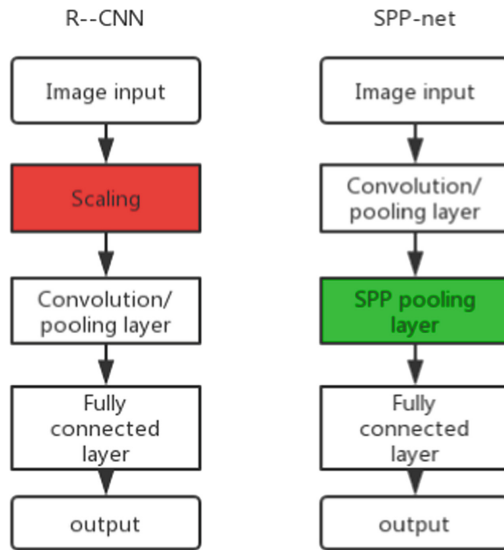


Fig. 2. Comparison of detection process between SPP-net and R-CNN

The design principle of the SPP pooling layer is shown in Fig. 3. This layer is usually added to the back of the CNN structure. At this time, the input size of the network can be arbitrary. Therefore, in the lower convolutional layer, the shape of the feature map extracted is arbitrary, and each frame is divided into 3 in the figure. Step pooling, the degree of pooling has nothing to do with the size and shape of the target window area. Set the output feature map dimension to d . In the pooling operation on the left, in order to obtain more detailed features, it is pooled with a size of $4 * 4$. After pooling, a one-dimensional feature with a size of $16 * d$ is obtained. Similarly, in the middle pooling area, a $2 * 2$ pooling operation is performed on it to obtain a one-dimensional feature vector with a size of $4 * d$, which is on the far right Perform a pooling of $1 * 1$ on the area of, and obtain a one-dimensional feature vector with dimension d . Therefore, a one-dimensional feature vector with a size of $21d$ will be output for feature maps of

different sizes. The SPP pooling layer adjusts the degree of pooling according to the size of the input feature map, and the final output feature vectors all have the same size.

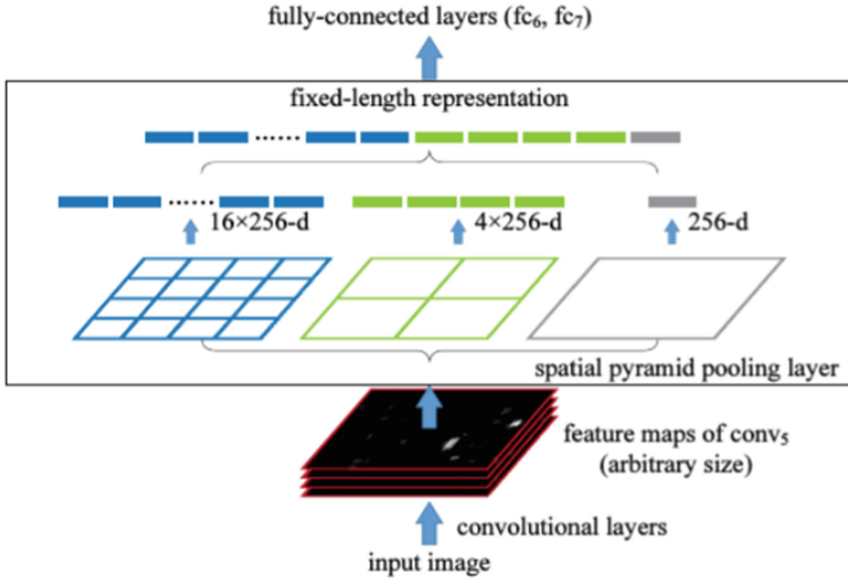


Fig. 3. SPP pooling principles

1.2 Gesture Key Point Positioning

The key point positioning technology is a technology to find the key points of the target object in the image and mark them. This technology is widely used in the field of computer vision and involves many subdivision fields. Common subdivision areas include gesture key point positioning, face key point detection, object key point detection and pose estimation. Among them, the commonly used loss function of the gesture key point positioning algorithm is the Euclidean loss function, that is, the Euclidean distance from the detected key point to the actual key point:

$$L_{i} = \|y_i - \hat{y}_i\|_2^2 \quad (2.1)$$

L_i is the loss value of the i -th key point, y_i is the coordinate of the detection key point i , \hat{y}_i is the actual coordinate of the key point i , and the Euclidean distance is the square of the L2 norm. The estimated loss for multiple key points is the arithmetic mean of the loss functions of all key points. The following formula is the loss function of N key points.

$$L = \frac{1}{N} \sum_{i=1}^N L_i \quad (2.2)$$

The CPM proposed by Shih-EnWe et al. in 2016 was an earlier model that combined artificial neural network and gesture key point positioning technology and achieved good

results [10–13]. The first model was used to solve the problem of single-person gesture recognition. The CPM input is a picture containing a single gesture, and the output is a response heat map of each joint point. CPM is a cascaded network structure. Figure 4 is a schematic diagram of a CPM network structure with three levels, each level predicts key points separately. At the same time, CPM is also an interactive network structure, and the prediction results of the previous level will provide auxiliary information for the prediction of the next level. This segmented response mechanism will output the confidence map corresponding to the prediction at each level, that is, the prediction result, and usually take the prediction result of the last level as the final result. Users can choose to use different levels of CPM network structure according to the actual situation. Generally, fewer levels have faster calculation speeds, but the detection accuracy of key points is poor; more levels have better detection accuracy, but the real-time performance of the model gets worse with the increase of levels.

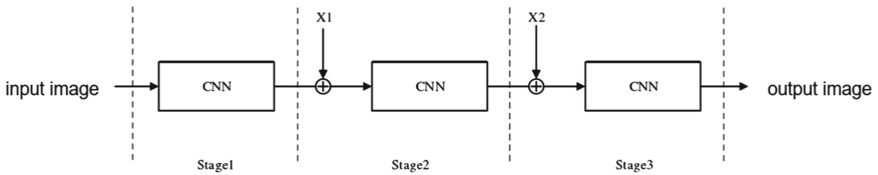


Fig. 4. Schematic diagram of CPM detection process

The CMU OpenPose framework developed by Carnegie Mellon University has good real-time performance and accuracy in the field of gesture recognition. It is the predecessor of the open source project OpenPose. The framework uses Part Affinity Fields (PAF) extraction technology to match gestures and key points, it can be used to recognize multiple gestures. Different from CPM, CMU OpenPose's key point positioning and key point association are realized through two different network structures. As shown in Fig. 5, CMU OpenPose first extracts the features of the input image, and then based on the feature map, through two network structures to extract the confidence map and partial affinity fields, and finally use the bipartite matching (Bipartite Matching, BM) technology to combine the key points of a hand. This method separates the key points and key point regions for solving, and finally links each key point. The accuracy of gesture key point positioning is higher than that of the CPM model.

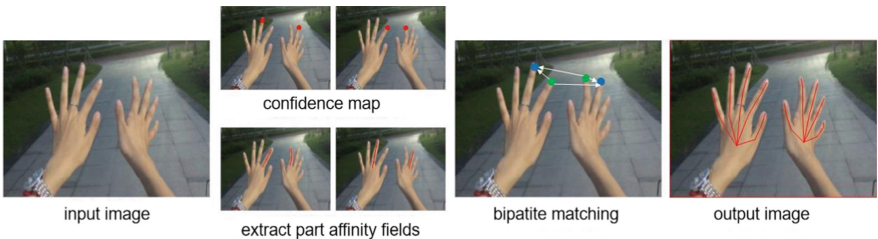


Fig. 5. Schematic diagram of CMU OpenPose

Eldar Insafutdinov et al. proposed the DeeperCut framework. Unlike the above framework that directly detects key points of gestures, DeeperCut first uses convolutional neural networks to extract hand candidate regions, no matter how many hands are in the picture, make each key point represents a joint, connect all joints two by two to form a dense map. As shown in Fig. 6, the weights of connections between nodes in a dense graph represent the degree of association between joint points. The framework then converts the key point location problem into an optimization problem, classifies all nodes, and the nodes belonging to the same hand are classified into one category. Finally, in detecting the same type of nodes, mark which part of the hand belongs to, and combine the classification result and the marking result to realize the gesture pose estimation. This method clearly divides the key point detection task into several steps: first, detect all the key points of gestures, and then optimize and classify the key points detected. This method has a good effect on detecting scenes with multiple gestures, but the real-time performance is also poor.

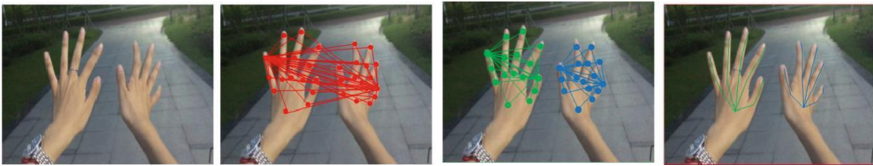


Fig. 6. Schematic diagram of deeper cut

The key point positioning algorithm for gestures based on deep learning is mainly implemented using the key point detection network structure. The performance comparison of the above network structure is shown in Table 1.

Table 1. Performance comparison of gesture key point positioning algorithms

Network structure	Real-time performance	Accuracy	Realize multi-gesture key point positioning
CPM	Good	Average	NO
CMU OpenPose	Average	Good	YES
Deeper cut	Bad	Good	YES

The hardware device models used in this article are shown in Table 2:

Table 2. Hardware environment

Device type	Device model
Algorithm test (laptop)	Lenovo Legion Y7000 2020
Raspberry pi	Raspberry pi 4B
Camera	Astra Pro

2 Conclusion

With the development of embedded devices, people's desire for human-computer interaction is becoming stronger and stronger. At the same time, research on human-computer interaction through gestures has become a hot spot in recent years. Therefore, this paper studies the vision-based gesture recognition system, which involves three parts: gesture detection, gesture key point positioning, and gesture classification. And finally the system is used in human-computer interaction to complete the unmanned vehicle control system based on gesture recognition.

The main content of this article is as follows:

First, introduced the basic concepts and development history of human-computer interaction, summarized different types of gesture recognition technology, and summarized several technologies based on visual gesture recognition.

Second, introduced three main part of hand gesture recognition: hand detection, hand key point extraction, gesture classification.

More, set up the gesture recognition and control algorithm, after successfully running on the computer platform, after debugging and modification, apply it on the Raspberry Pi platform of the unmanned vehicle.

Last, successfully output commands through gestures to control the basic movements of the unmanned vehicle.

Acknowledgements. This work are supported by the Chinese National Natural Science Foundation (No. 61773039), the Aeronautical Science Foundation of China (No. 2017ZDXX1043) ,and Aeronautical Science Foundation of China (No. 2018XXX).

References

1. Basilio, J.A.M., Torres, G.A., Pérez, G.S., et al.: Explicit image detection using YCbCr space color model as skin detection. In: Proceedings of the American Conference on Applied Mathematics and the 5th WSEAS International Conference on Computer Engineering and Applications. ACM Press, New York, pp. 123–128 (2011)
2. Bourke, A., O'Brien, J., Lyons, G.: Evaluation of a threshold-based tri-axial accelerometer fall detection algorithm. *Gait Posture* **26**(2), 194–199 (2007)
3. Bretzner, L., Laptev, I., Lindeberg, T.: Hand gesture recognition using multi-scale colour features, hierarchical models and particle filtering. In: Fifth IEEE International Conference on Automatic Face and Gesture Recognition, pp. 405–410 (2002)

4. Cote, M., Payeur, P., Comeau, G.: Comparative study of adaptive segmentation techniques for gesture analysis in unconstrained environments. In: IEEE International Workshop on Imagining Systems and Techniques, pp. 28–33 (2006)
5. Zhang, Y., Li, K., Li, K., Liu, J., et al.: Intelligent prediction method for updraft of UAV that is based on LSTM network. *IEEE Trans. Cogn. Develop. Syst.* (2020)
6. Haria, A., Subramanian, A., Asokkumar, N., et al.: Hand gesture recognition for human computer interaction. *Procedia Comput. Sci.* **115**, 367–374 (2017)
7. Kevin, N.Y.Y., Ranganath, S., Ghosh, D.: Trajectory modeling in gesture recognition using cybergloves and magnetic trackers. *IEEE TENCON* **10**, 571–574 (2004)
8. Bakar, A., Ke, L*, Liu, H.B., et al.: Multi-objective optimization of low Reynolds number Airfoil using convolutional Neural Network and non-dominated sorting genetic algorithm. *Aerospace* **9**(1), 35 (2022)
9. Li, T., Qin, Q., Chen, Z.: Interaction method based on visual gesture recognition. In: Second Target Recognition and Artificial Intelligence Summit Forum. International Society for Optics and Photonics, vol. 11427:114273C (2020)
10. Moin, A., Zhou, A., Rahimi, A., et al.: A wearable biosensing system with in-sensor adaptive machine learning for hand gesture recognition. *Nature Electron.* **4**(1), 54–63 (2021)
11. Rautaray, S., Agrawal, A.: Vision based hand gesture recognition for human computer interaction: a survey. *Artif. Intell. Rev.* **43**(1), 1–54 (2012). <https://doi.org/10.1007/s10462-012-9356-9>
12. Soriano, M., Martinkauppi, B., Huovinen, S., et al.: Skin detection in video under changing illumination conditions. In: Proceedings of the 15th International Conference on Pattern Recognition. IEEE Computer Society Press, Los Alamitos, vol. 1, pp. 839–842 (2000)
13. Turk, M., Athitsos, V.: Gesture recognition. *Comput. Vis. Ref. Guide* 1–6 (2020)



Research on Simulation Model System Integration and Interconnection Methods

Yan Hao^(✉), Jun Zhen, Ying Qu, and YaFei Zhang

System Engineering Research Institute of China State Shipbuilding Corporation,
Beijing 100036, China
282079961@qq.com

Abstract. Aiming at the application requirements of comprehensive integration of multi-source heterogeneous simulation resources in the construction of equipment system, the research on model integration and heterogeneous simulation system interconnection technology is carried out, the design ideas and technical approaches of the integration framework are proposed, and the application development toolset is developed to support the mixed assemblable and transparent interoperability of heterogeneous external simulation resources. Achieve consistent expression, unified management, hybrid assembly, and joint operation of heterogeneous resource integration.

Keywords: Heterogeneous integration · External simulation resources · Simulation model reuse

1 Introduction

Analyzing the main technical problem in the process of heterogeneous system interconnection integration, This article takes an object-oriented middleware and service-oriented architecture design approach. Heterogeneous external simulation systems, simulation models, and physical/semi-physical simulation models are all regards as external simulation resources. Before the simulation begins, classify it and register it and declare it as a simulation instance. When the registration statement is successful, it becomes a digital simulation resource of the simulation system, so that pure digital simulation and hybrid simulation can be unified in a consistent process, realizing the mixed assembly and transparent operation of heterogeneous simulation resources.

2 Research Methodology

2.1 Requirements Analysis

With the deepening application of modeling and simulation in many fields such as design verification, performance evaluation, program deduction, simulation training, etc., various disciplines and fields adopt different modeling methods, development tools

and simulation architectures according to their own business needs, resulting in a large number of heterogeneous simulation systems. Breaking through the barriers between simulation systems in different fields, different levels and different uses, comprehensively integrating infrastructure resources such as trial training bases, laboratories, and equipment simulation laboratories, continuously strengthening the interconnection and interoperability of different simulation systems, simulation systems, and command and control systems, and striving to build a comprehensive and integrated joint simulation environment is an important way to improve and give play to the efficiency of simulation system and resource construction.

2.2 Main Issues

Heterogeneous systems are interconnected and interoperable, giving full play to their respective functions and design advantages, and collaborative simulation, which is a natural requirement, but for different systems, their openness and standardization degree are different, and there may be problems in interconnection, interoperability, and interoperability between each other, such as openness and protocol consistency, which are reversed according to the severity [1].

- (1) There is no interconnect design when designing the object system. The system itself was not designed with the problem of co-computation simulation with other systems in mind, and was simulated independently using only interface input and only data files as input initial conditions.
- (2) The underlying network protocol is inconsistent, resulting in the inability to interconnect. For distributed simulation systems, each simulation node may run in different operating systems, may use different network communication protocols, and may even be just different configurations of network communication protocols, which may cause the most basic requirements of interconnection
- (3) Different syntax definitions make the data unable to communicate with each other. Due to the different data schemas, data types, and data structures, and different serialization methods, the data transmitted between inter-chained systems cannot be received or understood by each other.
- (4) The semantic definition is not clear, so that the data cannot be understood. The two systems that communicate with each other are able to acquire and parse communication data, but lack further understanding of semantics. In object-oriented system design, there is a lack of public object descriptions, and data objects cannot be constructed from the acquired data.
- (5) There is no pragmatic consensus that makes collaborative computation impossible. Interoperable heterogeneous systems can understand data and synchronize the state of remote objects, but lack consensus on information processing rules.

3 Findings

3.1 Model Library Organizational Structure (OA)

In response to the problems and needs of tool fragmentation, model reuse and intellectual property protection, the European Simulation Conference proposed the FMI [2] standard,

the full name of the FMI standard is The Functionary Mock-up Interface, which is a tool-independent standard that supports both model exchange and co-simulation of dynamic models through XML files and compiled C code combinations.

To support the service-oriented architecture, each simulation model can be considered a class of computing services, implemented by an interface FMU package that references the FMI standard, and each FMU package contains XML files that describe the model interface information and data, compiled binaries that implement the functions of the model computing service, and other necessary reference libraries or data files. The binaries in the FMU are compiled into DLL dynamic link libraries for the simulation model, and can also be regarded as a functional plug-in for the model service framework provided by the model running service software, loaded by the model service framework during runtime and instantiated according to the imaginary data for time-driven, event-excited, or direct function calls. XML files in FMU are used to support the resource manager or custom editor to generate model parameter settings during the resource configuration period or the custom editing period (Fig. 1).

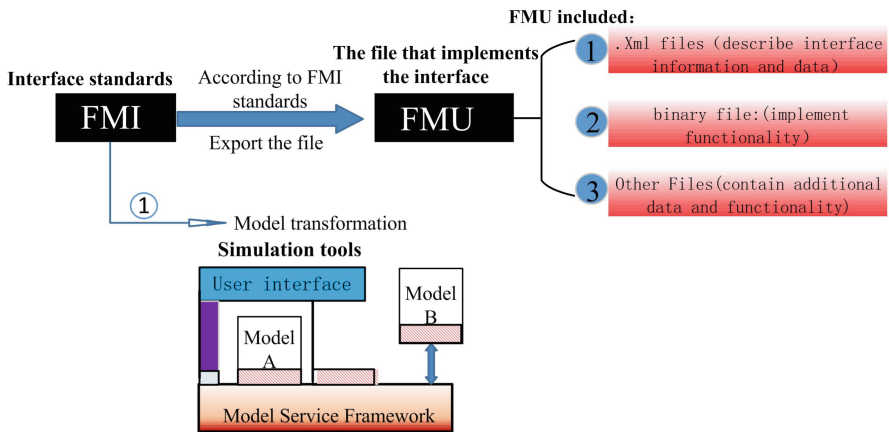


Fig. 1. Reference FMI architecture for the model library organization form

3.2 Encapsulation, Registration and Operation of Generalized, Heterogeneous Models

Hybrid assembly and joint operation of heterogeneous models are problems that must be solved by distributed simulation, and also an important indicator to test the openness and compatibility of the model library architecture. The FMI standard not only provides model exchange capabilities between homogeneous models, but also provides three co-simulation modes, which can complete the registration and joint application of heterogeneous models in the model library.

Generally speaking, heterogeneous simulation resource integration [3] can adopt different integration modes such as model wrapping, proxy mapping, and peer gateway according to the resource form and degree of openness.

(1) Model wrapping

Model wrapping refers to the development of a model to call the participating model, which is equivalent to adding a “shell” to the participating model that meets the requirements of the simulation platform interface. When the participating model provides a well-defined functional function interface that is not related to the simulation platform, or even directly gives the interface code that calls the model, and these models do not have independent time management, but give functional functions, so that any platform can use its own calling framework to call these business interfaces, encapsulate a “shell” model for these models, register the “shell” model, and these business computing models are published together with the “shell” model as additional resources of the “shell” model, and are associated and loaded into the same simulation process. This mode is equivalent to the joint simulation mode of “code export” under the FMI standard (Fig. 2).

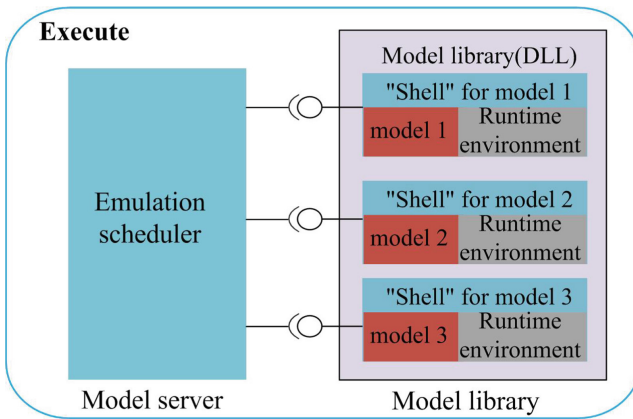


Fig. 2. Model wrapping pattern

(2) Proxy mapping

Proxy object mapping is when the connected model is a standalone application, or even a set of physical/semi-physical devices, at which time an interface adapter composed of modules such as proxy objects, control management and synchronization, data acquisition and conversion is developed. The proxy object is a model corresponding to the participating model function in the simulation platform model system, on the one hand, it maps the state of the participating model in real time, and on the other hand, it interacts with other models in the platform based on the standard interface of the simulation platform. The Control Management and Synchronization Module is responsible for combining the participating models and simulation engines to coordinate time synchronization and control. On the one hand, the data acquisition and conversion module receives the status, response and interaction of the acquisition and participation model, converts it into the standard interactive format of the platform, submits the simulation

system through the proxy object, and on the other hand, receives the interactive information provided by the proxy object, and converts it according to the protocol interface of the participating model itself.

In this mode, it is equivalent to the “tool coupling” joint simulation mode under the FMI standard (Fig. 3).

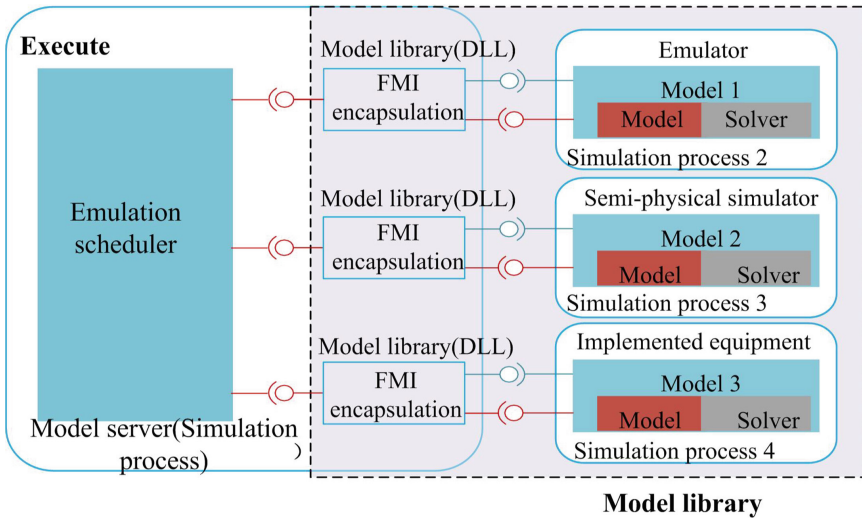


Fig. 3. How the proxy mapping pattern works

(3) Proxy gateway [4]

Both the model package and the agent mapping mode are to connect the simulation model and the physical/semi-physical device as a model to the specified simulation system, while the peer-to-peer gateway is often used for the equal interconnection of the two simulation systems, each system has its own model system, and has its own time promotion mechanism. In the peer-to-peer gateway mode, it is necessary to design an Internet gateway that connects multiple simulation systems, and construct an intermediate model in each simulation system, and there is a proxy model for each intermediate model in the Internet gateway. The data of each system is collected from the intermediate model subscription and sent to its own proxy model, and the agent model passes the data to the proxy model of the intermediate model of other systems, converts the data format, and passes it to other systems through the intermediate model. Time synchronization between systems is coordinated between agent models.

At runtime, the models in the two platforms only interact through the gateway and do not need to dynamically access each other’s objects; however, when you want to edit, the simulation model in the integration platform needs to be unified edited by the simulation model in the integration platform as a force template. Therefore, it is necessary to register the simulation model in the integrated platform into the integration

platform in accordance with the standards unified with the integration platform, so that the integration platform can refer to the simulation model in the integrated platform in the model library as a force template for force generation and deployment in the imagination (Fig. 4).

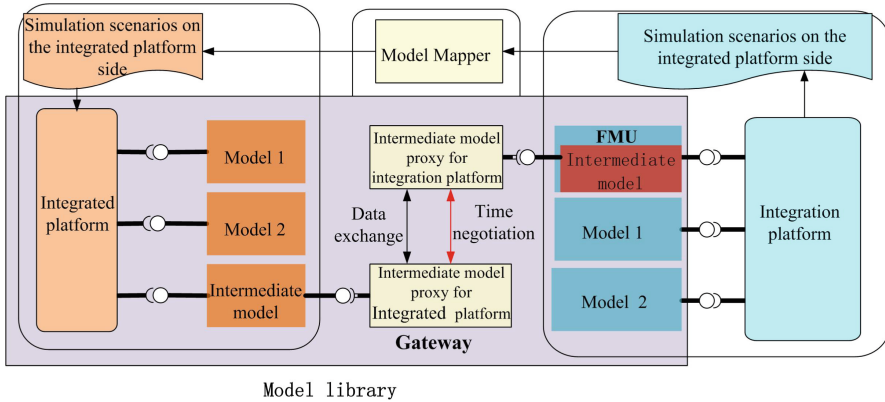


Fig. 4. The composition principle of the peer gateway

4 Conclusions of the Study

The model construction and integration standard proposed by this technology requires the external simulation model to be extended in the form of components and parameters, and supported by the external heterogeneous system access toolset. The integrated development of heterogeneous external resources follows the idea of hierarchical, modular and lightweight, decomposes the equipment according to the actual equipment composition, builds the functional components of each type of equipment based on component technology, and generates a model component library. When modeling equipment, different performance parameters are bound to each functional component, and the specific model of equipment is constructed by reconstruction, and simulation and evaluation are carried out. The component-based equipment modeling method can quickly generate equipment models and prototype systems, and users can reconstruct the equipment physical model according to the needs of the project, ensuring the portability, scalability and rapid efficiency of simulation model development.

5 Application Orientation

The reuse and combination of simulation resources, especially existing simulation models and simulation systems, is a comprehensive theoretical topic facing the field of modeling and simulation of large complex systems today. Combined with the reuse

and integration requirements of multi-source heterogeneous simulation resources in the construction of equipment system, this paper conducts an in-depth study on the integration technology of heterogeneous external resources based on standardized model specifications, which has certain theoretical and practical guiding significance for the construction of equipment system. In theory, the research of this technology belongs to the basic research of modeling and simulation methodology, and has a certain role in promoting the current combinatorial modeling simulation theory. In practice, the heterogeneous model integration technology proposed in this paper can be used to guide and support the system integration and model reuse in the overall design field of system research.

Acknowledgements. This work is supported by the: Hainan Province Major Science and Technology Program Grant (ZDKJ2019003).

References

1. Zhang, Y., Zhang, M., Hu, X.: A review of multi-system interconnection technology for LVC training, *J. Syst. Simul.* **25**(11) (2013)
2. Wang, H., Lian, D., Xu, J.: Research on distributed joint simulation technology based on FMI, *Comput. Simul.* **34**(4) (2017)
3. Lei, Y.: Simulation Model Reuse Theory, Method and Heterogeneous Integration Technology Research, Ph.D., National University of Defense Technology (2006)
4. Yao, Y.: Design of scalable software gateway architecture based on object model, M.S. thesis, South China University of Technology (2012)



Detection of VOCs in *E. Coli* Based on Gas Chromatography-Mass Spectrometry

Handong Yao¹, Shuang Nie², Shuxin Du¹, Qianqian Ni², Xun Liu²,
and Fengfeng Mo²(✉)

¹ School of Engineering, Huzhou University, Huzhou 313000, China

² Department of Naval Nutrition and Food Hygiene, Naval Medical University,
Shanghai 200433, China
edsenone@hotmail.com

Abstract. *Escherichia coli* (*E. coli*) is a common bacteria that belongs to the family Enterobacteriaceae, which is a ubiquitous microorganism in the environment and human intestinal tract. *E. coli* is one of the common foodborne pathogens which is a highly diverse species that include numerous types and strains with distinctive characteristics. Many methods are used to detect *E. coli* at present. Volatile Organic Compounds (VOCs) are all kinds of organic compounds with boiling points ranging from 50 °C to 260 °C at room temperature. Solid-phase Microextraction (SPME) and gas chromatography-mass spectrometry (GC-MS) are the main methods to detect VOCs at present. In this paper, we firstly evaluated the relationship between culture days and activity of three different *E. coli* strains in the early stage and verified optimal incubation time of the strains for VOCs analysis. Then, we studied VOCs products of *E. coli*, *E. coli* BL21 (*Escherichia coli* BL21) and Extraintestinal Pathogenic *Escherichia coli* (ExPEC) under extraction conditions of 37 °C and 80 °C respectively, and screened out several iconic VOCs, which provided a theoretical basis for further detection.

Keywords: *E. coli* · Volatile Organic Compounds (VOCs) · Gas chromatography-mass spectrometry (GC-MS) · Solid-phase Microextraction (SPME)

1 Introduction

Food is the most basic need for human survival, and the issue of food safety caused by foodborne diseases is one of the most prominent public health problems worldwide. As we all know, *Escherichia coli* (*E. coli*), a normal flora bacterium in the intestines of humans and animal, is a conditional pathogen that normally does not cause disease. However, pathogenic *E. coli* can cause gastrointestinal infections, gastrointestinal infections, urinary tract infections, arthritis, meningitis, and septic infections in humans or animals [1]. Therefore, it is urgent to develop a more convenient and safer detection methods to improve the efficiency and safety of detection.

In China, Volatile Organic Compounds (VOCs) refers to organic compounds with saturated vapor pressure greater than 70 Pa and boiling point below 260 °C at normal

temperature, or a vapor pressure greater than or equal to 10 Pa at 20 °C. *E. coli* in liquid medium of Luria-Bertani (LB) or gravy can decompose lactose to produce a certain number of VOCs. Harish Devaraj extracted, identified, and quantized VOCs in the headspace culture of *E. coli* by analysing the VOCs with high content [2]. Ratiu directly detected headspace samples above a series of *in vitro* bacterial cultures by inhalation ion migration spectrometer, and analysed the fingerprints of *E. coli*, *Bacillus subtilis* and *Staphylococcus aureus* (*S. aureus*), and identified the three bacteria to a certain extent through specific VOCs [3]. Therefore, detecting *E. coli* by the VOCs is expected to develop into a more reliable and safe detection technique.

Gas chromatography-mass spectrometry (GC-MS) can be used for quantitative analysis of some complex compounds and is suitable for the separation and identification of low molecular weight (about 50–600 Da) volatile compounds [4]. Solid-phase microextraction (SPME) technology is a pre-treatment technology that uses quartz or carbon fiber to enrich and extract samples. Buszewski combined SPME and GC-MS techniques to screen the characteristic VOCs of *E. coli* at 37 °C [5]. Fitzgerald also investigated VOCs products of *S. aureus* and *E. coli* strains by SPME coupled with GC-MS technology at 37 °C [6]. However, none of these studies have verified whether microbes can produce sufficient and reliable products under the extraction condition of 37 °C.

In this work, based on the stable activity of *E. coli*, *E. coli* BL21 and Extraintestinal Pathogenic *Escherichia coli* (ExPEC), we evaluated the relationship between the early culture days and activity of the three strains of *E. coli*, and determined the best culture time for VOCs analysis. After that, the VOCs products of the three strains were enriched under the extraction conditions of 37 °C and 80 °C, respectively. These VOCs were analyzed and detected by GC-MS, and several marker VOCs were selected to provide a theoretical basis for further detection.

2 Materials and Methods

2.1 Materials and Instruments

1XPBS, LB Broth Medium, Solid Phase Microextraction needle (50 µm CAR/PDMS) Supelco USA, Bacterial viability assay CCK-8 (BestBio).

2.2 Sample Processing

Bacterial strains	
<i>E. coli</i>	CCTCC AB 93154
<i>E. coli</i> BL21	CCTCC AB 204033
ExPEC	CCTCC AB 2013345

All the above strains purchased from China Center for Type Culture Collection.

Sample preparation: *E. coli*, *E. coli* BL21 and ExPEC with stable bacterial activity were taken, and their absorbance was tested under OD₆₀₀, and the unified bacterial

solution concentration was 10^9 cfu/mL. After that, the three bacterial strains were assessed by GC-MS. The experimental group was divided into two groups with extraction temperature of 37 °C and 80 °C, which were used to compare VOCs output under environmental temperature and heating conditions. Three parallel sets were set for each group.

2.3 Detection Method

2.3.1 Bacterial Activity Detection

Before the preparation of test samples, in order to determine the stable growth time of the three strains of *E. coli* and ensure the stable VOCs output of the bacteria, the relationship between the activity and culture days of the bacteria were tested first. After gradient dilution, the three strains of *E. coli* were spread in LB plate medium with 100 μ L inoculation and incubated in 37 °C constant temperatures incubators for 24 h. Then 3–5 colonies were selected and inoculated in 5 mL LB liquid medium and placed in 37 °C constant temperature incubators. The concentration of bacterial solution was measured and recorded every 24 h. Then selected 190 μ L of bacterial liquid cultured for day 1 to day 6, next added 10 μ L of CCK-8, and incubated in a shaker at 37 °C and 70 rpm for 30 min. Then, the absorbance at OD₄₅₀ from day 1 to day 6 was measured in a microplate tester. The higher the OD value, the higher the bacterial activity.

2.3.2 GS-MS Analysers

The two groups of samples to be tested were extracted at the set temperature of 37 °C and 80 °C for 35 min, respectively.

Chromatographic column: DB-624 capillary column (60 m*0.25 mm ID*1.40 μ m).

Heating procedure: injector temperature: 250 °C. Split ratio 50:1, injection volume: 100 μ L. Carrier gas and flow rate: helium, 1 ml/min. Heating procedure: keep at 50 °C for 3 min, then increase to 160 °C at a rate of 5 °C/min, and then increase to 250 °C at a rate of 13 °C/min.

Ms conditions: EI ion source temperature: 230 °C. Transmission line temperature: 250 °C. Electron energy 70 eV. Full Scan mode, scan range: m/z: 40–500, scan speed: 2 times/second. Solvent delay: 1.5 min.

3 Results and Discussion

3.1 Relationship Between Culture Days and Activity of the Three *E. Coli* Strains

This experiment results can be seen that the relationship between the culture days and the activity of the three strains is as follows: the trend was more consistent for *E. coli* and *E. coli* BL21, with the bacterial activity gradually increasing from the first day and continuing to increase with the increase in incubation time and reaching the highest activity on the fourth day. Unlike the trend of *E. coli* and *E. coli* BL21 activity, ExPEC bacterial activity reached its highest on the second day and then gradually decreased with increasing incubation time. Although the bacterial activity of ExPEC showed a

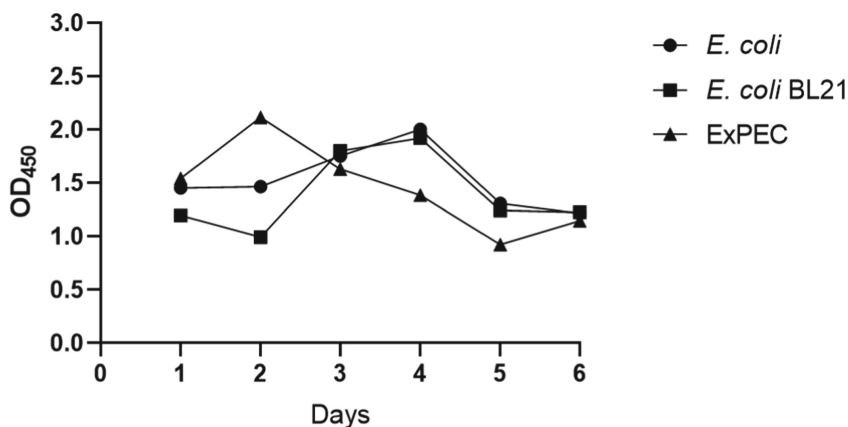


Fig. 1. Relationship between culture days and activity of the three *E. coli* strains

decreasing trend on the fourth day, the difference in OD₄₅₀ with the other two strains was within 0.5. Therefore, in order to ensure the best stability of the experiment, we selected the strains cultured for four days for subsequent GC-MS analysis (Fig. 1).

3.2 VOCs Product Analysis of Three Strains of *E. Coli*

VOCs products of blank group (pure LB medium), *E. coli*, *E. coli* BL21 and ExPEC were obtained by solid-phase extraction and GC-MS analysis. We first compared the VOCs products of the three strains with the blank group and screened out the products of these strains, then we compared the differences in the content of VOCs products between the three strains. The specific VOCs products at 37 °C and 80 °C are shown in Table 1 and Table 2 below:

Table 1. *E. coli* BL21, ExPEC and *E. coli* differential VOCs products at 37 °C

Bacterial strains	Component name	Retention time	Reference m/z	Avg score	Avg TIC	Formula (mol. ion)
<i>E. coli</i> BL21	Hydroxyurea	5.777	43.98	47.1	35634135	CH ₄ N ₂ O ₂
	Propanal, 2-methyl-	10.488	43.02	93.1	18809039	C ₄ H ₈ O
	Butanal, 3-methyl-	14.521	41.04	93.9	622112032	C ₅ H ₁₀ O
	Butanal, 2-methyl-	14.841	41.04	86.6	109505629	C ₅ H ₁₀ O
	2,3-Pentanedione	16.229	43.03	85.3	38214227	C ₅ H ₈ O ₂
	Octanal	28.453	56.07	81.8	6958126	C ₈ H ₁₆ O
ExPEC	1-Butanol, 3-methyl-	18.351	70.08	95.6	1914184378	C ₅ H ₁₂ O
	Furan, 2-(1,1-dimethylethyl)-4-methyl-	24.014	123.05	16.1	8804567	C ₉ H ₁₄ O
<i>E. coli</i>	Ethanol	7.559	45	93.8	1194177720	C ₂ H ₆ O

Table 2. *E. coli* BL21, ExPEC and *E. coli* differential VOCs products at 80 °C

Bacterial strains	Component name	Retention time	Reference m/z	Avg score	Avg TIC	Formula (mol. ion)
<i>E. coli</i> BL21	Propanal	8.311	58.05	90.6	12011436	C3H6O
	1-Propen-1-ol	10.862	57.03	96.1	227715861	C3H6O
	Butanal, 3-methyl-	14.521	41.04	93.9	622112032	C5H10O
	Butanal, 2-methyl-	14.841	41.04	86.6	109505629	C5H10O
	2,3-Pentanedione	16.229	43.03	85.3	38214227	C5H8O2
	meso-3,4-Hexanediol	21.793	59.06	80.4	5748710	C6H14O2
	Butane, 2,2,3,3-tetramethyl-	22.011	57.06	33.1	2502035	C8H18
	Pyridine, 3-methyl-	23.555	93.01	92.2	46144470	C6H7N
ExPEC	4-Pentanol, 3-ethyl-	27.65	87.07	61.5	14657184	C7H16O
	1-Butanol, 3-methyl-	18.351	70.08	95.6	1914184378	C5H12O
	1-Butanol, 2-methyl-, (S)-	18.463	41.06	86.8	196429902	C5H12O
<i>E. coli</i>	Cyclohexanone	25.479	55.02	92.8	89564871	C6H10O
	Ethanol	7.559	45	93.8	1194177720	C2H6O
	1-Octanol	30.343	56.08	96.3	307394402	C8H18O

According to the results, at two different extraction temperatures, the differential VOCs of *E. coli* BL21 are aldehydes, while *E. coli* are alcohols. In addition, at the extraction temperature of 37 °C, *E. coli* BL21, ExPEC, *E. coli* are less than those under extraction condition of 80 °C. It can be seen that the higher the extraction temperature, the more conducive the strain to produce the corresponding VOCs.

In addition, VOCs produced by the three strains were compared under extraction conditions at 37 °C and 80 °C as the Table 3 below:

Table 3. Differential VOCs shared by the *E. coli* BL21, ExPEC and *E. coli* at 37 °C and 80 °C

Bacterial strains	Component name	Retention time	Reference m/z	Avg score	Avg TIC	Formula (mol. ion)
<i>E. coli</i> BL21	Butanal, 3-methyl-	14.521	41.04	93.9	622112032	C5H10O
	Butanal, 2-methyl-	14.841	41.04	86.6	109505629	C5H10O
	2,3-Pentanedione	16.229	43.03	85.3	38214227	C5H8O2

(continued)

Table 3. (continued)

Bacterial strains	Component name	Retention time	Reference m/z	Avg score	Avg TIC	Formula (mol. ion)
ExPEC	1-Butanol, 3-methyl-	18.463	41.06	86.8	196429902	C5H12O
<i>E. coli</i>	Ethanol	7.559	45	93.8	1194177720	C2H6O

For these substances, due to the comparison of products at two extraction temperatures and the experimental results based on three parallel samples, they have high reliability as differential VOCs corresponding to these strains.

4 Conclusion

In this study, using the characteristic that microorganisms produce VOCs, we can identify and analyze microorganisms by detecting the differential VOCs produced by microorganisms. We selected the most suitable incubation time after verifying the relationship between incubation time and the activity of *E. coli*, *E. coli* 21 and ExPEC. The VOCs produced by the strains were enriched by SPME method at the time point of highest activity of the strains, and then the collected VOCs were identified and analyzed by GC-MS technique. We compared the various differential VOCs produced by different strains at the same temperature. In addition, we also summarized the common VOCs produced by each of the three strains at different incubation temperatures, and there were three common products of *E. coli* BL21, ExPEC and *E. coli* each had one product in common. This conclusion shows a good reliability of these overlapping products.

In conclusion, it is a very promising method to be able to achieve microbial identification analysis by detecting differential VOC of microorganisms. However, there are difficulties in the practical application of this method, for example, the concentration requirements of bacterial solution in complex environments and the culture environment cannot be fully guaranteed. In the next work, in addition to increasing the stability of VOCs produced, we will further analyse VOCs products of *E. coli* under the actual complex samples, laying a foundation for the practical detection technologies in the future.

Acknowledgements. This work is supported by the Military Biosafety Research Project (grant number: A3702022004). Handong Yao and Shuang Nie contributed equally to this work.

References

1. Shao, Z.: Research progress of *Escherichia coli*. *Cult. Feed* **20**(8) (2021)
2. Devaraj, H., et al.: Profiling of headspace volatiles from *E. coli* cultures using silicone-based sorptive media and thermal desorption GC-MS. *J. Sep. Sci.* **41**(22), 4133–4141 (2018)

3. Ratiu, I.A., et al.: Discrimination of bacteria by rapid sensing their metabolic volatiles using an aspiration-type ion mobility spectrometer (a-IMS) and gas chromatography-mass spectrometry GC-MS. *Anal .Chim. Acta.* **982**, 209–217 (2017)
4. Beale, D.J., et al.: Review of recent developments in GC–MS approaches to metabolomics-based research. *Metabolomics* **14**(11), 1–31 (2018). <https://doi.org/10.1007/s11306-018-1449-2>
5. Buszewski, B., et al.: The effect of biosilver nanoparticles on different bacterial strains' metabolism reflected in their VOCs profiles. *J. Breath Res.* **12**(2), 027105 (2018)
6. Fitzgerald, S., Holland, L., Morrin, A.: An investigation of stviability and species and strain-level specificity in bacterial volatilomes. *Front. Microbiol.* **12**, 693075 (2021)



Design Suggestion of Epidemic Prevention System for Shared Car Based on Scenario and Data

Zhouce Huang and Quan Yuan^(✉)

State Key Laboratory of Automotive Safety and Energy, School of Vehicle and Mobility,
Tsinghua University, Beijing 100084, China
yuanq@tsinghua.edu.cn

Abstract. Entering the post-epidemic era, the travel demand for shared cars is increasing day by day. In the normalized epidemic prevention and control, epidemic prevention in shared cars needs to be designed systematically. This paper analyzes the existing risk of COVID-19 propagation based on two perspectives: scenario and data, and discusses the existing means of protection. Then based on the existing measures, the design suggestions are given from two aspects: scenario-based and data-based. Based on the scenario, the layout design and disinfection is implemented in regard to various ways that COVID-19 is transmitted; based on data, travel data integration should be promoted to achieve macro-structural dynamic adjustment and integrated governance from the overall transportation system. In the context of the industries, the shared car industry should response to new trend immediately and implement innovative ideas to obtain a service that is better suited for individuals in the post-epidemic era. In the end, several major functions of design in terms of developing the urban transportation system are discussed.

Keywords: COVID-19 · Shared cars · Epidemic prevention system · Scenario and data · Urban transportation

1 Introduction

The sudden outbreak of COVID-19 caused the strict restriction on people's traffic. People are gradually resuming to travel in post-epidemic era, but urban transportation must be reflected and reformed accordingly in the face of small-scale epidemic outbreak. As the forefront of post-epidemic work resumption, traffic system shall demonstrate timely response speed and operation capacity to meet the requirements of complex and massive transportation during the resumption of work and production and epidemic control. The epidemic has not only touched the dead zone of original mechanism, but also promoted mechanism reform in time. In the post-epidemic era, it is necessary to use the reform period, combine with the development trend of urban transportation and the disadvantages from the epidemic response, actively reflect to improve the system,

promote the system and growth of the city, improve the effective supply, and enhance industry tenacity.

As an important role in urban transportation, shared cars (taxi, online ride-hailing, time-sharing rental) also play an important role in epidemic prevention. Prevention and control of the epidemic require drivers and passengers to take personal precautions for COVID-19, and require the targeted system design for shared cars.

XIAO W et al. [1], as well as SHEN J et al. [2] have analyzed the risks of COVID-19 transmission in traffic scenes. JIANG N et al. [3], as well as Bucsky P [4] have analyzed the crowd traffic behaviors of China and Budapest during the outbreak. Based on MNL regression model, ZOU S [5] has explored the effect factors of crowd travel modes. GAO Y et al. [6] have analyzed the changes in online car-hailing during the outbreak and put forward suggestions. Tirachini A [7] has analyzed the epidemic risk in public transport and put forward suggestions to reduce the risk of transmission. Based on SEIR model, CHEN J [8] has analyzed the spread of COVID-19 and put forward the coping strategy for online car-hailing. In view of traffic system, YAO J et al. [9] have put forward management strategies on regular epidemic prevention and control in railway passenger transport. LI M [10] has analyzed the development of urban transportation in the post-epidemic era, and putting forward suggestions to adjust the structure of urban transportation system and enhance industry tenacity. LI Y et al. [11] have analyzed the tenacity of urban transportation system, and put forward promotion strategies.

The research results of the above scholars have important reference significance on virus prevention and epidemic prevention of shared cars. Based on the scenario and data, and combined with epidemic prevention in the work scenario of shared cars and the epidemic prevention and control strategies based on travel data and epidemic risks, this paper has put forward design suggestion for epidemic prevention system of shared cars.

2 Analysis on Scenario-Based Epidemic Prevention

A working scenario of shared cars is a system consisting of man-machine- environment in the interaction process of shared cars. Taking online car-hailing as an example, the system consisting of driver, passenger, car and environment is analyzed in the process from the driver's order receiving and receiving passenger to letting of passenger. It is aimed at reducing the transmission of COVID-19 and the risk of infection in drivers and passengers based on the epidemic prevention of scenarios.

2.1 COVID-19 Transmission Routes in the Working Scenarios of Shared Cars

The main transmission routes of COVID-19 are droplet and contact transmission, and aerosol transmission can also happen in a relatively closed environment [12]. For the current working scenarios of shared cars, common transmission methods include: (1) Close contact between passengers and drivers, cough, sneeze, inhalation of respiratory droplets, resulting in droplets transmission. (2) The contamination of internal and external car surfaces and objects infected by persons during getting on or off the car becomes the transmission media, resulting in contact transmission. (3) For staying in a car for a long time, aerosol transmission may happen [1].

2.2 Current Scenario-Based Prevention Methods

The methods on COVID-19 prevention can also be classified by the transmission route of the epidemic.

For the prevention of droplet transmission, individuals shall wear masks, gloves and protection clothing; for vehicles and environment, common protection methods are to isolate in space and pay attention to ventilation. Where a driver isn't physically separated from a passenger, the passenger shall be forced to get on the car from the rear door in order to avoid contact between driver and passenger.

For the protection against contact transmission, it is necessary to focus on human, vehicle, environmental disinfection and space isolation. For individual disinfection, it is necessary to focus on hand disinfection of driver and passenger. For vehicles and the environment, common disinfection methods are UV disinfection and disinfectant disinfection.

For protection against aerosol transmission, it is necessary to strengthen ventilation, purify the air by natural ventilation and mechanical ventilation especially for the relatively closed environment in the car, so as to effectively reduce the concentration of suspended matters in closed space [2].

3 Analysis on Data-Based Epidemic Prevention

The data mainly refer to people's travel demand data, individual travel data and regional epidemic risk data during the outbreak. Data-based epidemic prevention and control are aimed at precise digital management from individuals to areas, timely investigating and controlling close contacts, timely predicting and preventing regional epidemic risks, and formulating the relevant strategies.

3.1 Travel Demands and Features During the Outbreak

Based on MNL regression model, ZOU found that residents' travel selection is mainly related to the effect of epidemic prevention and control after analyzing the effect factors of residents' travel under epidemic prevention and control. In the areas with high risk of outbreak, residents are more likely to select taxis and online car-hailing [5]. According to the related data after desensitization, GAO found that there is still a large demand of online car-hailing in the areas with high risk of outbreak [6]. It shows that the demand for shared cars is more common after the outbreak and that the shared cars will play an important role; especially for higher demand for shared cars in areas with high epidemic risk, more attention should be paid to COVID-19 prevention for shared cars and providing preventive measures for drivers.

3.2 Current Data-Based Prevention and Control Methods

The current prevention and control method of shared cars is to analyze and monitor trips with current health codes and travel cards according to big data of travel. The common process is as follows: Passengers shall show health codes when taking online

car-hailing, wear masks during the ride, conduct temperature measurement and code scanning registration while passenger travel records are made. At present, the whole urban transportation system, even the trans-regional traffic system, still have barriers between travel data and have a lack of data-based design of epidemic prevention system [10].

Each car-sharing enterprise shall adopt the current prevention and control method to establish prevention and control organization. Timely measure temperature for team drivers, disinfect vehicles and establish the logs of drivers and passengers. Further, establish the leading group of epidemic prevention and control and logistical group to ensure the normal operation of overall epidemic prevention.

4 Suggestions on Design of Shared Car Epidemic Prevention System

It shows that the current epidemic prevention design of shared cars is conducted only from scenario or data, and that the epidemic prevention design of shared cars in traffic system is lacked. Based on scenario and data, this paper will carry out the design recommendation for the epidemic prevention system of shared cars, which provides references for preliminary epidemic prevention.

4.1 Suggestions on Design of Scenario-Based Epidemic Prevention

For COVID-19 prevention in the working scenario, the design of space layout and disinfection method will be conducted to establish scenario-based COVID-19 prevention (see Fig. 1).

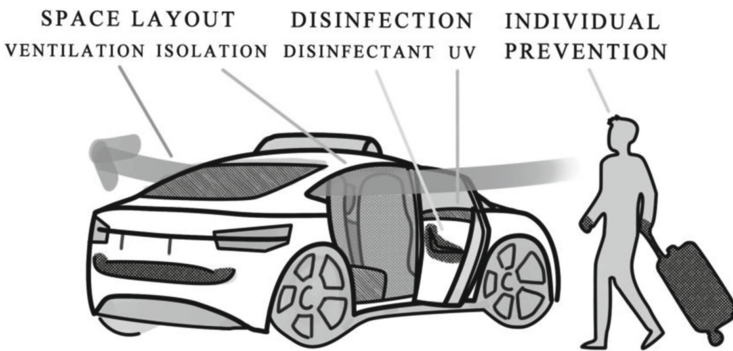


Fig. 1. Scenario-based epidemic prevention system

4.1.1 Suggestions on Space Layout Design

For personal prevention, drivers and passengers shall wear masks and keep a distance, which is the most basic guarantee to avoid the spread of droplets and is also the prevention

method outside the car. Further, encourage low-density travel, control the number of people in the car, shorten travel distance and time, and reduce transmission risks [8].

For the space in a car, separating passengers from a driver is the most efficient method. Baffle (such as transparent acrylic board) and protective film shall be installed between the front and rear seats and between the driver and co-driver to avoid direct contact between passengers and drivers. It is difficult to pay cash due to barriers. Online payment shall be encouraged to improve the digitization of shared cars during the outbreak. On the other hand, it is necessary to strengthen ventilation through mechanical ventilation and natural ventilation, improve the ventilation power and inflation rate of air conditioning, clean and replace the filter elements of air conditioning regularly, and open windows for ventilation at low speed or when the car is parking to lower the risk of droplet transmission and aerosol transmission.

4.1.2 Suggestions on Disinfection Design

During the regular epidemic prevention and control, shared cars shall be disinfected frequently through using UV lamps and disinfectants.

During the UV disinfection, the disinfection part must be fully exposed to ultraviolet ray, and the position of UV disinfection lamp in car must be adjusted to ensure the coverage of maximum area [13]. Automatic UV disinfection in the car may be designed. When no person is in the car, it will be automatically disinfected and automatically end after disinfection. At the same time, it will be automatically closed or manually closed when a person is close to the door, so as to achieve higher disinfection frequency. The UV lamp is placed according to the reading lamp and top lamp position.

For individual disinfection, drivers and passengers shall disinfect hands with alcohol or iodophor after getting on and off the car every time. Disinfection of disinfectants in cars shall be conducted three times a day. A driver must disinfect each part of the car before using the car every day.

4.2 Suggestions on Design of Data-Based Epidemic Prevention and Control

According to travel data and epidemic risk data, the epidemic prevention system is designed and suggested, combined with three aspects of individuals, enterprises and transportation systems. (Fig. 2).

4.2.1 Integrate Travel Data to Achieve Digital Epidemic Prevention

In scenario-based prevention, promote the level of network connection, achieve the digitization of drivers and passengers, record travel demands and trips, and unify scenarios and data. For epidemic prevention and control of urban transportation, break down data barriers, integrate the travel data of public transport and shared cars to promote the digital management level. At the same time, establish the unified travel data platform, achieve cross-regional epidemic prevention and control to ensure the effectiveness of epidemic prevention and control. Achieve digital epidemic control and multi-dimensional and cross-regional targeted epidemic prevention and control, and improve the tenacity of epidemic prevention and control of urban transport.

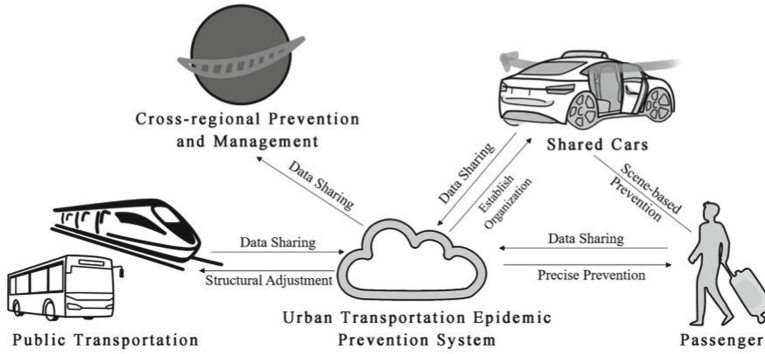


Fig. 2. Data-based epidemic prevention system

4.2.2 Carry Out Risk Prediction, Dynamic Adjustment of the Structure of Traffic System

In the post-epidemic era, the bearing pressure of urban transportation also increases with the increase in the demand of private cars. In the epidemic prevention and control of public traffic system and car-sharing companies, the model integrating traffic system with infectious risks shall be established on the basis of data integration in order to effectively predict epidemic risks. In different areas of epidemic risks, adjust structure according to travel demands, encourage to play an important role by means of digital, low density and travel mode of shared cars, make more contributions to congestion control and vehicle scheduling, and promote the supply tenacity of urban transportation.

4.2.3 Establish the Unified Epidemic Prevention Organization

As individualized travel needs, shared cars must actively take social responsibility. Car-sharing enterprises can systematically establish anti-epidemic organizations. The government can formulate the uniform standards for organization, and carry out epidemic prevention and control in a more active and dynamic manner combined with digital management.

4.2.4 Layout of New Four Modernizations, Innovation of Individualized Travel Services

Car-sharing industry shall grasp the reform opportunity in the post-epidemic era, promoting the new four modernizations of cars layout, upgrading infrastructure and vehicles, applying emerging technologies to promote the integration of shared cars in urban transportation system. On the other hand, it is necessary to actively explore future travel modes on the basis of integration. Epidemic prevention provides new scenes for autonomous driving, sharing and intelligence, so the car-sharing industry shall further explore and innovate the individualized travel service.

5 Summary

From the perspective of COVID-19 transmission risk, it is suggested that the systematic prevention of shared cars shall be designed according to scenario and data. In view of scenario-based design, the transmission mode of COVID-19 must be considered to achieve isolation, ventilation and disinfection in the working scenario; in view of data-based design, it is necessary to promote travel data integration, achieve digital management from the perspective of urban transportation system and whole transportation system, and achieve cross-regional comprehensive prevention and control. On the other hand, actively promote new four modernizations of shared cars, explore and innovate the individualized travel services to meet the travel requirements in the post-epidemic era. Finally, this paper discusses the significance of the design of epidemic prevention system, which is to improve the epidemic prevention system of urban transportation, grasp the reform opportunity of post-epidemic era, and actively take social responsibility.

This paper proposes the design of epidemic prevention system based on scenario and data, and puts forward the preliminary design and suggestions that can be used as the directional reference for the construction and reform of shared cars and urban transportation epidemic prevention system. However, there is no quantitative research on specific preventive means, technologies and specific structure and strategy of prevention system, which shall be further improved.

Acknowledgements. This work is supported by the 2020 project of China Society of Automotive Engineers.

References

1. Xiao, W., He, J., Yan, J., Deng, J., Li, X., Shi, J., et al.: Transmission risks and response strategies for land transportation under the epidemic of coronavirus disease 2019. In. *Med. (Electron. Ed.)* **9**(02), 1–8 (2020)
2. Shen, J., Duan, H., Zhang, B., Wang, J., Ji, J., Wang, J., et al.: Prevention and control of COVID-19 in public transportation: experience from China. *Environ. Pollut.* **266**, 115291 (2020)
3. Jiang, N., Li, S., Cao, S., Wei, J., Wang, B., Qin, N., et al.: Transportation activity patterns of chinese population during the COVID-19 epidemic. *Res. Environ. Sci.* **33**(7), 1675–1682 (2020)
4. Bucsky, P.: Modal share changes due to COVID-19: the case of budapest. *Transp. Res. Interdisc. Perspect.* **8**, 100141 (2020)
5. Zou, S.: Analysis the influence factors of residents' travel mode under the background of epidemic prevention and control based on multinominal logistic regression model. *Shandong Jiaotong Keji.* **04**, 98–102 (2020)
6. Gao, Y., Yu, Z., Qiu, D., Chu, Q.: Analysis and suggestions on changes of online car-hailing during COVID-19. *Traffic Transp.* **33**(S2), 173–178 (2020)
7. Tirachini, A., Cats, O.: COVID-19 and public transportation: current assessment, prospects, and research needs. *J. Public Transp.* **22**(1), 1 (2020)
8. Chen, J.: COVID-19 propagation process based on SEIR model and online car-hailing response strategy. *Intell. Comput. Appl.* **11**(7), 205–211 (2021)

9. Yao, J., He, J., Chen, X., Tang, Q.: Study on emergency management decision of safety supervision of railway transport of passenger in normalized COVID-19 epidemic prevention and control. *Logistics Sci-Tech.* **45**(02), 80–85 (2022)
10. Li, M.: Prospect of urban transportation development in post-epidemic period. *Ind. City.* **07**, 84 (2020)
11. Li, Y., Liu, X., He, Q.: Urban transportation system resilience during the COVID-19 pandemic. *Urban Transp. China* **18**(3), 80-87+10 (2020)
12. Diagnosis and Treatment Protocol for Novel Coronavirus Pneumonia (2020). <http://www.nhc.gov.cn/yzygj/s7652m/202003/a31191442e29474b98bfed5579d5af95.shtml>
13. Zhang, Y.: Guidelines for car ownership in the context of COVID-19. *Auto Maintenance Repair* **05**, 27–28 (2020)



Prediction Model of Accident Vehicle Speed Based on Artificial Intelligence Decision Tree Algorithm

Wei Ji¹, Tiantong Yang^{1(✉)}, Quan Yuan², Gang Cheng¹, and Shengnan Yu¹

¹ Key Laboratory of Evidence Science, China University of Political Science and Law, Ministry of Education, Fada Institute of Forensic Medicine and Science, Beijing 100088, China
joe@cupl.edu.cn

² State Key Laboratory of Automotive Safety and Energy, School of Vehicle and Mobility, Tsinghua University, Beijing 100084, China

Abstract. Speeding is not only an illegal act, but also an important cause of traffic accidents. Judging whether the accident vehicle is speeding is an important work in the process of accident handling. This paper analyzes 903 traffic accidents in Beijing, China in 2020, extracts the time of occurrence, road characteristics, collision types, casualties, vehicle types and driver characteristics as variables, and constructs a decision tree to analyze whether the vehicle is speeding. The sample cases are classified into training set and test set with the proportion of 3:1. The training set is used for artificial intelligence machine learning, and the test set is used as an actual case to verify the accuracy of the model for overspeed prediction. Results show that the accuracy of the decision tree model in predicting vehicle overspeed is 77%. This paper discusses the application of the decision tree model in the intelligent identification of vehicle speed in road traffic accidents, which provides a basis for peers to carry out in-depth research.

Keywords: Driving speed · Speeding · Artificial intelligence · Decision tree · Prediction

1 Foreword

Decision Tree [14] is a computer learning method and a predictive model algorithm that is widely used in the field of artificial intelligence. As early as the 1980s, Quinlan [10, 11] proposed the algorithm and use of decision tree. When there is a set of multi-attribute data sets and it is impossible to unify the data scale before modeling like a general algorithm, a decision tree that can preserve the data scale is the best choice. In addition, the decision tree algorithm saves data preparation time, the decision tree can effectively classify the data even if it contains outliers and incomplete data. Moreover, the visualization and the easy-to-understand composition of decision trees are also the reasons for the popularity of it [6].

In the research of traffic accidents, it is found in the paper that decision tree algorithm can be used for predicting whether the accident vehicle is speeding by modelling through

The original version of this chapter was revised: Chapter title has been amended. The correction to this chapter is available at https://doi.org/10.1007/978-981-19-4786-5_101

training. In fact, some scholars have been engaged in the research of decision trees in the field of traffic accidents for a long period. For example, Liang Sufang constructed a decision tree based on the fuzzy information of road accidents to predict the possibility of traffic accidents on curved roads [8]. Liu Xinyu used environmental factors and driver behaviors as variables to predict the severity of traffic accidents [9], Sun Yixuan et al. also built a decision tree model based on attributes such as driver type to predict the severity of traffic accidents [12]. In this paper, by studying the data of 903 traffic accidents in Beijing, China, adopting the accident time, road characteristics (speed limit, presence or absence of fixed monitoring probes), vehicle collision type, accident casualties, vehicle type, and driver-related attributes as the variables to discriminate the overspeed model, a decision tree model for overspeed analysis is built. The model can solve the problem of timeliness caused by program requirements, on-site investigation, data acquisition, etc., and uncertain errors caused by subjective reasons such as material data handover and vehicle speed calculation method selection in the speed identification of vehicles in current traffic accidents. The mature prediction model based on decision tree is expected to be adopted in the construction of artificial intelligence vehicle speed identification system, so as to predict the speeding behavior of the accident vehicle and provide help for the traffic accident handling of the traffic police.

2 Establishment of Decision Tree Model

2.1 Basic Algorithm of Decision Tree Model

A decision tree contains a root node, several internal nodes and several leaf nodes; The leaf nodes correspond to the decision results, and each other node corresponds to an attribute test; The sample set contained in each node is allocated to child nodes according to the result of attribute test; The root node contains the full set of samples [3]. The path from the root node to each leaf node corresponds to a decision test sequence. The purpose of decision tree learning is to generate a decision tree with strong generalization performance, that is, the ability to deal with unseen examples. Its basic process follows the simple and intuitive “divide-and-conquer” strategy [15], as shown in Fig. 1.

2.2 Construction and Classification of Decision Tree Model

The construction of decision tree has two steps: Construction and classification [1]. First, we construct a decision tree from top to bottom by letting the computer learn from the given training data set, and exploring each internal node starting from the root node until each leaf node is found. A good decision tree can minimize the mixed classification between each subset. Second, we use this decision tree to classify a new object. Starting from the root node, each attribute of the object will be evaluated by the decision tree and imported into the corresponding internal node, and finally enter a classification result, that is, a leaf node.

```

Putin:trainingsetD={(x1, y1), (x2, y2), ..., (xm, ym)}; attribute setA={a1,
a2, ..., ad}
Process:function Tree Generate(D, A)
01:Generate the node;
02:if D All of the middle samples belong to the same level C then
03:Mark the node as a class C leaf node;return
04:end if
05:if A=null OR D middle samples were given the same values on A
then;
06:mark node as a leaf node and its category as the class with the
largest number of samples in D;return
07:end if
08:Select each value a*vd of the optimal partition attribute a*;
09:for a*from A Generate a branch for node;
10:make Dv represent the subset of the value a*vd on a*;
11:The if Dv is an empty set then;
12:Mark the branch node as the leaf node with the largest number of
samples in D;return
13:else
14:Take Tree Generate(DvAl{a*}) as the branch node;
15:end if
16:end for
Output:A decision tree with node as the root node

```

Fig. 1. Basic algorithm for decision tree model, [15]

Taking the binary classification task as an example, we hope to learn a model from a given training data set to classify new examples. This task of classifying samples can be regarded as the “decision” or “judgment” process of the question of “Does the current sample belong to the positive class?”. Just as its name implies, a decision tree makes decisions based on the tree structure, which is a very natural handling mechanism for humans when facing with decision-making problems, and is also the embodiment of artificial intelligence logic in such operation process. As far as the research content of the paper is concerned, when determining “Is this car speeding?”, there is usually a series of judgments or “sub-decisions”: let’s start with “What type of car is it?”, if it’s a “car”, then we judge “what gender is its driver?”, if it is “male”, let’s judge “what is its collision form?”, and so on, and finally, we come to the final decision: the car is speeding.

2.3 Sample Set

The samples used in this research include 903 cases of data on whether there is an overspeed identification result. These samples are randomly allocated in a ratio of 3:1 and used as a training set and a test set respectively to train and test the algorithm model of decision tree.

The indicators used in the sample to judge overspeed, that is, the classification items in the decision tree, include vehicle type, road speed limit, collision type, driver gender, driver age, driver casualty, occupant casualty, etc. (as shown in Table 1).

Table 1. Indicator table of determining whether overspeed

Indicator name	Type of indicator	Indicator interpretation
Month of occurrence	Discrete indicator	January, February, March, ..., December
Time of occurrence	Discrete indicator	0, 1, 2, ..., 23
Vehicle type	Discrete indicator	Bus, motorcycle, electric car, van, sedan, other cars
Road speed limit	Continuous indicator	km/h, missing data was replaced with 200 km/h
Overload	Discrete indicator	Yes-overload, no-not overload
Video type	Discrete indicator	Fixed probe, dashcam, no video recording
Collision type	Discrete indicator	Front, side, rear-end
Driver gender	Discrete indicator	Male, female
Driver age	Continuous indicator	Integer type data
Driver casualties	Discrete indicator	No loss, property loss, injury, death
Casualty	Discrete indicator	No occupant, property loss, injury, death

2.4 Code Implementation

The decision tree code can be written in the python language. First, the test set and training set data are randomly divided, and then the information entropy is used as the dividing standard to train the decision tree; after the decision tree structure is written to the file, the decision tree will make judgments on new data and ultimately make predictions.

2.5 Accuracy, Recall, and Precision of Decision Tree

Decision tree classifies a data set, so a small branch often leads to multiple different decisions, and therefore, the prediction conclusion given by the decision tree will have a large error [3].

This decision tree model has a discriminative accuracy rate of 0.79 for the training set, that is, the number of correctly predicted samples accounts for 79% of all samples, and the recall rate is 0.56, that is, 59% of the overspeed samples are successfully predicted, and the precision rate is 0.69, that is, the precision of predicting overspeed sample is 69%; the discriminative accuracy rate on the test set is 0.77, the recall rate is 0.57, and the precision rate is 0.63 (as shown in Table 2).

Table 2. Table of accuracy, recall and precision

Accuracy	0.7921146953405018	0.7688172043010753
Recall	0.5568862275449101	0.5714285714285714
Precision	0.6888888888888889	0.6274509803921569
Accuracy	0.7921146953405018	0.7688172043010753

2.6 Prediction of Speeding

As shown in Fig. 2, the blue box in the decision tree indicates that the driver is highly possible of speeding. The darker the blue, the higher probability of speeding. The orange box indicates that the driver has a high probability of not speeding. In practice, it can be judged whether the driver has a high probability of speeding according to the relevant information of the driver. For example, for an accident vehicle with a road speed limit higher than 25 km/h, the driver is younger than 33.5 years old and drives a motorcycle. If there is a traffic accident, then the driver is highly possible of speeding, and the probability of speeding is 86.96%; for an electric bicycle accident, if the driver is older than 33.5 years old, then the probability of speeding before the speed is more than 25 km/h is relatively low, and the probability basically approaches 0.

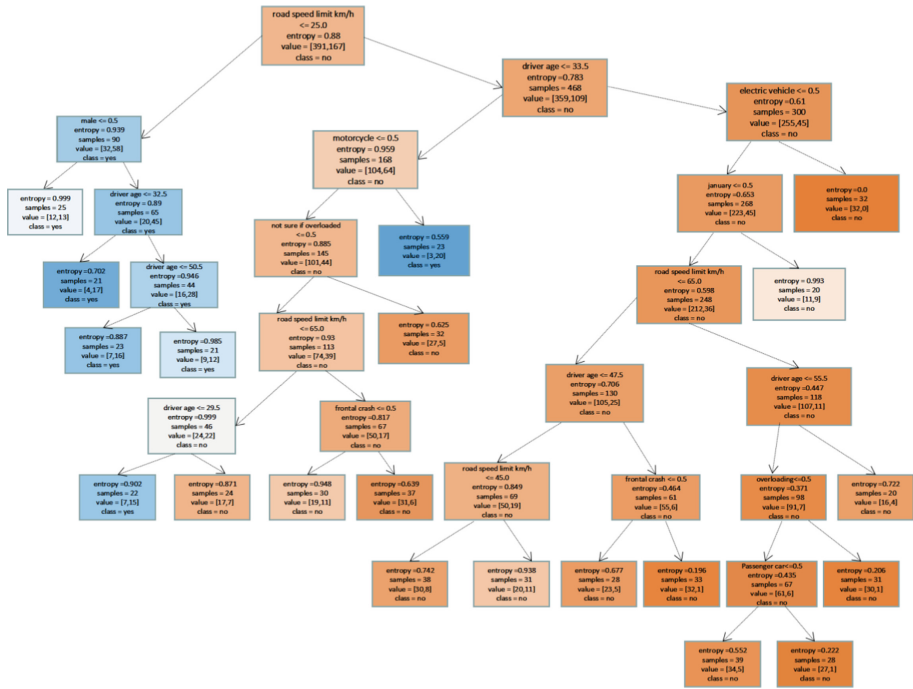


Fig. 2. Decision tree for predicting overspeed

3 Discussion

3.1 Application of Decision Tree Model

At present, in handling an accident, the police usually relies on the entrusted judicial expertise agency to determine whether the vehicle was speeding before the incident. However, due to the limitations of procedural requirements, on-site investigation and related standard methods, the timeliness and error range of judicial expertise are sometimes difficult to control. Research on the intelligent identification system of vehicle speed based on decision tree model can effectively solve the above problems. The decision tree model introduced in this paper can effectively predict whether a vehicle is speeding in a new actual case with limited sample data and fewer indicators (factors). The reason is that the internal relation of multiple factor data by artificial intelligence via a large number of calculations, which can be linked with the identification content (such as whether the accident vehicle is speeding), and finally make a judgment. Although the decision tree model is limited by factors such as the location and time of the sample cases, the results may be limited, but with the continuous increase of sample data of actual cases, its operation prediction results will be more accurate. Theoretically, artificial intelligence can continuously improve its discriminative accuracy for new cases through continuous learning. When its accuracy can cover the error range of current identification methods, its prediction results can be considered credible. The biggest advantage of artificial intelligence identification system is that the growth trend of data volume is irreversible, and the improvement of the accuracy of its prediction results is inevitable.

3.2 Implementation of Artificial Intelligence Vehicle Speed Identification System

The artificial intelligence vehicle speed identification system will eventually be presented in the form of open source software and use mobile terminals as the carrier. The front-line police of public security accident can enter the basic information of the accident such as accident month, accident time, vehicle type, road speed limit, speeding or not, video recording, collision type, driver gender, driver age, driver casualty, occupant casualty, etc. in the mobile phone or tablet computer, then the feedback of the artificial intelligence on speeding conclusion can be quickly provided, and the conclusion will be displayed in the form of percentage or specific judgment on speeding can be directly determined. Similarly, if there is no need to quickly draw conclusions on the spot, the system can be used in the information and data processing work of the public security system. With the strengthening of information-based office capabilities of the public security system and the construction of various information management platforms, the internal general traceability of basic road accident information can be improved, and the basic accident information shared within the public security system can be directly imported into the artificial intelligence vehicle speed identification system, and cases of certain speeding or not speeding can be excluded from the feedback results, only individual special cases which cannot be directly judged by artificial intelligence need to be manually identified, which can maximize the efficiency of judicial expertise entrusted by the public security, and reduce the financial expenditure incurred by purchasing judicial expertise services.

Theoretically, the ultimate goal of artificial intelligence vehicle speed identification is to replace manual identification, but this needs to be based on long-term learning and training and a huge data computing foundation.

3.3 Prospect of Artificial Intelligence Vehicle Speed Identification System

Artificial intelligence has been applied in many fields such as traffic engineering and vehicle engineering. There are relatively mature models or products in vehicle number plate recognition, vehicle body feature recognition, automatic (assisted) driving, etc. If there are channels, the interconnection of a variety of artificial intelligences can be established, which can give full play to the advantages of artificial intelligence itself. Combined with technologies such as vehicle electronic data, radar and visual recognition, it will provide new possibilities for human beings to realize fully automated intelligent transportation.

4 Conclusion

The paper analyzes and studies 903 traffic accidents that occurred in Beijing in 2020, extracts accident-related data to establish a decision tree model for predicting whether the accident vehicle is speeding, conducts artificial intelligence machine learning and training on the decision tree through the training set, and validates the accuracy of decision tree through the test set. Although the decision tree is limited by factors such as time, space and number of cases, in the validation stage, the prediction accuracy of decision tree on whether the accident vehicle is speeding can still reach 77%. The mature decision tree model can be used to build an artificial intelligence vehicle speed identification system. The contents of this research can provide research ideas for peers and provide a basis for in-depth research.

References

1. Amor, N.B., Benferhat, S., Elouedi, Z.: Qualitative classification with possibilistic decision trees. In: Bouchon-Meunier, B., Coletti, G., Yager, R.R. (eds.) *Modern Information Processing: From Theory to Applications*, pp. 159–69. Elsevier, Amsterdam (2006)
2. Bartosik, A., Whittingham, H.: Evaluating safety and toxicity. In: Ashenden, S.K., Bartosik, A. (eds.) *ERA of Artificial Intelligence, Machine Learning, and Data Science in the Pharmaceutical Industry*, pp. 37–119. United Kingdom: Academic Press, Cambridge (2021)
3. Dev, V.A., Eden, M.R.: Gradient boosted decision trees for lithology classification. *Comput. Aided Chem. Eng.* **47**, 113–118 (2019)
4. Kingsford, C., Salzberg, S.L.: What are decision trees? *Nat. Biotechnol.* **26**(9), 1011–1013 (2008)
5. Kotsiantis, S.B.: Decision trees: a recent overview. *Artif. Intell. Rev.* **39**(4), 261–283 (2011). <https://doi.org/10.1007/s10462-011-9272-4>
6. Kotu, V., Deshpande, B.: Classification. In: Kotu, V., Deshpande, B. (eds.) *Predictive Analytics and Data Mining: Concepts and Practice with Rapidminer*, pp. 63–163. Amsterdam Elsevier/Morgan Kaufmann, Amsterdam (2015)
7. Li, H.: *Methods of Statistics*, 2nd edn. Tsinghua University, Beijing (2019)

8. Liang, S.: Study on traffic accident and prediction in dangerous section [Master's thesis], Jilin University, Jilin, vol. 77 (2016)
9. Liu, X.: Study of road traffic accident sequence pattern and severity prediction based on data mining [Master's thesis], Beijing Jiaotong University, Beijing, vol. 109 (2016)
10. Quinlan, R.: C4.5: Programs for Machine Learning. Morgan Kaufmann, San Mateo (1993)
11. Quinlan, J.R.: Simplifying decision trees. *Int. J. Man Mach. Stud.* **27**(3), 221–234 (1987)
12. Sun, Y.X., Shao, C.F., Zhao, D., Ou, S.: Traffic accident severity prediction model based on C5.0 decision tree. *J. Changan Univ.* **34**(05), 109–116 (2014)
13. Reinders, C., Ackermann, H., Yang, M.Y., Rosenhahn, B.: Learning convolutional neural networks for object detection with very little training data. In: Murino, V., Rosenhahn, B., Yang, M.Y. (eds.) *Multimodal Scene Understanding Algorithms, Applications and Deep Learning*, pp. 65–100. Elsevier Science & Technology, San Diego (2019)
14. Tan, L.: Code comment analysis for improving software quality. In: Bird, C. (ed.) *The Art and Science of Analyzing Software Data*, pp. 493–517. Kauffmann, Amsterdam (2015)
15. Zhou, Z.H.: *Methods of Statistics*. Tsinghua University, Beijing (2016)



Control Design to Underwater Robotic Arm

Jiahong She¹, Shang Huan¹(✉), Shaoli Xie¹, Deli Zhang², Liangliang Han³,
and Jian Yang³

¹ China Astronaut Research and Training Center, Beijing 100094, China
huan_shang@126.com

² Nanjing University of Aeronautics and Astronautics, Nanjing 210016, China

³ Shanghai Aerospace System Engineering Research Institute, Shanghai 201109, China

Abstract. Objective. In order to improve the operation ability and response speed of the underwater robotic arm in simulation training mission of space station, this paper focuses on solving the arm's operability problem. **Methods.** Based on the man-machine ergonomic characteristics, the control design scheme is proposed from the aspects of control system architecture, motion control and human-computer interaction. **Conclusion.** The test and application results show that the arm has fine operability. It makes underwater training more efficient. Owing to the approximate function of the space station manipulator, it makes simulation training more realistic. At present, the underwater training missions are successfully completed from SZ-12 to SZ-14. It proves that the control design is reasonable and the goal of good operability has been achieved.

Keywords: Underwater · Control · Robotic arm

1 Introduction

In order to actually simulate the extravehicular activities of the space station, an economical and safe underwater training method has been adopted in China. The neutral buoyancy tank is equipped with the underwater robotic arm (the arm for short) and the whole space station model to carry out simulation training mission. Which can help astronauts experience and grasp the procedures and features of space operations, for example, installing & repairing the key components, transferring materials, patrolling & maintaining the space station [1]. During underwater simulation training, the astronauts wearing spacesuit, the arm and the tank have formed a special cooperative relationship, as shown in Fig. 1. Its high efficiency largely depends on the handling performance of the arm. Therefore, this paper focuses on the control system architecture, motion control and human-computer interaction to solve the problem of efficient operation for the arm.

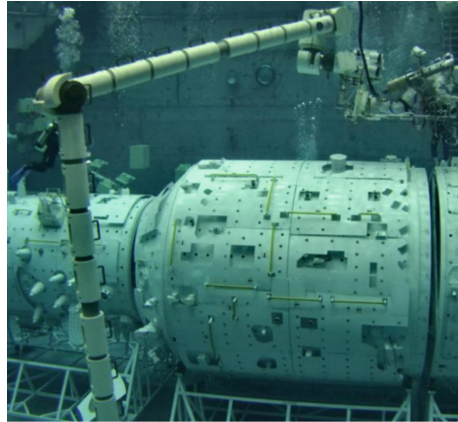


Fig. 1. Underwater robotic arm

2 Control System Architecture

According to the principles of easy operation, flexibility, safety and reliability, the control system of the arm adopted three-level distributed architecture of command & scheduling, motion planning and component execution[2, 3], as shown in Fig. 2.

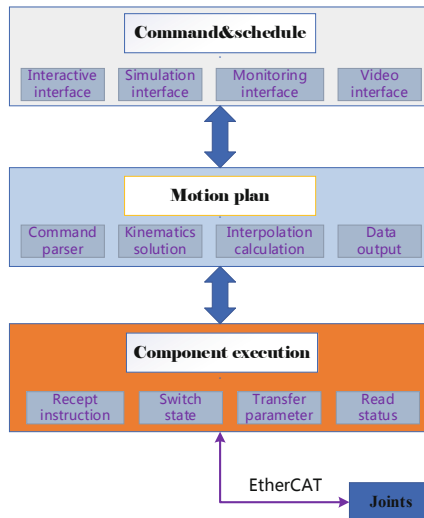


Fig. 2. Architecture of control system

The top layer is the command & scheduling layer, which mainly covers man-machine interface, monitoring interface, mission simulation interface and underwater monitoring video. The middle layer is the central controller, which is responsible for motion planning, mainly including the parsing of motion control instruction, positive and inverse

solution of kinematics, interpolation calculation, matrix transformation, etc. The bottom layer is the component execution layer, which is responsible for receiving the instructions of the central controller, driving the joint motor, and uploading the joint angle, current, temperature and other status data. Ethernet communication is adopted between the top-level application and the central controller to transmit interface data. EtherCAT bus communication is used between the central controller and actuators such as joints, sensors. Command & scheduling, and motion planning layer are developed based on VC++ development environment, which is convenient for algorithm implementation and later software maintenance; the component execution layer is developed by PLC to process the external signal logic and the terminal operation [3]. The key to the arm control is the establishment of kinematic coordinate system and the optimization of algorithm.

2.1 Positive Solution Algorithm

The arm is designed to have six degrees of freedom, with the “2 + 1 + 3” structure. Among them, three adjacent joint axes of wrist pitch, elbow pitch and shoulder pitch are parallel to each other, and three adjacent joint axes of wrist roll, wrist pitch and wrist yaw intersected at one point, as shown in Fig. 3. The kinematics equation of the arm had closed solution according to the principle of “pieper”. The D-H coordinate system is established by the connecting rod parameter d_i , a_{i-1} , α_{i-1} , θ_i , based on the arm deployment configuration, as shown in Table 1. Thus, the spatial transformation matrix from the base to the end and the kinematic equation of operating the arm can be established [4].

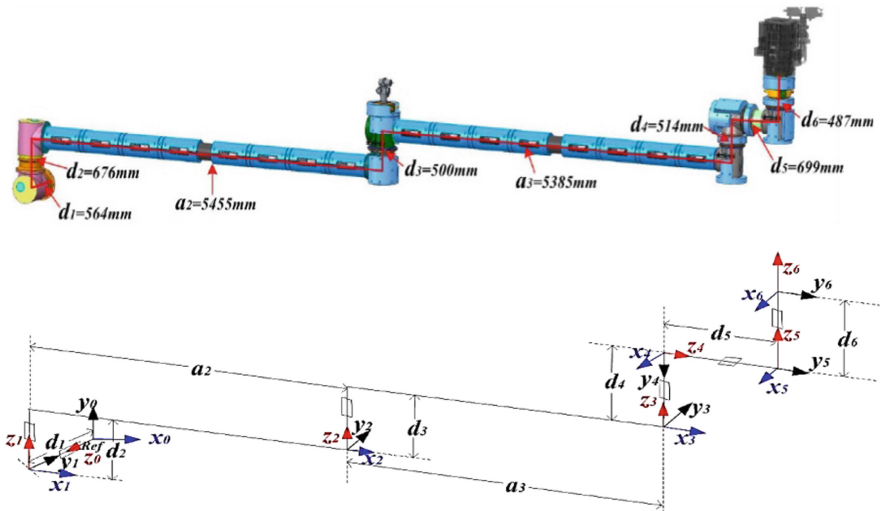


Fig. 3. DH coordinate system of underwater arm

Table 1. D-H parameter of underwater arm

i	Offset base d_i	Axle base a_{i-1}	Twist angle α_{i-1}	Offset angle θ_i
1	$d_1 = 0.564$	0	0	0
2	$d_2 = 0.676$	0	$-\pi/2$	$-\pi/2$
3	$d_3 = 0.5$	$a_2 = 5.455$	0	$\pi/2$
4	$d_4 = 0.514$	$a_3 = 5.385$	0	0
5	$d_5 = 0.699$	0	$\pi/2$	$\pi/2$
6	$d_6 = 0.487$	0	$\pi/2$	0

2.2 Inverse Solution Algorithm

The kinematics inverse solution of the arm is more suitable for engineering application, which is the basis of path planning and trajectory control. The rotation angle of each joint can be solved by the spatial transformation matrix. Because solving the inverse trigonometric function equation will produce many sets of solutions. For the arm, there is only one set of solutions corresponding to the actual situation. Generally, the appropriate solution is selected by joint motion space, or redundant solutions are eliminated successively. In order to reduce the probability of underwater collision, this topic is based on the principles of the shortest path, that is, the minimum amount of movement per joint. Therefore, the weighted sum of the joint angle motion angle value is adopted to select the optimal solution of the robot arm motion. Calculate $\delta[i]$ according to Formula 1, then the group with the smallest value is the optimal solution [5].

$$\begin{aligned} \delta[i] = & A_1 * \text{abs}(\theta'_1 - \theta_1^i) + A_2 * \text{abs}(\theta'_2 - \theta_2^i) + A_3 * \text{abs}(\theta'_3 - \theta_3^i) \\ & + A_4 * \text{abs}(\theta'_4 - \theta_4^i) + A_5 * \text{abs}(\theta'_5 - \theta_5^i) + A_6 * \text{abs}(\theta'_6 - \theta_6^i) \end{aligned} \quad (1)$$

Among them, the current joint angle values: $\theta'_1, \theta'_2, \theta'_3, \theta'_4, \theta'_5, \theta'_6$, possible solution: $\theta_1^i, \theta_2^i, \theta_3^i, \theta_4^i, \theta_5^i, \theta_6^i (i = 1, 2, 3, 4, \dots)$, weighted values: $A_1, A_2, A_3, A_4, A_5, A_6$.

3 Motion Control

The motion of the arm involved the linkage control of 6 joints. A series of measures such as motion pause, S-type acceleration & deceleration algorithm, end linear planning, and end arc planning are taken to ensure the smooth, safe and efficient operation of the arm.

3.1 Stop Control

From the perspective of safety and stability, the control system is equipped with motion pause and emergency stop buttons to deal with special situations. When the operator

cannot accurately predict the safety boundary in the process of operation, he can perform the pause operation immediately to slowly stop the arm, seriously observing the underwater video to further judge whether there is any collision risk. If not risk, click the start button to continue to execute the current path. 1 ton mass bring the arm a lot of inertia; 11m extension length bring the arm great torque. So the suspension control must stop and start slowly. The control program adopts the method of sectional deceleration, which divides the total pause time into ten sections, and each section decelerates one tenth of the speed in turn until the arm stops moving. If the motion is resumed, on the contrary, the growth rate of each section is one tenth in turn until it accelerates to the original speed. In case of emergency, press the emergency stop button, and the arm directly holds the brake to cancel the task and keep the current state.

3.2 Speed Control

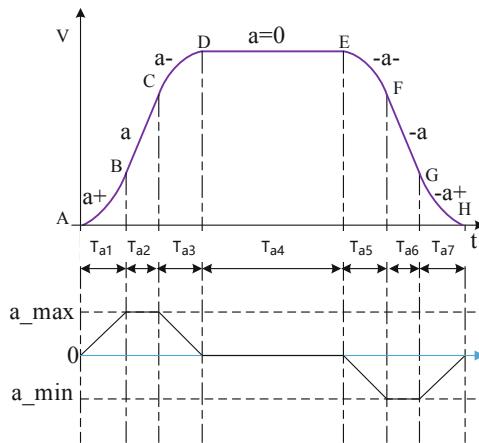


Fig. 4. S-type acceleration & deceleration

According to the S-type acceleration & deceleration algorithm, the controller calculates the position increment of each interpolation cycle, and then obtains the target angle of each joint through spatial transformation to ensure the stability and safety of motion. S-type acceleration & deceleration are divided into three stages, as shown in Fig. 4. The first stage is acceleration stage, including three small sections T_{a1} , T_{a2} and T_{a3} . The acceleration is increased from 0 to a_{\max} at “a+” in T_{a1} , running is accelerated at “ a_{\max} ” in T_{a2} , and acceleration is reduced to zero at “a-” in T_{a3} ; the second stage is the uniform speed stage, namely, running at a constant maximum speed in T_{a4} ; the third stage is the deceleration stage, including the sections T_{a5} , T_{a6} , T_{a7} . The acceleration is reduced from 0 to “ a_{\min} ” at “-a-” in T_{a5} , running is slowed down at “-a” in T_{a6} , and the deceleration is reduced from a_{\min} to 0 at “-a+”. On the other hand, to satisfy ergonomic requirements, the maximum translational speed of the end is limited to 200 mm/s, acceleration is 5 mm/s^2 , and the maximum rotational speed is $3^\circ/\text{s}$, acceleration is $0.15^\circ/\text{s}^2$.

3.3 Path Planning

For efficient path planning, the control system provided not only the end linear planning, but also the end arc planning. Among them, the algorithm of end linear planning is as follows:

Input the coordinates of starting and ending points $(x_0, y_0, z_0, \theta_0, \psi_0, \phi_0)$, $(x_1, y_1, z_1, \theta_1, \psi_1, \phi_1)$. Output the interpolate points of the end at the current time $(x_t, y_t, z_t, \theta_t, \psi_t, \phi_t)$.

Under normal circumstances, firstly, the distance between two points is calculated. Secondly, according to S-type speed planning, interpolation is performed by the planned distance “ d_{st} ” and the total distance “ d ”.

$$x_t = x_0 + k(x_1 - x_0)$$

$$y_t = y_0 + k(y_1 - y_0)$$

$$z_t = z_0 + k(z_1 - z_0)$$

$$\theta_t = \theta_0 + k(\theta_1 - \theta_0)$$

$$\psi_t = \psi_0 + k(\psi_1 - \psi_0)$$

$$\phi_t = \phi_0 + k(\phi_1 - \phi_0)$$

$$k = d_{st}/d$$

When two points are too close and the attitude changes a lot, two-point distance planning should be switched to the speed planning to avoid the rotation over speed of Euler angle [6–9]. Namely, speed planning is performed for the Euler angle vector length, and interpolation is performed by vector length “ $norm_{st}$ ” and total vector length “ $norm$ ”.

$$k = norm_{st}/norm$$

Similarly, the end arc path planning is as follows: the first step is to establish the local plane coordinate system according to the given three points, and calculate the center coordinate and radius. The second step is to define the mapping matrix “T” from the local plane coordinate to the base coordinate. The third step is to convert the three-point coordinates into the local coordinates, calculate the arc angle and the interpolation value by the S-type speed planning. The fourth step is to restore the interpolation results to the base coordinate.

3.4 Disposal of Singular Point

Although the end linear and arc path planning has the advantages of intuitive operation, clear target position and settable relative moving distance, it cannot solve the problem of singular point. Because the arm has no redundant joints, whether forward kinematics or inverse kinematics, when more than two axes are collinear, the Jacobian matrix is not completely linear independent, resulting in the reduction of the rank, the determinant value is zero, and the singular point inevitably occurs, leading to the failure of autonomous path planning. Moreover, there are many obstacles in the tank, and there are few effective roads that can be planned. In serious cases, the task may not be performed. The control system provides two solutions to solve the problem. First, when the two axes are collinear, directly drive corresponding joint to move and jump out of the singularity. Second, the joint walking algorithm is used to converge to the target angle value of each joint synchronously without using Jacobian matrix. It is especially effective to execute duplicate operation paths. Therefore, in the actual training process, record the Cartesian coordinate value and joint angle value of the path at the same time to deal with the special operation path.

4 Human-Computer Interaction

During the training, human-computer interaction is directly related to the operation efficiency and safety [10]. In this project, it is improved from the aspects of interactive interface, control mode and mission simulation to respond rapidly to various training needs.



Fig. 5. The console of the arm

4.1 Interactive Interface

The console of the arm is equipped with main control panel and four monitors. The main control panel is on the working table to be responsible for task scheduling, editing and simulation; the monitors are arranged at the front of the console for easy observation. The key parameters of joints and the end are monitored by lower right monitor; multiple



Fig. 6. Control & monitoring window

underwater operation videos with different perspectives are displayed from the remaining three monitors. See Fig. 5 for details.

The ergonomics and aesthetics are taken into account the whole interactive interface by industrial design. The controls layout such as tabs, notes, buttons and forms matches the habit of human cognition and behavior. The dynamic parameters are highlighted and given with red and green indicator states according to the threshold value, as shown in Fig. 6. In the normal state, the operator only needed to pay attention to the color of alarm light and didn't need to read specific data, which can greatly reduce visual fatigue and brain load.

4.2 Control Mode

The control system provides a variety of control modes, such as Descartes, single joint, pre-programming and handle [5–8] to satisfy demands of different operation scenes and different operator personalities.



Fig. 7. Descartes operation interface

Descartes operation interface is as shown in Fig. 7. The arrow group at the top control the robot end effector translation, and the arrow group at the bottom control the robot end effector attitude. This mode mainly takes the end effector as the control

object, and quickly responds to the temporary movement demand through the following design: First, for a temporary operation, the motion step and speed ratio can be set quickly through Descartes form. For example, the end moves up 0.5 m at 60% speed ratio and 5° to the right at 80% speed ratio. Second, the system provides two kinds of coordinate systems to motion control: one is the base coordinate. Its origin is located in the arm's base center, with +X facing forward, +Y facing left and +Z facing up, which is convenient for large-scale transfer of the arm; the other is the astronaut coordinate, which makes the end effector movement direction consistent with the movement direction of the astronaut body. For example, the astronaut moves forward in the horizontal operating posture, but actually the end effector moves downward. In this way, the operator can quickly respond to the astronaut's fine-tuning demand of position and attitude without coordinate conversion first.

Through the single joint operation interface, the operator can directly control single or multiple joints to meet the following requirements: first, assist to plan the specific path; second, manipulate the corresponding joint to jump out of the singularity in the path; third, quickly and accurately fine tune the end effector attitude. The arm's capacity is effectively expanded by this mode.

Pre-programming mainly carries out path planning and path storage for operation points in advance to achieve "What you see is what you get". It is especially suitable for repeat paths in training, which not only saves time and labor, but also is safe and efficient.

Handle is to directly control multi-joints linkage of the arm through translation handle and attitude handle to reach the operation point. In case of control system failure, the handles are still effective. Even if this method matches different working conditions such as no-load, manned and heavy load, it still needs to accurately grasp the motion inertia of the whole arm, so it requires certain operating skills.

4.3 3D Mission Simulation

There are two problems in predicting the safe working boundary of the arm only by video from underwater cameras: First, the operator needs to reconstruct the three-dimensional operation scene in his mind, which is few easy to use. Second, owing to no valid verification for planning path, there is risk of feasibility and safety. Therefore, the digital twin 3D models, including tank, arm, cabins and spacesuit, are used to build 3D mission simulation environment to achieve man-machine interaction with virtual-real fusion [9, 10], covering the following abilities.

First, the pre-programming path is simulated at five times speed to rapidly verify its feasibility and safety in 3D simulation environment. Second, the simulation and physics are executed synchronously. Front view, top view, side view and axial view can be selected from the 3D environment to observe the arm operation, which improves the operator's prediction ability greatly, and reduces the operator's brain load. Third, real-time software collision detection. In the process of 3D simulation, set the safety boundary value of the model, carry out collision detection and give safety precaution. This can make up for the shortcomings of video images and eliminate potential misjudgment (Fig. 8).

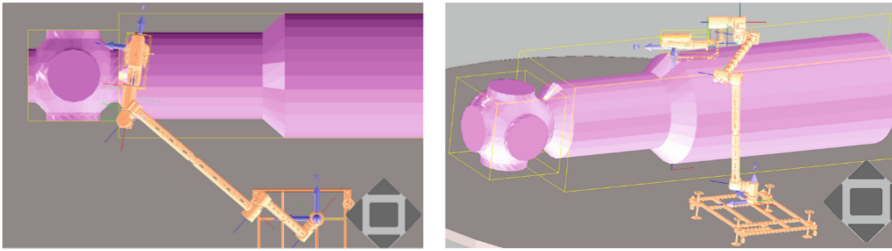


Fig. 8. 3D mission simulation

5 Testing Verification

The verification experiment on the arm ability was carried out simultaneously with the space station training tasks of TianHe module, MengTian module and WenTian module.

Test items are divided into three categories: Functional test, It mainly includes astronauts in spacesuit install and remove the foot restraint, get on and off the arm, transfer goods, and support operation at fixed-point, etc. Posture adjustment test, the astronauts' working orientation adjustment covered upright position, $\pm 180^\circ$ horizontal position, 40° forward tilt position. Training subject test, including lifting the extravehicular panoramic camera stand, installing the extension pump set, repairing solar panel, extravehicular emergency rescue, etc.

During this period, after 3 days of short-term training, four persons without background knowledge can also be competent for the operation post. The test results show that the human-computer interaction system is reasonable, the mission simulation is credible, the command response is rapid, transfer and operation support at fixed-point are smooth.

6 Conclusion and Prospect

Various measures in the aspects of control system architecture, motion control, and human-computer interaction and so on have been taken to improve the arm's operation ability and efficiency. At present, the underwater training missions are successfully completed from SZ-12 to SZ-14. The application results verify that the arm has fine operability. It makes underwater training more efficient. Owing to the approximate function of the space station manipulator, it makes simulation training more realistic.

Optimizing controller parameters, refining the granularity of the cabin model and enriching the operation object model is the next key work, which can further improve the arm operation ability.

References

1. Huan, S., Chao, J., Zhang, Y.J.: Safety design to underwater robotic arm. In: Long, S., Dhillon, B.S. (eds.) *Man-Machine-Environment System Engineering: Proceedings of the 21st International Conference on MMESE*. MMESE 2021. Lecture Notes in Electrical Engineering, vol. 800. Springer, Singapore. https://doi.org/10.1007/978-981-16-5963-8_55

2. Huan, S., Wang, S., Han, X., Bi, J.J.: Research on key technology to underwater robotic arm. In: Long, S., Dhillon, B. (eds.) *Man–Machine–Environment System Engineering*. MMESE 2019. Lecture Notes in Electrical Engineering, vol 576. Springer, Singapore. https://doi.org/10.1007/978-981-13-8779-1_41
3. Han, L., Yang, J.: Development summary report on underwater robotic arm . Shanghai aerospace systems engineering institute (2020)
4. Zhang, D.: Control system summary report on underwater robotic arm. Nanjing University of Aeronautics and Astronautics (2020)
5. Xiong, Y., Li, W.: Space robotics: modeling, control and vision. Huazhong University of science and technology press (2020)
6. Wang, Y., Tang, Z.: Research and software implementation of accuracy analysis of space manipulator. *Manned Spaceflight*, pp. 59–65 (2021)
7. Jiang, X., Feng, X.: Underwater vehicles. Liaoning Science and Technology press (2000)
8. Shen, Y.: The research of 6DOF robot trajectory planning and control algorithm. Nanjing University of Science and Technology (2017)
9. Jian, Y.: Working space and dexterity analysis and application for 6-DOF industrial robots. Huazhong University of science and technology press (2015)
10. Sun, J., Jiang, T.: Research on ergonomic evaluation indicator and methodology for interactive interface of spacecraft software. *Manned Spaceflight*, pp. 208–213 (2020)



Research on Development of Vehicular High Power Microwave Weapons

Bing Qian^(✉), Wei Yu, Heyuan Hao, and Haoran Zhu

Zhengzhou Campus, Army Academy of Artillery and Air Defense, Zhengzhou 450052, China
858563690@qq.com

Abstract. Vehicular high power microwave weapon is a kind of directional energy weapon which destroys electronic equipment by high power microwave beam. It has the advantages of fast attack speed, large attack range, both soft and hard killing, high cost-effectiveness ratio and so on. In the future, it has broad development prospect in the field of air defense operation. This paper summarizes the research status of high power microwave technology, introduces the latest progress of vehicular high power microwave weapons in the United States, Russia and China, and analyzes the future development trend of vehicular high power microwave weapons.

Keywords: High power microwave technology · Vehicular high power microwave weapons · HPM · HPMW · Development

1 Introduction

Vehicular high power microwave weapon (VHPMW) can launch high power microwave beam directionally, damage electronic equipment through ‘front door’ or ‘back door’ coupling. It has the advantages of fast attack speed, large attack range, both soft and hard killing, high cost-effectiveness ratio etc. It has broad development prospects in the field of future air defence operations, and may become the main weapon equipment for future information confrontation and air defense.

2 Research Status of Vehicular High Power Microwave Technology (VHPMT)

Typical vehicular high power microwave weapon system is usually composed of primary energy, pulse power source, microwave source, directional antenna, auxiliary system and others [1]. The basic working process is that the primary energy is compressed by the pulsed power source and transformed into a high-power pulsed electron beam, which generates high-power microwave radiation in the microwave source and irradiates the target through the high-gain directional antenna, thus producing interference and damage effects. With the high power microwave weapon attracting more and more attention, the research of high power microwave source technology, high gain directional antenna technology, high power pulse power source technology, high density primary energy technology and other key technologies has made great progress.

2.1 High Power Microwave Source Technology

High power microwave source is the core component of microwave weapon, and it is the key research direction of high power microwave technology. The power of microwave source fundamentally determines the killing ability of high power microwave weapon. High power microwave sources can be roughly divided into relativistic devices and non-relativistic devices. Relativistic devices mainly include relativistic klystron, relativistic magnetron, relativistic backward wave tube, magnetic insulation line oscillator and magnetic gyrotron. Non-relativistic devices mainly include Cyclotron oscillating tube, virtual cathode device, and multi-wave Cherenkov oscillator [2]. At present, the output power of various high-power microwave sources generally reaches several hundred megawatts to Gigawatt. Table 1 lists the advantages and main technical problems of various types of high power microwave sources.

Table 1. The advantages and main technical problems of high power microwave sources

Types	Advantages	Technical problems
Relativistic klystron	High power, high efficiency, phase stability	Complex structure and large volume
Relativistic magnetron	Simple structure, high power, repetition rate	Low efficiency, only 20–50%
Relativistic backward wave tube	High power, high efficiency, repetition rate	Secondary electron emission, field breakdown, pulse reduction
Magnetic insulation line oscillator	Low impedance, no need for external magnetic field	Low efficiency, pulse shortening problem
Magnetic gyrotron	High power, high efficiency	Single frequency band, narrow pulse width
Cyclotron oscillating tube	Fill the millimeter wave and submillimeter wave gaps, high efficiency	electron bombardment, secondary electron emission
Virtual cathode device	Simple structure, high power, easy tuning, light weight, wide pulse width	Low efficiency, single working frequency band, limited service life
Multi-wave Cherenkov Oscillator	High power, high efficiency	High requirement of working magnetic field, difficult to output power

2.2 High Gain Directional Antenna Technology

The equivalent radiation power of high power microwave weapons is proportional to the antenna gain in the radiation direction. The performance of the antenna determines whether the microwave can be effectively radiated, and directly affects the attack effect

of high power microwave weapons. The traditional large-aperture reflector antenna has huge volume and can only realize beam scanning through mechanical structure. So its application in high power microwave weapons has great limitations. The array antenna has the advantages of low profile, high gain, and easy to realize beam scanning, which is more suitable for high power microwave weapons. However, there are also some problems to be solved, such as power capacity, high power mode transformation and power distribution network, radiation beam scanning, and comprehensive design of high aperture efficiency array. In recent years, a variety of high power microwave antennas have been studied in China and abroad, including high power spiral antenna array based on radial power division, high power microwave antenna based on Rotman lens [3], and Linear array antenna based on the coupling feed of the narrow slot in a rectangular waveguide [4], which promote the development of high gain directional antenna technology.

2.3 High Power Pulse Power Source Technology

Pulse power technology is a technology that studies the generation and transformation of high-power electrical pulse through space-time compression of energy. New combat forces such as laser weapons, high power microwave weapons, electromagnetic railguns need the support of high power pulse power source technology. For vehicular high power microwave weapons, high power, high efficiency and repeatable pulse power source is the basis for its development towards higher power level. According to the technical route, the pulse power sources include Marx type, Tesla type, linear transformer type and inductive voltage superposition type [5]. In order to meet the mobility requirements of the vehicular high power microwave weapon system, it is necessary to greatly improve the power volume (weight) ratio and realize the miniaturization of the pulse power source. In recent years, the compact pulse power source based on LTD technology, double capacitance pulse shaping technology and solid-state wire pulse shaping technology have been developed, which promotes the development of the vehicular high power microwave weapon.

2.4 High Energy Density Primary Energy Technology

The energy storage of primary energy determines the 'silo' capacity of high power microwave weapons. The demand for mobility of vehicular high power microwave weapons also puts forward higher requirements for the energy density of primary energy. Common primary energy mainly includes chemical energy, chemical battery, super capacitor, fuel cell and nuclear battery. In recent years, with the rapid development of new energy electric vehicles, the chemical battery technology represented by lithium ion batteries has continued to develop. The battery energy density can reach 300 W·h/kg, which is expected to reach 500 W·h/kg by 2030 [6]. Chemical batteries have become a convenient solution for primary energy of high power microwave weapons. However, lithium ion batteries also have some limitations, such as slow charge and discharge speed, upper limit of energy density, easy ignition and explosion. Aluminum ion batteries, hydrogen fuel cells, nuclear batteries and other technologies may be applied to high power microwave weapon systems.

3 Development Status of Vehicular High Power Microwave Weapons

With the development of high power microwave technology, most countries around the world have started the development of vehicle high power microwave weapons. In terms of the overall development level, the United States, Russia and China have the highest research level.

3.1 The United States

The United States is at a leading level in the development of high power microwave weapons. In recent years, the United States Air Force Research Laboratory (AFRL), Raytheon, Leidos and Epirus have developed Several types of vehicular high power microwave weapon systems (VHPMWS).

Phaser anti-UAV system is integrated in the container, with diesel as the power source. By launch high power microwave to the target area, it can instantly damage the precise electronic components inside the UAV, and achieve the purpose of shooting down or blinding the enemy targets. The system can deal with not only a single target, but also a dense swarm of drone targets simultaneously. At present, the U.S. Air Force has deployed a small number of Phaser anti-UAV systems to counter asymmetric threats.

'Tactical High power Operational Responder' (THOR) is a high power microwave weapon dedicated to deal with the threat of small UAV swarms. The antenna of the system can quickly rotate and move up and down 360°, and use short pulse high power microwave to attack UAVs in different directions. The system can be transported on land by trucks or air by C-130 transport aircraft, and can be quickly assembled by two people within three hours [7]. The full capacity verification was completed in September 2019, and the overseas deployment assessment was carried out in 2020. In 2022, the next generation of high power microwave weapon system Mjолnir will be built on the basis of THOR.

Leonidas high power microwave system, which adopts solid-state GaN power amplifier, has the advantages of small size, light weight and low power consumption. It is the first miniaturized high power microwave system in the world. With an effective radiation power of 270 MW, it can achieve rapid launch, real-time interception of short-range and maneuvering threats, damage the electronic equipment carried by UAVs within 300 m. It can be integrated into ground combat vehicles to enhance the ability of maneuvering short-range air defense (SHORAD). In February 2022, Leonidas Pod was launched, which can be deployed on UAVs. Work with Leonidas ground systems to achieve greater power and scope and create layered defense areas.

3.2 Russia

With the deep accumulation and practice of microwave technology, Russia has developed many high power microwave weapons.

Krasukha series weapons are the latest representative of Russian electronic warfare weapons, including Krasukha-2 and Krasukha-4 models [8]. The Krasukha-2 transmitting system adopts the reflector antenna. The reflector is a parabolic surface with a

diameter of about 2.7 m. The antenna feed is composed of one main feed horn and two secondary feeds. The whole reflector antenna is installed on a 360° rotating platform, and the maximum pitch angle can reach 5°. In the range of 45° of the main lobe of the antenna, effective interference can be implemented through the side lobe, and the working distance to the warning aircraft can reach 150–300 km. The Krasukha–4 system can be remotely delivered by the IL-76 transport aircraft, and can be used to combat E–8C battlefield surveillance aircraft, ‘Predator’ unmanned reconnaissance attack aircraft, ‘Global Hawk’ unmanned strategic reconnaissance aircraft, and US Lacrosse radar spy satellites. Krasukha–2 and Krasukha–4 systems are an important part of Russia’s advanced electronic warfare capability. The joint use of the two systems can effectively prevent radar detection of enemy and make soft damage to electronic and communication equipment within hundreds of kilometers.

3.3 China

In recent years, China has also attached great importance to the research and development of vehicular high power microwave weapons. China Institute of Engineering Physics, National Defense University, University of Electronic Science and Technology, Northwest Institute of Nuclear Technology and other units have done a lot of research [9]. Currently it is transforming from laboratory research to practical application. The vehicular high power microwave weapon developed by China Weapons and Equipment Group was demonstrated at Zhuhai Aviation Exhibition in 2021.

4 The Trend of Future Development

At present, although high power microwave technology has made great progress and shows great potential, it is still not fully meet the needs, and there is still a considerable distance from putting into practice. The next step should focus on the following aspects to seek breakthroughs.

4.1 Miniaturization of Weapon System

The development trend of fast-paced and invisible warfare in the future puts forward higher requirements for the maneuverability and concealment of air defense weapons and equipment. The characteristics of silence and invisibility in the attack of high power microwave weapons meet the requirements of concealment. However, due to the current development of high power microwave sources, pulse power sources, primary energy and other technologies, vehicular high power microwave weapon system has large volume and weight, and poor operational maneuverability. In the future, it is necessary to break through the key technologies of solid-state microwave source, new materials with anti-penetration characteristic and high density energy storage, optimize the system integration design, solve the problems of large volume and high power consumption, and deal with the future complex battlefield environment.

4.2 Increase of Killing Distance

Limited by the power of high power microwave source, system energy storage capacity and energy conversion efficiency, the damage distance of vehicular high power microwave weapon is basically at the kilometer level, and the combat radius is small, which can only kill small UAVs or UAV colonies. With the in-depth study of high power microwave protection technology, the combat radius of existing vehicular high power microwave weapon systems may be further compressed. In the future, it is necessary to improve the output power of high power microwave sources and explore microwave power synthesis technology to achieve effective killing of medium and large UAVs and even manned aircraft at a farther distance.

4.3 Electromagnetic Compatibility Optimization

In the process of vehicular high power microwave weapons attacking targets, microwave radiation is mainly directed to the target through the antenna main lobe, but it is also inevitable to radiate part of the energy from the antenna side lobe. In terms of the high power microwave with output power of Gigawatt, a small part of the energy of the side lobe radiation is enough to cause damage or interference to other parts of the weapon system and even other air defense weapon systems. In the future, electromagnetic compatibility and combat coordination between vehicle-mounted high-power microwave weapons and other weapons and equipment can be realized through in-depth research on side-lobe suppression, high-power microwave protection, time-domain, space-frequency interleaving and other technologies.

4.4 Improvement of Detection and Perception Capability

At present, small UAV or the Swarms are the main killing targets of vehicular high power microwave weapons (VHPMW). Due to the low flight altitude, slow flight speed, less radar cross section (RCS) and weak electromagnetic signals, there are a series of problems in the process of resistance, such as hardly to detect, time-consuming to detect, nature of the target is difficult to confirm and not conducive to continuous and stable tracking. Unable to detect the sensing target means impossible to destroy the target. In the future, the detection information of radar, visible light, infrared, radio frequency, acoustics and sensor combination should be comprehensively used to realize the detection perception and real-time tracking of UAV.

5 Conclusion

This paper mainly introduces the research progress of high power microwave technology and the development of vehicular high power microwave weapons, and analyzes its research trend. As a weapon of electronic warfare, vehicular high power microwave weapons have attracted more and more attention from all countries and will play an important role in future air defense operations.

References

1. Ni, G., Gao, B.: Review of high power microwave weapon. *Fire Control Command Control* (08), 5–9 (2007)
2. Xu, Z., Feng, J.: Current situation and developments of high power microwave sources. *Vac. Electron.* (02), 18–27+1 (2015)
3. Zhou, X.: High power microwave antenna based on rotman lens. China Academy of Engineering Physics, M. A. dissertation (2018)
4. Yu, L.: Novel high power microwave scanning array antenna. Graduate School of National University of Defense Technology, Ph. D. dissertation (2019)
5. Qiu, Y.: Investigation of control system and EMC based on high power pulse generator. Graduate School of National University of Defense Technology, Ph. D. dissertation (2018)
6. Jin, W., Liao, M., Huang, J., Wei, Z.: The technological trend of high energy density Li-ion batteries for vehicles-based on data of global patents. *Energ. Storage Sci. Technol.* **11**(1), 350–358 (2022)
7. Niu, H., Wu, Y., Li, M.: Research on overseas high power microwave weapon development. *J. Aerodyn. Missile* (08), 12–16+23 (2021)
8. Wang, P.: A survey of the main research and development units for electronic warfare products and equipment development in contemporary Russia. *Nat. Defense Technol.* (06), 68–76 (2020)
9. Wang, Y., Binkai, Y., Wang, L.: Research on the development of high power microwave weapon based on patent analysis. *Aero Weaponry* (05), 19–25 (2019)



The Near-Infrared Forearm Vessel Image Segmentation and Application Using Level Set

Haoting Liu^(✉), Yajie Li, and Yuan Wang

Beijing Engineering Research Center of Industrial Spectrum Imaging, University of Science and Technology Beijing, Beijing 100083, China
liuhaoting@utsb.edu.cn

Abstract. A robust level set-based near-infrared forearm vessel image segmentation method is proposed. First, a near-infrared forearm image capture device is developed. More than 500 forearm images are accumulated by using this device. Second, an image segmentation algorithm is designed. The multiscale second order local structure of image is considered to enhance the vessel edges. The distance regularized level set evolution approach is used to implement the vessel segmentation. Third, the proposed algorithm is employed to assist the searching of the potential Arteriovenous Fistula Thrombosis (AFT). Many experiment results have shown the proposed system and method can locate the superficial vessels of forearm correctly; and the recognition rate of AFT is better than 95% .

Keywords: Near-infrared image · Vessel segmentation · Level set · Arteriovenous fistula thrombosis · Edge enhancement

1 Introduction

The arteriovenous fistula thrombosis (AFT) commonly happens to the dialysis patients [1]. Because the patients have to use the invasive therapy to clean their blood, it is very easy to form the thrombosis in their forearms. In recent years, the near-infrared imaging sensor together with its image processing method [2] are used to identify AFT. Comparing with other methods, the near-infrared imaging sensor can get the intuitive data, in addition its recognition accuracy is high; as a result, it has potential application value in medical device R&D. When implementing the AFT searching, the most important step is to enhance the vessel image and segment the vessel contour; then the image recognition method can be used. The current difficulties in this area lie in: the contrast of vessel image is low and the edge of vessel is blur. Therefore, it is necessary to develop a robust system and method to carry out the vessel segmentation task.

In this paper, the near-infrared vessel image segmentation [3] system and method of forearm are developed. First, a near-infrared forearm image capture device is designed and developed. This device include the light source, the infrared camera, and the structural support. Second, a robust vessel segmentation method is proposed. The multiscale second order local structure of image is considered to enhance the vessel edges [4]. Because the level set technique [5] has been proofed to be one of the best solutions

for non-rigid target segmentation, the distance regularized level set evolution approach [6] is used to implement the vessel segmentation. The main contributions of this paper include: 1) A near-infrared forearm vessel analysis system and its application method are developed. 2) A level set method together with the image edge enhancement technique is considered for a robust vessel segmentation.

2 Proposed Computational Method

2.1 Computational Flow Chart

Figure 1 presents the computational flow chart of proposed near-infrared vessel segmentation method. When the proposed method gets an image, first, the normalization processing and the denoising computational will be performed. The median filter is used to handle the system noises. Second, the image enhancement is carried out. Because the thicknesses of skin and fat are various, the region contrast and edge blur of near-infrared vessel are totally different among people. In this paper, the multiscale second order local structure of image is used as the vessel enhancement filter. Both the contour and the intensity of vessel can be strengthened after using the basis of eigenvalues of Hessian. Third, a distance regularized level set evolution technique is employed for image segmentation. The new evolution method of level set is used to improve the numerical accuracy of level set method. Finally, some image features and classifiers can be considered to carry out the AFT identification task.

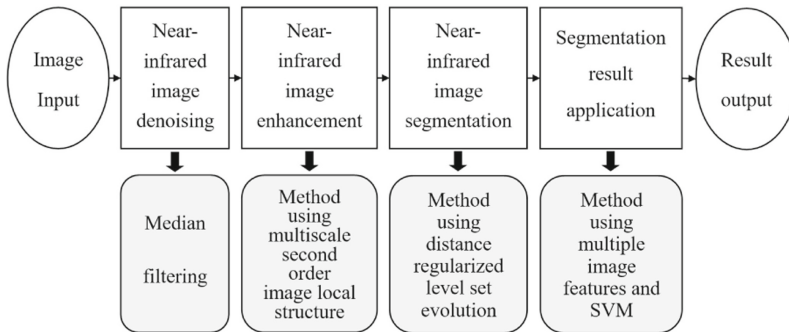


Fig. 1. The computational flow chart of near-infrared vessel segmentation and application

2.2 Key Computational Methods

As we have stated, the near-infrared image will have series of problems, such as the low region contrast, strong system noise, weak vessel edge, and blur vessel region, etc. To conquer these drawbacks, a multiscale second order local structure of image is computed to enhance the image details. An expansion approximates the structure of an image includes the gradient vector and Hessian matrix in this method; and then the

geometrical structures of vessel can be kept well. Other methods, including Retinex, Contrast Limited Adaptive Histogram Equalization (CLAHE), or Gammar correction can also be used for enhancement; however, because the weak edge of near-infrared image, the geometrical prior information is important in vessel enhancement, as a result only the method in [4] is utilized in this paper.

The level set method is a numerical technology for interface tracking and shape modelling. It is widely used in image segmentation area in recent years. The classic level set easily meets the problems of irregular evolution and slow convergence which will cause numerical errors and long term iteration. To improve the computational effect of level set method, a distance regularized level set evolution approach in [6] is considered. Equations (2.1) to (2.5) show its computational model. Clearly, the proposed level set method has a regularization term and an external energy term. A finite difference scheme is also used to implement the level calculation. More general initialization of level set can also be employed when using this model.

$$\varepsilon(\phi) = \mu \int_{\Omega} p(|\nabla\phi|)dx + \lambda \int_{\Omega} g\delta_{\varepsilon}(\phi)|\nabla\phi|dx + \alpha \int_{\Omega} gH_{\varepsilon}(-\phi)dx \quad (2.1)$$

$$\frac{\partial\phi}{\partial t} = \mu \operatorname{div}[d_p(|\nabla\phi|)\nabla\phi] + \lambda\delta_{\varepsilon}(\phi)\operatorname{div}\left(g\frac{\nabla\phi}{|\nabla\phi|}\right) + \alpha g\delta_{\varepsilon}(\phi) \quad (2.2)$$

$$g = \frac{1}{1 + |\nabla G_{\sigma} * I|^2} \quad (2.3)$$

$$\delta_{\varepsilon} = \begin{cases} \frac{1}{2\varepsilon} [1 + \cos(\frac{\pi x}{\varepsilon})] & |x| \leq \varepsilon \\ 0 & |x| > \varepsilon \end{cases} \quad (2.4)$$

$$H_{\varepsilon}(x) = \begin{cases} \frac{1}{2} [1 + \frac{x}{\varepsilon} + \frac{1}{\pi} \sin(\frac{\pi x}{\varepsilon})] & |x| \leq \varepsilon \\ 1 & x > \varepsilon \\ 0 & x < -\varepsilon \end{cases} \quad (2.5)$$

where $\varepsilon(\phi)$ is an energy function; ϕ is a level set function which is located in domain Ω ; p is an energy density function; symbol ∇ is the gradient operator; symbol $|\cdot|$ means the modulus; g is an edge indicator function of image; G_{σ} is a Gaussian kernel with a standard deviation σ ; I is an image; ε is a parameter and $\varepsilon = 1.5$ in this paper; symbol $\operatorname{div}(\cdot)$ is the divergence operator; d_p is the derivative of potential function $p(s)$, and $p(s) = s^2$ in this paper; symbols α , μ , and λ are the weights of model, $\alpha = 1.5$, $\mu = 0.04$, and $\lambda = 5.0$ in this paper.

3 Experiments and Discussion

A series of test and evaluation experiments were performed to assess the effectiveness of proposed method. All the simulation programs were written by Python (Pycharm 2020) in our PC (4.0 GB RAM, 1.70GHz Intel (R) Core(TM) i3-4005U CPU).

3.1 Experiment Data Source

A new near-infrared forearm image capture device was developed. Figure 2 presents its prototype photo and the corresponding image data. In Fig. 2, (a) is the device photo; (b) illustrates our near-infrared images of forearm vessel. From Fig. 2, the proposed system include at least three parts: the near-infrared camera, the light source, and the structural support. When using this device, the subject needs to put his or her forearm under the vision field of camera, then the image can be recorded. Because different people have different skins, body fats, and vessel sizes, the imaging effects of vessel present dramatically diversities. For example, some vessels have the bending structures, some vessels are obstructed by other vessels, and others are affected by the photography posture of forearm. As a result a robust vessel segmentation method should be studied.

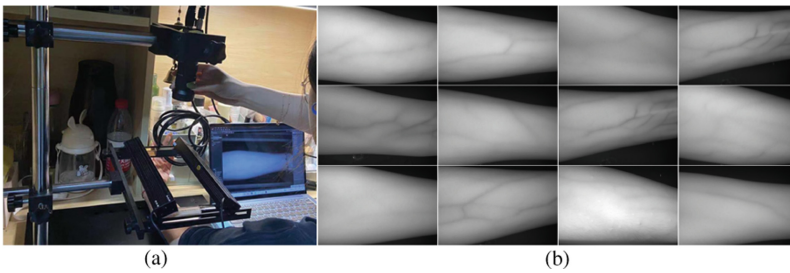


Fig. 2. The image samples of near-infrared vessel analysis device and image data

3.2 Evaluation of Vessel Segmentation

Figure 3 illustrates the image processing of vessel segmentation. In Fig. 3, (a) and (e) are the original images captured by the near-infrared camera; (b) and (f) are the results of image enhancement of (a) and (e), respectively; (c) and (g) are the 3D visualization processing results of initial segmentations of (b) and (f); and (d) and (h) are the final segmentation results of (a) and (e). From Fig. 3, the region contrast and the edge definition can be improved clearly after the image enhancement processing. The classic OTSU method is considered to get the initial segmentation of those images after enhancement. And the level set in [6] can find the accurate contour of vessel. Some other segmentation methods are also tested in this paper, such as the classic Vese's method [7] and the active contour model [8], etc. After a series of comparisons, our method can behave better computational stabilities in the weak edge and low region contrast images. This result may come from the fact that both the image enhancement and the robust contour segmentation are considered in our model.

After the vessel segmentation, the classifier can be used for AFT detection [9]. Because the size of near-infrared image is big, i.e., its size is 5472×3648 ; it is impossible to implement a global searching throughout the whole image to find the AFT in a real-time application. To control the processing speed of detection method, the searching regions only are set around the segmentation result of vessel. Multiple image features

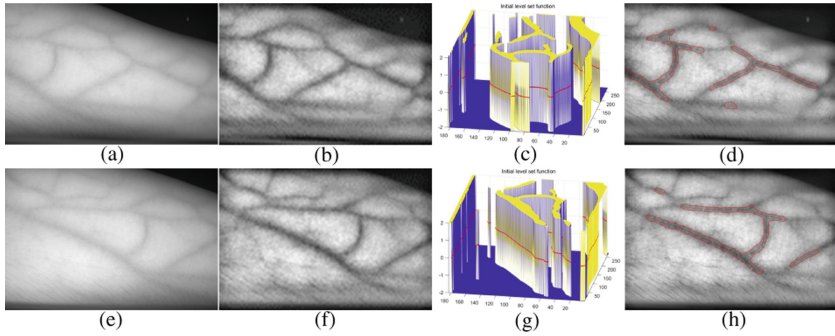


Fig. 3. The proposed computational flow chart of near-infrared vessel segmentation

are computed to identify the AFT, they are the geometric feature, the gray intensity feature, the edge gradient feature, and the Gray Level Co-occurrence Matrix (GLCM) texture features. All these features should be normalized before the further processing. Then the Support Vector Machine (SVM) is used to classify the AFT from the pixels near the vessel. The amount of training data set is 240, while the amount of test data is 160. After a series of test, the best correct classification rate can reach 96.25% if the model of distance regularized level set evolution approach is controlled properly.

3.3 Discussions

The chronic kidney disease has become a global public health problem in recent years. The dialysis is an effective treatment measurement however the AFT will be induced even only after a short-time intervene. The imaging technique can be used to detect AFT in its early time, thus a near-infrared forearm vessel image capture and segmentation system and its method are developed in this paper. The proposed system and method at least have three merits. First, its computational effect is good. Extensive experiment results have shown the superficial vessel can be segmented well by using this system. Second, its computational function is powerful. Both the segmentation and classification of vessel and AFT can be solved by our system and method. Third, the algorithm scalability is also well. The multiscale second order local image structure is used to enhance the vessel edges and the distance regularized level set evolution approach is considered to implement vessel segmentation. Actually, other image enhancement methods and level set models can also be utilized in future. Our method also has some drawbacks. For example, its processing speed is comparable slow, the average computational time is tens of seconds. In future, other fast algorithm will be designed in our method and the hardware acceleration technology will also be considered.

4 Conclusion

A near-infrared forearm vessel image segmentation method is developed in this paper. First, an intelligent device is designed to implement the near-infrared image collection task. This device at least includes the light source, near-infrared camera, and attitude

adjustment support. Second, a robust image segmentation method is proposed. The multiscale second order local structure of image is used to carry out the image enhancement mission; and a kind of distance regularized level set evolution method is utilized to realize the contour segmentation of vessel. Third, the detection task of AFT is performed by using the image segmentation result. Multiple image features and SVM are employed to detect the AFT. In future, the deep learning network will also be tested to improve the image effect of the near-infrared image; and more structure constrain functions will be considered in the level set model.

Acknowledgement. This work was supported by the National Natural Science Foundation of China under Grant No. 61975011, the Fund of State Key Laboratory of Intense Pulsed Radiation Simulation and Effect under Grant No. SKLIPR2024, and the Fundamental Research Fund for the China Central Universities of USTB under grant No. FRF-BD-19-002A.

References

1. Cattini, S., Rovati, L.: An optical technique for real-time monitoring of hemolysis during hemodialysis. *IEEE Trans. Instr. Meas.* **65**, 1060–1069 (2016)
2. Lee, S., Namgoong, J.M., Kim, Y., et al.: Multimodal imaging of laser speckle contrast imaging combined with mosaic filter-based hyperspectral imaging for precise surgical guidance. *IEEE Trans. Bio-med. Eng.* **69**, 443–452 (2022)
3. Li, Y., Qiao, Z., Zhang, S., et al.: A novel method for low-contrast and high-noise vessel segmentation and location in venepuncture. *IEEE Trans. Med. Imag.* **36**, 2216–2227 (2017)
4. Frangi, A.F., Niessen, W.J., Vincken, K.L., Viergever, M.A.: Multiscale vessel enhancement filtering. In: Wells, W.M., Colchester, A., Delp, S. (eds.) *MICCAI 1998*. LNCS, vol. 1496, pp. 130–137. Springer, Heidelberg (1998). <https://doi.org/10.1007/BFb0056195>
5. Sum, K.W., Cheung, Y.S.: Vessel extraction under non-uniform illumination: a level set approach. *IEEE Trans. Bio-med. Eng.* **55**, 358–360 (2008)
6. Li, C., Xu, C., Gui, C., et al.: Distance regularized level set evolution and its application to image segmentation. *IEEE Trans. Image Process.* **19**, 3243–3254 (2010)
7. Chan, T.F., Vese, L.A.: Active contours without edges. *IEEE Trans. Image Process.* **10**, 266–277 (2001)
8. Li, C., Kao, C.Y., Gore, J.C., et al.: Implicit active contours driven by local binary fitting energy. In: *IEEE Conference on Computer Vision and Patter Recognition*, pp. 1–7 (2007)
9. Roychowdhury, S., Koozekanani, D.D., Parhi, K.K.: Blood vessel segmentation of fundus images by major vessel extraction and subimage classification. *IEEE Trans. Biomed. Health* **19**, 1118–1128 (2015)



Evaluation of CCGA Solder Pillar Grinding Effect Based on End-Face Imaging Analysis

Mengmeng Wang¹, Haoting Liu¹(✉), and Shaohua Yang²

¹ Beijing Engineering Research Center of Industrial Spectrum Imaging, University of Science and Technology Beijing, Beijing 100083, China

liuhaoting@ustb.edu.cn

² Northwest Institute of Nuclear Technology, Xi'an 710024, China

Abstract. Due to the advantages of Ceramic Column Grid Array (CCGA) packaging technology such as the good thermal matching and vibration resistance, it is often used for the manufacturing of high-end chips. However, in practical engineering applications, CCGA has many process problems, such as the oxidation of bottom surface of lead column, and the poor coplanarity of welding column end. The CCGA welding column is manually ground for end face flatness processing, it is easy to lead to a poor end face coplanarity, skewing of the welding column and other issues, so that the grinding effect is difficult to be guaranteed. This paper proposes a CCGA column grinding effect evaluation method based on end face imaging analysis, and we use image processing, feature extraction, machine learning algorithms, and other technologies to achieve the binary classification of CCGA column grinding pictures. Compared with other related algorithms, the method proposed in this paper is highly targeted and its effect is stable. It puts forward solution ideas and methods for existing industrial problems.

Keywords: Feature extraction · Machine learning · SVM · CCGA

1 Introduction

With the development of microelectronic packaging technology in the direction of high density, large size and high performance, ceramic planar array packaging is widely used in aviation, aerospace as well as the military and other fields [1]. Ceramic Column Grid Array (CCGA) is one of the most widely used ceramic planar array packaging forms at present. At present, the production of CCGA-packaged chips has basically realized the automatic manufacturing process in China. However, during the processing of lead-out end of chip, manual grinding is still used to process the end surface flatness of CCGA. Obviously, the quality of manual grinding is closely related to the initial end face state of CCGA and manual operation experiences; thus the grinding effect is difficult to guarantee. In order to solve the above-mentioned problems, this paper proposes a method for evaluating the grinding effect of CCGA pillars based on the end-face imaging analysis. In this paper, image pre-processing and feature extraction are carried out on the grinding image of CCGA welding column end face. We choose three

features that can better reflect the characteristics of the pictures in the dataset. Then, we optimize the parameters of the Support Vector Machine (SVM), and use it to classify the grinding effect of the end face of CCGA welding column, which can provide a basis for the finalization of the manufacturing and assembly process of related aerospace products (Fig. 1).

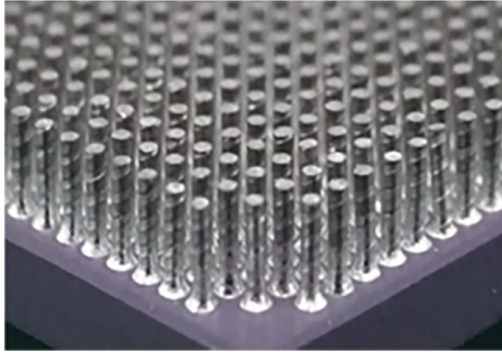


Fig. 1. Example of CCGA packaging product

2 Algorithm Flow Design

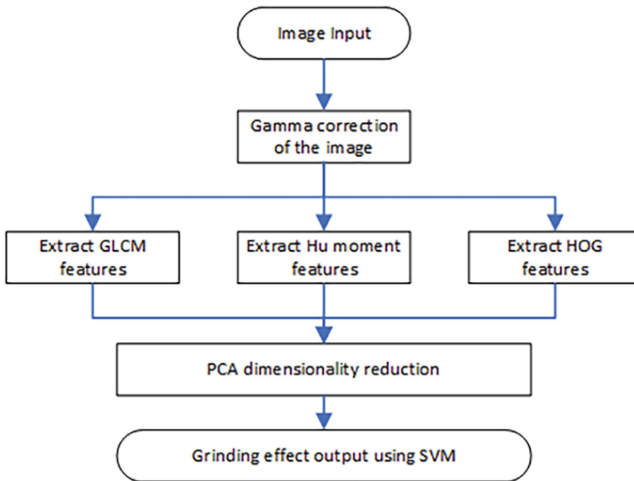


Fig. 2. Algorithm flow chart

The algorithm flow chart of CCGA solder post grinding effect evaluation based on end face imaging analysis proposed in this paper is as follows (Fig. 2):

1. The image of end face of CCGA solder post after grinding are collected.

2. The image feature parameters are extracted and normalized.
3. The Principal Component Analysis (PCA) method is used to reduce data dimensionality.
4. The trained SVM classification model is used to evaluate and classify the grinding effect of welding column end face.

3 Key Technologies

3.1 Grinding Image Features Extraction

In order to realize the evaluation and classification of grinding effect of CCGA column end face, and combine with the image characteristics of CCGA welding column end face before and after grinding, three image features are designed.

The first one is the Gray-Level Co-occurrence Matrix (GLCM), which uses the gray value distribution between pixels in the grayscale image to distinguish different textures. Since the dimension of GLCM is large, it is not directly used as a texture feature, but the statistic results calculated from the GLCM is selected as the texture feature. In this paper, four statistic values, the Angular Second Moment (ASM), Entropy (ENT), Contrast (CON), and Inverse Differential Moment (IDM), are used as texture classification features.

$$ASM = \sum_i \sum_j P(i, j)^2 \quad (3.1)$$

$$ENT = - \sum_i \sum_j P(i, j) \log(P(i, j)) \quad (3.2)$$

$$CON = \sum_i \sum_j (i - j)^2 P(i, j) \quad (3.3)$$

$$IDM = \sum_i \sum_j \frac{P(i, j)}{1 + (i - j)^2} \quad (3.4)$$

The second feature is the Histogram of oriented gradient (HOG) feature. The realization idea of HOG feature is to splice the local gradient statistical features of image as the total feature. Specifically, the image is divided into blocks in units of blocks as the basic feature extraction unit, and then the blocks are divided into $N \times N$ cells as the basic statistics. In the cell, the gradient direction of each pixel is counted in the cell to form a gradient histogram, and then the gradient histograms of all cells in each block are combined and normalized. Finally all the block features are combined to form the HOG feature.

The third feature utilizes the Hu moment of image, which is a moment group with translation, rotation and scale invariance constructed on the basis of ordinary moments. Seven invariant moment groups included in the Hu moment are composed of the linear combination of the second-order and third-order central moments.

3.2 PCA Method

Rich features will undoubtedly provide richer information, but not all features can effectively evaluate the grinding effect. In order to reduce the computational complexity and avoid the possible dimension disaster of subsequent classification, dimensionality reduction must be carried out before classification identification to improve the computational efficiency [2]. The method of principal component analysis in this paper is to calculate and subtract the average value of original data set. Then, we calculate the covariance matrix and its eigenvalues. The covariance matrix is defined in formula (3.5). Third, the eigenvalues are sorted from large to small, and the K largest eigenvectors are determined according to the reverse order of the sorting results. These eigenvectors will form a matrix for data conversion, which uses n features to convert the original data into a new space. In PCA dimensionality reduction, we need to find the maximum K eigenvectors of the sample covariance matrix XX^T , and then use the maximum K eigenvectors to form a matrix for low dimensional projection dimensionality reduction. According to the above principal component analysis, the dimension of 611 feature parameters extracted in this paper is reduced, and finally 48 main components are gotten.

$$\sum_X = \begin{bmatrix} \sigma_{X,1,1} & \cdots & \sigma_{X,1,n} \\ \vdots & \ddots & \vdots \\ \sigma_{X,n,1} & \cdots & \sigma_{X,n,n} \end{bmatrix} \quad (3.5)$$

$$\sigma_{X,i,j} = E[(c_{X,i} - \mu_{X,i}) - (c_{X,j} - \mu_{X,j})] \quad (3.6)$$

3.3 SVM Classifier Parameters Optimization

The SVM is a machine learning method based on statistical learning theory, which is famous for its advantages of small sample size and small structural risk [3]. Since the training data used in this paper is nonlinearly separable, it is necessary to map the sample data from the original space to the high-dimensional space by introducing a kernel function, so that the original sample data is transformed into a linearly separable case in the high-dimensional space. Kernel functions can be expressed as the inner product of two vectors in a feature space. The introduction of kernel functions can greatly simplify the calculation by implementing all operations in the feature space only through the inner product between points without having to know the coordinate form in the feature space. Commonly used kernel functions are linear kernel functions, polynomial kernel functions, radial base kernel functions, and Sigmoid kernel functions, etc. Different kernel functions and the same kernel functions with different parameters correspond to different mapped spaces, thus showing different properties, which determine different nonlinear problem solving capabilities, as well as different scopes and environments. In this paper, we select the radial basis kernel function:

$$k(x, y) = e^{-(\gamma \|x-y\|)^2} \quad (3.7)$$

Two parameters that have the greatest impact on the classification effect in the algorithm are the penalty factor C and the kernel function parameter γ . The penalty factor

C is a trade-off between the simplicity of the misclassified sample kernel interface. The larger the value of C , the greater the penalty for the classification error, and the easier it is to cause overfitting. The kernel function parameter γ will affect the action range of Gaussian function corresponding to the support vector, thereby affecting the generalization performance. The larger the value of γ , the more the Gaussian function acts near the support vector samples, and the worse the classification effect of unknown samples is. Therefore, choosing the appropriate penalty factor C and the Gaussian kernel function γ parameter value is crucial to the SVM classification accuracy [4].

In this paper, the grid search method is used to find the optimal parameter values. The grid search method is an exhaustive search method for specifying parameter values. The optimal learning method is obtained by optimizing the parameters of the estimated function through cross-validation [5]. That is to say, the possible values of the penalty factor C and the kernel function parameter γ are arranged and combined, and all the combined results are generated into a “grid”. Each combined parameter is used for SVM training, and cross-validation is used to evaluate the training effect. SVM classifier with optimal parameter combination.

4 Experiments and Discussion

4.1 Data Source Acquisition

Due to the high manufacturing cost and small quantity of aerospace-grade chips packaged in CCGA, it is difficult to obtain a large number of image data of solder post end face grinding currently. Therefore, this paper uses many pictures before and after laser cleaning of the alloy material surface similar to the end face of the welding column and a small number of grinding pictures of the end surface of CCGA welding column to build the data source to evaluate the grinding effect of the end surface of the CCGA welding column. The final training set data has 76 pictures. The test set data has 70 images. The data set used in this paper is the gray images, and the images need gamma correction before extracting features. In Fig. 3, (a) is the original image and (b) is the corrected image using gamma.

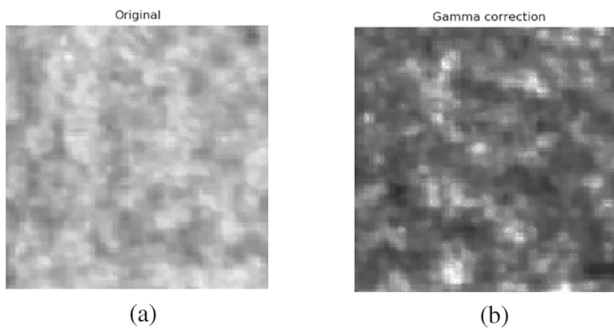


Fig. 3. Original images and preprocessing effects

4.2 Experimental Results

In this section, we will take an image from the dataset as an example. First of all, we will do gamma correction. And then four features of GLCM and HOG are extracted. At the same time, we will grayscale the image to extract Hu moment features. At this point, we get an eigenvector with 611 elements. After PCA dimensionality reduction, we finally get an eigenvector with 48 elements. Next, we put the feature vectors above into SVM. Through the grid search method, the optimal SVM parameters are obtained. The radial basis kernel function is selected as the kernel function, the penalty factor C is 1000, and the kernel function parameter γ is 1. The final training result accuracy rate is 87.50%, and the test result accuracy rate is 87.14%. Some classification results are shown in Fig. 4. Among them, the surface of (a) is smooth and the texture is uniform, which belongs to the category of good grinding effect. On the contrary, there are large black spots on the surface of (b) and large color difference and uneven texture on the surface of (c), which belong to the category of poor grinding effect.

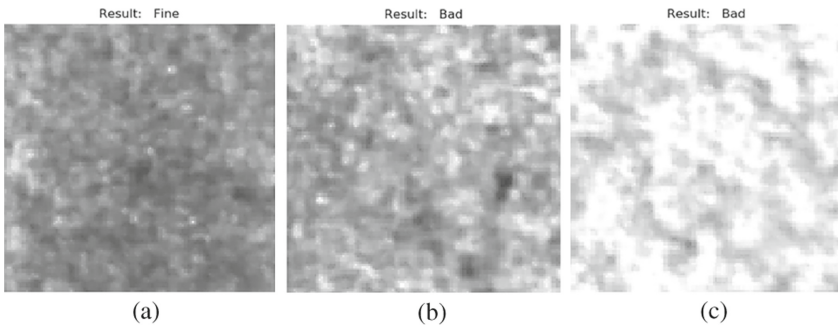


Fig. 4. Example of classification results

We perform some comparative experiments. Table 1 present the corresponding result. From these results, the final accuracy cannot meet the requirement whether one feature is selected or two are combined.

Table 1. Comparative experimental results

Features	Training accuracy	Test accuracy
Hu moment	50.00%	41.43%
HOG	50.00%	62.86%
GLCM Hu moment	75.00%	80.00%
GLCM HOG Hu moment	87.50%	87.14%

5 Conclusion

A method for evaluating the grinding effect of CCGA solder pillars based on end-face imaging analysis is proposed. Starting from the image features of CCGA end face grinding, the machine learning algorithm is applied to achieve the classification of different grinding effects. Using the trained SVM classifier to evaluate the grinding effect of chip CCGA, the experimental results show that the proposed algorithm is effective and feasible. The SVM method used has complete theoretical support, and can eventually be converted into a quadratic programming problem. Compared with methods such as neural networks, it is supported by more reliable mathematical principles. Due to the high cost of grinding end face of CCGA solder posts for aerospace-grade chips, the amount of data is small currently. The method proposed in this paper uses fewer samples with the feature extraction, PCA and machine learning algorithms to obtain better classification accuracy. To sum up, this method can provide accurate and efficient decision-making for the evaluation of grinding effect of CCGA solder column end face and provide a basis for the manufacturing and assembly of high-end chips.

Acknowledgement. This work was supported by the National Natural Science Foundation of China under Grant No. 61975011, the Fund of State Key Laboratory of Intense Pulsed Radiation Simulation and Effect under Grant No. SKLIPR2024, and the Fundamental Research Fund for the China Central Universities of USTB under grant No. FRF-BD-19-002A.

References

1. Reza, G.: CCGA packages for space applications. *Microelectron. Reliab.* **46**, 2006–2024 (2006)
2. Maldonado, S., Weber, R., Famili, F.: Feature selection for high-dimensional class-imbalanced data sets using support vector machines. *Inf. Sci.* **286**, 228–246 (2014)
3. Sanchez, V.: A advanced support vector machines and kernel methods. *Neurocomputing* **69**, 1754–1759 (2006)
4. Bacau, I., Kotropoulos, C., Pitas, I.: Demonstrating the stability of support vector machines for classification. *Signal Process.* **86**, 2364–2380 (2006)
5. Wang, X., Liu, Z.: Identifying the parameters of the kernel function in support vector machines based on the grid-search method. *Period. Ocean Univ. China* **35**, 859–862 (2005)



Near-Infrared Vascular Image Enhancement Using Deep Convolutional Neural Network

Yajie Li, Haoting Liu^(✉), and Yuan Wang

Beijing Engineering Research Center of Industrial Spectrum Imaging, School of Automation and Electrical Engineering, University of Science and Technology Beijing, Beijing 100083, China
liuhaoting@ustb.edu.cn

Abstract. Near-infrared vascular images play an important role in the diagnosis and treatment of vascular diseases. However, near-infrared vascular images often have problems such as low image quality and unclear vascular patterns. To solve these problems, we propose a Deep Convolutional Neural Network (DCNN) auto-encoder for image enhancement to enhance vascular structures and suppress non-vascular structures. We also collect a datasets of 156 images for the training and validation testing of the model; and further we use the full-reference image quality assessment metrics, i.e., Peak Signal to Noise Ratio (PSNR) and Structural SIMilarity (SSIM) to quantitatively evaluate the image enhancement effect of this model. The experimental results show: compared with the traditional image enhancement algorithm, the enhanced image quality of the Residual Convolutional Auto-Encoder (RCAE) model is better and more similar to the original image.

Keywords: Image enhancement · Vascular pattern · Deep Convolutional Neural Network

1 Introduction

Medical image processing plays a very important role in clinical diagnosis and participates in every important procedure of diagnosis and treatment. Compared with medical imaging methods such as the Digital Subtraction Angiography (DSA), Computed Tomography (CT), and Magnetic Resonance Imaging (MRI), the near-infrared imaging has the advantages of simple operation, low price, and contains superficial blood vessel information, which has a guiding role in the diagnosis and treatment of vascular diseases such as hemangioma, vascular embolism, arteriosclerosis, and varicose veins.

However, due to the influence of different experimental conditions, acquisition environment, subject's fatness, and skin colour, the quality of the obtained near-infrared blood vessel images is quite different. In order to solve the problems of low contrast, unclear blood vessel lines, and loss of blood vessel details in near-infrared blood vessel images, we propose a Deep Convolutional Neural Network (DCNN) auto-encoder for image enhancement to improve vascular structures and suppress non-vascular structures.

2 Proposed Method

2.1 Model Architecture

To enhance near-infrared vascular images, we employ a Residual Convolutional Auto-Encoder (RCAE) architecture for supervised training on the images [1]. RCAE consists of the encoder and decoder blocks that are linked through a residual connection. The encoder uses an input vascular image, and the decoder attempts to reconstruct its enhanced version. In our system, the input images are grey with a fixed-size of 320×240 pixels.

The encoder of RCAE consists of 3 blocks, where each block includes a convolution, activation, and normalization. These blocks are connected to each other in sequence through pooling operation which can reduce the spatial dimensions of the effective input at every stage. In this system, the max-pooling is performed over the window of 2×2 across the encoder.

On the decoder side, we have a succession of 3 decoding blocks: each consisting of a convolution and fractionally-strided convolution filters, along with activation and normalization layers. The convolutional layers consist 64 kernels in total, which have same size of 5×5 . And we retain the stride of 2 for fractionally-strided convolutions in the decoder. The network includes a residual transmission across every pair of blocks in encoder and decoder. This leads to a differential component that learns the difference between the input and target across layers. The Rectified Linear Unit (ReLU) has been chosen as the activation operator in the encoder and the decoder; and each block is interspersed with a batch normalization layer to reduce the dependence on the training datasets and help the generalization [2]. Details of the architecture and parameters of RCAE are showed in Table 1:

Table 1. Architecture and parameters of RCAE

RCAE	Encoder	Block1	Convolution ($64 \times 5 \times 5$) Activation (ReLU) Normalization Pooling (2×2)
		Block2	Convolution ($64 \times 5 \times 5$) Activation (ReLU) Normalization Pooling (2×2)
		Block3	Convolution ($64 \times 5 \times 5$) Activation (ReLU) Normalization
	Decoder	Block1	Convolution ($64 \times 5 \times 5$) Activation (ReLU) Normalization Fractionally-strided convolution (stride = 2)

(continued)

Table 1. (continued)

		Block2	Convolution ($64 \times 5 \times 5$) Activation (ReLU) Normalization Fractionally-strided convolution (stride = 2)
		Block3	Convolution ($64 \times 5 \times 5$) Activation (ReLU) Normalization Fractionally-strided convolution (stride = 2)

2.2 Training Procedure

Synthetically generated enhanced near-infrared vascular images are looked as the reference outputs during training. We consider the enhanced image (reference image) as the linear combination of actual input image and the binary mask of vessel labels [3]. Therefore, we manually annotated the vessel locations in the form of binary masks for the training datasets. If x is the input near-infrared vascular image with h as the binary mask with a description of vessel structure, then the reference image y , is obtained as:

$$y = \alpha x + (1 - \alpha)h \quad (1)$$

where α refers to the fixed weight parameter. It should be noted that x , h , and y have the same dimensions. Figure 1 shows the example of original image and its mask, along with the reference image.

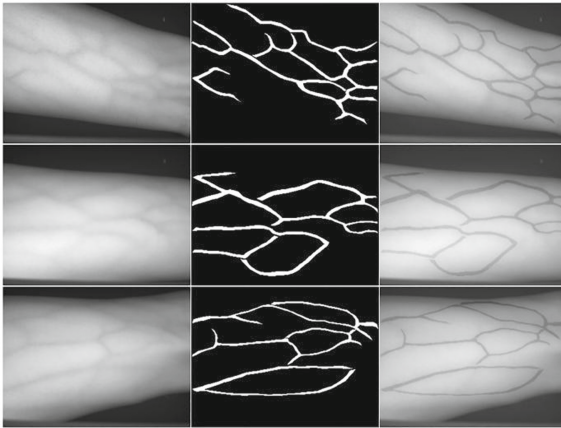


Fig. 1. From left to right are the original image, its mask, and the reference image.

Since the near-infrared vascular images are quite different from usual images in most common datasets, we have chosen a Mean Squared Error (MSE) loss for the training

RCAE. For the reconstructed image \hat{y} , and the reference image y , the MSE loss is computed as:

$$L_{mse} = \frac{1}{N} (y - \hat{y})^T \cdot (y - \hat{y}) \quad (2)$$

where N is the number of pixels in the image y .

For training the RCAE, we have chosen the Adam optimizer [4] with a learning rate of 0.001 to accomplish computation. In the beginning, the weights were initialized by random values normalized on a Gaussian centered around 0 with a bias of 0.05.

3 Experiments and Discussions

3.1 Datasets

Currently, there are few public forearm near-infrared vascular datasets available for testing. Therefore, we established a datasets in our laboratory for further research. We acquired the data using a near-infrared image acquisition system. The system consists of two strip lights, a near-infrared camera, and a lens with narrowband filter, as shown in Fig. 2. The collected datasets contains 156 images from 26 subjects, and each subject contains 6 images (3 from the left arm and 3 from the right arm). Some of the images in the datasets are shown in Fig. 3. At present, the majorities of subject in the datasets are young students aging between 20 and 30, but we are still expanding the datasets. We will continue to improve our datasets by considering factors such as gender, age, skin color, fat thickness, etc.

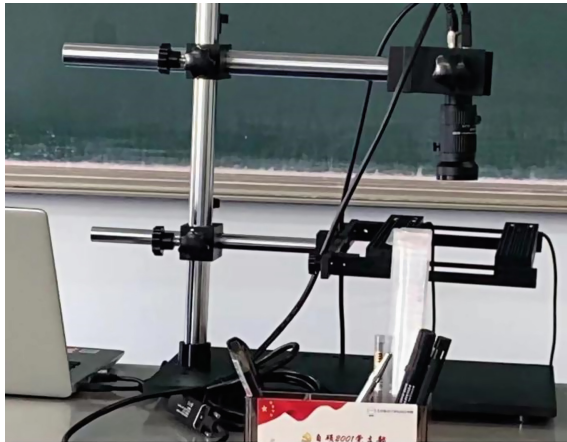


Fig. 2. The structure of near-infrared image acquisition system

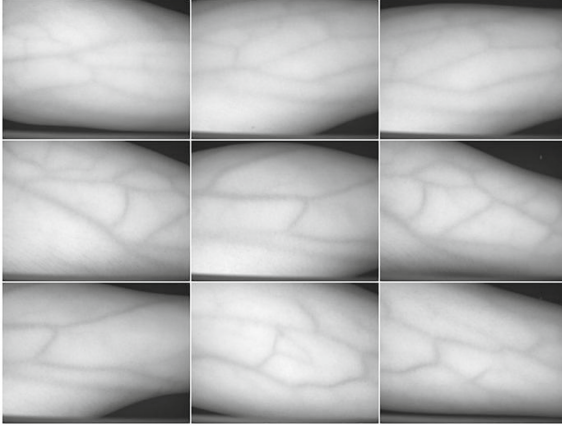


Fig. 3. Some near-infrared images from the datasets

3.2 Metrics for Evaluation

We use the full-reference image quality assessment metrics Peak Signal to Noise Ratio (PSNR) and Structural Similarity (SSIM) [5] to quantitatively evaluate the image enhancement effect of this model. A higher PSNR value indicates the similarity in terms of pixel-wise values, and a larger SSIM score indicates the result that is closer to the ground truth in terms of structural properties.

PSNR is a widely used image objective evaluation metric, which is defined as:

$$PSNR = 10 \log_{10} \frac{MAX_I^2}{MSE} \quad (3)$$

where, MSE is the Mean Square Error between the enhanced image and the original image, MAX_I is the maximum value of image pixel brightness. For the grayscale images, if each pixel is represented by 8-bit data, then $MAX_I = 2^8 - 1 = 255$.

SSIM is more consistent with human visual perception than other traditional methods, which is defined as:

$$SSIM(x, y) = [l(x, y)]^\alpha \cdot [c(x, y)]^\beta \cdot [s(x, y)]^\gamma \quad (4)$$

where α , β , and γ are the parameters used to adjust the relative importance of these three components, $\alpha > 0$, $\beta > 0$, and $\gamma > 0$. Symbol $l(x, y)$ is the luminance comparison function, $c(x, y)$ is the contrast comparison function, and $s(x, y)$ is the structural comparison function, which are defined as:

$$\begin{aligned} l(x, y) &= \frac{2\mu_x\mu_y + C_1}{\mu_x^2 + \mu_y^2 + C_1} \\ c(x, y) &= \frac{2\sigma_x\sigma_y + C_2}{\sigma_x^2 + \sigma_y^2 + C_2} \\ s(x, y) &= \frac{\sigma_{xy} + C_3}{\sigma_x\sigma_y + C_3} \end{aligned} \quad (5)$$

where μ_x and μ_y are the mean intensity of x and y , σ_x and σ_y are the standard deviation of x and y , and σ_{xy} is the covariance of x and y . And C_1 , C_2 , C_3 are the constants to avoid system errors caused by the denominator being 0.

In engineering calculations, we often set $\alpha = \beta = \gamma = 1$ and $C_3 = C_2 / 2$, then SSIM is simplified as:

$$SSIM(x, y) = \frac{(2\mu_x\mu_y + C_1)(2\sigma_{xy} + C_2)}{(\mu_x^2 + \mu_y^2 + C_1)(\sigma_x^2 + \sigma_y^2 + C_2)} \quad (6)$$

3.3 Experimental Results

We evaluated the performance of our RCAE model using some test images and compared with the experimental results enhanced by conventional Contrast Limited Adaptive Histogram Equalization (CLAHE). The original image and enhanced results are shown in Fig. 4. The enhanced results are evaluated using the above evaluation indicators, as shown in Table 2.

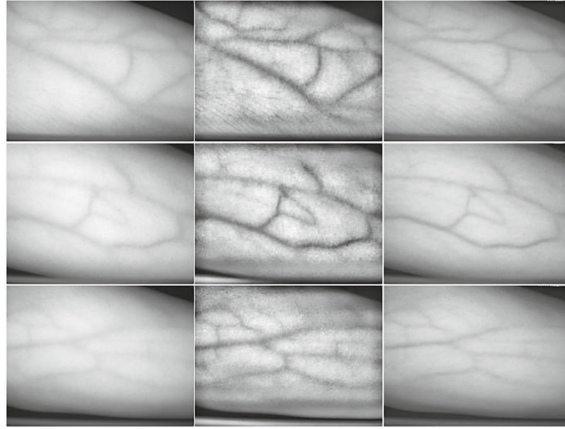


Fig. 4. From left to right are the original image, CLAHE enhanced results and RCAE enhanced results.

Table 2. Evaluation of CLAHE and RCAE enhanced results

Enhancement methods	Evaluation indicators	
	PSNR	SSIM
CLAHE	17.6687	0.6364
RCAE	22.7419	0.9571

From Table 2, compared with CLAHE, the PSNR value and SSIM value of the image enhanced by the RCAE model are higher, which indicates that the enhanced image quality of the RCAE model is better and more similar to the original image.

4 Conclusion

For near-infrared vascular images, we proposed a DCNN auto-encoder, i.e., a RCAE enhanced algorithm. The purpose of the RCAE is to learn the prominent as well as subtle vessel patterns in image, and improve the quality of presentation, in terms of a better contrast. The model is validated in our collected datasets. In addition, our model can be used to other image data. When the corresponding paired training data are available, it is a general model that can effectively enhance a specific target structure and has certain application value.

Acknowledgement. This work was supported by the National Natural Science Foundation of China under Grant No. 61975011, the Fund of State Key Laboratory of Intense Pulsed Radiation Simulation and Effect under Grant No. SKLIPR2024, and the Fundamental Research Fund for the China Central Universities of USTB under grant No. FRF-BD-19-002A.

References

1. Varastehpour, S., Sharifzadeh, H., Ardekani, I., et al.: An adaptive method for vein recognition enhancement using deep learning. In: Proceedings of the IEEE International Symposium on Signal Processing and Information Technology, pp. 1–6 (2019)
2. Ioffe, S., Szegedy, C.: Batch normalization: accelerating deep network training by reducing internal covariate shift. In: Proceedings of the 32nd International Conference on Machine Learning, vol. 37, pp. 448–456 (2015)
3. Bros, V., Kotwal, K., Marcel, S.: Vein enhancement with deep auto-encoders to improve finger vein recognition. In: Proceedings of the International Conference of the Biometrics Special Interest Group, pp. 1–5 (2021)
4. Kingma, D.P., Ba, J.: Adam: a method for stochastic optimization. In: The 3rd International Conference on Learning Representations, pp. 1–15 (2017)
5. Wang, Z., Bovik, A.C., Sheikh, H.R., et al.: Image quality assessment: from error visibility to structural similarity. *IEEE Trans. Image Process.* **13**, 600–612 (2004)

Research on the Environment Character



The Development and Suggests of Planetary Protection

Lantao Zhang^(✉)

Beijing Institute of Spacecraft System Engineering, China Academy of Space Technology,
Beijing 10094, China
zlt840208@163.com

Abstract. Planetary protection is significantly important for the earth safety and the exploration of the origin of life. In this article, its current history and development are systematically reviewed. The categories of planetary protection are divided according to the different tasks. Then, based on the whole process of the planetary exploration, the measures of planetary protection are analyzed, which include forwarding contamination and back contamination. Finally, the development and implementary suggestions of planetary protection are proposed.

Keywords: Planetary protection · Earth safety · The origin of life · Biological contamination

1 Introduction

With the gradual deepening of human exploration of planets, a new problem has emerged, that is, planetary protection, which refers to a series of control measures taken to prevent contamination of the earth by alien planets or alien life materials during the exploration of outer space. This includes two aspects. On the one hand, after the launch of the probe, it will carry part of the earth's living materials or organic macromolecules to the target planet, thus affecting the life detection of outer planets, so as to pollute the biological system of outer planets. It's called positive pollution. On the other hand, it refers to the risk to earth's biological system caused by biological material brought back from outer space when the probe of outer space planets returns to Earth. It is called reverse pollution [1].

2 Concept

The main purpose of planetary protection is to avoid the interaction between earth and outer planets when the biological hazard of the target planet is unknown. The connotation mainly includes two aspects: one is to ensure that the probe itself is as clean as possible, in order to ensure that the impact on the outer planet is minimized. It is realized by the clean control of the detector before launch. The second is to make sure that samples, and any returning probes that have made contact with other planets, are safe enough to look for life on other planets. The returned samples will be studied in absolute isolation from the Earth's environment, keeping earth safe from extraterrestrial life [2].

3 Categories

COSPAR defines the following five levels of planetary protection, based on missions and the probability of life on other planets [3] (Table 1):

Table 1. Classified of COSPAR planetary protection

Target	Type	Classified
The immediate goal of exploration of target planets is not to understand the origin of life or the process of chemical evolution, and there are no planetary protection requirements for orbiters or landers targeting these planets	Any	I
The goal of planetary exploration is to understand the origin of life or the process of chemical evolution, but the chance of contamination by spacecraft is so small that it would not jeopardize future exploration plans	Any	II
The specific mission objective is to explore the origin of life or the chemical evolution of the target planet, or scientists believe there is a greater chance that the spacecraft will cause pollution, thereby jeopardizing future biological experiments The specific mission objective is to explore the origin of life or the chemical evolution of the target planet, or scientists believe there is a greater chance that the spacecraft will cause pollution, thereby jeopardizing future biological experiments	Flyby, Orbiters	III
	Landers, Probes	IV
Any spacecraft on a return mission, focus on protecting earth	Earth-Return	V

4 Analysis of Control Methods

Planetary protection is an important work involving the development of spacecraft and the whole mission, including many aspects of control, such as material screening, product acceptance, clean assembly, pre-launch cleaning, control of returned samples and destruction of returned samples [4].

In Material screening, antibacterial mouldproof properties of material selection are needed. The screening methods take reference on ground antibacterial mouldproof performance testing methods, considering the test strains on the ground the microbial species, A comprehensive selection of the development and launch of the regional environment of the dominant strains, as the test strains in the material test, and formulated the antibacterial rate of higher than 90% index, fully ensure the follow-up good performance of the material.

When delivering the products, clean the products in advance. Suitable cleaning methods are adopted for different materials. Metal and non-metallic materials with smooth surface are wiped with 75% alcohol. Fabrics are sterilized by Co60 irradiation. Other

complex materials are irradiated by ultraviolet light. After the treatment is completed, the product shall be tested by a third party qualified for microbial testing, and then the product surface shall be covered with sterile film or stored in an antistatic bag [5–7].

In the delivery of the population, the population staff will review the microbial test report and extract 5% of the products according to the product delivery category for retesting, so as to achieve the purpose of supervision.

In the final assembly test process, personnel's hands, clothing, work shoes and so on will bring pollution in the process of touching the spacecraft. Therefore, in order to reduce pollution sources, personnel in contact with the spacecraft before disinfection, is conducive to keep the spacecraft clean. The secondary dressing room is an additional purification measure designed for the operator, requiring the operator to complete the cleaning again in the area of the clean room close to the spacecraft, so as to keep the operator as clean as possible. The design of the secondary dressing room is improved by using small containers, which are equipped with air filtration and purification system, ozone and ultraviolet sterilization system, as well as the whole body air shower and hand disinfection facilities. Personnel can enter the changing room, change clean work clothes and work shoes, hand disinfection and body wind shower, and then through a special channel into the spacecraft working area, this measure to keep the spacecraft clean during the final assembly test has played an important role.

Before the launch, because the spacecraft has been overall assembly for one, the spacecraft sterilization measures are very limited, mainly can be unified on the spacecraft hydrogen peroxide steam sterilization, or ultraviolet irradiation on the external surface sterilization. A disinfectant can also be used to wipe the surface [8].

For returned samples, there is an unpredictable risk to the earth. Therefore, it is necessary to transfer them to a P4 biosafety level laboratory for research in a sealed state, so as to ensure absolute isolation of samples from the earth's external environment.

5 Suggests

According to the information mentioned above, some measures should be taken to achieve the goal of planetary protection.

1) Establish the clean process environment: First, the design of (Assembly, Integrate and Test, AIT) workshop requires strictly compliance with specifications, in which the cleanliness can reach to ISO 8 level; second, set secondary dressing room and steriled room, which was used for cleaning work suit every day. Third, In order to avoid the contamination from vistors, a separate dressing room and channel should be built.

2) The management control of workers. It requires strengthening the personal hygiene of the workers before entrancing the AIT and operation on the spacecrafts, such as washing hands, washing head and even bathing; in addition, all the work suits, caps and shoes should be disinfected regularly, and the clothes needs unified management, which is the most important aspect of all the control measures.

3) Closed-loop control of the whole process. In the development of spacecrafts, appropriate measures should be taken to control the contamination in each part of the manufacture; The clean cloth should be stamped during storing; Furthermore, before installation, the

surface of the products should be wiped by the non-hazardous disinfectants, and during installation, gloves would be required to keep the contamination from hands; after installation, the inner surface of cabin should be wiped, and the gas of the entire cabin should be replaced, then seal the cabin before launching.

4) Assess probe the probability of collision or sterilization process was carried out on the aircraft: for all launched from earth orbit, and likely to collision with the outer planets may craft, precise calculation for the flight orbit, and analyzing the probability of collision with the planet, for aircraft collision probability is higher, it must be sterilization processing before launch.

5) Special microorganisms should be identified. In order to reduce the amount of microbial load on the surface of the aircraft, it is necessary to evaluate the microbial load of the aircraft several times during the final assembly test on the ground. If the number of microorganisms exceeds the specified range, the surface must be kept absolutely clean prior to launch by means of dry heat sterilization or radiation sterilization in order to meet the requirements of planetary protection documents.

6) The sample which was brought back should be carefully disposed. It should be put in a sealed box, and then transport to the highest bio-safety class laboratory-class 4. The sample should be totally disposed after the analysis, in case it would lead to some severe consequences [9–11].

6 Conclusion

In conclusion, planetary protection policy recommendations should be maintain and promulgated at the international level. In one hand, some efficient measures should be taken to keep our spacecraft clean to avoid the contamination from earth organisms and organics, on the other hand, the sample, which was carried by a spacecraft returning from other planets, should be disposed in right way, to protect our planet from potential harmful extra-terrestrial matter.

References

1. COSPAR Planetary Protection Policy. Approved by the bureau and council, World Space Council, USA 24 March 2011
2. Pierson, D.L.: Microbial contamination of spacecraft. *Gravit. Space Biol. Bull.* **14**(2), 1–6 (2001)
3. Rummel, J., Ehrenfreund, P., Peter, N.: COSPAR workshop on planetary protection for outer planet satellites and small solar system bodies. COSPAR, Paris, 41 (2009)
4. John, D., Rummel, J.: Planetary exploration in the time of astrobiology: protecting against biological contamination. *PNAS* **98**(5), 2128–2131 (2001)
5. Debus, A.: Planetary protection: Elements for cost minimization. *Acta Astronaut.* **59**, 1093–1100 (2006)
6. Biological Contamination Control for Outbound and Inbound Planetary Spacecraft. NPD (NASA Policy Directive)
7. Planetary Protection Provisions for Robotic Extra-terrestrial Missions. NPR (NASA Procedural Requirements) 8020.12B

8. Nefedov, Y.G., Shilov, V.M., Konstantinova, I.V., Zaloguyev, S.N.: Microbiological and immunological aspects of extended manned space flights. *Life Sci. Space Res.* **9**, 11–16 (1971)
9. Race, M.S., Kminek, G., Rummel, J.D.: Planetary protection and humans on mars: NASA/ESA workshop result. *Adv. Space Res.* **42**, 1128–1138 (2008)
10. Subject: Biological Contamination Control for Outbound and Inbound Planetary Spacecraft, 25 August 2011
11. Rummel, J.D., et al.: A draft test protocol for detecting possible biohazards in martian samples returned to earth. NASA/CP-2002–211842



Research on Calculation Method of Aircraft Cabin Inner Wall Temperature Based on Parameter Sensitivity Analysis

Yi Cao^(✉)

Shanghai Aircraft Design and Research Institute, Shanghai 200000, China
caoyi1@comac.cc

Abstract. Aiming at the factors affecting the aircraft cabin inner wall temperature, this paper starts from the basic theory of heat transfer, combined with the sensitivity analysis method, structure thermal resistance R , cabin internal ambient temperature T_I and external ambient temperature T_4 are determined to be sensitive factors within the scope of engineering experience. This paper innovatively proposes the dimensionless temperature θ , which is the ratio of the cabin inner wall temperature to the cabin air temperature difference and the external environment temperature difference. It provides a measurement of the relative temperature difference between the cabin inner wall temperature to the internal and external environments, which can characterize the temperature gradient along the heat transfer direction. Data dimensionality reduction is realized through dimensionless, and then the functional relationship between dimensionless temperature θ and skin thermal resistance R is obtained through data fitting. Finally, the calculation method of aircraft cabin inner wall temperature is deduced. This method fully considers the complete heat transfer link from the internal of the cabin to the external environment, and an estimation method of cabin inner wall temperature for designers is provided.

Keywords: Cabin inner wall temperature · Sensitivity analysis · Dimensionless

1 Introduction

With the improvement of economic requirements of civil aircraft, aircraft weight reduction design has gradually become an important research direction of civil aircraft manufacturers at home and abroad. Composite materials have been widely used in civil aircraft structural design due to the light weight, high strength and excellent properties [1]. Due to the low glass transition temperature of composites, structural thermal analysis must be carried out to ensure the safety of aircraft structure. The cabin inner wall temperature is an important boundary for aircraft structure thermal analysis.

In preliminary calculation, when the aircraft structure temperature reaches a steady state, it is generally considered that the cabin inner wall temperature is the same as the cabin air temperature, so it is taken as the cabin target temperature value in calculation. This simplified method ignores the heat transfer between the internal and external air and

the cabin wallboard, as well as the thermal resistance of the cabin wallboard. This oversimplification will affect the accuracy of temperature field calculation results of cabin, resulting in the problem of “frozen legs” in the cabin door area can not be reproduced. The inner wall temperature of cabin can also be obtained by calculating the structural temperature field for the whole aircraft structure, but this method is too complicated. At present, there is no simple and accurate method to calculate the inner wall temperature of aircraft cabin that can be applied to engineering practice.

Based on the basic theory of heat transfer, in view of the factors affecting the aircraft cabin inner wall temperature, combined with the sensitivity analysis method, an estimation method for temperature of the inner wall of the aircraft cabin is proposed in this paper, which fully considers the complete heat transfer link from the internal of the cabin to the external environment.

2 Heat Transfer Analysis for Cabin Inner Wall Temperature

As a structural parameter of the aircraft skin, the inner wall temperature of aircraft cabin is affected by convection and radiation heat transfer of the inside and outside of the cabin, and the thermal conductivity of structure. All the internal and external environments work together to form the inner wall temperature of the aircraft cabin [2, 3].

When the heat transfer between the aircraft structure and the internal and external environment is stable, according to the principle of no heat accumulation, the structural heat transfer process can be expressed as:

$$Q = (T_1 - T_4)/(1/K_1 + R + 1/K_2) = K_1 \times (T_1 - T_2) \quad (1)$$

where Q is structure heat flux, W/m^2 . T_1 is cabin internal ambient temperature, K. T_4 is external ambient temperature, K. K_1 is heat transfer coefficient inside the cabin, $W/(m^2 \cdot K)$. R is structural thermal resistance, $(m^2 \cdot K)/W$. K_2 is heat transfer coefficient outside the cabin, $W/(m^2 \cdot K)$. T_2 is cabin inner wall temperature, K.

According to the above formula (1), the inner wall temperature of aircraft cabin T_2 is only related to five parameters, namely T_1 , T_4 , K_1 , K_2 and R . In the following, the key parameters affecting the aircraft cabin inner wall temperature in the above five parameters will be determined based on parameter sensitivity analysis, and the estimation method based on the key parameters will be given.

3 Parameter Sensitivity Analysis

Parameter sensitivity analysis is to determine the key factors affecting the target parameters by evaluating the response level of the target parameters to the changes of the influencing factors. It usually includes single-factor sensitivity analysis and multi-factor sensitivity analysis. Single-factor sensitivity analysis was adopted in this paper, that is, only one factor was changed at a time, while other factors remained unchanged [4].

The values of five parameters affecting the inner wall temperature of aircraft cabin T_2 determined based on experience are shown in Table 1 below.

Table 1. Parameter value

No.	T_1	T_4	R	K_1	K_2
1	218	217	0.001	1	50
2	233	218	0.005	2.5	75
3	253	233	0.01	5	100
4	273	253	0.05	7.5	125
5	283	273	0.1	10	150
6	293	283	0.5	12.5	175
7	295	288	1	15	200
8	297	293	5	17.5	225
9	298	298	10	20	250
10	300	303	15	22.5	275
11	303	308	20	25	300
12	313	313	25	27.5	325
13	328	328	50	30	350

A full factorial test analysis was carried out for the 5 factors and 13 levels defined in Table 1, and the temperature value T_2 of cabin inner wall under each working condition was obtained, and then the functional relationship between T_2 and 5 related parameters was determined by the fitting method, as shown in the following formula:

$$T_2 = 0.91 \times T_1 + 19.59 \tag{2}$$

$$T_2 = 0.0904 \times T_4 + 271.1 \tag{3}$$

$$T_2 = -7.35 \times R^{-0.94} + 298 \tag{4}$$

$$T_2 = -44.41 \times K_1^{-0.59} + 301.9 \tag{5}$$

$$T_2 = 9.17 \times 10^{12} \times K_2^{-8.22} + 290.7 \tag{6}$$

According to the functional relationship between the target parameter T_2 and the five influencing factors, the sensitivity coefficient of each parameter is obtained [5], as shown in Fig. 1, 2, 3, 4 and 5.

Combined with the definition of parameter sensitivity in engineering [6], as can be seen from Fig. 1, 2, 3, 4 and 5 that within the scope of engineering experience, the sensitivity analysis conclusions of various factors are as follows:

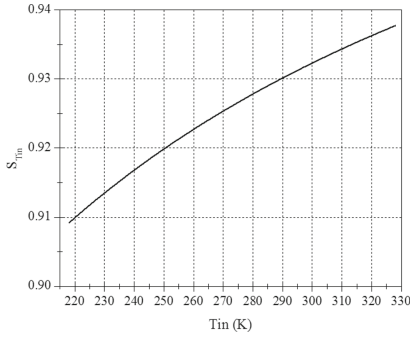


Fig. 1. Sensitivity coefficient - T_1

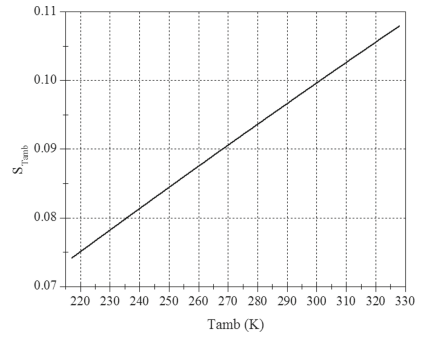


Fig. 2. Sensitivity coefficient - T_4

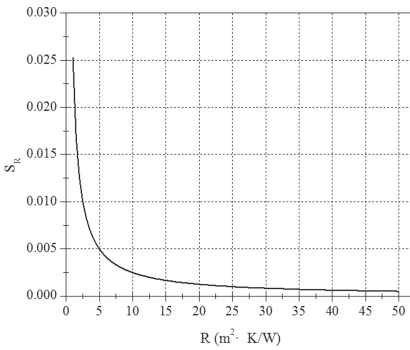


Fig. 3. Sensitivity coefficient - R

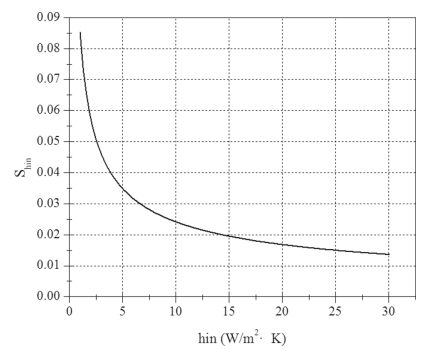


Fig. 4. Sensitivity coefficient - K_1

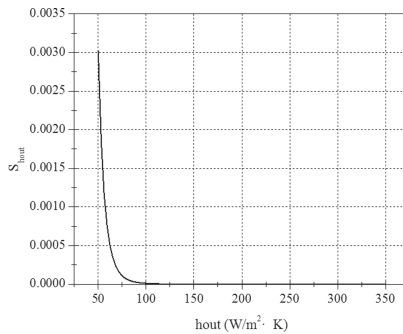


Fig. 5. Sensitivity coefficient - K_2

- 1) Both T_1 and T_4 are sensitive factors;
- 2) When the value of R is less than $0.148 \text{ (m}^2 \cdot \text{K)/W}$, that is, for the skin panel structure with poor thermal conductivity, the structure thermal resistance can be considered as a sensitive factor;
- 3) Except for factors R , T_1 and T_4 , all other factors are insensitive factors.

4 Calculation Method of Aircraft Cabin Inner Wall Temperature

The following is a quantitative analysis of three sensitive factors R , T_1 and T_4 to determine the formula for calculating the inner wall temperature of aircraft cabin. As skin thermal resistance R is only a sensitive factor in a local range, the upper limit of R value range for subsequent quantitative analysis is $5 \text{ (m}^2 \cdot \text{K)}/\text{W}$.

Firstly, the temperature is dimensionless to achieve dimensionality reduction of data. The dimensionless temperature θ is defined as shown in formula (7), which is the ratio of the cabin inner wall temperature to the cabin air temperature difference and the external environment temperature difference. It provides a measurement of the relative temperature difference between the cabin inner wall temperature to the internal and external environments, which can characterize the temperature gradient along the heat transfer direction.

$$\theta = (T_1 - T_2)/(T_2 - T_4) \tag{7}$$

Data fitting is carried out for dimensionless temperature and skin thermal resistance, and the fitting curve is shown in Fig. 6. The sum of residual square SSE is 0.0001254 and the decisive coefficient R-square is 0.9999, indicating a good fitting result. The relationship between dimensionless temperature θ and structure thermal resistance R is shown in formula (8).

$$\theta = 0.1014 \times R^{-0.955} \tag{8}$$

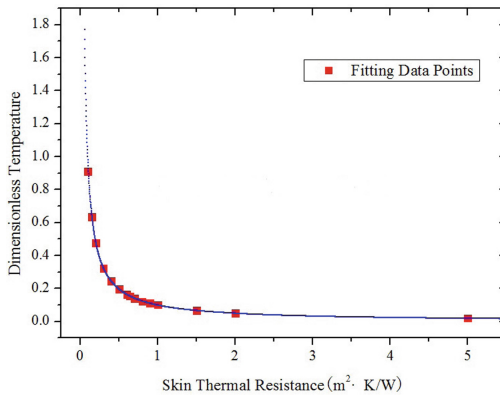


Fig. 6. Fitting curve of dimensionless temperature and skin thermal resistance data

Substituting formula (7) into formula (8) yields formula (9), that is the aircraft cabin inner wall temperature estimation formula.

$$T_2 = T_4 + (T_1 - T_4)/(1 + 0.1014 \times R^{-0.955}) \tag{9}$$

5 Conclusion

Aiming at the factors affecting the aircraft cabin inner wall temperature, this paper starts from the basic theory of heat transfer, combined with the sensitivity analysis method, structure thermal resistance R , cabin internal ambient temperature T_i and external ambient temperature T_e are determined to be sensitive factors within the scope of engineering experience. This paper innovatively proposes the dimensionless temperature θ , which is the ratio of the cabin inner wall temperature to the cabin air temperature difference and the external environment temperature difference. It provides a measurement of the relative temperature difference between the cabin inner wall temperature to the internal and external environments, which can characterize the temperature gradient along the heat transfer direction. Data dimensionality reduction is realized through dimensionless, and then the functional relationship between dimensionless temperature θ and structure thermal resistance R is obtained through data fitting. Finally, the calculation method of aircraft cabin inner wall temperature is deduced. This method fully considers the complete heat transfer link from the internal of the cabin to the external environment, and an estimation method of cabin inner wall temperature for designers is provided.

References

1. Cao, Y.: Research on calculation method of aircraft skin temperature based on parameter sensitivity analysis. In: Long, S., Dhillon, B.S. (eds.) MMESE 2020. LNEE, vol. 645, pp. 513–521. Springer, Singapore (2020). https://doi.org/10.1007/978-981-15-6978-4_60
2. Fu, Y., Chang, H.J., Wu, Y.Q., Xue, H.: Dynamic temperature predicted model for airplane platform based on measured data. *Acta Aeronautica et Astronautica Sinica* **35**(9), 2472–2480 (2014)
3. Aircraft Design Manual Total Editorial Board: Aircraft Design Manual: Life Support and Environmental Control System Design, vol. 15, pp. 3–8. Aviation Industry Press, Beijing (1999)
4. Zhang, G., Zhu, W.S.: Parameter sensitivity analysis and optimizing for test programs. *Rock Soil Mech.* **14**(1), 51–58 (1993)
5. Guo, L., Wu, Q.W., Yan, C.X.: Sensitivity analysis of thermal design parameters for focal plane assembly in a space spectral imaging instrument. *Heat Mass Transf.* **49**, 299–308 (2013)
6. Wei, L.X., Sun, C., Zhao, J., et al.: Sensitivity analysis of influencing factors on heat transfer coefficient calculation. *Sci. Technol. Eng.* **14**(20), 294–297 (2014)



Study on the Noise Control Technology in the Batching Room of a Dairy Production Enterprise

Zhenfang Chen¹, Jianwu Chen^{1,2(✉)}, Qing Zhang¹, Bin Yang^{1,2}, and Yanqiu Sun^{1,2}

¹ China Academy of Safety Science and Technology, Beijing 100012, China
cjh3000@126.com

² NHC Key Laboratory for Engineering Control of Dust Hazard, Beijing 100012, China

Abstract. Dairy products have become an important part of people's daily diet, but the noise in the batching room of the dairy production enterprise is harmful to workers' occupational health especially the hearing system. Take the batching room of a dairy production enterprise as this research object, and the sound pressure levels and frequency distribution were detected by the noise meter. The sound pressure level of the batching workbench with all the side plates was 7.5 dB higher than the occupational exposure limit under present conditions, and the sound insertion loss capacity of the existing side panel was only 4.9 dB. The sound distribution was mainly in 500 Hz to 8 kHz, which indicates that the sound belongs to medium and high frequency and broadband noise. Base on the analyzing the results of octave band sound pressure level detection and the cause of exceeding the limit, a sound insulation encasing was designed in detail to reduce the noise.

Keywords: Noise · Acoustic shield · Transfer pump · Dairy production · Batching

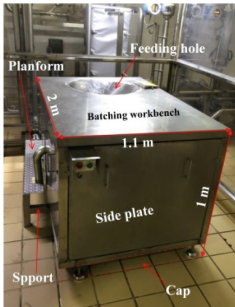
1 Purpose

Dairy products are the most nutritious food except breast milk. They have become an important part of people's daily diet, and the demand of them is increasing day by day [1, 2]. It is often necessary to put the solid milk powder into the batching workbench in the processing of liquid dairy products [3], which is manual operated by workers. The solid milk powder is transported to the production line by the transfer pump, which is set in the batching workbench. The transfer pump will produce high noise during operation, and the batching workers will be exposed to a certain intensity of noise for a long time, which is harmful to workers' occupational health [4, 5]. Noise can cause hearing loss and even deafness, while it can also affect the nervous system, endocrine system, work efficiency and even cause accidents [6, 7]. Therefore, the sound pressure level in the batching room of a dairy production enterprise were analysed in this paper, and the control measures were put forward, which can be used for reference in other similar workplace.

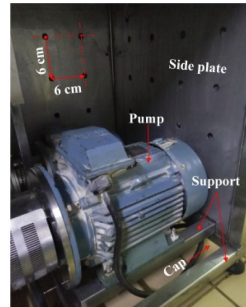
2 Research Object and Methods

2.1 Research Object

Takes the batching room of a dairy production enterprise as the research subject for this study, and a length 2 m × width 1.1 m × height 1 m batching workbench was set in the batching room as shown in Fig. 1 (a).



(a) Batching workbench



(b) Internal view of batching workbench

Fig. 1. The batching workbench in the batching room of a dairy production enterprise studied.

Workers stand on the support platform to feed milk powder into the feeding hole, and the milk powder and other auxiliary materials are mixed proportionally in the batching workbench. They are delivered to the process line by a material delivery pump built into the batching workbench. The outer surface of the worktable is stainless steel, and the inner surface of the workbench is multi-hole stainless steel orifice plate. Between the two stainless steel plates is empty. The holes of the porous stainless steel inner plate are arranged in a square shape, the space between the holes is 6 cm, and the diameter of the holes is 1 cm, between the two stainless steel plates is empty. The pump is fixed on the shell of the workbench by the stainless steel support as shown in Fig. 1(b), and it produces noise in the running.

2.2 Research Methods and Occupational Exposure Limits

The Quest Soundpro sound level meter was used to measure the sound pressure level, which was set to A-weighted sound pressure level, “Slow”, and “Octave” [8]. The noise was measured 0.5 m from the workbench and the tester, and the detector pointed in the direction of the sound source. The noise was detected with or without side panels of the batching workbench when only 1 batching workbench was in running without load of feeding materials. The octave band sound pressure level spectrogram was derived from Software of Quest Detection Management.

The occupational exposure limits of steady and non-steady noise is 85 dB (A) in the workplace [9], whether the limits is the normalization of equivalent continuous A-weighted sound pressure level to a nominal 8 h working day or 40 h working week, which was set in GBZ2.2-2007 “Occupational exposure limits for hazardous agents

in the workplace Part 2: Physical agents” [10]. That is the same as the requirements for noise limits in GB/T 50087–2013 “Code for design of noise control of industrial enterprises” [11]. In order to meet the requirements of occupational exposure limits, the noise of batching workbench is better less than 85 dB (A). Therefore, 85 dB (A) was taken as the noise control target of the workbench.

NR (Noise Rating) evaluation curve is recommended by ISO and widely used in China and Europe. According to the comparison between the results measured of each frequency band of noise value and NR evaluation curve, the noise value needed to be reduced at a certain frequency band and the main frequency band of noise exceeding the standard can be obtained. Sound insulation materials can be selected according to frequency distribution, and the thickness of sound absorbing material can be designed according to the sound pressure level.

3 Results and Analysis

3.1 Sound Pressure Level Detection Results and Analysis

The sound pressure level detection results of the batching workbench were as shown in Table 1 when only 1 batching workbench was in running without load of feeding materials, which shown the influence of side plate on the sound pressure level.

Table 1. The influence of side plate on the sound pressure level for the batching workbench.

Detection condition	Sound pressure level (dB(A))		
	Detection results	Control target	Noise reduction needed
Without one side plate	97.4	85	12.4
With all the side plates	92.5	85	7.5

As seen in Table 1, the sound pressure level with all side plates of the batching workbench was 7.5 dB higher than the occupational exposure limit under present conditions, and the sound insertion loss capacity of the existing side panel is only 4.9 dB. It shows that sound insulation effect of the present side plates in the batching workbench is very poor, which should be improved. According to the results of noise detection without one side plate, the sound insertion loss capacity of the newly designed plates is at least 12.4 dB to achieve the target sound pressure level of 85 dB (A). The octave band sound pressure level detection results are plotted and analyzed as shown in Fig. 2 in order to further analyze the sound frequency distribution characteristics, which is important basis for the subsequent selection of noise control techniques.

As shown in Fig. 2, the sound pressure level on each frequency is increased without one side plate of the batching workbench, but the increase is very small, which also shows that the sound insertion loss of the plates is very small. The sound distribution is mainly in 500 Hz to 8 kHz, which indicates that the sound belongs to medium and high frequency and broadband noise. The sound pressure level of batching table can be

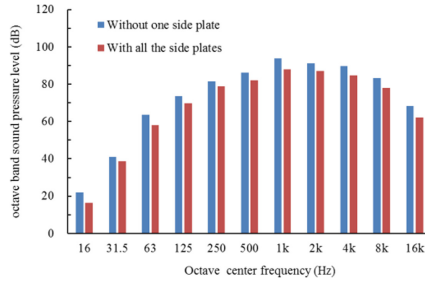


Fig. 2. The measured results of octave band sound pressure level of the batching workbench with and without side plate in the batching room of a dairy production enterprise studied. 1 k, 2 k, 4 k, 8 k and 16 k represent 1000, 2000, 4000, 8000 and 16000 respectively.

reduced to 85 dB (A) by adopting sound insulation measures. According to GB/T 50087–2013 “Code for design of noise control of industrial enterprises”, the sound transmission loss (TL_a) for each frequency band should be calculated by Eq. 1 [11].

$$TL_a = L_p - L_{pa} + 5 \quad (1)$$

where:

TL_a—The sound transmission loss, dB.

L_p—The measure results of sound pressure level at each frequency band, dB. The measured sound pressure levels of the batching workbench without side plate were used in this study as shown in Table 1.

L_{pa}—The limit sound pressure level of each frequency band, dB.

In order to get the control target of 85 Db (A) for the sound pressure level in this study, it is necessary to reduce 5 dB [11, 12] and take 80 dB (A) as the design target of sound pressure level. The reduced 5 dB is used to avoid the influence of reverberation noise sound on the results. When the design target of sound pressure level is 80 dB (A), NR75 evaluation curve data was used for the limit sound pressure level of each frequency band (L_{pa}) for this study. The NR75 evaluation curve data [11] as shown in Table 2 is that the sound pressure limits of each frequency when the sound pressure level is 80 dB (A) and the noise sound pressure level is 75 dB (A) at 1 kHz. The sound transmission loss of each frequency band for the batching workbench was shown in Table 2, when takes the NR75 evaluation curve data as the design target of sound pressure level.

Table 2. The sound transmission loss of each frequency band for the batching workbench

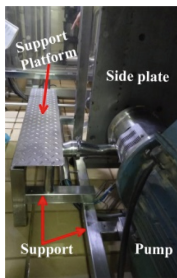
Sound pressure level (dB(A))	Octave center frequency (Hz)							
	63	125	250	500	1 k	2 k	4 k	8 k
Detection results without one side plate	63.7	73.4	81.5	86.0	93.7	91.2	89.8	83.1
NR75 evaluation curve data	95	87	82	78	75	73	71	69
Sound transmission loss	—	—	—	8	18.7	18.2	18.8	14.1

As shown in Table 2, in order to reduce the sound pressure level to 85 dB (A) for the batching workbench studied in this paper, it is about 19 dB needed to reduce between the frequency of 1 k to 8 k.

3.2 Cause Analysis of Noise Exceeding Standard

The noise of the batching workbench is mainly caused by the material transfer pump running. The sound insulation of the shell of the batching workbench is only 5 dB, which shows that the sound insulation effect of side plate of the batching workbench can't meet the requirements. The reasons for the noise exceeding the standard are as follows.

- (1) The pump and the support platform are connected to the workbench shell through stainless steel support, and no vibration isolation measures are set between them, which was shown in Fig. 1 and Fig. 3(a). The stainless steel support forms a solid sound bridge that transmits pump noise outside, and the sound was amplified by the shell of the batching workbench and support platform.



(a) Supports



(b) Cap on the front side plate

Fig. 3. The local pictures of batching workbench in the batching room studied.

- (2) There is a large gap in the front side plate and the bottom of the batching workbench as shown in Fig. 1 and Fig. 3(b), and they formed an air acoustic bridge, which forms an air bridge and causes the noise to come out.
- (3) There is no sound absorbing material between the inner and outer surfaces of batching workbench, and the layout and the diameter of the holes on the inner surface are not reasonable, which are shown in Fig. 1(b). So that the side plate of the workbench has no sound absorbing effect, and the noise reduction of it is only 4.9 dB.

3.3 Design of Noise Control Measures

Based on the analysis of the causes of noise exceeding the standard, the following measures can be taken to reduce the noise of the batching workbench.

- (1) The pump is set on a separate support which is set separately from the shell of the batching workbench. And the vibration reduction measures are taken between the support and the pump, and between the support and the ground. The support, pump and tube were set inside of the batching workbench, and they were isolated from the shell of the workbench with a distance of more than 10 cm. Thus reducing pump vibration transmission to the shell of batching workbench and the ground, so that the transmission of noise in solid was eliminated.
- (2) Replace the shell of the workbench with a new sound insulation encasing, which was shown in Fig. 4.

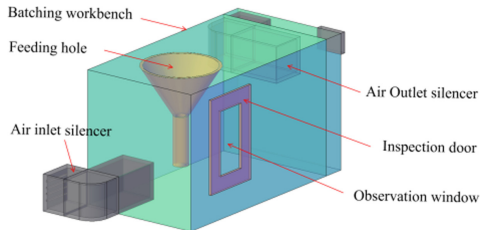


Fig. 4. The model of sound insulation encasing for the batching workbench.

The 1.5 mm thick stainless steel was used as the outer surface of the sound insulation encasing, and the multi-hole orifice stainless steel plate was used as the inter surface. The diameter of hole on multi-hole orifice plate was 2 mm, and the holes were arranged in 60° staggered. The polyurethane sound absorbing material of 5 cm thickness was arranged between the inner and outer surfaces of the batching workbench, which was used to absorb noise.

In order to exhaust the heat generated by the pump running in time, it is necessary to set up ventilation to reduce the temperature inside the workbench to ensure the normal operation of the pump. Therefore, an air inlet silencer is set at the lower side of the front plate of workbench, and an air exhaust silencer is set at the upper part of the back side plate of workbench, which is as shown in Fig. 4. The fan is set on the inlet of the air exhaust silencer, which is used to exhaust the heat air from the inside of the workbench.

For the convenience of maintenance and repair, an observation window and inspection door should be set on the side plate as shown in Fig. 4. Double glasses are used as the observation window, which is convenient to observe the inside conditions of the workbench through it. The inner glass is 3 mm thick with a 1° tilt setting, the outer glass is 5 mm thick with a vertical setting, and the layer of air is set between the two glasses is, which are used to increase the sound insulation of the observation window. The 5 mm thick rubber strip is set at the connection of the shell of the workbench with the inspection door and ground, which is used to avoid leaving a gap at the connection of them, thus causing the noise to spread out.

The tube is wrapped with soundproof cotton, and the soundproof is also used at the connection of the tube and the shell of batching workbench to prevent the sound spreading out.

4 Discussions

The air silencers of inlet and outlet are set on the batching workbench, but the exhaust air volume should be calculated later according to the heat dissipation of pump motor used in this process, and the specific structure size of air silencers should also be studied according to the exhaust air volume. Because the wind speed at the surface of air silencer should meet the design requirements, and the type and size of the air silencer also should meet the requirements of the batching workbench space.

The study object is only one batching workbench, but when there may be more than one batching workbench in the batching room for other dairy production enterprise, and the sound pressure level will increase. The sound pressure level should be calculated according to the sound superposition principle.

5 Conclusions

The sound pressure level of the batching workbench with all the side plates was 7.5 dB higher than the occupational exposure limit under present conditions, and the sound insertion loss capacity of the existing side panel was only 4.9 dB. The sound distribution was mainly in 500 Hz to 8 kHz, which indicated that the sound belongs to medium and high frequency and broadband noise.

Base on the analyzing the results of octave band sound pressure level detection and the cause of exceeding the limit, a sound insulation encasing was designed in detail to reduce the noise.

Acknowledgements. This work is supported by the National key R&D Program of China (No.2016YFC0801700) and the basic research funding of China Academy of Safety Science and Technology (No.2022JBKY02).

References

1. He, Z.: Analysis on the present situation and prospect of dairy industry in China. *China Dairy* **4**, 20–23 (2021). <https://doi.org/10.16172/j.cnki.114768.2021.04.005>
2. Kuznetsova, A.: Prospects for the development of the dairy industry in the republic of Belarus and in the Russian federation. In: Hradec Economic Days (2020). <https://doi.org/10.36689/uhk/hed/2020-01-048>
3. Wei, J., Lin, Y., Wei, J., et al.: Research progress of domestic fermented cheese products technology. *J. Guangxi Agric.* **36**(3), 67–71 (2020). <https://kns.cnki.net/kcms/detail/detail.aspx?FileName=GXLB202103017&DbName=CJFQ2021>
4. Atmaca, E.Y.Ü.P., Peker, I., Altın, A.: Industrial noise and its effects on humans. *Pol. J. Environ. Stud.* **14**(6), 721–726 (2005)
5. Ghuncha, F., Ateeque, A.: Impact analysis of urbanization on rural livelihood—an empirical study of an urban centre of Delhi. *India. Int. J. Urban Sci.* **16**(3), 147–160 (2011). <https://doi.org/10.1080/09709274.2004.11905735>
6. Wokekoro, E.: Public awareness of the impacts of noise pollution on human health. *World J Res Rev* **10**(6), 27–32 (2020)

7. Farooqi, Z.U.R., et al.: Assessment of noise pollution and its effects on human health in industrial hub of Pakistan. *Environ. Sci. Pollut. Res.* **27**(3), 2819–2828 (2019). <https://doi.org/10.1007/s11356-019-07105-7>
8. Burkard, R.: Sound pressure level measurement and spectral analysis of brief acoustic transients. *Electroencephalogr. Clin. Neurophysiol.* **57**(1), 83–91 (1984). [https://doi.org/10.1016/0013-4694\(84\)90010-5](https://doi.org/10.1016/0013-4694(84)90010-5)
9. Arenas, J.P., Suter, A.H.: Comparison of occupational noise legislation in the Americas: an overview and analysis. *Noise Health* **16**(72), 306–319 (2014)
10. Occupational exposure limits for hazardous agents in the workplace part 2: physical agents: GBZ 2.2–2007. National Health Commission of the PRC (2007)
11. Code for design of noise control of industrial enterprises : GB/T 50087–2013. Ministry of Housing and Urban of the People’s Republic of China (2013)
12. Bell, L.H., Bell, D.H.: *Industrial Noise Control: Fundamentals and Applications*. CRC Press, Boca Raton (2017)



Study on the Environmental Characteristics of UAV Swarm Anti-swarm

Zeliang Jiao, Qian Liu, Yanyan Ding, Hongyan Ou, Jiantao Liu, Hongyi Li, and Weixin Liu^(✉)

Zhengzhou Campus, CPLA Army Artillery and Air Defense Forces
Academy, 450052 Zhengzhou, China
2242127616@qq.com

Abstract. (Purpose) This paper is to study the environmental characteristics of the new combat style of UAV swarm and anti-swarm. (Methods) Conceptual analysis and comparative research methods are used in the research process. (Results) Three environmental characteristics of UAV swarm anti-swarm in battlefield, electromagnetic and social environment are sorted out, and the corresponding conclusions are drawn from the comparison with traditional anti-swarm methods. (Conclusion) It is concluded that the UAV swarm and anti-swarm has the features of wide range of battlefield environments, complex electromagnetic environment and social environmental safety. (Application direction) The research results of this paper can be applied to the construction of the UAV swarm anti-swarm system, which provides a certain reference for its operational use in different environments.

Keywords: UAV swarm · Environmental characteristics · Air defense operation

On the basis of integration of open architecture, UAV swarm is constructed by a large number of UAVs based on the combat capability of single platform UAVs, supported by the cooperative interaction ability of UAVs, centered on the emerging ability of swarm intelligence. A combat system with the advantages of survivability, low-cost function distribution, and intelligence features [1]. UAV swarm anti-see colony is a new concept and combat mode which uses its own UAV swarm to against the enemy UAV swarm. Compared with the traditional anti-drone methods such as missile and shell, the combat space of swarm and anti-swarm is more deeply intermingled with the external environment, and has some advantages in battlefield environment, electromagnetic environment and social environment.

1 Wide Range of Battlefield Environmental Characteristics, the “Active Lift-Off” Shows Its Role in

The systematic existence of UAV swarm gives it strong adaptability. When some individuals in the swarm are destroyed, the remaining individuals can change their behavior according to the battlefield situation, and realize the strategic and experiential learning, thus improving the survival rate of UAV swarm system [2]. Therefore, when the incoming UAV swarm infiltrates different battlefield environments, our UAV can also be projected into the corresponding environment to conduct interception operations.

1.1 Outstanding Low-Altitude Combat Capability

With the characteristics of small size and low noise, UAV swarm can penetrate the conventional air defense system in low altitude and ultra-low altitude. When UAV swarm flies below the near boundary of the air defense missile, the air defense missile cannot fire, and the anti-aircraft gun cannot rapidly cover the sudden attack with firepower. In actual combat, the UAV swarm also plays an important role of “decoy”, seducing enemy’s radar to turn on to expose itself, so that the swarm can destroy it as soon as discover. It can fight with the incoming swarms at low altitude with the advantage of “active lift-off” feature, and the fighting type of UAV in swarm can be used to destroy enemy’s swarm, which can enhance terminal air defense capabilities at low-altitude.

1.2 Effective Interception Capability at Sea

In the modern marine combat environment, UAV swarm operations have become a new “killer” for attacking large surface ships [3]. At this stage, the ship-borne air defense system is mainly aimed at aircraft and various missiles, and there is still a “blind zone” for the defense of “low, small and slow” scattered targets such as swarms. The U.S. military has conducted a simulation experiment of using the “Coyote” drone swarm to attack the “Aegis” system, and the swarm has worked well. When the swarms attack our large surface ships in the marine environment, we can use the ship-borne missiles as the platform to quickly launch a large number of drones to intercept the incoming swarms, effectively enhancing the ability of ships to fight against swarms and making up for the shortcomings.

1.3 Strong Adaptability to Complex Regions

UAV swarms are highly systematic and widely distributed. The RCS scattering area of a single UAV is small, and it is difficult to be detected by radar and other reconnaissance equipment in complex geographical environments such as rugged mountains and high-rise cities. In the tactical application of UAV swarm anti-swarm, the defender can use the various characteristics of the drone projection platform to use missiles or rockets for long-range cluster projection or use aircraft to “spray” to areas that are difficult to deploy with conventional air defense weapons in a variety of complex terrains (in cities, it can be directly launched into the air), according to the preset route based on intelligent flight control technology and path planning technology, it can carry out combat tasks such as patrolling, warning, reconnaissance and interception and destruction of enemy swarms that may strike.

2 The Electromagnetic Environment Has Complex Characteristics, and “Overcoming the Enemy and Saving Oneself” is Particularly Critical

The control, formation and autonomous capabilities of UAV swarms are completely based on airborne electronic equipment such as communication modules and flight control modules [4]. In the UAV swarm anti-swarm operations, the electromagnetic environment is relatively complex. The UAV swarms on both sides are not only subject to

mutual signal interference within their own swarms, but also face cluttered electromagnetic spectrum interference from the outside world and the electronic countermeasures attack by enemy swarms.

2.1 Outside Spectrum Clutter

In the use of drone swarms to fight against swarms, the external electromagnetic interference will interfere with both offensive and defensive sides indiscriminately, thus affecting the operational fluency of the swarms on both sides. On the one hand, there is civil frequency interference, which mainly includes civil radio devices such as civil satellites, communication relay stations, and broadcasting stations. This kind of interference usually does not have special pertinence and the interference intensity is small. On the other hand, military frequency interference complicates the complex electromagnetic environment in the modern battlefield environment by various command and control systems based on the interweaving of radio stations and various weapons such as shelters and pods with electronic countermeasures. Such interference is usually close to the UAV swarm anti-swarm operations, the interference intensity is large, and it may have high-power interference specifically aimed at UAVs.

2.2 Opposite Reactance Suppression

The “soft kill” with electronic countermeasures as the main type is an important means of fighting between the two sides in the UAV swarm anti-swarm operations. Both sides can use electronic interference or pulse shock to interfere or suppress each other. One is active interference. UAVs concentrate electromagnetic energy to actively transmit or forward targeted electromagnetic frequency bands to the other UAVs to suppress, interfere or even burn through the communication modules of the other UAVs. The second is passive interference. The UAV reflects the electromagnetic energy radiated by the enemy by releasing the chaff of the load to interfere and suppress the opponent, which is usually passive.

2.3 Mutual Interference of Own Signal

Since the swarm usually consists of dozens or even more individual clusters, the complicated radio signals during internal signal transmission will cause mutual interference, especially in the case of electronic countermeasures. Electromagnetic waves emitted by drones will often cause harm to their nearby counterparts. Therefore, how to intelligently concentrate and distribute electromagnetic energy and how to automatically avoid electromagnetic interference have a great impact on the practical application of UAV swarm anti-swarm.

3 Characteristics of the Social Environment Are Safe, and “Minimally Invasive Surgery” is Accurate and Reliable

According to the “five-ring strike theory” and the history of war, social and environmental factors such as people’s livelihood facilities and the will of the masses often play a crucial

role in the direction of the war. UAV swarms can sneak into cities to perform tasks such as “decapitation operations” and disrupt and destroy urban facilities. Compared with traditional conventional weapons, the “minimally invasive surgical interception” of UAV swarm anti-swarm is safer and more reliable for the social environment.

3.1 Few Casualties

The main factor that determines the outcome of the battlefield is people, and the number of casualties usually affects the morale of the combat troops and thus the outcome of the war. In swarm anti-swarm operations, our projection personnel often use projection platforms far away from the enemy swarm to project, and operators usually sit in the operation cabin or conduct command through satellites in a remote command post. In this way, there is a certain safe distance from the enemy swarm, thereby avoiding “short-hand weapon contact” with the enemy swarm, and weapons such as missiles, bullets and high-energy particle beams carried by the enemy swarm cannot harm our personnel. The safety of our personnel is guaranteed to the limit and social panic caused by casualties is avoided.

3.2 Small Impact on People’s Livelihood

People’s livelihood is an important factor affecting the development of human society and environment. In future wars, enemy drone swarms may penetrate into our cities to harass and destroy important targets such as our hydropower plants, communication centers, and local governments. If the traditional conventional weapons are used for fire interception, it is easy to cause accidental explosion and accidental injury. The use of high-power electromagnetic weapons for soft kill will affect civilian communication facilities early and cause a certain social panic. Instead, UAV swarms are used to intercept UAV swarms, and the advantages of miniaturization, distribution, and low cost of swarms, as well as the ability to precisely kill the incoming swarms, are used to precisely hunt and kill incoming swarms, so as to reduce damage to people’s livelihood facilities.

3.3 High Economic Benefits

Swarm operations has high economic benefits, the enemy needs to spend dozens or even hundreds of times the cost to attack and defend, which will greatly increase the enemy’s combat cost and indirectly bring advantage in cost-effectiveness exchange to our side [5]. Therefore, in the UAV swarms attack, when the defender uses missiles, artillery shells and high-power electromagnetic interference, the attacker will have an asymmetric economic advantage over the defense, thereby dragging the defender’s social-economic environment into the war mud. If the swarm anti-swarm method is adopted, both sides are low-cost, high-performance systematic combat weapons, which will weaken the enemy’s asymmetric economic advantages, thereby improving operational economic benefits, reducing logistical support pressure and reducing negative impact on the social and economic environment.

4 Conclusion

With the gradual application of UAV swarm operations, the means to combat UAV swarms are also more important. As a new anti-swarm method with certain advantageous environmental characteristics, the continuous research on it is a beneficial exploration in the field of anti-UAV swarm operations, so as to remain invincible in the future battlefield environment.

References

1. Lina, Y., Zeyang, C., Jianjun, W.: Demand analysis of anti-UAV swarm combat system. *Air Force Mil. Acad.* **1**, 37–40 (2019)
2. Zhongying, Y., Yulong, W., Chuanlong, L.: Research on the development status and trend of UAV swarm combat. *Aeronaut. Missile* **5**, 34–38 (2019)
3. Yong, H., Yue, W., Yuanfeng, L., Zao, Z.: Threat analysis of UAV swarms against sea operations. *Command Control Simul.* **6**, 1–6 (2019)
4. Hu, L., Li, Z., Qiu, Z.: Analysis of UAV swarm combat application. *UAV*, (28) (2018)
5. Chen, F., Huang, J., Zhao, Y.: Analysis on the development of U.S. unmanned bee colony combat technology. *J. Equipment Coll.* (4) (2016)



Research on the Comprehensive Evaluation of Environmental Comfort in Deep-Sea Confined Space Based on Entropy Weight Method

Chuan Wang¹, Juan Wang²(✉), Ziyang Wang¹, and Zhibo Lu²

¹ Naval Medical Center of PLA, Naval Medical University (Second Military Medical University), Shanghai 200433, China

² College of Environmental Science and Engineering, Tongji University, Shanghai 200092, China

wangjuan@tongji.edu.cn

Abstract. In order to provide a reference for improving the environment of deep-sea confined space and improving the comfort of the space environment, this study constructs a deep-sea confined space from four aspects: heat and ventilation environment, light environment, sound and vibration environment and comprehensive design according to the characteristics of deep-sea confined space environment. The environmental comfort evaluation index system has established a comprehensive index evaluation method, including index standardization, index weight determination based on entropy weight method, index comprehensive calculation and classification. A questionnaire survey was used to investigate and comprehensively evaluate the environmental comfort of a deep-sea confined space manipulation area (Area A), a residential area (Area B) and a dining area (Area C). The environmental comfort evaluation index system of deep-sea confined spaces is constructed from twelve dimensions, including temperature, ventilation, odor, humidity, noise, vibration, swing, lighting, color matching, space design, human factor design, and floor comfort. The research results put forward corresponding improvement suggestions for the environmental comfort of a certain deep-sea confined space manipulation area (Area A), living (B area) and dining area (C area).

Keywords: Entropy weight method · Confined space · Environmental comfort · Comprehensive evaluation

Preface

The cabin activity space in the deep-sea confined space environment is limited, and cabin environment is closed related to the safety and comfort of navigation, which affects the comfort and working efficiency of operators directly. This paper is aimed at establishing the comprehensive evaluation system of the comfort of deep-sea confined spaces through researching the comprehensive influence factors of confined spaces, and provides reference for improving the space environment of deep-sea confined spaces, and improving the comfort of space environment.

1 Evaluation Indicator System of Environmental Comfort of Deep-Sea Confined Space

Comfort refers to individuals' a peaceful and calm of mental state in space, and a comfortable feeling of physical and mental health without pain or fear [1]. Environmental factors of heat and ventilation mainly include temperature, humidity, ventilation, etc. Among them, temperature is an important factor [2]. Too high or low ambient environment will aggravate the sick building syndrome, reduce air quality, resulting in affecting work efficiency [3, 4]. Sound and vibration environmental factors mainly include sound intensity, vibration, etc. High-strength sound will cause distraction, increase psychological burden, and impair memory, resulting in reducing work efficiency [5]. Light environmental factors mainly include lighting, color, etc. The persons with higher illumination have higher attention levels than the persons with lower illumination. In conclusion, 12 indexes are selected to establish the evaluation index system of comfort degree of deep-sea confined space (Fig. 1).

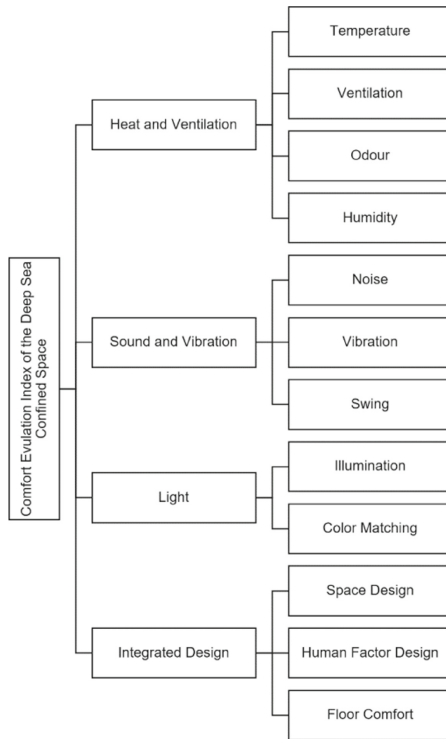


Fig. 1. Evaluation index system of comfort degree of deep-sea confined space

2 Determination of Index Weight

Entropy-right method (ERM) was used in this paper. Essentially, it adopted the effective value of the index to determine the weight coefficient.

- (1) When i evaluation objects (samples) and j indexes were selected to establish the decision matrix $X(n \times m)$

$x_{11} \cdots x_{1m} \cdots x_{n1} \cdots x_{nm}$, X_{ij} was the value of the j^{th} index of the i^{th} evaluation object (sample). ($i = 1, 2, \dots, n$; $j = 1, 2, \dots, m$).

- (2) Standardized treatment of index

$r_{ij}^* = x_{ij} / \max\{x_{1j}, x_{2j}, \dots, x_{nj}\}$ (forward index) ($i = 1, 2, \dots, n$; $j = 1, 2, \dots, m$).

$r_{ij}^* = \min\{x_{1j}, x_{2j}, \dots, x_{nj}\} / x_{ij}$ (contrary index) ($i = 1, 2, \dots, n$; $j = 1, 2, \dots, m$).

- (3) Calculate the proportion of the i^{th} evaluation object (sample) in the j^{th} index, and establish the standardized data matrix

$$y_{ij} = r_{ij}^* / \sum_{i=1}^n r_{ij}^* \quad 0 \leq y_{ij} \leq 1$$

$$Y = y_{ijn} \times m$$

- (4) Calculate the entropy of the j^{th} index.

$$e_j = -K_j \sum_{i=1}^n y_{ij} \ln y_{ij}, \quad K_j = 1 / \ln n$$

- (5) Calculate the information effectiveness of the j^{th} index.

$$d_j = 1 - e_j$$

- (6) Calculate the weight of the j^{th} index.

$$w_j = d_j / \sum_{j=1}^m d_j$$

3 Comprehensive Evaluation and Grading of Indexes

The method of weighted mean was used in the comprehensive evaluation of environment comfort of deep-sea confined spaces according to the calculation result of entropy-based weight. Calculation formula:

$$C = \sum_{i=1}^n w_i X_i$$

In formula: X_i represents the specific value of the standardized i^{th} index (0–1).

W_i represents the weight of this index.

n represents the number of indexes.

Environmental comfort is divided into five levels according to the result of comprehensive evaluation, including “extremely uncomfortable”, “uncomfortable”, “little comfortable”, “comfortable”, and “extremely comfortable”. Grading standard is shown in Table 1.

Table 1. Classification standard for environmental comfort in deep-sea confined spaces

C value	0–0.3	0.3–0.5	0.5–0.75	0.75–0.9	0.9–1.0
Comfort classification	Extremely uncomfortable	Uncomfortable	Little comfortable	Comfortable	Extremely comfortable

4 Validation Research

4.1 Data Sources

The environmental comfort of deep-sea confined space control area (Area A), residence area (Area B) and dining area (Area C) were investigated respectively. Each index was assigned with 1–10 points and was an integer. 10 scores indicated very comfortable, and 1 score was the lowest, indicating extreme discomfort. 240 valid questionnaires were collected (Fig. 2).

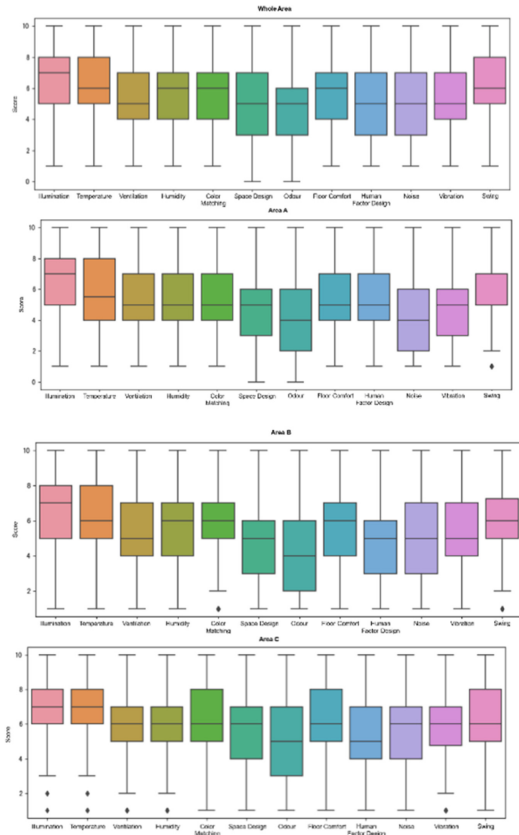


Fig. 2. Statistical chart of the original score of the questionnaire

Respondents generally gave higher evaluation on the comfort degree of indexes such as “illumination”, “humidity”, “swinging”, “color” and “floor comfort” in areas A, B and C, and gave lower evaluation on the comfort degree of “odor” and “space design” indexes.

4.2 Standardized Index

Indexes were standardized by the proportional transformation method. All indexes were forward indexes, namely, the higher the indexes, the better. 10 scores were the maximum. So the standardized formula of evaluation index was as follows:

$$X_i = x_i / 10$$

In formula: X_i -Standardized value of index, x_i -Actual score value of index.

The average values of all sample indexes in each area after standardization are shown in Table 2.

Table 2. Standardized values of indicators

Area	Heat				Sound			Light		Integrated Design		
	Temperature	Ventilation	Odour	Humidity	Noise	Vibration	Swing	Illumination	Color Matching	Space Design	Human Factor Design	Floor Comfort
A	0.57	0.52	0.42	0.55	0.39	0.45	0.57	0.66	0.51	0.47	0.52	0.54
B	0.60	0.52	0.42	0.56	0.51	0.55	0.59	0.67	0.56	0.47	0.48	0.56
C	0.67	0.59	0.51	0.59	0.57	0.58	0.60	0.71	0.60	0.54	0.53	0.60

4.3 Determination of Index Weight - Entropy Weight Method

The entropy value e_i and information utility value d_i were calculated according to the above calculation steps of entropy weight method, as shown in Table 3. Finally, the weight value w_i of each regional index was obtained, as shown in Table 4.

Table 3. The entropy value and information utility value of each regional evaluation index

Num	Index	Area A		Area B		Area C	
		e_i	d_i	e_i	d_i	e_i	d_i
1	Temperature	0.369	0.631	0.390	0.610	0.429	0.571
2	Ventilation	0.381	0.619	0.380	0.620	0.422	0.578
3	Odour	0.366	0.634	0.369	0.631	0.437	0.563
4	Humidity	0.385	0.615	0.390	0.610	0.409	0.591
5	Noise	0.323	0.677	0.406	0.594	0.446	0.554
6	Vibration	0.342	0.658	0.407	0.593	0.430	0.570
7	Swing	0.383	0.617	0.399	0.601	0.404	0.596
8	Illumination	0.387	0.613	0.390	0.610	0.414	0.586
9	Color matching	0.368	0.632	0.395	0.605	0.422	0.578
10	Space design	0.376	0.624	0.377	0.623	0.425	0.575
11	Human factor design	0.403	0.597	0.372	0.628	0.406	0.594
12	Floor comfort	0.377	0.623	0.389	0.611	0.418	0.582

Table 4. The weight value of each regional evaluation index

Classification	Num	Index	Area A	Area B	Area C
Heat	1	Temperature	0.084	0.083	0.082
	2	Ventilation	0.082	0.085	0.083
	3	Odour	0.084	0.086	0.081
	4	Humidity	0.081	0.083	0.085
Sound	5	Noise	0.090	0.081	0.080
	6	Vibration	0.087	0.081	0.082
	7	Swing	0.082	0.082	0.086
Light	8	Illumination	0.081	0.083	0.084
	9	Color Matching	0.084	0.082	0.083
Integrated design	10	Space design	0.083	0.085	0.083
	11	Human factor design	0.079	0.086	0.086
	12	Floor comfort	0.083	0.083	0.084
Sum			1.000	1.000	1.000

4.4 Comprehensive Evaluation and Grading

The standardized value and weight of each index were put into the comprehensive evaluation formula to obtain the comfort evaluation results of each area in the investigated deep-sea confined spaces, as shown in Table 5 and Fig. 3.

Table 5. Evaluation and classification of comfort in each area

Area	A	B	C
Evaluation	0.513	0.540	0.592
Classification	Little comfortable	Little comfortable	Little comfortable

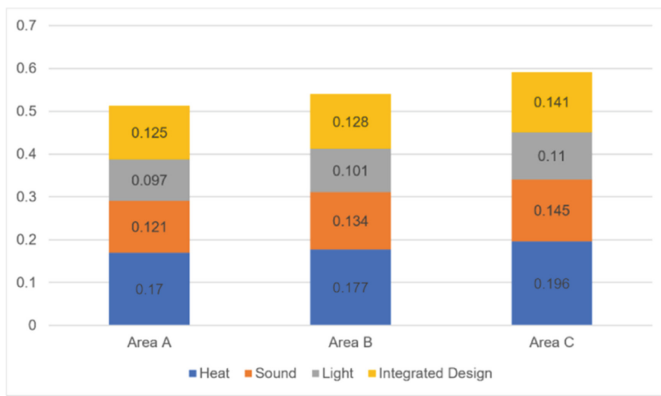


Fig. 3. Classification and evaluation of regional indicators

Single index evaluation for the radar in each region is shown in Fig. 4. The evaluation results of single index in areas A, B and C have similar change characteristics, as shown in the figure. Illumination, temperature and humidity are three indexes with high comfort evaluation level. However, the evaluation results of odor and noise in three areas are obviously low, which can be used as the key environmental factors to improve in the future.



Fig. 4. Comparison of evaluation results of individual indicators in each region

5 Conclusion

The evaluation index system of comfort degree of deep-sea confined space was established in this paper according to the environmental characteristics and work requirements of deep-sea confined spaces; the comprehensive evaluation model was established and applied to empirical study. The evaluation results have provided reference for improving the deep-sea confined space environment, and guiding researchers to independently design questionnaires, carry out data statistics and analysis, optimize the indicator system, and guide the design of human factor.

Acknowledgement. This work is supported by the “Thirteenth Five-Year Plan” key discipline professional construction project, No. 2020SZ21-5.

References

1. Mao, Z., Zhang, H., Sun, X.: Research progress on comfort care and its influencing factors. *Chin. Nurs. Res.* **5**(31), 513–516 (2017)
2. Lan, L.: Mechanism and evaluation of the effects of indoor environmental quality on human productivity. Shanghai Jiao Tong University (2010)
3. Pilcher, J.J., Nadler, E., Busch, C.: Effects of hot and cold temperature exposure on performance: a meta-analytic review. *Ergonomics* **45**, 682–698 (2002)
4. Fang, L., Wyon, D.P., Clausen, G., et al.: Impact of indoor air temperature and humidity in an office on perceived air quality, SBS symptoms and performance. *Indoor Air* **14**(Suppl 7), 74–81 (2004)
5. Jahncke, H., Hygge, S., Halin, N., Green, A.M., Dimberg, K.: Open-plan office noise: cognitive performance and restoration. *J Environ. Psychol.* **31**, 373–382 (2011)



Applicability Analysis of Adaptive Power and Thermal Management System

Junhao Zhang¹, A. Rong²(✉), Liping Pang¹, and Xiaodong Cao¹

¹ School of Aeronautical Science and Engineering, Beijing University of Aeronautics and Astronautics, Beijing 100191, China

347953610@qq.com, {pangliping, caoxiaodong}@buaa.edu.cn

² Institute of Manned Space System Engineering, China Academy of Space Technology, Beijing 100094, China

ivory_118@126.com

Abstract. With the development of electronic integration technology, the heating power of airborne electronic equipment increases gradually, thus the demand for cooling is higher and higher. Meanwhile, the aerodynamic heating effect of supersonic makes the cooling capacity of air as heat sink limited. In order to meet the requirements of the flight mission with Mach numbers from 1 to 4.4, an adaptive power and thermal management system is proposed, which can efficiently manage the heat by taking the external duct air and fuel as heat sink, taking engine bleed air and ram air as refrigeration to suit in wide Mach number flight. The system includes both closed and open operating modes. The heat sink and refrigerant are selected according to the mode to meet the energy requirements of the mission. By calculating the fuel penalty, it's provided a basis for system selection under cooling capacity and power generation requirements, analyzing the adaptability of each subsystem. Closed systems have less fuel penalty at low Mach numbers compared with open system, but require larger cooling capacity from fuel.

Keywords: High speed aircraft · Wide speed range · Heat sink · Thermal management system · Fuel weight penalty

1 Introduction

With the development of multi-electrochemistry of aircraft and the gradual development of electronic equipment integration technology, the airborne thermal load shows an exponential upward trend [1–3]. Especially, the high energy electronic equipment in the aircraft, such as laser weapons, long range radar, makes the requirements of airborne electronic equipment on temperature gradually increase, also, the demand for cold source is increasing. However, the external thermal environment of high-speed aircraft is more serious. With the increase of Mach number, the airframe temperature increases continuously with the increase of flight time because of aerodynamic heating. The heat problem is always the core problem to be solved for high-speed aircraft [4]. For the limited airborne heat sink, the heat problem severely limits the endurance time of high-speed aircraft and the service time of electronic equipment [5, 6]. Therefore, the thermal

management system of high-speed aircraft needs to be able to select and efficiently utilize suitable the limited heat sink according to different flight Mach numbers to ensure the stability of aircraft systems and the safety of aircraft.

The heat sink available for high-speed aircraft is limited, mainly including external air, fuel and carrying expendable coolant [7]. In low Mach number flight state, the temperature of the external ambient air is low, and the external air can also be selected as high-quality heat sink in this flight stage. However, when flying at high Mach number, aerodynamic heating is gradually strengthened, which will eventually lead to the loss of external air heat sink. As the large specific heat liquid that aircraft must carry and must be heated and discharged during flight, fuel is one choice of high-quality heat sink of high-speed aircraft [8]. However, with the increase of flight time, heat accumulates gradually in the aircraft. If fuel and ramjet air continue to be used as heat sink, it will cause overtemperature of electronic equipment due to insufficient fuel flow [9] and excessive ramjet air entrainment flow, resulting in a sharp increase in fuel compensation loss and shortening of flight time [10]. Therefore, the idea of heat-energy integrated design was applied [11, 12].

1.1 New Adaptive Power and Thermal Management System

In view of the different Mach number 1–4.4 flight mission requirements, this paper proposes an adaptive power and thermal management system, which uses external bypass air and fuel as heat sink, uses the engine bleed air and ram bleed air as refrigerating agent, to apply to wide Mach number flight. The adaptive power and thermal management system is divided into two work modes according to the different methods of cooling and power for airborne equipment: closed refrigeration-generating working mode and open refrigeration-generating working mode. Their working principles diagram of the model are shown in Fig. 1(a) and (b) respectively. In both modes, air is used as the refrigerant. Under the action of compressor and turbine, heat is transferred from high temperature heat source to low temperature heat sink, where heat sink can be selected from fuel or external air. The power generation adopts the method of engine air expansion through turbine. When the open system mode is adopted, the refrigeration part can also provide power.

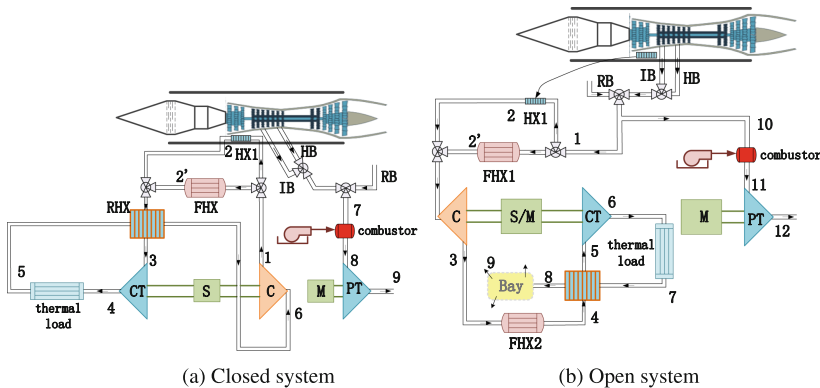


Fig.1. Working mode diagram of adaptive power and thermal management system

1.2 Subsystem Classification

For the closed and open working modes, due to the different selection of heat sink and air source, there are six sub-modes respectively. Because each mode has different influence on engine performance, that is, the cause of fuel weight penalty is different. In this paper, the equivalent system quality method is used to evaluate the system quality, energy consumption, gas source consumption and other costs as fuel weight penalty.

Table 1. Subsystem numbers for different heat sinks and air

Classification	number	Architecture	Cooling air	Heat sink	Power source
Closed system	1	1-2-3-4-5-6-1 7(IB)-8-9	—	External bypass air	Bleed air
	2	1-2'-3-4-5-6-1 7(IB)-8-9	—	High temperature Pao	Bleed air
	3	1-2'-3-4-5-6-1 7(RB)-8-9	—	High temperature Pao	Ram air
Open system	4	1-2-3-4-5-6-7-8-9 10(IB)-11-12	Bleed air	External bypass air High temperature Pao	Bleed air
	5	1-2'-3-4-5-6-7-8-9 10(IB)-11-12	Bleed air	Double Pao	Bleed air
	6	1-2'-3-4-5-6-7-8-9 10(RB)-11-12	Ram air	Double Pao	Ram air

2 Methods

2.1 Fuel Weight Penalty Evaluation Model

In order to analyze and evaluate the characteristics of each system, it's adopted the equivalent system quality method. The system quality, energy consumption, gas source consumption and other costs are equivalent to fuel weight penalty. The adaptive Mach number of each system was obtained by studying the fuel weight penalty of the six subsystems in Table 1 under various working conditions.

The total fuel weight penalty of each system can be calculated by the following formula (Table 2).

$$m_{all} = m_{bypass} + m_F + m_{rim} + m_E + m_{fuel}$$

Table 2. Sources and calculation of fuel weight penalty

Sources	Calculation
Inlet resistance	$m_{bypass} = \frac{\dot{m}_a(v-v_{out})K}{g} \left(\exp\left(\frac{C_e \tau_0 g}{K}\right) - 1 \right)$
Fixed mass equipment weight	$m_F = M \left(\exp\left(\frac{C_e \tau_0 g}{K}\right) - 1 \right)$
Ram bleed air	$m_{rim} = \frac{\dot{m}_e v K}{g} \left(\exp\left(\frac{C_e \tau_0 g}{K}\right) - 1 \right)$
Engine bleed air	$m_E = \left(\frac{\dot{m}_e H^* \left(\pi_0^{\frac{k-1}{k}} - 1 \right)}{H_u \varepsilon_c \left(\pi_c^{\frac{k-1}{k}} - 1 \right)} + \dot{m}_e v C_e \right) \frac{K \left(e^{\frac{C_e \tau_0 g}{K}} - 1 \right)}{C_e g}$
Fuel consumption	$m_{fuel} = \frac{f \cdot \dot{m}_e K}{C_e g} \left(e^{\frac{C_e \tau_0 g}{K}} - 1 \right)$

2.2 System Simulation Under Different Working Conditions

In the process of aircraft design, it is hoped that the adaptive power and thermal management system can meet the demand of cooling capacity and power supply while generating the minimum fuel weight penalty within the flight envelope. According to the refrigerating capacity and power generation range listed in Table 3, the minimum fuel weight penalty required by each system under different energy demands and flight conditions is studied under different refrigerating capacity and power supply, and then the application range of each system is analyzed.

Table 3. The simulation conditions of the adaptive power and thermal management system

Simulation variables	Refrigerating capacity/(kW)	[100,250] Step size 50
	Power generation/(kW)	[0,200] Step size 25
	Cruising Mach number	[1,4.4] Step size 0.2
Basic parameters	Cruise time/(s)	4200
	High Pao Initial temperature/(°C)	150
	Maximum temperature of equipment/(°C)	70
	Closed cycle turbine outlet pressure /kPa	100
	Lift-to-drag ratio	4.62
	Fuel consumption per unit thrust TSFC/(1/h)	3600Ct,1 + Ct,2Ma
	Constant Ct,1/(1/s)	1.1e-04
	Constant Ct,2/(1/s)	6.8e-05
	Inlet drag loss coefficient	0.9
	Adiabatic efficiency of turbines and compressors	0.75
	Mechanical efficiency	0.98
	Turbine maximum temperature/(K)	1400
	Maximum compressor final stage temperature/(K)	800

3 Results

3.1 Minimum Fuel penalty

Figure 2 shows the specific performance of the power supply increasing from 0 to 200 kW when the cooling capacity of the minimum fuel weight penalty of each system is 100 kW.

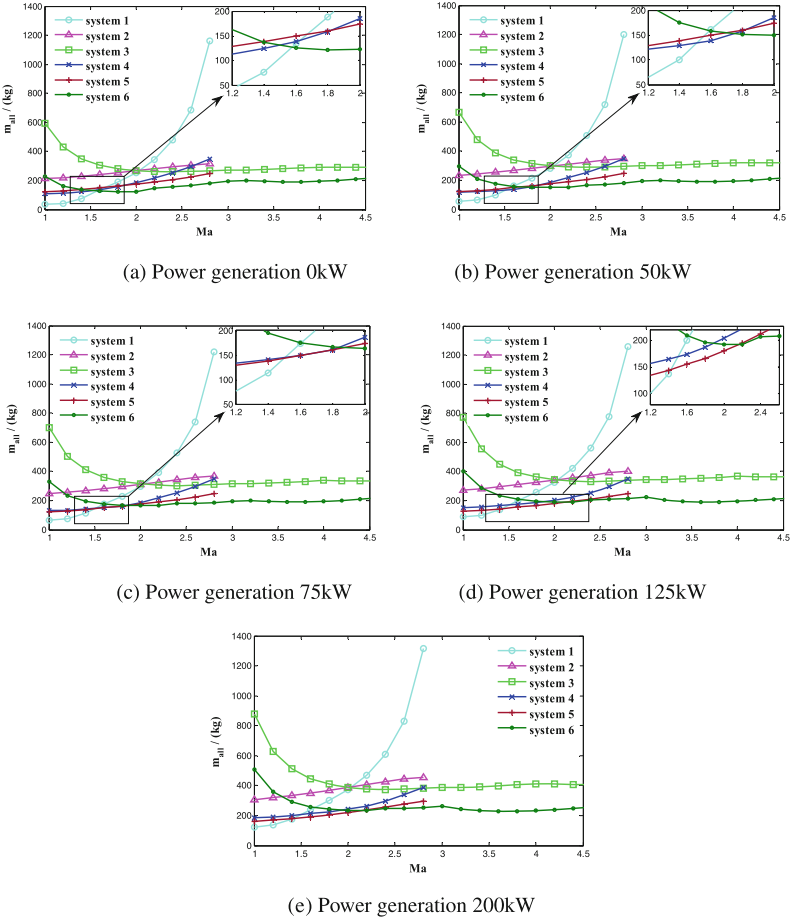


Fig. 2. The fuel weight penalty of each system when the cooling capacity is 100 kW

When the power supply demand is 0, as shown in Fig. 2(a), when $Ma \leq 1.6$, the m_{all} of system 1 is the smallest in all systems; when $Ma \geq 1.6$, the m_{all} of system 6 is the smallest in all systems. The situation at 50 kW is similar to that at 0 kW. When the power supply demand is 75 kW, as shown in Fig. 2(c), the minimum system of m_{all} changes. At this point, when $Ma = 1.6-1.8$, the m_{all} of systems 4 and 5 is the smallest.

As the power supply demand reaches 125 kW, as shown in Fig. 2(d), when $Ma = 1-1.4$, the m_{all} of system 1 is the smallest; when $Ma = 1.4-2.4$, the m_{all} of system 5 is the smallest; when $Ma = 2.2-5$, the m_{all} of system 6 is the smallest. As the power supply further increases, as shown in Fig. 2(e), the m_{all} of each system further increases. Currently, when $Ma = 1-1.4$, the m_{all} of system 1 is the smallest; when $Ma = 1.4-2.2$, the m_{all} of system 5 is the smallest; when $Ma = 2.2-5$, the m_{all} of system 6 is the smallest.

4 Conclusion

The adaptive power and thermal management system studied in this paper is not directly comparable due to the different air source, heat sink and performance of each component. In order to analyze and evaluate the characteristics of each system, the equivalent system quality method was adopted to evaluate the system quality, energy consumption, air source consumption and other costs as equivalent fuel weight penalty. The relationship between the system performance and Mach number under different flight conditions and different energy demands under different working modes was studied.

In the case of Mach number (<1.5), the operating mode of closed refrigeration and power generation is more suitable for the aircraft; In the case of high Mach number (>1.5), it is suitable to adopt the open adaptive power and thermal management system, and when the power supply demand is large, the open system is more competent.

References

1. Mahefkey, T., Yerkes, K., Donovan, B., Ramalingam, M.L.: Thermal management challenges for future military aircraft power systems. In: Power Systems Conference. SAE International, vol. 3204 (2004)
2. Mehta, J., Charneski, J., Wells, P.: Unmanned aerial systems (UAS) thermal management needs, current status, and future innovations. In: 10th International Energy Conversion Engineering Conference. AIAA, vol. 4051, pp. 1–14 (2012)
3. Ganev, E., Koerner, M.: Power and thermal management for future aircraft. In: SAE 2013 AeroTech Congress and Exhibition. SAE International, vol. 2273 (2013)
4. Anderson, J.D., Jr.: Hypersonic and High-Temperature Gas Dynamics, pp. 4–24. McGraw-Hill, New York (1989)
5. Fischer, A.: Design of a fuel thermal management system for long range air vehicles. In: 3rd International Energy Conversion Engineering Conference. American Institute of Aeronautics and Astronautics, vol. 5647 (2005)
6. Yu, S., Ganev, E.: Next generation power and thermal management system. SAE Int. J. Aerosp. **1**(1), 1107–1121 (2008)
7. David, B.D.: Optimal cruise altitude for aircraft thermal management. J. Guidance Control Dyn. **38**(11), 2084–2095 (2015)
8. Moore, A.L., Shi, L.: Emerging challenges and materials for thermal management of electronics (review). Mater. Today **17**(4), 163–174 (2014)
9. Maiorano, L.P., Molina, J.M.: Challenging thermal management by incorporation of graphite into aluminium foams. Mater. Des. **158**, 160–171 (2018)
10. Phillips, E.H.: Langley develops thermal management concept for hypersonic aircraft. Aviat. Week Space Technol. **134**(15), 41 (1991)

11. Newman, R.W., Dooley, M., Lui, C.: Efficient propulsion, power, and thermal management integration. In: 49th AIAA/ASME/SAE/ASEE Joint Propulsion Conference. American Institute of Aeronautics and Astronautics, vol. 3681 (2013)
12. Walters, E., Amrhein, M., O'Connell, T., et al.: Invent modeling, simulation, analysis and optimization. In: 48th AIAA Aerospace Sciences Meeting Including the New Horizons Forum and Aerospace Exposition. AIAA, vol. 287, pp. 1–11 (2010)



New Detection Technology for Food Pesticide Contamination

Handong Yao¹, Dawei Tian², Fengfeng Mo¹, and Shuang Nie¹(✉)

¹ Department of Naval Nutrition and Food Hygiene, Naval Medical University, Shanghai 200433, China
shuangnie94@smmu.edu.cn

² Air Force Medicine Center, PLA, Beijing 100142, China

Abstract. Food contamination is an increasingly serious social problem. It can be divided into microbial, chemical, and physical pollution according to its nature, among which pesticide pollution is the most common chemical pollution. The major constituents include organochlorine pesticides (OCP), organophosphorus pesticides (OPPS), carbamate, pyrethroid diphenyl, germicides, herbicides, etc. There are many technologies to detect pesticide pollution which can be roughly divided into laboratory and sensor detection technologies. Here, we briefly cover some new reports on laboratory detection and latest sensor detection technologies and summarized the advantages and disadvantages of these technologies. We aimed to examine articles, books, and reports that evaluated the future of pesticide detection technologies for food contamination through this paper.

Keywords: Pesticide contamination detection · Laboratory detection Sensor detection

1 Introduction

Food is the indispensable part of social development and the necessity for human survival. However, the problem of food contamination has gradually become a focus of attention in recent years. Food contamination sources are divided into pesticide, pathogen, and biological toxin pollution. Agricultural chemical inputs such as pesticides and synthetic fertilizers are the largest chemicals used in agricultural land [1] (Fig. 1).

Pesticides can be divided into inorganic, organic and biological pesticides by composition and source. There are a lot of fast detection technologies gradually emerging to solve increasingly serious food contamination problems. In this paper, we summarized new highly sensitive detection technologies for pesticide contamination and compared some existing laboratory technologies with portable rapid detection technologies.

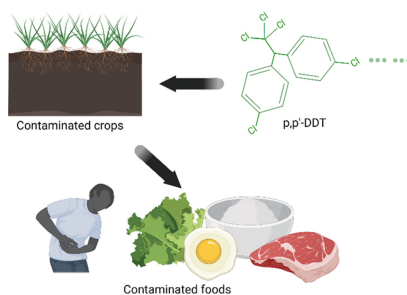


Fig. 1. Food pesticide contamination pathway

2 Laboratory Detection Technologies

2.1 Chromatography and Mass Spectrometry

According to the investigation, chromatography and mass spectrometry is the main detection technology used in pesticide residue monitoring systems in EU, US, and Japan. The derived technologies include gas chromatography-mass spectrometry (GC-MS), high performance liquid chromatography (HPLC) and other related technologies.

GC-MS is considered as a versatile analytical platform which can identify different substances in samples [2]. It is used in industrial testing, food safety, environmental protection, and many other fields. Szarka *et al.* developed a technique for the determination of pesticide residues in nutrient drops containing alcohol by dispersive liquid microextraction combined with GC-MS. The economical and fast program could detect up to 40 kinds of pesticide residues in samples. The limits of detection were 0.001 to $0.910\text{g}\cdot\text{L}^{-1}$, and the quantitative range was 0.004 – $3.003\text{g}\cdot\text{L}^{-1}$ [3].

Compared with gas phase, liquid chromatography (LC) is different in that the sample used for testing is a solution, which does not require the sample to be gas and is not limited by the sample volatility. Gonzalez *et al.* based on the combination of LC and nanotechnologies, developed a nano-flow LC system combined with high resolution mass spectrometry, which realized the detection of multiple pesticide residues in olive oil samples [4].

Although chromatography and mass spectrometry have some shortcomings in the pesticide detection field, they are still widely used in food safety detection with their strong advantages.

2.2 Enzyme Inhibition Technologies

Enzyme inhibition technologies are based on the principle of inhibition of acetylcholine activity by OPPs and carbamate pesticides. In addition to acetylcholinesterase, there are alkaline phosphatase, peroxidase, tyrosinase, laccase, urease, and aldehyde dehydrogenase can detect OPPs, carbamates, dithiocarbamates, triazines, phenylureas, diazines, or phenols [5].

Cacciotti *et al.* reported a multiplied and biopolymeric-based optical bioassay for organophosphate detections based on the use of acetylcholinesterase (AChE) which was

optically detected using Ellman colorimetric technology, and in a range of concentrations between 10 and 100 ppb, achieving a linear range up to 60 ppb and the detection limit of 10 ppb [6]. Jin *et al.* developed a flow injection system for the determination of OPPs and carbamate pesticides using free acetylcholinesterase, synthesized a fluorescent probe overly sensitive to pH and applied it to the flow injection system, and successfully applied to the determination of pesticide residues in vegetable samples [7]. However, due to the large loss of activity of natural enzymes and its poor thermal stability, this approach may become unstable [8]. In the future, the enzyme inhibition technologies will be further developed on improving the sensitivity and repeatability.

2.3 Surface-Enhanced Raman Spectroscopy (SERS)

SERS is a surface spectrum technology. Compared with Raman spectroscopy, SERS has improved the detection sensitivity, and it also has the advantages of no pre-processing, simple operations, and real-time rapid detections (Fig. 2).

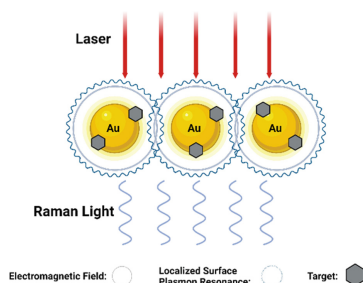


Fig. 2. Surface enhanced Raman Spectroscopy

Kang *et al.* developed a novel and overly sensitive metastable nanoparticles SERS based on amphiphilic polyurethane-silver nanoparticles. The limits of detection for thiabendazole, triazophos and phosmet were 0.02, 0.8 and 0.6 $\mu\text{g}\cdot\text{mL}^{-1}$, respectively [9]. Li *et al.* developed a high sensitivity and good reproducibility SERS sensor by hydrophobic modification of filter paper. The SERS sensor developed could be applied to the detection of Thiram with detection limits of 0.46 nM to 0.49 nM [10]. Zhang *et al.* reported a promising nanoparticle, flowerlike Ag nanoparticles were used as a SERS substrate, which could detect permeative pesticides compared with general detections from leaves, and the SERS data were in accord with the GC-MS results within error limits [11].

However, the disadvantage of SERS is that the target analyte should be separated or concentrated from the matrix before obtaining target spectrums in complex food matrix to ensure SERS can obtain the required spectrums completely.

3 Sensor Detection Technologies

At present, the technologies used for portable detections of pesticide residues are based on sensors. Sensors are detection devices that can feel the measured information and

transform the felt into electrical signals or other required forms of information output according to certain rules. The main sensors used for pesticide detections are electrochemical biosensors, fluorescence sensors, and nano sensors.

3.1 Electrochemical Sensors

Electrochemical sensors can convert chemical signals into electrical signals when chemical reactions occur. These sensors can be used as analytical tools easily and it also can be used in the outside laboratories by non-specialized personnel [12]. In recent years, there have been many developments in electrochemical sensors.

According to He *et al.* studied, he prepared sensing elements for detecting contaminated samples by physical drilling, magnetron sputtering and electrochemical deposition of Au nano dendrites. This sensor could quickly identify pollutants such as Sulfan-1, formicide and thiabendazole in real samples by direct sampling [13]. Noori *et al.* reported an electrochemical sensing system based on modified electrodes. The system could detect lindane in water within 20 s. This system had a sensitivity of $7.18 \mu\text{A} \cdot \mu\text{M}^{-1}$ and can be used for the determination of lindane in groundwater [14]. Electrochemical immunoassay is an analytical technology combining the immunoassay and the electrochemical detections. Bettazzi *et al.* reported an electrochemical competitive immunoassay, based on the use of antibody-modified magnetic particles to detect glyphosate. The calibration curve had been recorded in the 0 to 10,000 $\text{ng} \cdot \text{mL}^{-1}$ concentration range, with a detection limit of $5 \text{ ng} \cdot \text{mL}^{-1}$ and quantification limit of $30 \text{ ng} \cdot \text{mL}^{-1}$ [15].

However, many electrochemical sensors use time-consuming electrode preparation that will be difficult to scale up when commercialisation occurs [16]. So, as mature sensor detection technologies, electrochemical sensors future development trend will focus on reducing the cost of sensor production, improving the technology and so on.

3.2 Fluorescence Sensors

The fluorescence sensors have the advantages of high sensitivity, fast response, and flexible design. The greatest advantage of fluorescence sensors is the output results can be observed by eyes directly. Nowadays the main sensitive elements of fluorescence sensor for pesticide detections are enzyme, antibody, molecularly imprinted polymer, and aptamer.

Aptamers, as base sequences that can specifically bind to target molecules, have attracted increased attention. Ouyang *et al.* used a fluorescence resonance energy transfer technology to develop a fluorescent biosensor for carbendazim pesticide residues detection by observing the fluorescence transfer situation after the specific fluorescence adapter binds to the target. The detection limit of the sensor was $0.05 \text{ ng} \cdot \text{mL}^{-1}$ [17]. Chen *et al.* studied a high-throughput optical array system assembled by thiocholine sensor. It was also mentioned that the database was used to screen the unknown contaminated samples successfully, and the concentrations of pesticides screened were consistent with HPLC technologies [18].

The above two technologies indicates that there are many means to generate fluorescence at present and indicates the wide detection ability of fluorescence sensors.

3.3 Nanometer Materials Sensors

Nanometer materials are materials with a minimum unit size between 1 and 100 nm. There are a lot of nanometer materials that can be used as catalysts. They are highly sensitive to photoelectric signals and are used in modified electrodes to improve the detection performance of sensors [19].

Ganesamurthi *et al.* proposed a hydrothermal synthesis based cobalt oxide nanoparticles into graphite-carbon nitride composite, which was modified on the electrode surface of the sensor as an electrode catalyst, improving the detection ability of thiamethoxam. The detection limit was 4.9 nM, and the linear range was 0.01 to 420 μM [20]. Hu *et al.* designed a novel fluorescent probe consisting of a fluorescent carbon quantum dot, its excitation and emission light could be strongly absorbed by malachite green. Therefore, based on this principle, the author constructed a fluorescence sensor for detecting malachite green in fish. The detection limit of malachite green was 21 nM when the concentration of fluorescent carbon quantum dots ranges from 0.07 μM to 2.50 μM [21]. Similarly, Singh *et al.* reduced redox graphene oxide and ZnO-NFs were chemically synthesized and electrodeposited on a gold electrode, and studied an electrochemical biosensor based on the principle of AChE enzyme inhibition. The limit of detection for the present sensor was 0.01 nM for OPPs pesticides in visceral samples [22].

Nanometer materials have enormous potential for development, but their prohibitive cost makes them unable to be applied to large-scale practical detections.

4 Conclusion

Food contamination is an important problem that needs to be solved urgently today, and pesticide contamination is the main source of food contamination. Based on the laboratory detection technologies and portable pesticide detection technologies, we summarized some new ways appeared in the latest literature and simply explained the advantages and disadvantages of these technologies.

In terms of laboratory detection technologies, this paper lists GC-MS, enzyme inhibition and SERS detection methods. Among them, the GC-MS detection has the highest detection accuracy to achieve accurate quantification of contaminated products in tested samples. Until now, it has always been a relatively mainstream technology. However, one of the disadvantages is that the testing location is limited to the laboratory and other space, so it is easy to cause errors in the process of sample submission. The enzyme inhibition detection methods start with the mechanism of pesticide and have good response ability to the corresponding pesticides, but the detection accuracy is not high, make it can be disturbed by the sample matrix easily, then the result misjudgement occurs. SERS detection methods have the same shortcomings, which cannot make accurate detections in complex samples. Therefore, in conclusion, although the three laboratory detection techniques mentioned above can ensure good sensitivity and accuracy under optimized conditions, they cannot make a good response to complex samples.

The sensor detections' advantages depend on its portability and rapidness. Due to the small size which make them not only can be carry easily, but also can finish on-site detection quickly. But the drawbacks are equally obvious, such as the low-cost sensors cannot detect accurately in the actual complex environments but the sensors with high

detection accuracy are highly expensive, sensors like optical integral sensors or modified by nanomaterials cannot be mass-produced or widely used in daily practical detection. Therefore, the development trend of sensor detection methods is to make a balance between low cost and high detection performance.

Acknowledgements. This work is supported by the Military Biosafety Research Project (grant number: A3702022004). Handong Yao and Dawei Tian contributed equally to this work.

References

1. Gao, Y., Li, H.: Agro-environmental contamination, food safety and human health: an introduction to the special issue. *Environ. Int.* **157**, 106812 (2021)
2. Beale, D.J., et al.: Review of recent developments in GC-MS approaches to metabolomics-based research. *Metabolomics* **14**(11), 152 (2018)
3. Szarka, A., Turkova, D., Hrouzkova, S.: Dispersive liquid-liquid microextraction followed by gas chromatography-mass spectrometry for the determination of pesticide residues in nutraceutical drops. *J. Chromatogr. A* **1570**, 126–134 (2018)
4. Moreno-Gonzalez, D., et al.: Multi-residue pesticide analysis in virgin olive oil by nanoflow liquid chromatography high resolution mass spectrometry. *J. Chromatogr. A* **1562**, 27–35 (2018)
5. Bucur, B., et al.: Advances in enzyme-based biosensors for pesticide detection. *Biosens. (Basel)* **8**(2), 27 (2018)
6. Cacciotti, I., et al.: Reusable optical multi-plate sensing system for pesticide detection by using electrospun membranes as smart support for acetylcholinesterase immobilisation. *Mater. Sci. Eng. C Mater. Biol. Appl.* **111**, 110744 (2020)
7. Jin, S., et al.: Determination of organophosphate and carbamate pesticides based on enzyme inhibition using a pH-sensitive fluorescence probe. *Anal. Chim. Acta* **523**(1), 117–123 (2004)
8. Cao, J., et al.: An overview on the mechanisms and applications of enzyme inhibition-based technologies for determination of organophosphate and carbamate pesticides. *J. Agric. Food Chem.* **68**(28), 7298–7315 (2020)
9. Kang, Y., et al.: A novel metastable state nanoparticle-enhanced Raman spectroscopy coupled with thin layer chromatography for determination of multiple pesticides. *Food Chem.* **270**, 494–501 (2019)
10. Lee, M., et al.: Subnanomolar sensitivity of filter paper-based SERS sensor for pesticide detection by hydrophobicity change of paper surface. *ACS Sens.* **3**(1), 151–159 (2018)
11. Zhang, D., et al.: Detection of systemic pesticide residues in tea products at trace level based on SERS and verified by GC-MS. *Anal. Bioanal. Chem.* **411**(27), 7187–7196 (2019)
12. Pérez-Fernández, B., Costa-García, A., Muñiz, A.D.L.E.: Electrochemical (bio) sensors for pesticides detection using screen-printed electrodes. *Biosens. (Basel)* **10**(4), 32 (2020)
13. He, X., et al.: Microdroplet-captured tapes for rapid sampling and SERS detection of food contaminants. *Biosens. Bioelectron.* **152**, 112013 (2020)
14. Noori, J.S., Mortensen, J., Geto, A.: Rapid and Sensitive Quantification of the Pesticide Lindane by Polymer Modified Electrochemical Sensor. *Sensors* **21**(2), 393 (2021). Basel, Switzerland
15. Bettazzi, F., et al.: Glyphosate determination by coupling an immuno-magnetic assay with electrochemical sensors. *Sens. (Basel)* **18**(9), 2965 (2018)
16. Ferrari, A.G.M., Crapnell, R.D., Banks, C.E.: Electroanalytical Overview: Electrochemical Sensing Platforms for Food and Drink Safety. *Biosens. (Basel)* **11**(8), 291 (2021)

17. Ouyang, Q., et al.: A highly sensitive detection of carbendazim pesticide in food based on the upconversion-MnO₂ luminescent resonance energy transfer biosensor. *Food Chem.* **349**, 129157 (2021)
18. Chen, L., et al.: Broad-spectrum pesticide screening by multiple cholinesterases and thiocholine sensors assembled high-throughput optical array system. *J. Hazard. Mater.* **402**, 123830 (2021)
19. Willner, M.R., Vikesland, P.J.: Nanomaterial enabled sensors for environmental contaminants. *J. Nanobiotechnol.* **16**(1), 95 (2018)
20. Ganesamurthi, J., et al.: Electrochemical detection of thiamethoxam in food samples based on Co₃O₄ Nanoparticle@Graphitic carbon nitride composite. *Ecotoxicol. Environ. Saf.* **189**, 110035 (2020)
21. Hu, Y., Gao, Z., Luo, J.: Fluorescence detection of malachite green in fish tissue using red emissive Se, N Cl-doped carbon dots. *Food Chem.* **335**, 127677 (2021)
22. Singh, A.P., et al.: Nano-interface driven electrochemical sensor for pesticides detection based on the acetylcholinesterase enzyme inhibition. *Int. J. Biol. Macromol.* **164**, 3943–3952 (2020)



Noise Hazard Analysis and Sound Insulation Research of a Semiconductor Manufacturer

Zhenfang Chen¹, Jianwu Chen^{1,3}, Xiaotong Chen^{1,2(✉)}, Yanqiu Shun^{1,3}, Bin Yang^{1,3}, and Weijiang Liu^{1,3}

¹ China Academy of Safety Science and Technology, Beijing 100012, China
2428592766@qq.com

² Capital University of Economics and Business, Beijing 100070, China

³ NHC Key Laboratory for Engineering Control of Dust Hazard, Beijing 100012, China

Abstract. The demand for semiconductors is increasing day by day, but the noise hazard becomes more and more serious with the increase of semiconductor production. The noise was detected using sound level meter in semiconductor production workshop. The results shows that the noise intensity of a semiconductor workshop is about 93.1 dB (A)–94.7 dB (A), which exceeds the noise limit of 9.7 dB and mainly distributes in the frequency range of 1 k–8 k, so it is belongs to high frequency noise. A sound screen was set up at 0.7 m distance from the equipment for noise protection in this paper. On the basis of comparative analysis, the transparent PC board is selected as the sound insulation material. Through theoretical calculation, it is found that the height of sound insulation screen should be at least 1.6 m in order to achieve 20.5 dB sound insulation effect and meet the requirement of noise limit.

Keywords: Occupational health · Noise · Semiconductor plant · Sound insulation

1 Purpose

The demand for semiconductors is increasing day by day [1], but the noise is generated during semiconductor processing and production [2], which is often exceed occupational exposure limit. While the workers exposed to noise for a long time may cause noise hearing loss [3, 4]. In serious cases, it may lead to noise deafness of legal occupational diseases, which may damage workers' occupational diseases, reduce production efficiency and induce safety production accidents [5, 6]. Therefore, this paper takes a semiconductor processing enterprise as an example, divides the noise intensity, and studies its control technology.

2 Research Object and Methods

2.1 Research Object

The semiconductor production workshop is 30 m length × 12 m width × 6 m height, the workshop is equipped with 4 production lines, each production line is equipped with

13 sets of equipment, and a 4 m width passageway is set between the two production lines for the colleague of staff and material transportation. The workshop site is shown in Fig. 1.



Fig. 1. Semiconductor production workplace

The interior wall of the workplace is white limestone wall, the ceiling is made of glass and ordinary perforated aluminum plate, and the ground is epoxy resin. The main work content of the workers is to inspect the equipment and load and unload materials. The workers work for 8 h every day. Due to the long-time noise working environment, the hearing of the workers has decreased.

2.2 Research Methods

According to GBZ/T 189.8-2007 “Measurement of noise in the workplace”, the noise was measured by sound level meter (Quest Soundpro, 3M, America), which was set to “A-weighted sound pressure level”, “Slow” and “Octave”.

GBZ 2.2-2007 “Occupational Exposure Limits for Hazardous Agents in the Workplace Part 2: Physical Agents” requires that the occupational exposure limit of noise is 85 dB (A). The noise detection results are analyzed and evaluated by this limit, and it also is set as the noise control target of sound insulation screen design.

Compare the NR (Noise Rating) evaluation curve with the noise octave noise intensity test results to clarify the main frequency of noise distribution and the required noise reduction value of each frequency, because the NR (Noise Rating) evaluation curve is widely used. The calculation method of GB/T 50087-2013 “code for design of noise control of industrial enterprises” is used to design the sound insulation screen.

3 Noise Detection Results and Control Measures

3.1 Noise Detection Results and Analysis

According to the noise test results, the workshop noise intensity is 93.1 dB (A)–94.7 dB (A), exceeding the noise limit 9.7 dB. According to GB/T 50087-2013, in order to achieve the control target of 85 dB (A) [7, 8], the noise limit of each frequency with the noise limit of 80 dB (A) in the NR curve shall be selected. The NR (Noise Rating) is 80 dB (A), which is calculated by Eq. 1 [9].

$$NR = L_A - 5 \tag{1}$$

where:

NR—Noise Rating, dB.

L_A —Allowable sound pressure level of each frequency band, dB. 85 dB (A) in this study.

The comparison results between the noise intensity test results and the limit values [10] of each frequency are shown in Table 1, when $NR = 80$ dB.

Table 1. The comparison results between the noise intensity test results and the limit values of each frequency.

Sound pressure level (dB(A))	Octave center frequency (Hz)							
	63	125	250	500	1 k	2 k	4 k	8 k
Detection results	20.5	39.8	66.1	79	84.2	88.9	89.6	89.5
NR curve data	95	87	82	78	75	73	71	69
Sound transmission loss	/	/	/	1	9.2	15.9	18.6	20.5

As can be seen from Table 1, the frequency of noise exceeding the limit in semiconductor production workshop is 1 k–8 k. Therefore, the noise belongs to high-frequency noise. In order to reduce the sound pressure level to 85 dB (A) for the semiconductor production workshop studied in this paper, it is about 20.5 dB needed to reduce between the frequency of 2 k to 8 k.

3.2 Noise Control Measures

Workers are mainly engaged in patrol inspection, so it is necessary to set a sound insulation screen between the passageway and semiconductor production equipment to reduce the noise exposure level of workers. Therefore, a sound insulation screen [10] is arranged between the semiconductor production equipment and workers’ walking position, and a sound insulation door is arranged in the sound insulation barrier, which is used for carrying out inspection, maintenance and feeding operation of the equipment.

Assume that the device noise is a point source located in the center of the device. A sound insulation screen is arranged at a distance of 0.7 m from the equipment, at which

time the sound source is 1.1 m from the sound insulation screen. If the worker walks in the middle of the corridor, the sound point is at the middle of the corridor and 1.5 m above the ground and the sound point is 1.3 m from the screen. The width of the noise barrier is 26 m, with 4 m in the workshop length direction reserved for the movement of materials and the passage of people. The location of the noise barriers is shown in Fig. 2.

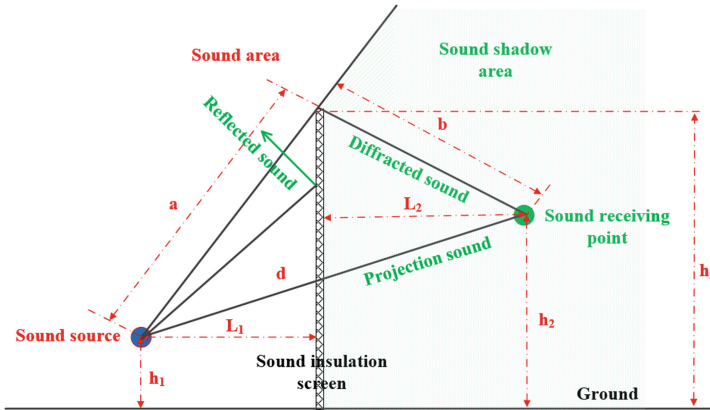


Fig. 2. Sound insulation screen

As seen in Fig. 2, h_1 is the height of the noise source from the ground; h_2 is the height of the sound receiving point from the ground; h_3 is the height of the sound insulation screen; a is the distance from the noise source to the top of the sound insulation screen; b is the distance from the noise source to the top of the sound insulation screen; d is the distance from the noise source to the sound receiving point.

Since workers need to inspect the equipment operation through the sound insulation barrier, transparent sound insulation materials should be selected for the sound insulation barrier, and the commonly used sound insulation materials are PC board (polycarbonate impact resistant board) and glass board. The glass plate is easy to break after impact, which may cause noise occupational injury. PC board has the characteristics of impact resistance and flame retardant, and has better sound insulation coefficient. Therefore, PC board is selected as sound insulation material.

Semiconductor manufacturing workshop is a clean workshop, and it is necessary to control the amount of particles in the air of the workshop in order to ensure product quality. Therefore, when selecting sound-absorbing materials, not only the sound-absorbing coefficient should be high, but also particles should not fall off from the sound-absorbing materials. Therefore, the commonly used sound-absorbing cotton with high sound-absorbing coefficient cannot be used. Polyurethane foam is made by polymerization and foaming of isocyanine and hydroxyl compounds. The material should have not only high sound absorption coefficient, but also excellent elasticity, softness, elongation, compressive strength, chemical stability and wear resistance. Therefore, polyurethane foam is chosen as the sound absorption barrier material.

3.3 Results of the Sound Insulation Screen Height

The sound insertion loss (IL) of sound insulation screen is calculated according to Eq. 2.

$$IL = 10 \log(N + 13) \tag{2}$$

where:

IL—sound insertion loss, dB.

N—Fresnel number. It can be calculated it by Eq. 3.

$$N = \frac{2}{\lambda}(a + b - d) \tag{3}$$

where:

λ —Acoustic wavelength, m. The acoustic wavelength is 0.0425 m when the frequency is 8000 Hz.

a —The distance from the point of sound source to the top of sound insulation screen, m. As shown in Fig. 2.

b —The distance from the point of sound receiving to the top of sound insulation screen, m. As shown in Fig. 2.

d —The distance from the point of sound source to t the point of sound source, m. As shown in Fig. 2.

Therefore, the position of 1.5 m high at 0.5 m, 1.3 m and 2.6 m from the screen is selected as the sound receiving point. 0.4 m of the center height and 0.8 m of the top of the equipment were selected as the noise sources. When the noise insertion loss of 20.5 dB is realized at 8000 Hz, when the sound source height is 0.4 m and 0.8 m respectively, and the receiving point is 1.5 m high at 0.5 m, 1.3 m and 2.6 m from the sound insulation screen respectively, the required height of sound insulation screen is calculated as shown in Table 2.

Table 2. The calculation results of the height of sound insulation screen when the sound source and sound receiving point are in different positions.

The height of sound insulation screen (m)		The distance from the sound receiving point to the sound insulation screen (m)		
		0.5	1.3	2.6
The height of sound resource (m)	0.4	1.6	1.5	1.5
	0.8	1.6	1.6	1.5

As can be seen from Table 2, the noise insertion loss of 20.5 dB can be realized when the sound source height is between 0.4 m and 0.8 m, and the sound point is between 0.5 m and 2.6 m, and the height of the screen is 1.6 m. Therefore, the minimum height of the screen shall be 1.6 m.

3.4 Effect of Sound Insulation Screen

The area of the whole screen is 41.6 m², the sound Absorption Coefficient is 0.02 and the projection coefficient is 0.001 when the frequency is 8 kHz. In order to ensure the workers can effectively carry out the operation of the equipment, it is assumed that the area of polyurethane foam is 20.0 m² of PC board, the Sound Absorption Coefficient is 0.82 and the transmission coefficient is 0.00 when the frequency is 8 kHz. According to Eq. 4 and Eq. 5, the average sound absorption and transmission are calculated as 0.56 dB and 0.0006 dB respectively.

$$\bar{\alpha} = \frac{\sum_{i=1}^n S_i \alpha_i}{\sum_{i=1}^n S_i} \quad (4)$$

where:

- $\bar{\alpha}$ —Average absorption coefficient.
- α_i —Absorption coefficient of substance i .
- S_i —The area of substance i .

$$\bar{\tau} = \frac{\sum_{i=1}^n S_i \tau_i}{\sum_{i=1}^n S_i} \quad (5)$$

where:

- $\bar{\tau}$ —Average transmission coefficient,
- τ_i —Transmission coefficient of substance i .
- S_i —The area of substance i .

According to Eq. 6, the insertion loss of the screen is calculated to be 29 dB, which can meet the requirement of insertion loss should be greater than 20.5 dB.

$$IL = 10 \times \log \frac{\bar{\alpha}}{\bar{\tau}} \quad (6)$$

4 Conclusion

The noise intensity of the semiconductor workshop is 93.1 dB (A)–94.7 dB (A), exceeding the noise limit of 9.7 dB, and mainly distributed in 1 k–8 k, which belongs to high frequency noise. The sound exceeds the limit of 20.5 dB at 8 kHz, which is the key point of noise control. Noise protection can be achieved by installing a sound insulation screen at a distance of 0.7 m from the equipment. The sound insulation screen is 26 m long and at least 1.6 m high. Using transparent PC board as the sound insulation screen material, the sound insulation effect of 20.5 dB can be achieved.

Acknowledgement. This work is supported by the National key R&D Program of China (No. 2016YFC0801700) and the basic research funding of China Academy of Safety Science and Technology (No. 2022JBKY02).

References

1. Chen, T.: Strengthening the competitiveness and sustainability of a semiconductor manufacturer with cloud manufacturing. *Sustainability* **6**(1), 251–266 (2014). <https://doi.org/10.3390/su6010251>
2. Amick, H., Yazdanniyaz, A.M., Pearsons, K.S., Nugent, R.E.: A review of noise issues in semiconductor clean rooms. In: *Proceedings of Noise-Con*, vol. 90, pp. 247–252 (1990)
3. Itoh, K.: The special issue on “the noise countermeasure of electronic equipment” demand for the manufacturer of semiconductor. *IEEJ Trans. Electron. Inf. Syst.* **123**(7), 1191 (2003)
4. Wokekoro, E.: Public awareness of the impacts of noise pollution on human health. *World J. Res. Rev.* **10**(6), 27–32 (2020)
5. Farooqi, Z.U.R., et al.: Assessment of noise pollution and its effects on human health in industrial hub of Pakistan. *Environ. Sci. Pollut. Res.* **27**(3), 2819–2828 (2019). <https://doi.org/10.1007/s11356-019-07105-7>
6. Arenas, J.P., Suter, A.H.: Comparison of occupational noise legislation in the Americas: an overview and analysis. *Noise Health* **16**(72), 306–319 (2014)
7. Occupational exposure limits for hazardous agents in the workplace Part 2: Physical agents: GBZ 2.2-2007. National Health Commission of the PRC (2007)
8. Bell, L.H., Bell, D.H.: *Industrial Noise Control: Fundamentals and Applications*. CRC Press (2017)
9. Code for design of noise control of industrial enterprises: GB/T 50087-2013. Ministry of Housing and Urban of the People’s Republic of China (2013)
10. Chen, C.H., Deen, M.J.: Direct calculation of metal–oxide–semiconductor field effect transistor high frequency noise parameters. *J. Vac. Sci. Technol. A* **16**(2), 850–854 (1998)



Acoustic Target Recognition Based on MFCC and SVM

Kai Ding¹, Shoujun Zheng¹, Xiaogang Qi², Shan Huang³, and Haoting Liu⁴(✉)

¹ Science and Technology on Near-Surface Detection Laboratory, Wuxi 214035, China

² School of Mathematics and Statistics, Xidian University, Xi'an 710071, China

³ Nanjing ATE Electronic Tech Co., Ltd., Nanjing, China

⁴ Beijing Engineering Research Center of Industrial Spectrum Imaging, University of Science and Technology, Beijing 100083, China

liuhaoting@ustb.edu.cn

Abstract. Feature extraction and classification are the main body of acoustic target recognition. Firstly, amplitude extraction based on harmonic set, MFCC and wavelet packet decomposition are selected as feature selection methods to extract the features of four kinds of measured sound signals respectively. Then, the feature vectors extracted by MFCC method with the best clustering effect are combined with GMM classifier, BP neural network, OVO-SVMs and multi-layer support vector machine as classifiers, and MATLAB is used for simulation recognition and classification. Finally, the recognition results are compared and analyzed. The results show that BP neural network has the best recognition effect, but its robustness is poor, the experimental results are unstable, and the selection of training and test data has a great impact on the recognition rate. The multi classification algorithm based on support vector machine has a better stable recognition rate.

Keywords: Acoustic target recognition · MFCC · Support vector machine · BP neural network

1 Introduction

Vehicle target recognition [1] has important academic value, can produce huge social and economic benefits, and is also an important task of intelligent transportation system. There are many methods to identify targets (optical means, sound, seismic wave, electromagnetic wave), and acoustic sensors have many advantages over other types of sensors. The sound sensor is a passive sensor, which can be arranged in a hidden place to avoid detection. It does not need very strict installation conditions, has low cost and low power consumption. Therefore, it has a good application in the intelligent city research field.

The common sound signal is a non-stationary signal, which is stable only for a short period of time (15 ms–30 ms). The analysis method combining time and frequency domain can extract the local time domain and frequency domain characteristics of the signal at the same time, such as short-time Fourier transform [2], harmonic set [3], Gabor

transform [4], wavelet transform [5], wavelet packet energy [6], which has been deeply studied and widely used. At the same time, in view of the good recognition of animal auditory system in bionics, the conversion and frequency response of analog auditory system to acoustic signal have also achieved good recognition effect. Among them, linear prediction coefficient, linear prediction cepstrum coefficient and Mel frequency cepstrum coefficients (MFCC) [7] are common descriptive features of acoustic signal recognition.

2 Design Ideas

The process of acoustic target recognition can be divided into three steps: signal preprocessing, feature extraction and classification and recognition. In this paper, amplitude extraction based on harmonic set, MFCC and wavelet packet decomposition are selected as feature selection methods to extract the features of four measured sound signals: bus, truck, wheel car and small UAV. Then cluster the features extracted by different methods to find the best clustering method. Then, using the feature vector extracted by this method, combined with Gaussian Mixture Model (GMM) classifier, BP neural network, One Versus One Support Vector Machines (OVO-SVMs) and multi-layer support vector machines as classifiers, Matlab is used for simulation recognition and classification, and the recognition results are compared and analyzed.

3 Simulation and Test

The simulation experiment collects the signals generated by four objects: bus, small UAV, truck and wheeled vehicle, and each type collects two sound signals under different conditions. Some signals will have some useless sounds at the beginning or end of a short period of time, such as voice noise, background noise and so on. Therefore, the pure data mentioned later in this paper refers to the useful sound signal segment recognized by the human ear, while the noisy data refers to the complete sound signal. In order to facilitate subsequent feature extraction, we convert sampling frequency of all types of data into 8192 Hz.

3.1 Signal Pre-processing

In this paper, the detection target is recognized by the most intuitive human ear, and the useful signal time period heard is recorded, that is, pure data. High pass filter is selected for MFCC and wavelet packet decomposition feature extraction, and 30 Hz FIR high pass filter is selected for wavelet packet decomposition to remove background noise; MFCC uses a high pass filter with a filter transfer function of $H(Z) = 1 - \alpha * Z^{-1}$, $\alpha = 0.97$ for pre emphasis.

3.2 Feature Extraction

In this section, the most representative harmonic set amplitude method, wavelet packet decomposition method and the feature vector extracted by MFCC are selected as the feature parameters. Due to the non-stationary and short-time stationary characteristics of the sound signal, three methods are based on frame division and windowing: the frame length L is set to 1024, the frame is moved to half of the frame length, and the Hamming window is selected as the window function. The harmonic set amplitude method, the wavelet packet decomposition method and MFCC feature extraction are shown in Fig. 1.

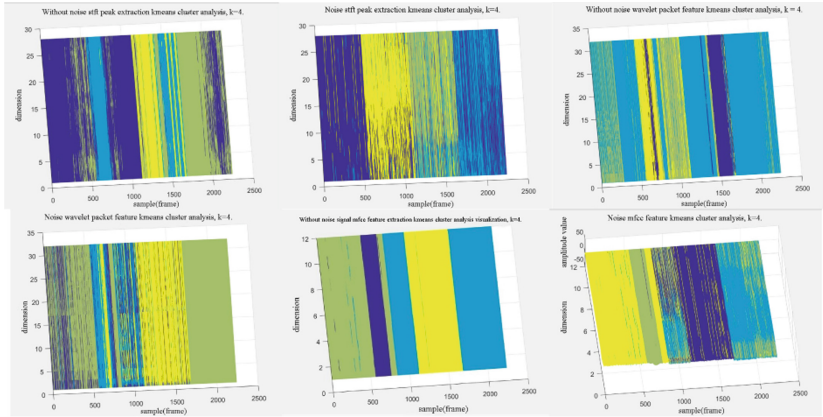


Fig. 1. Harmonic set amplitude method, wavelet packet decomposition method, MFCC feature extraction diagram

Three diagrams of the first layer in Fig. 1 respectively show the harmonic set amplitude method without noise, wavelet packet decomposition method and MFCC feature extraction diagram; three pictures on the second layer show the harmonic set amplitude method with noise, wavelet packet decomposition method and MFCC feature extraction diagram. It is easy to know from Fig. 1 that the colour aliasing of the second and third categories (the number of samples is from 560 to 1120) in the harmonic set amplitude feature extraction diagram is very serious. In addition, the clustering results of the second half of the first category (280 to 560 frames) and the second half of the fourth category (1960 to 2240 frames) are opposite. These show that the features cannot represent the characteristics of each category to distinguish them from other categories. In the wavelet packet decomposition method, a piece of data in the first category (before 560 frames), the second category (561–1120 frames) and the third category (1121–1680 frames) are classified into the fourth category. MFCC clustering effect is significantly better than the first two methods, only the second half of the second category and the fourth category are not clearly distinguished, and other clusters are clear. To sum up, the best clustering method is MFCC.

3.3 Classification and Identification

In this section, representative BP neural network, GMM and SVM multi classification in machine learning (including OVO-SVMs and multilayer support vector machine) are selected for classification and recognition. In order to compare these classification algorithms, MFCC feature vector with the best clustering effect is selected to verify the excellence of the classifier.

The features with good clustering effect are selected uniformly, combined with different classifiers, and the excellence of the classifier is analyzed and judged by calculating the total accuracy, total misjudgment rate and the accuracy and misjudgment rate of each type of acoustic target. The higher the accuracy is and the lower the misjudgment rate is, the better the classifier performance is. Where, the total correct rate = the number of correct classifications/the total number of samples in the test set; total misjudgment rate = average misjudgment rate = sum of misjudgment rates of each type/4; accuracy rate of each type = number of correct classification of the target/total number of the target; misjudgment rate of each type = number of non-targets judged as targets/total number of non-targets. The recognition results of different classifiers are shown in the following table (Tables 1, 2, 3, 4 and 5):

Table 1. Recognition results: MFCC features are extracted through neural network

Type	Bus	Small UAV	Truck	Vehicle	Total
Correct rate	0	86.07%	99.46%	67.86%	63.34%
Misjudgement rate	0	49.04%	1.22%	2.61%	13.22%

Table 2. Recognition results: MFCC feature are extracted through neural network (feature extraction vector with noisy data optional 5000 frame training 3000 test)

Type	Bus	Small UAV	Truck	Vehicle	Total
Correct rate	99%	96.02%	98.27%	99.9%	98.6%
Misjudgement rate	2.01%	0.49%	0.11%	0.7%	0.83%

Table 3. Recognition results: MFCC features are extracted by GMM classifier

Type	Bus	Small UAV	Truck	Vehicle	Total
Correct rate	98.93%	81.61%	98.57%	44.82%	80.98%
Misjudgement rate	22.74%	1.55%	0	0	6.072%

Table 4. Recognition results: MFCC features are extracted by hierarchical vector machine, kernelpar and c are the parameters of SVM classifier

Optimal c , kernelpar value	Performance standard	Bus	Small UAV	Truck	Vehicle	Total
Kernelpar5	Correct rate	97.68%	94.46%	99.82%	53.75%	86.43%
Kernelpar5	Misjudgement rate	5.06%	12.08%	0.83%	0.01%	4.495%
Kernelpar10	Correct rate	98.57%	90.36%	99.64%	50.89%	84.87%
Kernelpar10	Misjudgement rate	6.96%	12.14%	0.95%	0.12%	5.04%
Kernelpar15	Correct rate	98.93%	80.71%	99.82%	49.64%	82.28%
Kernelpar15	Misjudgement rate	11.13%	11.19%	1.19%	0.12%	5.91%

Table 5. Recognition results: MFCC features are extracted by OVO-SVMs, c and g are the parameters of SVM classifier

Optimal c value	Optimal g value	Performance standard	Bus	Small UAV	Truck	Vehicle	Total
$c = 32$	$g = 0.0078125$	Accuracy of each type of judgment	83.21%	96.96%	99.82%	59.1%	84.77%
$c = 32$	$g = 0.0078125$	Misjudgement rate	8.1%	10.18%	1.96%	0.06%	5.075%
$c = 0.5$	$g = 0.0078125$	Accuracy of each type of judgment	84.46%	96.96%	99.64%	60.7%	85.45%
$c = 0.5$	$g = 0.0078125$	Misjudgement rate	1.79%	16.07%	1.49%	0.06%	4.85%
$c = 128$	$g = 0.00048828125$	Accuracy of each type of judgment	82.86%	96.96%	99.82%	61.4%	85.27%
$c = 128$	$g = 0.00048828125$	Misjudgement rate	2.98%	14.35%	2.32%	0	4.91%

It can be seen from the above table that BP neural network has the best recognition effect, but its robustness is poor, the experimental results are unstable, and the selection of training and test data has a great impact on the recognition rate. When we use noisy signals for feature extraction to form a feature set, and then randomly select 8000 frames (including 5000 frames as the training set and 3000 frames as the test set), the recognition effect is very good, reaching more than 98%. However, if the data selection method in

this paper is used to select the data, the effect of BP neural network is not good, while the multi classification method OVO-SVMs and multi-layer support vector machine based on SVM have better recognition rate.

4 Conclusion

In this paper, the collected data of buses, small UAVs, trucks and wheeled vehicles are selected as acoustic targets. The harmonic set, wavelet packet decomposition and MFCC methods are used for feature extraction respectively, and then the features of all categories are combined to form a feature set for cluster analysis. It is found that the clustering effect of MFCC is better. It is found that BP algorithm depends on the selection of samples and test sets, and SVM has better stability and better classification and recognition effect.

Acknowledgement. This work is supported by the National Natural Science Foundation of China, Nos. 61501468, 61975011, the Foundations of Science and Technology on Near-Surface Detection Laboratory, No. 6142414210101.

References

1. Zhou, Y.: The research and implement of moving vehicle precognition based on acoustic signal. In: University of Electronic Science and Technology (2013)
2. Duarte, M.F., Hu, Y.H.: Vehicle classification in distributed sensor networks. *J. Parallel Distrib. Comput.* **64**, 826–838 (2004)
3. Dong, W.: Research on the application of feature extraction and feature optimization in vehicle acoustic classification. In: Zhongbei University (2010)
4. Tao, L., Zhuang, Z.Q.: Real valued discrete Gabor transform for speech analysis. *Electro-Acoustic Technol.* **12**, 3–6 (2000)
5. Yang, C.: Research and realization of acoustic target recognition based on DSP. In: Zhongbei University (2008)
6. Liu, H., Yang, J.A., Xu, X.Z.: A novel low altitude passive acoustic target identify approach research based on MFCC and HMM. *J. Missile Guidance* **5**, 217–219+222 (2007)
7. Lv, X.Y.: Recognition algorithm based on MFCC and GMM. In: Southwest Jiaotong University (2010)

Research on the Man-Machine Relationship



Description Strategy Selection in Collaborative Spatial Tasks

Ying Zhu¹, Duming Wang¹, Guangshan Liao², Liang Liu², Yunfei Chen²,
Lizhi Wang², Hanjun Yang², Wenhao Zhan², and Yu Tian²(✉)

¹ Department of Psychology, Zhejiang Sci-Tech University, No. 928, Second Avenue, Qiantang New Area, Hangzhou 310018, China

² China Astronaut Research and Training Center, No. 26, Beiqing Road, Haidian District, Beijing 100094, China
cctian@126.com

Abstract. *Objective*—To examine the efficiency of description strategies people used in collaborative spatial tasks. *Methods*—Study1 asked participants (N = 30) to describe the location of specific objects under different spatial conditions. The experimental conditions contained different spatial layouts (regular, irregular) and visibility of the interactive partner’s perspective (available, unavailable). We recorded all the utterances and categorized them by the description strategies involved. Study2 tested the efficiency of these strategies. Participants (N = 30) were guided by different kinds of descriptions to make spatial judgments. *Results*— (1) There are four spatial description strategies most commonly used: Addressee-centered, Exocentric, Object-based and Egocentric. (2) Participants’ spontaneous descriptions were affected by their partner’s viewpoint. When the partner’s viewpoint is unavailable, they tend to represent spatial information exocentrically. (3) Organizing spatial instructions in an exocentric way led to better task performance. *Conclusion*—If the collaborators have common cognition of spatial directions and references, exocentric reference frame could maximize the efficiency of spatial interactions.

Keywords: Spatial interaction · Human-robot interaction · Spatial description strategies · Reference frames · Perspective-taking

1 Introduction

As robotics penetrates every aspect of daily life, human and robots begin to work together. The ability of humans to complete collaborative tasks rests, at least partially, on our communication skills. When interacting with partners, we can imagine their viewpoints and describe spatial relationships from another perspective [1] (e.g., “please hand me the scissors on your left”). However, while humans have no difficulties in expressing or understanding spatial languages, it is not easy for robots [2, 3]. To elevate the efficiency of human-robot collaboration, researchers suggested that designers should use human-to-human interaction as a model [4]. Thus, it is essential to study how people spontaneously organize spatial information in natural dialogues.

Previous studies have indicated that the ways people present spatial information are various and dynamic. Researchers have concluded five different types of description strategies: Addressee-centered, Exocentric, Object-based, Egocentric, and Deictic [5]. Speakers dynamically adopt different description strategies, tailoring their spatial expressions to fit the circumstances. Even children from different cultural backgrounds can use these strategies flexibly [6]. Therefore, we assumed that people had a common knowledge of spatial directions and basic reference frames. Views on those spatial description strategies are divided. The first view believes that using Egocentric spatial expressions is the most immediate, while taking other perspectives may require extra mental work. The second view suggests that people can switch to partners' perspectives spontaneously and flexibly [7, 8]. Therefore, Addressee-centered spatial expressions are efficient and frequently used [9].

However, little research has systematically examined the efficiency of those strategies in collaboration. In addition, the communication environment [10–12] and the characteristics of collaborators [13–15] have been confirmed to affect strategy selection. But most of the previous studies fail to take these factors into account, which resulted in their findings being confined to specific communicative situations.

In this work, we set out to solve two problems: (1) What description strategies do people frequently use? Would the strategies vary from communicative situation to another? (2) Among those strategies, which one is the most efficient? Therefore, we conducted two studies. In study1, we collected utterances of participants in different situations and then coded them to calculate the frequency and proportion of different strategies. In study2, we selected the three most commonly used strategies obtained in Study1 as experimental conditions, evaluating their effectiveness in guiding participants to make spatial judgments.

2 Study1

2.1 Method

2.1.1 Subjects

Participants were 30 students (15 females; mean age 21.4 ± 1.2 ; range 17–23) from a local university.

2.1.2 Design

Study1 employed a 2 (Layout: Regular, Irregular) \times 2 (Partner's Viewpoint: Available, Unavailable) within-subject design. We manipulated: whether the spatial layout is Regular or Irregular; whether the partner's viewpoint was Available or Unavailable to the participants.

2.1.3 Materials

We used 12 scenes in Study1 (Fig. 1). Each scene involved a circular table and 4 Gray cubes. In the Regular condition, the objects were arranged in a symmetrical layout. In the Irregular condition, the objects were randomly arranged in an asymmetrical layout.

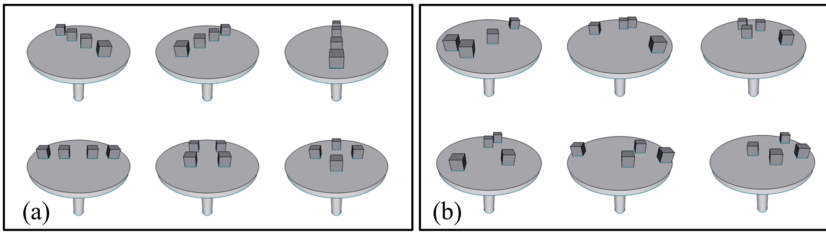


Fig. 1. Scenes used in Study 1: (a) Regular layout; (b) Irregular layout

2.1.4 Procedure

Before the experiment, we explained to the participants that they were going to describe the location of a red target to a partner (who does not actually exist).

During the experiment, participants observed the scenes and expressed their descriptions without a time limit. Each of the 12 scenes was described 4 times, for a total of 48 times. In each trial, the target object was randomly selected from 4 objects, and we highlighted it in red. Participants' utterances were recorded as they performed the task.

In the Unavailable condition, participants perform the task without knowing the partner's viewpoint; In the Available condition, we use an arrow to show the partner's viewpoint from a random direction.

2.2 Results

A total of 1440 utterances were collected. We eliminated 59 (i.e., 4% of the total) utterances for not containing a valid description and coded the rest according to the strategy they involved. Table 1 shows the proportion of four different types of descriptions.

Table 1. Proportion of different description strategies

Description strategies	Example	Percentage
Addressee-centered	"It's on your right"	45%
Exocentric	"It's in the east"	31%
Object-based	"It's beyond the table"	20%
Egocentric	"It's on my left"	4%

- (1) Overall, the most common ways that participants produced descriptions are Addressee-centered (45%), Exocentric (31%), and Object-based (20%).
- (2) Whether the spatial layout was regular or irregular, the commonly used strategies were consistent.
- (3) The speaker's spontaneous strategy is affected by the partner's viewpoint. Participants are more likely to use Addressee-centered descriptions when the partner's viewpoint was available than when it was unavailable (Fig. 2).

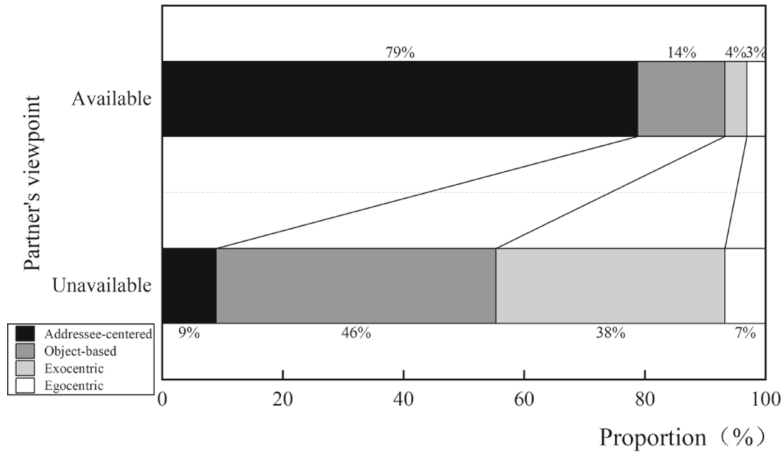


Fig. 2. Observed proportions of the strategies in the *Available* or *Unavailable* condition

3 Study2

3.1 Method

3.1.1 Subjects

Participants were 30 students (15 females; mean age 21.2 ± 1.4 ; range 18–23) from the local university.

3.1.2 Design

Study2 employed a 2 (Layout: Regular, Irregular) \times 3 (Description Strategy: Addressee-centered, Exocentric, Object-based) within-subject design.

We manipulated the spatial environments (Layout) and instructions (Description Strategy) that participants were exposed to. Dependent variables were Reaction time (RT) and Accuracy (ACC) of the target search task.

3.1.3 Materials

We used 12 scenes and 144 instructions in Study2. The scenes were identical with Study1 (Sect. 2.1.3). Spatial instructions are clues to the location of the targets (e.g., “The target is closest to you”). We compiled three sets of instructions based on the three most commonly used strategies (Sect. 2.2): Addressee-centered, Exocentric, and Object-based.

3.1.4 Procedure

Before the experiment, we explained to the participants that they were going to perform a visual search task.

In each trial, we first displayed a scene with an instruction in the center of the screen. Participants followed the instruction, spotted the target from 4 objects, and then typed in their answer. Each of the 144 instructions was randomly displayed 2 times, for a total of 288 times.

3.2 Results

Figure 3 shows the participants' performance (i.e., Reaction time and Accuracy) at each level of the independent variables. A repeated-measures ANOVA revealed that there was no significant difference between regular or irregular layouts, but there was a significant difference between different strategies.

In the Regular condition, a repeated-measures ANOVA showed a significant effect of strategies on Reaction Time ($F(2, 58) = 70.34, p < 0.05, \eta^2 = 0.71$) and Accuracy ($F(2, 58) = 7.09, p < 0.05, \eta^2 = 0.20$). In the Irregular condition, it also showed a significant effect of strategies on Reaction Time ($F(2, 58) = 36.36, p < 0.05, \eta^2 = 0.56$) and Accuracy ($F(2, 58) = 59.56, p < 0.05, \eta^2 = 0.67$).

Overall, the participants' performance differs over the three strategies conditions. The reaction time of Exocentric condition is the shortest, followed by the Addressee-centered, and Object-based. The accuracy of Addressee-centered condition is the lowest, while the Exocentric condition and Object-based condition have similar accuracy.

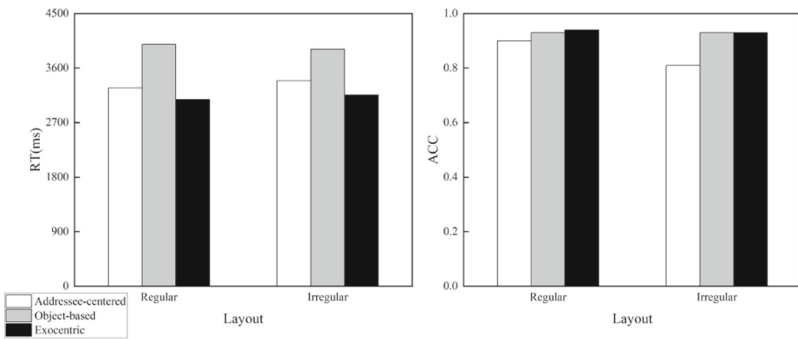


Fig. 3. Reaction Time (RT) and Accuracy (ACC) of three strategies in *Regular* and *Irregular* layout

4 Discussion and Conclusions

In this work, we revealed the description strategies people prefer in different situations and examined the efficiency of participants in comprehending those strategies.

Firstly, we found that there are four spatial strategies most commonly used, which is consistent with the previous findings [5].

Secondly, we found that people would choose different strategies under different situations. When participants know their partners' physical viewpoint, they would consequently use more partner-centered expressions. Otherwise, they would decrease partner-centered expressions and opt to use Object-based or exocentric expressions. This pattern

of effects is consistent with other research on perspective-taking, which similarly found that speakers would spontaneously choose another person's perspective, even when just perceiving the presence of another person [8].

Thirdly, exocentric reference frame (i.e., describe based on the external world) is the most commonly used strategy with the highest communication efficiency. In the traditional view, speakers do not have to switch their perspectives when generating Egocentric expressions. Likewise, for listeners, Addressee-centered expressions should be easy to understand. However, their advantages are limited by the user's role and lack of data support. Through our experiments, those two strategies both showed worse general performance than exocentric reference frame. As eliminating ambiguity is the basis for accurate positioning [3], exocentric expressions always have a clear meaning. Therefore, it causes less ambiguity and decreases the probability of making mistakes.

However, this study also has several limitations. We used an arrow to indicate the partner's perspective, which has relatively low fidelity. On the one hand, participants may not be able to successfully imagine a partner, especially in the Unavailable condition. On the other hand, previous researchers suggested that people's choice of spatial language differs between imagined partners and real-world partners [14]. Therefore, it may also limit the generalization of the results.

Moreover, we assumed that our participants, which were recruited from local universities, had a common understanding of spatial directions and basic reference frames. Nonetheless, their spatial cognition basis may not be completely identical (for example, there are differences in non-linguistic spatial cognition between southerners and northerners in China [16]). Fortunately, this potential issue won't interfere with human-robot interaction. We can select and train human workers while the parameters of the robots can be set manually, making humans and robots have the common sense of spatial directions and strategies. Therefore, we have a positive view on applying exocentric reference frame to human-robot collaborations.

In summary, to achieve better mutual understanding and higher cooperation efficiency, our findings recommend applying exocentric reference frame to the design of human-robot interaction systems.

Acknowledgement. This work is supported by the Space Medical Experiment Project of China Manned Space Program (No. HYZHXM03001), and Funding Project of National Key Laboratory of Human Factors Engineering (No. SYFD061902, No. SYFD061903).

Compliance with Ethical Standards. The study was approved by the Department of Psychology, Zhejiang Sci-Tech University. All subjects who participated in the experiment were provided with and signed an informed consent form. All relevant ethical safeguards have been met with regard to subject protection.

References

1. May, M., Wendt, M.: Visual perspective taking and laterality decisions: problems and possible solutions. *Front. Hum. Neurosci.* **7**, 549 (2013)
2. Sisbot, E.A., Ros, R., Alami, R.: Situation assessment for human-robot interactive object manipulation, pp.15–20 (2011)

3. Ros, R., Lemaignan, S., Sisbot, E.A., et al.: Which one grounding the referent based on efficient human-robot interaction, pp. 570–575 (2010)
4. Xiao Chengli, F.Y., Xu, L., Zhou, R.: Human-centered human-robot natural spatial language interaction (2019)
5. Trafton, J.G., Cassimatis, N.L., Bugajska, M.D., et al.: Enabling effective human-robot interaction using perspective-taking in robots. *IEEE Trans. Syst. Man Cybern. - Part A: Syst. Hum.* **35**(4), 460–470 (2005)
6. Li, P., Abarbanell, L.: Competing perspectives on frames of reference in language and thought. *Cognition* **170**, 9–24 (2018)
7. Tversky, B., Hard, B.M.: Embodied and disembodied cognition: spatial perspective-taking. *Cognition* **110**(1), 124–129 (2009)
8. Tosi, A., Pickering, M.J., Branigan, H.P.: Speakers' use of agency and visual context in spatial descriptions. *Cognition* **194**, 104070 (2020)
9. Tversky, B., Lee, P., Mainwaring, S.: Why do speakers mix perspectives? *Spat. Cogn. Comput.* **1**(4), 399–412 (1999). <https://doi.org/10.1023/A:1010091730257>
10. Mou, W., Zhao, M., McNamara, T.P.: Layout geometry in the selection of intrinsic frames of reference from multiple viewpoints. *J. Exp. Psychol. Learn. Mem. Cogn.* **33**(1), 145–154 (2007)
11. Gramann, K.: Embodiment of spatial reference frames and individual differences in reference frame proclivity. *Spat. Cogn. Comput.* **13**(1), 1–25 (2013)
12. Li, J., Su, X., Wang, Y., et al.: The effect of different object orientation conditions on the construction of intrinsic frame of reference system in virtual scene. *J. Psychol. Sci.* **40**(6), 1322–1327 (2017)
13. Mainwaring, S.D., Tversky, B., Ohgishi, M., et al.: Descriptions of simple spatial scenes in English and Japanese. *Spat. Cogn. Comput.* **3**(1), 3–42 (2003)
14. Duran, N.D., Dale, R., Kreuz, R.J.: Listeners invest in an assumed other's perspective despite cognitive cost. *Cognition* **121**(1), 22–40 (2011)
15. Galati, A., Michael, C., Mello, C., et al.: The conversational partner's perspective affects spatial memory and descriptions. *J. Mem. Lang.* **68**(2), 140–159 (2013)
16. Liu Lihong, Z.J., Huiping, W.: The effect of spatial language habits on people's spatial cognition. *Acta Psychol. Sin.* **37**(04), 469–475 (2005)



Research on Human-Robot Cooperative Target Recognition for Spatial Sampling Task

Shuqi Xue¹, Guangshan Liao¹, Lifeng Tan¹, Yu Tian¹, Yuan Wu¹, Yan Fu²,
Zhixian Zhang³, and Chunhui Wang¹(✉)

¹ National Key Laboratory of Human Factors, Astronauts Research and Training Center of
China, Beijing 100094, China
chunhui_89@163.com

² Huazhong University of Science and Technology, Wuhan 430074, China

³ China Academy of Space Technology, Beijing 100094, China

Abstract. Objective—A new type human-robot collaborative target recognition mode was designed to improve the performance of spatial sampling tasks. *Methods*—The new type not only presented the target attribute information recognized by the robot sensors to humans, but also expressed the credibility of the information determined by the algorithm through a designed interface. An experimental platform for simulating the physical and task environment of the lunar surface were constructed, on which the new type collaborative recognition mode as well as a traditional type mode were designed and simulated respectively. *Results*—The experiment results showed that the new type human-robot collaborative target recognition mode achieved a better accuracy of target recognition. *Conclusions*—In the new mode constructed in this research, the robot processed and presented the attribute information in a humanized manner which matched the human cognitive architecture, thereby achieving a better human-robot collaborative performance.

Keywords: Human-robot collaboration · Target recognition · Spatial sampling task · Human-computer interface

1 Preface

For space exploration tasks to the moon and Mars, the collection and sampling of samples (rocks, soil), etc. is an important task to be performed. The United States obtained a total of about 380 kg of lunar soil through the Apollo program [1], and China obtained 1731 g of lunar soil through the Chang'e 5 task in the form of automatic drilling technology [2]. At present, humans have not yet completed the sampling of Mars samples. It is reported that NASA is expected to realize this magnificent feat in 2031 [3].

With the development of robotics, computer processors, and algorithm technologies, the ability of robots to autonomously recognize the characteristics of specific objects continues to increase. However, for spatial sampling tasks, it is common to encounter the situations (such as illumination, occlusion, special terrain, radiation, etc.) that exceed the boundaries of preset conditions. At this time, in unstructured scenes, the excellent fuzzy

recognition and judgment capabilities of humans will play an important role [4]. Therefore, combining the recognition characteristics and advantages of humans and robots, collaborative target recognition is an important and effective mode. In traditional type target recognition, robots generally directly present the recognition results to humans, and humans cannot communicate with the robots at the knowledge level, and there isn't sufficient information fusion and collaboration.

The human-computer accurate/efficient collaborative work requires establishing a collaborative structure and information sharing mechanism at the system design level. NASA Ames Research Center proposed the Human-Robot Interaction Operating System, HRI/OS [5], which completes system integration through the communication and interaction mechanisms between different Agents. For human and robot teams to share the task planning that may be dynamically changed and the need to complete tasks collaboratively, Sandra and Rachid (2016) [6] proposed an agent implementation framework based on the Theory of Mind. Guided by the theory of situation awareness [7], Chen et al. established Situation Awareness-based Agent Transparency, SAT [8]. In this framework, the trust and workload of members were taken into account, and the transparency-enhanced interface design was carried out. The application test was performed in the simulated aviation flight.

In this research, for the spatial sampling task, we designed a new type human-robot collaborative target recognition mode, which visually presents the target attribute information recognized by the robot sensor to human operators, and the credibility of the information determined by the algorithm is expressed through display interface design. An experimental platform that simulates the lunar environment is constructed, and the traditional type human-robot collaborative target recognition mode and the new collaborative recognition mode are built on the experimental platform to verify whether the new mode can improve the accuracy of recognition.

2 Design

2.1 Target Recognition Ability of Robot

We built a simulated lunar scene and simulated target block with Unity3D, and set three attributes of color, size and roughness for the target block. The above attributes were identified by software through image recognition algorithms, which were used as the baseline of the robot's target recognition capability of this research.

- (1) Color. The in Range function is adopted to realize the binarization function. The inRange function sets the pixel value within the set threshold to white (255), contrarily, it is black (0), and initially extracts the area with black backplane. The image is preprocessed, so that each pixel on the output function is the weighted sum of the corresponding pixel on the original image and the surrounding pixels, and the original image is smoothed. The findContours is adopted to find out whether it contains the point of specified color, and if is adopted to judge whether the result of identifying the target is achieved.

- (2) **Size.** The maximum opening range of the mechanical arm jaws used in the model is 55 mm, which is used as the main reference size. When the maximum cross-sectional width of the target is smaller than the reference size, it is a small target, contrarily, it is a big target. The binocular camera is adopted to acquire the front-view image of the target, the parallax map of the target image is obtained through stereo matching, and the 3D point cloud coordinates corresponding to the parallax map is calculated; and then the cross-sectional area of the target is calculated with the improved OTSU threshold segmentation algorithm.
- (3) **Roughness.** The target image is divided into two parts of the target and the background by adopting the algorithm of gray image segmentation, and the gray image is converted into binary image. After separating the target from the background, it is necessary to calculate the gray value of the target. Since the task environment only needs to be divided into categories, the image gray variance can be used to make a rough classification and a variance limit of 5 shall be set according to the needs of the project. It is rough if the gray scale variance of the target is higher than 5, and smooth if it is lower than 5.

2.2 Design of a New Type Human-Robot Information Collaboration Mode

The computer will mark the target object determined by the robot with a white wire frame. When the cursor moves to the potential target block, a table of specific attribute information recognized by the robot through the sensor will pop up. The information includes not only the recognition results of color, roughness and size, but also the quantitative value of the corresponding attribute characteristics of the image obtained by the algorithm, and this quantitative information is displayed in the form of triangle mark as shown in Fig. 1. Considering the lack of intuitive reference for human to judge the size (big, small) of the block, it also presents the identification contour information of the robot to recognize the block, which is displayed in the form of a green wire frame.

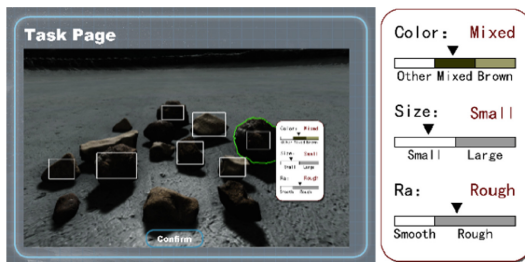


Fig. 1. The interface design of the new type human-robot collaborative target recognition mode

3 Method

3.1 Task of Experiment

There are 14 potential target blocks in the scene (as shown in Fig. 1), each block has its own 3 attributes, and each attribute has 2 characteristics: roughness (rough, smooth),

color (brown, mixed color), shape size (big, small). The block that satisfies the combination of the two attributes of “mixed color, rough, big” and “brown, smooth, small” is set as the target block (6 blocks in total). The goal of the task is to identify all the blocks as much as possible that meet the target attribute requirements.

3.2 Experimental Platform

The unity3D as an experimental platform tool is adopted to build the lunar surface human-computer collaborative operation system, which mainly includes: traditional type operation mode and new type operation mode.

3.3 Volunteers

A total of 31 volunteers were recruited in this experiment, 14 of whom were female, with an average age of 29.2 ± 4.6 years old. The volunteers have normal cognitive ability, operational ability, and hearing, and after standard training process, they could successfully complete various tasks. The experiment plan passed the review of the Ethics Committee of Astronauts Research and Training Center of China, and the volunteers signed the Informed Consent Form before the experiment.

3.4 Design of Experimental Factors

The experimental factors are mainly two interaction modes: traditional type human-robot collaboration and new type human-robot collaboration.

- (1) Human-computer interaction with traditional type human-robot collaboration: in the target recognition stage of the task, the operator needs to find and open the lower-level control page to call up the image of the target block. In the image of the target block, the computer marks the selected block that it has determined to be the target block, which is represented by a wire frame. The operator confirms the choice of the computer, or click with the mouse to cancel the choice, or add other subject blocks. The final confirmed target is the block with a wire frame. The data is saved in the background and the task ends.
- (2) Human-computer interaction with new type human-robot collaborative characteristics: Refer to the summary of Sect. 2.2 of this paper for its design. The operator can judge the result of the determined result of the computer system based on the attribute information presented by the robot and the degree of certainty of the graphic quantification, or assist it in confirmation and re-identification.

3.5 Data Acquisition

After each test time, the experimental platform will output the results, record the results of the initial robot recognition in this test and the final recognition results of the participant. The number in it is the default number of the object block in the system.

The performance indicator of this project is the correct rate of target recognition, which is broken down into the detection rate and false rate. The higher the correct rate

of target recognition, the higher the corresponding detection rate and the lower the false rate.

There are a total of $n_t = 6$ target blocks set by the experiment system; the total number of blocks in each experiment is $n_{total} = 14$, and the number of non-target blocks is $n_{nt} = 8$.

1) Detection rate

Through the output of the system, record the number a of the target block number in each recognition result, and the detection rate P_{dt} is:

$$P_{dt} = \frac{a}{n_t} \times 100\% \quad (1.1)$$

2) False rate

Through the output of the system, record the sum of the number b of non-target object block numbers that appear in each recognition result and the number c of non-target object block numbers that do not appear in each recognition result. The total false rate P_{ft} is:

$$P_{ft} = \frac{b + c}{n_{total}} \times 100\% \quad (1.2)$$

3.6 Experiment Process

Each volunteer has received the training of equal level, and then completed 4 times of target recognition test based on the combination of two task scenes and two operation modes, and the two adjacent scenes are different to avoid the learning effect from same scene.

4 Results

4.1 Performance Results

According to the calculation requirements of performance, the number of detections and false detections of single machine recognition and human-computer collaborative recognition under the new type and traditional type control modes are summarized, and the corresponding performance is calculated based on this. Based on the definition formula, the performance comparison table of under the new type and traditional type models is calculated, as shown in Table 1.

The detection rate of the two sets of experiments under the new type human-computer control and traditional type human-computer control modes was carried out by paired sample t test. The results showed that the detection rate of the new type human-computer control mode ($75.4\% \pm 12.2\%$) was significantly higher than that of traditional type human-computer control mode ($62.7\% \pm 17.2\%$), $t(22) = 4.669$, $p = 0.000$. That is, the new type human-computer control mode can better identify the target object block compared to the traditional type human-computer control mode.

Table 1. The comparison of the performance in different recognition modes

	Detection rate (M ± SD)	False rate (M ± SD)
New type human-robot	75.4% ± 12.2%	20.8% ± 6.2%
Traditional type human-robot	62.7% ± 17.2%	31.4% ± 8.6%

The false rate of the two sets of experiments under the new-human-computer control and traditional-human-computer control modes was carried out by paired sample *t* test. The results showed that the false rate of the new type human-computer control mode (20.8% ± 6.2%) was significantly lower than that of traditional type human-computer control mode (31.4% ± 8.6%), $t(22) = -5.856$, $p = 0.000$. That is, the new type human-computer control mode has a lower probability of incorrectly identifying the target object than the traditional type human-computer control mode.

From the results of performance indicators of detection rate and false rate, it is found that the performance of target object block recognition in the new type human-computer control mode is better than that of the traditional type human-computer control mode.

4.2 Target Attribute Recognition Analysis

The target object blocks in the experiment task have three attributes: color (brown, mixed color), roughness (rough, smooth) and size (big, small). Based on the judgement on three attributes of all object blocks by the volunteers in the questionnaire, the analysis of attribute recognition is carried out, and the analysis index is the correct rate of attribute recognition.

In the recognition of the three attributes of color, roughness, and size, the paired sample *t* test was performed on the recognition accuracy of the new type operation mode and the traditional type operation mode. Only the color recognition accuracy was significantly different ($t(30) = 3.318$, $p = 0.002$), there is no significant difference between the accuracy of roughness recognition and the accuracy of size recognition ($t(30) = 1.223$, $p = 0.231$; $t(30) = 0.440$, $p = 0.663$ (Table 2).

Table 2. The comparison of the accuracy rate of the 3 attributes

	The accuracy rate of color (M ± SD)	The accuracy rate of roughness (M ± SD)	The accuracy rate of size (M ± SD)
New type human-robot	89.4% ± 8.4%	79.3% ± 7.9%	79.3% ± 11.7%
Traditional type human-robot	81.3% ± 9.5%	76.0% ± 10.7%	78.1% ± 8.6%

5 Discussion and Conclusion

Compared with the autonomous recognition of robots, the recognition accuracy rate can be significantly improved after adding human recognition and judgment capabilities. This shows that the recognition ability of humans and the recognition ability of robot sensors complement each other, which can improve the recognition accuracy. In terms of the detection rate and false rate, the new type collaborative mode is significantly better than the traditional type mode by more than 10%. The new type collaborative mode presents the robot's attribute judgment and credibility to humans in a natural form, and is better than the traditional type mode in various correct recognition indicators.

In the traditional type mode, the operator can only obtain the final result of the robot recognition, and modify or confirm on this basis, but the operator cannot evaluate whether the result of the robot recognition should be trusted, or at which level the recognition result of the robot should be trusted. Therefore, it is generally necessary to perform subject block recognition again, which does not have the effect of superimposing the recognition ability of the robot and the recognition ability of the human.

In the new type mode, after the robot obtains the target attribute information that it recognizes, it is recalculated to feed back and prompt the information to the operator in a structured form. The operator can not only obtain the result of each attribute recognized by the robot, but also observe the degree of the recognition quantitative value close to the critical value from the pointer position. If it is closer to the critical value, it proves that the credibility of the image recognition result by robot is low, at that time, the operator can focus on identifying the corresponding attributes. In addition, the subject block contour identified by the green wire frame can be used for intuitive comparison between the operator and the image. If the contour identified by the robot is significantly different from the contour of the subject block recognized by the human, then combining the identification information in the target attribute table, the comprehensive judgment of human-robot identification information can be carried out.

In summary, through the new type human-robot collaborative target recognition mode constructed by this research, the robot will process and present its identification information in a humanized manner, matching the human cognitive architecture, thereby achieving better human-robot collaborative performance, which can improve the target recognition accuracy.

Acknowledgement. This work is supported by the Manned Aerospace Research Project of China, No. 030602, and Foundation Strengthening Project Technical area Funding, No. 2020-JCJQ-JJ-449.

Compliance with Ethical Standards. The research was approved by the Logistics Department for Civilian Ethics Committee of Astronauts Research and Training Center of China. All subjects who participated in the experiment were provided with and signed an informed consent form. All relevant ethical safeguards have been met with regard to subject protection.

References

1. Logsdon, J.M.: The decision to go to the moon: project Apollo and the national interest. *Int. Affairs* **47**(4), 876 (1971)

2. Qian, Y., Xiao, L., Head, J.W., Wilson, L.: The long sinuous rille system in northern oceanus procellarum and its relation to the chang'e-5 returned samples. *Geophys. Res. Lett.* **48**(11) (2021). <https://doi.org/10.1029/2021GL092663>
3. Excell, J.: On the mars path: this summer's hot destination is mars, and few people know more about the logistics of getting there than brian muirhead, flight system designer for the pathfinder and chief engineer at nasa's mars science lab. *Engineer* (2003)
4. Keller, J.M., Gader, P., Tahani, H., Chiang, J.H., Mohamed, M.: Advances in fuzzy integration for pattern recognition. *Fuzzy Sets Syst.* **65**(2–3), 273–283 (1994)
5. Schreckenghost, D., Milam, T., Fong, T.: A perspective on human-robot interaction for NASA'S human exploration tasks (2014)
6. Devin, S., Alami, R.: An implemented theory of mind to improve human-robot shared plans execution. In: 2016 11th ACM/IEEE International Conference on Human-Robot Interaction (HRI). ACM (2016)
7. Endsley, M.R.: Theoretical underpinnings of situation awareness: a critical review. *Situation Awar. Anal. Meas.* (2000)
8. Chen, J., Barnes, M.J., Wright, J.L., Stowers, K., Shan, G.L.: Situation awareness-based agent transparency for human-autonomy teaming effectiveness. In: SPIE Defense + Security. Society of Photo-Optical Instrumentation Engineers (SPIE) Conference Series (2017)



Interface Design of a Health APP Based on the Mentality of the Elderly

Yanhui Xue^(✉) and Jilei Yuan

Hohai University, Jiangsu, China
1203687701@qq.com

Abstract. The health management of the elderly population is a topic of extensive research around the world. Starting from the mental model of the elderly, this paper explores the pain points and unique needs of the elderly in using mobile phone software, and explores the unique thinking logic of the elderly through questionnaires, interviews, literature search, observation and other methods. Using factor analysis to summarize the design factors of mobile phone software for the elderly, this paper refines and summarizes the principles of software design for the elderly. On this basis, an interactive interface of health management software based on the mentality of the elderly is designed, which is suitable for the present and the future, and provides new strategies for the theory and practice of age-friendly design.

Keywords: Psychology of the elderly · Interface design · Ergonomics

1 Introduction

Elderly health is a global hot topic. The elderly are facing the digital divide in smart healthcare. This paper focus on the elderly's needs and propose a new strategy for the aging-appropriate APP design.

2 Preliminary Research

2.1 Research Status

Foreign research on health APP for the elderly is relatively in-depth and forms a theoretical system. Peyer. Gregor proposed the interface design structure of APP for the elderly and the design strategies at all levels according to the learning and cognitive characteristics of the elderly. Flavio. Ferreira investigate the medication situation of the elderly and establish a user role model, evaluating the feasibility of APP-assisted medication by prototype testing. Domestic research on human-computer interaction for the elderly has not yet formed a complete system, but there are still many applied theoretical achievements. Huang Sheng summarized the APP market demand document through interviews and the creation of user roles; Long Yingbing refined the interface design process based on interface design theory [1]. There are many theoretical results of domestic and foreign research and the conclusions are different, resulting in poor practical application effect.

2.2 User Research

In order to explore the physiological characteristics of the elderly and the problems encountered when using mobile phone software, the method of factor analysis was adopted, focusing on analyzing the needs of the elderly when using mobile phone.

According to Table 1, users' needs are divided into physiological needs and psychological needs, with a total of 13 sub-factors.

Table 1. User demand factors

Category	Content	
Physiological	Sight	Vision X1
		Can't see the text and pictures on the phone X2
	Hearing	Hearing X3
		Can't hear phone beeps X4
	Action force	Finger flexibility X5
		Flexibility of legs X6
		Can't keep up with the speed of the phone X7
		Inflexible finger operation X8
	Memory	Memory X9
		Can't remember the steps X10
Psychological	Worrying about safety and afraid to operate X11	
	Do not understand and dare not operate X12	
	Lack of guidance and don't know how to operate X13	

A total of 248 samples were obtained, with an effective rate of 85.08%, including 37 invalid samples and 211 valid samples. The results of reliability and validity test are shown in Table 2. Thus, factor analysis can be performed.

Table 2. Reliability test

Cronbach's α	Cronbach's α based on standardized projects	Number of projects
.674	.643	13

As shown in Table 3, the KMO test and the Bartlett sphericity test were used to test the correlation of variables. According to Table 3, the KMO value is 0.865, and the significance is less than 0.001, so it is suitable for factor analysis.

Table 3. KMO and Bartlett’s test

Kaiser-Meyer-Olkin measure sampling suitability		.865
Bartlett’s test for sphericity	Approximate chi-square	1487.589
	df	78
	Saliency	.000

As shown in the rotated component matrix (Table 4), the main factor F1 has a high load factor with factors X1, X3, X5, X6, and X9, which can be called the physical function factor; F2 has a high load factor with factors X2, X4, X10, which can be called the static usage factor; F3 has a high load factor with factors X11, X12, and X13, which can be called the learning force factor; F4 has a high load factor with factors X7 and X8, which can be called the dynamic usage factor.

Table 4. Rotation factor matrix

	Components			
	1	2	3	4
Flexibility of finger	.818			
Flexibility of leg and foot	.811			
Hearing	.791			
Vision	.760			.315
Memory	.657			– .320
Can’t see clearly		.820		
Can’t hear the sound		.751		.350
Can’t remember operation		.700	.452	
Lack of guidance			.832	
Don’t understand technical terms			.818	
Afraid to operate for fear of safety			.665	.404
Inflexible fingers and difficult to operate	– .310	.473		.663
Slow response and can’t keep up		.497	.396	.593

The cumulative contribution rate of variance of the first four main factors is 73.348%, which meets the requirements of factor analysis. According to the data above, it can be concluded that the design of mobile phone software for the elderly should fully consider the physical function factors of the elderly, such as audio-visual tactile ability; fully consider their static usage factors, such as the ability to accept pictures, texts and sounds; fully consider their learning force factors, such as short-term memory ability

and comprehension ability; fully consider their dynamic usage factors, such as operating habits and short-term response ability.

We conducted interviews and behavioral observations to obtain more user needs. We randomly selected 10 elderly people aged over 60. Interviews and their behaviors were recorded by video after obtaining their consent. The results show that most of the interviewees focus on their weight, blood pressure and blood sugar. They have an insufficient awareness of regular physical examination and ignore personalizing their examinations. They consider medical records, testing and personal files the most important. The software interface needs to be concise and easy to understand. The icons need text annotations and the response time needs to be longer. Through the observation of the behavior, the fingers of the elderly vibrate during the operation. They click on screen hard and squint their eyes. Their operation is hesitant and their reaction time is long.

In addition, the interviews with doctors show that the elderly should focus on their chronic diseases, especially sudden cardiovascular and cerebrovascular diseases. The regular physical examination of the elderly needs to be based on the four examinations of blood test, ECG, ultrasound, and X-ray. Other examinations should be added according to personal physical characteristics.

According to the analysis and summary of user interviews and behaviors, a variety of schemes are provided for the elderly to choose, and finally the best user process scheme is obtained, as shown in Fig. 1.

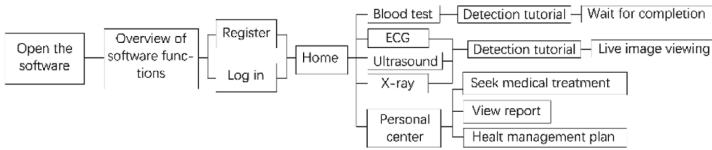


Fig. 1. User flowchart

2.3 Research Summary

According to market research and analysis, there are very few health management apps specially designed for the elderly. Among them, the interface interaction logic is based on the information framework of the software, which lacks in-depth analysis of the mental model of the elderly; the interface design does not completely break through the inertia of traditional design thinking, such as changing large buttons and large texts into large icons and buttons. According to user research and analysis, the needs of the elderly are mainly manifested in physiological factors such as audio-visual touch. For psychological factors such as understanding, memory, and learning, it is difficult for the elderly to directly express them, and they can only distinguish the pros and cons through selection. Therefore, the designer needs to experience the particularity of the thinking of the elderly, in order to fit the software process to the thinking of the elderly as much as possible.

3 Human-Machine Analysis and Effect Presentation

The physiological and psychological factors of the elderly should be fully considered to optimize APPs in logic, human-machine size and user experience.

3.1 Visual Specification Design

Text and pictures are the main information received by the elderly from phones. The following will elaborate on the design of font, color and icons.

For font size, as shown in Fig. 2, the font size can be determined by the word height, and the word height can be calculated according to the formula:

$$h = 2d \times \tan(a/2) \tag{1}$$

where a is the viewing angle; d is the distance between the eyes and the screen.

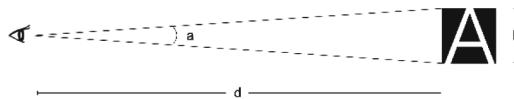


Fig. 2. Relationship between font and viewing distance

According to the literature search, the preferred minimum viewing angle a is 0.75° and the viewing distance d is 20–30 cm for the elderly. Considering the visual comfort, a is enlarged to 1.2° . When d is 30 cm, the minimum character height is 0.6283 cm, which is close to 18 pt in the national standard. Thus, all font sizes should be larger than 18 pt. The design specifications are shown in Table 5:

Table 5. Text specifications

Scenes	List title	Summary of list	Article title	Article body	Supplementary information
Font size (pt)	36	28	42	36	20
Line spacing (times)	1.4	1.2	1.4	1.4	–
Whether to bold	Yes	No	Yes	No	No

For font weight, the reading habits of the elderly are eye-catching and concise. The sans serif is clear and bold with a simple typeface. English fonts can be selected from San Francisco, Robot and Chinese fonts can be selected from Microsoft Yahei and Siyuan Black Body. When the text is long, serif fonts are conducive to the visual management [2]. Besides, the word weight should be increased to semi bold or bold.

For the color, considering the weakened color perception and yellowing of the eye lens, the elderly will selectively absorb blue light, failing to identify blue light. Therefore, use bright and warm colors or neutral colors without blue-based colors.

Considering the needs for high distinction between color and text, color contrasts should be suitable. According to the WCAG (Web Content Accessibility Guidelines), Level AA requires a contrast ratio of at least 4.5:1 for normal text and images and a contrast ratio of at least 3:1 for large text and images. Level AAA requires a contrast ratio of at least 7:1 for normal text and images and a contrast ratio of at least 4.5:1 for large text and images [3].

Considering that the old people’s inherent cognition of medical colors is blue and white, we choose the blue adjacent color purple and match its contrasting color yellow, supplemented by white. The color scheme is shown in the following Fig. 3:

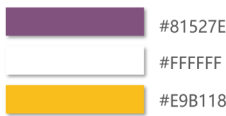


Fig. 3. Color scheme



Fig. 4. Icon design

3.2 Auditory Design Specifications

The elderly suffer from hearing loss and have a low sensitivity to volume. The software needs to automatically set the volume appropriately, which is 67.5–75.3 decibels [5]. A high decibel reminder is needed to avoid long-term high volume.

The elderly accumulates more hard earwax and their inner ear hair cells and the cells of the auditory nerve channel decline and die. So, their response sensitivity to high-frequency sounds is reduced. The gear setting of the video playback speed also needs to be modified according to the audio frequency, shown in Table 6.

Table 6. Speech speed gear

Speed	Slow	Normal	Fast
Multiple	0.75	1	1.25

3.3 Haptic Specification Design

For the two common ways of holding phones, the size of the distal knuckle of the index finger is selected as the minimum size of the button in the interface, which is 19 mm in the national standard GB10000-88. Considering the fingers of the elderly are thicker and more accurate, the size is enlarged to 24 mm, which is 46 pt. Thus, the minimal button size is 46 * 46 pt, and the adjacent spacing areas is 12 pt.

3.4 APP Structure

The APP structure should be close to the user flow of the elderly. According to the previous research, the APP structure is formulated as shown in Fig. 5:

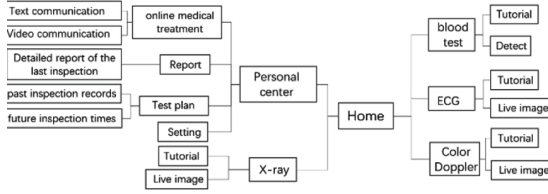


Fig. 5. APP structure

3.5 Other Design Specifications

Considering the comprehension decline of the elderly, the copywriting in the software needs to be easy to understand, as shown in Table 7:

Table 7. Copywriting modifications

Category	Personal center			Settings	
Before	Online consultation	Test report	Inspection schedule	Font size adjustment	Customer service
After	Doctor	Reports	Plan	Font size	Help

3.6 Design Presentation

The final design effect is shown in Fig. 6:



Fig. 6. Final effect

4 Conclusions

This paper obtains the use requirements of the elderly health management software through research and standardizes the visual specifications. According to the conclusions in the research and design process, the design principles of the APP interface for the elderly are obtained (Fig. 7), and we hope to provide new strategies for future aging-friendly design.

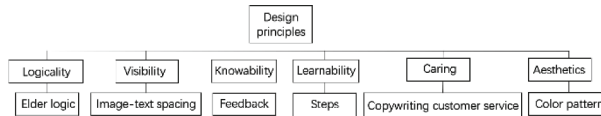


Fig. 7. Design principles

Compliance with Ethical Standards. The study was approved by the Logistics Department for Civilian Ethics Committee of Hohai University.

All subjects who participated in the experiment were provided with and signed an informed consent form.

All relevant ethical safeguards have been met with regard to subject protection.

References

1. Cui, C.: Research on mobile social application software design for urban elderly. *China Acad. Arts* (2021). <https://doi.org/10.27653/d.cnki.gzysy.2021.000003>
2. Xiao, Y.: Research on the interface design of mobile phone application for elderly health management based on mental model. Shandong University (2015)
3. WAI: Web Content Accessibility Guideline WCAG2.0[EB/OL]. <https://www.w3.org/WAI/>. Accessed 16 Oct 2015
4. Zhang, J., Li, Y., Zhu, L.: Research on the optimization design of APP user experience for the elderly based on logistic regression. In: *Packaging Engineering*, pp. 1–10, 10 Oct 2022
5. Huangnan, H.: A study on auditory aesthetic preference of the elderly: taking auditory dependence, sound type, volume, speed and timbre preference as examples. *J. Xinghai Conserv. Music* **3**, 98–106 (2016)



Flight Deck Layout Design of a SSBJ

Guiqing Liu¹ and Zheng Yang²(✉)

¹ AVIC Xi'an Aircraft Industry Group Company Ltd., Xi'an 710089, China

² AVIC XAC Commercial Aircraft Co., Ltd., Xi'an 710089, China

18709224769@139.com

Abstract. This thesis focuses on the design of the flight deck layout for a supersonic business jet (SSBJ). The main work written down is about following the whole design process to design the flight deck. The most critical design feature of the flight deck design is finding out the pilot's field of view and fixing the pilot's seat plane. Analysis and evaluation according to the ergonomics will be discussed in the thesis.

Keywords: SSBJ · Flight deck · Pilot's field of view · Ergonomics

1 Introduction

Technology had developed to a point where engineers were exploring the possibility of civil air travel at speeds of about Mach 1.2 or even as high as 1.8–2.0. With growing interest from many aircraft design companies, this is an appropriate time to investigate the viability of a new supersonic business jet, which is the E-19 project. The E-19 project aimed for a low-boom low-drag supersonic business jet which targets at 2025–2035. It is designed to travel at the cruise speed of Mach 1.8 with at most 10 passengers with baggage of 125 kg per passenger. The overview of E-19 is shown in Fig. 1. It has a slender body with delta wings and the wing span is about 14 m. There are some configuration challenges like the pilot's view that is obstructed by the slenderness of the fuselage forebody and the geometric constraints on the kinematics of the tailplane [1].

As mentioned above, the flight deck layout design of this supersonic aircraft is one of those challenges. This thesis focuses on the design process of the flight deck layout, including the three-dimensional model design. And one of the key points in the flight deck layout design is the design of the shape of the pilot's window, which will also be discussed in this thesis.

2 The Flight Deck Layout

2.1 Flight Deck Philosophy

The flight deck is the place from where the crew fly the aircraft. This task can be divided into two main functions: The control of the aircraft as a moving object in the space and the supervision of the aircraft as a system of systems.

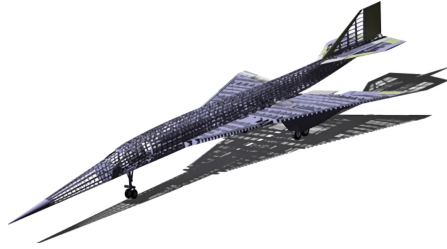


Fig. 1. E-19's overview

The flight deck is the interface between the pilots and the aircraft, the human organization and the environment. First, the pilot must be able to control the aircraft and its position and the aircraft's systems must be able to provide information to the pilot. And as a part of the air traffic, the pilot must be able to express its intentions or to answer controller's requests. Last but not least, the pilot must ensure the safety of the aircraft by avoiding obstacles or hazardous areas.

These are the main features that drive the design of the flight deck: Flight crew, Flight control system, Flight control inceptor, Windows, Display system. Among these features, classic flight deck design is driven by the position of the windows and the position of the pilot's eye.

2.2 Human's Field of View

Each pilot compartment and its equipment must allow the minimum flight crew to perform their duties without unreasonable concentration or fatigue.

To design the flight deck layout, the pilots and other crew must be positioned so that they can reach all controls comfortably. And they must be able to see all flight essential instruments without undue effort. So visibility from the flight deck must adhere to certain minimum standards.

The clear areas of vision should be determined by measurement of angles from the design eye position utilizing ambinocular vision, which is shown in Fig. 2. Ambinocular vision is the total area that can be seen by both eyes [2].

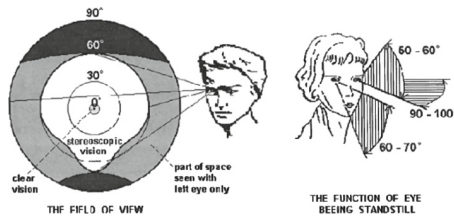


Fig. 2. Human's field of view [2]

According to the SAE ARP4101, the flight deck windshield must provide sufficient external vision to permit the pilot to safely perform any maneuvers within the operating

limits of the aircraft and, at the same time, afford an unobstructed view of the flight instruments and other critical components and displays from the same eye position [3]. Aircraft designers and manufacturers should make every effort to build windshields that offer the pilot more external vision.

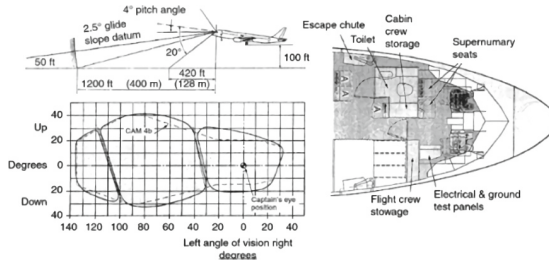


Fig. 3. Vision envelope and flight deck arrangement [4]

This figure shows the arrangement for a narrow-body flightdeck together with its crew vision envelope [4]. We can take it as a reference for E-19 (Fig. 3).

2.3 Pilot’s Field of View

Classic flight deck design is driven by the position of the pilot’s eye. The definition of designed eye point (DEP) is a point fixed in relation to the aircraft structure (neutral seat reference point) at which the pilots’ eyes should be located when seated at the normal position. The DEP is the principle dimensional reference point for the location of flight deck panels, controls, displays, and external vision. The definition of the seat point is the intersection of a tangent to the surface of the bottom of a seated person’s buttocks and a line through the seat back cushion representative of a back tangent line when in a compressed state under the load of a 50th percentile, 175 cm, 77 kg.

Although pilots generally see through both eyes, it is customary to construct the visibility pattern by assuming that point C is the DEP, which is the center of vision. Make sure that the distance labeled L_c is within the indicated range.

It is important to locate point C, which can be seen in Fig. 4(a). Point C can then be used to locate the pilot seat. The seat itself must be located relative to the floor and relative to the controls.

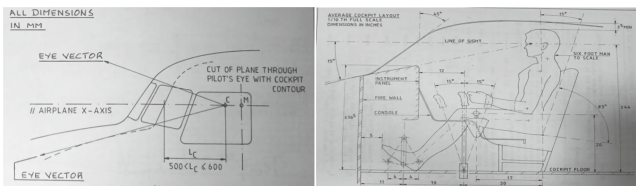


Fig. 4. (a) Center of vision (b) dimension of seat arrangement [5]

Figure 4(b) shows the normal arrangement of the pilot's seat. After orienting the pilot seat, the visibility rules can be used to check the minimum required visibility. Actually, in reality it is very difficult to achieve the "ideal" visibility pattern [5].

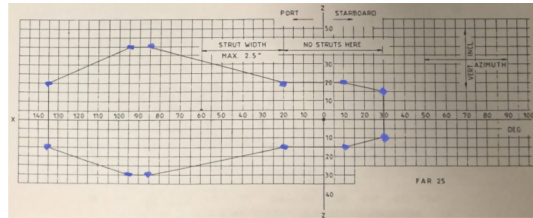


Fig. 5. Requirement for pilots' field of view [4]

The design of the vision has to take into account the requirement for a wide field of view. In Fig. 5, every point inside the boundary line represents a certain angle in vertical and horizontal vision direction. CATIA is used for this design. First adjust the floor plane of the flight deck and as well as the seat point, then select 12 points which are showed blue in the picture from the boundary line and draw 12 lines from the eye point of the portside pilot to make an intersection with the shape of the E-19. The range of the intersection is the ideal minimum range of the windows. And the position of the windows can be adjusted with the point C's adjustment. Then the same thing is done to the starboard side pilot.

Concerning the structure and surface design of the aircraft [6], the design of the shape of the pilot's window is shown in Fig. 6. Figure 7(a) shows the flight deck environment. The view from the portside pilot is shown in Fig. 7(b).

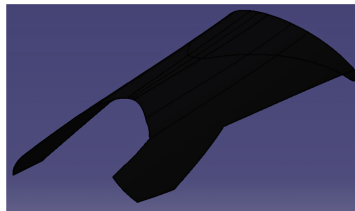


Fig. 6. Pilot's window

2.4 Pilot's Seat

The number of the flight crew is set to two. The E-19's pilot seat is designed following the SAE ARP4101 [3].

Based on the dimension in Fig. 8, the model of E-19's pilot seat is built by CATIA, as shown in Fig. 9. The pilot model chosen in CATIA is 95% American men.

All the controls in the flight deck should be approached easily when the pilots sit on the seats. So if not move the pilots seats, it will be difficult for the pilots to get into their

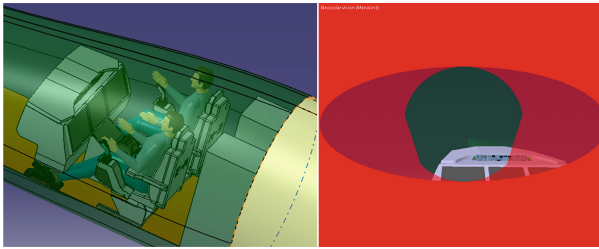


Fig. 7. (a) Flight deck environment (b) portside pilot's view.

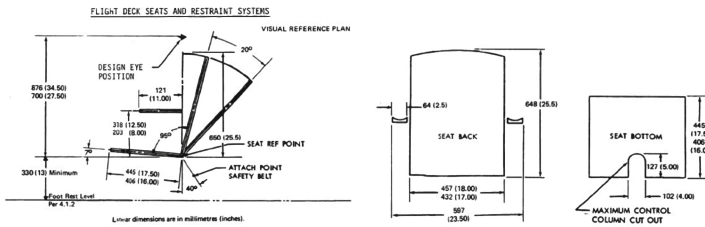


Fig. 8. SAE 4101 pilot seat requirement

seats since the limit space. To solve this problem, tracks can be used to make the pilot seats move [7]. As we can see in the CAD model of E-19's pilot seat, the track is also designed in E-19's pilot seat to move the seat so that it can make space for the pilot.

2.5 Flight Deck Panel and Control Design

A flight deck usually contains instrument panels and controls by which the pilot can fly the aircraft. The overall look of the E-19's flight deck is shown in Fig. 9. In E-19, the flight deck panel is divided into the glare shield, the main instrument panel and the pedestal. The three panels are arranged around the pilots. There are three main displays located in the main instrument panel which is the most critical part in the flight deck. The flight control unit locates in the glare shield, which is often used to control the navigation, altitude and speed [8]. The pedestal is in the centre of the flight deck, with a lot of functions including the landing gear controller, the flaps controller, the speed brake and the thrust control levers.

For the pitch and roll control, three solutions are used in already existing aircraft. There are the yoke, the central stick and the side stick. Given the size of the yoke, the central stick and the side stick, also the limit space of E-19's flight deck, the side stick is chosen to apply for the flight deck. There is no need of physical force to fly the aircraft and this solution provides a better view to the lower control panel, as well as a weight saving as compared to the yoke. It will also reduce the uncomfortable feeling of the pilot during the flight. The side sticks are assembled to the pilots' seats. As the CAD model shown, in the rear part of the flight deck are two black boxes of avionics instruments.

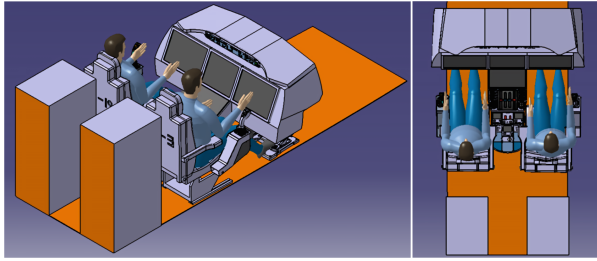


Fig. 9. E-19's flight deck layout

3 Conclusion and Future Work

The design of this flight deck layout is following the relevant regulations. And it still needs to be verified by primary safety assessment. This thesis shows the basic design process and understanding of flight deck layout of a supersonic business jet. In this process, there are some details needed to be discussed deeper and new areas which I am interested in and worthy to investigate further.



Fig. 10. E-19's concept design

In my own opinion, the slenderness of the fuselage brings the flight deck a space issue that the layout is a little bit crowded which is a flaw of this aircraft. However, currently for a supersonic aircraft, there must be one side to make the compromise [9], the concept design with the pilot's window on it can be seen in Fig. 10. So for the future work, I want to do more investigation on the flight deck layout for supersonic aircrafts to see if there's any better actuation solution. Besides, I want to do more research in the synthetic vision system design which can augment the pilot's view.

References

1. Smith, H., Sun, Y.: Low-boom low-drag supersonic business jet E-19 project specification. *Aeronaut. J.* **124**, 76–95 (2019)
2. Raud, G.: E-5 flight deck and synthetic vision (2006)
3. SAE International: Description of Pilot Seat, Report Number AIR4101, rev B, Society of Automotive Engineers (SAE), Warrendale, PA, USA (2001)
4. Fielding, J.P.: Introduction to Aircraft Design (2012)

5. Roskam, J.: *Airplane Design, Part III* (2006)
6. Giannopoulos, I.: *Stressing Data Sheets, Aerospace Vehicle Design Lecture notes AVT-AVD 9632, Cranfield University [Unpublished]* (2015)
7. Pratt, R.W.: *Flight Deck: Practical Issues in Design and Implementation* (2000)
8. Moir, I., Seabridge, A.: *Aircraft Systems: Mechanical, Electrical, and Avionics Subsystem Integration* (2009)
9. Falconer, J.: *Concorde: A Photographic History*. Haynes Publishing (2009)



Research on Man-Machine Interface Layout Method of Intelligent Command Cabin Based on GA-AA

Aiguo Lu^(✉), Bo Dong, Xiaoye Tong, and Wen Li

Wuhan Digital Engineering Institute, Wuhan 430205, China
laigwx@163.com

Abstract. Starting from the solution of man-machine interface layout problem, this paper proposes to combine GA and AA to form a GA-AA hybrid algorithm, which simplifies the actual problem into a mathematical model, through the cabin operator information processing model and the layout method based on cognitive characteristics, Research on the spatial layout technology of man-machine interface based on GA-AA: firstly, the genetic ant colony algorithm and the basic idea of layout optimization based on GA-AA are used to improve the solution efficiency; Secondly, through the evolutionary operation steps and the termination conditions of genetic algorithm, the layout scheme most in line with the law of cognitive characteristics is solved; Finally, ant cycle model is used to solve the best layout scheme.

Keywords: Man-machine interface layout · Intelligent command cabin · Genetic algorithm · Ant cycle model

1 Introduction

In the design of man-machine system, the spatial layout design of man-machine interface should fully consider people's cognitive characteristics, so as to make the operator's operation posture in the cabin more comfortable. From the perspective of cognitive psychology, the cognitive model of man-machine interface is established according to the information processing process, and the spatial layout principles of man-machine interface are summarized as the layout constraints. Then the genetic ant colony algorithm is applied to solve the layout optimization, and the man-machine interface spatial layout design model is established to realize the intellectualization of the cabin man-machine interface spatial layout [1].

2 Construction of Cognitive Model for Cabin Operators

2.1 Information

The relationship between the amount of information x contained in the message and the probability $p(x)$ of the message is as follows:

$$X = \log_a \frac{1}{p(x)} = -\log_a p(x) \quad (1)$$

The determination of information quantity unit depends on the logarithm base a in the formula. Bit is usually used as the unit of information, and the logarithm base $a = 2$. 1 bit information is the information needed for the uncertainty of events with two independent equal probability possible states to be eliminated.

$$X = \log_2 \frac{1}{1/2} = \log_2 2 = 1(\text{bit}) \tag{2}$$

If the information source outputs n messages with equal probability, the amount of information inf of one of the messages with equal probability is equal to the logarithm of the number of messages.

$$\text{Inf} = \log_2 n \tag{3}$$

2.2 Wichens Information Processing Model

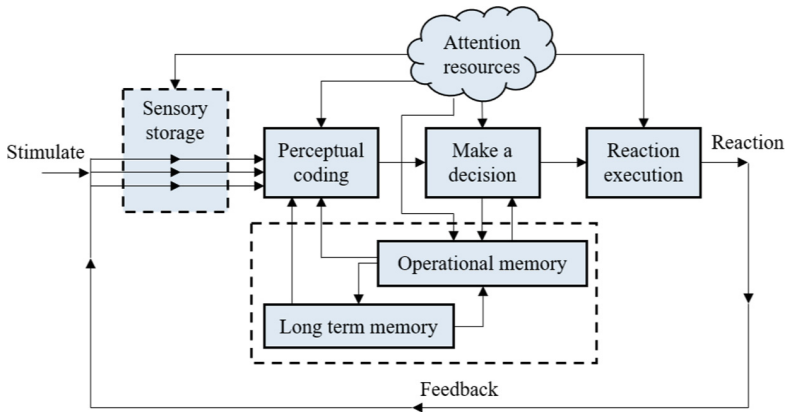


Fig. 1. Information processing model

In cabin operation, sensory information is mainly visual and auditory. Short term memory temporarily encodes, stores and retrieves oral and spatial information; Long term memory stores programs, rules, training, experience and other information. The function of feedback is to strengthen or inhibit the re input of information [2]. Attention runs through the whole process of information processing, and its role is to screen and filter a large amount of information in the outside world. As shown in Fig. 1.

2.3 Human Machine Interface Cognitive Model

As shown in Fig. 2, the design of man-machine interface involves three levels: physiology, cognition and spirit. Ergonomics research human-computer interface usually starts from the lowest physiological level, which is directly related to the difficulty of human-computer interaction [3]. The cognitive level is related to the effectiveness of information

communication design between man and machine, so that the designed man-machine interface can be easy to learn, easy to use, efficient and error avoidance [4]. The spiritual level is the high-level goal of man-machine interface design, focusing on the emotional expression, aesthetic experience, aesthetic structure and the manifestation of traditional culture of man-machine interface.

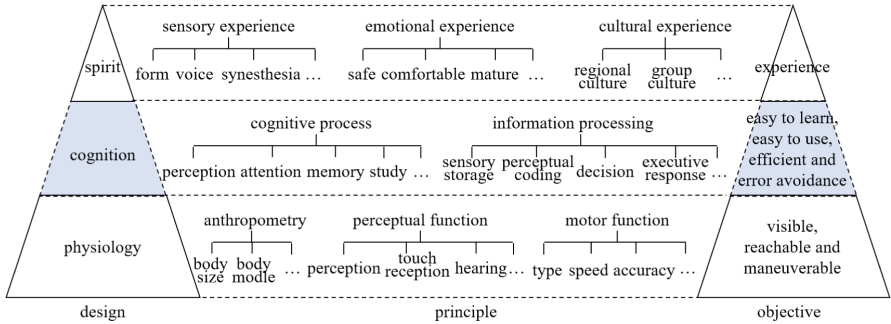


Fig. 2. Human machine interface cognitive model

The spatial layout design idea of man-machine interface is to build a cognitive model based on human information processing mechanism. Based on human thinking characteristics, it uses human information organization law, visual search law and user memory characteristics to make the man-machine interface conform to the cognitive ability of the operator to the interface information [5]. This paper proposes a cognitive model of cabin man-machine interface, as shown in Fig. 3.

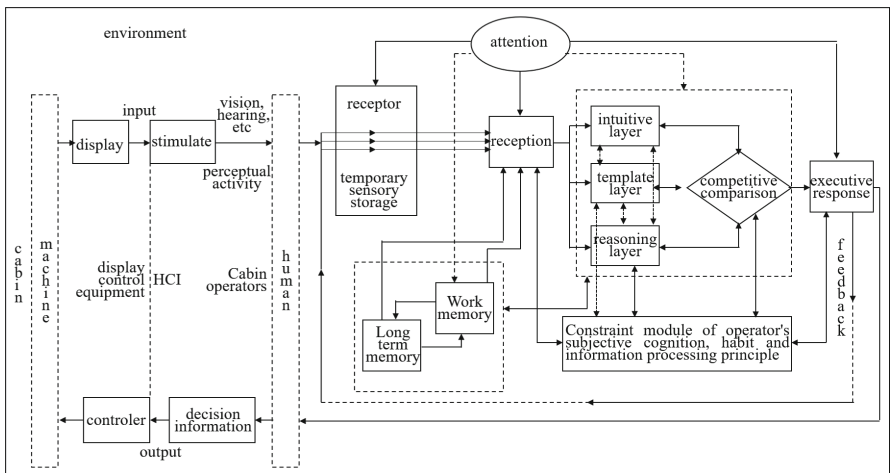


Fig. 3. Cognitive model of cabin man-machine interface

2.4 Research on Layout Method Based on Cognitive Characteristics

1. Cognitive characteristic law

The processing method in line with the habits of the operator can reduce the learning and memory time. For example, if manipulators with similar functions are arranged in the same area, the operator's attention will automatically search the familiar area.

2. Task flow design

According to the tasks that the operator needs to complete, analyze the main operation processes, and then merge, reduce and plan the operation actions according to the cognitive habits of the operator.

3. User cognitive strategy matching

According to the user's visual search characteristics, the key information and other information are displayed in different ways.

4. Information organization law

The principles of similarity, proximity and closeness of visual organization are used to guide layout design.

5. Layout design principles

Considering the above cognitive characteristics, the layout principles of display and manipulator are selected.

- Display layout

- The most frequently observed or important displays are arranged in the central viewing area.
- According to the observation frequency of the display and the correlation degree between the displays, they are reasonably and compactly arranged in different areas.
- Arrange the display in the clockwise rotation direction from left to right and from top to bottom according to the observation order.
- According to the function of the display, arranging the display related to the function together can improve the efficiency and accuracy of reading.

- Manipulator layout

- Arranged in the accessible area.
- Arrange according to the operation sequence.
- Arrange according to importance and operation frequency.
- Arrange by group correlation.
- Spacing requirements of manipulators.

3 Space Layout Technology of Man-Machine Interface Based on GG-AA

3.1 Genetic Ant Colony Algorithm

GA converges faster at the initial stage of search (t0 TA). When it evolves to a certain extent, its evolution rate will decrease significantly, that is, the efficiency will decrease

after t ; On the contrary, AA searches very slowly at the initial stage of search (t_0 TA), but when the pheromone accumulation reaches a certain intensity, the ant's search activities will show a certain regularity under the guidance of pheromone, that is, the speed will increase rapidly after TA. So, as shown in Fig. 4.

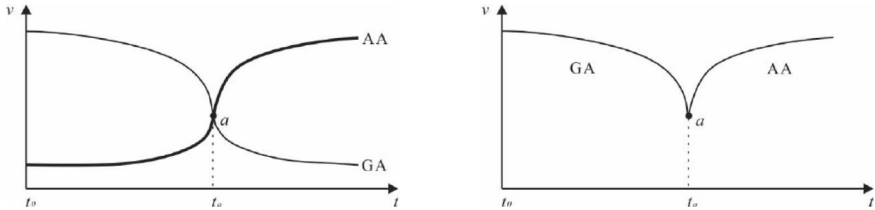


Fig. 4. Ant search law

GA and AA are fused. GA is used to generate the suboptimal solution of the layout scheme before point a , and AA is used to solve after point a .

The basic idea of applying ga-aa to layout optimization is shown in Fig. 5.

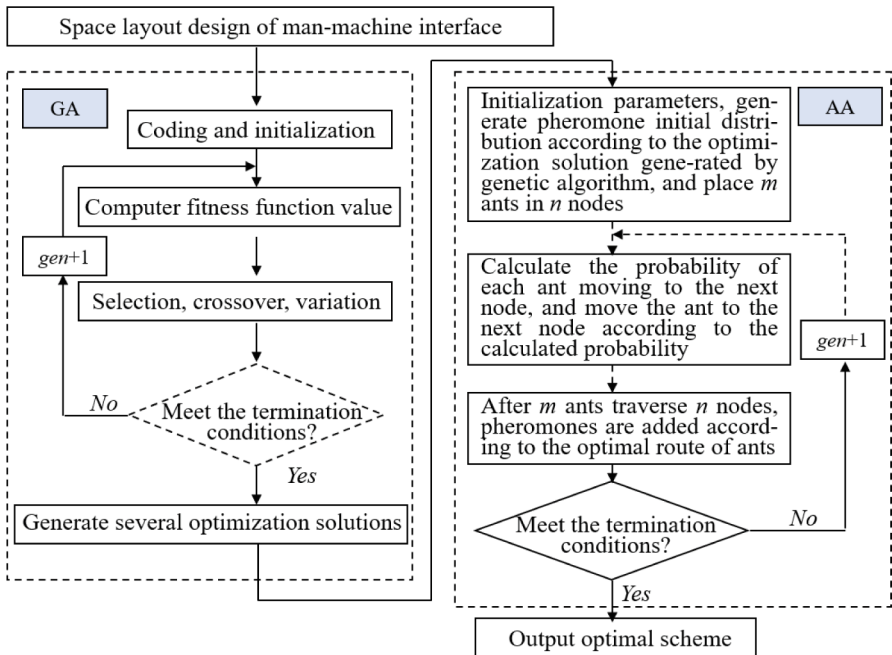


Fig. 5. Basic idea of layout optimization based on GA-AA

GA is used in the first part of the hybrid algorithm. Using the randomness and global convergence of GA, the initial solutions of several personal computer interface spatial layout schemes are generated and transformed into the initial pheromone trajectory

intensity distribution; In the latter part of the hybrid algorithm, AA is used to optimize the layout scheme again. When the initial pheromone trajectory intensity distribution is obtained by transforming the GA solution results, the parallelism and positive feedback mechanism of AA are used to output the optimal solution to improve the solution efficiency.

3.2 Generation of Suboptimal Solution of Genetic Algorithm

The layout of the objects to be solved is the optimal layout of the given space, that is, the layout of the objects to be solved conforms to the layout law of the given space.

Firstly, the fitness value of each individual is calculated, and then the probability that the individual is selected in the selection process is calculated according to the formula. For groups with SCA scale $Pop = \{chr_1, chr_2, \dots, chr_n\}$, the fitness value of individual chr_i is $f(chr_i)$, The selection probability is:

$$Pop(chr_i) = \frac{f(chr_i)}{\sum_{i=1}^{sca} f(chr_i)} \tag{4}$$

Because the sequential crossover has a repair program, this operator is used to crossover the parent individuals and exchange some genes with each other to form a new individual. The specific operation steps are shown in Fig. 6.

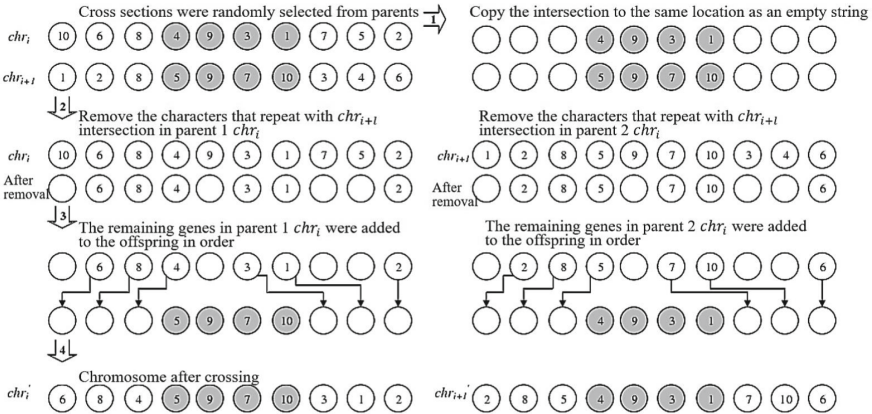


Fig. 6. Schematic diagram of evolution operation steps

The exchange mutation is used to operate the individual mutation, so as to ensure the diversity of the population and prevent immature convergence in Fig. 7.

During the operation of GA, the fusion time of GA and AA is dynamically determined. Firstly, the minimum number of genetic iterations $Genmin$ and the maximum number of genetic iterations $genmax$ are set in GA. Then, in the process of GA iteration, the evolution rate of offspring population is counted according to the formula, and the minimum evolution rate $genp$ of offspring population is set. Within the set number of iterations, if continuous $genq$ generations, the evolution rate of offspring population is

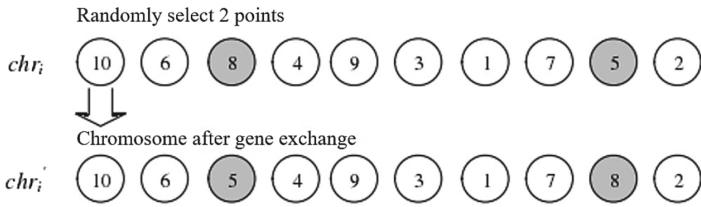


Fig. 7. Termination condition of genetic algorithm

less than gen_p , indicating that the GA optimization speed is very low at this time, so the GA process can be terminated and enter AA. According to the suboptimal solution generated by GA, the initial pheromone distribution of AA is carried out to further obtain the optimal solution.

$$EV^k = \frac{\sum_{i=1}^{sca} (f_i^k - f_i^{k-1}) / f_i^{k-1}}{sca}, k = 2, 3, \dots, n \tag{5}$$

In the formula, sca - population size; f_i^k -fitness value of individual I in the k -th iteration.

4 Conclusion

This paper establishes the cognitive model of man-machine interface, summarizes the principles of man-machine interface spatial layout, and constructs the intelligent design model of man-machine interface. Finally, it is feasible to solve the best layout scheme through the man-machine interface spatial layout technology based on GA-AA.

References

1. Chen, J., Cao, W.H., Zhao, H.: Application research of TAO in shipborne command and control system. *Comput. Eng.* **34**(11), 237–238 (2008)
2. Jia, P., Xiao-Gang, Z.W.T., et al.: Battlefield visualization research on shipborne command and control system. *Journal of System Simulation* **25**(10), 2355–2358 (2013)
3. Yang, Z., Fan, A.: Research on cloud resource scheduling algorithm based on ant-cycle model. *Artificial Intelligence and Application* (2016)
4. Zhai, R.J., et al.: Automated elimination of river based on multi-objective optimization using genetic algorithm. *J. China Univ. Min. Technol.* **35**(3), 403–408 (2006)
5. Jia, S., et al.: A Survey on Ship Intelligent Cabin (2020)



Research on the Recognition and Decision-Making of Carrier-Based Aircraft Interception and Landing Based on Visual Information

Xi Wan^(✉) and Wen Li

Wuhan Digital Engineering Institute, Wuhan 430205, China
lukelukeke@163.com

Abstract. This paper proposes to use image and video means to judge the blocking and landing status of carrier-based aircraft, and studies the intelligent sensing technology of carrier-based aircraft tail hook recognition and arresting cable mounting status based on visual information. First, identify and locate the tail hook of the carrier-based aircraft. Then, the neural network is used to learn the dynamic spatiotemporal deformation characteristics during the contact between the arresting cable and the tail hook and the drawing process, and then make a judgment.

Keywords: Adversarial-transfer · Dynamic deformation characteristics

1 Introduction

During the landing process of a carrier-based aircraft in a complex surface environment, the way of manual judgment directly affects the landing success rate and the escape and go-around success rate of the carrier-based aircraft [1]. With the help of visual information-based aircraft tail hook identification and arresting cable mounting status intelligent perception technology research, the automation and intelligence level of carrier aircraft landing operations can be greatly improved [2]. This paper studies the identification and decision-making of the arresting state of the carrier-based aircraft in the complex environment of the ship surface, and solves the two key problems of the identification of the tail hook and the determination of the arresting and pulling state [3].

2 Recognition of Tail Hook of Carrier Aircraft in Complex Environment of Ship Surface

The purpose of identifying the tail hook of the carrier aircraft in the process of blocking the landing is to obtain the starting time of the blocking landing event. On this basis, the spatiotemporal information is used to judge the state changes of the tail hook and the arresting cable of the carrier aircraft. Whether the carrier-based aircraft is successful in blocking and pulling.

2.1 Data Augmentation of Carrier Airplane Tail Hook Based on Generative Adversarial Learning

We use the “adversarial-transfer” learning method to generate enough datasets that are similar to the real carrier aircraft tail hook samples, and then uses the dataset to train a neural network object detector to collect the camera tail in the video.

The specific implementation method is as follows: using a two-level “adversarial-transfer” learning method [4]. At present, there are relatively few image data about the carrier-based aircraft tail hook. Therefore, a network carrier-based aircraft tail hook generator is obtained by using the “adversarial-transfer” method to learn on the basis of the carrier-based aircraft generator. This is the first Level “adversarial-transfer” learning. Finally, we use the actual carrier-based aircraft tail hook data to form two datasets, and then use the “adversarial-transfer” method to learn the actual carrier-based aircraft tail based on the network carrier-based aircraft tail hook generator. Hook generator, which is the second level of “adversarial-transfer” learning. Through the proposed two-level “adversarial-transfer” learning, we generate a large number of sample data similar to real tail hooks.

In order to enhance the ability of Generative adversarial Network (GAN) to generate images of different kinds of target objects, the Auxiliary Classifier GAN (AC-GAN) as shown in Fig. 1 is used to generate the adversarial network model. Its generator G has two inputs, one is the classification label c of the image, and the other is random data z , which generates an image $X_{fake} = G(c, z)$; at the same time, its discriminator D judges whether the input image is the probability distribution $P(S|X)$ for the real data, and the probability distribution $P(C|X)$ for the classification labels. Therefore, the objective function of AC-GAN consists of two parts: the first part L_s is the cost function for whether the image is true or not; the second part L_c is the cost function for the accuracy of data classification:

$$L_s = E[(\log P(S = real|X_{real}))] + E[(\log P(S = fake|X_{fake}))]$$

$$L_c = E[(\log P(C = c|X_{real}))] + E[(\log P(C = c|X_{fake}))] \tag{1}$$

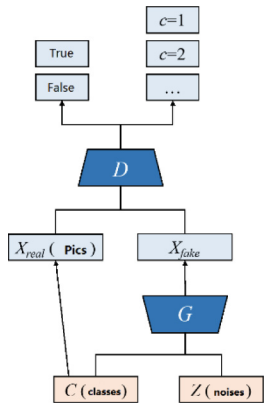


Fig. 1. Auxiliary classifier generative adversarial network (AC-GAN) model

In the process of network optimization, it is hoped that the discriminator D makes $L_c + L_s$ as large as possible, and the generator makes $L_c - L_s$ as large as possible, that is, the discriminator can distinguish between real images and generated images as much as possible and can effectively classify images. It is hoped for the generator that the generated images are considered to be real images as much as possible and that the images can be classified effectively.

2.2 Recognition of Carrier-Based Aircraft Tail Hook Based on Cascaded Neural Network

We designed a cascaded convolutional neural network detection framework. The detection framework is composed of two fully convolutional networks concatenated by the target pre-screening network Plane-FCN and the target accurate detection network Hook-FCN. Plane-FCN is a lightweight target detection network, which is responsible for fast pre-screening of possible carrier-based aircraft areas in captured scene images. It has a small number of layers and simple training, which can reduce the computational burden of subsequent networks. Hook-FCN is an improved U-Net neural network. By adding target mask and carrier-based aircraft tail hook orientation estimation layer to the traditional U-Net structure for multi-task learning, it realizes the fine-grained target of the carrier-based aircraft tail hook position. In general, Plane-FCN sends the aircraft candidate area into the Hook-FCN network for accurate carrier-based aircraft tail hook detection, and realizes the rapid detection of small targets in visual scenes through two cascaded networks.

Hook-FCND is an improved U-Net structure. It is divided into three parts: feature extraction, feature fusion and result output. In feature extraction, in order to avoid problems such as overfitting and gradient explosion that may occur in the training process, the transfer learning method is adopted to complete the initialization of the feature extraction network by borrowing from the ResNet50 model. The feature fusion part draws on the idea of U-Net. On the basis of FCN, it combines the high-dimensional and low-dimensional features of the convolutional network to achieve image pixel-level classification and improve detection accuracy. In the output part of the results, through three $1 * 1$ convolutional layers, a 1-channel confidence score map, a 4-channel rectangular box boundary information map, and a 1-channel shipboard aircraft tail hook rotation angle map are obtained respectively (Fig. 2).

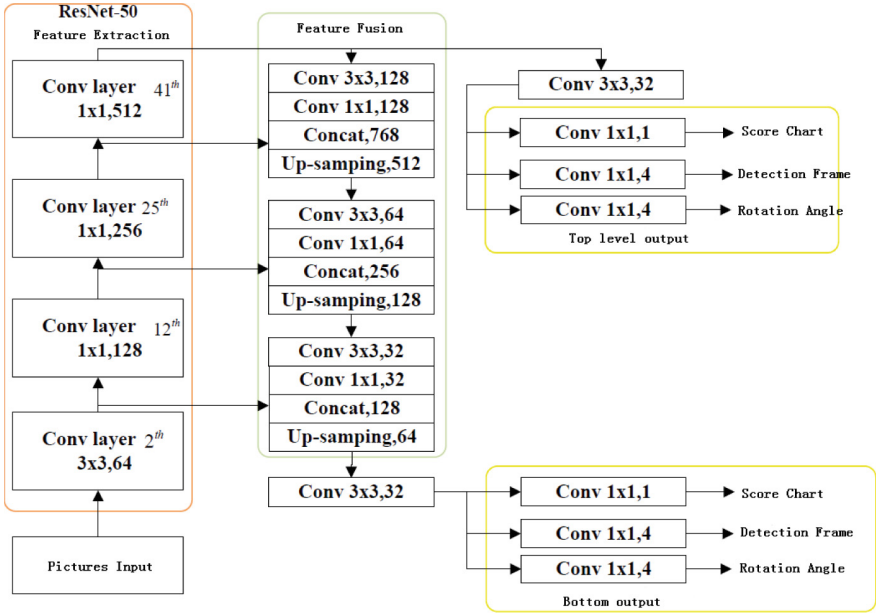


Fig. 2. Hook-FCN network structure diagram

3 Judgment of Arresting and Pulling State of Carrier-Based Aircraft

We use the visual information of space-time dynamic deformation during the pulling process of arresting cable and tail hook to judge whether the arresting and pulling of carrier-based aircraft is successful or not.

In this paper, a neural network based on spatial reasoning and temporal attention learning [5] is designed to learn the dynamic spatiotemporal deformation characteristics during the contact between the arresting cable and the tail hook and the pulling process. The key frame information to judge whether it is successful or not, and then judge. Specifically, as shown in Fig. 3, in view of the advantages of Long Short-Term Memory (LSTM) in modeling dependencies and dynamics in sequence data, the spatial reasoning sub-network uses an LSTM network layer to learn different frames. The spatial structure and shape information in the interaction process between the arresting cable and the tail hook, the temporal attention sub-network adopts an LSTM network layer to learn the specific timing dynamic information of this process, and assigns different attention weights to different frames. Based on the LSTM layer, the network performs feature extraction on video frames, utilizes temporal correlation, and determines whether the final drawing is successful or not.

Since the pulling and shedding states of the tail hook and the arresting cable of the carrier-based aircraft can be described by the spatial state of the arresting cable in the video frame, the spatial reasoning sub-network adopts the attention mechanism to assign the area where the arresting cable is located and other areas in the frame image. With

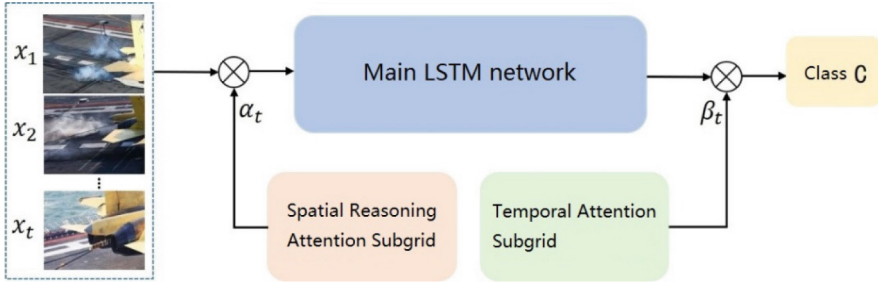


Fig. 3. The network for determining the success of carrier-based aircraft arresting and pulling

different attention weights, it consists of one layer of LSTM, two fully connected layers and one normalization layer. At each time frame t , the attention score of different regions of the image can be expressed as:

$$s_t = U_s \tanh(W_{xs}x_t + W_{hs}h_{t-1}^s + b_s) + b_{us} \tag{2}$$

U_s , W_{xs} and W_{hs} are network parameter matrices, and b_s and b_{us} are bias vectors. h_t-I_s represents the hidden variable of the LSTM layer. The normalized attention activation values for different regions in the image frame can be calculated as:

A set of gates of the attention sub-network controls the weight of the information of different regions entering the main LSTM network. The larger the weight, the greater the importance of the image frame region for judging the successful judgment of pulling, and the characteristics of the frame image entering the main network at time t . It becomes $x'_t = x_t \cdot \alpha_t$. After the spatial reasoning attention sub-network is trained together with the main network, it will learn a spatial attention model for blocking straightening discrimination.

Since only the frames that describe the state and relationship between the tail hook and the arresting cable of the carrier-based aircraft contain the most information of the pair-pulling discrimination in the collected video of the carrier-based aircraft blocking the landing, we plan to design a temporal attention module to automatically assign different frames to different frames. Different levels of attention weights β , the module consists of a layer of LSTM, a fully connected layer and a non-linear activation function layer to realize the discriminative selection of different frames. For sequence-level classification and discrimination, based on the output z_t of the main LSTM network and the temporal dynamic attention value β_t at each time t , the score output for different categories of blocking pull is:

$$o = \sum_{t=1}^T \beta_t \cdot z_t \tag{3}$$

Among them, $o = (o_1, o_1, \dots, o_c)^T$, C represents the total category of blocking and pulling, and T is the total frame length of the video frame. Then the predicted probability of each category of carrier-based aircraft arresting and pulling can be expressed as:

$$p(C_i|X) = \frac{e^{o_i}}{\sum_{j=1}^C e^{o_j}}, k = 1, \dots, C. \tag{4}$$

The activation value for the frame selection gate can be obtained by the following formula:

$$\beta_t = ReLU(w_x x_t + w_h h_{t-1} + b) \tag{5}$$

It can be seen that the value of β_t is determined by the current frame image x_t , the hidden variable h_{t-1} at the time $t - 1$ of the LSTM layer. This gate controls the frame selection per frame for the final blocking decision. Based on the frame selection gate, the main LSTM network and the temporal attention sub-network can be simultaneously trained to learn the dynamic temporal attention model.

The purpose of the attention model is to enable the network to assign different degrees of importance to different frames when the carrier’s tail hooks and arresting cables act. Spatial reasoning and temporal attention are concentrated in the same network. This item intends to use a sequence of regularized cross-entropy loss to represent the final objective function of the spatiotemporal attention network:

$$L = - \sum_{i=1}^C y_i \log \hat{y}_i + \lambda_1 \sum_{k=1}^k \left(1 - \frac{\sum_{t=1}^T \alpha \partial_{t,k}}{T} \right)^2 + \frac{\lambda_2}{T} \sum_{t=1}^T \|\beta_t\|_2 + \lambda_3 \|W_{uv}\|_1 \tag{6}$$

where $y = (y_1, y_2, \dots, y_c)^T$ denotes the true label, if it belongs to the i -th class, then for $j \neq i, y_j = 1$ and $y_j = 0$. \hat{y}_i represents the probability that the sequence is predicted to be class i , where $\hat{y}_i = p(C_i|X)$, the parameters λ_1, λ_2 and λ_3 balance the contributions of the three regularization terms. The first regularization project aims to encourage the spatial attention model to dynamically pay attention to more spatial information in the sequence, in order to prevent the spatial attention model from tending to ignore many regions all the time, i.e., being trapped in local optima. The second regularization item is to regularize the controlled learning time attention values with the l_2 norm instead of increasing them indefinitely. This mitigates vanishing gradients in backpropagation, where the gradient of backpropagation is proportional to $1/\beta_t$. The third regularization term with l_1 norm is to reduce overfitting of the network. W_{uv} represents the connection matrix in the network.

4 Carrier-Based Aircraft Block Landing Decision

Identify through the pulling state of the Carrier-based carrier’s tail hook. When the arresting cable is in successful contact with the carrier’s tail hook, a yellow signal light is given. When the arresting cable completely pulls the carrier aircraft successfully, a green signal is given. On failure, a red signal light is given. The signal lights are used to give timely feedback to the pilots of the carrier-based aircraft, so that the pilots have sufficient psychological and physiological reaction time to escape and go around or quickly get confirmation of the safe landing, and at the same time, they can quickly send the news of the success of the carrier-based aircraft landing. To the aviation management system, it is convenient to make relevant command decisions.

5 Conclusion

This paper proposes a method of judging the drawing state by using the spatiotemporal deformation pattern between the carrier-based aircraft tail hook and the arresting cable on the surface of the ship. Use video means to judge the status of carrier-based aircraft blocking the landing.

References

1. Zhibing, Z., et al.: Review on development in guidance and control of automatic carrier landing of carrier-based aircraft. *J. Nanjing Uni. Aeronau. Astronaut.* **50**(6), 734–744 (2018)
2. Ziyang, Z., et al.: Research progress in guidance and control of automatic carrier landing of carrier-based aircraft. *Acta Aeronautica et Astronautica Sinica* **38**(2), 1–22 (2017)
3. Wang Jie, W., et al.: Study on automatic carrier landing control configuration. *Flight Dynamics* **2**, 26–29 (2017)
4. Ganin, Y., et al.: Domain-adversarial training of neural networks, *The J. Machine Learning Res.* **17**(1), 2096–2030 (2016)
5. Rush, A.M., Chopra, S., Weston, J.: A neural attention model for abstractive sentence summarization. In: *Proceedings of the 2015 Conference on Empirical Methods in Natural Language Processing*, pp. 379–389

Research on the Man-Environment Relationship



Research on the Adaptability Drills of Special Forces in Swimming Across Low Temperature Seawater

Chunlai Wang^(✉)

Guangzhou College of Applied Science and Technology, Guangzhou 511370, China
wwwcl_1@163.com

Abstract. Armed swimming drill is a basic training content for special forces to cross the sea and land on the island. In actual combat, the seawater temperature around the swimming area shows seasonal and regular changes, especially the low temperature water environment can reduce the combat effectiveness of crossing the sea and land on the island, hindering or even destroying the completion of the combat mission. Carrying out swimming and swimming adaptation drills in low temperature water, especially the swimming and swimming adaptation drills in low-temperature waters at sea, can enable special forces to adapt to the sea environment in advance. Better grasp the characteristics of sea waves, ocean currents, tides, and sea horizons in low-temperature waters, and achieve pre-adaptation to the low-temperature sea environment, so as to improve combat effectiveness and successfully complete the mission of crossing the sea and landing the island.

Keywords: Special forces · Armed swimming · Adaptability drills · Low temperature seawater

1 Introduction

According to our army's global mobile operations policy and actual combat needs, special operations capabilities such as crossing the sea and landing on islands need to be further strengthened. The operation of crossing the sea and landing on the island may be deeply affected by severe weather, especially the low temperature of the sea in winter will weaken the actual combat effectiveness of special operations. The pre-war seawater adaptability training, especially the long-distance swimming adaptability training for low-temperature waters, can enable special forces to adapt to the marine climate in advance.

2 Theory of Low Water Temperature Effects

2.1 Definition

The low-temperature water environment is the water environment where the temperature is lower than the comfort level of the human body. However, the low-temperature water

that adversely affects human work efficiency is usually below 10 °C. Special Operation Forces (SOF) operate regularly in extreme environmental conditions that may affect tactical and physical performance [1].

2.2 Skin Temperature

Skin temperature (Fig. 1) initially increased and then slowly decreased to 36.3 °C by the end of the swim [2] When exposed to a low-temperature environment, the body's metabolic heat production is less than the body's heat dissipation, which reduces the core temperature and muscle temperature. Studies have found that for every 1 °C decrease in body core temperature and muscle temperature, the maximum aerobic work capacity decreases by 5% to 6%.

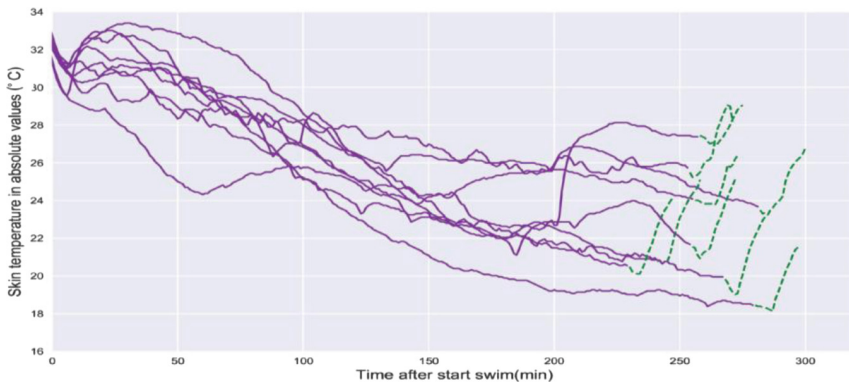


Fig. 1. Skin temperature changed when exiting in the seawater

2.3 Cardiovascular System Function

Maximum oxygen consumption and the rate of vasoconstriction (Fig. 2) are positively correlated. Rate of metabolic heat production, skin heat conductance, and the rate of vasoconstriction are also significantly correlated [3].

The cold water environment has an important influence on the cardiac output, peripheral resistance, mean arterial pressure, heart and sympathetic nerve function during exercise, mainly manifested in the maximum heart rate, cardiac output and peripheral tissue during exercise. Reduced blood flow. Studies have found that when the body's core body temperature drops by 0.6 to 2 °C, the maximum heart rate drops by 28 beats/min. The decrease in the maximum heart rate during exercise in a low temperature environment is the main reason for the decrease in the maximum aerobic working capacity. In addition, the reduction of blood flow in peripheral tissues caused by low-temperature water environment is one of the important reasons that affect sports performance.

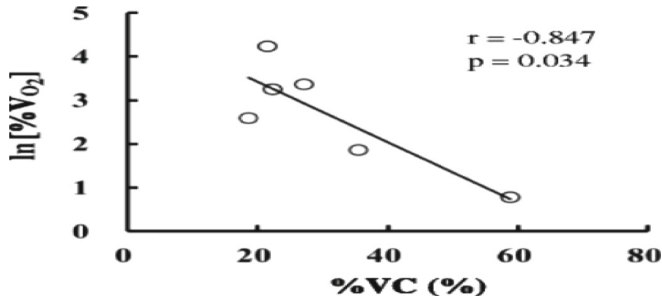


Fig. 2. Relationship between oxygen uptake and the rate of vasoconstriction

2.4 Oxygen Uptake and Oxygen Transport System

The increase in oxygen consumption when swimming in colder water (Fig. 3) is due to the super-imposition of shivering on swimming metabolism [4].

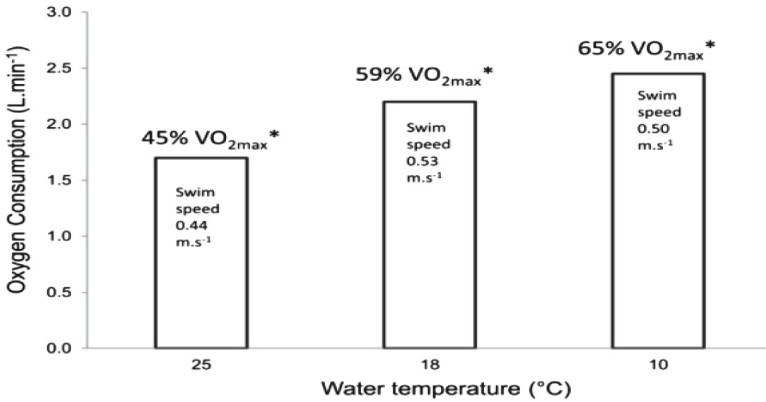


Fig. 3. Oxygen consumption in different seawater temperature

Studies have shown that when the human body’s stress response to low-temperature water exposure is insufficient to prevent core body temperature (drop $> 0.5\text{ }^{\circ}C$) and peripheral tissue temperature drop, it will have a negative impact on the human body’s maximum aerobic working capacity. On the one hand, low-temperature water environment stimulation causes myocardial contraction dysfunction, which reduces blood supply and affects the body’s maximum aerobic work capacity; on the other hand, low-temperature environment stimulates the body to reduce the perfusion of skeletal muscle blood volume during exercise, which affects peripheral skeletal muscles. The oxygen uptake level reduces the maximum aerobic work capacity [5].

2.5 Skeletal Muscle Energy Metabolism

Long-term exposure to low temperature environment will also affect the energy metabolism of skeletal muscle during exercise. Studies have found that when exercising in a low-temperature environment with an involuntary shudder response, the blood lactic acid concentration is higher than when the same exercise intensity is performed in a normal temperature environment. Therefore, the muscle groups that participate in the body’s involuntary shudder response in a low-temperature environment consume inositol Originally to meet the needs of its own energy metabolism [6].

3 Four-Week Adaptability Drill Scheme

The training purpose of this scheme is to promote the trainees to complete the acclimation to the seawater in low temperature and master in the shortest time the characteristics of the low temperature seawater through high-intensity adaptive training. And the practical significance of this adaptive training is that it can effectively improve the operational effectiveness of cross-sea landing and reduce the occurrence of non-combat attrition such as frostbite and drowning (Table 1).

Table 1. Four-week low-temperature seawater adaptability drill scheme

	Monday Water Temp 10 °C Full wetsuit with hood	Tuesday Water Temp 10 °C Full wetsuit with hood	Wednesday Water Temp 10 °C Full wetsuit with hood	Thursday Water Temp 10 °C Full wetsuit with hood	Friday Water Temp 10 °C Full wetsuit with hood
Week1 Endurance	Warming-up with 500 m	Warming-up with 500 m	Warming-up with 500 m	Warming-up with 500 m	Warming-up with 500 m
	Freestyle:100 mx5 Interval with10 sec	Freestyle:100 mx5 Interval with10 sec	Freestyle:100 mx5 Interval with10 sec	Freestyle:100 mx5 Interval with10 sec	Freestyle:100 m x 5 Interval with10 sec
	Breaststroke: 50 m-100 m-200 m Interval with 10 s	Breaststroke: 50 m-100 m-200 m Interval with 10 s	Breaststroke: 50 m-100 m-200 m Interval with 10 s	Breaststroke: 50 m-100 m-200 m Interval with 10 s	Breaststroke: 50 m-100 m-200 m Interval with 10 s
	Recovery	Recovery	Recovery	Recovery	Recovery
Week2 Strength and power	Warming-up with 500 m	Warming-up with 500 m	Warming-up with 500 m	Warming-up with 500 m	Warming-up with 500 m
	Freestyle: 100 mx5 Interval with 35 s	Freestyle:100 mx5 Interval with 35 s	Freestyle:100 mx5 Interval with 35 s	Freestyle:100 mx5 Interval with 35 s	Freestyle: 100 m x 5 Interval with 35 s
	Breaststroke:100 mx5 Interval with 35 s	Breaststroke:100 mx5 Interval with 35 s	Breaststroke:100 mx5 Interval with 35 s	Breaststroke:100 mx5 Interval with 35 s	Breaststroke:100 mx5 Interval with 35 s
	Recovery	Recovery	Recovery	Recovery	Recovery
Week3 Anaerobic	Warming-up with 600 m	Warming-up with 600 m	Warming-up with 600 m	Warming-up with 600 m	Warming-up with 600 m
	Freestyle: 100 m x 5 Interval with 20 s	Freestyle:100 m x 5 Interval with 20 s	Freestyle:100 m x 5 Interval with 20 s	Freestyle:100 m x 5 Interval with 20 s	Freestyle: 100 m x 5 Interval with 20 s

(continued)

Table 1. (continued)

	Monday Water Temp 10 °C Full wetsuit with hood	Tuesday Water Temp 10 °C Full wetsuit with hood	Wednesday Water Temp 10 °C Full wetsuit with hood	Thursday Water Temp 10 °C Full wetsuit with hood	Friday Water Temp 10 °C Full wetsuit with hood
	Freestyle: 100 m x 5 Interval with 30 s	Freestyle: 100 m x 5 Interval with 30 s	Freestyle: 100 m x 5 Interval with 30 s	Freestyle: 100 m x 5 Interval with 30 s	Freestyle: 100 m x 5 Interval with 30 s
	200 m relaxing swim	200 m relaxing swim	200 m relaxing swim	200 m relaxing swim	200 m relaxing swim
	Freestyle: 100 m x 5, Interval with 50 s	Freestyle: 100 m x 5, Interval with 50 s	Freestyle: 100 m x 5, Interval with 50 s	Freestyle: 100 m x 5, Interval with 50 s	Freestyle: 100 m x 5, Interval with 50 s
	500 m relaxing swim	500 m relaxing swim	500 m relaxing swim	500 m relaxing swim	500 m relaxing swim
	Recovery	Recovery	Recovery	Recovery	Recovery
Week4 Aerobic	Warming-up with 500 m	Warming-up with 500 m	Warming-up with 500 m	Warming-up with 500 m	Warming-up with 500 m
	Freestyle:200 mx5 Interval with 40 s	Freestyle:200 mx5 Interval with 40 s	Freestyle:200 mx5 Interval with 40 s	Freestyle:200 mx5 Interval with 40 s	Freestyle:200 m x 5 Interval with 40 s
	200 m relaxing swim	200 m relaxing swim	200 m relaxing swim	200 m relaxing swim	200 m relaxing swim
	Freestyle: 200 m x 5, keep distance pace, Interval with 10 s	Freestyle: 200 m x 5, keep distance pace, Interval with 10 s	Freestyle: 200 m x 5, keep distance pace, Interval with 10 s	Freestyle: 200 m x 5, keep distance pace, Interval with 10 s	Freestyle: 200 m x 5, keep distance pace, Interval with 10 s
	500 m relaxing	500 m relaxing	500 m relaxing	500 m relaxing	500 m relaxing
	Recovery	Recovery	Recovery	Recovery	Recovery

4 Discussion

4.1 Adaptive Training Effect

Long-term exercise training in a low temperature environment can improve the body's basal metabolism, increase the skeletal muscle chill threshold, and increase the body's heat production; on the other hand, it can improve the body's ability to regulate temperature and enhance the body's ability to withstand cold.

4.2 Choice of Technology

Mainstream experts at home and abroad believe that the basic technique used for long-distance armed swimming should be breaststroke. Because the breaststroke technique has the advantages of high buoyancy, strong weight-bearing ability, simple movement structure, labor-saving, stable, low sound, and easy observation, it is very suitable for armed swimming. In actual combat, you should flexibly choose other swimming techniques to avoid vortexes, rapids, etc. according to the actual situation.

4.3 Drill Methods

In armed swimming training, endurance training should be the mainstay and speed training should be supplemented. The heart rate is controlled between 140–180. Speed exercises mainly exercise the ATP-CP energy supply system. And anaerobic training mainly exercises blood lactic acid and ATP-CP energy supply system. Then aerobic exercise

energy supply system. Training methods include interval training method, high-strength training method, interval high-strength training method, Fatlake method, continuous training method and repetitive training method. Before the end of training, take active recovery methods to reduce fatigue. It is best to choose a slow swimming method with a heart rate of less than 50%.

5 Conclusion

This training plan can effectively improve the ability of special forces members to adapt to the low temperature environment of special waters when crossing the sea and landing on the island, and effectively improve their combat capabilities.

References

1. Melau, J., Hisdal, J., Solberg, P.A.: Impact of a 10,000-m cold-water swim on norwegian naval special forces recruits. *J Spec Oper Med.* Fall **21**(3), 55–59 (2021)
2. Alexander Rüst, C., Knechtle, B., Rosemann, T.: Changes in body core and body surface temperatures during prolonged swimming in water of 10 °C—a case report. *Extrem Physiol Med.* **1**(1), 8 (1 Nov 2012)
3. Maeda, T.: Relationship between maximum oxygen uptake and peripheral vasoconstriction in a cold environment. *Maeda Journal of Physiological Anthropology* **36**, 42 (2017)
4. Tipton, M., Bradford, C.: Moving in extreme environments: open water swimming in cold and warm water. *Tipton and Bradford Extreme Physiology & Medicine* **3**, 12 (2014)
5. Knechtle, B., Waśkiewicz, Z., Sousa, C.V., Hill, L., Nikolaidis, P.T.: Cold water swimming—benefits and risks: a narrative review. *Int. J. Environ. Res. Public Health* **17**, 8984 (2020)
6. Stocks, J.M., Taylor, N.A.S., Tipton, M.J., Greenleaf, J.E.: Human physiological responses to cold exposure. *Aviation, Space, and Environmental Medicine* **75**(5) (May 2004)



Impact of Continuous Night Shifts on Crew Performance in 9-day Isolated Environment Shift Experiments

Zezheng Qiu¹, Liang Guo², Chenyuan Yang², and Liping Pang²(✉)

¹ Wuhan 2nd Ship Design and Research Institute, Wuhan 430064, China

² School of Aeronautical Science and Engineering, Beijing University of Aeronautics and Astronautics, Beijing 100191, China
pangliping@buaa.edu.cn

Abstract. Continuous night shifts in isolated environments such as cabins, submarines, and space stations have a negative impact on the circadian and cognitive function of the crew. Therefore, 9-day simulated isolated environment experiments were conducted to reveal the negative impact of continuous night shifts on crew performance. A 6-shift-per-day schedule was established, in which there were 3-night shifts, namely a 0–4 shift, a 4–8 shift, and a 20–24 shift respectively. The operational performance was evaluated using the Multi-Attribute Task Battery II (MATB-II) platform. The subjective feelings were evaluated by NASA Task Load Index (NASA-TLX) questionnaire, Karolinska Sleepiness Scale (KSS), and job satisfaction scale. Generalized Additive Mixed Models (GAMMs) were established to test the fixed effect estimates of potential influencing factors on crew performance. The analysis results showed that subjects had the worst performance in the 4–8 shift and the later experimental periods, namely Day 7 to Day 9.

Keywords: Continuous night shifts · Operational performance · MATB

1 Introduction

Shiftwork in the long-term isolated environment has become common in the last few decades with the growing demands of human life [1, 2]. Approximately 20% of developed countries are engaged in shift work. It leads to disturbance of internal rhythms and causes serious behavioral, physiological, and performance problems [3]. Sleep disorder is the main behavioral problem faced by shift workers and often causes insomnia for the misalignment of working time with normal circadian phases [3–5]. When the circadian rhythm of the crew cannot adapt to abrupt changes in shift times, it most likely causes some physiological problems, such as disturbance of gastrointestinal function, increased incidence of cardiovascular and coronary heart disease [6]. Shortz et al. [7] proved that shiftwork adversely affected heart rate responses. Shiftwork also caused serious health issues including cancer and metabolic disorders, due to the disruption in the circadian clock system [8–10]. Shiftwork has been reported to show an increased accident risk due to low performance in recent years [11].

2 Experiment Description

2.1 Design

Two 9-day isolated environment shift experiments were carried out in an isolated experimental area. 15 and 12 subjects were recruited in the first and second experiments. Each 9-day experiment was divided into three periods, that is P_1 from Day 1 to Day 3, P_2 from Day 4 to Day 6, and P_3 from Day 7 to Day 9.

A 6-shift-per-day schedule was established, half of which were day shifts and half were night shifts. Night shifts included a 0–4 shift (S_{0-4}), a 4–8 shift (S_{4-8}), and a 20–24 shift (S_{20-24}). Day shifts included an 8–12 shift (S_{8-12}), a 12–16 shift (S_{12-16}), and a 16–20 shift (S_{16-20}).

In each simulated shift task, the subjects firstly filled in the KSS. Then half of the subjects performed MATB, and the other subjects carried on cognitive tests. It took about 110 min. After a short break of 8 min, two groups exchanged the tasks.

2.2 Platform

To maintain a stable living environment, diet, and lifestyle, the experiments were carried out in an enclosed cabin completely isolated from the external environment. The simulated shift tasks, sleep, rest, and leisure activities were restricted to the corresponding areas. The work area was divided into a MATB test area and a cognitive test area. While half of the subjects performed MATB, the others carried on the cognitive test.

MATB-II was developed by NASA and widely used for the study of the operational performance and mental workload of operators [12]. It contained 4 subtasks, namely system monitoring, tracking, scheduling, and resource management. In this study, MATB platform was used to simulate the shift missions and the task interface is shown in Fig. 1.

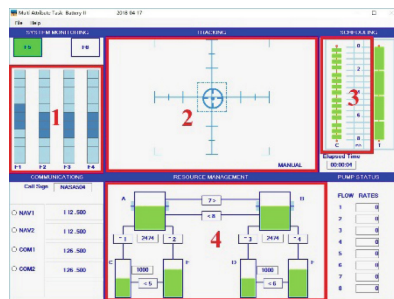


Fig. 1. MATB-II platform

2.3 Subjective Feeling Scales

NASA-TLX is widely used for subjective mental workload assessment. It combines 6 factors to derive a reliable estimation of mental workload, namely mental demand,

physical demand, temporal demand, performance, effort, and frustration level. It was filled after every mental workload test of MATB.

The KSS with a 9-point scale is widely used to assess sleepiness. In this study, KSS was used to measure the sleepiness of the crew at the beginning and end of 4h simulated shift tasks. Their scores were recorded as KSS_1 and KSS_2 , respectively.

Job satisfaction is the degree of crew satisfaction with work in both physical and psychological aspects. It is closely related to emotional exhaustion or burnout. In this study, a job satisfaction scale was used at the end of 4h simulated shift tasks.

2.4 Subjects

In our study, 27 subjects were all male postgraduates or undergraduates with an average age of 23.04 ± 1.49 years old. They all had normal vision or vision corrected to 1.0. To minimize the impact of practice effect on the experiments, subjects were trained until their operational performance met the requirements. All experimental protocols had been approved by the Biological and Medical Ethics Committee of Beihang University and all methods were carried out in accordance with relevant guidelines and regulations. All subjects signed the informed consent form before the formal experiment.

2.5 Data Processing and Methods

2.5.1 Preprocessing

MATB Performance

The ratio of the average response time to the accuracy is defined as the operational performance of the subjects, as shown in (1.1).

$$P_{MATB} = \frac{1}{4} \sum_{i=0}^4 (ACC_i / RES_i) \quad (1.1)$$

where P_{MATB} is the operational performance; ACC_i and RES_i are the accuracy and response time of subtask i , respectively; subtask i represents system monitoring, tracking, scheduling, and resource management, respectively, and $i = 1, 2, 3, 4$.

NASA-TLX Score

Subjects rated 6 factors of NASA-TLX during MATB test, including mental demand, physical demand, temporal demand, performance, effort, and frustration level³¹. The weights were calculated through the pairwise comparison of the importance of the 6 factors. Subjective mental workload is calculated with (1.2).

$$MW = \sum_{i=1}^6 Score_i \times Weight_i \quad (1.2)$$

where MW is subjective mental workload score; $Score_i$ and $Weight_i$ are the score and weight of factor i , respectively; subscript i represents factor i and $i = 1, 2, \dots, 6$.

2.5.2 Statistical Analysis

Statistical analyses are performed by setting up the GAMMs in the statistical package R version 3.6.1 (R Project for Statistical Computing, Vienna, Austria). The GAMMs are used to test the relationship between dependent variables and independent variables. y_i represents dependent variable, $i = 1, 2, \dots, 4$. In our study, y_1 – y_4 are MW score, P_{MATB} , KSS score, job satisfaction score, respectively. Independent variables are 6 shifts and 3 periods. The subjects are treated as a random effect. Differences are considered statistically significant when $p < 0.05$.

3 Results

In our analysis, “*” indicates $p < 0.05$, and “**” indicates $p < 0.01$. These marks will be used in Figs. 2, 3, 4 and 5.

3.1 Operational Performance Analysis

The GAMM results of P_{MATB} show no significant difference between P_1 , P_2 , and P_3 . But there are significant differences between the 6 shifts, as shown in Fig. 2.

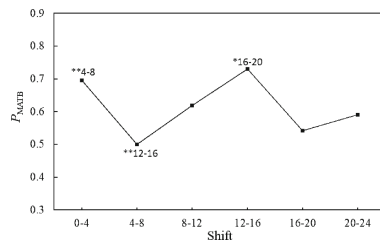


Fig. 2. Operational performance in 6 shifts

3.2 Subjective Feeling Analysis

The GAMM results of the NASA-TLX show that subjective mental workload has significant differences between P_1 , P_2 , and P_3 only in S_{4-8} , as shown in Fig. 3.

The GAMM results of KSS_2 show no significant difference between 6 shifts and 3 periods. KSS_1 is significantly lower than KSS_2 , which shows that the 4 h simulated shift tasks significantly increase the degree of sleepiness.

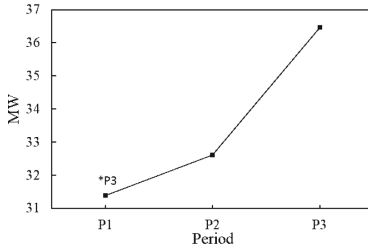


Fig. 3. The subjective mental workload in P_1 , P_2 , and P_3 in S_{4-8}

The relationships between KSS_1 shifts and periods are shown in Fig. 4.

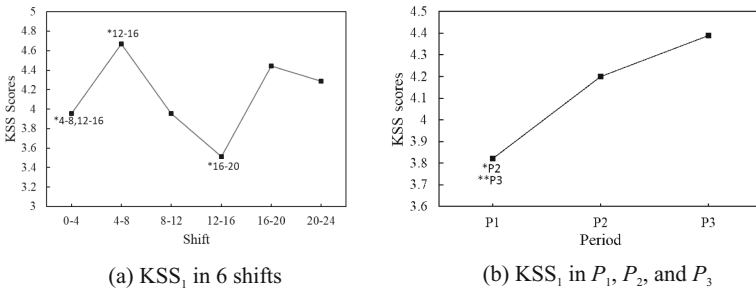


Fig. 4. GAMM results of KSS_1

The GAMM results of the job satisfaction scale are shown in Fig. 5.

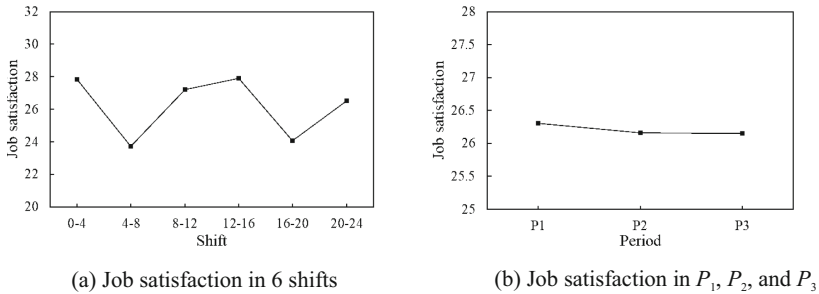


Fig. 5. GAMM results of job satisfaction

4 Conclusion

The risk of human error in S_{4-8} is the highest, which is based on GAMM results of operational performance. Specifically, operational performance and alertness were significantly lower in S_{4-8} than that in other periods. Job satisfaction is the lowest in S_{4-8}

with no significant difference. This study combines subjective evaluation and objective testing to achieve a comprehensive assessment of crew in continuous night shifts. We revealed the negative impact of continuous night shifts on crew performance in 9-day isolated environment shift experiments. It may contribute to reducing the risk of accidents during continuous night shifts and improving the safety of shiftwork.

Compliance with Ethical Standards. The study was approved by the Logistics Department for Civilian Ethics Committee of Wuhan 2nd Ship Design and Research Institute.

All subjects who participated in the experiment were provided with and signed an informed consent form.

All relevant ethical safeguards have been met with regard to subject protection.

References

1. Åkerstedt, T., Wright, K.P.: Sleep loss and fatigue in shift work and shift work disorder. *Sleep Med. Clin.* **4**(2), 257–271 (2009)
2. Barnes, R.G., Deacon, S.J., Forbes, M.J., Arendt, J.: Adaptation of the 6-sulphatoxymelatonin rhythm in shiftworkers on offshore oil installations during a 2-week 12-h night shift. *Neurosci. Lett.* **241**(1), 9–12 (1998)
3. Mizuno, K., et al.: Sleep patterns among shift-working flight controllers of the international space station: an observational study on the JAXA flight control team. *J. Physiol. Anthropol.* **35**(1), 19 (2016)
4. Arendt, J.: Shift work: coping with the biological clock. *Occup. Med.* **60**(1), 10–20 (2010)
5. Dijk, D.J., Czeisler, C.A.: Paradoxical timing of the circadian rhythm of sleep propensity serves to consolidate sleep and wakefulness in humans. *Neurosci. Lett.* **166**(1), 63–68 (1994)
6. Hampton, S.M., et al.: Postprandial hormone and metabolic responses in simulated shift work. *J. Endocrinol.* **151**(2), 259–267 (1996)
7. Shortz, A.E., Franke, M., Kilic, E.S.: Evaluation of offshore shiftwork using heart rate variability. *Proc. Hum. Factors Ergon. Soc. Annu. Meet.* **61**(1), 1036–1039 (2017)
8. Karlsson, B.H., Knutsson, A.K., Lindahl, B.O., Alfredsson, L.S.: Metabolic disturbances in male workers with rotating three-shift work. Results of the WOLF study. *Int. Arch. Occup. Environ. Health* **76**(6), 424–430 (2003)
9. Knutsson, A.: Health disorders of shift workers. *Occup. Med.* **53**(2), 103–108 (2003)
10. Kantermann, T., Juda, M., Vetter, C., Roenneberg, T.: Shift-work research: where do we stand, where should we go? *Sleep Biol. Rhythms* **8**(2), 95–105 (2010)
11. Folkard, S., Tucker, P.: Shift work, safety and productivity. *Occup. Med.* **53**(2), 95–101 (2003)
12. Wilson, G.F., Russell, C.A.: Operator functional state classification using multiple psychophysiological features in an air traffic control task. *Hum. Factors* **45**(3), 381–389 (2003)



Modeling of Human Cold Stress in Low Temperature Environment

Yuhong Shen, Chenming Li, Ting Zou, and Huilin Wei^(✉)

Institute of Quartermaster Engineering Technology, Beijing, China
154491268@qq.com

Abstract. In this paper, a physiological model of human cold stress was developed to analyze and study the stress response of human body in low temperature environment and to predict human injury. The physiological model of human cold stress includes two parts: passive system and active system. The passive system divides the human body into 22 segments and 98 nodes, which are used to simulate the heat conduction, heat convection and blood perfusion heat transfer of the human body. Among them, the active system mainly simulates four kinds of thermoregulatory responses, including skin blood perfusion rate, arteriovenous anastomosis (AVA) blood flow, tremor and sweating. The verification tests of core temperature and multi-site skin temperature under cold exposure condition (-5°C) were carried out by using environmental climate chamber. The tests confirmed that the physiological model of human cold stress accurately simulated the response of human cold stress and predicted the changes of human skin and core temperature.

Keywords: Human cold stress · Prediction model · Low temperature environment · Passive system · Active system

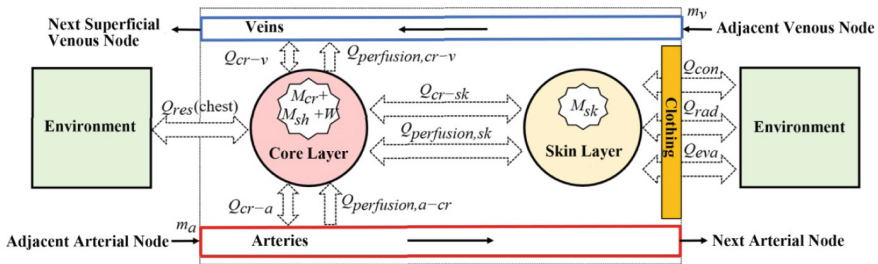
1 Introduction

The average skin temperature of the human body is usually maintained between 33°C and 34°C . In a low temperature environment, the average skin temperature will drop when the cold resistance of clothing cannot meet the needs of the human body. Low temperature can directly damage human skin tissue. When the skin tissue temperature is close to zero, it will cause non-freezing damage [1, 2]. In addition, if the skin tissue is exposed to cold water for a long time, the tissue damage can worsen or even develop pathological changes, such as causing trench foot disease. If the temperature of the skin tissue continues to drop to zero, it will cause freezing injury [3, 4]. A cold environment can also adversely affect mental work. Low temperature may reduce the attention, prolong response time and increase error rate of disaster relief workers, which will reduce work efficiency.

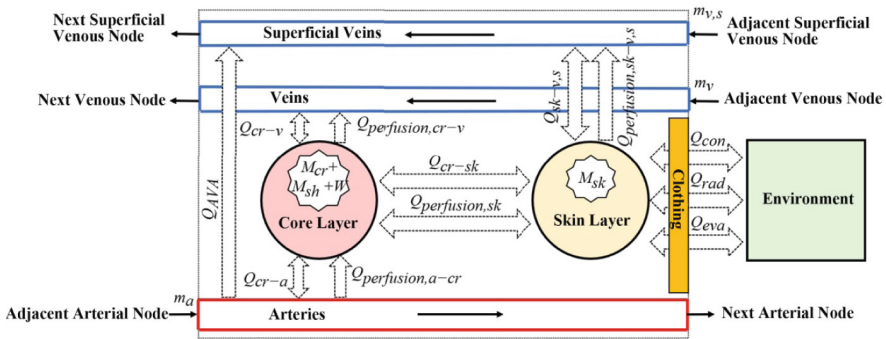
2 Cold Stress Modeling of Passive System

In the process of modeling, the human body is divided into 22 segments, including head, face, shoulder, chest, abdomen, upper arm, lower arm, palm, finger, hip, thigh, calf, foot, etc. Each segment of the human body consists of 4 layers: the core layer, arteries, veins, and skin layers, while the ends of the limbs (forearms, calves, hands, feet, and fingers) are divided into 5 layers that the superficial veins are added [5, 6], thus forming a 98-node human cold stress physiological model.

The physiological modeling of human cold stress is based on the heat conduction, heat convection and blood perfusion heat transfer process between each layer, as well as the heat convection and thermal radiation process between the skin and the external environment. For the heat transfer process and blood flow in different parts of the human body, see Fig. 1.



(A) Schematic diagram of the non-acral heat transfer process and blood flow in the human body.



(B) Schematic diagram of heat transfer and blood flow in human extremities (forearms, calves, hands, feet, and fingers)

Fig. 1. Schematic diagram of heat transfer process and blood flow in each partition of the human body.

Except for the extremities of the human body (forearms, calves, hands, feet and fingers), the heat balance equations of the rest of the body are expressed as follows:

Core layer:

$$CrdTcrdt = M_{cr} + M_{sh} + W - Q_{res} - Q_{cr-a} - Q_{cr-v} - Q_{cr-sk} + Q_{perfusion,a-cr} + Q_{perfusion,sk} - cr$$

(2.1)

Artery:

$$C_{bl,ad}T_{bl,adt} = Q_{cr} - a + m_{acbl}(T_{bl,a,adjacent} - T_{bl,a}) \quad (2.2)$$

Vein:

$$C_{bl,vd}T_{bl,vdt} = Q_{cr} - v + Q_{perfusion,cr-v} + m_{vcbl}(T_{bl,v,adjacent} - T_{bl,v}) \quad (2.3)$$

Skin layer:

$$C_{skd}T_{skdt} = M_{sk} - Q_{cr} - sk - Q_{perfusion,sk-cr} + Q_{sk-v,s} - Q_{con} - Q_{rad} - Q_{eva} \quad (2.4)$$

wherein, C_{cr} represents core layer specific heat, J/K; T_{cr} represents core layer temperature, °C; t represents time, s; M_{cr} represents core layer metabolic rate, W/m²; M_{sh} represents chilling heat production, W/m²; W represents heat generated by human work, W/m²; Q_{res} represents respiratory heat dissipation, W/m²; Q_{cr-a} represents respiratory heat dissipation, W/m²; Q_{cr-v} represents the convective heat exchange between the core and vein, W/m²; Q_{cr-sk} represents the core-skin heat conduction, W/m²; $Q_{perfusion,a-cr}$ represents the core blood perfusion heat exchange, W/m²; $Q_{perfusion,sk-cr}$ represents the skin blood perfusion heat exchange, W/m². $C_{bl,a}$ represents the specific heat of the arterial layer, J/K; m_a represents the blood flow of the segment, ml/h; c_{bl} represents the specific heat of the blood flow, J/K; $T_{bl,a,adjacent}$ represents the arterial blood flow temperature of the upper part flowing to this site, °C; $T_{bl,a}$ represents the arterial blood flow temperature of this part, °C. $C_{bl,v}$ represents the specific heat of the venous layer, J/K; m_v represents the venous blood flow of this segment, ml/h; $T_{bl,v,adjacent}$ represents the venous blood flow temperature of the upper part of the site, °C; $T_{bl,v}$ represents the venous blood flow temperature of this part, °C. C_{sk} represents the skin layer specific heat, J/K; T_{sk} represents the skin temperature, °C; M_{sk} represents the skin layer metabolic rate, W/m²; $Q_{sk-v,s}$ represents the convection between the skin and the superficial veins, W/m²; Q_{con} represents the heat exchange between the skin and the external environment caused by convection, W/m²; Q_{rad} represents the radiative heat exchange, W/m²; Q_{eva} represents the heat loss by evaporation from the skin to the external environment, W/m².

The energy balance equation of the superficial venous nodes at the ends of human limbs (forearms, calves, hands, feet and fingers) is expressed as follows:

$$C_{bl,v,sd}T_{bl,v,sdt} = Q_{sk-v,s} + Q_{perfusion,sk-v,s} + m_{v,scbl}(T_{bl,v,s,adjacent} - T_{bl,v,s}) + Q_{AVA} \quad (2.5)$$

wherein, $C_{bl,v,s}$ represents the specific heat of the superficial venous layer, J/K; $m_{v,s}$ represents the blood flow entering the segment from the upper superficial venous node, ml/h; $T_{bl,v,s,adjacent}$ represents the blood flow temperature of the upper superficial venous node flowing to this site, °C; $T_{bl,v,s}$ represents the superficial venous blood flow temperature of this part, °C.

3 Cold Stress Modeling of Active System

The active response to cold stress in human body includes trembling, sweating and dynamically regulating the blood perfusion rate of each segment of the skin layer. The active regulation control equation is determined by calculating the receptor signals and comprehensive signals of the local core and skin nodes. The average setting values of core and skin are $T_{cr,set} = 36.8\text{ }^{\circ}\text{C}$ and $T_{sk,set} = 33.7\text{ }^{\circ}\text{C}$, respectively. The temperature sensors in various parts of the human body receive the temperature signal, which forms a temperature difference with the preset value and a disturbance signal. The disturbance signal is calculated as follows:

$$\text{errorn}(i) = T_n(i) - T_{n,set}(i) \quad (2.6)$$

wherein, n represents the serial number of the body part, error_n represents the disturbance term, T_n and $T_{n,set}$ represent the actual temperature and preset temperature, respectively. When the perturbation is positive, the corresponding perturbation signal is identified as warm_n . Conversely, when the disturbance term is negative, the disturbance signal is considered cold_n . Secondly, the model assumes that the temperature receiver is located in the hypothalamus and skin, and the temperature sensor senses the external temperature, and then releases the disturbance signal, which is processed by the central nervous system of the hypothalamus and then converted into relevant instructions that prompt the human body to respond. The comprehensive sensor signal of the skin thermoreceptor can be determined in the following ways:

$$\text{warms} = i = 122(\text{warmsk}(i) \cdot \alpha_{sk}(i)) \quad (2.7)$$

$$\text{colds} = i = 122(\text{coldsk}(i) \cdot \alpha_{sk}(i)) \quad (2.8)$$

wherein, α_{sk} represents the weighting coefficient of integration.

The active control equation was applied to four thermoregulatory responses: skin perfusion rate, AVA blood flow, trembling and sweating.

3.1 The Amount of Blood Perfusion in the Skin Layer

In cold and extremely cold environment, local skin blood flow is reduced by vasoconstriction to reduce heat loss between the skin and the environment, which is very important for the human body to keep the core temperature within the normal range. In this model, the skin layer perfusion rate (m_{sk}) is calculated using the vasomotor governing equation:

$$m_{sk,dil} = m_{sk,basal} \quad T_{cr} \leq T_{cr,set} \quad (2.9)$$

$$m_{sk,dil} = 2.5(T_{cr} - T_{cr,set})(m_{sk,max} - m_{sk,basal}) + m_{sk,basal} \quad T_{cr} > T_{cr,set} \quad (2.10)$$

$$m_{sk,dil} = m_{sk,max} \quad T_{cr} \geq (T_{cr,set} + 0.4) \quad (2.11)$$

$$m_{sk,co} = m_{sk,min} \quad T_{sk} \leq (T_{sk,set} - 5.9) \quad (2.12)$$

$$msk,co = 0.17(Tsk - Tsk,set + 5.9)(msk,basal - msk,min) + msk,min \quad Tsk > (Tsk,set - 5.9) \& Tsk < 33.7^{\circ}C \quad (2.13)$$

$$msk,co = msk,basal \quad Tsk \geq Tsk,set \quad (2.14)$$

wherein. $m_{sk,basal}$, $m_{sk,min}$ and $m_{sk,max}$ represent the basal, maximum and minimum skin perfusion rates for various parts of the body, respectively.

Finally, the perfusion rate of the skin layer is calculated using the following formula:

$$msk = msk,dilmsk,co/msk,basal \quad (2.15)$$

3.2 AVA Blood Flow

In addition to communicating through arteries-capillaries-veins, the blood vessels of the human body can communicate directly with each other between arteries and arteries, veins and veins, and even between arteries and veins to form vascular anastomosis. In many parts of the body, such as fingertips, toes and other extremities, arterioles and venules can be directly connected by vascular branches to form AVA. This kind of AVA can shorten the circulation pathway and regulate local blood flow and body temperature, especially in extremely low temperature environment. Arteries in the fingers and feet deliver AVA blood flow directly to the superficial veins, and the AVA blood flow velocity (m_{AVA}) is controlled by the percentage of patency (AVA_{limb}), that is AVA_{finger} or AVA_{foot} :

Finger:

$$AVA_{finger} = 0.265(Tsk - (Tsk,set + 0.3)) + 0.953(Tcr - Tcr,set) + 0.9126 \quad (2.16)$$

Foot:

$$AVA_{foot} = 0.265(Tsk - (Tsk,set + 1.7)) + 0.953(Tcr - (Tcr,set + 0.2)) + 0.9126 \quad (2.17)$$

The AVA blood flow in the terminal section is calculated as:

$$m_{AVA} = msk,maxAVA_{limb} \quad (2.18)$$

wherein, m_{AVA} represents the AVA blood flow directly from the arterial node into the superficial vein. AVA_{limb} refers to the AVA opening factor for fingers (AVA_{finger}) or feet (AVA_{foot}), which varies between 0 and 1.

3.3 Trembling to Produce Heat

When the core temperature of the human body drops to a certain extent, and vasoconstriction cannot make the body temperature return to the normal level, the human body begins to tremble to adapt to the environment, and the increased heat production caused

by trembling can reach 5 times the metabolic rate of the human body at rest. The trembling heat production of the core layer of each body part is calculated using the following formula:

$$Msh(i) = (24.4colder(1)colds)\alpha sh(i) \tag{2.19}$$

wherein, αsh represents the tremor distribution coefficient for each body segment.

3.4 Transpiration, Evaporation and Heat Dissipation

When the human body temperature is higher than the ambient temperature, evaporative heat transfer becomes the only way for human body to dissipate heat. The amount of heat evaporated by perspiration is calculated by the following formula:

$$Esw(i) = \{371.2errorrcr(1) + 33.6(warms - colds)\}\alpha sw(i)2.0errorsk(i)/10 \tag{2.20}$$

wherein, αsw represents the sweat distribution coefficient for each skin node.

4 Model Verification

The verification tests of core temperature and multi-site skin temperature under cold exposure condition ($-5\text{ }^{\circ}\text{C}$) were carried out by using environmental climate chamber. The experiment recruited 12 healthy young male volunteers (mean \pm SD: 23.7 ± 1.1 years old, height: 172.5 ± 4.0 cm, weight: 72.1 ± 6.5 kg, BMI: 24.0 ± 1.4 kg/m). All the subjects had the experience of living in a cold climate, had no bad medical history, and were prohibited from smoking, drinking coffee, tea, alcohol and strenuous exercise within 24 h before and during the experiment. The details of the experimental process and related measuring equipment have been explained to each subject before the start of the experiment, and the subjects are required to sign a written informed consent form

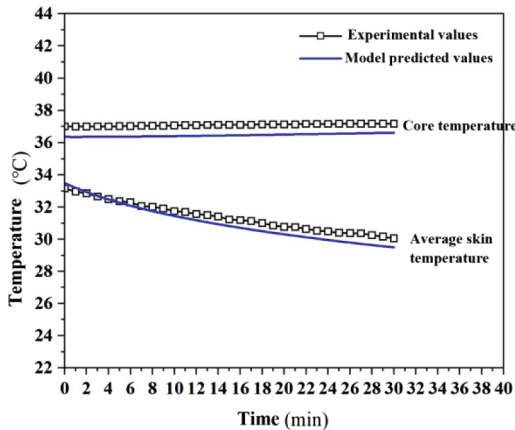


Fig. 2. Comparison of model predicted values and experimental measurement results

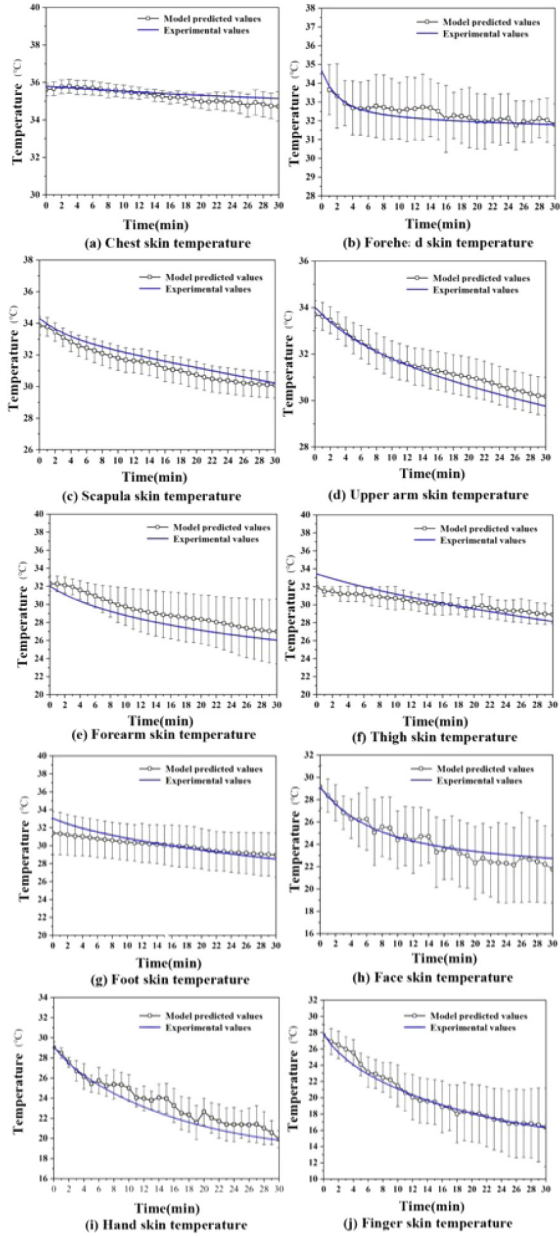


Fig. 3. Comparison of model predicted values and experimental results under -5°C environment

before the experiment can be carried out. In the experiment, the core temperature capsule of edible grade was used to continuously monitor the core temperature of human body. At the same time, the skin temperature of face, head, shoulder, upper arm, lower arm, hand, finger, thigh, calf and foot was measured by TT-K-30 (OMEGA, upper American). The precision is 0.2 °C and the sampling frequency is 15 s.

In order to further evaluate the accuracy of the prediction results of cold stress prediction and evaluation software, the above experimental data were used as a reference to quantitatively compare and analyze the temperature changes of different parts of the human body during cold exposure. Figure 2 shows the simulation results of the cold stress model of the human body at -5 °C and the core temperature and average skin temperature of the human body measured in the experiment. Figure 3 provides the quantitative comparison between the experimental data at the same low temperature (-5 °C) and the predicted results of 10 local skin temperatures calculated by the model.

The results suggest that the model can accurately predict the core temperature and average skin temperature during the whole test period. The maximum difference between the predicted results of the model and the experimental data is less than 0.67 °C, and the relative error is less than $\pm 2\%$. The calculated 10 local skin temperatures are in good agreement with the experimental data, and the relative error is less than $\pm 5\%$. The 10 parts of the human body include 7 parts covered by clothing, namely, chest, shoulder, upper arm, forearm, thigh, foot and forehead, and 3 exposed parts, namely face, hand and finger. For the parts covered by clothing (chest, forehead, shoulder, upper arm, forearm, thigh, foot), the temperature measurement of these parts is relatively stable, and the relative error is less than $\pm 4\%$. In particular, the relative error of each segment of the chest, scapula, upper arm and forehead is less than $\pm 2\%$, and the maximum difference between the measured value and the simulated value is not more than 0.65 °C.

Compliance with Ethical Standards. The study was approved by the Logistics Department for Civilian Ethics Committee of IQET, AMS.

All subjects who participated in the experiment were provided with and signed an informed consent form.

All relevant ethical safeguards have been met with regard to subject protection.

References

1. Lee, J.K.W., Kenefick, R.W., Chevront, S.N.: Novel cooling strategies for military training and operations. *The J. Strength Conditioning Res.* **29**, 77–81 (2015)
2. Potter, A.W., Blanchard, L.A., Friedl, K.E., Cadarette, B.S., Hoyt, R.W.: Mathematical prediction of core body temperature from environment, activity, and clothing: the heat strain decision aid (HSDA). *J. Therm. Biol.* **64**, 78–85 (2017)
3. Valk, P.J., Veenstra, B.J.: *Military Performance and Health Monitoring in Extreme Environments*. TNO Defence Security and Safety Soesterberg, Netherlands (2009)
4. Cain, B.: *A preliminary study of heat strain using modelling and simulation*. Defence research and development Toronto, Canada (2006)

5. Tikuisis, P., Keefe, A.A.: Effects of cold strain on simulated sentry duty and marksmanship. *Aviat. Space Environ. Med.* **78**(4), 399–407 (2007)
6. Xu, X., Rioux, T., Gonzalez, J., Hansen, E.O.: Development of a cold injury prevention tool: The Cold Weather Ensemble Decision Aid (CoWEDA). US Army Research Institute of Environmental Medicine, Natick, MA (2019)



Study on Prediction Model of Human Heat Stress in High Temperature Environment

Chenming Li, Yuhong Shen, Ruoshi Xu, and Huilin Wei(✉)

Institute of Quartermaster Engineering Technology, Beijing, China
154491268@qq.com

Abstract. In this work, the prediction model of human heat stress in high temperature environment was studied to evaluate the thermal physiological response and heat stress of personnel during all kinds of training activities in high temperature environment. The prediction model of human heat stress covers both passive system and active system. The passive system divides the human body into 21 sections, each of which is divided into three to five layers according to the structural characteristics to simulate the heat transfer process of the human body. Among them, the active system mainly simulates the regulation of human thermal physiological state by vasodilation, vasoconstriction, trembling and sweating. The thermal physiology and thermal stress prediction and evaluation model software were compared and verified by using human thermal response experimental data. The results verified that the model accurately predicts the average human skin temperature in a high temperature environment.

Keywords: Human heat stress · Prediction model · High temperature environment · Passive system · Active system

1 Introduction

The heat wave hit the entire land area of the Northern Hemisphere in 2018, killing hundreds of people; in the summer of 2019, many countries and regions in Europe experienced unprecedented heat waves. According to the French Ministry of Health, a total of 1435 people were killed in two consecutive rounds of hot weather between June 24 and July 27, 2019. In December 2019, the worst cold wave in India killed 42 people in a single day. In August 2020, high temperatures continued in many parts of Japan, and 103 people died of heatstroke in the capital Tokyo [1, 2]. In July 2013, a wide range of high temperatures occurred in Jiangnan, and Chongqing in China, covering 19 provinces and cities covering an area of 3.177 million square kilometers. The temperature in Hangzhou was the highest since 1951. In 2019, the ratio of extreme high temperature events in China is 0.38, which is 0.26 and 0.20 more than that in normal years and 2018, respectively. Past studies have confirmed that if the human body is exposed to high temperature for a long time, physiological reactions such as shortness of breath and rapid heart rate will occur, which will be accompanied by dull consciousness, inflexible movements, inattention and other reactions, resulting in prolonged reaction time and

increased error rate. In order to evaluate the thermal physiological response and thermal stress of personnel during all kinds of training activities in high temperature environment, this paper deeply analyzes the process of human thermal physiological response and its key influencing factors based on physiology, heat transfer principle and numerical simulation method. the purpose of this study is to establish a prediction and evaluation model of high temperature heat stress for young men.

2 Modeling of High Temperature Stress in Human Passive System

According to the physiological structure of the human body, the human body is divided into 21 parts, including face, head, left upper arm, right upper arm, left lower arm, left hand, right hand, chest, left shoulder, right shoulder, abdomen, back, left hip, right hip, left thigh, right thigh, left calf, right calf, left foot and right foot [3, 4]. Considering the layering of tissues, organs and bones in the human body, the layers of the head, chest and abdomen are redivided, in which the head is divided into three layers: brain (core layer), skeletal layer and skin layer; the chest is divided into five layers: lung (core layer), skeletal layer, muscle layer, fat layer and skin layer; the abdomen is divided into five layers: viscera (core layer), skeletal layer, muscle layer, fat layer and skin layer; and other parts are divided into four layers: core layer, muscle layer, fat layer, skin layer, and the central blood layer is set separately. The division of human body structure is shown in Fig. 1.

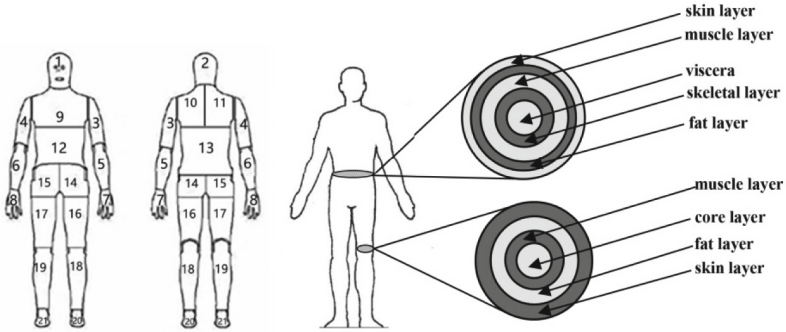


Fig. 1. Division of human thermophysiological structure.

The heat balance equation for each layer is as follows:

$$\text{Core layer: } C_{i,1} \frac{dT_{i,1}}{dt} = Q_{i,1} - B_{i,1} - D_{i,1} - Res_{i,1} \tag{2.1}$$

$$\text{Bone layers (head, thorax, abdomen): } C_{i,2} \frac{dT_{i,2}}{dt} = D_{i,1} - D_{i,2} \tag{2.2}$$

$$\text{Muscle layer: } C_{i,3} \frac{dT_{i,3}}{dt} = Q_{i,3} - B_{i,3} + D_{i,2} - D_{i,3} \tag{2.3}$$

$$\text{Fat layer: } C_{i,4} \frac{dT_{i,4}}{dt} = Q_{i,4} - B_{i,4} + D_{i,3} - D_{i,4} \tag{2.4}$$

$$\text{Skin layer: } C_{i,5} \frac{dT_{i,5}}{dt} = Q_{i,5} - B_{i,5} + D_{i,4} - Q_{i,5} - E_{i,5} \tag{2.5}$$

The heat balance equation for the central blood layer is as follows:

$$C_{86} \frac{dT_{86}}{dt} = \sum_{j=1}^4 B_{1,j} + \sum_{j=1}^3 B_{2,j} + \sum_{i=3}^8 \sum_{j=1}^4 B_{i,j} + \sum_{j=1}^5 B_{9,j} + \sum_{i=10}^{11} \sum_{j=1}^4 B_{i,j} + \sum_{j=1}^5 B_{12,j} + \sum_{i=13}^{21} \sum_{j=1}^4 B_{i,j} \tag{2.6}$$

wherein, C represents the heat capacity of each node of the human body, Wh/°C; T represents the temperature of each node of the human body, °C; t represents the exposure time, h; Q represents the heat production, W; B represents the blood heat exchange, W; D represents the conduction heat exchange between different layers in the same part of the human body, W; Res represents the respiration heat transfer, W; E represents the skin evaporation heat, W; M represents the conduction and radiation heat transfer, W.

2.1 Metabolic Heat Production

The heat production of human body consists of three parts: basic metabolic heat production, work production and trembling heat production. The calculation formula is as follows:

$$Q = Q_b + W + C_h \tag{2.7}$$

wherein, Q_b represents basal metabolic heat production, W; W represents work heat production, W; C_h represents tremor heat production, W. The basal metabolic heat production of the human body is calculated by the following formula:

$$Q_b = (58 \times BW + 1741 \times HT - 14 \times age - 470 \times sex + 227) \times \frac{1000}{24 \times 3600} \tag{2.8}$$

where, BW represents body weight, Kg; HT represents height, m; age represents age; sex represents gender, when the human body represents male, $sex = 0$, when the human body represents female, $sex = 1$. Heat production is calculated by the following formula:

$$W = CFB \times 58.2(met - Q_b)AM_f \tag{2.9}$$

$$CFB = \frac{Q_b}{Q_{bm}} \tag{2.10}$$

wherein, CFB represents the correction factor, dimensionless; Q_{bm} represents the total basic metabolic heat production of the original model human body, W; A represents

the surface area of various parts of the body, m^2 ; met represents the metabolic heat production of the human body, W ; M_f represents the distribution coefficient of muscle heat production between different regions and layers of the human body. When the human body is in a high temperature environment, the metabolism will increase. The formula for calculating the thank you rate in this era is as follows:

$$Q^* = Q + \Delta Q \quad (2.11)$$

$$\Delta Q = Q_b[2^{0.1(T-T_0)} - 1] \quad (2.12)$$

wherein, Q^* represents the metabolic rate of the human body in the high temperature environment, W ; ΔQ represents the increase of the metabolic rate caused by the high temperature of the environment, W ; T_0 represents the set point temperature of each layer of each part of the human body, $^{\circ}C$.

2.2 Blood Convection Heat Transfer

The convective heat transfer of blood is mainly the heat exchange between the central blood layer and the blood through various parts of the human body, which plays a very important role in the thermal regulation of the human body. the specific calculation is as follows [5, 6]:

$$B = apB_f(T - T_{81}) \quad (2.13)$$

wherein, a represents a constant, dimensionless; p represents the volumetric specific heat of blood, $Wh/(l \cdot ^{\circ}C)$; B_f represents blood flow, l/h ; blood flow is mainly affected by three factors: basic blood flow, work and trembling. The formula is as follows:

$$B_f = B_b + \left(\frac{W + C_h}{1.16} \right) \quad (2.14)$$

wherein, B_b represents basal blood flow, l/h .

When the human body is in a high temperature environment, the body will accelerate the heat loss of the human body to the outside world by increasing the blood flow. The calculation formula of the blood flow at this time is as follows:

$$B_f^* = B_f + \Delta B_f \quad (2.15)$$

wherein, B_f^* represents human blood flow, l/h ; ΔB_f represents the increase in blood flow caused by high temperature, l/h . The calculation expression of ΔB_f is as follows:

$$\Delta B_f = B_b[2^{0.1(T-T_0)} - 1] \quad (2.16)$$

wherein, T represents the temperature of each node of the human body, $^{\circ}C$; T_0 represents the set point temperature corresponding to each node of the human body, $^{\circ}C$.

2.3 Conduction Heat Transfer in Vivo

The formula for calculating the conduction heat exchange between adjacent layers in the same place is as follows:

$$D = C_d(T_j - T_{j+1}) \quad (2.17)$$

wherein, D represents the heat conduction between the adjacent layers in each zone of the human body 20, W; C_d represents the heat conduction coefficient between the adjacent layers in each zone of the human body, W/°C.

2.4 Respiratory Heat Transfer

Respiratory heat dissipation occurs only in the core layer of the chest. The formula is as follows:

$$Res = \{0.0014(34 - T_a) + 0.017(5.867 - p_a)\} \sum_{i=1}^{20} \sum_{j=1}^4 Q \quad (2.18)$$

wherein, T_a represents ambient temperature, °C; p_a represents ambient water vapor pressure, kPa.

2.5 Evaporative Heat Transfer on the Skin Surface

The evaporative heat loss from the skin surface is calculated as follows:

$$E = Eb + ESW \quad (2.19)$$

wherein, E represents the evaporative heat loss on the skin surface, W; E_b represents the heat loss from the diffusion of water vapor on the skin surface, W; ESW represents the evaporative heat transfer of the human body, W.

The heat loss of water vapor diffusion on the surface of human skin is calculated as follows:

$$E_b = 0.06 \left(\frac{1 - E_{sw}}{E_{max}} \right) E_{max} \quad (2.20)$$

E_{max} represents the maximum amount of heat removed by the human body due to evaporation of sweat, and the calculation formula is as follows:

$$E_{max} = h_e(p_{sk,s} - p_a)A \quad (2.21)$$

wherein, h_e represents the evaporative heat transfer coefficient of heat exchange between the skin and the environment W/m²·K; $p_{sk,s}$ represents the saturated vapor pressure on the surface of the skin, kPa; p_a represents the ambient water vapor pressure, kPa; A represents the surface area of each section of the body, m².

2.6 Sensible Heat Exchange on the Surface of the Skin

The sensible heat transfer between the skin surface and the environment includes convection, radiation and conduction heat exchange. The convection and radiation heat exchange on the skin surface is greatly affected by clothing. The calculation formulas of convection and radiation when wearing different clothing can be found in the clothing system below.

3 High Temperature Stress Modeling of Human Active System

In the aspect of active system, keeping body temperature relatively stable is an important sign that human beings and other constant temperature animals are different from variable temperature animals, and physiological regulation system plays an important role in maintaining human body temperature stability. The human thermosensory system is controlled by the hypothalamus and is realized by receptors, central controllers and effectors. Thermogenesis is regulated by vasodilation, vasoconstriction, trembling and sweating.

3.1 Temperature Sensing System

The temperature perception of the human body is characterized by the temperature error signal, and the set point temperature plays an important role in the process of temperature regulation. The temperature perception error signal is calculated as follows:

$$Err = (T - T_{set}) + R_{ate} F \quad (3.1)$$

wherein, T_{set} represents the set point temperature, °C; R_{ate} represents the sensitivity of thermal induction; F represents the rate of temperature change.

The heat signal and the cold signal can be calculated by the following formula:

$$Warm = Err, \quad Cld = 0 \quad (3.2)$$

$$Cold = -Err, \quad Wrm = 0 \quad (3.3)$$

The heat and cold signal of skin temperature is weighted to get the comprehensive signal of human body temperature perception:

$$Warm_s = \sum_{i=1}^{20} (SKINR(i) \times Warm(i,4)) \quad (3.4)$$

$$Cold_s = \sum_{i=1}^{20} (SKINR(i) \times Cold(i,4)) \quad (3.5)$$

3.2 The Mode of Thermoregulation

There are four ways of temperature regulation of the human body, namely, vasoconstriction, vasodilation, trembling and sweating. When the human body is in a high temperature environment, vasodilation and sweating regulate the body temperature, and when the human body is in a cold environment, vasoconstriction and trembling regulate human questions.

The blood flow of the human body is calculated as follows:

$$BF(i,j) = \frac{BFB(i,j) + (SKINV(i) \times D_L)}{1 + (SKINC(i) \times ST)} \times km(i,4) \tag{3.6}$$

wherein, *SKINV* and *SKINC* represent the control coefficient of thermophysiological regulation, dimensionless; *km*, *D_L* and *S_T* represent regional multiplier, vasodilation coefficient and vasoconstriction coefficient, dimensionless respectively. The region multiplier reflects the effect of local skin temperature on vasodilation and contraction, and the formula is as follows:

$$km(i,4) = 2.0^{Err(i,4)/RT(i,4)} \tag{3.7}$$

wherein, *RT* represents temperature difference, and the value is 10 °C.

$$D_L = C_{dl} \cdot Err(1,1) + S_{dl} \cdot (Warm_s - Cold_s) + P_{dl} \cdot Warm(1,1) \cdot Warm_s \tag{3.8}$$

$$ST = -C_{st} \cdot Err(1,1) - S_{st} \cdot (Warm_s - Cold_s) + P_{dl} \cdot Cold(1,1) \cdot Cold_s \tag{3.9}$$

The evaporative heat dissipation *E_{sw}* of human sweat is calculated as follows:

$$E_{sw}(i,4) = \left\{ \begin{array}{l} C_{sw} \cdot Err(1,1) + S_{sw} \cdot (Warm_s - Cold_s) \\ + P_{sw} \cdot Warm(1,1) \cdot Warm_s \end{array} \right\} SKINS(i) \cdot km(i,4) \tag{3.10}$$

The heat production of human tremor can be calculated by the following formula:

$$C_h(i,4) = \left\{ \begin{array}{l} -C_{ch} \cdot Err(1,1) - S_{ch} \cdot (Warm_s - Cold_s) \\ + P_{ch} \cdot Cold(1,1) \cdot Cold_s \end{array} \right\} Chilf(i) \tag{3.11}$$

when human skin is exposed or covered with clothing, the amount of sweat produced by the human body is calculated using the following formula. When human skin is exposed:

$$M_{sw} = \frac{E_{sw}}{wl \times A} \tag{3.12}$$

$$\frac{dm_s}{dt} = M_{sw} + \frac{P_{sat} - P_{sk}}{R_{esk} \times wl} - \frac{P_{sk} - P_a}{R_{ea} \times wl} \tag{3.13}$$

$$P_{sk} = \begin{cases} P_{sat} & m_s > 0 \\ \frac{M_{sw} \times R_{esk} \times R_{ea} \times wl + P_{sat} \times R_{ea} + P_a \times R_{esk}}{R_{ea} + R_{esk}} & m_s \leq 0 \end{cases} \tag{3.14}$$

wherein, *M_{sw}* represents the active regulation of perspiration by the human body, g/m²·s; *wl* represents the latent heat of evaporation of water, J/g; *m_s* represents the amount of

perspiration of the human body, g/m^2 ; P_{sat} represents saturated water vapor pressure, kPa; P_{sk} represents the surface water vapor pressure of the skin, kPa; P_a represents the ambient water vapor pressure, kPa; R_{esk} represents the skin moisture resistance, $\text{m}^2 \cdot \text{kPa}/\text{W}$; R_{ea} represents the air layer moisture resistance, $\text{m}^2 \cdot \text{kPa}/\text{W}$.

When human skin is covered with clothing:

$$\frac{dm_s}{dt} = M_{sw} + \frac{P_{sat} - P_{sk}}{R_{esk} \times wl} - Diffmc \times \frac{P_{sk} - P_{cl}}{L} \times 1000 \quad (3.15)$$

$$P_{sk} = \begin{cases} \frac{P_{sat}}{R \times T_{sk}} & m_s > 0 \\ \frac{P_{sat} \times L + M_{sw} \times L \times R_{esk} \times wl + 1000 \times Diffmc \times p_{cl} \times R_{esk} \times wl}{R \times T_{sk} \times L + 1000 \times Diffmc \times R_{esk} \times wl} & m_s \leq 0 \end{cases} \quad (3.16)$$

$$P_{sk} = p_{sk} \cdot R \cdot T_{sk} \quad (3.17)$$

wherein, $Diffmc$ represents the diffusion coefficient of water vapor, m^2/s ; p_{sk} represents the density of water vapor on the surface of the skin, kg/m^3 ; p_{cl} the water vapor density on the inner surface of the fabric, kg/m^3 ; L represents the air gap width between the skin and the fabric, m; R represents the water vapor gas constant, $\text{kJ}/\text{kg} \cdot \text{K}$; T_{sk} represents the temperature of the skin layer, K.

4 Model Verification

Furthermore, the thermal physiology and thermal stress prediction and evaluation model software were compared and verified by using human thermal response experimental data. The high temperature experiment was carried out as follows: before the beginning of the experiment, the subjects sat quietly in a climate room with an ambient temperature of 29°C and a humidity of 40% for one hour. The mean and variance of subjects' information were: age 25.4 ± 2.1 years old, height 173.6 ± 3.2 cm, weight 66.5 ± 5.0 kg, body surface area 1.8 ± 0.1 m^2 . During the experiment, the temperature of the two rooms in the climate room was set to 29°C and 45°C respectively, and the humidity was 40%. The subjects were exposed to four working conditions for two hours: from normal temperature environment (29°C), high temperature environment (45°C), and then back to normal temperature environment (29°C) and high temperature environment (45°C), each stage for half an hour. The laboratory subjects remained seated in the environmental cabin. Figure 2 provides the quantitative comparison of skin temperature, core temperature and average skin temperature in various parts of the body.

According to Fig. 2, the thermal physiology and heat stress prediction and evaluation model can better reflect the changes of human core temperature and skin temperature in high temperature environment. Specifically, the core temperature simulation results show the same upward and downward trend and amplitude as the experimental values at each stage of high temperature (45°C) and neutral temperature (29°C). The experimental measurement values fit well with the model simulation values, and the maximum deviation in the stable stage of 30–120 min is less than 0.4°C . The obvious deviation in 0–30 min minutes is due to the fact that the initial temperature of the model is too low compared with the experimental value. The maximum deviations between the simulated and experimental values of average skin temperature are 0.79°C , 0.80°C , 0.32°C and

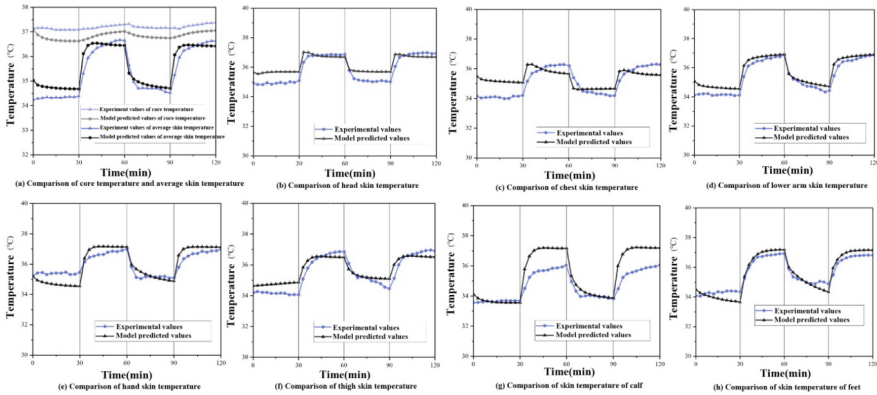


Fig. 2. Comparison of model predicted values and experimental results in high temperature environment.

0.81 °C, respectively, which are less than the acceptable range of 1 °C. The results show that the model can accurately predict the average skin temperature of human body in high temperature environment.

Compliance with Ethical Standards. The study was approved by the Logistics Department for Civilian Ethics Committee of IQET, AMS.

All subjects who participated in the experiment were provided with and signed an informed consent form.

All relevant ethical safeguards have been met with regard to subject protection.

References

1. Lee, K.W.J.: Acute, short and long term responses to heat stress—Implications for combatants' performance and health. *J. Sci. Med. Sport* **20**, 55–66 (2017)
2. Potter, A.W., Gonzalez, J.A., Looney, D.P.: Biophysical assessment of the US Army Improved Hot Weather Combat Uniform (IHWCU) and a comparison to the currently fielded Fire Resistant Army Combat Uniform (FRACU). Biophysics and Biomedical Modeling Division, US Army Research Institute of Environmental Medicine Natick United States (2019)
3. Hunt, A.P., Billing, D.C., Patterson, M.J., Caldwell, J.N.: Heat strain during military training activities: the dilemma of balancing force protection and operational capability. *Temperature* **3**(2), 307–317 (2016)
4. Sauter, D.: Hot Environment Assessment Tool (HEAT) User's Guide. Army research lab white sands missile range nm computational and information sciences directorate/battlefield environment div (2012)
5. Potter, A.W., Blanchard, L.A., Friedl, K.E., Cadrette, B.S., Hoyt, R.W.: Mathematical prediction of core body temperature from environment, activity, and clothing: the heat strain decision aid (HSDA). *J. Therm. Biol* **64**, 78–85 (2017)
6. Takada, S., Kobayashi, H.: Thermal model of human body fitted with individual characteristics of body temperature regulation. *Build. Environ.* **44**(3), 463–470 (2009)



Thermal Comfort Assessment of Occupants in Special Vehicle Cabin

Sijuan Zheng¹, Feina Shi², Fang Xie¹ (✉), Qiufang Wang¹, and Zhongliang Wei¹

¹ North Vehicle Research Institute, Beijing 100072, China
clubjully@sina.cn

² Beijing North Vehicle Group Corporation, Beijing 100072, China

Abstract. Due to the specific function and ventilation limitation, the cabin of special vehicles is generally narrow and enclosed, in which occupants are faced with uncomfortable conditions such as high heat load, less cold source, and lack of fresh air. The thermal comfort assessment method is a crucial research premise of thermal environment and thermal comfort. Therefore, it is necessary to study the thermal comfort assessment method of occupants in the special vehicle cabin. Firstly, this paper analyzed the distribution characteristics of a variety of typical environmental parameters and the subjective assessment results of the occupants on the surrounding air environment in order to obtain the thermal boundary conditions necessary for Computational Fluid Dynamics (CFD) steady-state flow field simulation of the special vehicle cabin. Then according to the research of occupants' thermal comfort in the special vehicle cabin, the changes in thermal comfort temperature due to thermal adaptation of the occupants are investigated to obtain the thermal comfort assessment model that meets the needs of different seasons and different mission phases.

Keywords: Thermal comfort · Assessment methods

1 Introduction

Human thermal comfort is a reflection of satisfaction with the surrounding air environment and an integrated determination of psychological and physiological factors. The principal factors that affect human thermal comfort depend on the air temperature, humidity, air velocity, and other environmental parameters to which a person is exposed. The thermal comfort of occupants cannot be measured directly with instruments but can only be collected in the form of questionnaires [1]. In addition, the human body is not completely passive to the ambient air environment but actively adapts and interacts with the environment, which explains why the human thermal adaptation is the reason for the discrepancy between the results of many artificial climate laboratory studies and those of actual research studies. In China, seasonal changes can cause wide variations in outdoor air temperature. Differences in individual dress and environmental adaptations make a single temperature control standard unable to satisfy the demands of the thermal environment in the special vehicle cabin during different seasons [2–4]. Particularly in the

northern regions, the atmospheric environment temperature varies considerably from season to season throughout the year, which may lead to adaptive changes of human thermal comfort under different outdoor atmospheric temperatures.

2 Cabin Environment Test

In order to obtain the seasonal influence, experiments were carried out once a month in 12 months, and a total of 158 questionnaires were carried out. Gender and age are also important factors affecting human thermal comfort, and many studies have pointed out that women and the elderly have higher requirements for temperature and thermal comfort than other groups. However, considering the particularity of the vehicle, this paper only selects adult men as the test object.

2.1 Subjective Questionnaire Data

The thermal comfort of occupants cannot be measured directly with instruments but can only be collected in the form of questionnaires. Therefore, the analysis of subjective questionnaire data is very important, which is an important basis for evaluating the thermal environment comfort of vehicle cabin. As shown in Tables 1 and 2, the subjective questionnaire mainly studies and analyzes the thermal sensation in the cabin and the satisfaction of three environmental parameters, namely wind speed, temperature and humidity [5, 6].

Table 1. Method of thermal voting results

Thermal sensitivity						
Cold	Cool	A little cold	Moderate	A little warm	Warm	Hot
-3	-2	-1	0	1	2	3

Table 2. Environmental parameter satisfaction voting method

Environmental parameters satisfaction (wind speed, temperature, humidity)		
Hope to be lower	Moderate	Hope to be higher
-1	0	1

Through the analysis of the subjective questionnaire of heat feeling, it is considered that the current thermal environment in the vehicle cabin still does not fully meet the requirements of passengers for thermal comfort, and about half of passengers are not satisfied with the heat feeling in the cabin. On the other hand, the thermal environment in the cabin often makes the passengers in a hot state. In most cases, the cabin temperature control is generally high.

Through the analysis of the subjective questionnaire on the satisfaction of environmental parameters, it can be seen that the percentage of questionnaires that are dissatisfied with the temperature in the cabin and wanting the air temperature in the cabin to increase or decrease is lower than the percentage of questionnaires that the thermal feeling vote is not 0, which are 41.7% and 58.8% respectively. This shows that not all passengers who feel uncomfortable with heat have the expectation of adjusting the air temperature in the cabin. In order to analyze the causes of this phenomenon, the temperature expectation voting of passengers and thermal voting are combined to further analyze the temperature expectation of passengers in the cabin in different thermal voting value ranges [7]. Through the analysis of the subjective questionnaire on the satisfaction of environmental parameters, it can be seen that the percentage of those who are not satisfied with the cabin temperature and want the air temperature change in the cabin is lower than the percentage of those who do not have a thermal vote of 0, and the former is 41.7%, while the latter is 58.8%. This shows that not all passengers who feel uncomfortable with heat have the expectation of adjusting the air temperature in the cabin. In order to analyze the causes of this phenomenon, the temperature expectation voting of passengers and thermal voting are combined to further analyze the temperature expectation of passengers in the cabin in different thermal voting value ranges, as shown in the figure below (Fig. 1).

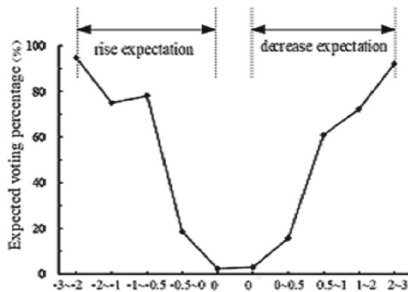


Fig. 1. Expected voting percentage of temperature in each thermal voting interval

Therefore, the tolerance of passengers to the indoor thermal environment is an important reason for the formation of “not all passengers who are uncomfortable with thermal voting have the expectation of adjusting the indoor air temperature”. The tolerance of passengers have a great impact on their temperature expectation voting, especially in the range of $-0.5\sim 0$ and $0\sim +0.5$. On the other hand, when the cabin thermal environment is in the partial heat state, the percentage decreases significantly from $+1\sim +2$ interval to $+0.5\sim +1$ interval, while when the cabin thermal environment is in the partial cold state, the percentage does not decrease from $-2\sim -1$ interval to $-1\sim -0.5$ interval. The passengers still have high temperature rise expectations in the $-1\sim -0.5$ thermal sense interval. This may be due to the fact that the body itself is more sensitive to cold than the heat. Cold sensation makes it easier for passengers to feel unbearable, which is similar to the results of other body heat sensation studies.

2.2 Objective Environmental Measurement Data

In addition to the subjective questionnaire, the objective environment in the cabin was monitored and recorded, mainly including the temperature change rule of each wall of the cabin, which is the necessary thermal boundary condition for obtaining the CFD steady-state flow field simulation of the cabin in a stable state.

Each wall in the cabin is an important boundary for radiative heat exchange with the passenger’s body in the cabin. The measurement of the temperature of each wall in the cabin can help to understand the radiative heat transfer environment of the passenger. Therefore, the temperature of each wall in the cabin is monitored and recorded, and the thermal boundary conditions necessary for the steady-state CFD flow field simulation of the cabin in a stable state are obtained from its variation rules. In this paper, the steady-state calculation is only carried out for the cabin environment in the numerical simulation, so only the measurement results in the stable stage are selected. Take the average number of test states such as ceiling, floor and sidewall temperature for calculation. According to the test results, the average temperature values of ceiling, floor and side wall in the stable stage are 24.1 °C, 22.3 °C and 23.1 °C, respectively.

2.3 PMV Index of Human Thermal Comfort

PMV value is an important index of human thermal comfort, representing the average cold and hot sensation of most people in the same environment. In a limited space, the thermal comfort of personnel is determined by six main factors, among which air temperature, average radiation temperature, partial pressure of water vapor in the air (or relative humidity), and air flow are determined by the environment, while the other two factors including the metabolic rate of the human body and clothing thermal resistance depend on human themselves.

Danish Professor Fanger established the famous PMV thermal comfort prediction and evaluation model based on the theory of human thermal balance and a large number of artificial climate experiments, which has been recognized internationally. PMV model can predict and calculate human PMV under the influence of human metabolic volume, clothing thermal resistance, ambient air temperature, flow rate, humidity and other factors. The PMV equation can be written as:

$$\begin{aligned}
 PMV = & 0.303e - 0.036M + 0.0275 \times M - W - 3.05 \times 10^{-3} \\
 & \times 5733 - 6.99M - W - Pa - 0.42 \times M - W - 58.15 \\
 & - 1.7 \times 10^{-5} \times M \times 5867 - Pa - 0.0014M34 - ta - 3.96 \times 10^{-8}fcl \\
 & \times tcl + 2734 - tr + 2734 - fclhctcl - ta
 \end{aligned}
 \tag{1}$$

Outer surface temperature of clothing can be written as:

$$tcl = 35.7 - 0.028M - W - Icl \times \{3.96 \times 10^{-8} \times fcltcl + 2734 - ta + 2734 + fclhctcl - ta\}
 \tag{2}$$

Convective heat transfer coefficient can be written as:

$$hc = hc1 = 2.38tcl - ta0.25, hc1 > hc2hc2 = 12.1va, hc1 < hc2
 \tag{3}$$

where M is Human metabolic rate, W/m2;

W is the work done by the human body, W/m^2 ;
 I_{cl} is Clothing thermal resistance, $m^2 \cdot K/W$;
 P_a is water vapor partial pressure in the surrounding environment, Pa;
 t_a is the temperature of the air around the body, $^{\circ}C$;
 t_{cl} is outer surface temperature of clothing, $^{\circ}C$;
 t_r is the average radiation temperature of the surrounding environment, $^{\circ}C$;
 f_{cl} is area coefficient of human clothing,
 h_c is convective heat transfer coefficient, $W/m^2 \cdot K$.

3 Thermal Comfort Assessment

In this paper, data from 10 adult male occupants under operating conditions at three different vent layout locations were measured, and the thermal comfort assessment function values at each measuring point were analyzed. The comparison of PMV value under different operating conditions is shown in the following table, from which it can be seen that the average thermal comfort of operating condition one is the best (Table 3).

Table 3. Comparison of PMV values under different condition

	Condition 1	Condition 2	Condition 3
Occupant 1	-0.541880	-0.622669	-0.551913
Occupant 2	-0.403320	-0.619861	-0.713797
Occupant 3	-0.538620	-0.603890	-0.504080
Occupant 4	-0.289780	-0.198996	-0.252513
Occupant 5	-0.521500	-0.626236	-0.626244
Occupant 6	-0.189910	-0.226786	-0.134982
Occupant 7	-0.164970	-0.338291	-0.261541
Occupant 8	-0.166170	-0.225226	-0.114887
Occupant 9	-0.207000	-0.148893	-0.287032
Occupant 10	-0.323740	-0.572772	-0.213723
Average PMV value	-0.334690	-0.418362	-0.366071

According to the measured results and test data of special vehicle cabins, covering different seasonal climate conditions throughout the year, the iterative calculation formula of PMV under different seasonal conditions is obtained through regression analysis. The thermal comfort assessment PMV values of the corresponding locations of coordinates were calculated by bringing the corresponding air temperature, mean radiation temperature, air relative humidity, air flow rate, human metabolic rate, and clothing thermal resistance from the simulation into the established PMV functional relationship. The closer this PMV value is to 0, the better the thermal comfort of the cabin.

4 Conclusion

In this paper, a subjective questionnaire survey on the thermal sensation and environmental satisfaction of the special vehicle cabin was carried out on 158 adult males in 12 months, which demonstrated the temperature expectation of the occupants in different thermal sensation voting ranges. Besides, the thermal boundary conditions essential for the simulation of the cabin CFD steady-state flow field were obtained by monitoring and recording the cabin environment, especially the temperature variation patterns of the cabin surfaces. The results showed average temperature values of 24.1 °C, 22.3 °C, and 23.1 °C for the ceiling, floor, and sidewalls of the cabin during the steady-state phase respectively. The thermal comfort analysis of the cabin occupants and the change in thermal comfort temperature caused by occupants' thermal adaptation was investigated to obtain the thermal comfort assessment model for the needs of different seasons and different mission phases. Finally, the PMV assessment method was applied with the input of results and data from actual vehicle measurements, which were used to guide the optimal design of the vehicle's air supply temperature and air supply air volume in different seasons and task phases, ultimately realizing a thermal adaptation control strategy for the special vehicle's thermal environment.

Compliance with Ethical Standards. The study was approved by the Logistics Department for Civilian Ethics Committee of North Vehicle Research Institute.

All subjects who participated in the experiment were provided with and signed an informed consent form.

All relevant ethical safeguards have been met with regard to subject protection.

References

1. Kok, J.C., Muijden, J.V., Burgers, S.S., Dol, H., Spekreijse, S.P.: Enhancement of aircraft cabin comfort studies by coupling of models for human thermoregulation, internal radiation, and turbulent flows. In: Proceedings of the European conference on computational fluid dynamics, pp. 1–19 (2006)
2. Tejsen, P.S., Zukowska, D., Jama, A., Wyo, DP.: Assessment of the thermal environment in a simulated aircraft cabin using thermal manikin exposure. In: Proceedings of the 10th international conference on air distribution in rooms, pp. 227–34 (2007)
3. Kok, J.C., Muijden, J.V., Burgers, S.S., Dol, H., Spekreijse, S.P.: Enhancement of aircraft cabin comfort studies by coupling of models for human thermoregulation, internal radiation, and turbulent flows. In: Proceedings of the European conference on computational fluid dynamics, pp. 1–19 (2006)
4. International Standard ISO/FDIS 7933: 2004(E). Ergonomics of the thermal environment-analytical determination and interpretation of heat stress using calculation of the predicted heat strain (2004)
5. International Standard ISO 7730: 2005(E). Ergonomics of the thermal environment-analytical determination and interpretation of thermal comfort using calculation of the PMV and PPD indices and local thermal comfort criteria (2005)
6. Pang, L.P., Gong, M.M., Qu, H.Q.: Moisture prediction for aircraft cabin based on a lumped virtual moisture source. *Acta Aeronaut Astronaut Sin* **33**(6), 1030–5 (2012). [Chinese]
7. de Dear, R.J., Arens, E., Hui, Z., Oguro, M.: Convective and radiative heat transfer coefficients for individual human body segments. *Int J Biometeorol* **40**(3), 141–156 (1997)



Research on the Selection of Cognitive Status Test Items and Indicators for Workers in Confined Spaces

Chuan Wang¹, Ting Wang², Yi Chen³, Xiaojun Wang⁴, and Ziyang Wang¹(✉)

¹ Naval Medical Center of PLA, Naval Medical University (Second Military Medical University), Shanghai 200433, China
wangziyingwzy@sina.com

² Wuhan Second Ship Design and Research Institute, Wuhan 430000, China

³ School of Biological Science and Medical Engineering, Southeast University, Nanjing 210096, China

⁴ Naval Equipment Department, Beijing 100089, China

Abstract. The working environment in the confined space is harsh, and long-term continuous operation may lead to the depression of the mood and the decline of cognitive ability of the operator, which affects the operation performance and operation safety. In this paper, from the six aspects of reaction time, attention function, working memory, time perception, spatial perception, and operational stability, the indicators for the identification of abnormal cognitive status of operators in confined spaces are selected to monitor the cognitive status of operators in real time, so as to reduce operational risks and ensure safe control. By reviewing the existing neurobehavioral testing tools, combined with the actual test situation of this paper, a set of work ability indicator system is screened out to evaluate different cognitive states, including a total of 8 tests, namely: simple reaction time, discriminative reaction time, choice response time, attentional stability, working memory ability, time perception ability, spatial perception ability, operational stability.

The research results can better identify abnormal states of various basic cognitive abilities under the influence of emotion, fatigue, stress, mental or neurological disease, thereby helping operators reduce human errors and improving the operation safety and performance, which has practical significance for the evaluation of operator's work ability and the prevention of human error.

Keywords: Confined space · Workers · Cognitive status · Test indicators

1 Foreword

Abnormal cognitive status is generally occurred for the confined space operators, which is prone to human error and brings great hidden dangers to operational safety. It is the most important exploration of space research to maintain complete cognitive ability [1]. The applicability of existing cognitive assessment tools is limited by educational and cultural differences in this context [2]. The cognitive function assessment scale has

significant value in the early identification of disease, the evaluation of curative effect and nursing guidance [3]. To study the impact of confined space on the cognitive function of operators, first, a set of qualified neurocognitive measurement tools is needed [4]. In this paper, from the aspects of reaction time, attention function, working memory, time perception, spatial perception, operation stability, etc., the indicators for abnormal recognition of cognitive status of operators in confined spaces are selected to monitor the cognitive status of operators in real time, reduce operational risks, and ensure safe operation.

2 Reaction Time

Reaction time, also known as response latency, refers to the time it takes for the body to respond to a stimulus. Reaction time (RTs) is a natural data to investigate cognitive processes under performance on cognitive tests [5]. Reaction time is an important indicator for evaluating human activity, and is also one of the most widely used indicators of mental activity in neurobehavioral research. Reaction time, as a reliable indicator of psychological activity, is able to measure the excitatory and inhibitory functions of the cerebral cortex, and analyze various psychological activities such as human feeling, attention, learning and memory, thinking, and personality differences. At present, reaction time measurement is widely applied in basic research and practical work in medicine, pharmacy, hygiene, psychology and so on.

Reaction time measurement was first researched and applied by Donders, a Dutch physiologist and psychologist, in 1968. Donders classified the reaction time into three categories according to specific tasks, namely:

(1) Simple reaction time

Also known as A reaction time. For example, when the subject presses the left mouse button immediately when seeing the red signal, this reaction time is a simple reaction time;

(2) Choice reaction time

Also known as the B reaction time. For example, the subject presses the left mouse button immediately when seeing the red signal, and presses the right mouse button immediately when seeing the green signal.

(3) Recognition reaction time

Also known as C reaction time. For example, the subject presses the left mouse button immediately when seeing the red signal, and do not need to operate when seeing the green signal. This reaction time is the recognition reaction time.

From the angle of physiology, each reaction time is composed of three processes: the first stage is the time when the stimulus causes the receptor to cause the nerve impulse to be transmitted to the sensory neuron; the second stage is the time when the nerve impulse is transmitted from the sensory neuron to the sensory center and motor center of cerebral cortex, and then from the center to the effector through the motor nerve; the third stage is the time when the effector receives the impulse to cause movement. The sum of the time consumed of the above three stages is the reaction time. For the neural behaviors corresponding to advanced cognitive functions, the difference in the

reaction time of different tasks and different groups of people is mainly reflected in the second stage, especially the time when nerve impulses are transmitted in the central nervous system, which reflects the degree of complexity required for processing the motor instructions of sensory information in the nervous system. Generally speaking, the more complex the stimulus, the more complex the task, the longer it will take. For example, for the same recognition task, the reaction time used to recognize high-level attributes such as faces or words is often longer than that of basic attributes such as shape, color or direction, because the former involves more and complex information processing processes. Therefore, in order to assess the processing state of the subjects in each stage of visual cognition as much as possible, this topic selected three reaction time indicators, namely simple reaction time, choice reaction time, and recognition reaction time.

There are many factors that affect the measurement of reaction time. From the internal factors of the subjects, the influencing factors include age, intelligence level, emotional state, fatigue state, and even some personality traits; from the external factors, the presentation method of the stimulus, the stimulus intensity, and the signal transmission characteristics of the electronic equipment also affect the measurements and calculation of reaction time. Therefore, when designing test tasks, try to keep as consistent and standardized as possible.

3 Attention Function

Attention is a basic mental state of human beings, and is the orientation and concentration of mental activities or consciousness to specific objects; therefore, it has the following two characteristics:

(1) Directivity

Directivity means that at each given moment, human mental activity or consciousness must be directed to a certain (or some) object, while ignoring other objects;

(2) Concentration

Concentration refers to the intensity or tension with which mental activity or consciousness moves in this definite direction.

Attentional states have the following four characteristics, also known as attentional qualities:

(1) Attention span

Attention span refers to the number of objects that a person can clearly perceive or grasp at the same time. In 1956, Miller, an American psychologist, found that the attention span of people in simple tasks is generally 7 ± 2 blocks (including numbers, letters or words, etc.), and later researchers found that attention span was also related with the block type and length. For example, the attention span to numbers or letters is usually greater than that of words, and the longer the word, the smaller the attention span.

(2) Attention stability

Attention stability refers to the duration that the attention state remains on the same object or the same activity. During this process, it is normal to be aware of some fluctuations.

(3) Attention allocation

Attention allocation means that a person can direct the attention to several different objects at the same time, or engage in several activities at the same time.

(4) Attention transfer

Attention transfer refers to the active transfer of attention from one object or activity to another according to the change of task requirements. Attention transfer is not contradictory to attention stability, because attention transfer is carried out actively by people and is controlled by the will of people; on the contrary, attention distraction means that attention is attracted by irrelevant objects and leaves the original directed objects or activities, also known as “absent-minded”.

Attention, as one of the most basic and important cognitive activities of human beings, participates in the whole process of information processing from perception to action reaction. Various complex operation tasks are highly dependent on the effective choice and reasonable allocation of attention. Attention function is also easily affected by various factors, the root of which lies in the changes in the structure or function of the human nervous system. The most typical example is attention deficit hyperactivity disorder (commonly known as “ADHD”). In addition, studies have shown that adverse physiological and psychological states such as fatigue and stress, and mental disorders such as depression or anxiety can lead to abnormal cognitive status, and the first manifestation is the deficit of attention function, such as decrease of attention span, stability and transfer flexibility, difficulty of concentrating, etc. Therefore, the measurement of attention state is also an important indicator of recognizing cognitive state abnormality.

4 Working Memory

Human memory can be roughly divided into three types: short-term memory, long-term memory and working memory. The retention time of short-term memory is usually about a few seconds to one minute, and the content of short-term memory can be converted into long-term memory after repetition and consolidation, which can be maintained for more than one minute until life. However, working memory is the temporary monitoring, processing and retention of task-related information during the execution of a specific task. The content retention time of it is between short-term memory and long-term memory, and the memory will be erased after the completion of the current task. Working memory is also one of the important basic cognitive functions of human body. It plays a vital role in the formation of advanced cognitive functions such as reasoning, learning, decision-making, and speech comprehension. It is also one of the important indicators reflecting the intellectual ability of human. It can be divided into visual working memory and auditory working memory according to the different sense organs involved in the task.

One of the more influential theory to explain the mechanism of working memory is the Baddeley’s model of working memory. The model argues that the working memory system can be divided into four modules:

(1) Central executive system

The central executive system is the core of working memory system, responsible for coordinating and integrating the functions of various subsystems, controlling memory encoding and retrieval strategies, and regulating the attention system.

(2) Phonological loop

The phonological loop is mainly responsible for processing auditory and speech-based information. It can not only store and control this information, but also keep the decaying speech representations continuously activated through “silent reading”, and can convert written language (text information) into speech representations.

(3) Visuo-spatial sketch pad

The visuo-spatial sketch pad is mainly responsible for the storage and processing of information related to visual and spatial perception.

(4) Episodic buffer

Episodic buffer communicate working memory and long-term memory, and store information from multiple dimensions, allowing the integration and temporary storage of information received and processed by phonological loop, visuo-spatial sketch pad, and information extracted from long-term memory for subsequent processing operations by the central executive system.

Visual working memory has also been found to be distributed in the central nervous system, involving multiple encephalic regions in the cerebral cortex and subcortical region, among which, the important nodes include the hippocampus, the fronto-parietal network, and the prefrontal lobe. Therefore, working memory function is also very sensitive to variations in human neurological function. Stress state, mental disorders, neurological diseases and degenerative diseases will also cause obvious defects in working memory function of human beings.

For the measurement of working memory, typical task paradigms include N-back paradigm, proactive interference paradigm, etc. Here, we choose N-back paradigm, its general flows are as follows: A random sequence of letters is presented at constant speed (e.g. one/second), one letter is presented each time; the subjects need to judge whether the current letter is the same as the Nth letter presented retrospectively, and if they are the same, they need to press the button immediately. Obviously, the larger the N, the higher the requirements for working memory ability and the higher the task difficulty.

5 Time Perception

Time perception is the reaction of individual to the continuity and sequence of objective things, and it is a basic cognitive function that plays an important role in evolution. Humans are able to perceive the length of time without resorting to a time scale, relying only on their own proprioception (internal clock level). In some operational tasks that require high time accuracy, it is crucial for the operator to accurately estimate and control the duration and judge the timing.

There are four main task paradigms for studying time perception:

(1) Time discrimination

The subjects were presented with two time intervals and asked which time interval was longer (or shorter).

(2) Time generation

Inform the subjects for a specified period of time (such as 10 s), and let the subjects subjectively estimate and express this objective number.

(3) Verbal estimation

In contrast to time generation, subjects are presented with a stimulus that lasts for a period of time (e.g. using visual, auditory, or tactile stimuli, etc.), and then ask the subject to verbally estimate the duration of this period of time.

(4) Time reproduction

The subjects are presented with a stimulus that lasts for a certain period of time, and then the subjects are asked to reproduce the duration subjectively.

The time perception of human being fundamentally depends on the level of its internal clock, but the processing of time information cannot be free from the influence of external factors and the constraints of specific tasks. Among the above methods, the time reproduction task is least affected by the level of the internal clock of the subjects, and more reflects the attention and working memory of the subjects. Therefore, the time reproduction method is adopted in this paper.

Studies have shown that people's time perception is significantly affected by factors such as attentional state, emotional state, personality traits, etc. In the study of time reproduction method, the duration of stimuli reproduced by patients with anxiety disorders is often short, while the opposite is true for patients with depressive disorders. Therefore, the time perception measured by the time reproduction method can also be used as an effective evaluation index of cognitive state.

6 Spatial Perception

Spatial perception ability reflects the subject's ability to recognize, identify and compare objects in space, as well as the spatial imagination ability to perform various transformations of objects in the mind, such as folding, rotating, etc. In engineering practice, if the operator cannot correctly perceive and judge the spatial relationship, human error may occur in the operation, which will damage the safety of operation. Especially in the operation tasks that need to be completed by observing the space indicating instrument, the operator must have the ability to correctly map the actual object position in the three-dimensional space to the space indicating instrument in the mind, which requires the operator to have strong spatial representation processing and psychological rotation ability.

Mental rotation is a classic paradigm in the study of spatial perception and spatial representation. It can be traced back to the research conducted by American psychologist Shepard in the 1970s. Its task was to present a pair of two-dimensional or three-dimensional graphics at random directions to the subjects, and the subjects were asked to judge whether the pair of graphics could coincide with each other after being rotated.

As shown in Fig. 1, the two sets of building blocks in the first and second columns can be overlapped after being rotated, while the two sets of building blocks in the third column are mirror-symmetrical after being rotated, so they cannot be overlapped.

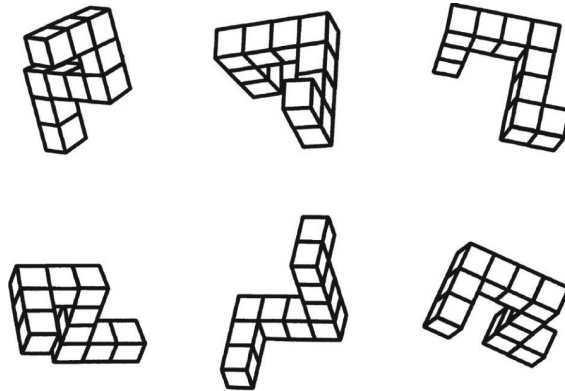


Fig. 1. A typical mental rotation task

Studies have shown that fatigue, stress, and mood changes can significantly affect the performance of mental rotation tasks. For example, the mental rotation ability of drivers in fatigue state is significantly reduced; acute stress state is helpful for mental rotation task, while chronic stress state impairs the processing of mental rotation task.

7 Operation Stability

Operation stability mainly reflects the ability of the operator to control the operator when performing a certain action, especially a relatively fine operation action. Many realistic operation tasks require high accuracy and stability for the operation of operators, such as positioning operations with small targets, rendezvous and docking, or remote control operations. Although operation stability is ostensibly an action indicator, it measures not only motor control functions, but also eye-hand coordination and attention state, which also reflect neural functions. In the state of tension, fatigue or stress, the body often suffers from distracted attention, impairment of limb coordination, abnormal completion of fine movements and misoperation. Some nerve damage or diseases can also lead to unstable movements and tremors.

Considering the special test situation involved in this paper, it is proposed to use some kind of ship simulation maneuvering task to examine the operational stability of the subjects, and let the subjects complete the operation tasks with the joystick, so as to increase the realism of the task and improve the involving degree of the subjects.

8 Conclusion

By reviewing the existing neurobehavioral testing tools, combined with the actual testing situation of this paper, a set of job ability indicator systems is screened to evaluate different cognitive states, including a total of 8 tests, as shown in Table 1:

Table 1. Test tasks and corresponding cognitive functions

Task paradigm	Cognitive function
Simple detection task	Simple reaction time
Recognition task	Recognition reaction time
Selective response task	Choice reaction time
Simple detection task	Attention stability
N-back task	Working memory
Time repetition task	Time perception
Mental rotation task	Spatial perception
Simulated operation task	Operation stability

This set of task indicator system can better recognize abnormal states of various basic cognitive abilities under the influence of emotion, fatigue, stress, mental or neurological diseases, thereby helping operators reduce human errors, improve operation safety and performance.

Acknowledgement. This work is supported by the Innovation Zone Project, No.20AH0702.

References

1. Strangman, G.E., Sipes, W., Beven, G.: Human cognitive performance in spaceflight and analogue environments. *Aviat. Space Environ. Med.* **85**(10), 1033–1048 (2014)
2. Rosli, R., Tan, M.P., Gray, W.K., Subramanian, P., Chin, A.V.: Cognitive assessment tools in Asia: A systematic review. *Int. Psychogeriatr.* **28**(2), 189–210 (2015)
3. Zongshan, L.I., Lili, W.E.I., Yaxing, G.U.I., Wei, C.H.E.N.: Development and application progress of cognitive assessment scales. *Chin J Contemp Neurol Neurosurg* **21**(11), 927–933 (2021)
4. Tu, Z., Li, H., He, J., Zhao, H., Qu, J., Shen, X.: Exploration of standardized neurocognitive test battery for personnel in military isolated and confined environments. *Acad. J. Second Mil. Univ.* **41**(06), 673–679 (2020)
5. Paul, D.B., Minjeong, J.: An overview of models for response times and processes in cognitive tests. *Front. Psychol.* **10**, 1–11 (2019)



Research on the Evaluation of Abnormal Cognitive Status of Workers in Confined Spaces

Chuan Wang¹, Qianxiang Zhou², Xiaojun Wang³, and Ziyang Wang¹(✉)

¹ Naval Medical Center of PLA, Naval Medical University, Second Military Medical University, Shanghai 200433, China

wangziyangwzy@sina.com

² School of Biological Science and Medical Engineering, Beihang University, Beijing 100191, China

³ Naval Equipment Department, Beijing 100089, China

Abstract. The operating environment in the confined space is harsh, and the long-term continuous operation leads to the depression of the operator and the decline of cognitive ability, thus affecting the operation performance and operation safety. In order for the operator to receive, transmit and execute instructions normally, cooperate as a team, and thus complete the operational tasks he is responsible for, the cognitive state of the operator, such as perception, attention, memory function, etc., is indispensable. The identification of abnormal cognitive state of operators has always been an important subject in the field of ergonomics and human factors engineering, which involves the integration of multiple fields of physiology, psychology, neuroscience and behavioral science. According to the actual situation of workers in confined spaces, this paper explores the evaluation methods of abnormal cognitive state from two levels of neurobehavioral core test and computerized neurobehavioral evaluation, and provides reasonable suggestions for cognitive state testing tools for workers in specific environments and specific positions. The research results provide theoretical guidance for the evaluation of cognitive abnormalities of operators in confined spaces, and have practical significance for the evaluation of operators' operational ability and the prevention of human errors.

Keywords: Confined space · Operator · Cognitive state · Abnormal recognition

Preface

With increasing public awareness of brain health, the people with unimpaired cognitive function are increasingly worrying that their cognitive function has weakened [1]. Mild cognitive impairment is a core feature of many mental disorders [2]. The feasibility of implementing comprehensive nerve psychotherapy is in the scanner, and the brain activation pattern of specific task improves the predictive ability of demographic information [3]. The results of many brain science experiments show that cognitive training can improve brain function and reduce attention deficit and other diseases of brain [4]. The abnormal cognitive states of operators in confined spaces are caused by two factors: On the one hand, there are external causes, namely, long-term exposure to more special or worse working environments, such as extreme physical factors (too high or too low

temperature and humidity), hypoxia, noise, vibration, electromagnetic field, exposure to toxic and harmful environmental pollutants (including biological pollutants, chemical pollutants, radioactive substances or radiation), etc.; on the other hand, there are internal causes, which are caused by physical or mental trait of operator, such as decreased arousal, fatigue, tension or anxiety, low mood or poor mood caused by long-time or irregular work.

Immersive virtual environment is using to evaluate human response variable for design increasingly [5]. Behavioral function indexes are highly sensitive and nondestructive, which can be tested repeatedly by non-invasive methods, so they are widely used to test cognitive states.

Human basic cognitive function and work capacity are called neurobehavioral ability. Neurobehavioral ability is the ability of the central nervous system to integrate and process external information and send movement commands and is the core and basic components of cognitive function, which is used to reflect cognitive level and mental work. There are many methods for the test and evaluation of neurobehavioral ability, with representative results such as: WHO-NCTB (Neurobehavioral Core Test Battery) developed by WHO (World Health Organization), NES (Neurobehavioral Evaluation System), etc.

In this paper, the evaluation methods of abnormal cognitive state of workers in confined spaces were analyzed from two aspects of WHO-NCTB and NES, and test methods and test items were summarized, compared and researched. Finally, it recommended the tool suitable for testing abnormal cognitive state of operators in confined spaces.

1 WHO-NCTB

Emerging WHO-NCTB is inseparable from the vigorous development of chemical industry, toxicology and neuroscience and behavioral science in the 20th century. After World War II, the developed countries in Europe and America have concerned about the pathological effects of exposure to toxic chemicals in operators, successively developing toxicology psychology, behavioral toxicology, neurobehavioral toxicology and other interdisciplinary to research the functional changes and relevant behavioral effects of toxic chemicals in the environment on the human nervous system, and taking relevant control measures. With the emergence of related theories and methods, WHO organized experts to analyze the current state of neurobehavioral toxicology in 1983 in order to solve the problem of information inconsistency and lack of comparability caused by all kinds of research methods and instruments used by scholars in various countries, and developing a set of evaluation test methods for professionals on this basis, namely, WHO-NCTB.

WHO-NCTB consists of 7 sub-tests:

(1) Mood state test

Emotional state test is a profile of mood states (POMS) consisting of 65 items. Each item includes a word describing a mood state. Participants were required to select the item which was most closely matched their subjective feelings for the previous week according to Rickert Five-point Scale. 65 subjects were divided into

six type of mood attributes -- “tension - anxiety”, “gloomy - depression”, “anger and hostility”, “fatigue - inert”, “strong - active” and “panic and confused”. The score of each attribute was calculated according to the tested selection.

(2) Simple response time test

Simple response time test adopted a special response time tester, and the subject pressed the specified switch immediately to turn it off when the red lamp on the instrument was on. This required high concentration and rapid eye-hand coordination of the subject. The average value, standard deviation, maximum value and minimum value of response time of the subject were calculated.

(3) Digit span test

Digit span test was taken from WAIS (Wechsler Adult Intelligence Scale), which was aimed at measuring the subject’s attention concentration and auditory working memory function. Each time, the experimenter clearly read a digit sequence at the rate of one digit per second, and the subject repeated them immediately in order or in the reverse order according to the requirements. Each sequence contained 2–9 digits and was tested according to sequence length (or “digit span”). For each digit span, two different digit sequence were tested, as shown in Table 1. Count the number of sequences that were repeated by the subject correctly.

Table 1. Digit span test

Positive sequence		Negative sequence	
Num	Test sequence	Num	Test sequence
1	5-8-2	1	2-4
	6-9-4		5-8
2	6-4-3-9	2	6-2-9
	7-2-8-6		4-1-5
3	4-2-7-3-1	3	3-2-7-9
	7-5-8-3-6		4-9-6-8
4	6-1-9-4-7-3	4	1-5-2-8-6
	3-9-2-4-8-7		6-1-8-4-3
5	5-9-1-7-4-2-8	5	5-3-9-4-1-8
	4-1-7-9-3-8-6		7-2-4-8-5-6
6	5-8-1-9-2-6-4-7	6	8-1-2-9-3-6-5
	3-8-2-9-5-1-7-4		4-7-3-9-1-2-8
7	2-7-5-8-6-2-5-8-4	7	9-4-3-7-6-2-5-8
	7-1-3-9-4-2-5-6-8		7-2-8-1-9-6-5-3

(4) Hand agility test

Hand agility test is also known as portable agility test, Santa Ana hand agility test, which is aimed at measuring eye-hand coordination and operation agility. This test adopted a wood board with 48 holes, each hole was embedded with a wooden plug of a round top and a square bottom. The surface of wooden plug was painted in black and white, as shown in Fig. 1. The subject was required to pull out each wooden plug in turn through using strong hand and weak hand respectively within 30 s as fast as possible, and to rotate it 180°, so that two colors on the surface of wooden plug were reversed and inserted into the hole. Keep the scores according to the number of wooden plugs correctly operated by each hand within the required time.

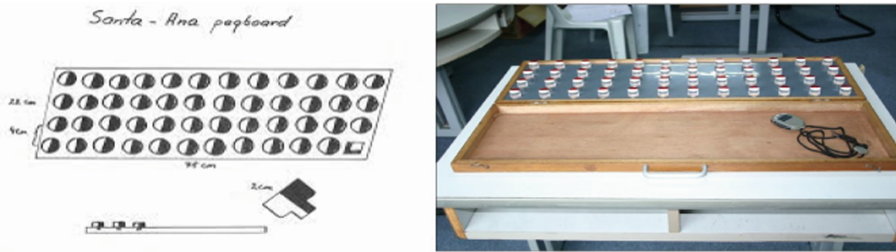


Fig. 1. Equipment used for hand agility tests

(5) Digit coding test

Digit coding test is taken from Wechsler Adult Intelligence Scale, which is mainly used to measure visual discrimination, memory and learning ability. Each digit from 1 to 9 was matched with a meaningless symbol as a code. After reading digits and codes for 20 s, the subject filled in a series of sample digits for 20 s, and filling in the corresponding symbol in the space below each digit (namely, “decode”); then filling in the formal test form and decode each digit as fast as possible, with a total of 90 s. Keep the scores according to the correct number of symbols decoded within the required time.

(6) Visual memory retention test

Visual memory retention test is also known as Benton visual retention test, which is mainly used to measure the subject’s visual discrimination and working memory function. This test adopted 10 sets of pictures. The first picture in each set consisted of a number of simple geometric figures. The second picture contained 4 small pictures, one was consistent with the first picture, and the other three pictures were similar but slightly different, as shown in Fig. 2. In each set of tests, the subject looked at the first picture for 10 s to remember the above picture, and then looked at the second picture for 10 s to point out which of small pictures is exactly the same as the first picture. Keep the scores according to the number of pictures correctly identified by the subject.

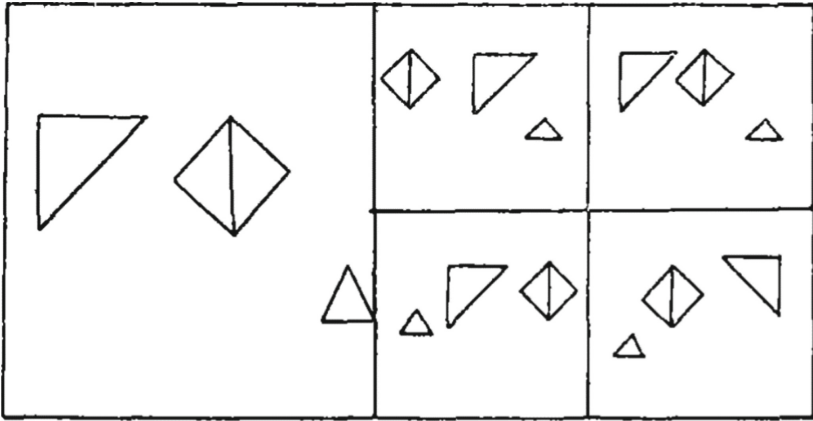


Fig. 2. Example of pictures used for visual memory retention tests

(7) Target pursuit test

This test is mainly used to measure the speed and precision of the subject's hand movements. The paper had a number of small circles, on which line feeds were arranged like S; the subject was required to make dots with a pencil in the center of each circle as fast as possible within 60 s. Draw dots should be visible, but not touch the edge of circle. Test twice, and then calculate the total number of correct dots, the total number of wrong dots, and the total number of dots in two tests.

In the above seven sub-tests, the rest of sub-tests were completed with paper and pen and scored manually, except for the special equipment used in response time test and hand agility test. With technical progress, these sub-tests can be integrated into a computer and judged and scored automatically by the system.

The neurobehavioral core test was originally used in toxicology research, but the later research has shown that the contents of these tests are highly sensitive to changes in neural function, so it is used in the clinical evaluation of nerve injury and rehabilitation.

2 Neurobehavioral Evaluation System (NES)

In order to overcome the shortcomings of neurobehavioral core tests, further reduce human influence and improve the degree of objectivity and stability of the test, the U.S. scientists have developed NES in the 1980s to make neurobehavioral test more programmed, standardized and automated. On this basis, Chinese scholars first developed a Chinese edition of NES (NES-C1) in 1988. Since then, the system has been modified and updated to the fourth Chinese edition (NES-C4). Taking the third edition of NES-C3, test items are divided into 5 categories, each category contains 2-7 sub-test items, with a total of 21 sub-test items:

(1) Mood

It mainly includes: ① Mood state scale, ② semi-structure projection test;

(2) Intelligence

It mainly includes: ① Mental arithmetic, ② series addition and subtraction;

(3) Learning and memory

It mainly includes: ① Visual retention, ② Twin words association, ③ Memory scanning, ④ Continuous recognition memory;

(4) Perception

It mainly includes: ① digital retrieval, ② symbol decoding, ③ line judgment, ④ attention transfer, ⑤ digit span, ⑥ stereoscopic vision;

(5) Psychological movement

It mainly includes: ① Simple visual response time, ② simple listening response time, ③ complex visual response time, ④ curve matching, ⑤ target tracking, ⑥ continuous operation, ⑦ digital filtering.

The above categories have reflected a certain type of neurobehavioral ability function respectively, and each sub-test item has tested human neurobehavioral function from different angles. In addition, the analysis of results has also shifted from calculating the original rough score to a more accurate and detailed scientific statistical index -- Neurobehavioral Ability Index (NAI).

The above two measuring tools are widely used in military medicine, marine medicine, aerospace medicine and other special medical fields by Chinese scholars, such as: health evaluation and competency selection of sailor, pilot, plateau soldier, aircrew, operator of communications force, etc.

In addition, national researchers have developed many neurobehavioral test tools, such as: CANT (Cambridge Neuropsychological Test Automated Battery), NCSE (Neurobehavioral Cognitive Status Examination), AENTB (Adult Environmental Neurobehavioral Test Battery), etc., which have been widely used in toxicology, pharmacology, psychology and clinical research, and used to evaluate the neurobehavioral state of people. The specific test items of measurement tools are different, but the basic function modules have many common points, namely, sensory perception, learning and memory, comprehensive ability, athletic ability, etc.

3 Conclusion

According to the above features of current tools, and considering that the cognitive test of the operators in confined spaces isn't a general screening test with strong commonality, but is used in the operators in a specific environment and in a specific position, and considering that the resources of professional testers and test equipment are limited in test situations, it is necessary to pay attention to the following points when selecting indexes and organizing behavioral test tools for abnormal cognitive status:

- (1) Operation is easy and simple, and can be completely by the subject independently after a simple explanation. There is no need for complex testing procedures and instruments;
- (2) Test contents are easy to be understand and accept, and are less affected by cultural difference;
- (3) Full consider the sensitivity, reliability and validity of indexes;

- (4) Total test time shall not be too long lest the subject feels tired and affects the test results;
- (5) Sub-test items reflect the basic neurobehavioral function, which is used to look at possible future intervention means in addition to evaluating the cognitive status of subjects.
- (6) It is recommended that the cognitive test items consist of 13 items, including mood state scale, visual retention, memory scanning, continuous recognition memory, digital retrieval, symbol coding, switching attention, simple visual response time, simple auditory response time, complex visual response time, target tracking, continuous operation, and digital filtering.

Acknowledgement. This work is supported by the Innovation Zone Project, No. 20AH0704.

References

1. Jessen, F., et al.: The characterisation of subjective cognitive decline. *Lancet Neurol.* **19**(3), 271–278 (2020)
2. Zhong, N., Zhao, M.: The cogstate computerized cognitive battery and its usability. *Psychol. Commun.* **2**(01), 67–70 (2019)
3. Roalf, D.R., et al.: Neuroimaging predictors of cognitive performance across a standardized neurocognitive battery. *Neuropsychology* **28**(2), 161–176 (2014)
4. Hu, Y.: Research and development of cognitive ability detection and training system. University of Chinese Academy of Sciences (Shenzhen Institutes of Advanced Technology, Chinese Academy of Sciences) (2020)
5. Kalantari, S., Rounds, J.D., Kan, J., Tripathi, V., Cruz-Garza, J.G.: Comparing physiological responses during cognitive tests in virtual environments vs. in identical real-world environments. *Sci. Rep.* **11**(1), 10027 (2021)

Research on the Machine-Environment Relationship



Analysis on Loitering Attack Missile Application in Nagorno-Karabakh Conflict

Lingpeng Kong, Heyuan Hao^(✉), and Lin Liu

Zhengzhou Campus, Army Academy of Artillery and Air
Defense Zhengzhou, Zhengzhou 450052, He Nan, China
13592517010@139.com

Abstract. In the Nagorno-Karabakh conflict, “Harop” as the representative of the loitering attack missile record is not bad, the precision strike effect is prominent. This paper briefly introduces the situation of the loitering attack missile used by Azerbaijan in the Nagorno-Karabakh conflict, analyzes the performance characteristics of the loitering attack missile and discusses the impact of the loitering attack missile on Armenia from the aspects of detection and identification, tracking and strike, survival and protection, and analyzes the reasons for the failure of Armenia in fighting the loitering attack missile from the aspects of air defense system, air defense strength and electronic warfare.

Keywords: Nagorno-Karabakh conflict · Loitering attack missile · Man-in-the-loop(MIL)

In Nagorno-karabakh conflict, Azerbaijan defense department issued a “Harop” loitering attack missile/suicide drone (also known as “Hubby - 2” unmanned aerial vehicle (UAV) or cruise missile) precision attack Armenia the ground target video, especially the destruction of S-300PS-the long-range air defense and missile defense system. It has drawn high attention from all of the world. Loitering attack missile has been widely used in the Nagorno-Karabakh conflict and achieved remarkable results, which is bound to have an important impact on air defense.

1 Brief Introduction of Azerbaijan Loitering Attack Missile

Azerbaijan’s loitering attack missile are mainly the Israeli-made “Harop” loitering attack missile and the indigenous “Iti Qovan” (tiKovan) loitering attack missile, which are mainly used to carry out point-killing precision strikes on Asian tanks, armored vehicles, artillery guns, air defense systems, vehicles, fortifications and bunkers, personnel and other effective forces.

1.1 Harop Loitering Attack Missile

The loitering attack missile, developed by Israel Aircraft Industries (IAI), is based on the Harop anti-radiation UAV, also known as Hubby-2, which was displayed at the 7th

Seoul International Aviation and Defense Exhibition (ADEX) in October 2009. The body length of “Harop” is 2.5 m [1] (The other documents is 2.06 m [2]), wingspan is about 3 m, height is about 0.5 m, full weight is about 135 kg, and the warhead weight is 32 kg. It can be launched by vehicle and 6 sortie by single vehicle. Its cruising speed is not less than 185 km/h, its dive speed can reach 48 km/h, endurance time of 6 h, and its maximum range can reach 1000 km. The combat radius is 250 km, manual control range is 150 km. It can be control by remote, and also have the independent attack capability and recyclability. It can carry out anti-radiation attack on radar, and can also carry out accurate reconnaissance and attack on other targets [1]. With stealth design and radar absorbing composite materials on the body surface, the radar echo reflection cross-sectional area is very small, and the infrared and optical characteristics are also small, so it has strong survivability.

1.2 Iti Qovan Loitering Attack Missile

The Iti Qovan is made in Azerbaijan, and can carry a payload of 1 kg–2 kg with a flight time of 2 h–3 h, a wingspan of 2.2 m, a maximum flight speed of 70 knots (126 km/h) and an operational radius of 100 km. And it can carry all-weather multi-sensor camera, also perform reconnaissance, detection, attack missions, recoverable.

In addition, several other types of loitering attack missile have been used in conflicts. For example, Israel’s Elbit Systems company’s “Sky Shooter”, size is similar as human body, weight up to 35 kg, can carry 5 kg–10 kg load, flight time of 2 h.

2 Characteristic Analysis of Loitering Attack Missile

2.1 Small Size and Strong Survival Ability

The body diameter of the loitering attack missile is generally 120 mm–330 mm, and the length is 0.5 m–1.5 m, and the larger one is generally less than 3 m. Composite materials are widely used, and stealth design is often adopted. The radar echo reflection area is small, making it difficult to be detected by radar, and infrared and optical features are reduced to improve the survival probability [3, 3]. Azerbaijan use loitering attack missile -”Harop” has the property, from the video of both the public and the results, the missiles like get into an unguarded environment. When Armenia being attacked, except very few battle field detected the enemy the others are like in the darkness. The Armenia only show few video for intercepting the kind of missile.

2.2 Long Endurance, Wide Range of Action

The cruising speed of the cruiser is generally 50 m/s, which is slow, but the body is relatively light, with long endurance and long flight range. For example, the “Iti Qovan” cruiser flies at a speed of about 35 m/s, with no less than 2 h in the air, and the flight distance can reach 100 km. The cruise speed of “Harop” missile is about 51 m/s, the dive attack speed is about 133 m/s, the hang time is no less than 6 h, the maximum range is up to 1000 km, and the combat radius is up to 250 km. Small, portable missiles such

as Israel's "Hero-20", "Skylite" and the U.S. "Switchblade" also have an operational radius longer than 10 kms. It was the Harop missile that Azerbaijan used to penetrate deep into Armenia to attack on its S-300 air defense weapon system.

2.3 Intelligent and Strong Attack Ability

Loitering attack missile is mainly divided into two types of reconnaissance and attack, the biggest difference between the two is the attack loitering attack missile increased the warhead and attack system, can be hard killing to the target. This kind cruise missile versatile, capable of carrying the photoelectric, radar, color TV camera, chemical or biological detection sensor, the meteorological instrument, non-lethal device and kill warhead. It has the target reconnaissance search and surveillance positioning, target designation, air alert, communications relay, precision attack, battle damage assessment, and other functions. It can be through the use of advanced data link and real-time intelligent processing, Provides critical situational awareness and provides Man-in-the-loop(MIL) capabilities to further enhance mission performance. For example, "Harop" loitering attack missile can fly along the designed track to the target area, hover in the air standby, attack the target or return to base. Human intervention can also be used to abort and reset tasks. The attack missile can carry out precision strike, can realize the discovery namely attack, attack namely destroy. From the public video of the Nagorno-Karabakh conflict, the "Harop" and the "Iti Qovan" loitering attack missile both accurately attack and destroyed the target, among which the s-300 air defense and anti-missile system and several SA-8 air defense missiles were be in the spotlight [5].

2.4 Low Price, High Cost-Efficiency Ratio and Flexibility

2.4.1 Low Cost and High Cost-Effectiveness Ratio

Loitering attack missile can be considered as the product of the organic combination of UAV technology and ammunition technology. Compared with cruise missile, its cost is low. For example, the Unit price of the British "Fire Shadow" loitering attack missile is about \$100,000, the U.S. WASP gun launched loitering attack missile is about \$10,000, and the "Harop" loitering attack missile is only several hundred thousand dollars. However, the efficiency and cost ratio is high. Loitering attack missile are usually used to attack high-value targets, and use one can achieve the purpose. For example, The Azerbaijan side destroyed the S-300PS long-range air defense and missile defense system [6] and SA-8 system with the "Harop" loitering attack missile.

2.4.2 The Launch Mode is Flexible and Varied

Some lunched by vehicle, such as the "Harop" used by Azerbaijan; Some are launched by small launchers, such as Azerbaijan's "Iti Qovan" cruiser; Some are launched by barrel artillery/rocket launcher, such as the American LAM loitering attack missile; Some use airborne delivery, such as the American "Air Master"; Some are launched by individual soldiers or portable launchers, such as the "Switchblade" individual soldier loitering attack missile of the US army, the "Lark" individual soldier loitering attack

missile of Israel, and the suicide UAV transformed by Armenia which can be launched from narrow alleys, Windows, rooftops or various field sites without site restrictions.

2.4.3 Operational Flexibility

Loitering attack missile has reconnaissance, monitoring, identification and positioning functions, and can change the flight path and mission independently or remotely according to battlefield conditions. It can also hover over the target area for a long time to guide fire attacks or launch suicide precision strikes. Both sides in the Nagorno-Karabakh conflict adopted this method of attack, which caused long-term threat and psychological pressure on the other side. Comparatively speaking, the Azerbaijan side is more superior because of its loitering attack missile performance and number advantage.

3 The Impact of the Loitering Attack Missile on Armenia

From the perspective of the Nagorno-Karabakh conflict, the cooperation of loitering attack missile and UAV caused great losses to Armenia whose tanks, rocket launchers, armored vehicles and even air defense systems were attacked by loitering attack missiles. In addition to the limited air defense capability of Armenia, which can not effectively deal with such targets as cruiser, the characteristics of the loitering attack missile making it a difficult problem to defense.

3.1 Difficult to Identify

The first problem to be solved is detection. However, as described in 2.1, RCS is small and some use stealth technology, so radar detection is very difficult. Loitering attack missile also applies a lot of infrared stealth technology, infrared characteristics are reduced, the difficulty of infrared detection is increased, through infrared detection to find the target distance is greatly shortened. With the decrease of RCS and infrared features, visual features become an important direction for detection. However, in complex battlefield conditions, the size of loitering attack missile is relatively small, with a wingspan of 1016 mm–1700 mm, so it is difficult to find it by visual or optical equipment. The video issued by Azerbaijan's in this conflict also shows that the target defections probability is low, not to mention an effective intercept.

3.2 Target Tracking Difficulty

The flying altitude of the missile is generally 100 m–1000 m, the flying speed is 35 m/s–100 m/s, which is a typical “low-slow-small” target. The radar echo is very weak, so it is difficult to lock and track stably. At the same time, it is often accompanied by the close interference and decoy of UAV, which can effectively interfere with the other side's air defense radar, combat communication and combat command equipment, paralyze the enemy's “eyes” and communication, making tracking more difficult. In the public video of the conflict, the radars of several Armenia air defense weapon systems were destroyed while working. One possibility is that the target was not found, and the other possibility is that although the target was found, it could not be locked and tracked effectively.

3.3 Fire Attack Difficult

Attack cruisers can strike at any time after finding sensitive targets, shortening the completion time of the kill chain, making the preparation time of Armenia's ground air defense system too short to fire in the air. Loitering attack missile in the flight process, can be controlled by the operator "MIL" in real time, can use the way of image and information transmission, through remote control or pre-installed flight path, to control the flight state of the missile, or change the target of the loitering attack missile. The flexible change of target increases the accuracy of threat judgment of Asian air defense system and the difficulty of air defense firepower attack.

4 Analysis on the Main Reasons of Armenia's Failure in Fighting Loitering Attack Missile

4.1 Air Defense is not Systematic

In this conflict, the reason why The Armenia side was helpless in the face of the Azerbaijan loitering attack missile is that the various services and arms have not formed a systematic ability to fight on their own, and even the field air defense forces are not systematic. Armenia seriously lacks effective air surveillance system, especially in the mountainous and hilly terrain of Nagorno-Karabakh region, where the field air defense situational awareness system is covered by the terrain, and there are no early warning aircraft, mobile radar stations and other supplementary situational awareness units, so it has no sense of the movements of Azerbaijan UAVs. The field air defense system is not suitable to undertake the current field air defense mission because of its backward performance and firepower collocation.

4.2 Air Defense is Weak and Backward

Armenia's main air defense forces include SA-8, SA-13, SA-15, ZSU-23-4, SU-23-2, etc. They are mainly manufactured by the former Soviet Union in the 1970s and 1980s, with relatively backward performance and insufficient quantity. The relatively advanced S-300 air defense weapon system is not mainly used to fight against targets such as loitering attack missile. The s-300 system was destroyed by the Harop missile. Moreover, in recent years, compared with Azerbaijan, the defense budget of Armenia is less than a quarter of that of Azerbaijan, the national defense construction is relatively lagging behind, and the update of air defense weapon system is almost stagnant. Using such air defense equipment to deal with Afghanistan's relatively advanced and sufficient number of loitering attack missiles, the outcome can be imagined.

4.3 Electronic Warfare Systems are Performing Poorly

Repellent-1, a Russian-made anti-UAV electronic warfare system, will be able to suppress unmanned systems such as loitering attack missile, but its electronic warfare effects are surprisingly limited. In the early days of the Nagorno-Kabakh conflict, The

Repellent-1 anti-UAV electronic warfare system of Armenia was destroyed in a raid by Azerbaijan's missile, indicating the weakness of Armenia's electronic warfare capability. The success of Azerbaijan's loitering attack missile and other unmanned systems is directly related to Armenia's lack of electronic warfare capabilities and limited role.

References

1. Wen, J.: Improved design and Operational Use of "Harop" loitering attack missiles UAV. *Unmanned Aerial Vehicle (UAV)* **5**, 12–13 (2016)
2. Zhang, G.Y.: The son of "Habi" – Israel "Harop" anti-radiation UAV. *China Air Force* **12**, 72–73 (2015)
3. Loitering attack missiles-baidu encyclopedia (entry), 19 October 2020. [https://baike.baidu.com/item/cruise missile](https://baike.baidu.com/item/cruise_missile)
4. Liang, H., Shanzeng, Y., Yintao, Z.: Research on combat method of anti-loitering attack missiles. *Sci. Technol. Inform.* **33**, 40–74 (2010)
5. Loitering attack missiles in the Nagorno-Karabakh conflict are UAV or not? ? Drones heroes list (WeChat public no.), 19 October 2020. https://mp.weixin.qq.com/s/YxNwddUfyc_m6L3TIMJzmQ
6. She, H.: UAV confrontation in Nagorno-Karabakh conflict. *China Defense News* (04), 20 October 2020



Research on UAV Swarm Operations

Lingpeng Kong, Zaochen Liu, Li Pang, and Ke Zhang(✉)

Zhengzhou Campus, Army Academy of Artillery and Air Defense, Zhengzhou 450052, China

13674920330@139.com

Abstract. In recent years, UAV swarm technology has become more and more mature, it has been a kind of newly-typed operations to conduct air strike by applying UAV swarms, and UAV swarm operations are leading the developmental trend of combat mode all over the world with the rapid development of artificial intelligence and big data. Combined with the concept on UAV swarms, This paper analyzes the advantages and disadvantages of UAV swarm operations. From the two aspects of information war and offensive war it discusses the main combat means and actions of UAV swarms centering on electronic warfare, cyber warfare, psychological warfare, formation attack and collaborative operations. It has a certain reference and significance for further analyzing counter-UAV swarm operations.

Keywords: Intellectualization · Countermeasure · UAV · Swarm · Air defense

In 2018, the Russian military base in Syria was attacked by the militants through a formation of 13 UAVs. Although the Russian garrison air defense forces responded in time and destroyed the enemy's offensive plan, the formation UAV offensive operations have attracted extensive attention in the military field, and the UAV swarms are developing into a new offensive means and constantly being applied. At present, all countries around the world focus on intelligent UAVs and UAV swarm tactics in order to maximize the war benefits. Through intelligent control, UAVs can complete combat tasks such as attacking, spying and reconnaissance with resort to the advantage of its smaller size and lighter weight. With the emergence of various forms of war such as air and space integrated warfare, Cyber Warfare and public opinion warfare, the main body of war and battlefield space are constantly changed by science and technology, and the operations of intelligent formation UAVs are also developing into the mode of swarm operations. From the perspective of practical application, through employment of systematic module UAVs can complete different tasks such as decapitation action on the battlefield, information data transmission, battlefield environment detection under the circumstance of carrying various weapons, equipment and high-tech apparatus. The UAV Swarm operations are to decompose the complex system into an integrated, replaceable, universal and single module through the innovation of information data link, and then configure it on the UAVs according to the actual combat requirements. The whole UAV swarms form a complete combat system through the central control terminal, that is the data chain with closed-loop information based on reconnaissance, control, strike and evaluation. Compared with individual UAV or formation UAVs it is more flexible and changeable.

1 Concept on UAV Swarm

UAV swarm technology imitates the bee flying mode in nature, connects a single UAV through the information system, and establishes a data link to complete the information transmission between a single individual and the central control terminal so as to realize the real-time processing of information and facilitate the strategic decision-making of the central control terminal. After receiving the instruction, the UAV swarms carry out task configuration, internal combination and implementation action. Finally, the original conception and purpose of swarm UAVs are realized. UAV swarm information sources and data fusion are also diversified. For example, the operator scouts the information with resort to scientific and technological means such as satellite reconnaissance and radar detection, and then transmits it into the system, develops the maximum efficiency of the data link finally [1].

2 The Characteristics of UAV Swarm

2.1 Advantages of UAV Swarm

2.1.1 Lower Combat Cost

When UAVs are developed in various countries, they are basically made of light-weight composite materials, which makes the cost of most UAVs remain at about thousands of dollars. Compared with air defense weapons like missiles, the manufacturing cost is much lower [2], which can reduce the comprehensive cost compared with other combat modes. At the same time, with the continuous innovation of UAV swarm carrier platform, the UAVs can be transported either by large-sized military transport vehicles on land, or by warships on the sea or by transport aircraft in the air, and then they are put into operations in a given area. Hundreds of micro UAVs can be transported at one time, they are grouped to swarms further, and then they complete their combat tasks respectively, which greatly reduces their transportation cost.

2.1.2 More Possible Combat Victory

In modern war, the quality of weapons and equipment is important, but the quantitative advantage can also play an important role. According to the actual combat cases in recent years, the combat swarms composed of UAVs can even penetrate the enemy defensive system under certain circumstances, and can develop great advantages in the three-dimensional battlefield of land, sea and air, the swarms composed of micro UAVs perfectly show their role as a “scout” with their unique concealment ability and flexible maneuverability. They are effective means to realize strategic reconnaissance and information acquisition. If they carry miniature and large equivalent bombs to conduct suicide operations, they can also achieve great combat effectiveness; if a swarm is grouped by large or medium-sized UAVs, it will be more available for the operations of the front battlefield, and destroy enemy’s confidence on the battlefield by applying battlefield advantages. The great superiority of swarm operations on the battlefield is that there is a quantitative advantage over the enemy on the increasing UAV targets stroke by the enemy, so that the enemy’s firepower is saturated and ultimately it is difficult for the enemy to conduct effective defense.

2.1.3 Much Higher Systematic Survivability

At present, the UAV swarms studied in various countries are becoming more miniaturized and intelligentized, thus the radar cross section of the UAV swarms is becoming much smaller. Even if the enemy radar system is fully turned on, it is difficult to detect the UAV swarms in the distant sky. In addition, the UAVs are characteristic of “dynamic centrality”, so it can not induce the enemy detection system to focus on striking a focal point of the body, thereby it reduces the possibility of being found and destroyed. Similarly, according to the design and application of swarm operations, the individuals within the swarm can autonomously cooperate with each other, and any task can also be dynamically allocated. Even if a few individuals are damaged, their own tasks can still be allocated to other individuals, which can make the individuals support with each other so as to ensure that military tasks are re-executed.

2.1.4 Much Higher Combat Efficiency

In the Syria war, 145 of the 397 air strikes conducted by the US military were completed by UAV formations, and achieved great combat effectiveness. It can be seen that the technical application of UAV formations has become much more mature, which provides more valuable reference for UAV swarm operations. Such a new combat mode with strong interaction, autonomy and flexibility is widely accepted by all countries under the increasingly complex modern battlefield environment. After the internal combination of UAV swarms, each performs its own functions, and ensures the overall combat capability. Compared with other combat means, the advantages of fire strike, information acquisition and enduring operations are becoming more prominent.

2.2 Disadvantage of UAV Swarm

2.2.1 Control Program is Fixed and Rapid Reaction Capability Declines

The UAV swarms are controlled by the system in flight and instructions are sent with resort to satellite signals and data links by inserting programs in advance, its flight path is relatively fixed. The current information technology and processor technology are not enough to realize the *adaptability* of the battlefield, which means that UAVs can not handle the emergent situation of war, Or effectively prevent the risk. Even if the ground control station can operate and control the UAVs, however, the information and data transmission of the whole war can not be *timely* in the case of much longer distance, which makes perception capability of the control station to the battlefield weak and the reaction time lags. Moreover, after loading various weapons and equipment or special ammunition, the flight weight of UAVs will increase, the enduring capability will also decrease, and the speed and maneuverability thereby will go down, which greatly reduces the actual combat significance of UAV swarms.

2.2.2 Information Link is Open and Stability Goes Down

The UAV swarm relies on the ground control station or the maritime control center to send flight instructions. The internal individuals send signals, flight status information

and transmit reconnaissance information to the center through the data link so as to complete the information interaction. All information and data are transmitted through the electromagnetic wave in the air, however, the internal communication system of the UAV swarms are a fully open one, thus it is easily subject to complex electromagnetic environment. In the process of electronic countermeasures, if the enemy conduct jamming against the satellite positioning signals of our ground control station or sea-based platform, this will seriously affect the flight stability of the UAV swarms and it will become a *blind man* on the battlefield. In addition, the shortage of network communication bandwidth is also a problem faced by swarm operations. During information interaction, there are multiple *parallel data packets* on the transmission line, and the detection equipment generates a large amount of repeated information to result in congestion of network links, which reduces the stability of the system.

2.2.3 Space Density is Expanded and *Obesity Targets* Are Easily Exposed

While the UAV swarms take advantage of the quantity to achieve operational superiority, the large quantity and high density have also become a major disadvantage of the UAV swarm attack. When entering the air defense area in the form of the UAV swarms, the whole swarm is exposed under the enemy's firepower and is easy to be destroyed. At the same time, the radar signal generated by the individual UAV during flight is very weak, which is not easy to attract the *attention* of the enemy. However, when a swarm enters the enemy's air defense area, the radar signal overlaps continuously, which increases the possibility of being detected, and it is easy to be intercepted and destroyed by the enemy air defense fire network.

3 The Main Combat Application of UAV Swarm

3.1 Information Warfare

3.1.1 Electronic Warfare

Electronic warfare is that the countermeasure scheme is formulated, and countering electronic equipment is carried by the UAV swarms to conduct anti-electronic reconnaissance, jamming and destruction in the light of the performance and characteristics of the enemy targets. At the same time, it is also possible to conduct strike with graphite bombs and shock wave bombs. With the continuous optimization of the whole combat strength, the air power of various countries are continuously strengthened, and the corresponding air defense system is becoming more and more rigorous. Under such circumstances, it is possible to cause huge losses if manned fighters or bombers penetrate the territorial airspace of the enemy. However, if the low-cost UAV swarms can be applied to penetrate the enemy's air defense system and jam their radar detection and optical infrared detection capabilities, if weapons carried by the UAV swarms can destroy their key targets and further weaken their combat capabilities, then our effective attack and survivability will be guaranteed in actual combat.

3.1.2 Cyber Warfare

Cyber warfare is a kind of combat mode that combines scientific and technological means with cyber system to strike the enemy's network communication. It is the characteristics of fast transmission, great efficiency and large damage. After this combat mode is combined with the UAV swarms, it overcomes the limitation of information transmission and can enter the target field to conduct strike. The US special operations command studies how to make use of micro UAV groups to launch a propaganda war, which is to turn UAVs into pseudo base stations and enter the enemy's air defense area to release a large amount of information for paralyzing the enemy's communication. In the meantime, it can also spread propaganda information to various electronic product interfaces through base stations so as to achieve the purpose of subduing the enemy without fighting. The war in the field of network has always been a kind of *invisible* one, and It is also the key research direction of various countries for the UAV swarms to break the limitation of cyber warfare.

3.1.3 Psychological Warfare

Psychological warfare has been a unique means on the battlefield since ancient times. Once being successfully applied, it will inevitably bring unexpected gains. In modern battlefield, the UAV swarms conduct multi-frequency and high-intensity fire strike against the enemy at interval, disturb their normal rest and demoralize them, and directly affect the decision-making organization so that they can not make effective decisions. The combination of psychological operations and the UAV swarms is also under continuous research, and it is believed that it must create good stories in military history in the future.

3.2 Offensive Warfare

3.2.1 Formation Attack

When a large number of UAVs are grouped into a swarm to conduct attack, the individual UAV can be installed radar, photoelectric, infrared and other reconnaissance equipment and various types of attack ammunition on its fuselage to group a formation and enter the enemy's airspace, ultimately the UAV swarms saturate the detecting, tracking and intercepting capabilities of countering air defense and missile system of the enemy, after that, we will dispatch manned aircrafts to conduct fire attack, and finally realize the combat intention at a lower cost. In the future, the more intelligent UAV swarms can conduct task allocation by itself according to the battlefield situation, carry a variety of accurate ammunition, analyze the combat situation according to real-time intelligence, and then conduct fire strike to make the enemy difficult to deal with it.

3.2.2 Collaborative Operation

UAV swarms can be grouped together with manned aircrafts firstly. According to the needs of the mission, small UAVs undertake the front-line assaulting and scouting mission, and then in the rear manned aircrafts will command and control them, and the

manned aircrafts pilot UAV swarms carrying a large number of sensors and highly-destructive explosive to attack the complex targets with serious threat and high value in the enemy territory, at the same time the UAV swarms can also provide maneuverable cover for subsequent manned aircrafts entering the battlefield, reduce the whole combat risk and cost, and realize the strategic intention [3, 4]. In the future, they should also conduct real-time collaboration and adjust the combat action according to the changing situation so as to develop own advantages and achieve combat effectiveness.

4 Conclusions

As a kind of subversive combat mode, UAV swarm operations have greatly changed the mode of future war [5]. The developmental trends of the future is increasingly changing, either UAVs can be networked internally, or UAVs can network with manned aircrafts, or even UAVs can network with satellites and ships. Therefore, the current exploration of efficient and practical UAV swarm theory is an urgent problem to be solved. In recent years, UAVs have frequently been the pioneer in local wars all over the world and achieved unexpected results. For example, in 2019, Saudi oil facilities were raided by UAVs from Houthi rebel group, resulting in major losses [6], and 70 swarm UAVs raided Israel, which achieved great effectiveness. A series of combat cases has shown that the integrated operations of swarm UAVs has been the necessity of the development of air defense weapons. Thereby, Focusing on the development of swarm UAVs and studying its countermeasures are of great significance to china's air defense security. At the same time, based on our current equipment we can take the initiatives in the battlefield by continuously improving technology and raising UAV swarm combat level.

References

1. Li, H., Sun, H., Li, H., Wang, H.: General description of UAV swarm operations and its countermeasure on early-warning & detection. <http://zf.qjw.jw/article/2019/12/24/4522.html>. 24 Dec 2019
2. Hu, J., Chen, H., Fu, Y., Mi, D.: The present situation of UAV swarm technology and the countermeasure against counter-UAV swarms. *Aerodyn. Missile* (9), 32–36 (2020)
3. Jiao, S., Liu, J., Wang, B., Tian, W.: Exploration on counter-UAV swarm combat application. *Aerodyn. Missile* (2), 50–53 (2019)
4. Wan, H., Zhang, Y.: Research on swarm UAVs' influence against battle environment and the countermeasure technology. *Aerodyn. Missile* (4), 68–72 (2019)
5. Chen, J.: The combat characteristics of UAV swarms and the conception of the countermeasure system. *Radio Eng.* **50**(7), 586–591 (2020)
6. Liu, J., Tang, X., Wei, G., Jiao, S., Hu, Q.: UAVs' influence on future war and analysis of the countermeasures. *Aerodyn. Missile* (9), 28–31 (2020)



Analysis on the Operation of Bionic UAV in Tropical Mountain and Jungle

Jiwen Sun, Heyuan Hao^(✉), Jianfeng Li, Junlong Guo, and Tao Li

Army Academy of Artillery and Air Defense Zhengzhou (Zhengzhou Campus),
Zhengzhou 450052, Henan, China
13592517010@139.com

Abstract. In view of the tropical mountain jungle environment to the traditional combat forces in surveillance reconnaissance, ground operations, coordination command, combat support aspects of negative effects, using bionic unmanned aerial vehicle (UAV) in stealth missions, accurate battlefield awareness, reduce casualties and adapt to extreme environment and efficient implementation of combat support aspects of superior performance, the bionic UAV combined with traditional combat power, explore the methods of fighting against the threat of high-tech weapons and the specific application in combat operations, so as to provide suggestions for optimizing the operational application of bionic UAV in future battlefield operations.

Keywords: Bionic UAV · Tropical mountain jungle · Operational application

Bionic UAV is an unmanned aerial vehicle that imitates the external shape and movement principle of flying creatures in nature, and it is engaged in biological characteristics. Different from common rotor-craft and fixed wing UAV, it is mainly flapping wing type, with strong camouflage, small size and light weight. As the product of unmanned and intelligent technology development in the new era, the bionic UAV not only enriched the combat system, innovated the combat method, but also overturned the traditional thinking mode. Tropical mountain jungle environment complex, the operation movement limits, command and communication difficulties, bionic UAV has strong concealment capability so hardly be found by the enemy, which can be widely used in all kinds of tactical operation. It is easy to use in air reconnaissance, guiding, attack, safeguard actions. Exploring the cooperation and application between bionic UAV with traditional combat forces has strong reference value for future land combat operations triggered by conflicts in the South China Sea, may in the future.

1 The Main Features of Tropical Mountain Jungle Operations

1.1 Communication is Limited, Terrain is Divided and Command Coordination is Difficult

Communication command: mountains and jungles are wet, and communication equipment components are prone to damp, mildew and damage. Affected by terrain and environment, the technical performance of communication equipment is reduced, communication distance is shortened and even communication efficiency is lost, which reduces the wireless communication effect [1]. It is difficult to set up, maintain, withdraw and transfer the wire communication line.

Organizational coordination: the improvement of troop mechanization and the limitation of terrain become contradiction, which brings great difficulties to organizational coordination; It is difficult for the artillery to find suitable firing positions, and the flexibility, rapidity and striking power of fire maneuvering are obviously reduced. Infantry and tank combat formations are easily divided by gullies and valleys. It makes troops are difficult department on time and carry out the overall coordination hardly [2].

1.2 Mountain is Slope and Steep, Gully is Deep and Narrow, the Ground Action is Slow

Tropical mountain and jungle are steep and continuous, with many crags and rain-cracked gullies, with an average slope of more than 40°. The amount of road construction is large and it is not convenient to use mechanical operations. The road is built along the river and valley, rugged and narrow, mostly soil and sand pavement. The road conditions is complex like follow: many passes, dangerous road, steep slope, bend, lack of detour, rainy season muddy difficult to travel, once the collapse, debris flow or enemy implementation of engineering blasting will make the mountain collapse and block the road, the team is difficult to detour or turn around [3]. If the off-road maneuvering needs to go through the forest, cross the river, and sometimes need to cut down the trees to open the way forward, it will cause large personnel physical consumption so the maneuvering speed is also slow. It is easy to lose direction and the fire attack effect will not good even the damage assessment is difficult.

1.3 High Temperature and Rain, Venomous Insects, People Prone to Disease

Tropical mountain jungle environment dense vegetation, poisonous plants everywhere breeding, poisonous insects and wild animals. The overgrown weeds and warm and rainy environment are conducive to the proliferation of bacteria and pathogenic microorganisms, resulting in the prevalence of various diseases. Such as dysentery, malaria, hepatitis, encephalitis, cholera and all kinds of insect bite dermatitis, combined with the comprehensive fatigue, and Crotch rot, hand rot, feet rot as “Three rot”. It will cause the operational staff morale down and even a large number of non-combat reduction that severely weakened battle effectiveness. During the Vietnam War, non-combat reduction of the U.S. army achieved 9%. According to the survey conducted by the per-Kunming Military Command troops who participated in the 1979 war, the ratio of the sick and wounded reached as high as 5:1.

2 The Main Influence of Tropical Mountain and Jungle Environment on UAV

2.1 Vegetation Luxuriant, Visible Light Reconnaissance is Difficult to Identify the Target

In the tropical mountain and jungle environment, the roads are rugged, the rivers are criss-crossing, the forest is dense and the grass is deep. It is difficult for the ground teams to maneuver and carry out the ground reconnaissance. However, this special operational environment also brings difficulties to UAV aerial reconnaissance. In tropical mountain jungle environment, trees are tall, vines are interwoven and trees are abundant. The vegetation coverage rate of nearly 80% has a certain impact on thermal imaging system, radar and other reconnaissance equipment, especially on optical reconnaissance equipment, which is not convenient for aerial observation, identification, indication and reception of targets. Tropical mountain jungle environment combat, enemy ground forces action, fortification construction, firepower collocation, obstacle setting, fire position configuration that can rely on the natural environment nearby, the use of convenient equipment for rapid camouflage, target identification by UAV aerial reconnaissance be greatly increased [4].

2.2 The Rain and Fog Are Not Conducive to UAV Flight and Operation

Areas south of the Border between Yunnan and Guangxi which in rainy season is from May to October every year. The annual average rainfall is more than 2000 mm. There are often heavy showers and heavy rains. In the northeast monsoon period, there will be even cloudy light rain, which lasts for four to five days, as long as a month. Usually morning with fog, visibility is very low, it is not only conducive to visual and optical equipment observation, but also brings great difficulties to UAV control. Air in this environment is humidity. Thunderstorms cause complex natural electromagnetic environment, interference signal transmission is bigger, communication between UAV and ground control station is susceptible. It is hardly to take of when rotor and fixed-wing UAV encountered thunderstorm and strong wind weather. It can easily crash out of control in thunderstorms weather during it flying.

2.3 The High Mountain and Deep Valley Pose a Great Threat to the Survival of UAV in the Battlefield

Tropical mountain jungle terrain, steep mountain slope, vertical and horizontal gullies, enemy organization and defense often rely on mountain fortifications, using gullies, rivers and other natural obstacles to defend against danger. Tropical mountain jungle warfare, the natural environment is relatively complex. It gave drone operators greater difficulty, because of the UAV is mainly rely on the ground for over-the-horizon remote control, the operator of the battlefield awareness relies mainly on the real-time transmission of video images, this inevitably lead to operator's battlefield perception ability is abate, delay the operation reaction, ability to respond is also reduced, so it will be more easily detected by enemy detector. The enemy can set up fake targets in advance

or temporarily and carry out electronic decoys or set up air obstacles and traps in the complex terrain such as the tall mountain pomp and dense forest valley where the air route must pass through, and trap and strike the UAV, which poses a great threat to the safety of the survival of the UAV in the battlefield.

3 Application of Bionic UAV in Tropical Mountain and Jungle Warfare

The unique battlefield environment of tropical mountain and jungle combat, such as horizontal and horizontal water systems, high mountains and deep valleys, lush vegetation and many caves, restricts and affects the traditional combat forces and modes. The addition of bionic UAV is bound to significantly improve the quality and efficiency of combat.

3.1 Swarm Search Can Eliminate Deadzone of Jungle Cave

The characteristics of high vegetation coverage and numerous caves in the tropical mountain and jungle environment had a great impact on the reconnaissance operation. In the self-defense and counter-attack against Vietnam, the Vietnamese army not only used vegetation for concealment, but also broke up into a large number of parts and hid in caves to disperse guerrilla raids, causing many casualties to our army. Modern tropical mountain jungle warfare, with a large number of equipment of all kinds of small bionic UAV, take the swarm tactics, micro infrared and visible light load close up search budgeting implementation, combining with large wide-area of SAR radar reconnaissance UAVs, effectively eliminate the jungle cave corner blind area, to overcome the warfighter psychological barriers, greatly enhance surveillance monitoring efficiency [5].

3.2 Bionic UAV Can Act as a Node to Ensure Command Coordination Smoothly and Orderly

The difficulty of command coordination of tactical operations in tropical mountain and jungle environment is mainly reflected in the occlusion of terrain and vegetation, which greatly affects the VHF communication mode featuring line-of-sight communication between teams [6]. In specific combat operations, bionic birds, bionic bats and other small bionic UAVs can be equipped with communication relay modules, and assigned to each task team. In case of any situation, each task team can quickly fly the bionic UAVs to the high ground and the top of tree for concealment, and use the communication relay function in time. For the problem of poor overall communication in local areas, the bionic UAV can also be used to quickly establish AD hoc network communication to ensure internal communication in local areas, so as to effectively improve the influence of tropical mountain and jungle environment on command communication.

3.3 Break the Barrier to Clear the Explosion and Open a Path Before Position then Lead Formation Crossing the River

Tropical mountain jungle water system in length and breadth largely restricted the action of forces. The first battle against Vietnam was break through the Red River in the Western Front. In the early stage, it created conditions for the subsequent troops to cross the river by smuggling. During the period, after being discovered by the enemy, it was changed into a forced crossing. Although the battle was won in the end, but a large number of personnel were sacrificed.

In modern combat operations, it can be use the bionic birds to conduct concealed reconnaissance on river waters and the other side of the river, and then cooperate with ground artillery and suicide UAV to discharge obstacles on the surface of the fire until effectively guiding and guaranteeing the safe crossing of the river for the subsequent task teams.

In the attack battle of ground position, bionic UAV can also be used to clear the obstacles and minefields at the front of position, quickly open up marked paths, and greatly reduce casualties.

3.4 Man-Machine Cooperation and Efficient Implementation of Forest Combat Tasks

In the battlefield environment of mountains and jungles, it is inevitable to fight in the forest, which is summarized as: "Fight in the forest, either without meeting or face to face." Its suddenness and unpredictability are self-evident, which is why 58,000 U.S. troops were killed and 304,000 wounded in Vietnam. In tropical mountain jungle forest fight, first to "swarm" multi-dimension reconnaissance, establish local real-time accurate battlefield transparency, create information advantage for the subsequent action, and then use suicide drone to attack enemy, efficient coordination team cooperation to follow up, Capture and attack on complex key areas, so as to effectively reduce casualties in forest battles.

References

1. Zhong, G., Tian, S., Long, T.: Application of information communication in tropical mountain and jungle offensive combat. *Natl. Defense Sci. Technol.* (6) (2016)
2. Liu, J.: A study on the characteristics of mountain and forest operations. *Natl. Defense* (6), 36 (1991)
3. Zheng, S.: Research on vehicle equipment support for tropical mountain jungle combat troops. *Automot. Appl.* (5), 17 (2012)
4. Yu, G.: Research on maneuvering combat communication operation application in mountain. *Mil. Commun. Technol.* (2), 72–76 (2009)
5. Luo, B., Huang, Y., Zhou, W.: Review on the development status of anti-UAV system abroad. *Airborne Missile* (9), 24–28 (2017)
6. Han, W., Ma, Z., Qin, C.: Confrontation and development of radar detection technology. *Dual-use Technol. Prod.* (16), 6 (2016)



Energy System Simulation for Low-Altitude Solar-Powered UAVs

Dapeng Zhou^{1,2}, Yang Zhang¹, Ke Li¹(✉), Bin Zhao¹, Meixian Wang¹, Ning Wang¹, and Lijing Wang²

¹ Avic Shenyang Aircraft Design & Research Institute, Shenyang, China
like@buaa.edu.cn

² School of Aeronautical Science and Engineering, Beihang University, Beijing, China

Abstract. Due to the special energy type of solar aircraft, the endurance capability of the long-haul aircraft type is very prominent. However, the solar vehicle energy system has a significant impact on performance. This paper studies the energy system design optimization and system simulation of low-altitude solar aircraft. Firstly, an optimization method for low-altitude long-endurance UAV energy system is proposed, which fully considers the influence of date and environmental factors on energy harvesting and consumption of solar aircraft. Secondly, according to the energy optimization method, the UAV energy system is optimized, and the simulation results verify the ability and reliability of the UAV's continuous long-haul flight.

Keywords: UAV · Solar-powered · Simulation · Energy system

1 Introduction

Solar-powered unmanned aerial vehicles (UAVs) can significantly increase the flying endurance of electric vehicles [1]. Under suitable environmental conditions, a solar powered UAV collects excess solar energy during the day and stores it in the battery so that the aircraft can fly at night and use it in the following day and night cycle. This long-time capability of UAVs, especially the ability to fly for multi-days or to fly permanently, can be used in missions such as large-scale surveying, observation, or telecom relaying. These functions can be applied to search and rescue missions, industrial or agricultural inspections, meteorological investigations, border patrols, etc. [2].

At present, after many years of development, solar aircraft have formed two major categories: high-altitude large aspect ratio long-endurance aircraft and low-altitude small aspect long-endurance aircraft. The former is represented by the Zephyr [3] and the Solara [4]. Low-altitude solar aircraft are rarely developed because of more meteorological challenges. Most studies have focused on conceptual design without extensive flight experience. Noth presents the conceptual design method, realization and experimental flight results of the 3.2-m wingspan SkySailor [5]. In 2008, the solar-powered flight was completed for 27 h' continuous flight without using thermals. SoLong [6] took advantage of solar energy and at the same time searched for and used the upwelling heat flow

for a continuous flight of 48 h. However, the deliberate search for heat flow restricted the freedom of the aircraft's track and weakened the practicability [7–11].

The following sections of this article are as follows. The third part briefly describes the composition of the energy system of the solar unmanned aerial vehicle. The Sect. 4 is the design of the UAV energy system management method. The fifth part is the energy system optimization method. Studying the relationship between the important parameters of the UAV's structure provides a feasible reference for the design of solar aircraft. The sixth part is a simulation example to verify this method, and some results. The last part is some concise conclusions and discussion of follow-up work.

2 Solar UAV's Energy System Composition

Figure 1 shows the composition of the energy system. The solar cells are connected in a fixed structure, covering the given surface of the wing, or other parts of the aircraft, such as tail or fuselage. During the day, solar cells convert light energy into electricity. The Maximum Power Point Tracker (MPPT) ensures that the solar cell operates at the maximum power point [12]. The generated energy is first used to power the motor and on-board electronics, and the second is to use the remaining energy to charge the battery. At night, solar panels cannot provide energy. The energy consumed by each component is provided by the battery. Until the next day, the solar cells work again to provide energy to the system, that is a new cycle begins.

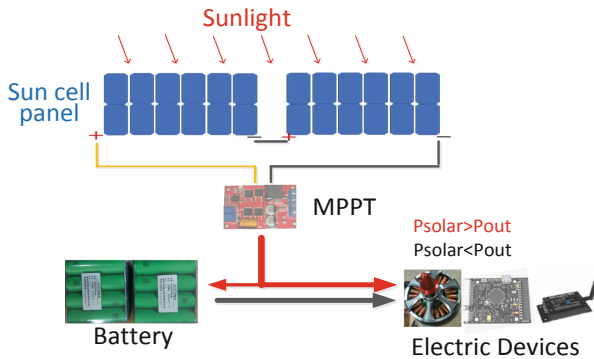


Fig. 1. Solar UAV energy system composition

Solar arrays are a key component in UAV energy systems. At the maximum power point, the available solar power is the largest, equal to $P_{max} = V_{MPPT} I_{MPPT}$. Solar cells should work exactly at this point, when the ratio between P_{max} and light intensity exactly represents the efficiency of solar cells. The current of a solar cell is proportional to its area, and it is almost linear with the change in light intensity. Temperature also affects the characteristics of solar cells. In general, considering the same irradiation conditions, solar cells can provide higher power at low temperatures [13].

Photovoltaic cells used by solar aircraft in energy systems can be classified in different ways, such as the type of material, manufacturing process, substrate, etc. [14].

The most widely used material is silicon because of its rich materials and low cost. The types of silicon solar cells for crystals [15] include: single crystals, polycrystals, etc. Compounds from Groups III to V of the periodic table can also be used to produce compound cells such as gallium arsenide, copper indium diselenide compounds, and cadmium, which have higher yield efficiency but are costlier to produce [16]. In addition, polymer solar cells and dye-sensitized solar cells made of organic materials are a promising technology and their manufacturing cost is not high [17], however, these technologies have yet to be resolved due to the instability of efficiency, and they cannot be used in industrial applications.

One of the equipment in the energy system is MPPT (Maximum Power Point Tracking), which is an upgraded new product of traditional solar charge and discharge control. By adjusting the working status (voltage, current) of the solar panel, the solar panel is always operated at the maximum power point of the V-A characteristic curve, and more solar power is output to obtain greater efficiency [18]. A considerable amount of research has been devoted to the development of more efficient and easy-to-use MPPT devices [19]. For example, studies in the literature [20] show that the MPPT efficiency can reach 0.97. Therefore, for the use of MPPT in solar-powered UAVs, the technical foundation is very mature [21].

Energy storage equipment is extremely important for solar aircraft that achieve long-endurance or permanent flight. The energy in the energy storage device is used to supply the aircraft with low solar power or sustained flight at night. Therefore, there are several important features of the equipment, stable charge-and-discharge performance, and greater energy density to minimize battery quality.

3 UAV Platform Parameter Design Method

The third part gives a detailed description of the energy system management method of solar aircraft. It can be understood that the design parameters of the aircraft are different, which will greatly affect its long-term or permanent flight performance. As shown in Fig. 2. The wingspan of an aircraft influences the solar power obtained, and the quality of the carried battery determines the energy that can be stored.

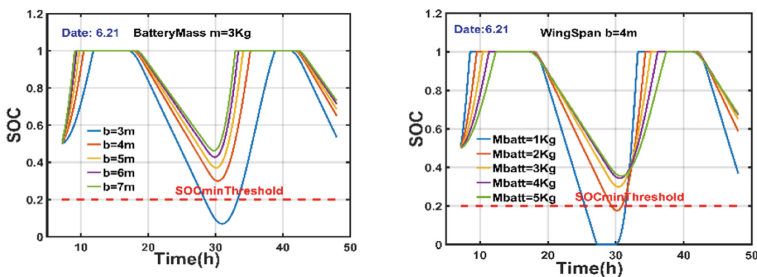


Fig. 2. Effect of aircraft wingspan (left) and battery mass (right) changes vs. SOC (Date 6.21)

According to Fig. 2 (left), when the battery quality is fixed, the wing span of the aircraft changes, the charging time of the aircraft battery, the battery full time, the flight

duration, and the SOC status value will change. The specific performance is that when the wing span of the aircraft increases, the battery charging speed gradually increases, and the time for full battery charging increases. At this point the aircraft will have the remaining power for the aircraft to climb, convert the energy into potential energy storage, and when the solar power is low, it can be used for low power gliding of the aircraft, increasing the flight time of the aircraft. At lower solar power or at night, the larger wingspan allows the aircraft to fly at lower power, so it takes longer to continue flying and the minimum SOC of the battery state of charge increases accordingly. Figure 2 (right) shows the effect of the battery quality carried by the aircraft on the permanent flight performance of the aircraft when the aircraft wingspan is fixed. The quality of the battery carried is too small, although the charging speed is faster, the stored energy is less, and it is impossible to maintain the continuous flight of the aircraft across the day and night. Therefore, it is necessary to increase the quality of the carried battery. However, as the battery quality increases, the speed of charging will also be reduced. To avoid overloading the battery, led to battery will not be fully charged, and the remaining uncharged battery will become an additional burden on the aircraft and increase the power consumption of the aircraft. Therefore, the optimization of the wingspan and battery quality of the aircraft must be carefully optimized.

4 The Method Simulation Results

According to the expansion criteria, the nominal latitude determined in this paper is 40° (N), and the test flight date is June 21. The aircraft's life time window is required to be relative to the flight date, that is, April 21st to August 21st. The battery used in this article is a high energy density lithium-ion battery, model SONY18650VTC6, 6S configuration (21 V), energy density $k_{\text{batt}} = 243 \text{ Wh/Kg}$.

Then, according to the literature, calculate the night time of the date window, $\text{Date}.6.21$, the minimum night time $\text{tnightmin} = 9.2 \text{ h}$, $\text{Date}.4.21$, and the maximum night time $\text{tnightmax} = 10.7 \text{ h}$. Thus $\text{texcDate} = 1.5 \text{ h}$. The influence of factors such as cumulus clouds in the early morning and evening on the charging process of the aircraft is selected $\text{texcWeather} = \text{tnightmax} \cdot k_{\text{ccf}} = 2.1 \text{ h}$, $k_{\text{ccf}} = 0.2$, among which k_{ccf} is the cloud layer or fog thickness factor [21]. For nighttime flight, the ambient air flow disturbances and the additional power loss caused by the model correction are chosen $\text{texcPLevel} = 0.1 \cdot \text{tnightmax} = 1.1 \text{ h}$. Therefore, the minimum surplus time $\text{texcreq} = 4.7 \text{ h}$ required to ensure that the aircraft flies during a long flight in the date window. The aircraft carries the battery quality E_{batt} , $\text{minreqk}_{\text{batt}} \approx 3.0 \text{ kg}$.

4.1 UAV Input/Output Power

Validate the performance of the energy system design method stated in the second part of the method. Keeping the model flying at a fixed altitude during the simulation can obtain the required power for the aircraft's level flight, from which the nominal output power of the aircraft can be calculated. The nominal output power can be used to calculate the battery capacity required for day-night flight on the corresponding date. Combined with the surplus time of the date, the capacity of the battery needed for the date window to

maintain a stable and continuous flight can be obtained. Simulation test aircraft model parameters, as shown in Table 1.

Table 1. Aircraft model parameters

Parameter	Value
Wingspan	5 m
Aspect ratio	13.3
Length	1.6 m
Height	0.4 m
Wing area	1.875 m ²
Total mass	6.8 kg
Battery mass	3 kg
Level velocity	8 m/s

As shown in Fig. 3, (a) is the aircraft’s leveling power at $H = 200$ m. The nominal output power is illustrated. The design requires a power of 35 W–50 W. The main factor is to consider the effect of gusts, vertical air currents on the model, and to correct the model. (b) is the solar power curve of the aircraft on the date of 6.21. In the figure, the maximum solar power, solar power changes over time.

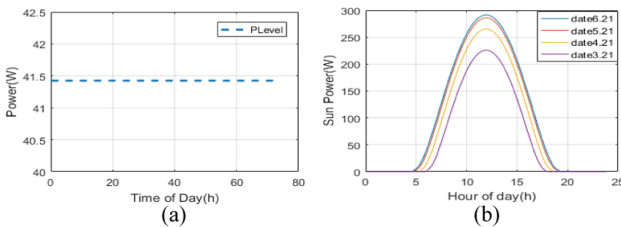


Fig. 3. Level flying power (a) and solar power (b) curves

4.2 Power Balance Simulation Test of System

The first step for a solar-powered aircraft to achieve a multi-day flight is to complete a single day-night flight. Therefore, first describe the state of the aircraft on the first day of launch. As shown in Fig. 4, it is the energy power curve of date 6.21. The solar-powered aircraft took off at 7 o’clock and the battery power status was 0.5. At this time $P_{solar} > P_{Level}$, when maintaining the aircraft’s level flight, while charging the battery, the SOC curve can be observed. After less than 3 h, the battery is full. The aircraft can climb the height to convert energy into potential energy storage.

Second, the performance of the aircraft continued to fly for several days. Figure 4 shows the flight simulation of the aircraft for three days, using the SOC status level to evaluate the ability of the aircraft to continue flying during the day and night. The SOC shown in the figure is at a minimum value of 0.3. That is, when the solar input power is equal to the output power on the second day, about 30% of the battery remains. The solar power is then greater than the output power, which can gradually charge the storage battery. The surplus time of the remaining battery power and the full battery time of the battery meet the basic requirements for day and night flight.

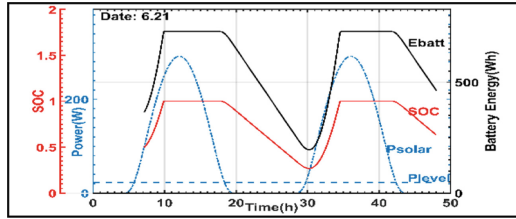


Fig. 4. Energy power curve of date 6.21 simulated continuous flight

Finally, the energy input and output energy performance curves for different days are analyzed, as shown in Fig. 5, which is the energy curve of date 4.21. The flight environment conditions are the same as the date 6.21. Due to the influence of the date change on the radiation intensity of the light beam, the solar output power is significantly reduced, so that the time for charging the battery is longer and the full battery time of the battery is reduced. At the same time, due to the change of the date, the time of the day becomes shorter and the time of the night increases. The discharge time of the battery is also greatly increased, and the residual value of the battery’s power decreases, and the surplus time. The lowest value of the state of charge parameter SOC is 0.21, which also decreases synchronously and approaches the SOC design threshold. Therefore, the date change has a significant influence on the parameters of the solar aircraft.

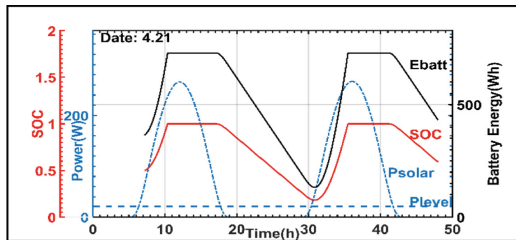


Fig. 5. Energy power curve of date 4.21 simulated continuous flight

5 Conclusion

This paper describes the design of energy system management methods for low-altitude and long-time solar-powered spacecraft, and the criteria for the expansion of the method, which increases the stability and robustness of the aircraft's multi-day flight performance. In the part of UAV platform design, the influence of the parameters of the solar-powered vehicle on the continuous flight performance is analyzed, and the design reference method of the solar UAV platform is given. In the simulation test, the aircraft was taking off from 7 o'clock on the first day to verify the aircraft's complete inter-day and night-flying capability and achieve the long-time flight of the 6.22 aircraft on the date to meet the mission requirements for multi-day flights. In addition, it also analyzes and verifies the ability of the aircraft continuous flight at date 4.21, the edge of the time window selected in this paper. The feasibility of this method is verified in this paper. Future research work will focus on the development of actual flight equipment to verify the validity of the practical application of this theoretical method and apply the solar-powered flight platform to the required scene.

Acknowledgements. This work are supported by the Chinese National Natural Science Foundation (No. 61773039), the Aeronautical Science Foundation of China (No. 2017ZDXX1043), and Aeronautical Science Foundation of China (No. 2018XXX).

References

1. Hening, S., Baumgartner, J., Teodorescu, M., et al.: Distributed sampling using small unmanned aerial vehicles (UAVs) for scientific missions. In: AIAA, InfoTech and Aerospace Conference (2013)
2. Malaver, A., Motta, N., Corke, P., et al.: Development and integration of a solar powered unmanned aerial vehicle and a wireless sensor network to monitor greenhouse gases. *Sensors* **15**(2), 4072–4096 (2015)
3. QinetiQ: QinetiQ files for three world records for its Zephyr Solarpowered UAV. QinetiQ Press Release (2010)
4. Zhang, Y., Li, K., Li, K., Liu, J., et al.: Intelligent prediction method for updraft of UAV that is based on LSTM network. *IEEE Trans. Cogn. Dev. Syst.* (2020)
5. Noth, A.: Design of solar powered airplanes for continuous flight. Ph.D. thesis, ETH Zurich (2008)
6. Cocconi, A.: AC propulsion's solar electric powered SoLong UAV. AC Propulsion, Technical report (2005)
7. Laurenzo, R.: Soaring on a solar impulse. *Aerosp. Am.* (5), 32–36 (2009)
8. Ke, Ch., Zhongwei, W., Zhou, Zh.: Exploring effects of solar-powered airplane operating conditions on solar cell performance. *J. Northwestern Polytech. Uni.* (4), 535–540 (2012)
9. Gao, X.Z., Hou, Z.X., Guo, Z., et al.: Energy management strategy for solar-powered high-altitude long-endurance aircraft. *Energy Convers. Manag.* **70**, 20–30 (2013)
10. Al-rabghi, O.M., Akyurt, M.M.: A survey of energy efficient strategies for effective air conditioning. *Energy Convers. Manag.* **45**, 1643–1654 (2004)
11. Ipsakis, D., Voutetakis, S., Seferlis, P.: Power management strategies for a stand-alone power system using renewable energy sources and hydrogen storage. *Int. J Hydrogen Energy* **34**(16), 7081–7095 (2009)

12. Soon, T., Mekhilef, S., Safari, A.: Simple and low cost incremental conductance maximum power point tracking using buck-boost converter. *J. Renew. Sustain. Energy* **5**(2), 1777–1790 (2013)
13. Castaner, L., Markvart, T. (eds.): *Photovoltaic Engineering. Solar Electricity*, pp. 74–114 (1994)
14. Lorenzo, E.: *Solar Electricity. Engineering of Photovoltaic Systems*. Progensa, Seville (1994)
15. Markvart, T., Castaner, L.: *Practical Handbook of Photovoltaics: Fundamentals and Applications*. Elsevier, Oxford (2003)
16. Mikoshiba, S., Sumino, H., Yonetsu, M., Hayase, S.: Highly efficient photo-electrochemical cell with novel polymer gel electrolytes. In: *Proceedings of the 16th European Photovoltaic Solar Energy Conference, Glasgow*, pp. 47–50 (2000)
17. Bakar, A., Ke, L., Liu, H.B., et al.: Multi-objective optimization of low Reynolds number airfoil using convolutional neural network and non-dominated sorting genetic algorithm. *Aerospace* **9**(1) (2022)
18. Weidong, X., Elnosh, A., Khadkikar, V., Zeineldin, H.: Overview of maximum power point tracking technologies for photovoltaic power systems. In: *IEEE Conference Publications*, pp. 3900–3905 (2011)
19. Ishaque, K., Salam, Z., Amjad, M., Mekhilef, S.: An improved particle swarm optimization (PSO) based MPPT for PV with reduced steady state oscillation. *IEEE Trans. Power Electron.* **27**(8), 3627–3638 (2012)
20. Safari, A., Mekhilef, S.: Implementation of incremental conductance method with direct control. In: *IEEE Conference Publications*, pp. 944–948 (2011)
21. ESRAM, T., Chapman, P.L.: Comparison of photovoltaic array maximum power point tracking techniques. *IEEE Trans. Energy Convers.* **22**, 439–449 (2007)



Research on the Configuration of Radar Jamming Force in Air Defense Operation

Xilian Tan, He Wu, Yanyan Ding^(✉), and Yujin Wang

PLA Army Academy of Artillery and Air Defense,
Zhengzhou Campus, Zhengzhou 450052, China
yzfdyy2010@163.com

Abstract. (Purposes) Radar jamming force is an important part of electronic air defense force, and its effect of covering targets is highly related to whether its configuration is correct or not. This paper proposes a solution for the configuration of radar jamming force through research, and gives full play to the combat effectiveness of radar jamming force. (Method) According to the operational characteristics of radar jamming force, it analyzes the configuration basis and studies the configuration method. (Results) Moreover, three typical configuration styles and specific configuration methods are proposed. (Conclusion) These configuration styles can adapt to different combat needs, and configuration methods can ensure that the radar jamming force can complete the combat mission. (Application direction) This paper can provide reference for radar jamming force commander to configure weapons and equipment.

Keywords: Air defense operation · Radar jamming force · Configuration

Radar, as the main sensor of air raid system, undertakes key tasks such as obtaining information, fire control and damage assessment, and is the key equipment of air raid system to attack important military targets. Due to the characteristics of long operational range, high detection accuracy and all-weather operation, airborne radar has become the main air threat faced by important military targets on the ground, and how to effectively reduce the reconnaissance capability of enemy aircraft has become an urgent problem to be solved [1]. The jamming force of ground-to-air radar is mainly used to deceive and suppress the airborne multi-function radar, reduce its operational efficiency, and help the air defense operation system to compete for information superiority. Because of the special operational mechanism of radar jamming weapon equipment, its efficiency is highly dependent on scientific and reasonable configuration. This paper studies configuration problems of radar jamming force from configuration basis, configuration styles and configuration methods, which can provide reference for air defense operation under conditions of informationization.

1 Configuration Basis of Radar Jamming Force

The main basis of radar jamming force configuration include air raider's situation, air defender's situation and battlefield environment, etc. The influence of various factors on

the operational efficiency of radar jamming force should be comprehensively considered, specific problems should be analyzed in detail, radar jamming force should be correctly configured on the basis of overall consideration.

1.1 Air Raider's Situation

In terms of operation timing, the air raider is always on the active side, so the air raider's situation is the basis in the air defense operation planning. In the configuration of radar jamming force, in order to improve the pertinence of the air defense system, it is necessary to consider main operational directions of air raider, dispatched force, standoff strike and accurate attack means, anti-reconnaissance and anti-jamming measures, as well as the performance, quantity, configuration and threat degree of the electronic information system of air raid weapons, and focus on the configuration of troops and weapons.

1.2 Air Defender's Situation

Under conditions of informationization, the air defense side relies on the network information system and aggregation system to fight against the air attack weapons, so the situation of air defense side is the realistic condition for air defense operation. In configuration of radar jamming force, some important factors such as main directions of air defense operation, intention at all levels, covered target, weapon equipment war, technical performance should be considered, moreover, the situation of friendly neighbors such as aviation, surface-to-air missile and electronic countermeasure is also an important reference factor in the system.

1.3 Battlefield Environment

The battlefield environment includes natural environment, social environment and electromagnetic environment. If used well, the battlefield environment can have a positive effect on air defense operations. In the configuration, the battlefield environmental factors, including topographic conditions, meteorological hydrology, roads, high-voltage lines, high-power transformers and other electronic information equipment facilities, should be analyzed and utilized. The air defense side should extensively collect all kinds of information on the battlefield, analyze and judge it on the basis of the above detailed information. In the course of configuring radar jamming power, make full use of favorable conditions, avoid unfavorable factors, ensure the effectiveness of radar jamming force, and make sure the formation of radar jamming force is scientific and reasonable.

2 Configuration Styles of Radar Jamming Force

The formation of radar jamming force must ensure that radar jamming forces can detect radar aerial targets in time, so that it can achieve the best suppression effect with the least force and provide comprehensive and focused cover for defending targets. While facilitating the command and coordination, the formation should avoid mutual interference of air defense electronic equipment. Typical configuration styles include: linear

configuration, circular configuration, ladder configuration. In combat, the appropriate configuration should be chosen according to the mission, the attacking direction of air raid weapons, covered targets conditions and the capability of radar jamming force.

2.1 Linear Configuration

Linear configuration is to deploy radar jamming force in linear or arc formation in the main attacking direction. It is usually used for reconnaissance actions in the main combat direction or areas where the air raider's electronic equipment is denser, or when the covered target has linear features, and is restricted by terrain conditions. When determining the location of radar jamming station, it is necessary to ensure that the maximum exposure radius is less than the minimum effective jamming range required by tactics, so as to protect the target effectively.

2.2 Circular Configuration

Circular configuration refers to deploy the radar jamming force in circular formation by taking the covered target as the center. The formation can carry out reconnaissance and interference to targets attacking from different directions, and help each other in exposed area and headspace blind area. It is generally used when covering small-sized targets or conducting all-round jamming and covering tasks. In the circular configuration, the distance between radar stations and the covered target, and covered angles of multiple radar stations cannot be the same in a bid to prevent the specific location and direction of the cover target from being exposed actively [2]. When determining the location of radar jamming station, it is necessary to ensure that the maximum exposure radius is less than the minimum effective jamming range required by the tactics, moreover, the cover angle range of each station can be overlapping in two and the whole coverage range is more than 360° .

2.3 Ladder Configuration

The ladder configuration refers to carry out the multilayer arc configuration for the main attacking direction of the air raid side, forming a large depth of the suppression area. This style is suitable for covering larger targets when the main attacking direction is clear. The ladder configuration is to deploy more forces and weapons in layers in a certain direction, which is a configuration style that highlights the key point. Usually, the covering effect is excellent in the direction where the radar jamming force is mainly configured. Two factors should be taken into account in determining locations of radar jamming stations. One is that the maximum exposure radius is less than the minimum effective jamming range required by the tactics [3], and the other is that the jamming force should ensure reliable communication, so that the multiple jamming vehicles can organically combine with each other and form a system.

3 Configuration Methods of Radar Jamming Force

The basic task of the radar jamming force is to suppress the airborne radar of the air raid weapon, so that the air raid weapons cannot see and aim accurately, and is difficult to conduct standoff strike or accurate attack. Therefore, when configuring the radar jamming force, generally follow the steps of determining the key covered point, judging the main attacking direction, selecting configuration locations and making sure configuration formations.

3.1 Determining the Key Covered Point

Key covered points of radar jamming force should be analyzed synthetically according to the operational mission, actions of combined arms forces, the position, function, quantity of the covered targets and terrain conditions in areas of covered targets, and the most important target can be selected as the key point of cover. Generally, command posts at all levels are the key points in the operation as well as the main targets of the air raid side and the cover of the air defense side at all stages. In addition, artillery which provides the main fire output in the offensive combat, combined units responsible for assault, the important defense support points and communication hubs in defensive operations, in the process of maneuvering, the key bridges and passes on the way are key covered targets.

3.2 Judging the Main Attacking Direction of Air Raid Weapons

The main attacking direction of air raid weapons refers to the direction of the air raid weapon attacking target. Generally, the air raid weapon is chosen to enter in the direction with the shortest range, which is convenient for concealed approach, target discovery, combat support and good attack effect, and the air defense firepower is spared and there are obvious landmarks. But in actual combat, in order to attack surprisingly, attacking directions of the air raid side is not fixed. Especially with the wide application of high-tech in the field of air raid operations, the choice of air raid attacking direction becomes more and more flexible. Technically, high-tech air raid weapons have the ability to strike targets from multiple directions; tactically, in order to disperse air defense fire, the air raid side usually uses small formation, multi-directional assault. The main attacking direction has a great influence on the configuration of radar jamming force. In the course of configuration, it is necessary to put emphasis on the main attacking direction on the basis of considering all possible attacking directions.

3.3 Selecting Configuration Locations

Locations of radar jamming force shall be determined comprehensively according to the interference responsibility direction zone of each jamming station, the minimum effective jamming range and effective jamming zone required by tactics.

(1) Interference responsibility direction zone of each radar jamming station

It refers to the jamming angle range which the station is mainly responsible for, usually expressed in ω . If all-round direction cover is needed, $\omega = 360^\circ$.

(2) Minimum effective jamming range required by tactics

When the air raid weapon is far from the covered target, its airborne radar receives a weak echo signal, which is easily suppressed by radar jamming station. As the air-raid weapon gets closer and closer to the target, the echo signal received by the airborne radar increases rapidly. At a certain distance, the target may be exposed from the interference mask. This distance is known as the exposure radius [4], also known as the minimum effective jamming range or burn-through range. At this moment, even if the radar jamming station jams the airborne radar, the airborne radar can still find the target, and the station cannot provide effective cover. The minimum effective jamming range required in tactics should be judged and obtained according to the parameters such as the direction of attack, flight speed and bomb-release height, etc. As the arms of air raid weapons tracking fire control become longer and longer, the minimum effective jamming range required for radar jamming force is higher and higher, which is also the key parameter in the configuration.

(3) Effective jamming zone of the jamming station

After being disturbed, the airborne radar of air raid weapon receives two signals at the same time: one is the echo signal reflected by the covered target; the other is the jamming signal transmitted by the radar jamming station. It is obvious that airborne radar will be disturbed when the intensity of the jamming signal emitted by the radar station is greater than that of the echo signal emitted by the covered target. Outside the exposure distance, the area within the effective jamming range is called the effective jamming zone. According to the relationship of signal intensity above, the relationship between the location of radar jamming station and the exposed area and the effective jamming zone can be obtained by mathematical calculation [5]. In combat, taking the minimum effective jamming range required by the tactics as the starting point for calculation, specific parameters of radar jamming station configuration can be obtained, including the distance between the configuration location and the covered target and the configuration angle, etc.

3.4 Determining Configuration Formation

Based on the basic principle of giving full play to the operational performance of radar jamming station, configuration styles should be determined reasonably according to covering abilities and characteristics of each configuration style of radar jamming force, in consideration of the factors such as the characteristics of the covered target and the main attacking direction of air raid weapon. On this basis, combining the tactical and technical performance of radar jamming station and airborne radar of the air raid weapon and the tactical requirements of air defense operation, analyze and determine the configuration parameters of each radar jamming station, and form the configuration formation of the radar jamming force.

References

1. Li, N.: Simulation of reconnaissance radar interference suppression area and exposed area. *J. Rocket Guidance* **3**(6), 31–34 (2020)
2. Luo, J.: *Principle of Radar Countermeasures*. People's Liberation Army Press, Beijing (2003)
3. He, J., Xi, Z.: Research on the configuration method of air defense radar jamming stations in important positions. *Mod. Defense Technol.* **10**(5), 103–107 (2008)
4. He, J., Xi, Z.: An algorithm for rapidly plotting interference areas. *Mod. Radar* **27**(3), 15–17 (2005)
5. Zhang, X., Xiao, K., Gu, J.: *The New System Radar Confrontation Theory*. Beijing Institute of Technology Press, Beijing (2020)



The Research on Optimal Design of Drawing Die for Non-circular Long Parts in Processing Environment

Wobo Zhang^(✉), Jianguo Shi, and Huichao Liu

Jinan Vocational College, Jinan 250014, China
wbz156@126.com

Abstract. The shape of the outer contour of the non-circular elongated part is not formed by the rotation of the bus bar around the axis. The first condition for the optimal design of this kind of mold is to avoid the lateral accumulation of materials or breakage due to excessive thinning. By discussing the three transition modes for deep drawing of non-circular elongated parts, namely oval transition, elliptical transition, and circular transition, it is determined that circular transition is adopted, from circular blank to cylindrical, and then to Oval, finally to oblong pieces, The number of times of drawing and the process parameters of each drawing were further determined, and an optimized design system for drawing dies for non-circular long parts under the processing environment was constructed. The use of this system framework can effectively solve the problems of mold utilization and adaptability, and realize the matching of workpiece requirements and functions, thereby expanding mold functions and optimizing system performance. It maximizes the performance of the die and provides users with an optimal design method for the drawing die for non-circular elongated parts under the processing environment that meets the goals of safety, efficiency, economy, health and comfort. The research has certain practical significance and theoretical value, and provides a guiding method for the optimization design system of the drawing die for non-circular elongated parts under the processing environment.

Keywords: Processing environment · Non-circular long piece · Deep drawing · Optimized design

1 Introduction

Modern man-machine-environment system research focuses on the interaction between man, machine and environment in the system to achieve the purpose of safe, comfortable and efficient production. Processing refers to the general term for machines or processing processes controlled by humans; environment refers to specific working conditions where humans and machines coexist. Optimum design of drawing dies for non-circular elongated parts in the processing environment aimed at the entire life cycle of the drawing [1], The design goal is product development, material selection, safe production, use and maintenance, recycling, product packaging and other technical aspects, Focus on

product environmental attributes (removability, recyclability, maintainability, reusability, etc.), with the help of technical information, environmental coordination information, economic information, etc. Using various advanced design theories such as concurrent design, it is a systematic design method that makes the designed products have advanced technology, good environmental coordination and reasonable economy, function, service life, quality [2], etc. Make the designed machine and environmental system suitable for the performance and characteristics of the processing process and actual use, to achieve the purpose of improving efficiency, safety, health and comfort in the processing process, and to achieve the goals of safety, efficiency and economy [3].

The optimal design of the processing environment consists of three parts: Part 1: Workpiece and machine operability; Part 2: Maintainability of workpieces and process equipment: including the maintainability of tools, fixtures, measuring tools, abrasives, cutting tools, auxiliary tools, and workstations for processing products; Part 3: Safety of workpieces, machines and computer systems and software, storage and transportation equipment.

The optimal design of the key “environment” mainly involves: the influence of the living environment (general environment, special environment), man-made environment and safety environment on people and machines. Including the research of environmental detection technology and environmental control technology.

2 Man-Machine-Environment System Analysis of Drawing Die for Non-circular Elongated Parts

Under normal circumstances, the goal of human-machine-environment system design mainly focuses on the design of three indicators of safety, efficiency, and economy, and tries to optimize the system as reasonably as possible [4]. The ultimate goal of human-machine-environment system design is to ensure the safety, efficiency, and economical conditions between humans and machines and the environment system, and to maximize human health and comfort [5].

Therefore, the objective analysis of the man-machine-environment system for drawing dies for non-circular elongated parts under the processing environment mainly carries out optimization analysis and design from the three objectives of “safety”, “high efficiency” and “economy”.

2.1 Research on the Influence of Environment on Machine Performance

In the human-machine system, the normal operation and performance of the machine, and the influence of environmental factors such as low temperature and high temperature play a crucial role in the performance of human working ability. If the processing environment is harsh, vibration, noise, human hypoxia, low pressure and other undesirable phenomena will result in machine damage and workpiece scrapping. Therefore, the optimal design of drawing dies for non-circular elongated parts under the processing environment should fully consider the intrinsic safety of the machine and the influence of environmental factors on the human-machine system, and establish a processing environment and drawing dies for non-circular elongated parts interface relationship.

2.2 Analysis of Deep Drawing Die System for Non-circular Elongated Parts Under Processing Environment

The shape of the non-circular elongated part perpendicular to the axial projection plane is non-circular, and the shape of the outer contour is not formed by the rotation of the bus bar around the axis. It is a typical non-rotating body drawing part, parts as shown in Fig. 1, its thickness $t = 0.3$ mm, Due to the deep drawing of a non-rotating body, the shape is very irregular, and the stress and strain states of each point along the edge are different. During the forming process, the tensile stress of the section increases, and the stress-strain state is very complicated. When the blank is locally too large, this part will protrude from the deformation zone during the deep drawing process, which not only reduces the deformation of the part itself, but also makes it difficult to deform the material adjacent to it. At the same time, the deformation degree of the large part of the blank is reduced, which will inevitably cause the deep drawing deformation to concentrate more on the rest of the blank, and increase the unevenness of the deformation distribution along the periphery of the blank. In this way, the drawn parts have uneven wall thickness, which is easy to cause excessive deformation. Localized wrinkling in the concentrated area. When the force state is not controlled properly, the quality of the workpiece is reduced and waste products are generated [6]. There are no mature design methods and steps for such oblong parts. In order to obtain qualified deep drawing parts, the following steps are often used to determine the design method of oblong parts under actual production conditions.

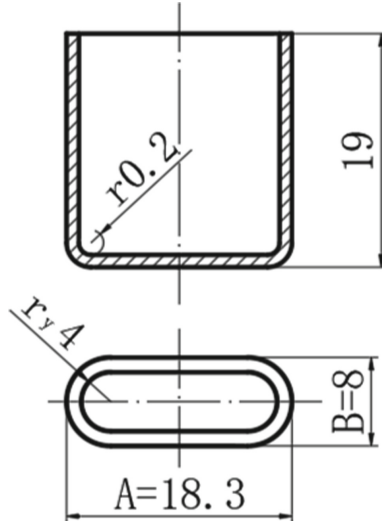


Fig. 1. Dimensions of the oblong piece

3 Deep Drawing Mode for Oblong Pieces

A reasonable transition form should be selected when the oval part is deep drawn, so that the deformation state and degree of deformation of the material at the surrounding points tend to be consistent, and the lateral accumulation of the material or the rupture due to excessive thinning is avoided [7]. This is a non-rotating body. Basic conditions for deep drawing. Therefore, the transition forms often used are oval transition, elliptical transition and circular transition.

The oval transition is the transition from a round blank to an oval to an oval piece. The material at the highest point A1 of the arc deforms the most, moving the material in the height direction, but also in the tangential direction C of the arc, while the material at B1 has only the displacement in the height direction pile up.

The oval transition is the transition from an oval blank to an oval to an oval part. This form is better, and the deformation of the material at each point tends to be the same, which can reduce the process, but the manufacturing of the mold is more difficult [8].

The circular transition is the transition from a circular blank to a cylindrical shape to an oval shape and finally an oblong piece is formed. The essence is the deep drawing of cylindrical parts, which can greatly simplify the difficulty of mold manufacturing and provide convenient conditions for automatic feeding [9]. However, the difficulty of circular transition lies in the transition from cylindrical to elliptical, and the difference between the margin b_x and a_x is large, which will increase the material flow velocity difference [10].

The conditions used for circular transitions are:

$$H/A > 0.9 \quad (1)$$

In the formula: H—The total height of the piece, in mm.

A—The length of the piece, in mm.

$$m_x = 1.14r_y / 1.14r_y + a_x > 0.8 \quad (2)$$

In the formula: m_x —circular transition drawing coefficient.

r_y —The inner diameter of the molded part, in mm.

4 Optimization Calculation of Deep Drawing (Calculation Unit is mm)

4.1 Determine the Blank Shape

It can be seen from Fig. 1 that $H = 19$, $A = 18.3$, and substituting into formula (1), we get: " $H/A = 1.04 > 0.9$ " belongs to high long round parts. Check the design manual for the blank area of the tall oblong part, it can be seen that the workpiece adopts a circular blank.

4.2 Calculate the Blank Diameter D

It can be seen from Fig. 1 that the radius of the inner arc of the oblong part is $r = 0.2 < 0.5$, and it can be seen from Fig. 1 that $B = 8$; B—the width of the non-rotating body part. Then bring into the calculation of the blank diameter D: $D = 38.7$, take $D = 38.5$.

4.3 Determine the Deep Drawing Mode

- (1) Determine whether the conditions for use of the circular transition are met,
From H0A, the m_x value can know that this workpiece satisfies the circle transition.
- (2) According to the above calculation, the circular blank, the intermediate process adopts a circular transition, and the $r = 0.2$ shown in Fig. 1 is obtained from the final shaping process.

4.4 Calculate the Technological Dimension of the n–1th Ellipse Drawing

After calculation $r_{an-1} = 29.5$, r_{an-1} —the radius of the short side of the n–1th deep drawing ellipse.

After calculation $H_{n-1} = 16.8$, H_{n-1} —the piece height of the n–1th deep drawing.

It can be seen from Fig. 1 that the inner fillet radius of the workpiece is $r = 0.2$. According to experience, $r_{n-1} = 1$, the size of the n–1th drawing process of the workpiece.

4.5 Calculate the Diameter of the n–2th Cylinder Drawing

After calculation $d_{n-2} = 22.2$, d_{n-2} —the workpiece diameter.

4.6 n–2th Cylindrical Deep Drawing

$$m_{total} = dD = 22.238.5 = 0.577$$

Look up table and get $m_1 = 0.55 < m_{total} = 0.577$, which can be stretched at one time. It takes one deep drawing from the blank to the n–2th time.

4.7 Calculation of the Size of the First Deep Drawing Process

Look-up tablet $D \times 100 = 0.78$, $m_1 = 0.55$.

r_1 —Inner fillet radius during the first deep drawing $r_1 = 3.5$

H_1 —The piece height of the first deep drawing is calculated.

The dimensions of the first drawing process of the workpiece are shown.

To sum up, the deep drawing process of this workpiece needs to be from a circular blank to a cylindrical, oval, and then an oblong part. The final oblong part is shown in Fig. 2.

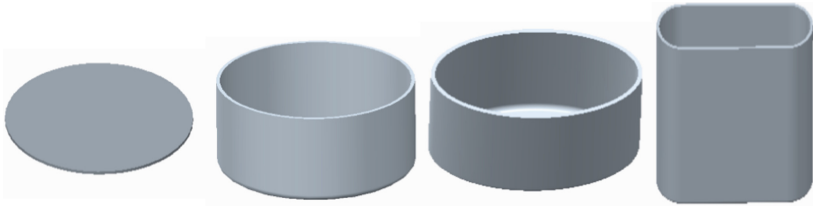


Fig. 2. Optimal design of oval piece

5 Conclusion

1. The optimal design of the drawing die for non-circular elongated parts under the processing environment should fully consider the impact of environmental factors on the safety of the human-machine system, the machine, and the workpiece itself. The optimization of the environment is particularly important.
2. The optimization design objectives mainly focus on three indicators: safety, high efficiency and economy.
3. The key to the optimal design of the deep drawing die for non-circular elongated parts is to establish a reasonable transition shape. In this paper, through a case, through analysis and calculation, circular and oval shapes are used as the transition to oval parts. The actual proof, which can avoid the lateral accumulation of materials or rupture due to excessive thinning, change the local wrinkling in the excessively concentrated deformation, and improve the quality of the workpiece.

References

1. Zhao, X.: Stamping Process and Die Design. Harbin Engineering University Press, Harbin (2010)
2. Roxann, D., Rocio, Q., Sara, H., Jennifer, B.: Promoting oral health in nursing education through interprofessional collaborative practice: a quasi-experimental survey study design. *Nurse Educ. Today* **82**, 93–98 (2019)
3. Yoo, S.J.: Connectivity-preserving design strategy for distributed cooperative tracking of uncertain nonaffine nonlinear time-delay multi-agent systems. *Inf. Sci. Press* **6**, 35–49 (2019)
4. Rosa, D., et al.: Designed asymmetric coordination helicates with bis- β -diketonate ligands. *Dalton Trans. (Cambridge, England: 2003)* **48**, 16844–16847 (2019)
5. Alessio, G., Pietro, I.: Better end points needed in primary sclerosing cholangitis trials. *Nat. Rev. Gastroenterol. Hepatol.* **16**, 143–144 (2019)
6. Peter, B.: Ten ways to optimize evidence-based policy. *J. Comp. Effectiveness Res.* **6**, 113–128 (2019)
7. Li, L., Liu, K.: Coordination contract design for the newsvendor model. *Eur. J. Oper. Res.* **6**, 118–129 (2019)
8. Chen, G., Bau, H.H., Li, C.H.: In-situ TEM liquid cell 3D profile reconstruction and analysis of nanoscale liquid water contact line movements. *Langmuir ACS J. Surfaces Colloids* **6**, 115–128 (2019)
9. Xue, Q.: Difficulties and Tips in Design and Manufacture of Stamping Die. China Machine Press, Beijing (2005)
10. Ding, J.: Design of Cold Stamping Die. China Machine Press, Beijing (2005)

Research on the Overall Performance of Man-Machine-Environment System



Correlation Analysis of Traffic Accident Severity of the Heavy Trucks Based on Logistic Model

Rufen Jiang, Xuejun Niu^(✉), and Huairui Zhang

School of Traffic Management, People's Public Security University of China, Beijing 100038, China

gadxxnj@sina.com

Abstract. With the increase of truck ownership year by year, traffic accidents involving heavy trucks occur frequently and the consequence is more serious. The accident is the result of the maladjustment of various factors in the “man-vehicle-environment” system. In this context, using the data of 305 traffic accidents of heavy truck in a province of China in 2020, 11 influencing factors are selected from the three aspects of people, vehicle, and environment. The scientific analysis of the factors affecting the severity of heavy truck accidents is carried out by the Logistic regression model. Mining the influence of “man-machine-environment” system disharmony on the severity of the accident. The result shows that the main factors affecting the severity of heavy truck accidents are driving on the wrong side of the road, failing to yield as required, involving pedestrians, vehicle fault and without traffic control. Based on the above five factors, countermeasures to prevent heavy truck traffic accidents are put forward in order to reduce casualties and property damage caused by accidents. It is of great theoretical significance and practical application value to improve the level of road traffic safety in China.

Keywords: Man-machine-environment · Heavy goods vehicle · Accident severity · Logistic regression models

1 Introduction

With the rapid development of social economy in China, the logistics industry has gradually developed, and the national freight demand shows an upward trend year by year. In 2020, the number of heavy trucks in China is 8.43 million, an increase of 750000 over 2019, a year-on-year increase of 9.765%, reaching the highest level in a decade. The number of heavy trucks in 2010–2020 is shown in Fig. 1 [1].

The increase in the number of heavy trucks has strengthened the close cooperation among various regions of the country to a certain extent. However, traffic accidents involving heavy trucks have seriously damaged the safety of people's lives and property. According to the road traffic accident statistics of the traffic administration bureau of the Ministry of public security, 17947 heavy truck accidents occurred in 2017, accounting for 51.12% of the total number of operating vehicle accidents. The direct property loss caused by heavy truck accident is 248384224 yuan, accounting for 56.37% of the total

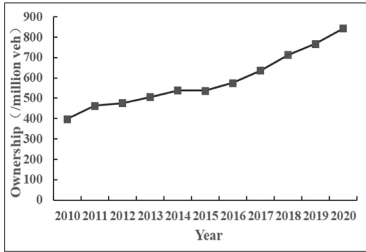


Fig. 1. Ownership of heavy trucks in 2010–2020



Fig. 2. Example of heavy truck

property loss caused by operating vehicle accident. The number of injuries is 17974, accounting for 45.73% of the number of injuries caused by operating vehicles. The number of deaths is 10739, accounting for 59.80% of the total number of accident deaths [1]. The frequency and severity of heavy truck accidents are significantly higher than other operating vehicles. It is urgent to prevent heavy truck traffic accidents and implement road traffic safety management scientifically.

In order to effectively prevent and control road traffic accidents, scholars all over the world have studied the influencing factors of accident severity. Sun proves that the main factors affecting the severity of motor vehicle crashes are collision type, road attribute, accident cause and driver type [2]. Qin et al. scientifically studied the factors affecting the severity of two-lane motorcycle accidents in mountainous areas by establishing ordered Logit model and multiple Logit models [3]. Hu et al. studied the coupling relationship between people, vehicles, environment, management factors and accident severity by establishing ordered Logit model and ordered Probit model [4]. Fang analyzed the accident severity through Bayesian network [5]. Lin et al. studied the impact of driver's fault on the severity of non-motor vehicle traffic accidents through Logistic regression, and learned that whether motor vehicle drivers have fault is closely related to their gender, the kind of vehicles, road type and weather [6]. Using the complex network, Hu found the traffic accident risk factor network of operating trucks has complex characteristics, which proves that the truck accident is the result of the coordination imbalance of “man-vehicle-environment” system [7]. Because of its own characteristics and professional characteristics of drivers, the accident consequences of heavy trucks are more serious. It is necessary to carry out a separate study on heavy trucks.

Traffic accident is a comprehensive reflection of the coordination imbalance of various elements of “person-vehicle-environment” in the road system under a specific environment [8]. The severity of the accident is affected by many factors such as driver, vehicle and environment [9]. Based on the traffic accident data of heavy trucks in a province in 2020, selecting 11 key factors from the perspective of human, machine and environment. A binary Logistic regression model was established to analyze the influence of various factors on the severity of heavy truck traffic accidents.

2 Data Selection

This paper extracts the detailed data of traffic accidents related to heavy trucks in a province of China in 2020 from the traffic accident database of the public security traffic integrated management application platform. After sorting and screening the data, we obtain the detailed data of 305 heavy truck traffic accidents.

2.1 Definition Standard for Heavy Goods Vehicles

GA802-2019 stipulates that trucks include heavy, medium, light, micro, low-speed trucks and three wheeled vehicles. A heavy truck is defined as a truck with a total mass greater than or equal to 12000 kg [10]. An example of a heavy truck is shown in Fig. 2.

2.2 Independent Variable Selection

The severity of heavy truck accidents is affected by many factors. 11 influencing factors are selected from the perspective of people, vehicles and environment.

3 Methodology

Logistic regression is a widely used supervised statistical method. It has fast training speed, does not need too much calculation, and has good interpretability. It is the basis of other complex algorithms. Because the output results are discrete values between 0–1, Logistic regression model has unique advantages in binary classification [11]. It has been well applied in many fields [12–14].

3.1 Model Interpretation

Logistic regression estimates probability with its inherent function to measure the relationship between research objectives and influencing factors. The employed Logistic model assumes a discrete dependent variable y with probability P ; the specific form of the Logistic model is given by:

$$P = \frac{\exp(\beta_0 + \beta_1x_1 + \beta_2x_2 + \cdots + \beta_mx_m)}{1 + \exp(\beta_0 + \beta_1x_1 + \beta_2x_2 + \cdots + \beta_mx_m)} \quad (1.1)$$

Carry out Logistic transformation on Eq. (1.1) to obtain multiple Logistic regression models. Expression (1.2) is given by:

$$\ln \frac{P}{1 - P} = \beta_0 + \beta_1x_1, \beta_2x_2 \dots, \beta_mx_m \quad (1.2)$$

Here, logit is the natural logarithm of the odds where dependent variable y is fatal ($y = 1$) versus non-fatal ($y = 0$), P is the probability of fatal crash occurrence, β_k is the model coefficient value, and x_m denotes the independent variables used in the study.

In order to make the results of model analysis easier to understand, it is necessary to analyze the OR value of each dependent variable when using the model. The specific form of the OR value is given by:

$$OR_j = \exp[\beta_j(c_1 - c_0)] \quad (1.3)$$

where c_1 and c_0 respectively represent the two exposure levels under the x_j independent variable. If the OR value is greater than 1, the corresponding independent variable is more likely to cause fatal traffic accidents.

3.2 Model Application

Using SPSS26.0 to analyze the processed heavy truck traffic accident data.

In Omnibus test, the significance obtained by Logistic regression model analysis is 0.029, less than 0.05. It shows that the OR value of at least one variable in the fitted model is statistically significant.

The significance of Hosmer-Lemeshow test result is 0.896, greater than 0.05. It can be seen that the goodness of fit of the model is high. It is feasible to analyze the severity of heavy truck traffic accidents by using Logistic regression model.

Logistic regression model is used to analyze the data. The results of each variable are listed in Table 1:

Table 1. Variable selection and logistic regression analysis results

Factor	Introduction	Count	Contribution	p-value
Human factor				
Driving on the wrong side of the road	Yes = 1	22	7.30%	0.030
	No = 0	283	92.7%	
Behavior that hinders safe driving	Yes = 1	46	15.1%	0.459
	No = 0	259	84.9%	
Speeding	Yes = 1	32	10.5%	0.411
	No = 0	273	89.5%	
Failing to yield as required	Yes = 1	54	17.8%	0.047
	No = 0	251	82.2%	
Involving pedestrians	Yes = 1	38	12.5%	0.029
	No = 0	267	87.5%	
Machine factor				
Vehicle condition	Good = 1	275	90.2%	0.041
	Bad = 0	30	9.80%	
Environmental factor				
Traffic control type	Controlled = 1	205	67.3%	0.051
	Uncontrolled = 0	100	32.7%	

(continued)

Table 1. (continued)

Factor	Introduction	Count	Contribution	p-value
Physical isolation of roads	Physical isolation = 1	58	19.1%	0.608
	Without isolation = 0	247	80.9%	
Road location type	Ordinary section = 1	219	71.9%	0.845
	Special stages = 0	86	28.1%	
Lighting conditions	Good = 1	213	69.9%	0.422
	Bad = 0	92	30.1%	
Weather	Sunny = 1	263	90.1%	0.812
	Bad = 0	42	9.90%	

It can be seen from Table 1 that the p-values of overspeed, behavior hindering safe driving, physical isolation of road, type of intersection section, good lighting and weather conditions are greater than 0.1. The above six variables failed to pass the significance test at the 90% level. Therefore, these variables need to be removed for further analysis.

The p-values of the five variables in Table 2 were lower than 0.1, which was statistically significant.

Table 2. Logistic regression analysis results after excluding some variables

Factor	Coefficient	Standard error	p-value	OR
Driving on the wrong side of the road	1.033	0.487	0.034	2.809
Failing to yield as required	0.649	0.316	0.040	1.913
Involving pedestrians	0.757	0.368	0.039	2.132
Vehicle condition	-0.840	0.317	0.044	0.440
Traffic control type	-0.474	0.254	0.063	0.623

3.3 Model Results

3.3.1 Driver Aspects

Speeding behavior has no significant impact on the severity of the accident, and the three independent variables of retrograde, failing to yield as required and involving pedestrians are more significant. When other independent variables are the same, the probability of fatal accident of retrograde vehicles is 2.809 times higher than that of non-retrograde vehicles. The probability of fatal traffic accident of non-yielding vehicles is 1.913 times that of yielding vehicles. The probability of fatal accidents involving pedestrians is 2.132 times that of accidents not involving pedestrians.

3.3.2 Machine Aspects

When other independent variables are the same, fatal traffic accidents are more likely to occur when there are problems in vehicle safety, and the accident probability is 2.273 times that when the vehicle safety is good.

3.3.3 Environmental Aspects

The type of intersection section and the existence of road physical isolation have no significant impact on the severity of traffic accidents. The existence of traffic control has a significant impact on the severity of traffic accidents. When other independent variables are the same, the probability of fatal traffic accidents of heavy trucks on roads without traffic control is 1.605 times that on roads with traffic control. Whether the lighting is good and weather conditions have no significant impact on the severity of traffic accidents.

4 Conclusion

- (1) According to whether there are deaths in heavy freight vehicle traffic accidents, the accident severity is divided into non-fatal accidents and fatal accidents, and a binary Logistic model is established. The results show that the accident severity is higher under the conditions of retrograde, failure to yield according to regulations, involving pedestrians, poor safety performance of vehicles and no traffic control.
- (2) At the driver management level. Regularly carry out publicity and education activities to strengthen drivers' awareness of traffic safety and improve drivers' driving skills and emergency response ability; Improve other traffic participants' understanding of the structural characteristics of heavy trucks, consciously stay away from heavy trucks in traffic activities, reasonably protect themselves and reduce traffic accidents.
- (3) At the level of vehicle safety management. Relevant law enforcement departments regularly inspect heavy trucks, strengthen the inspection and management of vehicle technical performance, and strictly review the vehicle safety performance in the sales link of heavy trucks from the source, prohibit unqualified heavy trucks from entering the market, and avoid road traffic accidents caused by vehicle safety performance from the source. In addition, strengthen the driver's understanding of the performance and structure of motor vehicles, make it clear the importance of daily vehicle inspection and maintenance, and form the habit of regular inspection and maintenance of heavy trucks to ensure the safety and stability of driving vehicles.
- (4) At the level of improving road traffic facilities. Relevant departments need to improve road traffic management measures and timely give early warning to drivers in high-risk sections, so as to facilitate them to make timely judgment and decision-making in complex roads and reduce the occurrence of traffic accidents. In addition, heavy trucks can be protected through guardrails and other facilities, so as to effectively reduce the consequences of vehicle out of control or accidents, and ensure the transportation safety of heavy trucks.

Acknowledgement. This work is supported by the Public security theory and soft science research program, No. 2020LLYJGADX020.

References

1. Traffic Management Bureau of the Ministry of Public Security: Road Traffic Accident Statistics Annual Report of the People's Republic of China. Traffic Management Science Research Institute of Ministry of Public Security, Wuxi (2017)
2. Sun, Y., Shao, C., Zhao, D., et al.: Traffic accident severity prediction model based on C5.0 decision tree. *J. Chang'an Univ. (Nat. Sci. Ed.)* **34**(5), 109–116 (2014)
3. Qin, Y., Xie, B., Yang, W., et al.: Comparative study between an ordered Logit model and the multinomial Logit model for analysis of motorcycle accidents on the mountainous two-lane roads. *J. Saf. Environ.* **21**(4), 1397–1404 (2021)
4. Hu, J., Yan, Z., Lu, X., et al.: Analysis for the influential factors of the accident severity based on the ordinal Logit and Probit models. *J. Saf. Environ.* **18**(3), 836–843 (2018)
5. Fang, Z., Xu, H., Zhang, H.: Prediction for traffic accident severity: comparing the Bayesian network and regression models. *Math. Probl. Eng.* **34**(3/4), 353–366 (1997)
6. Ling, Q., Deng, Y., Hu, J.: Logistic regression analysis of driver's fault and accident motorcycle accidents. *Saf. Environ. Eng.* **26**(5), 187–193 (2019)
7. Hu, L., Yang, H., He, Y., et al.: Driving risk identification of commercial trucks based on complex network theory. *J. Transp. Eng. Inf.* **26**(5), 1–8 (2019). <http://kns.cnki.net/kcms/detail/51.1652.U.20210428.0832.002.html>. Accessed 21 Oct 2021
8. Song, D., Yang, X., Zu, X.: Examination of driver injury severity in urban crashes: a random parameters Logit model with heterogeneity in means approach. *J. Transp. Eng. Inf.* **21**(3), 214–220 (2021)
9. Li, G., Zhang, F., Wang, Y.: Influencing factors analysis of multiple vehicle accidents in mountainous expressway based on SVM model. *J. Wuhan Univ. Technol. (Transp. Sci. Eng.)* **44**(6), 1046–1051 (2020)
10. Huang, X., Zou, P.: On the inspection of motor vehicles based on the frequent occurrence of “large ton and small standard” accidents of light trucks. *Auto Saf.* (5), 45–48 (2021)
11. Su, L., Pan, B.: Sharing on two kinds of fitting methods of condition logistic regression model. *Strait J. Prevent. Med.* **27**(03), 91–93 (2021)
12. Sun, X., Liao, W., Cao, D., et al.: A logistic regression model for prediction of glioma grading based on radiomics. *J. Cent. South Univ. (Med. Sci.)* **46**(04), 385–392 (2021)
13. Hu, D., Zhao, W.: Change point detection of multiple response regression model and its application. *Stat. Decis.* **37**(02), 34–38 (2021). <https://doi.org/10.13546/j.cnki.tjyj.2021.02.007>
14. Zhu, Y., Huang, W., Chen, S., et al.: Application of logistic regression model in runoff wetness-dryness prediction. *Water Resour. Power* **38**(12), 16–19+23 (2020)



Thoughts on Strengthening the Management of Dangerous Sources in Air Defense Force Training

Lie Wang, Zhenguo Mei^(✉), Chunxin Wang, Kun Cao, and Weifei Wu

Artillery and Air Defense Forces Academy (Zhengzhou Campus), Zhengzhou 450052, China
meizg_zz@sina.com

Abstract. Military training is the basis for the construction and development of air defense forces and the fundamental way to improve combat effectiveness. At present, our army is setting off an upsurge of military training and war preparation. All levels attach great importance to training safety, and training accidents are particularly sensitive. The most fundamental and effective way to prevent training accidents is to effectively curb hazard sources. Therefore, strengthening the research on the management of hazard sources in the training of air defense forces is of great significance to ensure the safe and smooth training of air defense forces. This paper summarizes the significance of hazard source management in air defense force training, combs the main problems existing in hazard source management in air defense force training, and puts forward countermeasures to strengthen hazard source management in air defense force training from four aspects: strengthening organization and leadership, strengthening publicity and education, paying attention to team construction and perfecting system.

Keywords: Air defense forces · Force training · Hazard management

Military training is the basis for the construction and development of air defense forces and the fundamental way to improve combat effectiveness. At present, our army is setting off an upsurge of military training and war preparation. All levels attach great importance to training safety, and training accidents are particularly sensitive. The most fundamental and effective way to prevent training accidents is to effectively curb hazard sources [1]. Therefore, strengthening the research on the management of hazard sources in the training of air defense forces is of great significance to ensure the safe and smooth training of air defense forces.

1 The Significance of Danger Source Management in Air Defense Force Training

1.1 Beneficial to Enrich and Perfect the Theory System of Air Defense Force Training Safety Management

At present, the theory of Hazard Management of Air Defense Forces has not been established, and the research on the problem of hazard management is still at the initial

stage. Carrying out the research on the management of dangerous sources will help to fill up the gaps in the theory of the management of dangerous sources in the training of air defense forces, and further enrich and perfect the theoretical system of the training safety management of air defense forces, it provides the theory basis and method support for the Air Defense Force Training Hazard Management.

1.2 Beneficial to Improve the Quality and Level of Hazard Source Management in Air Defense Force Training

With the gradual deepening of the actual combat training of air defense forces and the dispatch of all personnel and equipment, the risk factors of personnel, equipment and environment are becoming more and more complex, and the problem of training safety is becoming more and more prominent. Training hazard sources is one of the important contents of safety management. Its management directly affects the quality of safety management, and is related to the consolidation and improvement of the combat effectiveness of the army and the completion of combat tasks. Therefore, the research on the training hazard management of the army air defense force plays a positive role in improving the accuracy and quality of the training hazard management of the air defense force.

1.3 Beneficial to Improve the Quality of Safety Risk Management of Officers and Soldiers in Training

In military practice, officers and soldiers still lack sufficient understanding and understanding of hazard sources. Carrying out the research on the training hazard source management of air defense forces and constructing the theory and method system of training hazard source management of air defense forces can enable the officers and soldiers of the forces to understand the relevant knowledge of hazard sources in a short time, be familiar with the content and process of training hazard source management, and master the methods and precautions of training hazard source management, This has a certain practical value for improving the training safety risk management quality of military officers and soldiers.

2 Problems in Hazard Source Management of Air Defense Force Training

2.1 Ideological Neglect

Leaders not pay enough attention to the training of hazard management and did not conduct in-depth research. It believed that hazard management was similar to risk management and safety management. There was no need to specialize in hazard management and pay attention to safety management. The ambiguity and deviation in understanding lead to the formality of hazard source management. Although there are clear provisions in the rules and regulations, it is mainly to cope with the superior inspection, walk through the stage and shout slogans, which greatly affects the quality and effect of hazard source identification, assessment and management.

2.2 Education is not Deep

At present, there are two main problems in the process of organizing training and hazard source management education in the Army: one is that the education is not systematic enough. In the daily education, the education on hazard source management is too few, the content is relatively loose, and the regular education is not paid close attention to. Only the surprise education is carried out before the commencement of major training activities and safety inspection, resulting in a large gap in the understanding of hazard source management and the mastery of relevant knowledge, and there is always a vague understanding. Second, the professionalism of education is not enough. The education of officers and soldiers only stays on the safety requirements. The majority of officers and soldiers do not understand and master the relevant theoretical knowledge of hazard source management. The identification, control and basic risk response ability of hazard sources are relatively lack, resulting in the value of theoretical guidance and practice of hazard source management not being reflected in practice.

2.3 Lack of Talents

The training of hazard management is highly technical and the work is complex. The hazard management personnel need to reach a relatively professional technical level in order to effectively carry out hazard management. At present, the air defense forces are in short supply of hazard management talents with a certain professional and technical level. The reasons can be summarized as follows: first, there is little professional training. From the army organs, colleges and universities to the army, there are few professional training related to hazard source management, resulting in the lack of professional backbone in the army. Second, the pertinence is not strong. The knowledge and skill requirements of hazard source management are different for personnel in different positions. Only by carrying out targeted education and training in combination with the actual situation of the post can we effectively enhance the hazard source management ability of all kinds of personnel.

2.4 Imperfect System

At present, the air defense forces' training hazard source management is not standardized and unscientific. The reason is the lack of perfect hazard source management system and mechanism and the lack of standardized guidance of basic processes and methods. In the work, the troops can only rely on experience and explore themselves. It is inevitable that there will be work omissions, unscientific management and procrastination, As a result, the effect of hazard source management is greatly reduced. When carrying out training hazard source management, officers and soldiers simply have no way to start, because there are only the requirements of documents and leaders, there is no system and norms to be based on, and there are few successful experiences and practices. Therefore, the army urgently needs to establish and improve the system and mechanism in order to provide basic norms for the army to carry out training and hazard source management practice.

3 Countermeasures of Hazard Source Management in Air Defense Force Training

3.1 Strengthen Organizational Leadership

Leaders should recognize the importance of hazard source management, strengthen the organizational leadership of hazard source management, put hazard source management in the same important position as safety risk assessment, conduct synchronous research and overall consideration, rely on the organizational leadership of risk assessment, endow hazard source management with functional tasks, sort out and summarize relevant theories and systems of hazard source management, and establish their own hazard source database.

3.2 Strengthen Publicity and Education

Leaders at all levels should repeatedly educate the trained officers and soldiers. Use various occasions and forms to publicize the knowledge of hazard sources, improve the understanding of hazard sources, make officers and soldiers understand relevant knowledge and remember the identified training hazard sources; Pay attention to cultivating the safety awareness of officers and soldiers. We should always think about safety and ensure safety everywhere; Pay attention to the education of safety laws and regulations, let officers and soldiers learn the relevant systems and regulations of hazard source control, remember the control responsibilities, master certain hazard source control skills, and help improve the confidence of hazard source control training [1].

3.3 Pay Attention to Team Building

According to the characteristics of hazard source management, integrate high-quality resources from colleges, universities, troops and local governments to build an excellent hazard source management team with “safety managers as the main body and external experts as the supplement”. First, build a strong professional hazard management team. Combined with the actual training and construction of the unit, improve the quality of hazard source management of personnel through business training, visiting and learning, counseling and lectures, etc.; Focus on the tasks in charge, carry out post practice, accumulate experience, regularly exchange experience, share work experience and promote common improvement; Insist on incorporating the performance of hazard source management into the assessment, rely on promoting training, extend post training to the construction of talent team, stimulate the enthusiasm of personnel, and effectively improve the professional quality and management level of safety talents [2]. Second, make good use of high-quality military and local resources. Carry out in-depth co construction and co education activities, invite hazard source management experts to give guidance and lectures, and learn about the latest research results and laws and regulations of hazard source management; Employ military management experts as “distinguished experts” to participate in and guide the formulation of hazard identification management plan in a timely manner; Relying on military and civilian colleges, research institutions and training institutions to carry out cooperative research on the practical problems of

hazard management in training [3], and solve the problems of hazard management in time.

3.4 Improve the System

The training hazard source management of air defense forces is a complex systematic project, which is inseparable from the joint efforts of all departments at all levels. Therefore, it is necessary to establish and improve relevant systems and systems to ensure the cooperation of all departments at all levels to carry out the training hazard source management. The hazard source management system shall include the division of responsibilities, work flow, evaluation standards, objective strategies, management systems, etc. First, we should clarify the division of relevant responsibilities, focusing on the responsibilities of organs, grass-roots units and responsible personnel. Second, we should standardize the work flow and make officers and soldiers familiar with the methods and procedures of scientifically carrying out hazard source management. Third, it is necessary to establish hazard source evaluation standards to enable officers and soldiers to clarify the hazard level of relevant hazard sources, so as to facilitate hierarchical management and key control [4]. Fourth, we should clarify the management objectives and strategies, break the absolute safety concept of zero risk, and select appropriate control methods (risk avoidance, risk mitigation, risk dispersion, risk bearing, etc.) according to the identification and evaluation of hazard sources, Take effective control measures (preventive control, supplementary control, preventive control to prevent accident expansion, maintenance control, regular control and emergency control) Fifth, we should establish and improve the hazard source control system, mainly including registration and filing system, identification and evaluation system, inspection and supervision system, training and drill system and emergency rescue system, and build a “four in one” comprehensive prevention and control system of risk early warning, management standards, whole process monitoring and emergency rescue [5], so as to provide institutional basis and basic norms for the military to carry out training hazard source management.

References

1. Luo, Y., Yang., G.: Control of major hazard sources in air defense training. *J. Air Defense Acad.* **08** (2013)
2. Lu, D.: Study on Safety Management of Gold Troops under Decentralized Conditions. Chang’an University (2019)
3. Jing, Y., Wang, Y.: On promoting the development of military security by strengthening risk management. *J. Command* **04** (2010)
4. Hao, R., Zhou, L.: Identification and hierarchical management of major hazard sources in Armed Police Force. *J. Sichuan Ordnance Ind.* **04** (2013)
5. Li, X., Gao, J.: Building a four in one military hazard prevention and control system. *Force Manag.* **12** (2019)



Prominent Problems and Management Countermeasures of Military Safety Work

Kun Cao¹, Zhenguo Mei¹(✉), Yanjiao Wang², Weifei Wu¹, and Peng Gong¹

¹ Artillery and Air Defense Forces Academy (Zhengzhou Campus), Zhengzhou 450052, China
meizg_zz@sina.com

² Henan Foreign Economic and Trade Vocational College, Zhengzhou 450052, China

Abstract. In recent years, with the continuous deepening of the army's military struggle preparation and the gradual normalization of actual combat training, some prominent problems in safety work have increasingly become important factors affecting the generation of the combat effectiveness. How to solve these problems based on the existing conditions, so as to realize management itself is for war and improve the combat effectiveness has become a practical problem faced by the army. Therefore, starting from the reality of military safety management, this paper analyzes the current prominent problems related to safety education, hidden danger, laws and regulations, safety quality; explores the reasons behind, and puts forward countermeasures, which provides basic methods and ideas for the army to solve these security problems.

Keywords: Safety management · Safety education · Hidden danger · Laws and regulations · Safety quality

Military activities are full of risks. The process is not only the process of completing military tasks, but also the process of generating and improving combat effectiveness, and the process of fighting against various risks [1]. In recent years, with the continuous deepening of military struggle preparation and the normalization of actual combat training of the army, the security risks of the army have increased significantly, and some difficult problems in security work have gradually become prominent. Therefore, how to solve the security problem under the existing conditions has become a practical problem faced by the army.

1 Prominent Problems Faced by the Current Military Security Management

1.1 Safety Education is Difficult to Enter the Thoughts of Officers and Soldiers

Safety education is an important work that we often talk about. However, due to the lack of feeling of times and charisma, the problems of heart-to-heart talk going through the motions have not been effectively solved. Officers and soldiers often reflect that the safety education is difficult to enter their thoughts, and some are even mechanical, which makes people sleepy. While analyzing the root causes of some accidents and cases,

the most fundamental thing is that safety education has not been effective, resulting in a small number of officers and soldiers wavering ideals and beliefs, ideological and moral decline, breakthrough in the bottom line of law and discipline, and weak safety awareness.

1.2 Early Warning of Hidden Danger is Insufficient

Xun Yue of the Eastern Han Dynasty once said, “Prevention is to take precautions before things happen, succor is to rescue when the accidents happen, punishment is to blame after the accidents. The first thing to do is to prevent, the second thing is to rescue, and the last thing to do is to blame.” It can be seen that the focus of safety work is on “prevention”. The key to prevention is to predict in advance, formulate plans and take the initiative. In some units, the characteristics of no early warning, insensitivity and slow response are common. The root cause is that officers and soldiers lack a sense of active prevention, turn a blind eye to potential safety hazards, or even be insensitive, resulting in weak prevention ability and lack of response measures.

1.3 The Implementation of Laws and Regulations is not Strict

Practical practice has repeatedly proved that the failure to implement laws and regulations is the most common and profound lesson in military accident cases. At present, breakthroughs have been made in the reform of national defense and the army, and the corresponding laws and regulations are also being issued in full swing. For the army, the key is to implement these systems and make them play a guiding role in its work. However, in the actual implementation process, there are still phenomena of low quality, incomplete coverage and even non implementation, resulting in many safety problems and potential accidents.

1.4 Safety Quality and Job Suitability Are Poor

Improving the safety literacy of officers and soldiers is a basic project to prevent major safety problems. Building a strong professional team capable of safety theory research, equipment research and development, education and training and qualification certification is an important guarantee to solve the security problems of the army from the source [2]. However, from the actual situation of the army, the safety quality of some officers and soldiers is far from the post requirements, which is mainly reflected in: Firstly, safety awareness is lacking. The belief that safety work has nothing to do with themselves, the emphasis on work rather than management, and the inability to straighten out the relationship between safety and war preparation is existing to a certain extent. Secondly, there is a lack of safety knowledge. Some safety common sense and necessary risk avoidance knowledge are not mastered enough, resulting in the face of dangerous situations ignorantly or even “active” creation of dangerous situations. Thirdly, the safety skills are not qualified. On the one hand, the enthusiasm of officers and soldiers to participate in skill training is not high. On the other hand, the skill training organized is also lack of pertinence and effectiveness, resulting in the inability to deal with emergencies effectively.

2 Countermeasures for Solving Security Management Problems

Safety work is not the central work, but affects the center, also it is not the overall work, but affect the overall situation. The security management issues summarized above are all prominent factors affecting the stability of the army. Therefore, we should resolutely proceed from the actual situation of the army and do the following work well.

2.1 Highlight Safety Education and Strengthen the Safety Awareness of Officers and Soldiers

To ensure the safety and stability of the army, the first thing is to lay a solid foundation for the safety thought of officers and soldiers and truly put the safety concept into their thoughts. Firstly, find out the real matters. To increase the effect of safety education, we should first grasp the real ideas of officers and soldiers, not only adopt the traditional methods of listening, watching, asking, talking and checking, but also use modern “big data + networking” for accurate arrangement analysis. We should not only rely on ordinary observation and understanding, but also strive to provide information for the backbone of security and the families of officers and soldiers. In addition, we should also pay attention to getting together with officers and soldiers to further enhance their mutual identity, so that they can open their hearts and communicate with you. Secondly, we should make accurate decisions. The thinking and behavior of officers and soldiers are changing dynamically. We do not need one-size-fits-all safety education. We should clarify the actual thinking and psychological changes of individuals, through analyzing specific problems. Thirdly, create a safety culture atmosphere. Culture is implicit education and education is explicit culture. Safety culture is the long-term accumulation of safety education and the internal support of safety education [3]. We should use the platform carrier close to the officers and soldiers to build a strong safety culture, pay great attention to the construction of safety culture, integrate culture into safety, make safety a culture, make officers and soldiers form the habit of consciously grasping safety in the edification of safety culture for a long time, and realize the transformation from “He wants me to be safe” to “I want to be safe”. Fourthly, make good use of accident cases. The price paid with blood is even more alarming. Therefore, it is necessary to carry out warning education in a normal way. Once organized, the hearts and minds of officers and soldiers will be shaken and baptized once, so as to truly let them know awe, guard against fear and abide by the law and discipline. Fifthly, we should innovate means. The 5G era has come, and it is difficult to catch the officers and soldiers blindly using traditional educational means. Therefore, according to the characteristics of “online generation” officers and soldiers, we should catch the online express, integrate modern elements, enrich and expand mobile app, microblog, WeChat and other methods, and speak with fresh data, examples and cases, so as to make safety education more contemporary and grounded, and further enhance the pertinence and effectiveness of safety education.

2.2 Do a Good Job in Safety Prediction Scientifically and Highlight the Key Points of Safety

Putting prevention first is the basic policy of doing a good job in safety and stability. Firstly, we should pay attention to the opportunity of combination. Whenever the task

changes, seasonal changes, environmental changes and other major opportunities, we should predict in advance, study and come up with countermeasures. Whenever major international and domestic events occur, the state and the army issue major policies, and major social problems occur in the garrison, we should analyze and judge the impact in time and do a good job in education and guidance. Secondly, we should pay close attention to risk assessment. When organizing major activities or activities with high risks, the army should implement the safety risk assessment system in strict accordance with the requirements of the regulations, study and formulate targeted preventive measures and implement them. Thirdly, we should thoroughly investigate potential safety hazards. No accident is not really safe; no hidden danger is really safe. Only by eliminating the potential problems affecting safety, the probability of accident cases will be reduced. We should adopt more methods such as spot check, dragnet investigation and cross inspection, implement continuous inspection and guidance, and find out the existing hidden dangers and problems in time [4]. Fourthly, we should be good at using laws. There are objective laws to follow in grasping safety work, such as Hain Rules, Murphy's Law, Cannikin Law and The Butterfly Effect. For the army, it is necessary to strengthen the research on the characteristics and laws of accident cases, grasp the internal mechanism, scientifically predict and prevent in advance, and do a good job in safety work.

2.3 Strictly Implement the Safety System and Standardize the Safety Behavior of Officers and Soldiers

Facts have proved that the stricter the implementation of laws and regulations, the better the effect of the safety and stability work. Firstly, we should earnestly grasp the common sense of laws and regulations. Learning and understanding the law is the premise of abiding by the law. Most of the problems of violation of discipline and law are related to the long-term failure of officers and soldiers to learn and understand the law. We should adopt a flexible way to educate officers and soldiers to understand that laws and regulations are the main compliance of army construction, the basic basis for carrying out work, the fundamental guarantee of the rights and interests of officers and soldiers and the protective weapon for life safety, so as to truly learn and use them. Secondly, we should create an atmosphere of handling affairs according to law. Practice has proved that no matter how many difficult and miscellaneous diseases and historical relics that restrict safety, they can be properly solved sooner or later as long as they are handled according to law and fairly. Therefore, we should effectively put the thinking and mode of the rule of law into all links of our work, so that people are used to do things according to their duties and the rules. Thirdly, we should strengthen inspection and supervision. Without strict inspection and supervision, laws and regulations have become furnishings. To this end, we should pay enough attention to both normal inspection and special inspection, and fully cover the leading organs and grass-roots units. We should not only highlight safety management, but also cover all fields of war preparedness training, and do not give any opportunities to those who leave things to luck. Fourthly, discipline and punishment should be strictly enforced. To grasp the work of safety and stability, we must always adhere to rigid discipline and strict law enforcement, respond promptly to adverse tendencies and problems, and deal with them in time, so as to make laws and regulations an untouchable bottom line. Fifthly, leading cadres should take the lead.

Party committees and leaders at all levels are the main body of enforcing the rule of law, the protagonist of practicing the rule of law and the main force of promoting the rule of law. They should earnestly lead the above, stand as the flag, and consciously abide by rules and disciplines and act in accordance with the law.

2.4 Highlight and Strengthen Safety Training and Strive to Improve Safety Quality

People are the core of safety management, and the quality of officers and soldiers is the basis of safety management [5]. Firstly, we should pay attention to training, so that professional people can be proficient in professional things. On the basis of selecting the right person, the army should take various forms such as pre-job training, post training, learning and training, and pay great attention to the professional training of key targets such as airports, military ports and caverns and safety personnel in key posts, so that they can master the necessary professional knowledge and skills. Secondly, we should pay attention to the drill, and improve the ability of backbone to deal with special situations. The safety plan should be revised in time according to the changes of the situation, and emergency drills should be carried out regularly. Through the training of command, disposal, rescue, coordination and other subjects, the troops can rush to the scene and handle problems safely, so as to minimize losses and impacts. Thirdly, we should highlight the importance of knowing and avoiding risks and strengthen the safety and prevention literacy of all staff. We should pay close attention to the learning and training of safety common sense and skills. In particular, it is necessary to take the learning of safety common sense as a compulsory course in combination with the opportunities of new recruits, new students, new officers and new civilian staff entering the army, so as to enhance the safety awareness and ability of all staff.

References

1. Mei, Z., Xiang, Y., Tao, Y., et al.: Air Defense Unit Management. Zhengzhou Campus, Army Artillery Air Defense College (82) (2021)
2. Wang, M., Zhao, M.: Practical problems and countermeasures of army force safety training. *J. Gun Sci.* (3), 57–59 (2016)
3. Cheng, F.: “Paradox” phenomenon and countermeasures in military safety education. *Army Manag.* (3), 36–37 (2017)
4. Li, Z., Zhang, T., Wang, Y.: Thoughts on military security prevention during the period of deepening national defense and military reform. *Eng. Mil. Acad.* (2), 71–72 (2017)
5. Liu, C., Tao, B., Kong, L.: Adhere to improving the quality of military safety work in strict accordance with the law. *J. Gun Sci.* (1), 48–50 (2016)



Safety Risk Prevention and Control in Army Training: Model and Strategy

Zhenguo Mei^(✉), Qian Shen, Weifei Wu, Kun Cao, and Peng Gong

Artillery and Air Defense Forces Academy (Zhengzhou Campus), Zhengzhou 450052, China
meizg_zz@sina.com

Abstract. With the continuous advancement of real combat training, unsafe factors have increased. Safety risks become increasingly prominent, and accidents occur from time to time. Therefore, it is imperative to strengthen safety risk prevention and control in training. At present, safety risk prevention and control in army training still lacks science and rationality and relies on experience, which lead to low quality and efficiency. The root causes of this problem include unclear understanding of complex training safety risk factors, inaccurate recognition of the causal mechanism of training accidents, and lack of theoretical guidance on training safety risk prevention and control. Based on the modern risk management concept, this thesis sorts out three types of safety risk factors in training, analyzes the cause of training accidents from the perspective of prevention and control shield failure, explores the construction of training safety risk prevention and control model, and innovatively proposes a three-level training safety risk prevention and control system featuring “personnel, material and technology prevention”, “management prevention” and “cultural prevention” and relevant strategies. The thesis provides theoretical guidance and basic principles for the army to carry out training safety risk prevention and control scientifically.

Keywords: Army training · Safety risk · Prevention and control model · Prevention and control strategy · Prevention and control system

In recent years, with the continuous advancement of real combat training, unsafe factors have increased. Safety risks become increasingly prominent, and accidents occur from time to time. Therefore, it is imperative to strengthen safety risk prevention and control in training [1]. To scientifically carry out safety risk prevention and control in army training, it is necessary to re-divide safety risk factors, build a training safety risk prevention and control model, and explore innovative training safety risk prevention and control system and strategies, so as to provide direction and guidance for the army to carry out prevention and control scientifically.

1 Division of Army Training Safety Risk Factors

The safety risk factors in army training are very complex, involving personnel, task, equipment, material, facility, training field, road, weather, and management, etc. Based on their nature and roles in the formation of training accidents, these factors can be

divided into three categories: root risk factors, direct causative factors, and indirect causative factors. Here they are called the first type of risk factors, the second type of risk factors, and the third type of risk factors [2], as shown in the Fig. 1.

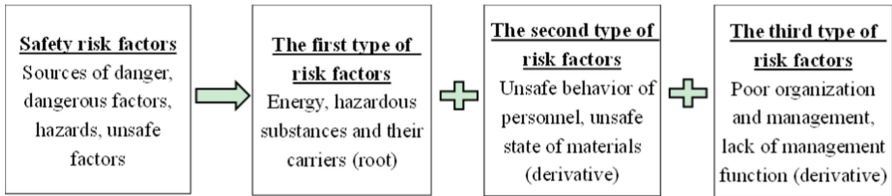


Fig. 1. Division of army training safety risk factors

1.1 The first type of risk factors: root risk factors

This type of risk factors refer to various energy, hazardous substances and their carriers in army training. They are inherent sources of danger, and the root risk factors of training safety risks. They include missile, cannonball, bullet, grenade, detonator, explosive, oil and other ammunition material (energy and carrier), light weapon, artillery, missile launching equipment, motor vehicle, facility and equipment (energy carrier), poisonous food, poisonous liquid, poisonous gas and the pathogenic microorganism and toxin it produces, electromagnetic radiation, and other harmful substances (harmful substances and carriers). Most of these risk factors belong to the material conditions of army training, which exist objectively in the training process. They are the source of training safety risks and the material premise and internal cause of training accidents, affecting the occurrence of training accidents and the severity of consequences. The existence of root risk factors in training makes accidents possible. Without these root risk factors, accident would never happen.

1.2 The second type of risk factors: direct causative factors

Such risk factors refer to human behavior errors and material failures (including physical environmental factors such as poor training field environment) during army training, which can be summarized as unsafe behavior of officers and soldiers, unsafe state of equipment and materials, and unsafe training field environment. They are the direct causative factors that trigger the uncontrolled and accidental release of the first type of risk factors (ie, energy or harmful substances and carriers). There are many direct causative factors in army training, among which the unsafe behavior of officers and soldiers is mainly manifested in operational error and command error, including illegal organization, illegal command, illegal safeguard, illegal operation, and various unsafe habits and other human error factors. The unsafe state of equipment and materials is mainly manifested in the safety defect of equipment (in design), the failure of equipment (caused by improper maintenance), the safety defect of facilities and equipment (caused by improper design and maintenance), etc. The unsafe training field environment is mainly manifested in complex terrain, poor geological conditions, rough roads, bad weather, etc. Such safety risk factors are various unsafe factors that lead to the failure or destruction of shielding measures (shields), which are used for constraining and limiting energy. They are the defects and loopholes of shields, the external cause of

training accidents, also the direct cause. The existence of direct causative factors induces the accidental release of energy or harmful substances and makes accidents possible. Without these direct causative factors, even if energy or harmful substances exist, when released according to normal demand, accidents will not happen.

1.3 The third type of risk factors: indirect causative factors

This type of risk factors refers to organizational and management problems and factors in army training, such as unscientific organization, unstandardized management, and inadequate supervision. They cause the second type of risk factors (direct causative factors) to happen, and are the indirect cause of accidents, so they are called the indirect causative factors. Indirect causative factors in army training mainly include unscientific preparation, unreasonable plan, imprecise organization, loose management, unstandardized order, inadequate inspection, lack of supervision and other management problems or loopholes. They are not the direct cause of training accidents, but the reason behind direct cause, which belong to the deep-level organizational and management reasons for the occurrence of accidents. Because there are various organizational and management problems in army training, organizational and management function fails, causing unsafe behaviors of officers and soldiers, unsafe state of equipment and materials, and unsafe environment, making training accidents possible. (However, it must be admitted that some unsafe states and conditions of equipment, materials and training field environment exist objectively and are difficult to be completely eliminated.)

2 Training Safety Risk Prevention and Control Model

2.1 Analysis of the cause of training accidents

By dividing the safety risk factors in army training, it can be seen that the occurrence of training accidents is the result of the accidental release of energy and harmful substances such as equipment and ammunition. Energy and harmful substances exist objectively, and their accidental release is due to the unsafe behavior of officers and soldiers and unsafe conditions of equipment and facilities, resulting in the loss of control of energy and harmful substances. The existence of unsafe behaviors of officers and soldiers and unsafe conditions of equipment and facilities indicates that the preventive ability of operators, namely “personnel prevention” and the preventive condition of equipment and facilities, namely “material prevention” and “technology prevention”, have failed. This is failure of the first level prevention and control.

The failure of the first-level prevention and control shield is essentially a problem of “personnel prevention”, “material prevention” and “technology prevention”. Existing loopholes result in unsafe behavior of officers and soldiers and unsafe conditions of equipment and facilities. Weak organization, poor management, and failure of management function also lead to the occurrence of unsafe behavior of officers and soldiers and the emergence of unsafe conditions of equipment and facilities. This is the failure of second prevention and control measures (shield) [3].

The failure of the second-level prevention and control shield is essentially a problem of organization and management, that is, the management foundation is not solid, the organizational system is not sound, and the supervision is incomprehensive. Existing loopholes result in the failure of organizational and management functions, but the

failure also reflects deeper contradictions behind the organization and management, that is, the safety atmosphere is not strong, the safety environment is poor, and the safety culture is lacking. The core problem lies in the construction of safety culture in army. This is the failure of the third-level prevention and control shield.

2.2 Construction of safety risk prevention and control model

According to the analysis of the cause of training accidents, it can be seen that the failure of the first, second and third-level prevention and control shields during training process results in the occurrence of unsafe behavior of officers and soldiers and unsafe state of equipment and facilities. This then triggers the root risk factors, which lead to uncontrolled and accidental release of energy or harmful substances, and finally result in casualties, damage to equipment and materials or property losses. Based on this, a training safety risk prevention and control model can be constructed, as shown in Fig. 2.

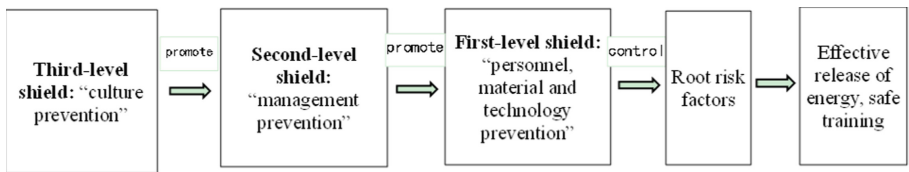


Fig. 2. Army training safety risk prevention and control model

The model contains the first-level prevention and control shield featuring “personnel, material and technology prevention”, the second-level prevention and control shield featuring “management prevention”, and the third-level prevention and control shield featuring “culture prevention”.

3 Training Safety Risk Prevention and Control Strategies

According to the training safety risk prevention and control model, the strategy for safety risk prevention and control is: to improve and perfect the three-level training safety risk prevention and control system featuring “personnel, material and technology prevention”, “management prevention” and “culture prevention”; to strengthen the three-level training safety risk prevention and control function, and to do a solid job in training safety risk prevention and control, so as to ensure that training is carried out safely and smoothly [4].

3.1 Build a solid first-level prevention and control shield: strengthen the quality cultivation of officers and soldiers, do well in construction and maintenance of equipment and facilities, and focus on improving the level of “personnel, material and technology prevention”

The first-level prevention and control shield is the most direct and important shield for safety risk prevention and control in army training. It directly affects and determines the behavior of officers and soldiers and the state of equipment and facilities. Only when the weapons and equipment are in good condition and facilities are sound and complete can they provide a good material basis for army training. Only if officers and soldiers

attach great importance to safety and possess good operational skills and qualities can they demonstrate standardized and safe operations and correct behaviors in training. On that premise they can further correctly use equipment and ammunition, and make sure ammunition and other root risk factors are under control, so that all kinds of energy can be safely released and used in a highly-effective training.

To this end, the army should start from the following four aspects to improve the level of “personnel, material and technology prevention”, and build a solid first-level prevention and control shield [4]. First is to strengthen education and training. The army should improve the safety awareness of officers and soldiers, focus on enhancing the training safety awareness in air defense forces, and build a “ideological defense line” for training safety. Second is to strengthen skill training. The army should improve the skills and quality of officers and soldiers, focus on ensuring their safe operation, and build a “capability defense line” for training safety. Third is to strengthen the management of weapon, equipment and facilities. The army should do a good job in maintenance to make sure the equipment and facilities maintain a good condition, and build a “material defense line” for training safety. Fourth is to strengthen technical means. The army should improve the level of safety technology, improve conditions that guarantee training safety, and build a “technology defense line” for training safety.

3.2 Strengthen the second-level prevention and control shield: adhere to scientific planning, organization and command, strict and precise management, monitoring, inspection and supervision, and focus on strengthening the “management prevention” function

The second-level prevention and control shield is the key shield for training safety risk prevention and control. It is the core of the three-level prevention and control shield and plays a linking role. “Linking role” means the second-level shield is restricted and influenced by the third-level shield, and can also directly affect and the first-level shield and its effect. With the premise that the training planning is well organized, the training command is precise, the training management are strict, the training inspection and supervision are in place, and the training process is orderly, the army can guarantee the behavior of officers and soldiers be effectively controlled, the equipment is in good condition, and the facilities are complete and perfect. In this way, the energy and harmful substances such as ammunition can be effectively controlled and released, in order to achieve the goal of safe and efficient training.

To this end, the army should start from the following four aspects to strengthen the “management prevention” function, and build a solid second-level prevention and control shield. First is to strengthen overall planning and coordination, make scientific plan, arrange training progress reasonably, and avoid reckless decision. Second is to follow training rules, organize and implement the training scientifically, command and control precisely, and eliminate empiricism. Third is to manage strictly according to regulations, standardize training order, and avoid chaotic training. Fourth is to strengthen training supervision, inspect and solve problems timely, and eliminate illegal behavior.

3.3 Strengthen the third-level prevention and control shield: strengthen the construction of safety culture, continuously enrich the content of training safety culture, and strive to create an atmosphere of “culture prevention”

The third-level prevention and control shield is the core of training safety risk prevention and control. It is an important measure and the fundamental approach for training safety risk management, and directly affects the first and second-level shields and their effects. With the premise that in the army, safety culture is well established, safety conditions have been improved, safety environment and atmosphere are strong, the army can fully exert the penetrating and infectious power of safety culture, make sure the culture affects the organization and management system, and use the system to affect the consciousness and behavior of officers and soldiers and the state of equipment and facilities. In this way, the army can achieve the goal of “safety for everyone, safety in everything, safety at any time”, and ensure the safety and smoothness of the training process.

To this end, the army should start from the following four aspects to create a “culture prevention” atmosphere and build a third-level prevention and control shield. First is to firmly establish the concept of safety development, learn safety common sense and scientific theory, improve working mechanism, and constantly enrich the content of safety system. Second is to establish safety conditions, improve training safety technology, and continuously enrich the forms of safety materials. Third is to strengthen the management of standard operation, develop good behavior habits of officers and soldiers, and continuously enrich the forms of safety behavior [5].

4 Conclusion

Based on the modern risk management concept, this thesis focuses on the status quo and problems of safety prevention and control in army training, sorts out the first, second and third types of safety risk factors in training, analyzes the cause of training accidents from the perspective of prevention and control shield failure, explores the construction of training safety risk prevention and control model, and innovatively proposes a three-level training safety risk prevention and control system. The thesis provides theoretical guidance and basic principles for the army to carry out training safety risk prevention and control scientifically.

Compliance with Ethical Standards. The study was approved by the Logistics Department for Civilian Ethics Committee of Artillery and Air Defense Forces Academy (Zhengzhou Campus).

All subjects who participated in the experiment were provided with and signed an informed consent form.

All relevant ethical safeguards have been met with regard to subject protection.

References

1. Mei, Z., Wu, W., Gong, P., Shen, Q., Cao, K.: Research on workflow of safety risk management in army training. In: Long, S., Dhillon, B.S. (eds.) MMESE 2021. LNEE, vol. 800, pp. 719–725. Springer, Singapore (2022). https://doi.org/10.1007/978-981-16-5963-8_97
2. Hu, Y.: Safety Risk Prevention and Control. Unity Press, Beijing (2018)
3. Wang, Z.: Risk Management. China Machine Press, Beijing (2020)
4. Fu, G.: Safety Management Science: Behavior Control Methods for Accident Prevention. Science Press, Beijing (2019). (12)
5. Mei, Z., et al.: Research on Important Issues and Difficulties in Air Defense Force Management. PLA Press, Beijing (2020)



Discussion on the Control of Major Hazard Sources in Unit Training

Weifei Wu, Zhenguo Mei^(✉), and Kun Cao

Artillery and Air Defense Forces Academy (Zhengzhou Campus), Zhengzhou 450052, China
meizg_zz@sina.com

Abstract. With the continuous increase in the intensity and difficulty of actual combat training, the training of unit has also shown the characteristics of normalization and frequency, and the sources of danger involved in training have become more and more numerous and more complex, and it is an important task to strengthen the effective control of major sources of danger and ensure the safety of the training of unit at present and even in the coming period. Based on the actual situation of unit training, this paper puts forward targeted countermeasures and measures for the control of major hazard sources in unit training, providing scientific reference for the control of major hazard sources in unit training, in order to improve the safety management level of unit training.

Keywords: Unit training · Major hazard sources · Controls

In recent years, under the guidance of the goal of strengthening the army, the PLA has set off a boom in real-combat training, and all levels of the PLA attach great importance to training safety. President Xi Jinping has specifically pointed out in the No. 1 Order of the Central Military Commission in 2022 that safety training should be carried out. To ensure the safety of training and reduce the impact of training accidents, the most effective and direct way is to take practical and effective control measures on the hazard sources that may cause accidents.

Article 96 of the Work Safety Law stipulates that a major source of danger refers to a unit (including premises and facilities) in which the quantity of dangerous goods is produced, handled, used or stored for a long time or temporarily equals or exceeds the critical amount. Military units, as the main body of long-term use of dangerous goods, may cause accidents are much more likely. Therefore, we can define the major hazards of unit training as: the collection of various factors that may lead to accidents of general and higher level in the course of unit training [1].

Hazard source is the premise of accident and the main body of energy and material release in the process of accident. Effective control of hazard sources, especially major hazard sources, is great important to ensure the safety of officers and soldiers and training safety [3]. In the research, this paper will also closely combine the actual situation of unit training, put forward targeted measures for the control of major hazard sources in the training of unit, in order to improve the safety management level of unit training.

1 Determine Control Principles [4]

According to the definition of major hazard sources, hazard sources are potential unsafe factors that may lead to accidents. In practical training, hazard sources are of various types and very complex, and their roles in causing accidents and causing personal injury and property loss are also quite different. Accordingly, the principles governing them are markedly different.

1.1 Hierarchical Management Principles

The danger level of the major hazards in unit training can be divided into four levels. The danger level of the major hazards in different levels is also different. The danger level of the major hazards in grade 1 is the highest, and the danger level of the major hazards in grade 4 is the lowest. According to the danger grade classification of major hazard sources, it is necessary to effectively control the major hazard sources according to the principle of hierarchical management and control.

1.2 Key Control Principles

The importance degree of major hazards in unit training is different, so it is necessary to distinguish and control them according to their importance degree. On the basis of risk level control, the unit should also distinguish key, sub-key and general risk sources according to their importance.

1.3 Principle of Differentiated Liability

For the control of major hazards in unit training, responsibilities should be differentiated according to the actual situation, mainly to clarify the specific responsibilities of relevant control personnel. The principle of differentiated responsibility requires that responsibility be refined and reward and punishment be distinct. Responsibilities, control standards and relevant requirements of control personnel at all levels of battalion, company and platoon should be clarified in detail, and corresponding rewards and punishment measures should also be clarified to further improve the sense of responsibility of control personnel.

2 Improve the Control System [2]

In order to effectively reduce the occurrence of accident cases, teams at all levels should improve the control system of major hazard sources, mainly from the following aspects.

2.1 Registration and Filing System

Major hazards involve a wide range of sources, and their basic information and impact consequences should be recorded in detail. If there is no registration and filing, when controlling major sources of danger, it is easy to leak pipes, less management, and inadequate control. Once these situations occur, a major hazard out of control, it is likely to cause accidents, and bring a very adverse impact to the unit. Therefore, all levels of the unit should register and file all the major hazard sources under control one by one, which is an important guarantee to ensure the safety and efficiency of the unit training, and also a prerequisite for the safety management of major hazard sources.

2.2 Safety Assessment System

Major hazards can be classified into grades and degrees. According to the identification and analysis results of major hazard sources, the unit should choose appropriate evaluation methods, conduct qualitative and quantitative evaluation of the possible consequences of major hazard sources, and grade them to determine the focus of control. The establishment and implementation of safety assessment system can timely and effectively grasp the location and dynamic change information of major hazard sources, and effectively take corresponding control measures for major hazard sources.

2.3 Practice and Drill System

Practice is the only standard to test truth, and practice is also the best way to acquire skills. In carrying out practical exercises, the emphasis should be placed on improving the emergency response capabilities of officers and soldiers, ensuring not only the implementation of training time, sites and equipment, but also the actual mastery of skills. Perfecting and implementing the practice and drill system is a reliable guarantee to prevent training accidents effectively.

3 Strengthen Learning and Education

To strengthen safety awareness, it is necessary to strengthen safety education and study, which is also the fundamental measure to prevent training accidents. From the perspective of training accidents in recent years, there are objective reasons, but more of them are subjective reasons of the parties involved.

3.1 Strengthen Safety Concept Education

Safety is not the center but affects the center, this sentence is familiar to everyone, but at present, most officers and soldiers are not familiar with the relevant content of safety concepts, safety regulations, major sources of danger, etc., and their connotation characteristics are not firmly grasped. Therefore, it is necessary to strengthen education and learning of the safety concept, safety regulations and major hazard, so that officers and soldiers firmly establish safety training awareness and keep in mind the provisions of training and operating procedures, which can improve the understanding of major hazard and enhance safety prevention awareness.

3.2 Strengthen Theoretical Knowledge Learning

In the survey, it was found that most officers and soldiers had a wrong view of paying more attention to practical operation than to theoretical learning. If the theoretical knowledge of the accident is not fully grasped, it is very prone to irregular operation behavior in training. Therefore, it is necessary to strengthen the study of training theory, safety knowledge and accident prevention skills, so that officers and soldiers can improve their ideological understanding, increase theoretical knowledge, master skills and methods, so as to further improve the reliability of training safety and effectively reduce or prevent the occurrence of training accidents.

4 Implement Whole-Process Control [5]

Major hazard sources exist at all times and in all links of training. To strengthen the control of major hazard sources in training, it is necessary to control the whole process, all posts and all equipment. To implement whole-process control means that every link, every officer and every piece of equipment should not be neglected. Only in this way can we ensure the safety, order and efficiency of the training.

4.1 Check the System Before Training

Before the training begins, we should focus on systematic investigation. First of all, it is necessary to check whether the thought, body and psychological factors of the training personnel meet the requirements of participating in the training, especially in the live ammunition training. The personnel with unstable thoughts, physical discomfort and poor psychological quality should carry out targeted training in advance. Secondly, the inspection of weapons and equipment should be done well, including training equipment and support equipment, so as to meet the needs of training at all times. Thirdly, the training site should be investigated one by one in strict accordance with the requirements to ensure the safety of training.

4.2 Inspection and Supervision During Training

Training is also an important stage in which accidents are most likely to occur. Unit commanders should attach great importance to and strictly inspect and supervise the training, and correct the problems found in time to ensure safety in training. First of all, it is necessary to supervise and inspect whether the trainees strictly implement the operation rules, and resolutely put an end to subjective assumptions, flexible and simplified command procedures, soil training laws, experience and habits instead of laws and regulations and other violations of the rules and regulations. Secondly, it is necessary to inspect and supervise whether the support personnel seriously perform their duties. War in the information age is fighting support, and its status cannot be ignored. The smooth implementation of training is closely related to support personnel. Thirdly, the security control of weapons and equipment should be inspected and supervised, focusing on whether the control measures of guns, ammunition and artillery equipment are effective, and whether there are problems such as ineffective control, weapons loss and equipment littering in training.

4.3 Summarize After Training

The end of training does not mean that the security alert can be dismissed. First of all, the detachment should organize a summary and appraisal, summarize the basic situation of the training, the achievements made, point out the existing problems, and clarify the next step, focus on highlighting the problems, especially the personnel who are ineffective in controlling major sources of danger, and carry out criticism and education for those who operate in violation of the law and do not obey the command; Secondly, the safety status of the equipment should be checked and accepted, and the damage should be sent for repair in time, the cause of the loss should be identified, and the responsibility of the relevant personnel should also be investigated for guns and other dangerous goods; Thirdly, It is necessary to attach great importance to the safety of returning to the camp, do a good job in the ideological education of personnel, and keep abreast of the changes in the thinking of personnel, especially after high-intensity training, whether there are personnel with large fluctuations in ideological changes, and treat them in a timely manner.

References

1. Mei, Z., et al.: Research on Key and Difficult Problems of Air Defense Force Management. PLA Press, Beijing (2020)
2. Luo, Y., Yang, G.: Control of major hazards in air defense training. Zhengzhou: J. Air Defense Force Coll. 65–67 (2013)
3. Wang, Q.: Safety Assessment of Major Hazard Sources. China Meteorological Press, Beijing (2010)
4. Guo, X., Zhang, W., Gao, H.: Research on problems existing in the management of major hazard sources. Charm China (3), 210 (2011)
5. Hu, D.: Security Theory of Military Training. National Defense University Press, Beijing (2010)



Risk Assessment in Air Defense Forces Unit Training

Qian Shen, Zhenguo Mei^(✉), Xuechen Yao, and Weifei Wu

Artillery and Air Defense Forces Academy (Zhengzhou Campus), Zhengzhou 450052, China
meizg_zz@sina.com

Abstract. As an essential effort in air defense forces (ADF) unit training risk management, risk assessment plays an central and critical part in ADF unit training risk management. To conduct proper and effective risk assessment, some certain basic principles should be followed, and an overall assessment process need to be clarified, thus providing scientific basis for ADF unit to control training risks, as a contribution to the effective control of training risks, to promote safety in ADF unit training. In this context, this thesis focused on the principles for risk assessment in ADF unit training, the basic steps included in risk assessment process, and some issues needed particular attention in risk assessment as attentions to Longford Trap, distortion of assessment conclusion, and identification of critical risk points.

Keyword: Air defense forces · Training risks · Risk assessment

1 ADF Unit Training Risk Assessment Principles

ADF training risk assessment principles, were basic guidelines for ADF units to execute training risk assessment. To conduct ADF training risk assessment properly, it is necessary to follow such principles as integrity, accuracy and dynamics [1].

1.1 Integrity

Risks in unit training involved multiple potential causes as training tasks, participants, materiel, environment, and administration, and presented in forms as accidents, disasters or hazards, which existed in multiple risk points through the entire training process [5]. Rather than assessment on a certain risk factor or sampling on some of the factors, risk assessment in ADF training should be an integrated assessment on all risk factors. Therefore, risk assessment in ADF training should follow the principle of integrated assessing, based on the analysis and judgment of all risk factors in training, to focus on the comprehensive assessment of the hazard source, level and probability, and to conduct overall assessment on the entire training operation, thus producing scientific and accurate assessment conclusions.

1.2 Accuracy

Accuracy is where the central tenet and value of training risk assessment laid in [3]. Without accurate assessment, unit leaders may misjudge the risks in training, leaving uncontrolled primary risk points, ineffective risk control, and significant accident potentials in unit training; while considerable resources were diverted to those risk points of less importance for prioritized control, with less effectiveness and waste of personnel, assets and finance. Therefore, risk assessment in ADF training should follow the principle of accuracy, to employ an array of scientific assessment methods comprehensively, execute scientific risk assessment with adequate and reliable data and information, and to make assessment conclusion accurate and objective, and corresponded with unit training practice, providing basis for training risk control.

1.3 Dynamics

As the progressing of ADF unit training activities, and changing of time and environment, factors in training activities would change; some risk factors may decline or disappear; while some factors may escalate; and some new factors may even emerge, which caused unit training risk changing dynamically. However, as risk assessment were typically conducted before training progress to estimate risks in unit training activities, which were understanding and reflection of unit training risk situation at that time, the risk assessment conclusion were characterized with relativity and timeliness. Therefore, training risk assessment should follow the principle of dynamics, and unit leader would both highlight the prediction, estimation and evaluation of future training risks before the training progress to enhance risk control in advance, and prioritize the dynamic follow-up assessment through the training progress to modify assessment conclusions in time and respond properly and effectively.

2 ADF Unit Training Risk Assessment Process

As a progress involved an array of activities, ADF unit training risk assessment consisted of four major steps as follow.

2.1 Identify Assessment Subject and Establish Assessment Tenets [4]

Identifying assessment subject and establishing assessment tenets would be the first step in training risk assessment process. The assessment subject referred to the risks in unit training, including risk causes, risk points, training activity risks, etc. Based on identification of training risk, to conduct assessment on critical risk points, it should be noted that some minor risk points may be clearly concluded early in risk identification stage without further risk assessment. In accordance with risk identification conclusions, analyze those risk points may impose critical effect on unit training as the subject for risk assessment.

2.2 Select Assessment Method and Execute Itemized Assessment [4]

Itemized assessment involved risk assessment across every single training risk points identified, to determine risk degree, level, and probability. It included such three actions as selecting assessment method, estimating index values, and conducting assessment calculation. First, select proper method for risk assessment according to various situation of all risk points. Specifically, it is to consider requirements as assessment operators proficiency, competence, and timeliness based on various situation of all risk points and characteristics of each assessment method, to screen an assessment method that was practical for the subject. Second, estimate index values. Estimated index values provided important basis for calculating risk degree and determining risk level. It involved analysis and judgment on assessment indexes of possible risk events, comparison with index value intervals of certain assessment method, thus determining the assessment index value of each risk points. Finally, to conduct assessment calculation. With estimated assessment index value of each risk points and established assessment method, to calculate the risk degree and probability, to determine the risk level of each risk points according to risk level criteria.

2.3 Conduct Comprehensive Assessment and Produce Assessment Conclusions [4]

Comprehensive risk assessment involved assessment activities throughout the entire unit training progress, including segmental risk assessment, overall risk assessment and assessment conclusion production.

First, segmental risk assessment. Segmental risk assessment involved comprehensive calculation to identify the risk level and probability based on itemized assessment. According to assessment results of each risk items, segmental risk assessment would follow the principle of “risk level prefers high to low and probability prefers high to low”, to calculate and assess the risk situation of each risk points.

Equation to calculate the risk level of each training stage (first category one index):

$$D_i = \max\{D_{ij}, j = 1, 2, \dots, n_i\} (i = 1, 2, \dots, N) \quad (1-1)$$

where D_i is the risk level of the No.i first category index in training; and D_{ij} is the risk level of the No.j risk point of the No.i first category index in training; n_i is the number of risk points of the first category index in training.

Equation to calculate the risk probability of each training stage (first category one index):

$$P_i = \max\{P_{ik_i} | \max[D_{ij}, j = 1, 2, \dots, n_i], k_i = 1, 2, \dots, m_i\} (i = 1, 2, \dots, N) \quad (1-2)$$

where P_i is the risk probability of the No.i first category index in training; and P_{ik_i} is the risk probability of the No.k_i highest risk level risk point of the No.i first category index in training; k_i is the serial number of highest risk level risk point of the first category index in training; m_i is the number of highest risk level risk points of the first category index in training.

Second, overall risk assessment. Overall risk assessment involved calculation and assessment of the overall training risk situation based on assessment of each first category index (assessment subject), in accordance with the principle of “risk level prefers high to low and probability prefers high to low”.

Equation to calculate the overall training risk level:

$$D_z = \max\{\max[D_{ij}, j = 1, 2, \dots, n_i], i = 1, 2, \dots, N\} \quad (1-3)$$

where D_z is the overall training risk level.

Equation to calculate the overall training risk probability:

$$P_z = \max\{\max\{P_{ik_i} | \max[D_{ij}, j = 1, 2, \dots, n_i], k_i = 1, 2, \dots, m_i\}, i = 1, 2, \dots, N\} \quad (1-4)$$

where P_z is the overall training risk level.

Third, assessment conclusion production. It involved determining the overall risk level and probability in training based on overall risk assessment calculation result, and determining risk warning employment and critical risk points according to the risk level of each risk points and the overall training process. Typically, to determine the critical risk points, risk points and critical risk source above risk level 3 would be categorized as critical risk points.

2.4 Propose Recommendations and Present Assessment Report [4]

As risk assessment conclusions were produced, then the assessment personnel may propose preliminary risk control recommendations according to assessment conclusion. For example, to propose recommendation to correct mistakes concerning violation of safety regulations and technical standards; to propose recommendations to optimize flaws in safety control organization and manning; to propose recommendations and measures on technical prevention of those risk factors may cause accident or even major accident.

3 Issues Needed Attention in ADF Unit Training Risk Assessment

In ADF unit training risk assessment, there were such three facets needed attention as avoidance of Longford Trap, attentions to distortion of assessment conclusion, and identifying critical risk points carefully.

3.1 Avoidance of Longford Trap

Longford Trap referred to the tendency of purely reliance on risk assessment conclusions, focusing on those “minor accident risk” of high probability and high risk level, rather than control of those “major accident risk” of low probability and low risk level and resulted in major accidents [2].

This was same for ADF units. To conduct risk assessment for those major training evens as “Three Live” training, live exercise along with other training activities of high

risks, especially for those analysis on the probability of risk factors which may cause major training accident, it should be particularly aware of the lowered probability due to rigid control and it is a must to put its serious aftermath into consideration, in order to avoid Longford Trap.

3.2 Attentions to Distortion of Assessment Conclusion

Training risk assessment was the risk level estimation based on the seriousness of each risk point and their probability. Both the seriousness of risk aftermath and their probability, were subjective estimation and judgment base on risk assessment personnel's understanding of the risk point situation. As they were subjective judgment, the result may be inaccurate and the estimated value may be higher or lower, especially when it was hard to estimate the probability and the result may be even more inaccurate. The inaccuracy in estimated assessment index value may lead to distortion of assessment conclusion. Therefore, when conducting training risk assessment, assessment personnel must pay additional attention to distortion of assessment conclusion.

3.3 Identify Critical Risk Points Carefully

Identification of critical risk points was an important part of training risk assessment conclusion. To identify critical risk points in training, it is to conduct in the following three aspects. First, identify critical risk points based on training risk level. Pay attention to those risk points above risk level 3, and pick up those risk points of above risk level 3 as critical risk points at first glance. Second, to identify those critical risk source of low probability as critical risk points. Third, to identify those risk points with high sensitivity and low robustness as critical risk points to pay additional attention. Although some of the risk points in training would be estimated as lower risk level, as their high sensitivity and low robustness, once situation changed, the risk probability may increase a lot bit, and the risk level may increase up to level 3 and above. Therefore, these risk points need to be leveled as critical risk points with special care and to be controlled rigidly.

References

1. Yan, C.: Basic Knowledge of Risk Management. Economy & Management Publishing House, Beijing (2018)
2. Hu, Y.: Risk Prevention and Control. Economy & Unity Press, Beijing (2018)
3. Shao, H., et al.: Risk Management Principles and Methods. China Petrochemical Press, Beijing (2010)
4. Sun, X.: Risk Management. Economy & Management Publishing House, Beijing (2007)
5. Zhao, T.: Research on Combat-Oriented Training for ADF. PLA Press, Beijing (2017)



A Framework of Aircraft Error-Prevention Verification Based on Routine Maintenance During Flight Test

Yuqi Zhang^(✉), Feimin Li, and Hongjiao Wu

Chinese Flight Test Establishment, Xi'an 710000, China
214106366@qq.com

Abstract. The Proportion of flight accidents caused by human error is increasing year by year. error-prevention design, as the most fundamental way to overcome human error, is very important for aviation equipment. However, at present, the error-prevention verification during flight test is mainly aimed at single equipment, which lacks systematicness and comprehensiveness. In this paper, we firstly analyzed the characteristics of routine maintenance and the correlation between it and error-prevention evaluation. Secondly, a multi-dimensional error-prevention evaluation criterion is constructed, and on this basis, an error-prevention daily verification system is formed, which can not only effectively improve the systematicness and comprehensiveness of error-prevention verification, but also improve the efficiency and accuracy of error-prevention verification. At present, this method has been applied to a type of helicopter, and the evaluation results can strongly support the maintainability design improvement.

Keywords: Error-prevention · Flight test · Routine maintenance · PFMEA

1 Introduction

Since the 21st century, the reliability of aircraft have been increasingly improved, and human error has gradually become one of the main causes of aviation accidents [1]. The proportion of accidents and symptoms caused by maintenance errors is also increasing year by year [2, 3]. To solve the problem caused by human error, error-prevention is the most direct method. Flight test is an important stage for a new aircraft. The error-prevention problem in this stage will be exposed at the first time, and becoming an important factor affecting flight safety [4, 5]. At the same time, flight test is an important maintenance stage of aviation equipment. Therefore, it is very necessary to provide an efficient, comprehensive and systematic error-prevention verification method for flight test stage.

The contents of the routine maintenance work during flight test almost covers all the inspection and maintenance of aircraft, this paper gave an error-prevention qualitative verification framework based on routine maintenance, and transform the verification from special to daily. This framework is effective to save manpower material resources of error-prevention verifying, and it can improve the systematicness and comprehensiveness of error-prevention verification.

2 The System of Routine Maintenance During Flight Test

2.1 Main Contents of Maintenance Work During Flight Test

The routine maintenance work during flight test mainly includes pre-flight preparation, re-flight preparation, direct-flight preparation and post-flight maintenance. In addition, there are periodic inspection, special inspection, ground experiment and fault removal, etc., as is shown in Fig. 1. Flight day work is the work carried out every flight, which is characterized by high frequency, high repeatability and changeable working environment. Other ground work is interspersed in the flight task and has no direct relationship with the daily flight. It is characterized by low repeatability and relatively fixed working environment.

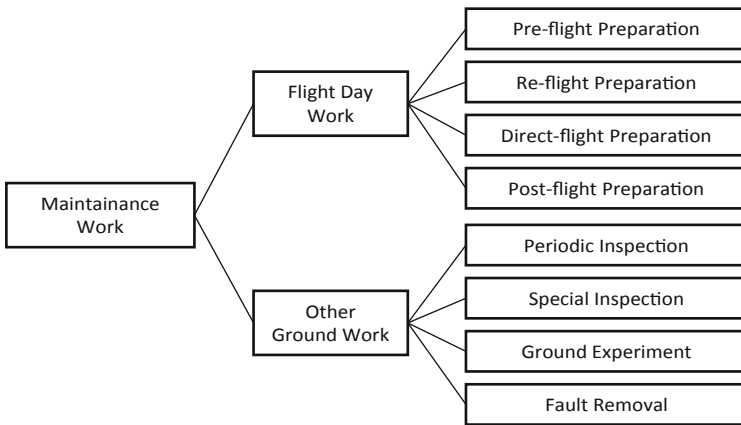


Fig. 1. Diagram of maintenance system during flight test

2.2 PFMEA-Based Decomposition of Routine Maintenance

Process Failure Mode Effect Analysis (PFMEA) is a method to analyze potential process risks in FMEA. It is a bottom-up inductive analysis method based on process decomposition. PFMEA is a systematic tool, which can be used for product of maintenance, production and operation process [6, 7].

The routine maintenance work during flight test involves different systems. Different system may have same work content and steps. In this paper, based on the process decomposition idea of PFMEA, the routine work of maintenance is divided from the aspects of work scene and maintenance content including maintenance steps, as shown in Fig. 2. Take the re-flight preparation for example, The process of maintenance task decomposition is presented in Fig. 3.

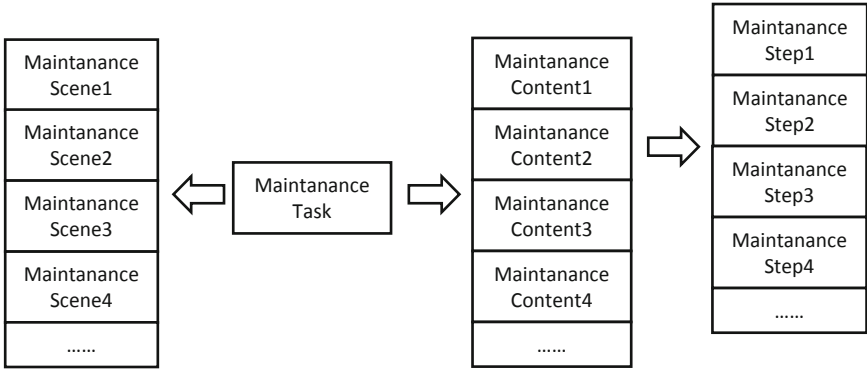


Fig. 2. Maintenance task process decomposition diagram

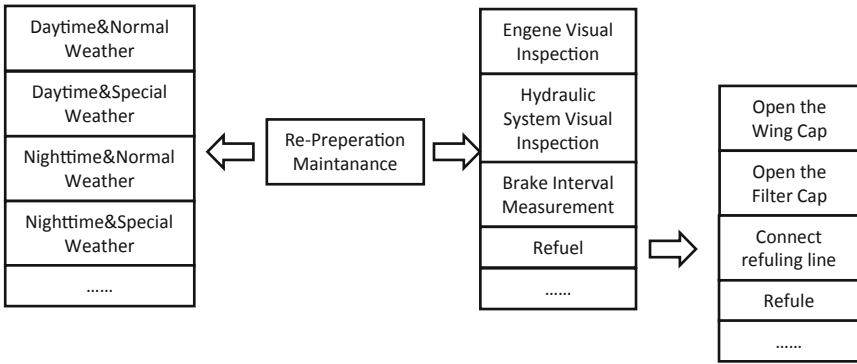


Fig. 3. Re-preparation maintenance process decomposition diagram

3 Multi-dimensional Matrix Error-Prevention Evaluation Criterion

We classified the requirement of error-prevention to form the matrix criterion which is shown in Table 1, so that we can directly cut out the error-prevention requirements according to the systems or hierarchicals and develop effective verification forms. So, the error-prevention design problems of the whole machine system can be investigated according to the evaluation criteria to prevent omission.

First of all, the evaluation requirements of aviation equipment error-prevention are sorted out. Then, the requirements are analyzed by multi-dimension and hierarchies, to form the evaluation criterion. The construction idea is showed in Fig. 4. We extracted requirements which can be verified in re-flight preparation work and make a table for verify error-prevention. Part of the table is showed in Table 2.

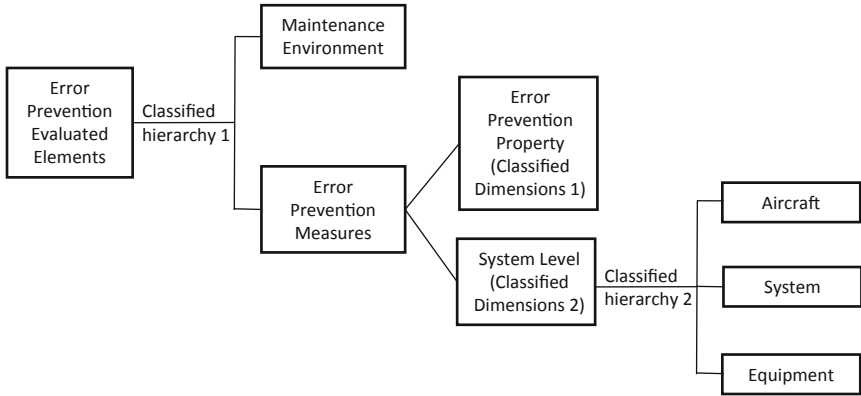


Fig. 4. Construction of multi-dimensional error-prevention evaluation requirement matrix

Table 1. Multi-dimensional error-prevention evaluation matrix for error-prevention attribute and system dimension

	①	②	③	④	⑤	⑥	⑦	⑧	⑨
(1)	●	●	●		●	●	●	●	●
(2)	●	●	●	●	●	●	●	●	●
(3)	●			●	●	●			●
(4)	●			●			●		
(5)		●	●	●	●	●	●		●
(6)	●							●	
(7)		●	●	●	●				
(8)	●			●	●		●		

The typical systems:①Structure; ②Flight Control System; ③Engine system; ④Fuel System; ⑤Hydraulic System; ⑥Environmental Control System; ⑦Avionics System; ⑧ Ground Support System; ⑨Electromechanical system;
 The error-prevention properties: (1)Installation mode/position; (2)Cables and connectors; (3)Pipes and valves; (4)Cap; (5)Switch/button/manipulator; (6)Ground equipment; (7)Protection/safety ; (8)Fastenings

4 The Verification Method of Routine Verification Test for Error-Prevention

The maintenance scene of flight day work is outdoor. The meteorological and climatic conditions vary greatly. The error-prevention verification framework should take specific different maintenance scenes into account to ensure the adequacy of verification. At the same time, the flight day highly repeated during flight test. Therefore, the error-prevention verification of flight day work is planned by orthogonal test method, which not only ensures the adequacy of verification, but also improves the efficiency of verification. The environment of other ground work is mostly indoor, which is relatively stable. So the influence of working environment on the verification test would not be taken into considered.

Table 2. Error-prevention verify table of aircraft maintenance re preparation

Error-prevention check table of re-preperation maintenance				Qualified or not
Working area: landing gear area				
System	Content	Steps	Requirements	
ECS	Ram air valve inspection	Check no damage and blockage	The installation direction of one-way valve should be error-proof	
Landing gear	The body check	Check landing gear hubs, brakes, etc.	Installation of landing gear ducts, hoses and wires should be error proof	
		The upper lock is located in the unlocking position	The landing gear should have interlocking safety device in ground state to prevent misretract landing gear	
Working area: hydraulic system and surrounding area				
Hydraulic	Check hydraulic system and hydraulic components in the vicinity	Hydraulic pump leak inspection	Hydraulic pump design should ensure that there is no wrong connection or installation	
			Hydraulic pump oil inlet, oil outlet, oil return port, oil leakage port should be obvious permanent marks	

(continued)

Table 2. (continued)

Error-prevention check table of re-preparation maintenance				Qualified or not
Working area: landing gear area				
System	Content	Steps	Requirements	
		Leakage inspection of hydraulic accessories	The screw hole of the socket shall have sufficient depth or have a joint limit device to prevent the joint from being screwed too far into the socket and damaging the internal mechanism or blocking the flow of oil	
			If the hydraulic fittings are likely to fail or damage parts due to the reverse or misplacement of the fittings on the aircraft, the design of the hydraulic fittings shall ensure that no incorrect connection or installation occurs	
.....(Other Requirements)				
Questions record for not qualified items				

Orthogonal test considers the maintenance working environment under meteorological conditions, day and night conditions and climate conditions, each factor has two different levels. Adopt the orthogonal test design method [8, 9], we establish experimental table (L₄2₃) as shown in Table 3.

5 The Framework of Routine Error-Prevention Verification

For a maintenance task, the error-prevention verification framework is formed as shown in Fig. 5. Firstly, the PFMEA method is used to decompose the tasks into contents and steps. According to the system and equipment involved in the maintenance steps, we index the corresponding task effective verification requirements from the error-prevention requirement matrix and generate the error-prevention verification table of

Table 3. Orthogonal test table of routine maintenance error-prevention verification (L_42^3)

Number of test	Factors		
	The meteorological environment	Climatic conditions	Day and night conditions
1	Normal weather	Normal climate	Daytime
2	Special meteorological	Special climate	Daytime
3	Normal weather	Special climate	Nighttime
4	Special meteorological	Normal climate	Nighttime

the maintenance task, as is shown in Table 2. Then, combined with the maintenance work on the aircraft, the error-prevention verification table is used to carry out the on-board verification, and the error-prevention requirement matrix is supplemented from the check results.

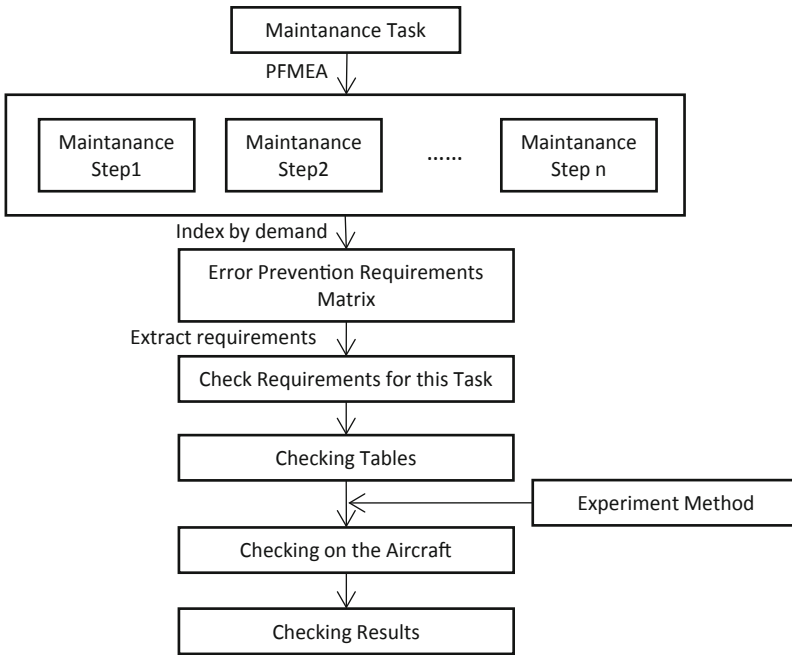


Fig. 5. Error-prevention verification framework of a maintenance task

6 Application

The method of this paper has been applied to a type of helicopter. We found 49 error-prevention problems, mainly involving environmental control system, flight control system, avionics system and airframe system, among which avionics system had the most error-prevention problems. What’s more, 4 error-prevention properties are involved: cables and connectors, fasteners, installation mode/position, and controllers, among which cables and connectors had the most error-prevention problems. Basing on the results, further quantitative analysis and improvement suggestions will be given (Fig. 6).

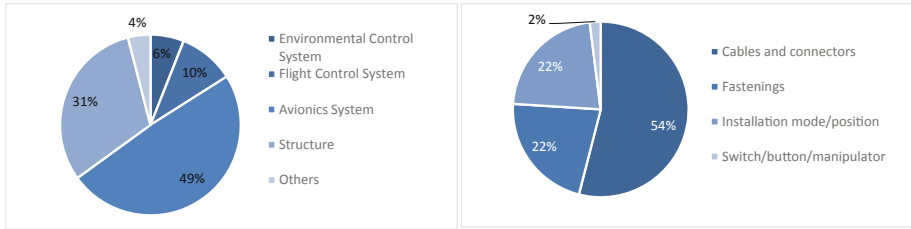


Fig. 6. Error-prevention verification results problem classification

7 Conclusions and Analysis

A new idea of error-prevention verification was presented in this paper. It can effectively improve the comprehensiveness, systematicness and efficiency of error-prevention verification by integrating special verification into routine verification. Based on PFMEA method, the characteristics of routine maintenance work during flight test and its correlation with maintenance error-prevention evaluation was analyzed. A multi-dimensional error-prevention evaluation criterion is constructed, and an error-prevention daily verification framework is formed, which can effectively improve the system and comprehensiveness of error-prevention verification, and what’s more enhance the detection rate of error-prevention problems and the accuracy of verification. This method has been applied to the maintainability evaluation of a type of helicopter, and the evaluation results can strongly support the maintainability design improvement.

Now electronic maintenance work card is gradually popularized. error-prevention requirements can be included in the maintenance work card, on the one hand, to remind maintenance staff of the problems that need to be paid attention to in the work process, on the other hand, to carry out error-prevention verification in the maintenance process, to improve efficiency. This method can be used to collect error-prevention problems not only during flight test, but also in the military use stage and the commercial aircraft operation stage.

References

1. Statal summary of commercial jet aircraft accident-worldwide operations. Boeing commercial airplane group, 1991–2001. Accessed 23 Feb 2022

2. AC-121-7 Maintenance error management for aviation personnel flight standards division, CAAC (2002)
3. International civil aviation organization (ICAO). Safety Management Manual. The U N Secretariat, New York (2006)
4. Changye, Q.: Research on Flight Test Technology Development. Aeronaut. Sci. Technol. Dev. Rep. (2010–2011) (2011)
5. Xu, X., Song, H., Guo, Y.: Development status of general quality characteristics of aircraft from flight Tests. Measur. Control Technol. (S2) (2018)
6. Hu, K.: Research on PFMEA technology of multi-varieties and small batch customization production mode. Nanchang University of Aeronautics and Astronautics (2017)
7. Zhang, Z.: Research on PoKA-Yoke application of danfoss compressor assembly line. Tianjin University (2012)
8. Zhao, V.: Experimental Design Method. Science Press, Beijing (2006)
9. Cheng, W.: Numerical simulation of supercombustion chamber design based on orthogonal experiment. Nanchang University of Aeronautics and Astronautics (2014)



Study on Quantitative Evaluation Method of Aviation Equipment Error-Prevention

Yuqi Zhang^(✉), Tao Ma, and Bao Lv

Chinese Flight Test Establishment, Xi'an 710000, China
214106366@qq.com

Abstract. The proportion of flight accidents and accident symptoms caused by human error is increasing year by year. Error prevention design, as the most fundamental way to overcome human error is very important for aviation equipment. At present, the error prevention level evaluation method during flight test is mostly qualitative, for single equipment, lacking of systematicness and quantitation. So, based on the theory of the man-machine ring and maintenance event, we established the evaluation indicator system. Then, from the perspective of security, combined with the incorrect consequences, aviation equipment error prevention quantitative evaluation method is established. The method has been applied to the maintainability evaluation of some aviation equipment, and scientific and reasonable evaluation results have been obtained.

Keywords: Flight test · Error-prevention · Risk assessment

1 Introduction

Since the 21st century, human error has gradually become one of the main causes of aviation safety accidents [1]. The proportion of accidents and symptoms caused by maintenance errors is also increasing year by year [2, 3]. Error-prevention design, as the most direct and effective way to solve human error, has been paid more and more attention. There are few researches on error-prevention evaluation control technology in the use and maintenance stage. What's more, error-ssprevention evaluation technology during flight test is very important for the evaluation of the reliability, maintainability and safety of aviation equipment. Therefore, it is very important to accurately evaluate the error-prevention level of aviation equipment to reduce security risks and improve system reliability.

In this paper, based on relevant standards and engineering examples, the error-prevention indicator system of aviation equipment is constructed according to the evaluation requirements. Then, the comprehensive quantitative evaluation method of aviation equipment error-prevention was given, and the safety analysis was carried out according to the evaluation results. At last, improvement suggestions were put forward.

2 The Indicator System of Aviation Equipment Error-Prevention Evaluation

2.1 The Influencing Factor and the Evaluation Indicator System

This paper analyzes relevant standards and engineering examples, to form the evaluation elements of aviation equipment error-prevention [4–6]. On this basis, combined with the concept of maintenance events, analysis of aviation equipment error-prevention factors, to reasonably define and classify the influencing factors.

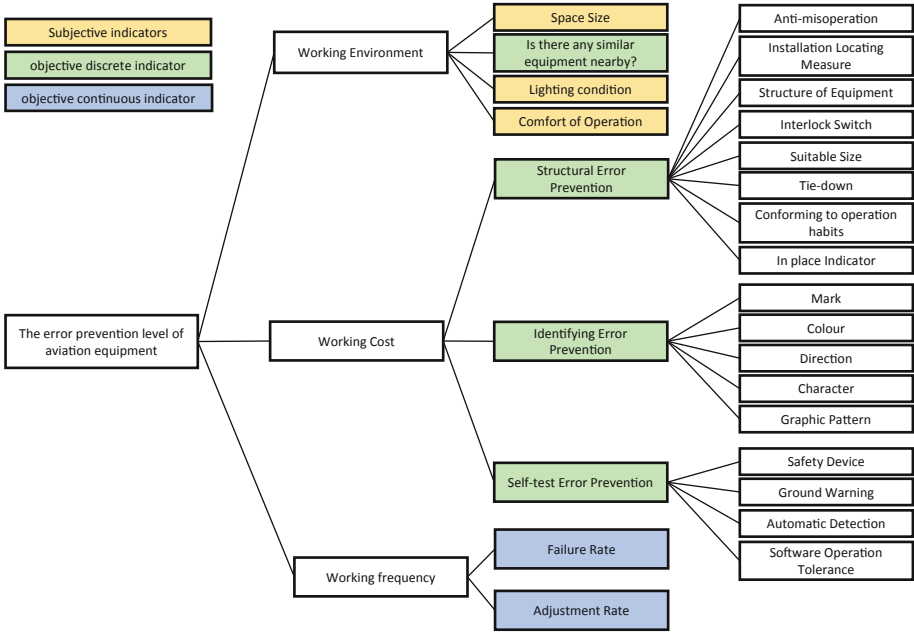


Fig. 1. Aviation equipment error prevention evaluation indicator system

The maintenance event is maintenance activities due to a failure, warning, or scheduled maintenance, etc. [7]. From the perspective of maintenance events, the influencing factors of error-prevention are divided into three categories: maintenance cost, maintenance frequency and maintenance environment. The higher the working frequency is, the better error-prevention are required. The maintenance frequency of maintenance events is affected by the failure rate and the adjustment rate in daily maintenance. At the same time, based the concept of “man-machine-environment”, the operating environment of is also taken into considered. Then, the improved Delphi method is adopted to expert consultation so that we obtained the results of indicators system [8], as is shown in Fig. 1.

2.2 Weight of the Indicator System

Grey correlation method is used to quantify the correlation degree of various factors in the system. It can find the main relationship between various factors of a system without the requirements of the sample size and regulation [8]. However, it ignores the influence of system factors. Entropy weight theory comes from thermodynamics and it is an objective measure of system state. Information entropy analysis can solve the entropy of each indicator of system, correct the importance degree and increase the reliability of data [9, 10].

In this project, information entropy algorithm is adopted to analyze the utility value of each group of data for the evaluation elements in the aviation equipment error prevention indicator system. Then, the utility value is brought into the grey correlation method as the importance degree, so that we can improve the objective accuracy of the overall correlation degree analysis of the system. This method can make up for the deficiency of equal weight processing of importance degree of data of traditional grey correlation algorithm.

2.3 Information Entropy Analysis

The sample data constitute a matrix X, Formula (1) is used for standardization. The entropy weight W is obtained by using Formula (2)–(4), where x_{\max} and x_{\min} are the maximum and the minimum element in matrix X. H_j is information entropy.

$$y_{ij} = \frac{x_{ij} - x_{\min}}{x_{\max} - x_{\min}} \beta + (1 - \beta) \quad 0 < \beta < 1 \quad (1)$$

$$f_{ij} = \frac{y_{ij}}{\sum_{i=1}^m y_{ij}} \quad (2)$$

$$H_j = -\frac{1}{\ln n} \sum_{i=1}^m f_{ij} \ln y_{ij} \quad (3)$$

$$w_j = \frac{1 - H_j}{\sum_{j=1}^n (1 - H_j)} \quad (4)$$

2.4 Grey Correlation Algorithm

The mother sequence Q_0' and comparative series Q_i' ($i = 1 \dots n$) which is formed by the indicator data constitute matrix Q' together. Formula (7)–(9) is used for calculating the correlation coefficient and correlation degree. According to the least information principle, we order the resolution coefficient $\rho = 0.5$ [8]. The correlation degree between the comparison sequence and the parent sequence is reflected by correlation coefficients

r_{0i} . Experts were invited to score the effective degree of the third level of the indicator on the error-prevention. The final weight of each indicator is shown in Table 1.

$$q_i(k) = \frac{q'_i(k)}{q'_i(1)}, i = 1, 2, \dots, n, k = 1, 2, \dots, N \tag{5}$$

$$\varphi_{0i}(k) = \frac{\min_i \min_k |q_0(k) - q_i(k)| + \rho \max_i \max_k |q_0(k) - q_i(k)|}{|q_0(k) - q_i(k)| + \rho \max_i \max_k |q_0(k) - q_i(k)|} \tag{6}$$

$$r_{0i} = \sum_{k=1}^N w(i) \cdot \varphi_{0i}(k) \tag{7}$$

Table 1. Weight table of each indicator

The goal indicator	Secondary indicator	Third indicator
Error-prevention level of equipment	Maintenance cost (error-prevention measures) 0.399	Structural error-prevention 0.139
		Identifying error-prevention 0.196
		Self-test error-prevention 0.064
	Maintenance environment 0.303	Lighting condition 0.106
		Space size 0.035
		Comfort of operation 0.151
		Is there similar equipment nearby 0.011
	Maintenance frequency 0.298	Failure rate 0.162
		Adjustment rate 0.136

3 Comprehensive Evaluation Method of Error-Prevention

3.1 Classification of Error-Prevention Evaluation Indicators

Different indicators have different evaluation methods. This paper classifies the indicators according to their characteristics and gives out the evaluation methods for different indicator respectively.

The indicators that can be evaluated objectively are defined as objective indicators. If there are only three evaluated results “Yes” and “No”, “Does not involved”, we defined them as the objective discrete indicator including structure error-prevention, self-test error-prevention and whether there is a similar equipment nearby. The failure rate and

adjustment rate of the equipment can be evaluated by the frequency of field maintenance, which is defined as an objective continuous indicator. Indicators described using natural language variables are defined as subjective indicators, such as lighting conditions. Subjective indicators mainly include the lighting situation in the operating environment, the comfort degree of operating posture and the size of installation space.

3.2 The Method of Subjective Indicator Evaluation Based on Fuzzy Evaluation

The subjective indicator is evaluated by fuzzy evaluation method. The basic idea of fuzzy comprehensive evaluation is to use fuzzy linear transformation and maximum membership degree to make a reasonable comprehensive evaluation. We choose the rectangular distribution as the membership function (8).

$$\mu_i(x) = \begin{cases} 1 & x \in v_i \\ 0 & x \notin v_i \end{cases}, i = 1, 2, \dots, 5 \tag{8}$$

The fuzzy vector of single factor is $R = (r_1, r_2, \dots, r_n)$, $r_j = x_{ij}/X$, where X is the number of experts, x_{ij} is the times for u_i has been rated to v_j . Five Grade comments and corresponding quantitative scores for fuzzy evaluation are shown in Table 2.

Table 2. Evaluation grades of lighting conditions

Evaluation indicators	Description of assessment grade				
	Optimal (v_1)	Good (v_2)	Middle (v_3)	Poor (v_4)	Bad (v_5)
Lighting condition	Perfect lighting	Good lighting condition which does not affect operations	Lighting condition is ordinary but acceptable	The lighting condition is not good. Corrective measures is recommended	Poor lighting conditions which is necessitated to improve

The evaluation matrix R is converted into the fuzzy comprehensive evaluation set of V by multiply the fuzzy operator and the weight of each indicators. The corresponding score is shown in Table 3.

Table 3. Quantization assignment table of comments set

Comments	Optimal	Good	Middle	Poor	Bad
Value	1	0.8	0.6	0.4	0.2

3.3 Objective Indicator Evaluation Method

The method of switching evaluation is adopted for the objective discrete indicator, and some evaluation grades are shown in Table 4. We quantify all the fourth indicators by two points. Then all the fourth indicators involved are evaluated by OR gate to obtain the evaluation results of the third objective discrete indicators. As for the objective continuous indicator, the failure rate and adjustment rate are divided into three grades according to the annual failure times and adjustment times of field maintenance during flight test, as is shown in Table 5.

Table 4. Description of **evaluation** grades of objective discrete indicators

Evaluation indicators			Assessment Grade		
Second indicators	Third indicators	Fourth indicators	1	0	/
Operation cost	Structural error-prevention	Mooring	Yes	No	N/A
		Place instructions	Yes	No	N/A
		...			
	Identifying error-prevention	Colour	Yes	No	N/A
		Direction	Yes	No	N/A
		...			
	Self-test error-prevention	Ground warning	Yes	No	N/A
		Self-protection	Yes	No	N/A
		...			
Operation environment	Is there any similar equipment nearby	/	No	Yes	N/A

Table 5. Quantitative evaluation grade table of objective continuous indicators

Failure rate/adjustment rate evaluation grade	Low	Middle	High
Number of outfield repairs/maintenance	zero	1–3 times	More than 3 times
The corresponding score	1	0.5	0

Then, the normalization of the evaluation results of all the above third indicators, and the evaluation results of the error prevention level of aviation equipment are finally obtained by weighted summing of the third indicators.

3.4 Analysis of Error-Prevention Risk Control Measures for Aviation Equipment

The safety analysis of error-prevention results is carried out after the quantitative evaluation of error prevention. The possible error consequences are taken as the risk severity,

and the classification standard refers to the risk severity classification table in GJB900A [11]. The quantitative evaluation result of error prevention is taken as the possibility of risk occurrence in safety evaluation. The higher the evaluation result is, the better the error-prevention design is, and the lower the possibility of error occurrence is. The corresponding error prevention level is shown in Table 6.

According to the risk indicator matrix in GJB (National military standard of China) 900A [11] (Table 7), improvement suggestions for aviation equipment error prevention are put forward based on risk indicator.

Table 6. Classification of danger possibility

Level	Descriptions	Error prevention level evaluation results
A	Often	[0, 0.2] The error may occur frequently
B	Likely	[0.2, 0.4] The error may occur several times
C	By chance	[0.4, 0.6] The error may occur occasionally
D	Few	[0.6, 0.8] The error is rarely, but possible
E	Very few	[0.8, 1] The error is very rare and can be considered unlikely to occur

Table 7. Preventive and control measures for different risk indexes

Risk index	Risk acceptance principle
1–5	Unacceptable, design improvements must be made
6–9	Do not want to have the risk, suggest the design improvement, need the ordering party to decide, consider the complexity of change and change cost and so on
10–17	Accept risks in a controlled manner, accept after review by the ordering party, and consider changes when they are less complex and cost effective
18–20	You can make improvements without making them, but for efficiency when the change costs are low

4 Application

The method of this paper was carried out on a type of helicopter. Among 49 error prevention problems found in qualitative verification, then quantitative evaluation method in this paper was used to evaluate 49 problems respectively. The evaluation results were as follows: There are 10 problems with risk index ≤ 17 which should be improved in design process (by physical error prevention measures or software modification); There are 39 items with risk index > 17 , among which 17 items are suggested to be improved by adding marks to prevent errors or improving technical data, and the remaining 22 items are limited to the difficulty of change and the risk level is low, so the change can be considered when the cost is not very high.

5 Conclusions and Analysis

Aiming at the problem that the qualitative evaluation of error prevention is not convincing at present, this paper constructs a scientific and reasonable error prevention indicator system and gives the indicator weight. At the same time, aiming at the problem that there are many kinds and scattered contents of error prevention evaluation indicators, this paper forms a comprehensive evaluation method for error prevention with different indicators. What's more, this paper analyzes the safety of evaluation results. In a word, the method in this paper improves the objectivity of error prevention evaluation results and provides technical support for ensuring the safety during flight test.

References

1. Statal summary of commercial jet aircraft accident- worldwide operations. Boeing Commercial Airplane Group, 1991–2001. Accessed 23 Feb 2022
2. AC-121-7 Maintenance error management for aviation personnel, flight standards division, CAAC (2002)
3. International civil aviation organization (ICAO). Safety Management Manual. The U N Secretariat, New York (2006)
4. Bai, N.: Cause analysis of aviation maintenance errors based on Bayesian network. *J. Binzhou Univ.* (2) (2015)
5. Changchun, Z., Fangjian, S., Yonggang, C.: Research on influencing factors of civil aviation maintenance personnel's errors based on ISM-AHP. *J. Binzhou Univ.* (4) (2015)
6. Wang, Y.: Research on safety analysis and evaluation of civil aviation maintenance based on human factors. Nanjing University of Aeronautics and Astronautics, Nanjing (2012)
7. Li, J., Deso, D., Li, Q.: Verification and evaluation indicator system of maintainability qualitative requirements based on maintenance events. *Army Off. Acad. J. Equip. Acad.* **26**(5), 4 (2015)
8. Song, H., Tao, M., et al.: Evaluation of influencing factors of human error in aircraft maintenance during flight test. *Mod. Def. Technol.* **44**(6), 7 (2016)
9. Xing, Z.: Risk assessment of debris flow in Bailong River Basin based on information entropy and AHP model. Lanzhou University, Lanzhou (2012)
10. Chen, T., Ting, M., Li, R.: Quantitative analysis of causes of aviation maintenance errors based on grey relational entropy. *Aeronaut. Comput. Technol.* (2) (2016)
11. GJB (National military standard of China) 900A Equipment Safety general requirements



Improvement of Work Efficiency of Intelligent Manufacturing Operator 4.0 from the Perspective of HCPS

Chaoan Lai and Ruobing Zhao(✉)

School of Business Administration, South China University of Technology, Guangzhou 510006, Guangdong, China
202020131176@mail.scut.edu.cn

Abstract. “Human- Cyber- Physical System” (HCPS) provides a theoretical basis for the development of human-centered intelligent manufacturing. Human has also changed its role with the development of modern information technology. Operator 4.0 was born under this background. It emphasizes man-machine cooperation with production equipment more, and its work efficiency greatly affects the process of the whole intelligent manufacturing system. This paper expounds the connotation and system composition of HCPS for the new generation of intelligent manufacturing, analyzes 11 key technologies of operator 4.0, and further explains how the emerging technologies improve work efficiency and corresponding technical limitations, then put forward the path and mechanism model of intelligent manufacturing technology empowering enterprises and promoting the transformation of enterprise business model. Finally, based on HCPS, put forward three suggestions for the development of related fields: paying attention to man-machine symbiosis, promoting human factors into system design and promoting system integration.

Keywords: New generation of intelligent manufacturing · HCPS · Operator 4.0

1 Introduction

With the rapid development of new generation cyber technology, human, physical and cyber system are becoming three indispensable components of intelligent manufacturing system. The traditional “human machine environment” system theory are gradually upgraded to “Human-Cyber-Physical System” (HCPS).

In the whole system, human is the most important and dynamic element, which determines the efficiency and effect of intelligent manufacturing. Operator 4.0 is produced with the emergence of new technology. The technology applied to the new generation of operators has greatly affected the work efficiency of workers and the development of intelligent manufacturing system.

2 Connotation and System Composition of HCPS for the New Generation of Intelligent Manufacturing

From the perspective of system composition, HCPS is a comprehensive intelligent system organically integrated by human, cyber system and physical system to achieve one or more manufacturing value objectives. The most essential difference from traditional manufacturing is that it adds a Cyber system - C between the original human and physical systems. In the whole system, human is the key master. Human is not only the creator of physical system and cyber system, but also the “intelligence” endowed by human, but also the manager, user and operator of the system; Physical system is the main body, which is the executor of manufacturing material flow and activity energy flow; Cyber system is the leading, which is the core of the cyber flow of manufacturing activities. It assists or replaces people’s cognition, perception, analysis, decision-making and control activities of the physical system, so as to make the physical system run in an optimal way.

The new generation of intelligent manufacturing technology is the deep integration of the new generation of artificial intelligence technology and advanced manufacturing technology. Its rapid development and wide application will reshape the technical system, industrial form and production mode of manufacturing industry. The cyber revolution marked by artificial intelligence has become the core driving force of the new round of industrial revolution [1].

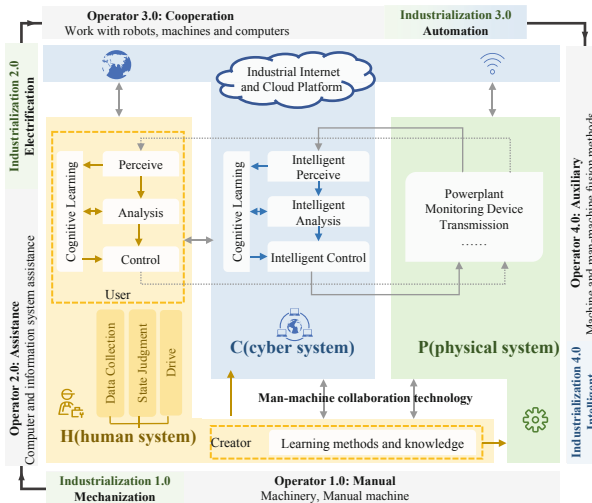


Fig. 1. New generation intelligent manufacturing based on HCPS

With the rapid development and upgrading of the new generation of intelligent manufacturing system, the cyber system that plays a leading role in HCPS has undergone essential changes: the learning and cognition part based on the new generation of artificial intelligence technology is added, which greatly enhances the ability of perception, decision-making and control of the cyber system, and makes it have the ability

of learning, cognition and knowledge generation, namely “artificial intelligence”; The learning and cognitive system of human beings and the cyber system together constitute the “knowledge base” in the cyber system, which contains the knowledge that human beings are difficult to accurately describe or process. Moreover, through continuous use and learning, the knowledge base can be continuously accumulated, improved and optimized. The essence of HCPS for the new generation of intelligent manufacturing system is shown in Fig. 1.

Facing the new generation of intelligent manufacturing, HCPS not only revolutionizes the production, utilization, transmission and accumulation efficiency of manufacturing knowledge, but also improves the operation and decision-making effect of manufacturing system to a great extent, and greatly improves the ability to deal with the uncertainty and complexity of manufacturing system.

3 4.0 Operator 4.0 of Intelligent Manufacturing System

In the whole manufacturing and production activities, human is always the most dynamic and energetic factor, and human’s central position is further highlighted in the new generation of intelligent manufacturing. Intelligent manufacturing improves the quality and efficiency of people’s use of physical tools to convert raw materials into products and services that can meet people’s production and living needs, but its ultimate service goal is still people. Therefore, the new generation of operators put more emphasis on “human-oriented”.









3.1 Connotation of Operator 4.0

Operator 4.0 gradually build a human-machine symbiosis system from single task operation to the planning of the whole intelligent manufacturing system. Romero et al. put forward the concept of operator 4.0 under HCPS semantics and looked forward to its development prospect [2]. It does not replace the operator with various equipment or technologies, but enhances the technology and ability of the operator in all aspects through intelligent methods or equipment. The new generation of operators constantly update and improve their technical level through learning in different complex problems and tasks. It is not a linear stack of new intelligent technologies, but a new concept of the integration of human, cyber system and physics, which together constitute the HCPS of human-machine symbiosis.

3.2 Classification of Operator 4.0

With the development of industry 4.0, operators’ production tasks are more personalized, professional and customized. They serve different business scenarios, and jointly promote the transformation and upgrading from “human-oriented” to intelligent manufacturing system (Table 1).

Table 1. Classification of operator 4.0

Type	Scenario	Description	Application
Cooperative Operators		Engage in non ergonomic or repetitive work in collaboration with cooperative robots (cobots)	Cobots; Collaborative manufacturing
Analysis Operators		Applying big data to analyze intelligent manufacturing process and results	Identify valid cyber and make predictions
Super Operators		Wearable, flexible and lightweight load-bearing robots mostly have power assisted devices	Exoskeleton technology enhances the strength of human operators; Jidoka (Lean production)
Intelligent Operators		Making full use of artificial intelligence to provide solutions for intelligent manufacturing	Assist the operator to interact with the machine, database computer or other cyber systems; Intelligent Manufacturing
Social Operators		The mobile network system assists the intelligent operator connecting the intelligent workshop	Social industrial Internet for building ecosystem; Agile manufacturing
Health Operators		With the aid of wearable monitors and devices, measure various human physiological health indicators, GPS positions or other personal data	Bracelet, smart watch, etc; Remote operation and maintenance; Cloud manufacturing
Augmented Reality Operators		Use AR to enrich the factory environment and improve the cyber transmission mode between cyber system and physical system	Smart phones and tablets are used as RFID identifiers. Space AR projector supports automobile manufacturing; virtual manufacturing
Virtual Operators		Using computer simulation reality technology, create a digital replica of design, assembly or manufacturing environment and interact with it	Using virtual reality technology to train ball games; virtual manufacturing

3.3 Business Model Transformation of Operator 4.0 Under HCPS

The three input factors of intelligent manufacturing capital investment K , skilled labor supply L_H of operator 4.0 and labor supply L_L of unskilled labor are included in the unified analysis framework. In order to distinguish the substitution elasticity of intelligent manufacturing capital for skilled labor and unskilled labor, this paper selects $(KL_H)L_L$ nesting method and assumes the production function corresponding to intelligent manufacturing enterprises, that is:

$$Y_i(K, L_H, L_L) = [((A_iK)^{\frac{\sigma-1}{\sigma}} + (B_iL_H)^{\frac{\sigma-1}{\sigma}})^{\frac{\sigma-1}{\sigma} \cdot \frac{\varepsilon-1}{\varepsilon}} + (C_iL_L)^{\frac{\varepsilon-1}{\varepsilon}}]^{\frac{\varepsilon-1}{\varepsilon}} \quad (1)$$

where: Y represents the manufacturing output of the enterprise; K represents the intelligent manufacturing capital of the enterprise; LH is the labor supply of operator 4.0 man-machine integration operation, and LL is the supply of unskilled labor; A is a variable to measure the maturity of intelligent manufacturing technology, representing the enterprise's intelligent manufacturing capital and promoting technical efficiency; B represents the ability level of the operator, that is, the technical efficiency of skilled labor; C represents the operating mode of the operator, i.e. unskilled labor to improve technical efficiency; σ represents the substitution elasticity between intelligent manufacturing capital and skilled labor; ε represents the substitution elasticity between intelligent manufacturing system and unskilled labor force.

When intelligent manufacturing technology advances, there will be neutral technological progress and biased technological progress. This paper constructs the biased technological progress parameter φ_i and Ψ_i to represent the relative intensity of labor-augmenting technical progress between intelligent manufacturing capital and skilled labor force or unskilled labor force of enterprise i . Let $A_i = \varphi_i M_i$, $B_i = (1 - \varphi_i) M_i$, $C_i = (1 - \Psi_i) N_i$, $M_i = \Psi_i N_i$, where M_i and N_i represent the neutral technical progress of intelligent manufacturing system and skilled labor force or unskilled labor force respectively. Then the production function is converted to:

$$Y_i(K, L_H, L_L) = N_i \left\{ \Psi_i^{\frac{\varepsilon-1}{\varepsilon}} \left[(\varphi_i K)^{\frac{\sigma-1}{\sigma}} + ((1 - \varphi_i) L_H)^{\frac{\sigma-1}{\sigma}} \right]^{\frac{\sigma-1}{\sigma} \cdot \frac{\varepsilon-1}{\varepsilon}} + ((1 - \Psi_i) L_L)^{\frac{\varepsilon-1}{\varepsilon}} \right\}^{\frac{\varepsilon-1}{\varepsilon}} \tag{2}$$

Generally speaking, when elements replace elasticity $\sigma > 1$, there is a substitution relationship between intelligent manufacturing capital and skilled labor force. At this time, the growth rate of technical efficiency of skilled labor force is less than that of intelligent manufacturing capital; When elements replace elasticity $\sigma < 1$, there is a complementary relationship between intelligent manufacturing capital and skilled labor force. At this time, the technical efficiency growth rate of skilled labor force is greater than that of intelligent manufacturing capital.

4 Key Technologies to Improve Work Efficiency and Promote Business Model Change

According to the introduction of the operation framework of operator 4.0 [3], it can be seen that during the operation of the operator 4.0, these 11 key technologies can greatly enhance operators' perception, cognition and control ability, so as to improve their work efficiency.

1. *Perception Ability.* The perception ability of the operator 4.0 starts from the equipment layer of the physical system and collects various equipment status cyber that is difficult or unable to be perceived by human beings through sensors, wearable devices or the cyber system of the physical device. Therefore, the operator can not only directly sense the equipment status at the production and manufacturing site, The manufacturing state can also be deeply perceived with the help of the cyber collected by these auxiliary devices and cyber systems.

- *Wearable Device (WD)*. It is a portable device designed to collect workers' health data and track the action trajectory of operators. This technology is mainly used for healthy operators. However, to a certain extent, it will also lead to the problem of user privacy disclosure.
 - *Sensors for Environment and Machines (SENS)*. When it is used in the Internet of Things, sensors can detect the state of objects, transmit information to a wider network system to help operators find useful information. However, it has high investment and requirements for the connectivity of equipment network.
 - *Augmented Reality Technology (AR)*. It is a technology that integrates 3D virtual objects into 3D real environment in real time. However, it may cause visual damage and the operator's skill level is required to be relatively high.
 - *Digital Twin Technology (DT)*. It is a technology to complete the whole life cycle mapping of corresponding physical equipment in virtual space. Wang et al. developed a human-computer interactive welding and technology analysis platform based on DT technology to improve the work efficiency of operators [4]. The related technical bottleneck mainly lies in the improvement of spatial reliability and accuracy.
2. *Cognition Ability*. Cognition ability is the extension of perception ability. The cognitive basis of operator 4.0 comes from its own intuitive perception and the analysis results of cyber system. After collecting the status of the auxiliary equipment or system at the intelligent manufacturing site, it collects the perceived information by using the bus and uploads it to the cloud with the help of the industrial Internet. Multi-source and continuous collection forms industrial big data, and then cognition is carried out with the help of the intelligent system.
- *Virtual Reality Technology (VR)*. Malik et al. developed a human-machine simulation integration framework based on VR by using robots in virtual environment to interact with operators, forming a human-centered production system [5]. VR technology can improve operators' cognition ability and simulate and create new solutions intuitively, but more research is needed on the comfort and safety of equipment use and more actual manufacturing scene simulation.
 - *Big Data Analysis Technology (BDA)*. Yang et al. summarized the development process, key technology and application of BDA in intelligent manufacturing system [6]. This technology greatly provides support for dealing with a variety of complex situations in the operation process. How to promote the independent analysis ability of the system are the focus of the next research.
 - *Computer Vision and Visual Analysis Technology (CV & VA)*. It can help operators expand their cognition of data in a shorter time, reduce the requirements for workers' attention and eyesight, and improve the accuracy of task execution, but it needs to update the fast iterative algorithm for technical support.
 - *Industrial Social Network (ISN)*. This technology greatly reduces the training curve of new employees; Reduce the incidence of recurring problems; Promote continuous improvement process, but there are also problems of information reliability and intellectual property protection.

3. *Control Ability*. To control the equipment in the intelligent manufacturing process, one of the key issues is from the simple analysis and direct real-time control of the auxiliary equipment after collecting the state information. The other is that in the complex manufacturing process, the cyber system analyzes the collected perceptual data to form the optimization decision, and then completes the relatively complex regulation through the control command; Third, in the more complex manufacturing process in which the automatic and intelligent system cannot complete the control independently, the operator 4.0 can comprehensively deal with various complex activities on the manufacturing site with the help of various means, and can implement the necessary intervention for the first two controls at the same time.
 - *Exoskeleton (EXO)*. It is a lightweight wearable mechanical auxiliary device mainly used in power operators. In nature, Collins et al. published the research on the use of EXO to reduce human physical consumption, emphasizing the importance of integrated design of human structure [7]. However, it has weight limitation in use.
 - *Artificial Intelligence (AI)*. Zolotova et al. expounded that AI technology can improve the human-computer interaction performance of operators by analyzing the enhancement mode and different ability of intelligent factory operators [8]. AI technology is an effective tool to support dynamic decision-making, but it may bring some ethical problems when used.
 - *Intelligent Decision Support System (IDSS)*. This technology combines the traditional decision support system and AI-based decision support system to make a rapid response to emergencies in production. However, the deployment of the whole system is time-consuming, labor-intensive and of high cost.

The above explains how technologies have a positive impact on people's perception, cognition and control ability and promote the formation of new business models. However, there are also some restrictions on their use. If these key technologies can be reasonably selected and combined, the ability of operator 4.0 can be enhanced, so as to improve work efficiency.

5 Conclusion and Suggestions on Intelligent Manufacturing Based on HCPS

Based on the theory of HCPS, operator 4.0 is the soul of human-centered intelligent manufacturing. Emerging technologies have greatly improved the working ability and efficiency, but there are also some use restrictions and defects. Based on this, the following suggestions for further research and development of Intelligent Manufacturing Based on HCPS are put forward.

1. *Pay attention to human-machine symbiosis*. In order to maximize respective advantages of human and intelligent machine to achieve the optimal system performance, we need to allocate the division of them better, and achieve deep integration and harmonious symbiosis with information physical system (intelligent machine). In

the process of division of labor and cooperation, we also need to define the boundary of privacy and ethical issues as soon as possible, so that it can serve mankind more safely.

2. *Promote the integration of human factors into system design.* At present, the design and application of many technologies still lack “human” factors, such as the low comfort of VR glasses and the weight limitation of exoskeleton technology, which limit the efficiency and effect of production and manufacturing. We should continue to promote the human factors design principle as a necessary step in the design of intelligent manufacturing system, and integrate human factors engineering into the design, construction and use of the whole intelligent manufacturing system. If necessary, some mandatory regulations can be adopted to promote the transformation and upgrading of intelligent manufacturing.
3. *Promote system integration.* For the development of the whole industry, the integration of intelligent manufacturing system plays a key role, such as smart energy, smart parking and smart voice. It is suggested to absorb the system integration experience of the integrated development of intelligent machines and people, promote the integrated development of intelligent manufacturing industry chain, talent chain and innovation chain.

The new round of industrial revolution provides a good environment for the development of various theories and technologies to be comprehensively applied and tested. We should seize the wave of manufacturing development and accelerate the development of relevant emerging technologies of operator 4.0, so as to further realize human-oriented intelligent manufacturing and promote the intelligent transformation of manufacturing industry.

Acknowledgement. This work is supported by the Guangdong soft science project, No. 2019A101002006 and China University Industry–University–Research Innovation Fund: Ministry of Education – “Alibaba Cloud University Digital Innovation Project”, No. 2021ALA04002.

References

1. Zhou, J., Li, P., Zhou, Y., et al.: Toward new-generation intelligent manufacturing. *Engineering* **4**(4), 11–20 (2018)
2. Romero, D, Bernus, P., Noran, O., et al.: The operator 4.0: human cyber-physical systems & adaptive automation towards human-automation symbiosis work systems. In: Nääs, I., et al. (eds.) APMS 2016. IFIP Advances in Information and Communication Technology, vol. 488, pp. 677–686. Springer, Cham (2016). https://doi.org/10.1007/978-3-319-51133-7_80
3. Zhou, J., Zhou, Y., Wang, B., et al.: Human cyber physical systems (HCPSs) in the context of new-generation intelligent manufacturing. *Engineering* **5**(4), 13 (2019)
4. Wang, Q., Jiao, W., Wang, P., et al.: Digital twin for human-robot interactive welding and welder behavior analysis. *IEEE/CAA J. Autom. Sinica* **PP**(99), 1–10 (2020)
5. Malik, A.A., Masood, T., Bilberg, A.: Virtual reality in manufacturing: immersive and collaborative artificial-reality in design of human-robot workspace. *Int. J. Comput. Integr. Manuf.* **33**(1), 22–37 (2019)

6. Yang, F.: A review of systematic evaluation and improvement in the big data environment. *Front. Eng. Manag.* **7**(1), 27–46 (2020)
7. Sawicki, G.S., Collins, S.H., et al.: Reducing the energy cost of human walking using an unpowered exoskeleton. *Nature* **522**, 212–215 (2015)
8. Zolotová, I., Papcun, P., Kajáti, E., et al.: Smart and cognitive solutions for operator 4.0: laboratory H-CPPS case studies. *Comput. Ind. Eng.* **139** (2018). Document number:105471



Research on the Mechanism of Intelligent Operations Command

Haimin Hu, Weixin Liu, Hao Liu^(✉), Lei Tang, Hongyan Ou, and Junfei Wang

Zhengzhou Campus, CPLA Army Artillery and Air Defense Forces Academy,
Zhengzhou 450052, China
hmhu@163.com

Abstract. Based on the application background of artificial intelligence technology in the military field, this paper studies the conceptual system of intelligent operations command; uses theoretical analysis and system engineering design methods to discuss the conceptual connotation of intelligent operations command and the relationship of man-machine intelligence integration. It focuses on operations command needs to study and design the functional framework of intelligent operations command, and explores the characteristics and mechanism of intelligent operations command. The research results effectively promote the research on the conceptual system of intelligent operations command, which can promote the deepening of intelligent operations command in modern operational systems.

Keywords: Intelligence operations command · Intelligent fusion · Intelligent algorithm · Data-driven

1 Introduction

As the core link of the whole operational system, intelligent operations command is the key to the success of “man + machine” intelligent integration in the future battlefield [1]. An in-depth study of the operational conceptual system of intelligent operations command and a grasp of its conceptual connotation, functional characteristics and internal mechanism will help to promote the application and development of intelligent operations command in modern operational system, effectively improve the operations command level of “man + machine” intelligent integration in modern war, and accelerate the in-depth evolution of intelligent warfare.

2 Connotation of Intelligent Operations Command

Intelligent operations command is an organizational activity conducted by commanders and command organs to combat troops by means of intelligent command information system under the support and application of intelligent technology [2]. Through the cooperative operational mode of “human brain + intelligent system”, intelligent operations command is based on intelligent technology groups such as warfighting cloud, database

and Internet of things to smoothly calculate the communication between computers and commanders, so that commanders can cope with rapidly changing complex battlefield conditions and complete command tasks smoothly and efficiently [3]. Intelligent operations command is a new concept based on operations command in the information age. It is the inevitable direction for the penetration and expansion of cutting-edge technology with intelligent data processing as the core in the field of operations command.

3 Functional Architecture of Intelligent Operations Command

According to the mission requirements of the operational system under the intelligent condition, the functional elements of the intelligent operations command are mainly reflected in the activities of intelligence, decision, control and evaluation. By comprehensively analyzing the logical relationship and operation requirements between the intelligent operations command elements, the functional architecture of the intelligent operations command is designed, as shown in Fig. 1.

3.1 Intelligent Battlefield Perception

Intelligent battlefield perception is also called intelligent battlefield situation awareness. Through the integration of artificial intelligence human-like characteristics and battlefield perception system, it can complete the tasks of detection and analysis and improve the ability and efficiency of battlefield perception.

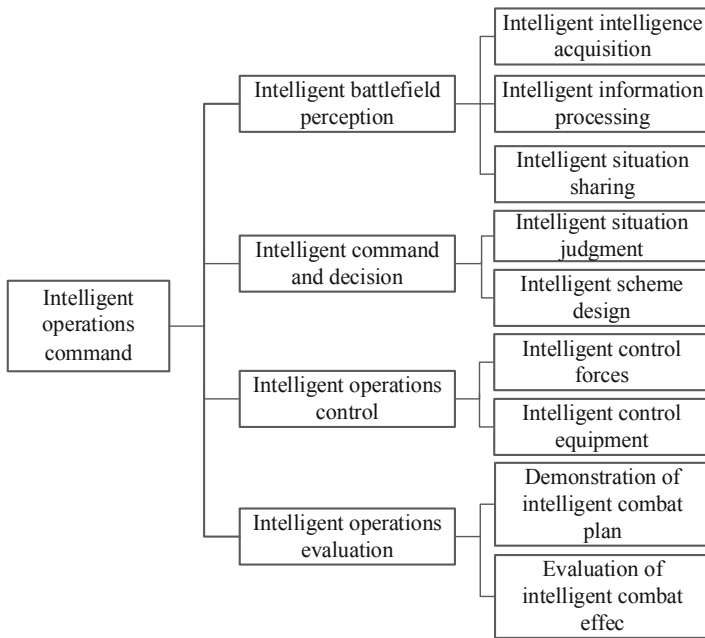


Fig. 1. Functional architecture of intelligent operations command

3.1.1 Intelligent Intelligence Acquisition

To realize of intelligence acquisition function, first, the sensor itself is equipped with a special intelligent identification processor and microprocessor, which can adaptively adjust its own working parameters according to the mission requirements, preprocess the data information, and transmit it to the command and control center or weapon system in time, accurately and safely. The second is to make full use of the networking application advantages of sensors to build an intelligent sensor task command and assignment system to solve sensor task assignment, multi-source information fusion and processing information distribution [4]. According to the battlefield intelligence reconnaissance situation and operational requirements, sensors in the optimal position are actively assigned to carry out reconnaissance or maneuver to the appropriate position for reconnaissance.

3.1.2 Intelligent Information Processing

Information intelligent processing is to intelligently fuse the data, that is, to fuse multi-source situation information through format conversion, elimination of redundancy and information complementarity, so as to form consistent and accurate situation information [5]. And it is to the intelligently mine the intelligence, that is, to select, associate, compare, screen and grade all kinds of situation information in the whole battlefield environment, and transform the fused information into credible, valuable, important and urgent information.

3.1.3 Intelligent Situation Sharing

Intelligent battlefield situation sharing is to constructs a new information sharing mode by using artificial intelligence technology, so that battlefield information flows in a safe and orderly manner, and realize the goal of “the right information is shared by the right personnel at the right time and place in the right way”. Intelligent battlefield situation sharing greatly improves the ability of battlefield situation information distribution and promotes the change of combat behavior, which is mainly reflected in the two links of information intelligent push and information intelligent acquisition.

3.2 Intelligent Command and Decision

Intelligent command and decision is based on the intelligent decision support system as the basic means, the integrated qualitative and quantitative method as the basic method, and the combination of man-machine decision as the basic method to continuously improve the speed and efficiency of command and decision and realize the scientization and efficiency of command and decision. The two core functions of intelligent command and decision are intelligent situation judgment and intelligent scheme design.

3.2.1 Intelligent Situation Judgment

Intelligent situation judgment is to automatically identify, analyze, judge and reason on complex battlefield situations, realize intelligent early warning and research and judgment, and assist commanders in making battlefield decisions accurately, in real time

and effectively by utilizing massive data fusion, rapid perception and cognition, powerful analysis and reasoning, adaptive and self-optimization that provided by artificial intelligence.

3.2.2 Intelligent Scheme Design

Intelligent scheme design is to form several sets of candidate schemes according to the conclusion of situation research and judgment and with the help of intelligent scheme rapid generation and evaluation technology, and make final decision through deduction, analysis, evaluation and optimization. Intelligent scheme design can realize the standardization, process and refinement of operation organization and management, and support commanders and staff to complete the operation scheme design scientifically and efficiently according to the standardized operation process.

3.3 Intelligent Operation Control

Intelligent operation control is the command activities of various combat forces effectively driven by intelligent man-computer interaction with the help of intelligent control system under the condition of comprehensive perception of the battlefield and its related conditions. Intelligent combat control includes two core functions: intelligent control of troops and intelligent control of weapons and equipment.

3.3.1 Intelligent Control Forces

With the help of the intelligent operations command system, the commander carries out various battle calculations and generates battle plans and battle documents. Through the intelligent command and control system, the commander issues instructions to all combat forces in real time and displays them on tactical terminals at all levels, so that the forces can carry out combat operations accordingly. The focus of regulation and control is the command institutions and combat units at all levels. The object of regulation and control is “man”. Under special circumstances, instructions can also be input into the weapon system to start the combat procedure.

3.3.2 Intelligent Control Equipment

According to the assigned combat tasks, each combat unit drives the intelligent weapons and equipment to carry out operations through the task planning, action control and other command activities of various intelligent weapons and equipment through the intelligent control terminal in the form of programs, instructions or independent ways. The focus of regulation is on weapon systems such as intelligent unmanned operational system and intelligent ammunition, and the object of adjustment is “objects”.

3.4 Intelligent Operation Evaluation

Intelligent operation evaluation mainly combines virtual space and real space to realize the simultaneous development of actual combat evaluation and system virtual combat

evaluation [6], solve the problems of cross modal, cross domain and cross scale combat modeling and simulation, and analyze, identify and evaluate complex combat phenomena through simulation experiments, so as to make the physical domain, information domain Cross domain assessment between cognitive domain and social domain is possible.

4 Characteristics and Mechanism of Intelligent Operations Command

Intelligent operations command is the extensive application of intelligent perception and information processing, intelligent command and control and auxiliary decision-making, and multi-functional expert system platform, which promotes the development of operations command from the information development stage focusing on digital network information system to the cross interaction between virtual and real space, coordinated command between man and unmanned The stage of intelligent operations command characterized by machine autonomy and man-machine integration.

4.1 Intelligent Man-Machine Integration

Intelligent operations command realizes the integration of “man” intelligence and “machine” intelligence through reasonable man-machine cooperation, gives full play to the respective advantages of human brain and machine, and realizes the integration of command art and technology [7]. Relying on the battlefield situation awareness system, it can accurately analyze and judge a large amount of battlefield information with the help of big data, cloud computing, artificial intelligence and modeling and simulation technology, and realize the transformation of operations command from “centered on human experience” to “centered on data model” intelligent decision.

4.2 Network Distribution and Interconnection

In the network-based operations system, information runs through all links of the operations command process, and the basic implementation carrying the coupling of various elements of the operations is also called distributed cloud [8]. By building a distributed system and multi-point fault-tolerant backup mechanism, the cloud platform has strong intelligence sharing ability, data processing ability, anti-attack and self-repair ability. It can provide fixed and mobile, public and private cloud services, greatly reduce the links of information flow, and promote the flat and fast command process.

4.3 Intelligent Algorithm Autonomous Learning

The intelligent algorithm represented by deep learning, by establishing a model simulating brain neural network, guides the computer to understand the battlefield in a learning way, master the law of operations command, dynamically identify the battlefield and predict the development trend of the battlefield. The intelligent algorithm fundamentally improves the intelligent operations command pattern recognition ability, making it reach or even exceed the excellent commanders, and has the ability to conduct independent operations command.

4.4 Battlefield Big Data Driven

Battlefield big data implies the quantitative characteristics of the battlefield, and data has become an indispensable key resource for intelligent operations command [3]. On the one hand, battlefield big data can overcome the imperfection of complex battlefield data; On the other hand, it is easy to find the correlation between different phenomena in the battlefield complex big data with rich types and growing orders of magnitude, so as to provide decision basis for commanders to accurately judge and predict the development and change of combat situation. Big data drives the update and improvement of intelligent operations command model and the optimization and innovation of operations command process.

5 Conclusion

Based on the application and development trend of artificial intelligence in the military field, this paper discusses the concept and connotation of intelligent operations command according to the background of intelligent combat requirements, designs the functional composition and operation mechanism of intelligent operations command, and studies the characteristic mechanism of intelligent operations command. The research results can effectively promote the research on the conceptual system of intelligent operations command and provide theoretical methods for the application of intelligent operations command.

References

1. Pang, H.: Intelligent Warfare. Shanghai Academy of Social Sciences Press, Shanghai (2020)
2. Kuai, Z., Zhao, X., Chen, K.: Research on the Application of Military Intelligence. Ordnance Industry Press, Beijing (2021)
3. Song, Y., Li, Z.: Analysis of intelligent battle command in DT Era. *J. Command* **2018**(7), 38–39 (2018)
4. Tan, T.: Artificial Intelligence: Creating an Intelligent Future with AI Technology. China Science and Technology Press, Beijing (2019)
5. Zhou, S., Zhang, G.: Initial intelligent battle command. *Milit. Acad. Air Force* **2018**(3), 42–47 (2018)
6. Zhang, X., Cao, X.: Research on military aided decision making based on deep learning. *Fire Control Command Control* **45**(3), 1–6 (2020)
7. Ying, Z., Li, Y.: Research on the Form of Future War. Ordnance Industry Press, Beijing (2021)
8. Wu, M.: Intelligent Warfare. National Defense Industry Press, Beijing (2020)



Research on Operational Effectiveness Evaluation of a Certain Type of Equipment

Hongyan Ou, Qian Liu, Di Wu, Junfei Wang, Shuxin Wang, and Weixin Liu^(✉)

Zhengzhou Campus, CPLA Army Artillery and Air Defense Forces
Academy, Zhengzhou 450052, China

Abstract. (Purpose) By comparing different evaluation methods, find a better method to evaluate the operational effectiveness of a certain type of equipment. (Method) AHP is used to construct the model, expert evaluation and step-by-step evaluation of the operational effectiveness of a certain type of equipment. (Results) An evaluation method is selected, the hierarchical evaluation model of operational effectiveness of a certain type of equipment is established, the judgment matrix of operational effectiveness evaluation is constructed, and the hierarchical ranking of operational effectiveness evaluation is carried out, and the basic conclusions and targeted countermeasures are put forward. (Conclusion) It is feasible to evaluate the operational effectiveness of a certain type of equipment by AHP, and the results are consistent with the actual application results of the equipment. This paper have theoretical significance for evaluating and improving the operational effectiveness of a certain type of equipment.

Keywords: A certain type of equipment · Operational effectiveness · AHP

1 Introduction

A certain type of equipment can provide timely, accurate and continuous information support, which provides an important guarantee for effectively defending enemy weapons attacks and ensuring the safety of important targets. So-called multi-planning will win; less planning will fail, let alone not planning? [1] Strengthening the research on equipment operational effectiveness evaluation is an important basis for realizing the optimal design and scientific use of equipment.

2 Application of AHP in Operational Effectiveness Evaluation of a Certain Type of Equipment

2.1 Method Characteristics of AHP

Each method has its own advantages and disadvantages. For example, the advantage of neural network evaluation method is that it has no strict assumptions, it has the ability to deal with nonlinear problems, and the disadvantage is strong randomness. The advantage

of D-S evidence theory evaluation method is that it is possible to obtain new reliability allocation output through comprehensive multi-sensor reliability allocation, which is more suitable for the case of small evidence conflict. The disadvantage is that it is easy to produce wrong conclusions when there is a large conflict between evidences [2]. AHP decomposes the components of the problem according to the nature of the problem and the expected goal, and forms a hierarchical structure model according to the relationship between the factors. Then, the importance weights of the lowest level factors for the highest level factors are obtained by layer analysis, and the pros and cons are sorted. The method combines qualitative and quantitative methods to deal with various decision factors, which is systematic, flexible and concise.

2.2 Evaluation Advantages of AHP

By comparing the advantages and disadvantages, combined with the characteristics of a certain type of equipment, AHP is more suitable for evaluating the operational effectiveness. We can judge each factor and provide a multi-scheme decision-making method from the various factors affecting the operational effectiveness of a certain type of equipment.

2.3 Evaluation Process of AHP

AHP decomposes complex unstructured problems into several factors. The elements are divided into different hierarchies according to different attributes. The upper hierarchy dominates all or some elements of the next adjacent hierarchy, forming a top-down layer-by-layer relationship between the layers. This hierarchical structure is of decisive significance to solve the problem successfully. AHP evaluates the advantages and disadvantages of each index in the system through pairwise comparison between indexes, and uses the evaluation results to comprehensively calculate the weight coefficient of each index, so as to sort the influencing factors or schemes [3].

3 Operational Effectiveness Evaluation Model of a Certain Type of Equipment Based on AHP

First, AHP determines the factors contained in the problem, for a certain type of equipment operational effectiveness evaluation is to select the appropriate evaluation index. Then the indexes are arranged in the form of the highest layer, the middle layer and the bottom layer, and the hierarchical structure model reflecting the correlation membership relationship of each index is established [4].

3.1 Establishing Hierarchical Model of Effectiveness Evaluation

Through the the exchange and consultation with experts in related fields, there are three first-order capabilities B1, B2 and B3 that affect the operational effectiveness of a certain type of equipment, and the second-order capabilities corresponding to B1 are C1, C2 and C3. B2 corresponds to C4, C5 and C6. B3 corresponds to C7, C8 and C9, these capabilities constitute the hierarchical structure of the operational effectiveness evaluation of this type of equipment.

3.2 Constructing Effectiveness Evaluation Judgement Matrix

In order to ensure the scientificity of assignment and lay a foundation for quantitative analysis, it is necessary to score all the evaluation indexes from multiple experts in this field and establish the pairwise comparison matrix of the operational effectiveness indexes of this type of equipment. Five members from the field form an expert group.

Assuming that taking the upper layer element M as the criterion and the next layer element is dominated by W_1, W_2, \dots, W_n , the corresponding weights of W_1, W_2, \dots, W_n are given according to the relative weights of criterion M . In the hierarchical structure model of operational effectiveness evaluation of a certain type of equipment, the membership relationship has been determined. Since there is no definite quantitative relationship between W_1, W_2, \dots, W_n , it is necessary to judge which is important between W_i and W_j according to criterion M , and assign the importance according to the scale method of 1–9 (1, 3, 5, 7, 9 are equally important, slightly important, obviously important, strongly important, and extremely important, 2, 4, 6, 8 are intermediate values of 1, 3, 5, 7, 9), so as to construct a pairwise comparison judgment matrix of operational effectiveness evaluation of a certain type of equipment.

Table 1, Table 2, Table 3, Table 4 are the scoring of experts on evaluation indexes. The pairwise comparison scores of experts 1 to 5 on B1 and B2 are (5, 5, 4, 6, 5) respectively, and the average value of B1–B2 is 5. Similarly, through experts scoring, the other evaluation score of indexes and the relative weight of indexes can be obtained. In this table, W_{A-B} represents the relative weight between the operational effectiveness and the first-order index, and $W_{B_1-C}, W_{B_2-C}, W_{B_3-C}$ represents the relative weight between the first-order index and the second-order index.

Table 1. Judgement matrix of layer A–B

A	B1	B2	B3	W_{A-B}
B1	1	5	6	0.7225
B2	1/5	1	2	0.1741
B3	1/6	1/2	1	0.1033

Table 2. Judgement matrix of layer B₁–C

B1	C1	C2	C3	W_{B_1-C}
C1	1	1/3	5	0.2746
C2	3	1	8	0.6571
C3	1/5	1/8	1	0.0682

Table 3. Judgement matrix of layer B₂–C

B2	C4	C5	C6	W_{B_2-C}
C4	1	3	1/2	0.320
C5	1/3	1	1/4	0.123
C6	2	4	1	0.557

Table 4. Judgement matrix of layer B₃–C

B3	C7	C8	C9	W_{B_3-C}
C7	1	4	3	0.6232
C8	1/4	1	1/2	0.1373
C9	1/3	2	1	0.2395

3.3 Hierarchical Single Ranking of Effectiveness Evaluation and Consistency Test

The geometric average approach is used to calculate the eigenvectors. First, calculate the multiplication of all elements per row in a pairwise judgment matrix B: $M_i = \prod_{j=1}^n b_{ij}$, n is the number of factors at all hierarchies, Then calculate the n-th root of M_i $\bar{W}_i = \sqrt[n]{M_i} (i = 1, 2, \dots, n)$, and take the geometric average value of all elements per row and getting the vector: $\bar{W} = (\bar{W}_1, \bar{W}_2, \dots, \bar{W}_n)^T$, then normalize to obtain formulas: $W_i = \frac{\bar{W}_i}{\sum_{i=1}^n \bar{W}_i}$, we

can judge that the matrix feature vector is: $W = (W_1, W_2, \dots, W_N)^T$, W_i is a single ranking weight for each hierarchy factor [5].

Consistency test of judgment matrix. Coincidence indicator $CI = \frac{\lambda_{\max} - n}{n - 1}$, the maximum characteristic root $\lambda_{\max} = \sum_{i=1}^n \frac{(BW)_i}{nW_i}$ is implanted as the eigenvalues of each judgment matrix, it can be seen from the definition of judgment matrix that the first-order and second-order judgment matrices are completely consistent. The higher the order n ($n \geq 3$) of the general judgment matrix, the larger the estimation deviation and the worse the consistency, the average random consistency index RI of the corresponding

n-order is introduced as the evaluation value (Table 5). Calculating the consistency ratio $CR = \frac{CI}{RI}$, when $\lambda_{max} = n$, $CR = 0$, which indicates that the pairwise judgment matrices are completely consistent; the larger the CR value is, the worse the complete consistency of the judgment matrix is; when $CR < 0.1$, it is considered that the consistency of the judgment matrix is acceptable; otherwise, the judgment matrix needs to be appropriately modified to ensure a certain degree of consistency.

Table 5. Average random consistency index RI

Order of matrix n	1	2	3	4	5	6	7	8	9	10	11
RI	0	0	0.52	0.89	1.12	1.26	1.36	1.41	1.46	1.49	1.52

For the judgment matrix layer A-B, $\lambda_{max} = 3.0291$, $CI = \frac{\lambda_{max}-n}{n-1} = 0.0146$, $RI = 0.52$, $CR = \frac{CI}{RI} = 0.0281 < 0.1$, Consistency is acceptable. Similarly, we can get judgment matrix layer $B_1 - C$ $\lambda_{max} = 3.0441$, $CI = 0.0221$, $RI = 0.52$, $CR = 0.0425 < 0.1$, Consistency is acceptable. The judgment matrix layer $B_2 - C$ $\lambda_{max} = 3.0183$, $CI = 0.0092$, $RI = 0.52$, $CR = 0.0177 < 0.1$, Consistency is acceptable. Judgment matrix layer $B_3 - C$ $\lambda_{max} = 3.0183$, $CI = 0.0092$, $RI = 0.52$, $CR = 0.0177 < 0.1$, Consistency is acceptable.

3.4 Effectiveness Evaluation Hierarchy Ranking and Consistency Test

Hierarchical total ranking is the composite weight. After obtaining the ranking weight vector of each hierarchy, the composite weight of each hierarchy for the total target is calculated layer by layer from top to bottom, and then the total ranking of the scheme is obtained. The hierarchical total ranking of a certain type of equipment operational effectiveness factors is shown in Table 6.

The random consistency ratio of hierarchical total ranking is: $CR = \frac{\sum_{i=1}^n \omega_{B_i} CI_i}{\sum_{i=1}^n \omega_{B_i} RI_i}$, CI_i is the consistency index of judgment matrix in hierarchy B corresponding to ω_{B_i} , RI_i is the consistency index of judgment matrix in hierarchy B corresponding to ω_{B_i} , when $CR < 0.1$, the hierarchical total ranking passes the consistency test, otherwise it does not pass. we can know that $CR = 0.0358 < 0.1$ from Table 6, all judgment matrices in the whole system analysis model meet the consistency requirements.

3.5 Conclusions and Countermeasures

By comparing the data in Table 6 with the evaluation index system, the conclusion can be drawn: among the factors affecting the operational effectiveness of a certain type of equipment, the three most influential factors are C_2 , C_1 and C_6 , accounting for 47.48%, 19.84% and 9.7%, respectively. According to this conclusion, in order to improve the operational effectiveness of this type of equipment, the following countermeasures can

Table 6. General ranking table of effectiveness factors of a certain type of equipment

Second-order index	ω_{A-B_1}	ω_{A-B_2}	ω_{A-B_3}	Total scale	General ranking
	0.7225	0.1741	0.1033		
C1	0.2746	0	0	0.1984	2
C2	0.6571	0	0	0.4748	1
C3	0.0682	0	0	0.0493	6
C4	0	0.320	0	0.0557	5
C5	0	0.123	0	0.0214	8
C6	0	0.557	0	0.0970	3
C7	0	0	0.6232	0.0644	4
C8	0	0	0.1373	0.0142	9
C9	0	0	0.2395	0.0247	7

be taken: First, standardizing operation, precision operation, reducing error rate and improving success rate of structural components related to C₂, C₁ and C₆ performance in daily use; second, timely maintenance and careful maintenance should be carried out in operation and training to ensure good quality and normal performance of components; third, further strengthening system design, focusing on enhancing the performance of C₂, C₁ and C₆, in order to achieve the goal of improving the overall efficiency of equipment.

References

1. Sun, W.: The Chapter of Ji in the Art of War, vol. 16. Zhong Hua Book Company (2016). (translated by Chen X)
2. Zhang, J., Tang, H., Su, K., et al.: Research on Effectiveness Evaluation Method. Defense Industry Press, Beijing (2009)
3. Duan, S.: Application of analytic hierarchy process in effectiveness evaluation of electronic weapons. Electron. Inf. Countermeas. Technol. (1), 38–40 (2006)
4. Li, D., Xu, T.: Analysis and Application of Navy Operational Research. Defense Industry Press, Beijing (2007)
5. Cheng, Q.: Command Effectiveness Evaluation and Risk Management Based on Information System, pp. 7–93. Defense Industry Press, Beijing (2011)



An Analysis of the U.S. Red Flag Military Exercises

Weixin Liu, Hao Jiang, Hongyan Ou^(✉), Shuxin Wang, and Kang Yu

Zhengzhou Campus, CPLA Army Artillery and Air Defense Forces
Academy, Zhengzhou 450052, China
2242127616@qq.com

Abstract. Red Flag is one of the most successful training exercises in the history of the world. By simulating the realistic actual combat environment, it has made outstanding contributions to maintaining the air superiority of the U.S. military in the high-intensity and difficult military exercises, by testing weapons and equipment, studying tactical methods of operation, and tempering the technical, tactical and psychological quality of pilots. The paper introduces the basic overview of the Red Flag from the perspectives of exercises purpose, confrontation form, battle-field condition, information support and evaluation method. The paper focuses on analyzing the distinctive characteristics of the Red Flag exercises, so as to provide a mirror for our exercises.

Keywords: Red flag · Military exercises · U.S. Air Force

1 Introduction

Red Flag is currently the world largest air combat training exercises and one of the annual routine exercises of the U.S. Air Force. It is held at Nellis Air Force Base in Nevada and Elson Air Force Base in Alaska, other U.S. military services (including the National Guard and Reserve) and U.S. military allies will attend. During the past 47 years of development, the Red Flag exercises have always been adjusted to adapt to the ever-changing threats and evolving environment, and has made outstanding contributions to improving the technical and tactical level of pilots, promoting air combat frontier research and developing experimental weapons and equipments.

2 Basic Information of the Red Flag Exercises

For the U.S. military, the exercises can be divided into demonstration exercises and effect-based exercises. Obviously, what is really positive for combat forces is effect-based exercises. Among all the effect-based exercises of the U.S. military, Red Flag can be called a “model of actual combat”.

2.1 Take Real Practice as the Purpose

Red Flag has its roots in the defeat of the U.S. Air Force during the Vietnam War. During the Vietnam War, the air force exchange rate hit an all-time low. The main reasons are as follows. Pilots were overly superstitious about equipment (air-to-air missiles and electronics) and ignored basic air combat skills. The information about the characteristics and tactical characteristics of enemy aircraft was far from enough, and no targeted drills were carried out in daily training. At the same time, the data also showed that 80% of combat losses occurred in the pilot's first 10 combat missions [1]. Based on the results of the Vietnam War, the U.S. military began to rethink that the traditional skill-based training mode can produce skilled pilots, but the lack of combat experience is the main cause of pilots' combat loss. In response, the Air Force began to reform pilot training to focus more on professionalism and authenticity. In April 1975, the Air Force Tactical Command officially announced the decision to organize the Red Flag exercises.

2.2 Take Red-Blue Confrontation as the Form

Red Flag adopts a typical form of "red and blue" confrontation. The 414th Combat Training Squadron subordinate to the 57th Wing is the main organization and execution unit of the exercises.

The main task of the "Red Force" is to act as imaginary enemies by using the paint of Russian fighters and imitating the air actions and combat methods of Russian aircraft to play the role of the air force of Russia and other countries, and to conduct air confrontation with the Blue Force. If the Red Force are shot down in battle, they can be "resurrected". In the battle, they often show "doing whatever they want" [4]. Their task is to play the enemy as realistically as possible, posing a real threat to the Blue Force pilots. Only by approaching the real battlefield to the greatest extent can pilots avoid facing such a crisis situation for the first time in an engagement.

The "Blue Force" is made up of a diverse mix of U.S. air Force, the NAVY, Air National Guard, Air Force Reserve (AFR) and NATO Allies. The types of units involved include Fighter Squadron, Electronic Warfare Squadron, Anti-submarine Warfare Squadron, Air Force Base Squadron, Navy Carrier Aircraft Squadrons, Helicopter Squadron, Transport Aircraft Squadrons, Reconnaissance Aircraft Squadrons, Early Warning Aircraft Squadrons, etc. They cover almost all arms of the U.S. military's air operations [2].

2.3 Take Joint Shooting Range as the Battlefield

Red Flag combines multiple shooting ranges, bases, command centers and simulation centers of various services and arms of the U.S. Army. These shooting ranges bear the main part of the Red Flag exercises. The surveillance, control and guidance assessment of the exercise were jointly completed by Nellis Air Force Base in Nevada, Herbert range in Florida, Fort bris in Texas, Kirtland Air Force Base in New Mexico and White Sands Missile Range [1].

Nellis Air Force base is located about 13 km northeast of Las Vegas, the famous casino city in the United States. With a complete overall training facilities, it is the

first choice for the U.S. Air Force to conduct air training. The base is equipped with a number of complete digital equipments, such as automatic action coordination system, air combat training system, joint engagement evaluation system, engagement display system, data recording system and integrated information display system. It's more of an integrated digital air battlefield than a base. The Nevada Test and Training Range is the main exercise area. The shooting range has four areas: areas No. 1 and No. 2 filed are electronic warfare shooting ranges, and their facilities mainly simulate the enemy's comprehensive ground air defense system, including early warning radar, fire control radar and electronic jamming; No. 3 field is ground-attack live ammunition shooting range, with large engineering facilities, static or dynamic simulation equipment and other types of simulation facilities. LVC can also be used to provide training for scenes that cannot be realized in the physical shooting range; No. 4 field is an air combat shooting range [2]. Most of the shooting range is located in the vast deserts and mountains, inaccessible and with good concealment.

2.4 Take Data Information as the Support

To organize such large-scale exercises, if the commander cannot intuitively see the situation of each season of the exercise. Then the effect of the exercise will be greatly reduced. The U.S. military uses its advanced technology to have a panoramic view of the war situation. Over the vast desert, a U-2 reconnaissance aircraft is cruising in the target airspace, and it will transmit relevant intelligence and information to E-8A early warning aircraft in real time [1]. The early warning aircraft is the air combat control commander, who is the brain of the exercises. He is responsible for guidance and control during the exercises. The special computer software system and radar equipment on the early warning aircraft can display the aircraft data in the operational airspace on the computer screen in real time in a three-dimensional dynamic way. In addition, the exercise also adopts advanced interactive intelligence broadcasting services, monitoring and control data links, joint air defense operation control systems and other types of tactical data links. Various tactical data, the telemetry data of unmanned reconnaissance aircraft, the location of threat targets, missile launch actions, and the evaluation results of damage effects for instance, are transmitted between the battle command center and weapons, as well as between equipment and equipment. The use of these data links makes the war truly one-way transparent, safe and efficient.

2.5 Take the Effect as Evaluation Basis

In Red Flag, the U.S. military uses information-based means to evaluate the effect of the exercises. By collecting panoramic situation data and adopting a variety of automatic analysis and processing systems, real-time adjudication and post-event evaluation of the tactical actions of trained troops are conducted in realistic confrontation situations and threat environments. In Red Flag of 2015, Command posts, combat simulation centers and weapon systems at all levels transmit battlefield situation data and engagement process data to Kirtland Air Force Base in real time through various wireless data links and wired communication networks. After these data are fused and processed by Robbins

Air Force Base, they are quickly transmitted back through the distributed mission combat network. Kirtland Air Force Base converts the data protocol, synthesizes it with the virtual ground target data generated by the local joint construction tactical simulation system, and transmits it to Nellis Air Force base through the joint test and test network, and Nellis Air Force Base performs necessary format conversion on the received synthetic data and sends it together with the real ground target data of Nellis shooting range measured by Nellis Air Force Base [2]. It forms a panoramic air ground battlefield situation combining real, virtual and structural, and truly ensure that there is no leakage of data.

3 Distinctive Characteristics of the Red Flag Exercises

There is no doubt that Red Flag has a wide impact all over the world. In addition to its great success, the Red Flag has explored a mature and effective exercises mechanism and established an invisible standard for the actual combat training of the Air Force.

3.1 Design Exercises for Short Board and Closely Target the Needs of War

The subjects and contents of the Red Flag exercises have different focuses each time according to the needs of current and future wars. During the Vietnam War, in order to solve the problem that F-4II was at a disadvantage in the air battle with Mig-17 and Mig-21 of North Vietnam, the content of the exercises highlighted the air-to-air combat. During the war in Afghanistan and in Iraq, a large number of village targets were set up in the shooting range, so the content of the exercises focused on how to find targets in the environment with more urban terrain characteristics and the pilots' consideration of collateral damage. With the U.S. strategy re-targeting competition among great powers, the exercises have become more prominent in a competitive, degraded and Constrained Operational (CDO) environment. In order to simulate the interference of China and Russia on the U.S. military's satellite communication and GPS system in the future war, the U.S. Air Force Space Command (AFSPC) even ordered the Colorado Satellite Control Center to deliberately "degrade" the communication link between spacecraft and aircraft [3]. Through the setting of these training subjects, the U.S. military can reduce its dependence on space support and ensure that the inertial navigation system, compass and mapcan be used to win the war.

3.2 Focus on the Construction of Imaginary Opponents and Build a Professional "Red Force"

In order to improve the authenticity of the Red Flag exercises, the U.S. Air Force has formed a professional imaginary enemy force to simulate the opponent as much as possible. During the cold war, the 64th and 65th Aggressor Squadron all adopted Soviet-style tactics and procedures, with aircraft painted in Soviet aircraft livery, pilots using Soviet Air Force tactical acronyms, and even the take-off and landing strips and dormitories of both squadrons changed to Soviet style. After 2000, in order to simulate the increasing space confrontation and cyber warfare capabilities of China and Russia, the U.S.

military has successively established the 527th Space Aggressor Squadron (transferred to the Space Force in April 2020) and the 26th Space Aggressor Squadron (Reserve) [4]. Squadron members are specially trained and can skillfully operate GPS jamming system and satellite communication system, so as to simulate the possible threat of the enemy to the U.S. space system and space system in training and testing. At the same time, the squadron also undertakes the task of developing new tactics, technologies and procedures (TTP) for combat against space-capable opponents.

3.3 Involve Multi-platform and Multi-model, and Highlight System Confrontation

The Red Flag exercises have paid more and more attention to system confrontation from stand-alone confrontation to group confrontation, from fighter aircraft to multi-aircraft types, and from a few countries to multinational joint participation. Even F-22 and F-35A play the role of main nodes in the system. Taking Red Flag 20-1 as an example, 21 units, 91 aircraft, 317 air force, space and cyber personnel, 461 aircrew, 912 maintenance personnel and 242 support personnel from three countries participated in the military exercises. Based on the information of all parties, it is obvious that the number of support aircraft represented by EA-18G, RC-135V and HH-60G in the exercise is equal to or even slightly more than that of fighter aircraft [2].

3.4 Exercise Military Diplomacy and Serve the Need of Strategy

The Red Flag exercises, as the largest exercise of the U.S. Air Force, not only play the role of the exercises themselves, but also expand their military diplomacy function and play an active role in national strategy by inviting other countries to participate in the exercises. As of 2020, a total of 27 countries have participated in the Red Flag exercises. In addition to traditional allies such as Britain, Australia and Canada, they also include countries that maintain friendly relations with the United States such as India, Egypt and Singapore [3]. On the whole, the multi-country joint exercises have played the following roles. The first is as a tool of national strategy. The Second is to increase the understanding of foreign aircraft. The third is to improve the level of joint operations among allies. Although the United States, Britain, France and other countries belong to the “NATO” military group, the specific tactical doctrine and command structure are not the same, and the exercise can just enhance the familiarity of both sides.

4 Conclusion

There is no doubt that Red Flag has gone far beyond the scope of the air force and has left an indelible mark on the history of the development of world military exercises. As an exercise born from war, a series of exercise principles introduced and developed by it have been absorbed and used for reference by almost all practical exercises in the future. What is even more valuable is that Red Flag has not been complacent after its great achievements, but has always been in a “negative” attitude of continuous self-innovation and keeping pace with the times.

References

1. Rininger, T.V.: Red Flag: Air Combat for the 21st Century. China Market Press, Beijing (2021)
2. Xu, Z.: Research on the joint red flag exercises of the U.S. military. *Command Control Sinul.* **36**(3), 137–142 (2014)
3. Hu, Z.: Current situation and development trend of. Red Flag. *Aerodyn. Missile J.* **2015**(12), 74–77 (2015)
4. Li, H., Wang, X., Liu, Y.: The aggressor force of U.S. air force. *Foreign Air Force Train.* **2017**(6), 16–18 (2017)



Demand Analysis of Air Defense Unit Training Evaluation System

Hao Liu, Yanyan Ding, Haimin Hu(✉), Hongyan Ou, Weixin Liu, and Junfei Wang

Zhengzhou Campus, CPLA Army Artillery and Air Defense
Forces Academy, Zhengzhou 450052, China
807111052@qq.com

Abstract. The construction of digitalization and informationization has put forward higher requirements for the training of air defense unit in scientific evaluation, correct decision-making and rapid response. At present, the manual evaluation method is not easy to query, classify, summarize and analyze the data information scientifically, and it cannot meet the needs of the modernization of the army. It is of great practical significance to study and establish the training and evaluation system of air defense unit to guide the training of troops and make scientific decision.

Keywords: Training · Evaluation · Demand analysis

Military training is an important basis for the generation of the army's combat effectiveness, and training evaluation is an important part of the army's training and management. At present, there are still some problems in the training of air defense units: first, the scientific evaluation and quantification of the training quality of units and individuals are not accurate; second, the arrangement of training plan is not scientific; third, the assignment of task to the team personnel is not reasonable; fourth, the combat grouping is not intelligent. Therefore, the scientific evaluation of the air defense unit training, and on this basis to provide practical assistance decision-making has become an important and difficult problem in military training.

1 Training and Evaluation of Air Defense Units

1.1 Training and Characteristics of Air Defense Units

The training of air defense unit refers to that the unit completes the training content within the prescribed scope in accordance with the provisions of the training program, and achieves the prescribed training target, so as to achieve the purpose of improving the combat effectiveness. It has the following characteristics:

Phased. Training of air defense unit is carried out in stages, and each stage of the training content has clear provisions. Unit and individual will transfer to the next stage after completing the training content of one stage and meeting the prescribed standards after assessment. If they fail to pass the assessment, they will take supplementary training until reaching the standard.

Repeatability. As long as the content of the military training program remains unchanged, the training content of each arm of service remains essentially unchanged, only repeating the previous training content.

Timing. All contents of the training are carried out in strict order. Only when unit and individual complete all the training contents in the first stage and reach the prescribed quality target can they carry out the training in the second stage.

1.2 Training Evaluation and Characteristics of Air Defense Units

The training evaluation of air defense unit refers to the evaluation of the training results of units and individuals according to the evaluation standards stipulated in the military training program, and a reasonable estimate of the training quality is excellent, good, pass or fail. Training evaluation consists of three items: individual annual training performance evaluation, unit annual training performance evaluation, and unit single-subject training performance evaluation. It has the following characteristics:

Integrity. Training evaluation can only be carried out on the premise that the evaluation subject has completed all evaluation contents. Individuals can only be assessed on their individual annual training performance after they have completed all the training subjects stipulated in the training program. The integrity of the training evaluation of air defense unit ensures the comprehensiveness and accuracy of the evaluation results [1].

Strictness. Military training program specifies strictly the evaluation standards for training results, different years, different arms and different professionals as well as different levels of units have different evaluation standards.

Scientific. The evaluation standard of military training results stipulated in the military training program is derived from the scientific calculation and summary of many years' experience data of the army, which are fully in line with the actual work of the army and has a strong scientific nature.

Accuracy. In strict accordance with the evaluation standards of military training results, the evaluation results obtained by scientific calculation of military training performance of units and individuals are accurate.

2 System Basic Function and Business Requirement Analysis

2.1 Basic Function

1. Collect and permanently store all the data needed for military training
2. Data sharing. Able to quickly and accurately provide all kinds of data needed for military training evaluation, and support basic activities in system operation.
3. It has the functions of single transaction processing, integrated transaction processing and auxiliary decision-making.

4. It has the effective functions of data management and data communication to ensure the accuracy, reliability, confidentiality and security of data.
5. In order to ensure the uninterrupted operation of military training and management of troops, it is necessary to have the function of continuous operation.
6. The system should have the capable of scalability.

2.2 Business Requirement

The overall task of system development is to realize systematization, standardization and automation of various information. System business requirement analysis is based on the overall task of system development. The system must deal with the following services:

1. The input, deletion, modification and inquiry of basic information such as arm, professional, subject, unit, site, personnel, etc.
2. Selection of subjects and their grading standard. Each year at the beginning of the year to select professional training courses and their grading standards.
3. Entry, modification, inquiry of scores. Including the entry, deletion, modification, and inquiry of score of units and individuals selected for each subject, and entry, deletion, modification and inquiry of the re-examination results of units and individuals who failed the assessment.
4. Training results evaluation. Including personal annual training performance evaluation, unit single-subject training performance evaluation and unit annual training performance evaluation.
5. The combat effectiveness index of units and individuals is generated according to the professional technical level of individual, training quality, combat experience, military age, etc.
6. Scientific task assignment system, according to the nature of tasks and combat effectiveness index of each unit, scientifically formulate the task assignment plan that is most conducive to the completion of tasks for the user [3].
7. Intelligent the combat grouping. According to the combat effectiveness index of individuals and requirements of the users, the system realizes the intelligent combat grouping of individuals, and the grouping plan ensures that the whole combat effectiveness of the army can reach to its maximum.

3 System Structure Requirement Analysis

According to the training content and evaluation requirement, the system can be divided into several functional modules, such as system management, basic information management, military training evaluation management and decision-making management. The modules are not completely independent, and can complete data sharing and interactive operations as required. The system structure diagram is shown in Fig. 1.

3.1 System Management Module

Set user rights, user management and user group management functions. Personnel with administrative rights can add, modify, delete, query, browse and set user rights through this module.

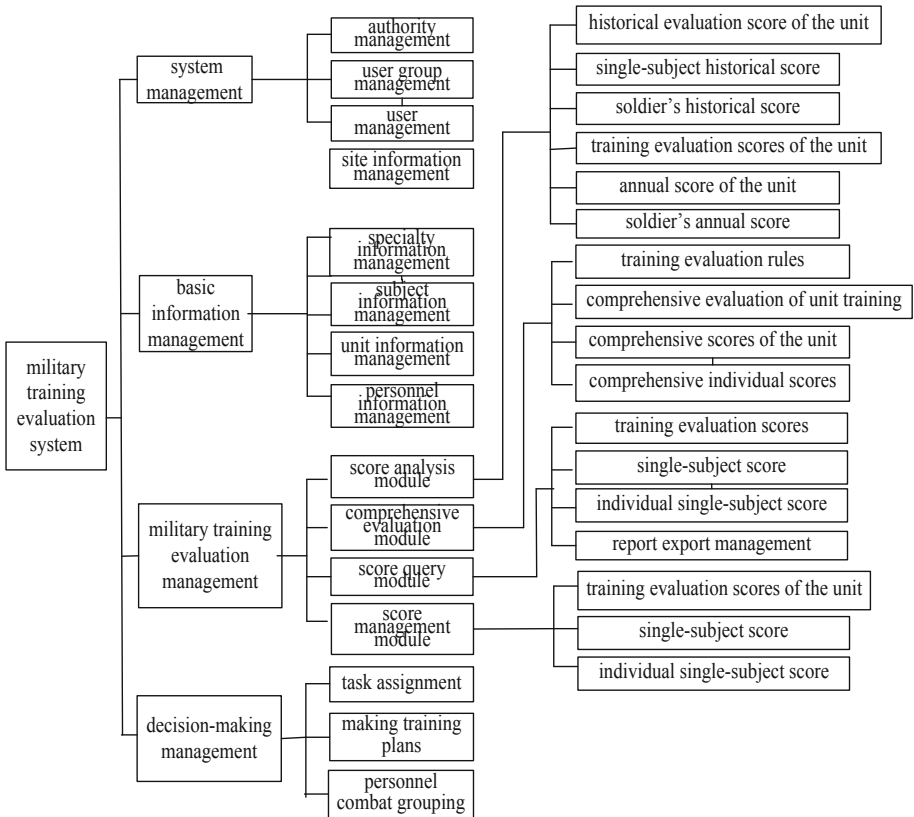


Fig. 1. System structure diagram

3.2 Basic Information Management Module

The basic information management module can input, delete, query and modify the basic information of specialty, subject, unit, site and personnel. To realize the operation of the data such as the number, name, number of officers, number of non-commissioned officers, number of conscripts, total number of personnel, number of technical grades, etc. of the arms, specialties and units, the operation of the results of the selected personnel of each subject, the excellent number and excellent rate of the assigned subjects, the good number and good rate, the number of passing officers, and the rate of passing officers, the number of failed students, the rate of failure, etc., Operation of personnel's identification

number, name, position, rank, political status, etc. The basic information management module facilitates the data administrator to modify the basic information of the system.

3.3 Training Evaluation Management Module

It mainly includes four sub-modules: score management, score query, comprehensive evaluation and score analysis. Comprehensive evaluation module: according to the evaluation rules of the training results and the military training comprehensive evaluation model, it automatically synthesizes the individual and unit's comprehensive scores of each item, carries on the comprehensive evaluation to the unit military training, updates and preserves each kind of comprehensive scores and training evaluation results, and may carry on the maintenance to evaluation rules and the evaluation model. The premise of system training comprehensive evaluation function is to have a comprehensive and reasonable training evaluation index system and a scientific and feasible evaluation calculation model. [2] Therefore, it is necessary to establish an objective and comprehensive evaluation index system and a scientific and feasible evaluation model to ensure the realization of the comprehensive evaluation function of military training system. Score management module: maintain and update individual single-course scores, unit single-subject scores, evaluation results information and units, personnel received rewards and punishment information, including the above information to add, modify, delete, etc. Score inquiry module: complete the inquiry and browsing of individual single-subject scores, unit single-subject scores, unit training evaluation results, provide the user with common information in the form of report form, complete the function of browsing, printing, exporting and so on. Score analysis module: users at all levels may, according to their authority, carry out comprehensive evaluation of individual scores, unit scores and unit training, and operation and training department conducts maintenance and management of score evaluation rules, mainly realizing the following functions:

1. Analysis shows the distribution of training scores of units or personnel in the current year.
2. Analysis shows the distribution of units or personnel's scores over the years.
3. Analysis shows the distribution of single-subject scores in this year.
4. Analysis shows the distribution of single-subject scores over the years.
5. Analysis shows the comprehensive evaluation of the unit's training in this year.
6. Analysis shows the comprehensive evaluation of the unit's annual training.

3.4 Decision-Making Management Module

Decision-making management module realizes the assistant decision-making in three aspects: training plan arrangement, task assignment and personnel combat grouping, which is divided into three sub-modules: training plan arrangement, task assignment and personnel combat grouping. The sub-modules of the training plan shall be prepared according to the specific conditions of each unit, profession and site and the specific requirements of each training course, and shall be used for reference by the training units in organizing and implementing the training. [4] The task assignment sub-module develops a scientific task assignment plan to meet the requirements of each unit's various

combat effectiveness indexes and tasks to ensure that the task is most beneficial to the completion of the task. The sub-module provides the auxiliary decision-making scheme according to the combat effectiveness index of the personnel and units produced by the statistics of the results, conversion coefficient of the professional technical grade of the combat grouping, conversion coefficient of the combat grouping age, conversion coefficient of the operational experience of combat grouping, conversion coefficient of the training quality of the combat grouping, conversion coefficient of the combat grouping unit, the number of the combat grouping and the requirements of the users.

4 Conclusion

The realization of the training and evaluation system of air defense unit is a complicated work, and it is also a work of great significance and value to the construction of the army. In this paper, the basic conception and thinking of the training and evaluation system of the air defense unit is very important for the construction of the training and evaluation system to guide the training and scientific decision-making of the troops.

References

1. Wu, Q.: Military Training. Military Science Press, Beijing (2003)
2. Ren, L.: An Introduction to System Operations Capability Based on Information Systems. Military Science Press, Beijing (2001)
3. Xiao, B., Zhao, C.: Military Training Management. Haichao Publishing House, Beijing (2001)
4. Li, H., Wang, X., Liu, Y.: The aggressor force of U.S. air force. Foreign Air Force Train. **2017**(6), 16–18 (2017)



Application of Grey AHP in Occupational Health Risk Assessment of Maintenance Operation in Xi'an Subway

Miao Zhang¹, Jianwu Chen^{2,4}, Zhenfang Chen^{2(✉)}, Hong Yang¹, and Yan Wang³

¹ Xi'an Rail Transit Group Co., Ltd., Xi'an 710016, Shanxi, China

² China Academy of Safety Science and Technology, Beijing 100012, China
czf1c7922@126.com

³ Beijing MTR Co., Ltd., Beijing 100068, China

⁴ NHC Key Laboratory for Engineering Control of Dust Hazard, Beijing 100012, China

Abstract. With the increasing number of subway lines and subway workers, their occupational health risks should be paid attention to. As the workplace, operation content, operation time, operation frequency and operators of metro operation and maintenance posts are determined according to the actual needs, the type, concentration or intensity, number of people, time and frequency of occupational hazards factors exposed are uncertain, and the risk is in a gray state, so it is difficult to evaluate their occupational health risk by quantitative evaluation method. Therefore, this paper takes a maintenance operation of Xi'an subway as the research object. The occupational health risk AHP model of subway maintenance operation was established from four aspects, which were occupational hazard factors, environmental factors, human-computer interaction factors and management factors. The gray analysis method was used to evaluate its uncertain risk. The comprehensive risk assessment results of occupational health for subway maintenance workers is between low and low risk level, which shown that the grey AHP can be used in the occupational health risk assessment of subway maintenance workers.

Keywords: Risk assessment · Occupational health · Subway · Grey AHP · Maintenance worker

1 Purpose

With the development of economy, the number of subway has become more and more. In order to ensure the safe of the subway running, the running, operation and maintenance workers are increasing day by day [1, 2]. Maintenance workers exposed to dust, poisons, noise, radio-frequency radiation, power-frequency radiation and other occupational hazards, because they worked in a variety of locations for maintenance [2, 3]. And the living habits, equipment used and maintained, as well as the surrounding environment also affected their occupational health and even induce accidents in operation [4], because they needed to work underground in night. Therefore the maintenance workers' occupational health should be paid enough attention to.

Mai S. et al. [5] analysed the occupational hazards in 18 representative subway tunnel construction sites in a city, and pointed out that noise was the key point of prevention and control in tunnel construction. Lai Y. et al. [6] compared and analysed the impact of ICM (International Council on Mining and Metals) method, UQ (the University of Queensland) method and MLSP (the Romania Labour and Social Protection Department) method of occupational health risk assessment on the results of dust occupational health risk assessment during the construction of subway. Risk Assessment is carried out for the workers exposed to chemical harmful factors in subway operator, and the applicable scope and conditions of the Composite Index method were also discussed [7]. The occupational health risk assessment methods were compared and analysed by Li Y. et al. [8] in the petroleum industry.

As the location, content, time, frequency and personnel of the operation and maintenance posts of the subway depend on the actual needs, the type, concentration or intensity, number, time and frequency of occupational hazards are uncertain. The risk of occupational health is in gray state, so it is difficult to evaluate the occupational health risk by quantitative evaluation method. The method of grey AHP (analytic hierarchy process) can be used to solve those problems. Li Y. [9] used the Grey System Theory to evaluate the occupational hazards of a sewage plant. Zhou W. et al. [10] also verified the effectiveness and feasibility of grey AHP in the safety risk assessment of three major emergencies, which were subway station fire, stampede and elevator failure. Therefore, this article takes the subway maintenance work as the research object, studies the application of grey AHP in occupational health risk assessment of maintenance workers, discusses and analyses the scientific and feasibility of the results.

2 Research Object and Method

2.1 Research Object

Because the maintenance work needs to adjust the work content according to the task needs, there are great uncertainties in the work location, work time, work frequency, occupational hazards and so on. It is difficult to evaluate scientifically by quantitative method, but the problem can be solved by GAHP. Therefore, this study takes a maintenance operation of Xi'an subway as the research object.

2.2 Research Method

Based on the full investigation of the research object, the occupational hazards factors exposed to subway maintenance operation are classified from four aspects, which were occupational hazards factors, environmental factors, human-computer interaction factors and management factors. The AHP is used to establish the evaluation index system, build the judgment matrix, determine the priority relationship and calculate the weight coefficient of each index. Finally, the consistency test was carried out, because the AHP is more subjective. As the AHP adopts pairwise comparison, it may lead to inconsistent judgment matrix. It is necessary to ensure the overall consistency according to the consistency ratio.

Base on AHP, grey theory was used to evaluate the uncertainty. According to the grey theory, the grey matrix is established. According to the index weight of risk matrix and evaluation index matrix, the weight set of primary evaluation index is calculated. The comprehensive evaluation value of occupational health hazard factors of subway maintenance posts was obtained by multiplying the primary index weight vector and the evaluation weight matrix. According to the comprehensive evaluation value, the occupational health risk of iron maintenance post was determined. The implementation process of grey analytic hierarchy process can be seen in literature [10].

3 Results and Analysis

3.1 Hierarchical Model and Weight of Occupational Health Risk Assessment of Subway Maintenance Operation

Based on the investigation of the research object, the hierarchical model of occupational health risk assessment of subway maintenance operation as shown in Fig. 1 was established from four aspects, which were occupational hazard factors, environmental factors, human-computer interaction factors and management factors.

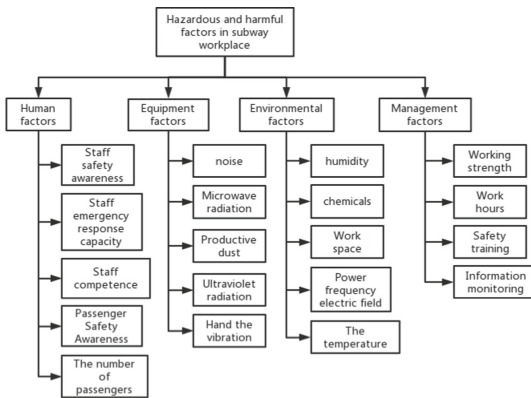


Fig. 1. Grey analytic hierarchy process flow chart.

3.2 Construct Judgment Matrix and Determine Index Weight

On the basis of determining the evaluation indicator system, a judgment matrix is established, and the scale in literature [10] is used to scale the indicators at the same level in the two levels to determine the priority relationship between them, and then the weight of each indicator can be calculated. After the consistency was test, C.R. All values are less than 0.1, as shown in Tables 1, 2, 3, 4 and 5, indicating that the constructed judgment matrix is reasonable.

Table 1. Judgment matrix and weight analysis of the first-level indicators.

<i>T</i>	<i>T₁</i>	<i>T₂</i>	<i>T₃</i>	<i>T₄</i>	<i>W_T</i>
<i>T₁</i>	1	3	3	2	0.4392
<i>T₂</i>	0.3333	1	3	0.5	0.1855
<i>T₃</i>	0.3333	0.3333	1	0.3333	0.0984
<i>T₄</i>	0.5	2	3	1	0.2769

$\lambda_{\max} = 4.1451$, C.R. = 0.0543 < 0.10, Consistency can be accepted

Table 2. Judgment matrix and weight analysis of *T₁*.

<i>T₁₁~T₁₅</i>	<i>T₁₁</i>	<i>T₁₂</i>	<i>T₁₃</i>	<i>T₁₄</i>	<i>T₁₅</i>	<i>W_{T1}</i>
<i>T₁₁</i>	1	3	3	3	3	0.4139
<i>T₁₂</i>	0.3333	1	2	2	2	0.211
<i>T₁₃</i>	0.3333	0.5	1	2	2	0.1642
<i>T₁₄</i>	0.3333	0.5	0.5	1	1	0.1055
<i>T₁₅</i>	0.3333	0.5	0.5	1	1	0.1055

$\lambda_{\max} = 5.1368$, C.R. = 0.0305 < 0.10, Consistency can be accepted

Table 3. Judgment matrix and weight analysis of *T₂*.

<i>T₂₁~T₂₅</i>	<i>T₂₁</i>	<i>T₂₂</i>	<i>T₂₃</i>	<i>T₂₄</i>	<i>T₂₅</i>	<i>W_{T2}</i>
<i>T₂₁</i>	1	1	0.5	0.3333	0.5	0.1126
<i>T₂₂</i>	1	1	0.5	0.3333	1	0.1348
<i>T₂₃</i>	2	2	1	1	1	0.2434
<i>T₂₄</i>	3	3	1	1	1	0.2907
<i>T₂₅</i>	2	1	1	1	1	0.2184

$\lambda_{\max} = 5.1091$, C.R. = 0.0244 < 0.10, Consistency can be accepted

Table 4. Judgment matrix and weight analysis of T_3 .

$T_{31} \sim T_{35}$	T_{31}	T_{32}	T_{33}	T_{34}	T_{35}	W_{T3}
T_{31}	1	2	2	0.5	0.25	0.1505
T_{32}	0.5	1	0.5	0.5	0.3333	0.0904
T_{33}	0.5	2	1	0.5	0.3333	0.1222
T_{34}	2	2	2	1	0.25	0.1909
T_{35}	4	3	3	4	1	0.446

$\lambda_{\max} = 5.2764$, C.R. = $0.0617 < 0.10$, Consistency can be accepted

Table 5. Judgment matrix and weight analysis of T_4 .

$T_{41} \sim T_{44}$	T_{41}	T_{42}	T_{43}	T_{44}	W_{T4}
T_{41}	1	2	0.3333	0.5	0.1653
T_{42}	0.5	1	0.5	0.3333	0.1254
T_{43}	3	2	1	3	0.4484
T_{44}	2	3	0.3333	1	0.2609

$\lambda_{\max} = 4.2610$, C.R. = $0.0977 < 0.10$, Consistency can be accepted

3.3 Grey Matrix Establishment

After obtaining the weight value of each indicator, the security risk level of the secondary evaluation index is divided into five levels: A, B, C, D and E. Where A is low risk; B is Lower risk; C is ordinary risk; D is high risk; E is High risk. A questionnaire survey was conducted with K experts to score the grade of the occupational hazard index of subway maintenance operation. According to the scoring table of each expert, the occupational health risk evaluation value of subway maintenance operation was obtained, and each column was an expert’s evaluation of each secondary index as shown in Eq. 1.

$$D = \begin{pmatrix} d_{11}^{(1)} & d_{11}^{(2)} & \dots & d_{11}^{(k)} \\ d_{12}^{(1)} & d_{12}^{(2)} & \dots & d_{12}^{(k)} \\ \vdots & \vdots & \ddots & \vdots \\ d_{21}^{(1)} & d_{21}^{(2)} & \dots & d_{21}^{(k)} \\ \vdots & \vdots & \ddots & \vdots \\ d_{ij}^{(1)} & d_{ij}^{(2)} & \dots & d_{ij}^{(k)} \end{pmatrix} \tag{1}$$

As the occupational health risk level of subway maintenance operation has been set as five grades A-E, the value of safety risk evaluation index can be determined as five gray numbers: low, lower, ordinary, higher and high, and e is used to represent the gray category, that is, $e = A, B, C, D$ and E , which are respectively assigned as 1, 2, 3, 4 and

5. Then the whitening weight functions $y_A(x)$, $y_B(x)$, $y_C(x)$, $y_D(x)$, $y_E(x)$ corresponding to each evaluation grey class are defined as follows.

The low-risk grey number is $\otimes 1 \in [0, 1, 2]$, and the whitening weight function is as shown in Eq. 2.

$$y_A(d_{ij}^{(k)}) \begin{cases} 1 & d_{ij}^{(k)} \in [0, 1) \\ 2 - d_{ij}^{(k)} & d_{ij}^{(k)} \in [1, 2) \\ 0 & d_{ij}^{(k)} \notin [0, 2] \end{cases} \quad (2)$$

The lower risk gray number is $\otimes 2 \in [0, 2, 4]$, and the whitening weight function is as shown in Eq. 3.

$$y_B(d_{ij}^{(k)}) \begin{cases} d_{ij}^{(k)}/2 & d_{ij}^{(k)} \in [0, 2) \\ (4 - d_{ij}^{(k)})/2 & d_{ij}^{(k)} \in [2, 4) \\ 0 & d_{ij}^{(k)} \notin [0, 4] \end{cases} \quad (3)$$

The gray number of common risk is $\otimes 3 \in [0, 3, 6]$, and the whitening weight function is as shown in Eq. 4.

$$y_C(d_{ij}^{(k)}) \begin{cases} d_{ij}^{(k)}/3 & d_{ij}^{(k)} \in [0, 3) \\ (6 - d_{ij}^{(k)})/3 & d_{ij}^{(k)} \in [3, 6) \\ 0 & d_{ij}^{(k)} \notin [0, 6] \end{cases} \quad (4)$$

The grey number of higher risk is $\otimes 4 \in [0, 4, 8]$, and the whitening weight function is as shown in Eq. 5.

$$y_D(d_{ij}^{(k)}) \begin{cases} d_{ij}^{(k)}/4 & d_{ij}^{(k)} \in [0, 4) \\ (8 - d_{ij}^{(k)})/4 & d_{ij}^{(k)} \in [4, 8) \\ 0 & d_{ij}^{(k)} \notin [0, 8] \end{cases} \quad (5)$$

The gray number of high risk is $\otimes 5 \in [0, 5, \infty]$, and the whitening weight function is as shown in Eq. 6.

$$y_E(d_{ij}^{(k)}) \begin{cases} d_{ij}^{(k)}/5 & d_{ij}^{(k)} \in [0, 5) \\ 1 & d_{ij}^{(k)} \in [5, 10) \\ 0 & d_{ij}^{(k)} \notin [0, \infty] \end{cases} \quad (6)$$

Five metro scholars scored the occupational health evaluation index of the subway maintenance operation based on the principle of 10 points. The higher the score, the higher the risk level. The evaluation sample matrix is as follows:

$$D_1 = \begin{pmatrix} 3 & 4 & 5 & 4 & 4 \\ 3 & 4 & 3 & 4 & 3 \\ 3 & 5 & 4 & 3 & 2 \\ 4 & 3 & 3 & 4 & 3 \\ 3 & 4 & 3 & 3 & 2 \end{pmatrix} \quad D_2 = \begin{pmatrix} 2 & 4 & 3 & 2 & 4 \\ 5 & 3 & 2 & 2 & 3 \\ 3 & 4 & 4 & 3 & 2 \\ 3 & 3 & 5 & 3 & 4 \\ 3 & 4 & 2 & 2 & 2 \end{pmatrix} \quad D_3 = \begin{pmatrix} 2 & 2 & 3 & 5 & 2 \\ 1 & 3 & 2 & 2 & 2 \\ 4 & 3 & 3 & 2 & 2 \\ 2 & 3 & 3 & 2 & 2 \\ 2 & 4 & 3 & 3 & 4 \end{pmatrix} \quad D_4 = \begin{pmatrix} 5 & 3 & 2 & 2 & 3 \\ 3 & 5 & 4 & 5 & 2 \\ 3 & 3 & 2 & 2 & 4 \\ 3 & 2 & 3 & 2 & 2 \end{pmatrix}$$

The grey evaluation coefficient $n_{11}e$ of T_{11} index belonging to the e grey evaluation category are as follows calculated by Eq. 7.

$$\begin{aligned}
 e = 1 : n_{111} &= \sum_{k=1}^5 f_A(d_{11k}) = f_A(d_{111}) + f_A(d_{112}) + f_A(d_{113}) + f_A(d_{114}) + f_A(d_{115}) \\
 &= f_A(3) + f_A(3) + f_A(5) + f_A(4) + f_A(4) = 0
 \end{aligned}
 \tag{7}$$

And there, $e = 2: n_{112} = 0.500, e = 3: n_{113} = 3.333, e = 4: n_{114} = 4.500, e = 5: n_{115} = 4.000$. Therefore, the total grey evaluation coefficient of T_{11} is $n_{11} = 12.333$.

Similarly, the total grey evaluation coefficient of the other 18 indicators can be calculated, and finally the evaluation weight matrix P of the second-level indicators for each grey category can be obtained, and the standard matrix P' can be obtained after normalization.

$$P = \begin{pmatrix} 0.000 & 0.500 & 3.333 & 4.500 & 4.000 \\ \vdots & \vdots & \vdots & \vdots & \vdots \\ 0.000 & 3.500 & 3.333 & 3.000 & 2.800 \\ 1.000 & 4.000 & 3.333 & 2.500 & 2.000 \\ \vdots & \vdots & \vdots & \vdots & \vdots \\ 0.000 & 4.000 & 4.000 & 3.000 & 2.400 \end{pmatrix} \quad P' = \begin{pmatrix} 0.000 & 0.041 & 0.270 & 0.365 & 0.324 \\ \vdots & \vdots & \vdots & \vdots & \vdots \\ 0.000 & 0.277 & 0.264 & 0.237 & 0.222 \\ 0.078 & 0.312 & 0.260 & 0.195 & 0.156 \\ \vdots & \vdots & \vdots & \vdots & \vdots \\ 0.000 & 0.299 & 0.299 & 0.244 & 0.179 \end{pmatrix}$$

3.4 Comprehensive Assessment

In combination with the determined weight values, the evaluation weight matrix of grade 1 occupational health risk index of subway maintenance operation on various evaluation gray scales can be calculated from Eq. 8.

$$A_i = x_i \cdot P_i = (b_{i1}, b_{i2}, b_{i3}, b_{i4}, b_{i5})
 \tag{8}$$

And there,

$$A = \begin{pmatrix} A_1 \\ A_2 \\ A_3 \\ A_4 \end{pmatrix} = \begin{pmatrix} 0 & 0.0617 & 0.1395 & 0.1345 & 0.1099 \\ 0 & 0.0588 & 0.0826 & 0.0771 & 0.0666 \\ 0.0052 & 0.0554 & 0.0599 & 0.0508 & 0.0420 \\ 0 & 0.0129 & 0.0162 & 0.0144 & 0.0126 \end{pmatrix}$$

According to the weight value of the first-level index in Table 1, the comprehensive evaluation value of each gray category of occupational health risk in subway maintenance operation can be calculated by Eq. 9.

$$\begin{aligned}
 S &= X \cdot A = (S_1, S_2, S_3, S_4, S_5) \\
 &= (0.0005, 0.0470, 0.0870, 0.0824, 0.0682)
 \end{aligned}
 \tag{9}$$

The grey class rating has assignment 1, 2, 3, 4, 5, then each grey class evaluation level threshold vector is: $Y^T = (1 \ 2 \ 3 \ 4 \ 5)$, the subway maintenance job occupational health risk comprehensive evaluation value of $W = S \cdot Y = 1.0261$.

Therefore, it can be concluded that the comprehensive risk level of hazardous and harmful factors in the workplace of Xi'an subway is between *A* and *B*, that is, between low and low risk level, that is, close to safety. The results of the evaluation were compared with the results of the evaluation report on the status of occupational hazards in the subway workplace.

4 Discussions

The Occupational Health Risk Assessment Hierarchy model of subway maintenance work is divided into four aspects, which were occupational hazards factors, environmental factors, human-computer interaction factors and management factors. The second level index and its weight are determined by investigation and scoring by experts. The occupational hazards factors didn't cover all possible occupational hazards, but only the related occupational hazards with the maintenance work in the subway were listed. The types of dust were not subdivided, but were evaluated according to the type of dust. If the conditions change, the model and index should be revised before application in the future.

This paper is mainly to verify the feasibility and feasibility of grey AHP in occupational health risk assessment, so the assessment indexes are only determined by 5 experts and the sample size is small. The follow-up should also supplement and improve the sample size of the scoring experts.

5 Conclusions

The occupational health risk assessment of AHP model was constructed from occupational hazard factors, environmental factors, human-computer interaction factors and management factors, and the secondary evaluation indicators were also listed. Based on the AHP, the grey matrix was constructed, and the results of occupational health risk assessment for subway maintenance work were put out.

It verified in this study that the application of grey AHP to occupational health risk assessment of subway maintenance work was scientific and feasible. The results of this study mainly focused on the subway maintenance work and listed the related factors of occupational hazards, work environment, human-computer interaction and management factors. If there are differences between other work and occupational disease risk factors, so the evaluation index and model of AHP should be revised when the results of this study are used on it.

Acknowledgements. This work is supported by the National key R&D Program of China (No. 2016YFC0801700) and the basic research funding of China Academy of Safety Science and Technology (No. 2022JBKY02).

References

1. Liu, H.: Occupational hazards and prevention in subway operation enterprise. *Mod. Occup. Saf.* (1): 96-97 (2019)
2. Su, Y., Wang, J., Zhang, Y., et al.: Current status of occupational health in urban rail transit enterprises in China. *China Occup. Med.* **45**(4), 517–520 (2020). <https://doi.org/10.11763/j.issn.2095-2619.2018.04.022>
3. Guo, S., Chen, H., Su, S., et al.: Analysis of occupational hazards and preventive and control measures in subway industry. *Henan J. Prev. Med.* **27**(06), 444–446 (2016). <https://doi.org/10.13515/j.cnki.hnjpm.1006-8414.2016.06.015>
4. Fan, X., Shu, Y., Feng, Y., et al.: Analysis of occupational hazards and preventive and control measures in subway industry. *Occup. Health* **38**(3), 413–416 (2022). <https://doi.org/10.13329/j.cnki.zyyjk.2022.0043>
5. Mai, S., Zhang, J., Wu, D., et al.: Analysis of occupational hazards in metro construction workplace. *Chin. J. Ind. Med.* **32**(4), 320–322 (2019). <https://doi.org/10.13631/j.cnki.zgg yyx.2019.04.033>
6. Lai, Y., Ai, L., Tian, Y., et al.: Application of dust occupational health risk assessment during subway construction. *Chin. J. Ind. Hyg. Occup. Dis.* **38**(4), 197–299 (2020)
7. Chen, L., Fan, X., Cen, Z., et al.: Application of comprehensive index method in assessment of occupational health risk in subway industry. *Occup. Health Emerg. Rescue* **38**(3), 250–253 (2020). <https://doi.org/10.16369/j.oher.issn.1007-1326.2020.03.009>
8. Li, Y., Guo, Y., Cai, X., et al.: Current situation and advantages and disadvantages of occupational health risk assessment technology. *Occup. Health* (11), 83-86 (2021)
9. Li, Y.: Discussion on the application of risk assessment of occupational disease hazards in a wastewater treatment plant based on grey system theory. *Manag. Technol. SME* (6), 140–141 (2021)
10. Zhou, W., Wang, J., Zhou, J., et al.: Research on safety risk assessment of metro station based on grey analytic hierarchy process. *Saf. Secur.* **42**(2), 25–30 (2021). <https://doi.org/10.19737/j.cnki.issn1002-3631.2021.02.004>

Theory and Application Research



Human Factors Design for Space Station

Wei Zhang^(✉), Yongqing Hou, Jian Jin, and Bing Wu

Beijing Institute of Spacecraft System Engineering, Beijing 100094, China
yuhang30@163.com

Abstract. Manned spacecraft provides the necessary environment for astronauts' survival, life and work. In order to meet the requirements of astronauts' long-time work and life in the space station, it is necessary to study the human factor design method for the space station. Combined with the human factor design characteristics of China space station, this paper puts forward the human factor design principles of manned spacecraft, and puts forward the human factor design methods for configuration layout, safety, maintainability and livability. These methods are applied in the human factor design of China Space Station. Astronauts have lived and worked in the core module of the China space station for about seven months, which shows that the proposed human factor design method ensures the efficient work and life of astronauts on orbit, and improves the livability and reliability of manned spacecraft. It provides a practical engineering method for human factors.

Keyword: China space station · Human factors · Design

1 Introduction

The Mir space station has worked on orbit for 15 years, and the International Space Station's design life is 15 years. At present, it has been working on orbit for 19 years [1].

The on-orbit working time of manned spacecraft has gradually increased from a few days to a few years or more. The human factor design has also gradually developed with the evolution of manned spacecraft. In order to meet the requirements of astronauts' long-time work and life in the China Space Station, it is necessary to study the human factor design method for the space station.

2 Human Factors Design Characteristics of Space Station

Human factor engineering is an interdisciplinary discipline that studies the relationship between human, machine and environment, also known as ergonomics [2].

Human factor design of manned spacecraft is a realization process under various constraints. It is also a man-machine design for astronauts in weightless environment.

(1) The system is complex

Space station have the natural ecological functions such as atmospheric environment control, temperature and humidity control and material recycling. It also provide the modern urban functions such as power supply, communication, diet and sleep and health exercise. Because it work on orbit, so it have the normal spacecraft functions such as attitude & orbit control, rendezvous and docking. So, the functions are complex and deeply related.

At the same time, human and equipment coexist and influence each other. On the one hand, the electromagnetic radiation, high pressure, high temperature, noise and harmful gases generated during the operation of the equipment, which are harmful to human. On the other hand, the moisture generated by human metabolism will lead the equipment to the risk of condensation. At the same time, the moisture will also breed microorganisms, and people's activities may cause mal operate.

(2) Multi-constraints

The constraints of mechanical environment, carrying envelope, carrying weight and space environment of low orbit bring difficulties to ergonomic design.

Constrained by the volume and weight of the launch vehicle, the product loading density of the space station is large, resulting in increased noise and reduced operating space. At the same time, because the products need to meet the mechanical environment requirements of the rising section, the firm mechanical connection is used. These factors increase the difficulty of on-orbit disassembly and assembly operation.

While operation on orbit, astronauts are in environment, so the research on the weightless operating characteristics is necessary. At the same time, it is necessary to consider the astronauts' body fixation, equipment limit and anti drift in the weightless environment. The operability of extravehicular equipment also needs to consider the influence of vacuum, alternating cold and heat environment.

(3) There are many types of on orbit operations

Astronauts on orbit need to carry out many operations such as daily life, station management, maintenance and special tasks. There are many types of operations.

- Daily life: diet, hygiene, exercise and entertainment;
- Station management: use of life support system, platform monitoring and cargo management;
- Maintenance and repair: regular maintenance, planned maintenance, and repair;
- Special tasks: human controlled rendezvous and docking, manipulator control and extra-vehicular activity.

(4) High safety requirements for on orbit operation

It has high requirements for the safety of astronauts' in orbit operation. It is necessary to carry out forward design to facilitate astronauts' correct operation, and reverse design to prevent astronauts' misoperation.

3 Design Principles

The outstanding feature of manned spacecraft is the participation of astronauts in space missions. Therefore, the basic principle of human factors design is to ensure human safety and platform safety, improving comfort and convenience. The spacecraft should fulfil human factors requirements by the lowest engineering cost.

4 Human Factors Design Method

4.1 Safety Design

(1) Emergency safety

The emergency tools shall be put at the easy-get position such as emergency breathing devices, fire extinguishers and plugging tools. At the same time, space station will give voice and light alarm in case of fire, loss of pressure and other emergencies on orbit, so that astronauts can quickly identify the emergency position and quickly find the fire-fighting and plugging tools.

At the same time, the passage to the manned spaceship shall be unblocked, and emergency escape signs (fluorescent) and emergency light lighting shall be set, so that astronauts can quickly escape the space station for refuge or withdraw to the ground (Fig. 1).



Fig. 1. Emergency escape

(2) Interface security

The equipment and instrument board which can be touched by astronauts in their daily work and life shall be chamfered [3].

For example, space station crimped J36, j14t and other conventional connectors commonly used in spacecraft, which improved the interface safety (Fig. 2).

(3) Power safety

The astronauts shall repair and maintain the equipment while turned off. The equipment that cannot be turned off and daily operation shall be powered by a safe voltage less than 36 V.

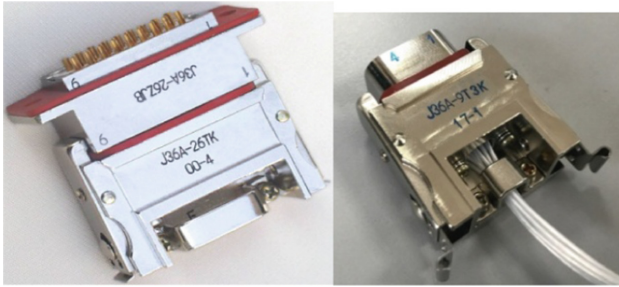


Fig. 2. Interface security of connector

(4) Pipeline product protection

The working medium of space station pipeline includes ethylene glycol aqueous solution, urine distilled water, urine containing strong corrosive pretreatment agent, as well as hydrogen, which are harmful to humans. The danger during operation comes from the leakage. Through the use of quick disconnector, the leakage rate of connection state is $\geq 1 \times 10^{-6} \text{Pam}^3/\text{s}$, the leakage at the moment of plugging is $\geq 0.1 \text{ ml}$, and the leakage rate in disconnected state is $\geq 1 \times 10^{-5} \text{Pam}^3/\text{s}$.

In addition, during maintenance, the upstream valve is closed and the downstream valve is opened to vent the gas in the pipeline. There is no high-pressure risk during operation and will not cause danger to astronauts.

4.2 Anti-misoperation Design

The tail cover of the electrical connector shall be provided with an eye-catching flag sign to facilitate the observation of astronauts and reduce the possibility of misoperation (Fig. 3).

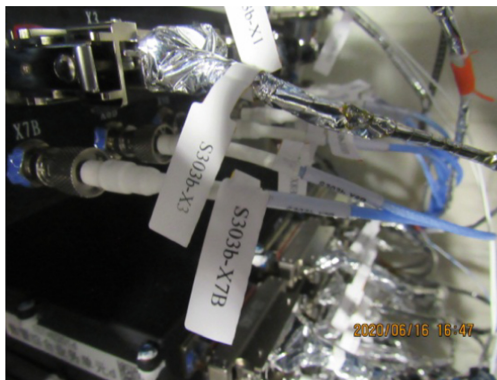


Fig. 3. Electrical connector identification

The shell of the electrical connector is equipped with anti misinsertion accessories for structural anti-misoperation (Fig. 4).

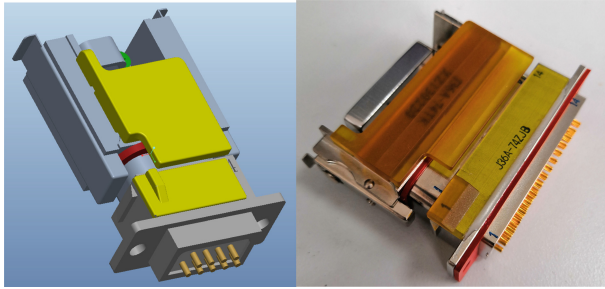


Fig. 4. Anti misinsertion design of cabin connector

4.3 Livability Design

(1) System configuration layout

Space station carries various needs of astronauts' on orbit work and life. It is necessary to reasonably arrange all kinds of living areas and working areas to separate the living area from the working area, so as to ensure that the living area is relatively quiet and private. At the same time, the sleep area needs to be closer to the manned spaceship for emergency evacuation [4].

Taking the core module of China Space Station as an example, the sealing area of the core module includes the node module - small column section - large column section from front to back. The node module is connected to the manned spaceship, and the end of the large column section is connected with the cargo spacecraft. The sleeping area, health area and exercise area are arranged in the small column section, the kitchen and dining area are arranged at the connecting area between the large column section and the small column section. The working area is arranged in the large column section. In this way, the living area is separated from the working area. At the same time, the sleeping area is closer to the manned ship and the working area is closer to the cargo ship, which is convenient for taking and placing goods (Fig. 5).



Fig. 5. Livable layout

In order to reduce the interaction between people and equipment, partitions are used in the working area to isolate the human activity area from the equipment, forming a $2\text{ m} \times 2\text{ m}$ activity area. Lighting lamps are installed in the corner (Fig. 6).



Fig. 6. Working area and living area

The sleeping area is arranged in the small column section, far away from the equipment area, and a number of measures are taken to control the noise within 50 dba; Micro ventilation system shall be set to ensure the circulation of oxygen and CO₂. Porthole, lighting lamp, reading lamp and storage box are also provided (Fig. 7).

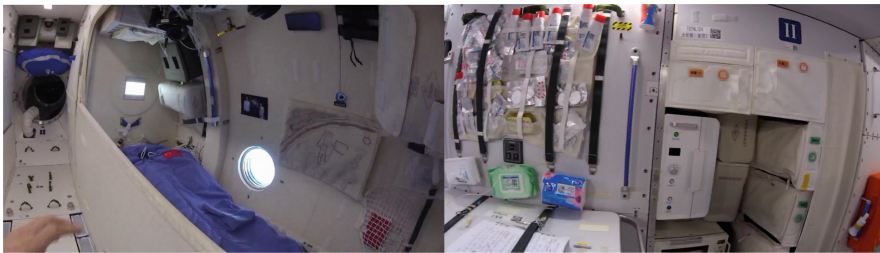


Fig. 7. Sleeping area, kitchen and dining area

The space kitchen is close to the dining table, which is convenient for food storage, processing and dining. Garbage storage is set under the table.

(2) Smart home

All kinds of living equipment can be controlled by smart terminals such as mobile phones. The astronauts can get the working condition of kitchen equipment and control the scene lighting. At the same time, the astronauts can also be reminded of phones, such as the empty and full state of the water tank, e-mail messages, alarms, etc.

Through the cargo management system, the storage location, use and material information of on orbit materials are managed, which is convenient for astronauts to find and understand the material status.

4.4 Operation Visibility and Accessibility

The operating objects should be seen and operated directly to avoid additional operation of other equipment. Equipment, which should be operated in a short time or have high operation frequency, shall be put in the area with good visual accessibility [5, 6].

Manned environmental regeneration system has the characteristics of strong correlation between internal components and products and high loading density. Turn the whole regeneration system into the human activity channel before operation. This can meet the loading space constraints and facilitate the astronauts' on orbit operation (Fig. 8).



Fig. 8. On orbit turnover integrated assembly

5 Summary

Human factors engineering design must be regarded as an important part in the design of space station system. At the same time, it is organically integrated with the multidisciplinary of the space station to achieve the harmonious unity of “man machine environment”.

Astronauts have lived and worked in the core module of the China space station for about seven months, which shows that the proposed human factor design method ensures the efficient work and life of astronauts on orbit, and improves the livability and reliability of manned spacecraft. It provides a practical engineering method for human factors related design of the subsequent manned spacecraft.

References

1. Li, X., Wei, C., et al.: On-orbit maintainability design system for manned spacecraft. *Syst. Eng. Electron.* **38**, 84–89 (2016)
2. Jiang, Z.: *Human Factors Engineering*, pp. 1–3. Science Publishing, Beijing (2011)
3. Wang, Q.F., Liu, W.B., Zhong, X.: Development and application of equipment maintenance and safety integrity management system. *J. Multivar. Anal.* **24**(4), 321–332 (2011)
4. Glor, P.J., Boyle, E.S.: Design evaluation for personnel, training and human factors(DEPTH). In: *Proceedings of the Annual Reliability and Maintainability Symposium*, Atlanta, pp. 18–25 (1993)
5. Fernando, T., Marcelino, L., Wimalaratne, P.: Constraint-based immersive virtual environment for supporting assembly and maintenance tasks. In: *Proceedings of the 9th International Conference on Human Computer Interaction*, New Orleans, pp. 943–947 (2001)
6. Marcelino, L., Murray, N., Fernando, T.: A constraint manager to support virtual maintainability. *Comput. Graph.* **27**(1), 19–26 (2003)



Man-Machine-Environment System Engineering in System of Systems Content

Baiqiao Huang (✉), Peng Zhang, and Kunfu Wang

System Engineering Research Institute, China State Shipbuilding Corporation, Beijing, China
seafury@buaa.edu.cn

Abstract. Aiming at the problem that the traditional man-machine-environment system engineering (MMESE) revolves around system, there is a lack of consideration in the design process of the new form of man-made engineering system, the system of systems (SoS). On the basis of summarizing and analysing the new characteristics of SoS and SoS engineering, a man-machine-environment system engineering model in the content of the SoS is proposed, which focus on the social network constructed by men in the SoS, the system network constructed by machines, the adversary system in the environment, and the mission planning and command and control of the commander's use of the SoS, and some main points of consideration of the above contents are analysed This paper provides a reference for carrying out man-machine environment system engineering work in the content of the SoS.

Keyword: MMESE · System of systems · SoS engineering · Social network

1 Introduction

Man-made engineering systems are people's integration and application of existing technologies, built through the engineering management process, and serve the purpose of transforming the objective world [6]. A man-made engineering system involves the interaction and coexistence between the system and the environment, and involves the information interaction process between people and the system and the decision-making process of people when they use the system. Therefore, man-made engineering systems are often typical man-machine-environment integrated systems, and the human-machine-environment system engineering is used as the design method. The human-machine-environment system engineering is a discipline that uses system science theories and system engineering methods to correctly handle the relationships between the three elements of human, machine and environment, and further study the optimal combination of the man-machine-environment system. [1] Man-machine-environment system engineering was proposed by Long Shengzhao and developed under Qian Xuesen's recognition and concern.

Man-machine-environment systems engineering plays an important role in improving the efficiency of man-machine interaction and ensuring the safe coexistence of people, systems, and the environment. However, as the scale of man-made engineering

systems becomes larger and the composition becomes more and more complex, a super system composed of multiple independent systems appears, which is called a system of systems or a system. Especially in the process of joint operation design of the US military, the independent operation and management of weapons platforms from different arms and arms need to work together. The traditional systems engineering method has obvious deficiencies in the process of building the management system, so it is emphasized that the system is different from the general system development process, the theoretical research of system and system engineering is vigorously promoted. At present, system engineering has become two new directions of INCOSE system engineering development together with MBSE [2].

A system of systems is a collection of multiple independent collaboratively interacting systems. The new features of the SoS that are different from general systems bring new challenges to human-computer interaction in the context of the SoS. First of all, the system is a socio-technical system. The influence of the organizational relationship between human during the operation of the system, and the cooperation between machines through information and control, has not been considered for the system operation process. Secondly, the SoS is not only network-centric, connects and cooperates through the network, but also needs to consider the self-organization ability in the case of unreliable network. Thirdly, the addition of a large number of unmanned equipment has brought about subversive changes in the traditional human-computer interaction-based human factors engineering design.

The application of human factors engineering in the analysis of accident causes is studied in [7], and in [8], the London bombing is also used as an example to analyze the content of human factors analysis in the context of the SoS. While the research of human factors in SoS content is really less. Therefore, on the basis of analyzing the new features of the SoS that are different from general systems, this paper puts forward the key consideration that need to be considered in man-machine environment systems engineering in SoS content, which providing reference guidance for the application of human-machine environment system engineering in SoS design, especially in military equipment SoS design.

2 SoS and SoS Engineering

2.1 Characteristic of SoS

It is an inevitable trend of technological development to connect multiple independent systems to form larger systems through collaboration and interaction. It is the US military that put the system concept on the research agenda. In 1996, Manthorpe [3] clearly proposed that SoS is a new opportunity and challenge for systems engineering in the military field. The U.S. Department of Defense takes joint operations as the main guiding ideology of its equipment development, and has developed a series of SoS-oriented technical and management standards from the aspects of equipment development requirements (JCIDS), SoS architecture design (DoDAF), and SoS engineering guidelines (SE for SoS) [4]. Mayer [5] proposed five characteristics for how to distinguish the SoS from the general system, namely Operational Independence, Managerial Independence, Evolutionary Development, Emergent Behavior and Geographic Distribution. We take the

NIFC-CA SoS of the US military as an example to illustrate these basic characteristics. First of all, the NIFC-CA SoS is composed of multiple weapon platforms whose operation and management are independent of each other, such as the F35 fighter jet, early warning aircraft, CEC network communication system, Aegis missile launch platform, etc. They are connected through the network and cooperate with each other through information exchange to achieve over-the-horizon strike targets, and they are also deployed in different geographical locations.

2.2 Characteristic of SoS Engineering

The SoS requirements analysis, design, integration, verification and validation process is called SoS engineering. Compared with traditional systems engineering, SoS engineering has two distinct characteristics. First, because the SoS consists of multiple independent systems, the SoS engineering is divided into two levels: SoS level and system level. At the SoS level, the mission of the SoS is mainly decomposed into the requirements for constitute systems, which are used as the input for systems development. After the development of the constitute systems are completed, the integration and verification of the SoS will be carried out. At the system level, the requirements of the system are implemented, and this process is guided by traditional systems engineering. Second, the constitute systems that make up the SoS are heterogeneous and are in different engineering stages. Most constitute systems reuse existing systems, and some need to be modified, and there are only a small number of systems that need to be developed as a new one.

3 MMESE in System of Systems Content

3.1 Traditional MMESE Design

There are many concepts for studying the design of human-system interaction, which are called Ergonomic in Europe, Human factor or man-machine engineering in the United States, and Human Engineering in Japan. These concepts are relatively close with man-machine-environment system engineering, and the difference is that the man-machine-environment system engineering emphasizes the highest principle of economic benefits after the comprehensive balance of the three, reflecting the characteristics of systems engineering. Man-machine-environment system engineering research focuses on human characteristics, machine characteristics, environmental characteristics, man-machine relationship, human-environment relationship, machine-environment relationship, and the overall performance of the man-machine-environment system [1].

The traditional man-machine environment system engineering is centered on human characteristics, and also considers the human-computer interaction factors of the operator in the process of using the system, the interaction factors between humans and the environment, the system are restricted by the environment, and the system output affects the environment. influence, etc. Human characteristics mainly study human physical characteristics, physiological characteristics, psychological characteristics, and social characteristics. Human physical characteristics refer to the dimensional characteristics

of the human body as a motion system. This characteristic determines the range of motion of the human body when operating the equipment, and is a necessary reference for equipment design. Human physiological characteristics refer to the physiological phenomenon characteristics exhibited by the human body in the process of maintaining its own life functions and interacting with equipment and the environment. Human psychological characteristics refer to the characteristics of human information processing and decision-making process in the process of human interaction with equipment and the environment, as well as psychological factors such as human values, personality, motivation, and emotions in this process. The social characteristics of human refer to the characteristics that people show when they are influenced by other members in a social group, mainly including social facilitation effect, social standardization tendency, social concern tendency, and social conformity tendency [9].

These all belong to the design category of a single system, and in the context of the SoS, which consists of multiple independent systems with different geographical distributions (in different environments), The relationship between people and between systems in the process of interaction between the constituent systems is a new addition to the traditional man-machine environment system engineering, and for the system, the environment is not limited to the natural environment and the microclimate environment where the systems are located, but also includes external systems. In terms of the military combat SoS, the enemy's combat SoS should also be counted as its environment, and the capabilities displayed by the SoS are different for different adversary.

3.2 Man-Machine Environment System Engineering Model in SoS Content

Considering the relationship between SoS engineering and system engineering and their essential differences, first of all, in the context of the SoS, man-machine environment system engineering also has two levels, one is the level of all constituent systems in the SoS, at this level, in the process of each member system design, it is necessary to consider the content of man-machine-environment system engineering, and carry out comprehensive trade-off design of man-machine-environment characteristics; one is the SoS level, at this level, the operators of different member systems form a social network, in this network there is a relationship between commanding and being commanded, and there is also a relationship of collaborative operation. The constituent systems form a system network with a certain topology structure, realize information exchange through different connection approach, and complete specific tasks that cannot be completed by a single system. Although due to the geographical distribution of the SoS, different member systems are in different geographical environments, however, for the SoS, the environment also includes the objects that the system tasks deal with. For the combat system as example, it is the combat adversary SoS. Different the combat adversary SoS, different the performance of own SoS. Another important feature of the SoS is the application. The composition and structure of the SoS are limited, but the application of the SoS is infinite, and the application of the SoS is the embodiment of human intentions. Through mission planning, command and control, the SoS as a whole can give full play to the mission efficiency of $1 + 1 > 2$. The man-machine-environment system engineering model in the content of SoS is shown in Fig. 1.

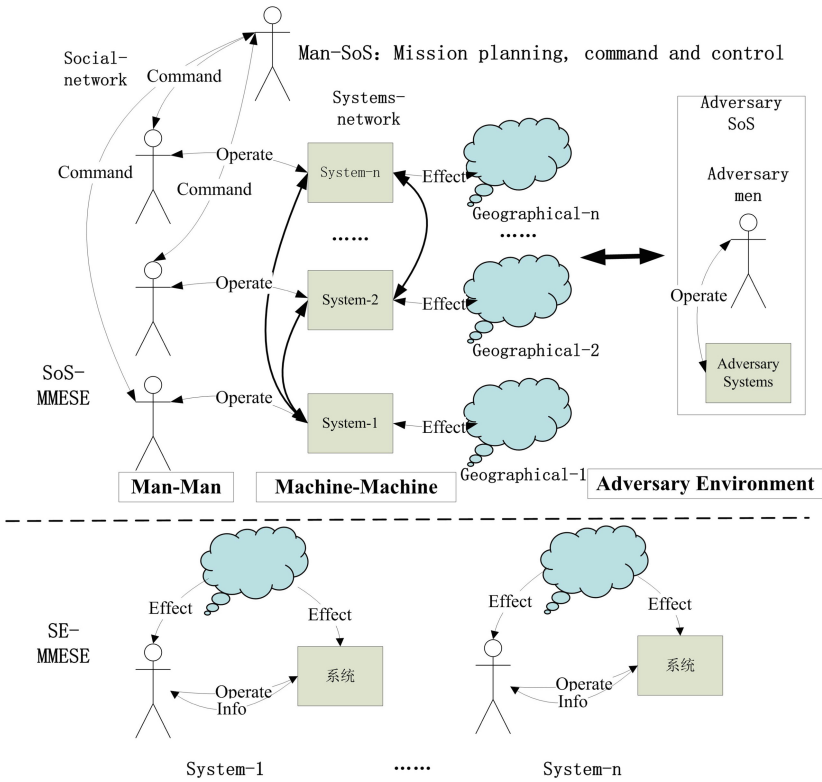


Fig. 1. Man-machine-environment system engineering model in the content of SoS

3.3 Consideration of MMESE in SoS Content

According to the contents of Fig. 1, we sorted out the important design points to be considered in man-machine environment system engineering in the content of SoS, as shown in Table 1.

Table 1. Consideration points table of MMESE in SoS content

Level	Category	Consideration points
System	Man	Physical characteristics, physiological characteristics, psychological characteristics and social characteristics
	Man-machine	Efficiency, comfort and error prevention of human-computer interaction
	Man-environment	Influence of environment on human physiology, operation efficiency and correctness

(continued)

Table 1. (continued)

Level	Category	Consideration points
	Machine-environment	Adaptability of system equipment to environment and impact of system output on environment
	Man-machine-environment	The comprehensive efficiency of human, machine and environment
SoS	Man-man	People in the SoS form a social network, and each operator in the network is not only affected by his responsibilities in the constituent system, but also by his social functions, such as his position, family responsibilities, and country and national consciousness
	Machine-machine	The systems in the SoS are connected through various networks to form a system network with a certain topology. In the SoS design, the relationship between machines and machines focuses on the following three points: 1) To realize the interconnection between multiple heterogeneous systems, the standardized design of the interface is the key point. Considering that most of the systems in the system are already developed, it is usually realized by the middleware interface translation; 2) Since there are multiple reachable paths between two points in the network, it provides convenience for the reconstruction of network connection between machines. In the case of some node failures, the system function can be restored through the structural reconstruction of the network. This is the core idea of the engineering resilient system theory; 3) With a large number of unmanned platforms, the autonomous decision-making of unmanned systems has become a new technological key point
	Adversary environment	The design of the SoS is always aimed at transforming the objective world, and the SoS always operates in an adversary's environment, especially for the military combat system, the member systems that make up the SoS are selected according to the strength of the adversary. Therefore, in the SoS design process, the system demonstration, requirement analysis and simulation verification process are inseparable from the support of the opponent's environmental simulation model
	Man-sos	The SoS is integrated by a limited number of member systems according to a specific architecture, but the application of the SoS is infinite. A specific commander formulates a mission plan for the use of the SoS according to the mission intent, and commands the operators of each member system to achieve the mission intention

4 Conclusion

The system of systems has become a common new form of man-made engineering system. The traditional man-machine-environment system engineering around the system design lacks the consideration of the new characteristics of the SoS. On the basis of analyzing the basic characteristics of the SoS and the SoS engineering, this paper constructs the man-machine-environment system engineering model in SoS engineering, and proposes that the man-machine-environment system engineering under the SoS background should focus on the social network constructed by humans in the SoS, the system network constructed by the machines in the SoS, the adversary SoS in the environment, and the application of the whole SoS by the conductor people. It provides a reference for carrying out man-machine-environment system engineering work in the content of SoS.

Acknowledgement. This work is supported by the **National Natural Science Foundation of China**, No. **61973282**.

This work is partly supported by the **Major science and technology plan of Hainan Province**, No. ZDKJ2019003.

References

1. Long, Z.: Man-machine-environment system engineering theory and its significance in productivity development. *Prog. Man Mach. Environ. Syst. Eng. Res.* **1**, 2–13 (1993)
2. Incose. *Systems Engineering Handbook*. Incose (2015)
3. Manthorpe, W.H.J.: The emerging joint systems of systems: a systems engineering challenge and opportunity for APL. *John Hopkins APL Tech. Dig.* **17**(3), 305–310 (1996)
4. DOD. *Systems Engineering Guide for Systems of Systems*. Department of Defense Office of the Deputy Under Secretary of Defense (2008)
5. Maier, M.W.: Architecting principles for system-of-system. *Syst. Eng.* **1**(4), 267–284 (1998)
6. Zhang, H., Huang, B., Ju, H.: An improved SoSE model—the “V+” model. In: *15th Annual Conference System of Systems Engineering*, Budapest, Hungary, pp. 403–409 (2020)
7. Stanton, N.A., Rafferty, L.A., Blane, A.: Human factors analysis of accidents in system of systems. *J. Battlefield Technol.* **15**(2), 23–30 (2012)
8. Dogan, H., Pilfold, S.A., Henshaw, M.: The role of human factors in addressing systems of systems complexity. In: *2011 IEEE International Conference on Systems, Man, and Cybernetics*, Anchorage, AK, USA, pp. 1–7 (2011)
9. Huang, B., Zhang, P.: Application of man-machine-environment system engineering in ship-board equipment. In: Long, S., Dhillon, B. (eds.) *Man-Machine-Environment System Engineering*, vol. 527, pp. 711–719. Springer, Cham (2018). https://doi.org/10.1007/978-981-13-2481-9_82



Man-Machine-Environment System Engineering Based Mine Ventilation System Safety Analysis Method Study

Hanqin Su¹(✉) and Baiqiao Huang²

¹ North China Institute of Science and Technology, Langfang, China
1369131857@qq.com

² System Engineering Research Institute, China State Shipbuilding Corporation, Beijing, China

Abstract. The traditional safety analysis of mine ventilation system is mainly based on empirical analysis, lacks systematic method guidance, and the focus of safety analysis is on ventilation technology and environmental factors, and does not pay enough attention to human factor analysis. In order to ensure the safe and efficient production of coal mines and improve the safety and economic benefits of mines, the human-machine-environment system engineering method is introduced, and the three aspects of “human”, “machine” and “environment” affect the operation of the mine ventilation system. The safety factors are systematically sorted out, and the failure mode influencing analysis method is used to analyze the failure mechanism and countermeasures of the safety factors. Finally, taking a mine ventilation system as the application object, the method proposed in this paper is used to carry out the safety analysis of the mine ventilation system, and the feasibility of the method is verified.

Keywords: Man-machine-environment system engineering · Mine ventilation system · Safety analysis · Failure model effect analysis · Object-FMA

1 Introduction

Mine plays an important role in our country’s national economic production and construction, but with the gradual improvement of mine production capacity, mine-related safety accidents have further increased the depth and scope of mine mining, resulting in an increase in mine air demand, mine ventilation resistance, The further increase in the wind resistance of the mine and roadway has brought about a series of safety problems, such as poor ventilation in the mine, the wind speed in some areas even exceeding the limit, The route of incoming and outgoing air at the wind site is longer, the large loss of ventilation pressure, the difficulty of air volume deployment, and the weakening of the mine’s disaster resistance capability. Therefore, the mine ventilation system is an important means to ensure the safety of the mine.

Mine ventilation system is composed of ventilation power and its devices, ventilation shaft network, wind flow monitoring and control facilities, etc. Its task is to use ventilation power to remove harmful gases in the mine and floating mine dust floating in the air, and

keep the air fresh, ensures the working conditions of construction personnel, maintains a reasonable range of wind speed and wind pressure in the mine, and can effectively and timely control the wind direction and volume in the event of a disaster to prevent the expansion of the disaster. Therefore, the mine ventilation system is of great significance to ensure the safety of the mine.

The safety analysis and evaluation of the mine ventilation system is an important part of the overall safety analysis of the mine, and the key to the safety analysis is to sort out the factors that affect the safety associated with the mine ventilation system. Based on the method of accumulation of experience, Bu Changsen et al. proposed the safety analysis of human-machine-environment system engineering [2–4], emphasizing the analysis of safety factors from three aspects of human, machine and environment. Engineering is a science that uses systems science theories and systems engineering methods to correctly handle the relationship between the three elements of human, machine and environment, and deeply study the optimal combination of human-machine-environment systems [1]. There is still a lack of methodological guidance on safety factors, which may result in incomplete analysis of safety factors.

Aiming at the lack of a method for systematically analyzing safety influencing factors in the safety analysis of mine ventilation system, this paper proposes a combination of human-machine environment systems engineering and object failure mode analysis method (Object-FMA) [5]. The analysis method analyzes the safety factors from the three aspects of people, ventilation system and mine environment, and regards them as objects with attributes and functions, and regards their violations of attribute and function constraints as their failure modes. And according to the FMEA method [6], the analysis of the failure mode of the analyzed safety factors is carried out, and the solution measures to alleviate the failure mode are proposed, so as to improve the safety of the analysis object. Finally, taking the safety analysis of the ventilation system of Tangshan mine as an example, the safety analysis method based on human-machine environment system engineering proposed in this paper is verified by an example, and the feasibility of the method is verified.

2 A Comprehensive Analysis Method of Safety Based on Human-Machine Environment Engineering

2.1 Man-Machine-Environment Model Analysis of Mine Ventilation System

Mine ventilation system is a typical man-machine-environment system. “Human” refers to the operators in the mine and the operator of the mine ventilation system. “Machine” refers to the ventilation system, and “environment” refers to the environment in the mine. Figure 1 shows the interaction among the people, the ventilation system and the environment in the mine. The operator receives the status information and feedback information received by the monitoring equipment of the ventilation system, and makes an operation output after thinking and processing in the brain, which acts on the equipment of the ventilation system. The device executes the operation according to the command given by the operator and outputs the expected operation. The activities of mine operators and ventilation system operators will be affected by harmful gases (gas, CO, CO₂, hydrogen

sulfide and other floating mine dust), air pressure and heat, and the environment in the mine will also affect the state of the ventilation equipment and the physiological and the psychological state of the operator.

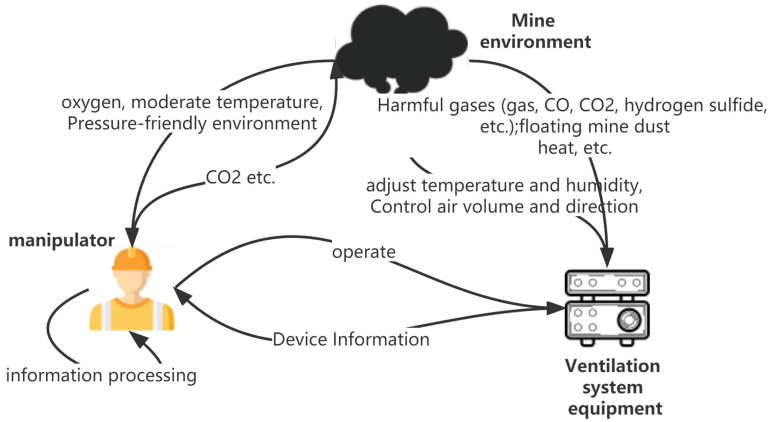


Fig. 1. Information interactive of human-machine-environment system

2.2 Analysis of Safety Factors Based on Human-Machine Environment System Engineering and Object-FMA

Failure refers to the state in which the analysis object cannot meet the established requirements under the specified conditions and time. Human-Machine-Environment Systems Engineering defines the scope of failure analysis, including human characteristics, machine characteristics, environmental characteristics, human-machine relationship, human-environment relationship, machine-environment relationship, and overall performance of the human-machine-environment system. Object-FMA guides the specific method of failure mode analysis, including the following steps: 1) analyze the properties and methods of the “object”; 2) analyze the constraints that these properties and methods need to meet; 3) constrain the “object” to itself Violation of the condition is considered a failure mode for that “object”.

Failure Mode Analysis of Object “Human”. In the human-machine environment, the operator is regarded as an object with three attributes of information receiver, information processor and executor, and the method of action operation. The operator first receives information through visual, auditory and other information receivers, and through the information processing of the brain, directs the limbs to perform corresponding operations, and the staff is affected by the information processor, such as psychological quality, ability, motivation, and at the same time by the body. Condition and the effect of the physiological state at that time. The analysis results are shown in Table 1.

Table 1. Failure mode analysis table for object “human”

object	property/method		constraint	failure mode	
Human	property	Information receiver	visual	Identify information, colors	cannot read/read wrongly/cannot distinguish colors
			hearing	Identify correct sound	Cannot hear/hear wrongly
		Information processing	Psychological quality	Meet job’s requirement	not be firm; impatience; Careless;
			ability	Meet occupational requirement	unskilled operation
			Motivation	Good attitude, good motives	Good attitude, good motives;
		Actuator	physical condition	meet job’s requirements	Physical condition does not meet;
			Physiological condition	meets job requirements	long-term or temporary illness;
		method	specific operation	Meet requirements	Operation wrongly

Failure mode analysis of the object “machine”. “Machine” means that the mine ventilation system consists of a power source (fan), a ventilation network (inlet, return air shafts and branch roadways), sensors and monitoring systems. The failure mode was analyzed by the Object-FMA method, and the results are shown in Table 2.

Failure analysis of the object “Environment”. Mine environmental factors are divided into harmful gases, microclimate environment and mine dust. Harmful gases affect the health of workers, such as gas, carbon monoxide, carbon dioxide, nitrogen oxides, sulfur dioxide, hydrogen sulfide, etc.; microclimate environment refers to the environmental conditions in which equipment and operators usually work, which should not only adapt to the survival of operators, but also The function of equipment is affected; mine dust (coal dust, rock dust, accumulated dust, etc.) affects human health, causes pneumoconiosis and skin diseases, accelerates mechanical wear, reduces use time, etc.; the failure mode analysis results of “environment” are shown in Table 3 shown.

Table 2. Failure mode analysis table for object “machine”

object	property/method		constraint	failure mode
Ventilator: power source	property	working condition	In working conditions	Beyond working conditions
		energy	Power Unicom/Energ y enough	Power cut-out/Energy enough exhausted
	method	ventilation work	ventilation efficiency meets requirement	Low ventilation efficiency
Ventilation network	property	ventilation line	Ventilation line is normal	Ventilation line block-ed;
		Ventilation Network Structure	network structure good and wind pressure stability	Unreasonable ventilation network structure , resulting in unstable wind pressure
Sensors	Property	working condition	In working conditions	Beyond working conditions
		category	meet control requirements	Some types of sensors are missing
	method	Perceive environmen tal information	conform to environmental reality	abnormal output; no output
Monitor System	property	UI	Displayed information is consistent with the status of the monitored object	monitoring status display is unclear or wrong
	method	Audible alert	Sound alarm is normal	The report is not reported or falsely reported

Table 3. Failure mode analysis table for object “environment”

Object	Property/method			Constraint	Failure mode
Environment	Property	Harmful gas	Gas, carbon monoxide, carbon dioxide, etc.	Be suitable working environment for operators	Excessive concentration of harmful gases and low oxygen
				concentration monitoring function is normal and timely alarm	Not timely warning
		Microclimate	Temperature, humidity, Wind pressure	Be suitable working environment for the operator	Excessive concentration of microorganism affects the health of workers
	Mine dust	Coal dust, rock dust, dust, etc.	Be suitable working environment	Mine dust concentration exceeding the standard	

3 Example Verification of Mine Ventilation System

This paper takes the safety analysis of the mine ventilation system of Tangshan Mine as an example, and based on the proposed safety analysis method, the safety analysis and verification of the coal mine ventilation system are carried out.

3.1 Tangshan Mine Introduction

Tangshan Mine is located in Tangshan City, Hebei Province. The mine field extends from the city center through the southwestern suburbs to Fengnan City. The mine basically realizes mechanized coal mining, and the mining method mainly adopts the longwall working face. The ultra-thick coal seam adopts the mining methods such as inclined stratification, metal mesh false roof or fully mechanized top coal caving. The mine has 4 ventilation levels, 5 air inlet shafts and 2 return air shafts. The mine ventilation adopts the central mechanical extraction ventilation mode. The return air shaft is equipped with two centrifugal fans, one for operation and one for standby.

3.2 Safety Analysis of the Ventilation System of Tangshan Mine

First of all, a standardized work flow is formulated, which mainly includes 4 processes: 1) Investigation of the analysis object. First, the relevant information of the Tangshan mine ventilation system is collected, and the layout and operation of the mine ventilation system are inspected on the spot. 2) MMESE-based safety factor analysis, based on

the method proposed in this paper, analyze the influencing factors of safety from three aspects of “people”, “machine” and “environment”, and establish the safety factor failure of mine ventilation system schema database. 3) Failure mode impact analysis, using the FMEA method to analyze the causes and effects of the failure modes analyzed in the previous process, and formulate improvement measures. 4) Evaluation and design of improvement measures, evaluate and weigh the proposed improvement measures, design and implement the selected suitable improvement measures, and improve the safety of the mine ventilation system.

According to the above work flow, the safety analysis of the ventilation system in Tangshan mine was carried out. According to the actual environment of Tangshan mine, the design and layout of the ventilation system and the actual situation of the operators, the failure mode was determined, and the FMEA analysis method was used to analyze the failure mode. The reasons and effects of the analysis are presented, and specific improvement measures are proposed. Figure 2 is a security workflow diagram based on MMESE. An excerpt of the analysis results is shown in Table 4.

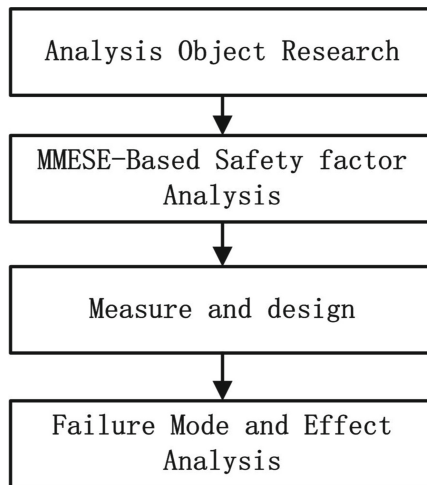


Fig. 2. MMESE-based security workflow diagram

Table 4. FEMA analysis of Tangshan mine expresses its meaning(excerpt)

Object	Invalid model	Invalid reason	Failure impact*	Severity	Measure
Human	Alarm color recognition error	Color blindness or color weakness	Failed to detect alarm information in time	II	1) Screening suitable operators; 2) Replace the red warning information with eye catching pic
	Slow emergency response	Fatigue work	Failure to deal with emergencies in a timely manner	II	Avoid fatigued work
Machine	Incomplete sensor type	Sensors are not set for key factors in the mine	Failure to warn in time when environment-al conditions exceed the limit	I	Add corresponding sensors and integrate data into monitoring system
environment	Mine dust concentration exceeding the standard	Ventilation efficiency is not up to standard or working hours are inappropriate	Health harm; long term cause pneumoconiosis	I	1 Add protective equipment; 2 Increase mine dust detection and early warning
...

4 Conclusion

This paper proposes a safety analysis method of mine ventilation system based on human-machine environment system engineering, which systematically sorts out the safety influencing factors from three aspects of human, machine and environment, and adopts the object failure mode analysis method to analyze the attributes and methods of the object. The failure modes of the influencing factors are analyzed in two aspects, and the failure mode analysis method is used to analyze the causes and effects of the analyzed safety failures. Finally, improvement measures are proposed to provide input for optimal design for improving the safety of the analyzed objects. In this paper, the method is verified by an example in the safety analysis of Tangshan Mine, which proves the feasibility of the method.

References

1. Long, Z.: Man-machine-environment system engineering theory and its significance in productivity development. *Prog. Man Mach. Environ. Syst. Eng. Res.* **1**, 2–13 (1993)
2. Bu, C., Cheng, W., Zhou, G., et al.: Safety analysis and assessment for human-machine-environment systematic engineering. *Ind. Saf. Environ. Prot.* **35**(2), 44–46 (2019)
3. Zhou, Z.: The security, stability and reliability appraisal and application study of the ventilating system of mine. Liaoning Technica University (2004)
4. Du, W., Jing, G., Shi, Q.: Preliminary discussion on safety analysis of man-machine-environment system for underpit transportation. *China Saf. Sci. J.* **7**(3), 34–37 (1997)
5. Huang, B., Zhang, H., Lu, M., et al.: Object-FMA based software code inspection approach. *J. Beijing Univ. Aeronaut. Astronaut.* **36**(12), 1473–1479 (2010)
6. GJB/Z 1391-2006 Procedure for failure mode, effects and criticality analysis (2006)



Design of Artificial Intelligence Monitoring and Early Warning System in Safety Manufacturing Based on Man-Machine-Environment System Engineering

Peng Zhang^(✉), Baiqiao Huang, Kunfu Wang, Wei Feng, and Jun Zhen

System Engineering Research Institute of China State Shipbuilding Corporation, Beijing 100094, China
my2ndemail@126.com

Abstract. Manufacturing safety has increasingly become a concern of the whole society. Existing manufacturing safety measures are inefficient and costly, which no longer meet the requirements of modern large-scale manufacturing. The latest development of artificial intelligence technology provides new solutions for intelligent monitoring and early warning in manufacturing. By analyzing the needs of manufacturing safety, this paper proposes the design of artificial intelligence monitoring and early warning system in manufacturing safety based on human-machine-environment system engineering, aiming to improve the manufacturing safety level of the whole society.

Keywords: Man-machine-environment system engineering · Manufacturing safety · Artificial intelligence · Early warning

1 Introduction

Industrial production has the characteristics of tight coupling of production equipment, coherent production process, cooperation of production personnel, and complex production management. Industrial production is a typical man-machine system [1]. In this system, if there is a problem in any link, the problem may be amplified by the system over time, resulting in irreparable losses. For example, in 2021, there will be 34,600 production safety accidents of various types and 26,300 deaths in China, with an average of more than 70 deaths per day [2]. Production safety has increasingly become a concern of the whole society. People are constantly seeking advanced technologies and measures for safe, stable, efficient and continuous production.

In the past, a lot of research has focused on hardware fault diagnosis, and there are many excellent results in this area [3]. However, the research on safety production accident remains on the simple statistical analysis, and there are few studies on the formation and development process of the accident and the pre-forecast of the accident.

The latest development of intelligent technology and the combination of mature information technology provide new solutions for intelligent monitoring and early warning of safe production. The popularization of this intelligent technology will improve the safety production level of the entire industry, reduce the cost of safety management, and increase the competitiveness of enterprises.

2 Inadequacies of Existing Manufacturing Safety Monitoring Measures and Technologies

There are many existing measures to reduce manufacturing safety accidents, such as standardization of processes, standardized operation of equipment, setting up safety management departments, regular training of personnel and so on. However, many accidents occur not because there are no specifications and standard requirements in the production process, but due to various subjective and objective factors. The existing manufacturing safety monitoring measures and technologies mainly have the following deficiencies:

(1) Insufficient timeliness.

At present, the monitoring of manufacturing safety is that after a problem occurs on the production site, it is uploaded to the high-level production scheduling center layer by layer through communication tools. When the high-level production scheduling center makes a decision, the accident has already occurred. The time from problem discovery to problem resolution is too long.

(2) The monitoring coverage is narrow

Limited by the number of personnel and costs, the monitoring of existing manufacturing safety can only cover a part of the entire production process. Full coverage of the entire process cannot be achieved. Many accidents occur in the blind spots of manufacturing safety monitoring.

(3) The influence of human factors

Human beings have their own limitations, such as fatigue, forgetfulness, tension, etc. These factors may lead to an increase in the number of production accidents. According to statistics, more than 70% of accidents are caused by human factors [4]. If the impact of the human factor can be reduced, the accident rate will be greatly reduced.

(4) Poor portability of experience in manufacturing safety

The level of manufacturing safety varies between industries, and between companies in the same industry. If the experience of a company with a high level of manufacturing safety can be transplanted to a company with a high level of manufacturing safety, the manufacturing safety level of the whole society will be improved. However, the current situation is that there is a lack of comprehensive statistical analysis and summary of the existing manufacturing safety experience and lessons, and the portability of experience is poor, and the cost of transplantation is high.

(5) Insufficient accident early warning capability

Any accident does not happen suddenly, and the occurrence of accidents has its own laws. Small violations often occur before a major accident, then develop slowly,

and finally break out. The existing manufacturing safety monitoring measures are insufficient to prevent these minor violations, and cannot give early warnings and take effective measures.

3 Artificial Intelligence Technology has Huge Application Potential in the Field of Manufacturing Safety

Artificial intelligence is a new technical science that studies the theory, method, technology and application system of simulation, extension and expansion of human intelligence. Current artificial intelligence technology is based on computer science. The main contents of artificial intelligence research include: knowledge representation, automatic reasoning and search methods, machine learning and knowledge acquisition, knowledge processing systems, natural language understanding, computer vision, intelligent robots, automatic programming, etc. [5]. Most research in artificial intelligence can be used in manufacturing safety.

Artificial intelligence technology, such as machine vision, posture recognition, abnormal behavior analysis and early warning, and so on, can be applied to safety prevention, supervision implementation, and quality inspection and production process management to realize real-time monitoring of the manufacturing process, automatic problem discovery, and active early warning. This method solves the outstanding problems of relying on low labor efficiency, small coverage and short monitoring time in the past, and ensures the safety and efficiency of production and the low cost of supervision.

Artificial intelligence has gradually played an increasingly important role in the field of industrial production safety. It has changed the previous mode of “post-processing” of safety management work, and turned to a scientific management method of pre-identification, analysis and control of hazards, and finally achieves the purpose of prior control and prevention. Compared with the traditional monitoring and early warning system, the artificial intelligence monitoring and early warning system of manufacturing safety has the following advantages:

(1) The AI system responds quickly.

The artificial intelligence monitoring system built on the basis of modern information system can quickly transmit and analyze data. In the entire production process, various sensors can be arranged to provide monitoring data 24 h a day. The artificial intelligence system can quickly analyze the data, make quasi-real-time decisions, and transmit various instructions through modern information systems. Decisive measures were taken to stop the expansion of the accident at the beginning of the accident.

(2) Comprehensive coverage of the entire production process

Various sensors such as audio, video, temperature, humidity and other sensors can provide continuous high-precision input for AI-based security monitoring and early warning systems. Only need to arrange enough sensors to monitor the whole process of production. Compared with the traditional increase in the number of personnel, the cost is greatly reduced.

(3) Greatly reduce the impact of negative human factors

The artificial intelligence-based monitoring and early warning system is different from the traditional security system. The system replaces humans with machines and programs. This system can monitor and warn the entire process 24 h a day, greatly saving human resources and making disposal methods possible, more efficient and diversified. For example, video surveillance, computer vision AI technology with deep neural network as the core technology, using machine vision to replace the supervision of human eyes, the system will not suffer from fatigue, distraction, forgetting and other shortcomings like humans. Tired of strictly performing tasks. Therefore, AI-based monitoring and early warning systems can greatly reduce the impact of negative human factors.

(4) Good portability of manufacturing safety experience

The artificial intelligence-based monitoring and early warning system stores some manufacturing safety experiences that are manually designed and systematically learned in the database. These experiences can be easily transferred to the systems of production enterprises in the same industry, and some macro experiences can be transferred to other industries. In addition, the software in the system can be easily upgraded to quickly improve performance. For example, with a better image recognition algorithm, it can be quickly upgraded and replaced in the original system, and the related capabilities of the entire system can be improved.

(5) Accident early warning can be realized

Current machine learning techniques can help early warning of accidents by mining the implicit relationships between events, especially causal relationships. For example, deep learning has the ability to automatically extract features, which is a kind of learning for representation. Deep learning allows multiple processing layers to compose complex computational models that automatically obtain representations of data and multiple levels of abstraction. These methods have greatly advanced the fields of speech recognition, visual recognition of objects, object detection, drug discovery, and genomics. By using the BP algorithm, deep learning has the ability to discover the underlying complex structures in large datasets. Tens of thousands of accidents occur in China every year. If the accident data over the years is used as training data, and the current machine learning technology is used to train, it is possible to discover the relationship between many hidden events, and use the related events that occurred before the accident as the training data. The signs of an accident can be used for early warning of an accident. The early warning of many faults has been achieved by means of machine learning and other methods, and the same method can also be used for early warning of accidents.

(6) The system is easy to operate

The designed manual interactive interface is very friendly to the operator, and can easily control various equipments of the system. And the client can integrate various functions such as control panel video playback, query, etc., and all operations can be realized through the same software.

(7) The system has strong scalability

The interface of the system is open and can be seamlessly connected with other related systems. In addition, today's intelligent technology can understand natural

language to a certain extent, and the system can communicate with the operator. The openness of the system makes it highly scalable.

(8) Good compatibility

For the original monitoring equipment or systems that have been installed and used, the interface can be set to be compatible in the new system, so as to achieve the purpose of saving costs and prolonging the service life of the equipment.

4 Design of Artificial Intelligence Monitoring and Early Warning System for Manufacturing Safety

Through the establishment of a set of manufacturing safety intelligent monitoring and management system based on the human-machine environment system engineering theory, the monitoring and management of the entire production process can be strengthened, and the safety hazards in each production link can be warned and discovered in time, and the safety hazards can be analyzed and quickly dealt with. Ultimately, achieve manufacturing safety. The system is responsible for the command and control, communication, data collection, data storage, monitoring and early warning of the production process. It is the key and link of enterprise manufacturing safety and management informatization. The design principle must ensure that the entire system has high reliability, strong stability, Advanced technology, friendly man-machine interface, simple operation, convenient maintenance, convenient upgrade and so on. This system needs to meet these requirements:

- (1) The artificial intelligence-based manufacturing safety intelligent monitoring system is combined with the operation permit management system to realize real-time monitoring of the entire process of on-site operations, and to realize the monitoring and management of intelligent identification and identity verification of construction workers at the construction site. It can monitor whether people in the operation area have dangerous behaviors, whether there are unauthorized people or things that cross the border and other irregular behaviors.
- (2) All kinds of data in the whole production process can be traced, so a database is needed to store the data. For example, the operation status of the production process equipment when a safety accident occurs, and the on-site video playback are all data required for accident analysis.
- (3) With a variety of intelligent identification technologies. Such as machine vision recognition, speech recognition and other intelligent recognition technologies. For example, machine vision recognition technology based on artificial intelligence is used to replace the traditional artificial visual recognition method to identify the roles of personnel on the job site. If the staffing of the job site does not meet the manufacturing safety requirements, the system will automatically and intelligently identify and warn.
- (4) The system interface can view the video images of each monitoring point in real time and in all directions, and call, warn and broadcast the remote video of key monitoring points. You can view various recent operations, hidden dangers, and video alarm processing through video playback. The system can communicate with everyone on the job site.

- (5) The monitoring and warning rules can be modified. Human experience can be combined with artificial intelligence to monitor and warn the production process. The rules and standards for manufacturing safety are constantly improving, which requires monitoring and alerting rules within the system to keep pace with the times. In addition, humans have accumulated a lot of experience in the monitoring and early warning of manufacturing safety. Combining these experiences with artificial intelligence can achieve better monitoring and early warning effects.

Based on these requirements, the system is designed as Fig. 1 follows:

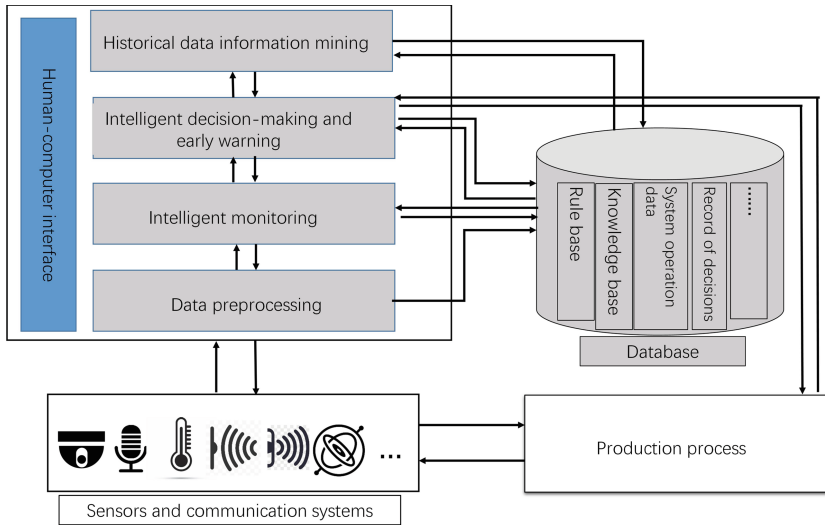


Fig. 1. Design of artificial intelligence monitoring and early warning system for manufacturing safety

The sensors and communication systems distributed in the whole production process input all kinds of data in the production process into the system. After the data is preprocessed, the data is backed up and uploaded. The intelligent monitoring system will analyze and monitor the data to find violations and dangers behavior, and then further transmit the data to the intelligent decision-making and early warning module. After the intelligent decision-making and early warning module makes a decision, it will directly affect the production process, eliminate dangers, and ensure production safety. In addition, the system itself will continue to learn through historical data to generate new knowledge and store it in the database.

5 Conclusion

This paper summarizes the shortcomings of existing manufacturing safety measures, analyzes the needs of new manufacturing safety monitoring and early warning systems,

and proposes a design scheme for manufacturing safety artificial intelligence monitoring and early warning systems based on human-machine-environment system engineering. This design can greatly improve manufacturing safety level.

Acknowledgement. This work was partially supported by the major science and technology projects in Hainan Province, No. ZDKJ2019003.

This work was partially supported by the National Natural Science Foundation of China, No. 61973282.

References

1. Long, Z.: Man-Machine-Environment System Engineering Theory and its Significance in Productivity Development. Progress in Man-machine-environment System Engineering Research, vol. 01, pp. 2–13. Beijing Science and Technology Press, Beijing (1993)
2. https://www.mem.gov.cn/xw/xwfbh/2022n1y20rxwfbh/wzsl_4260/202201/t20220120_407016.shtml
3. Wang, X.-F., Mao, D.-Q., Feng, S.-C.: Review on modern fault diagnosis technologies. China Meas. Test **39**(6), 93–98 (2013)
4. Wei, Q., Gu, X., Li, L.: Analysis of human factors behind the accident and research on countermeasures. China Sci. Technol. Overv. (18), 2 (2019)
5. Lucci, S., Kopec, D.: Artificial Intelligence in the 21st Century, 2nd edn. Mercury Learning and Information (2015)



Application of Man-Machine-Environment System Engineering in Yacht Driving Simulator

Kunfu Wang^(✉), Li Guo, Wei Feng, Peng Zhang, and Baiqiao Huang

System Engineering Research Institute of China State Shipbuilding Corporation,
Beijing 100094, China
wangkunfu1166@163.com

Abstract. The design of yacht driving simulator includes yacht driving operation space design and human psychological space design. Based on the theory of man machine environment system engineering, this paper analyzes the main factors affecting the space design of yacht driving simulator, and further analyzes the human-computer interaction connotation and typical design process of display and control equipment. This paper explores the application research of yacht driving simulator based on man-machine environment system engineering. In this method, the factor classification of man-machine interaction design, man-environment interaction design and machine-environment interaction design is fully considered. Finally, an application example shows that the design of yacht driving simulator based on man-machine environment system engineering can improve the work efficiency of yacht drivers, It can provide theoretical guidance for the interactive operation of yacht driving simulator.

Keywords: Man machine environment system engineering · Yacht driving simulator · Space design · Humanization

1 Introduction

The use process of yacht driving simulator is a typical man machine environment system engineering process, in which “man” refers to yacht driving operators, “machine” refers to yacht driving simulator itself, and “environment” includes the environment of yacht driving simulator. At present, the yacht driving simulator has gradually developed from focusing on the realization of pure three-dimensional visual function to focusing on “suitable for human nature”. For the design of yacht driving simulator, the design of driver’s operation space and human psychological space is an important means to meet the requirements of “suitable for human nature”. Therefore, in order to improve the “humanization” level and operation efficiency of yacht driving simulator, it is necessary to fully consider the influencing factors in man machine environment system engineering.

According to the practice of manned space pre research, long shengzhao and others put forward the concept of man machine environment system engineering, trying to bring human factors, ergonomics, engineering psychology, ergonomics, man machine system and other disciplines into the scientific framework of system engineering, study

the advantages and disadvantages of various combination schemes of man machine environment system from the overall height of the system, and change the previous dispersion The isolated research situation has pushed the practical activities of designing and developing man-machine-environment system to a new stage.

2 Analysis of Man-Machine-Environment Characteristics in Space Design of Yacht Driving Simulator

Human characteristics include human physical characteristics, physiological characteristics and psychological characteristics. Physical characteristics refer to the size characteristics of the human body as a motion system, which determines the activity range of the human body when operating the equipment, and is the basis for the design of the operation space of the yacht driving simulator. Human physiological characteristics refer to the physiological phenomenon characteristics of human body in the process of maintaining its own life function and the interaction between human and equipment and environment. It is mainly affected by the system load and mental load in the operation process of yacht driving simulator, and does not affect the spatial design of yacht driving simulator. This paper focuses on the influence of human physical characteristics on the operation space design of yacht driving simulator, and the influence of driver's psychological space characteristics on the layout of yacht driving simulator.

3 Application of Man-Machine-Environment System Engineering in Yacht Driving Simulator

3.1 Yacht Driver Anthropometric Data

The main anthropometric data of male yacht drivers are shown in Table 1:

Table 1. Human size data of male crew (mm)

	%			
	Raw data		Modified data	
	P5	P95	P5	P95
a	1630.7	1794.3	a(1)1660.7	a(1)1824.3
b	1513.2	1674.8	b(1)1543.2	b(1)1704.8
c	868.6	958.4	–	–
d	761.2	857.6	–	–
e	520.7	602.7	e(2)533.7	e(2)615.7
f	483.3	548.5	f(1)513.3	f(1)578.5
g	382.0	438.0	g(1)412.0	g(1)468.0
h	130.3	169.5	h(2)143.3	h(2)182.5
i	419.7	499.3	–	–

3.2 Control Range Design of Yacht Driving Simulator

Visual search is an important research content in the field of human-computer interaction in human-computer-environment system engineering. Visual search can be divided into structural area and non structural area according to the search area, and can be divided into random search and system search according to the search strategy. For the structured area, the system search strategy is generally adopted, which will have a faster speed. The research shows that the complex background will reduce the speed of target search and improve the discrimination between target and background, which can improve the speed of search. Visual search strategy is also related to the law of eye movement (Fig. 1).

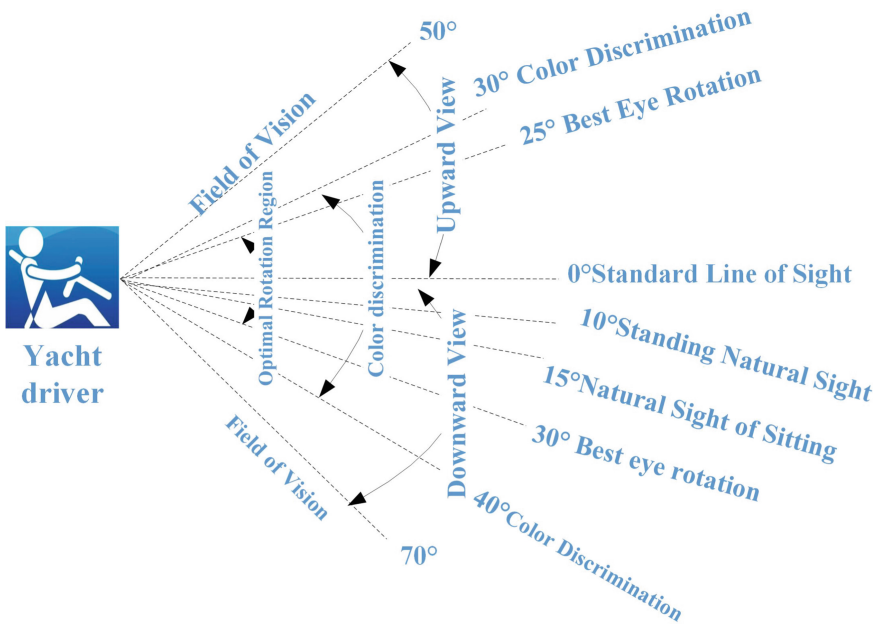


Fig. 1. Range of vision in human-computer interaction in yacht driving

According to the best visual field of yacht driver's visual search and the accessible area of daily yacht driver's hand, the specific operation space design conclusions are as follows:

1. The main controller shall be placed between shoulder height and waist height, and all controllers shall be placed within the reach range of yacht driver's hand;
2. The position of the controller shall ensure that the driver can operate two controllers with two hands at the same time without crossing or exchanging two hands. The frequently used controller shall be installed in the left or right front of the driver;
3. Frequently used controllers shall be installed within a radius of no more than 400 mm from the normal working position, and infrequently used controllers shall be installed within a radius of no more than 700 mm from the normal working position;

3.3 Control Range Design of Yacht Driving Simulator

Personal psychological space is an invisible area around the yacht driver's body. It is the space expected by people's psychological feelings, rather than the physical space required for normal work. The yacht driver's personal psychological space can be roughly divided into four areas from the center to the outside: tight area, close area, social area and public area, as shown in the Fig. 2.

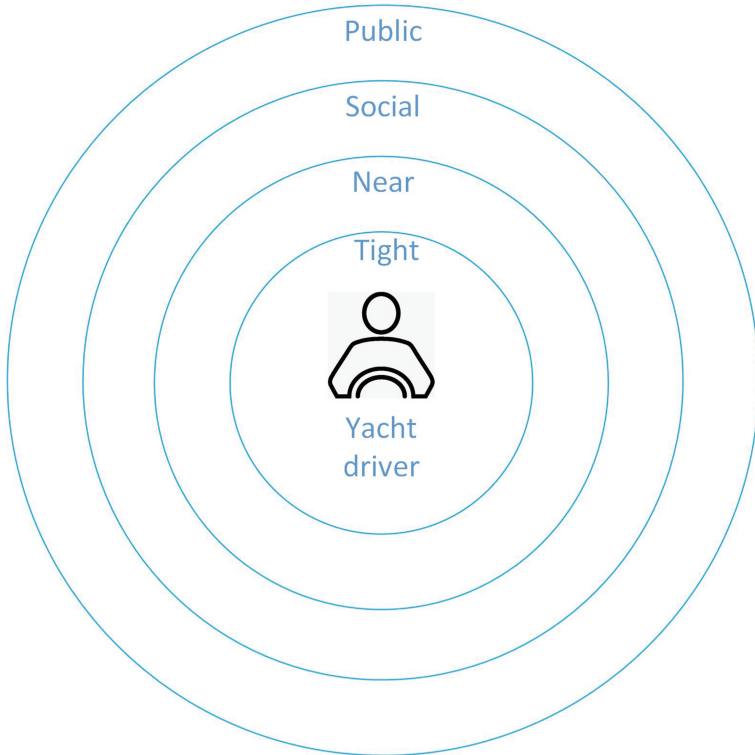


Fig. 2. Psychological space of crew

- 1) **Tight area:** It is the area closest to the human body, and its range includes the area around the human body within about 45 cm from the human body. The area about 0–15 cm away from the human body is characterized by direct contact with or close to the body, and ordinary people are not allowed to invade. The area about 15 cm–45 cm away from the human body is characterized by the reduction of the possibility of physical contact (hands can hold or touch), but it will still perceive the existence of others visually.
- 2) **Near area:** The close body area refers to the area about 45 cm–120 cm away from the human body. An area about 45 cm–76 cm away from the human body. This is the distance between acquaintances. The intrusion of strangers will make people

feel embarrassed or want to avoid, and even be regarded as a threat. An area about 76 cm–120 cm away from the human body. The distance that fingertips can touch when two people stand opposite each other. It is an area where people can talk and contact.

- 3) Social area: Social area refers to the area about 1.2 m–3.5 m away from the human body. An area about 1.2 m–2.1 m away from the human body. This is the distance people keep when working together or talking to their superiors and subordinates. An area about 2.1 m–3.5 m away from the human body. This is the area of general work contact, with formal social nature. For example, formal talks and etiquette are mostly carried out at this distance. It can keep a certain distance between people. In this area, it will not be considered impolite to work as usual in the presence of others.
- 4) Public area: Outside the social area is the public area, which refers to the distance maintained in public places, which has exceeded the spatial scope of direct contact and communication between individuals. An area about 3.5 m–7.5 m away from the human body. The size of personal mental space is a rough value, which varies from individual to individual. Individual differences include people's gender, age, culture, identity and closeness (Fig. 3).

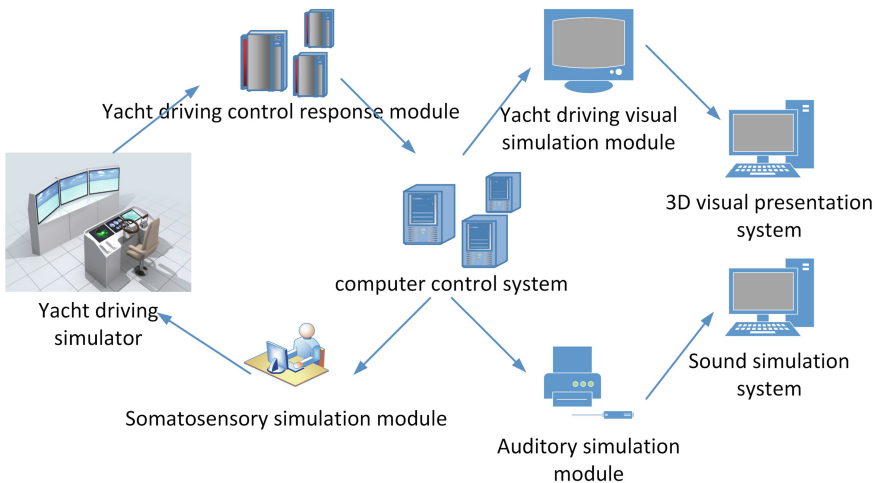


Fig. 3. Architecture of yacht driving simulator simulation system

4 Conclusions

Based on the man machine environment system engineering method, this paper analyzes the main factors affecting the spatial design of yacht driving simulator, including human physical characteristics and human psychological spatial characteristics. The operation space design of yacht driving simulator based on anthropometry and the spatial layout

design based on personal psychological space are carried out. It provides theoretical guidance for improving the “humanization” of yacht driving simulator.

Acknowledgement. This work is supported by Major science and technology plan of Hainan Province, No. ZDKJ 2019003.

This work is partly supported by the National Natural Science Foundation of China, No. 61973282.

References

1. Long, S.: Human-Machine-Environment System Engineering Theory and its Significance in productivity Development. Progress in Human-Machine-Environment System Engineering Research, vol. 01, pp. 2–13. Beijing Science and Technology Press, Beijing (1993)
2. Ying, S.: Human Factors, pp. 179–184. Tsinghua University Press, Beijing (2011)
3. Study on human-machine interface design of nuclear power plant control room. In: 19th International Conference on Man-Machine-Environment System Engineering, Shanghai, P.R. China (2019)
4. Wang, S.: Ergonomic Design and Application of Ship Wheelhouse Layout. Harbin Engineering University (2012)
5. Chen, C.: Humanized design of display control panel of radar. *Electro-Mech. Eng.* **22**(3), 39–41 (2006)



Emergency Search and Rescue Command Simulation Equipment Based on Man-Machine-Environment System Engineering

Ruolin Xing^(✉), Jun Zhen, Yan Hao, and Yafei Zhang

System Engineering Research Institute of China State Shipbuilding Corporation,
Beijing 100094, China
xr10515@126.com

Abstract. Man-Machine-Environment System Engineering (MMESE) has been widely used in engineering problem. In this paper, we introduce the interactive characteristics of emergency search and rescue command simulation equipment first. Then we analyze the relationship between emergency search and human-computer interaction. We propose a method to form a framework about emergency search and rescue command simulation equipment with MMESE. In our method, the relationship among man, environment and machine is considered in design process. From the examples, it is shown that the efficiency of MMESE and the advanced performance in emergency search and rescue command simulation equipment.

Keywords: Emergency search and rescue command simulation equipment · MMESE · Human factors engineering · Interaction design

1 Introduction

Man-Machine-Environment System Engineering, built in 1970s, is a scientific framework of system, which takes advantage of human, machine, environment and their relationships. Comparing with the isolated research situation, The MMESE prefers to design the system in practice [1, 2]. In this paper, we build the system framework on emergency search and rescue command simulation equipment. “Man” refers to the commander; “machine” refers to emergency search and rescue command simulation equipment; “Environment” includes the environment and the related equipment [3, 4].

2 Factors of Emergency Rescue Simulation Equipment

As a complex system, three basic elements, named man, machine and environment [5]. To describe the composition characteristics of each subsystem of man, machine and environment in the cab in detail, we should concern about the relationship between them [6], which is shown in Fig. 1:

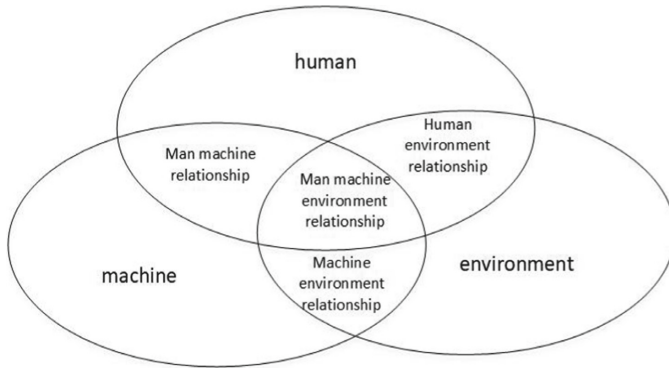


Fig. 1. Relationship between man machine and environment

3 Emergency Search and Rescue Simulation Training Equipment

3.1 Man Machine Relationship Design

In our system, the outstanding feature is that the realization of system functions often requires the interaction of human-computer, which exchange the information and process between human and machine, including information receiving, sending, transmission, processing, storage. The activities of human computer interaction can be described in Fig. 2:

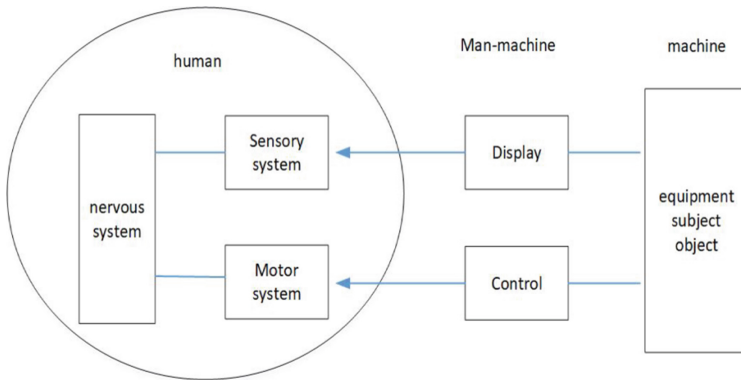


Fig. 2. Man machine relationship design

3.2 Design of Human Environment Relationship

The environmental factors on the psychological level of human body can lead to the changes of human body in work ability and efficiency. The adverse environmental factors on work efficiency is mainly manifested in the weakening of visual, auditory and other sensory information ability, which makes people have a long reaction time, reduced accuracy and higher error rate during the driving time.

The influence of environmental factors on the physiological level includes the influence on the cardiovascular system, respiratory system, digestive system and other systems. The physiological level change of longitude can return to the original normal state after the adverse environment stops working. A serious coup at the physiological level may lead to the reaction at the pathological level.

3.3 Design of Man Machine Environment Relationship

The human machine environment system constitutes an organic whole. The basic purpose of studying the relationship between human machine and environmental increase is to obtain the optimal effect of the whole system, that is, the whole system has high work efficiency, high safety, high comfort and good life guarantee. The main research contents include:

1. The components directly operated or used by people in the machine system shall be convenient for the operator to use effectively, so as to ensure the optimal working efficiency of the man-machine system.
2. Put forward the design requirements of environmental control and safety protection devices to ensure human safety, health, comfort and high work efficiency.
3. Optimization of the design of man-machine system.

The search and rescue command training simulation equipment adopts a two-level network structure, in which the main network is the network communication engine based on HLA to realize the data exchange between various subsystems in the simulator, and the second level network is the hardware network, which is used for the state acquisition of search and rescue environment simulation drive, search and rescue simulation dynamic system, motion capture analysis, as well as the control of instruments, indicators and other equipment (Fig. 3).

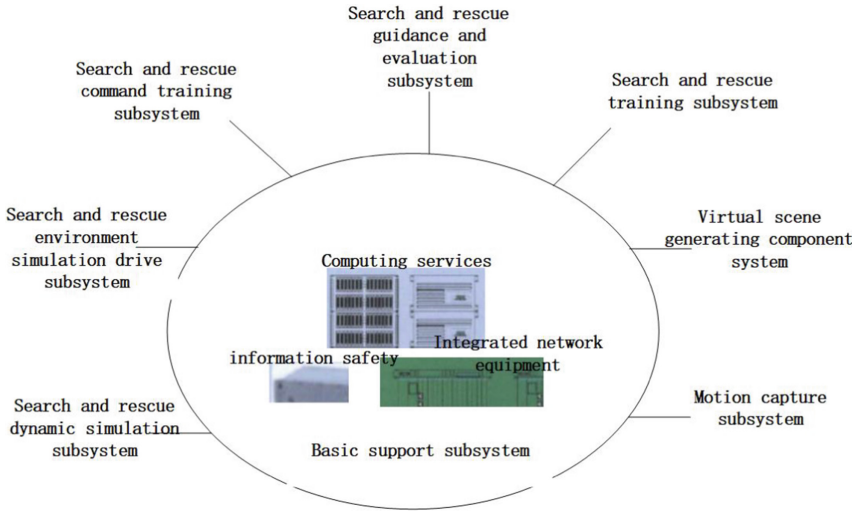


Fig. 3. Network structure design of search and rescue command training simulation equipment

It mainly considers the information interaction relationship between subsystems. The main interactive information involves information interaction such as battle position setting information, training command information, business status information, communication information and so on (Figs. 4 and 5).

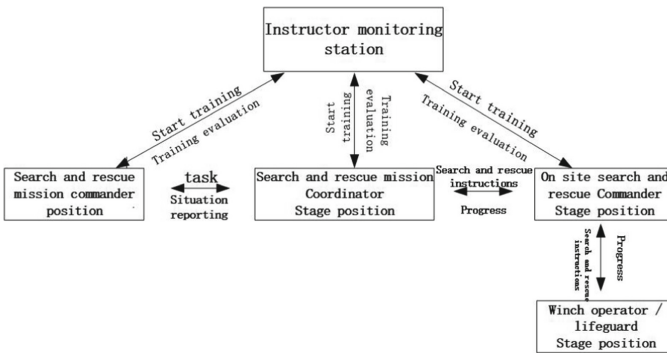


Fig. 4. Information relation design of emergency rescue command training task simulation system

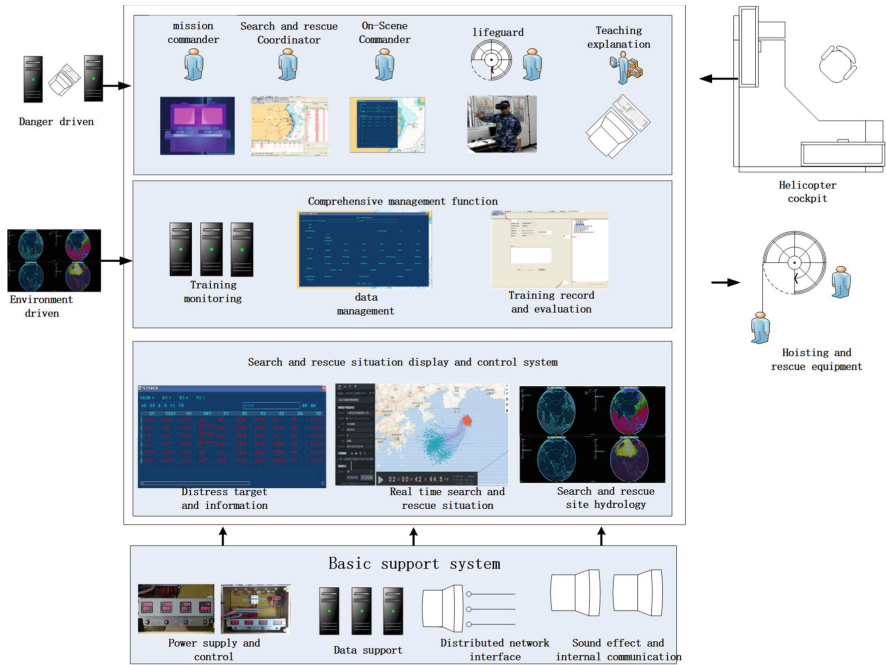


Fig. 5. Emergency search and rescue simulation training equipment based on MMESE

4 Conclusions

Firstly, this paper introduces and puts forward a design method of emergency rescue simulation equipment based on MMESE. In the process of design, we consider the classification of factors in both man machine and man ring interaction design. Considering the character of emergency rescue simulation equipment, we build a framework within the MMESE theory. Finally, an application example shows the efficiency of MMESE and the advanced performance in emergency search and rescue command simulation equipment.

References

1. Long, S.: Human-Machine-Environment System Engineering Theory and its Significance in productivity Development. Progress in Human-Machine-Environment System Engineering Research, vol. 01, pp. 2–13. Beijing Science and Technology Press, Beijing (1993)
2. Yang, Y.X.: 2018 China Food Composition Tables-Standard, 6th edn. Peking University Medical Press, Beijing (2018)
3. Catino, M., Patriotta, G.: Learning from errors: cognition, emotions and safety culture in the Italian air force. *Organ. Stud.* **34**, 437–467 (2013). 8. Fornette, P., Bardel, H., Lefrançois, C., et al.: (2012)
4. Kelly, D., Efthymiou, M.: An analysis of human factors in fifty controlled flight into terrain aviation accidents from 2007 to 2017. *J. Saf. Res.* **69**, 155–165 (2019)

5. Tianxue, Y.: On giving play to the initiative of seafarers under the new circumstances of ship management. *China Marit.* **2019**(8), 31–33 (2019)
6. Wang, X., Xiao, W.: Research on modeling design of industrial robot based on perceptual image. *Mech. Des.* **33**(08), 117–120 (2016)



Perceptual Evaluation on the Man-Machine-Environment System of Music Library

Kunzhu Zhang¹ (✉), Haoyu Yang², and Quan Yuan²

¹ Tsinghua University Library, Beijing 100084, China
zhangkz@tsinghua.edu.cn

² School of Vehicle and Mobility, Tsinghua University, Beijing 100084, China

Abstract. Music library is not only a library with artistic characteristics, but also an integrated system of man-machine-environment. This research takes the music library of Tsinghua University Library as an example to evaluate and analyze the corresponding man-machine-environment system. Firstly, the man-machine-environment system of the music library is established and classified. Then, the environment, including the luminous environment, the thermal environment, the acoustic environment and the spatial environment is evaluated in terms of the human comfort in applications. This paper discusses the improvement of thermal environment for superior human comforts and the coordinated control of acoustic and luminous environment in the library. The results of this paper may provide a significant reference for the humanized service improvement of music library.

Keywords: Music library · Man-machine-environment system · Perceptual evaluation · Environmental ergonomics

1 Introduction

In recent years, the application of the human-machine-environment system theory in the library has obtained certain attention [1–4], which has played a positive role in the optimization of the overall performance and comfort of the library. The library has various man-machine systems and man-machine interfaces. In the process of improvement, it is necessary to evaluate and analyze human perception factors.

The music library in universities is an important place for cultivating the musical literacy of college students, and is also an important part of college music education. Music libraries are divided into different types according to their resource characteristics and audience types. Relevant scholars at home and abroad have studied the human-machine-environment of music libraries from different perspectives [5–10], and put forward many R&D objectives and practices that can be used for reference. Research innovations include: database interconnection to realize automatic data integration, optimization of music on reading environment, operability of functional modules of Koke digital music library, multimedia reading in the context of big data, library music type selection and volume control skills etc. Existing researches show the rapid development of domestic and

foreign music libraries in recent years, and also reflects the development and construction experience of many large and medium-sized urban music libraries in China, and explored the development ideas of the music library in aspects such as user demands, function orientation, characteristic services, facilities and resources construction [11–15].

At present, few researches focus on the physical environment evaluation of music library in the human-machine-environment optimization of music library. However, the physical environment is very important to the users of library, and a comfortable environment helps to improve the user's work efficiency and the user's overall impression of the library. This research classifies and evaluates the physical environment of the music library of universities. Taking the music library of Tsinghua University as the starting point, the relevant research methods of human-machine-environmental system engineering science is adopted to test, evaluate and analyze the human-machine-environmental system, and put forward some suggestions on the improvement of audio-visual effects and comfort.

2 The Man-Machine-Environment System of Music Library

The main body of the music library of Tsinghua University is composed of three parts: the comprehensive zone of the music hall, music seminar room and music lecture hall. The three spaces are connected by the music culture corridor as a harmonious structure. Among which, the comprehensive area of the music library is about 500 m² with more than 100 seats and a total of 5 areas, namely the single appreciation area (M), group audio-visual area (U), electronic reading area (S), music book area (I) and book reading area (C), as shown in Fig. 1 and Fig. 2, with silent computers, audio decoders, high-quality headphones, LCD TVs etc., it provides readers with services such as high-definition lossless music and video appreciation, multimedia electronic reading, group music appreciation, music book reading through the self-built network platform.



Fig. 1. The interior scene of the music library **Fig. 2.** Typical equipment for the single appreciation area

This research mainly analyzes and evaluates the single appreciation area (M area) in the comprehensive zone of the music hall. This area is set with 8 groups of seats, and each 2 groups are divided into relatively independent areas by bookshelves. The distance between each seat is 1.1–1.2 m, the entire zone is equipped with 64 silent computers, and the audio decoders, high-quality headphones are provided for each computer for readers to enjoy music.

As shown in Fig. 3, the man-machine-environment system of the music library is composed of corresponding human, machine and environment. For the music library system, human is mainly the users of the library, including the user’s hearing, vision and touch or other senses that can interact with the environment. The machine includes various computers, speakers, multimedia equipment, network platform and workbench, seats and bookshelves; the environment includes luminous environment, acoustic environment, thermal environment and air, spatial environment, etc., among which the acoustic environment is the most important function of the music library.

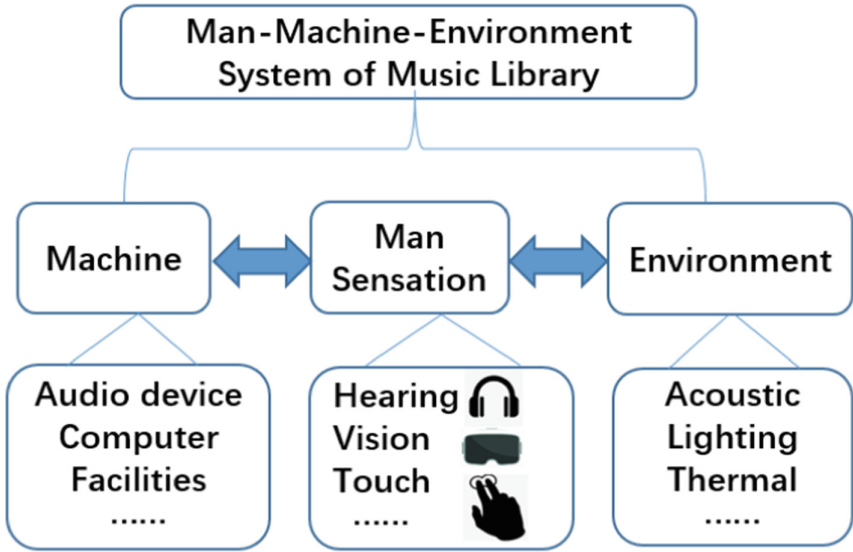


Fig. 3. Man-machine-environment system of music library

3 Perceptual Evaluation on the Man-Machine-Environment System of Music Library

The comprehensive zone of the music hall of Tsinghua University Library is taken as an example, a number of basic environmental data of the man-machine-environment system are measured, after comparing with the corresponding comfort indicators given in the national standard, the environment perception and comfort evaluation results of the music hall is obtained; moreover, supplemented by the actual observation method, a certain description and evaluation of the actual user’s feeling in the process of use is carried out.

3.1 Luminous Environment

The luminous environment is essential condition to the users of the library. Low illumination may cause damage to human eyes. Therefore, this research takes a music library

as an example to evaluate the indoor illumination intensity and human comfort. The evaluation basis used in this research is GB50034-2013 Standard for Lighting Design of Buildings [16]. It is stipulated in the Standard that in the library, the standard value of illuminance in the reading room should be higher than 300 lx (with the 0.75 m horizontal plane as the reference plane). In this research, the curtains next to the seats were pulled up to obtain a minimal luminous environment. The illumination intensities at different points on the desktop (about 0.75 m in height) were measured with light intensity measuring instrument. The result showed that the illuminance in the habitual reading area on the desk ranged 500–600 lx, which was higher than the national standard.

Since the screen will generate illumination during the use of device, when the screen is turned on (default brightness), the illuminance at the human eye was measured, and the illuminance value was about 520–530 lx, which was within the comfort range specified by the national standard.

3.2 Thermal Environment

The temperature and humidity control of the thermal environment is crucial for the users of the music library and the preservation of the books, image documents and instruments. Too high or too low temperature and humidity will cause discomfort to users, reduce the work efficiency, and is also not conducive to documents preservation. In the indoor thermal environment conditions of GB/T5701-2008, the indoor space temperature and humidity comfort curve suitable for most people is given, and the temperature and humidity range suitable for human work is marked, which provides an important basis for evaluating the indoor temperature and humidity of music library [17].

In this research, the indoor temperature in the comprehensive zone of the music library was measured with thermometer. The result was that the indoor temperature in spring was 23–26 °C with low fluctuation. This value is just within the recommended temperature range, which is due to the perfect central air-conditioning system of the music library; and in the winter heating environment, the indoor temperature was 25–30 °C. This is related to the adequate central heating system of the university.

The humidity value in the music hall was measured with hygrometer. The results showed that the humidity in the hall in spring was 30–35%, while in the heating environment in winter, the humidity in the hall was lower than 20%. Although this is conducive to the preservation of books in the library, and the national standard does not set the lower limit of humidity, too low humidity still has a certain impact on the comfort of readers in the library.

3.3 Acoustic Environment

The acoustic environment is one of the important elements of the library, and appropriate volume control can improve the use efficiency of library. The comprehensive zone of music hall is different from the music seminar room and music lecture hall in terms of orientations and functions. The former is only for individual appreciation and small-scale group appreciation, and users enjoy music through headphones; while the latter two are for group music appreciation and group discussion, as the medium and small concert halls, conference rooms, etc., the acoustic effect of the entire building is more

important, which has higher requirements not only for audio equipment, but also for the acoustic design of the space and the acoustic performance of building materials.

For the comprehensive zone of the music hall, only the quality of the sound source and the noise factor in the entire environment need to be considered. In terms of the quality of the sound source, the sound source of the self-built platform is mainly lossless audio resources, and two brands of professional audio decoders and SENNHEISER's semi-surrounding headphones are adopted, and these professional facilities bring users the ultimate hearing delight.

For the noise in the library, it can be quantitatively evaluated via measurement with noise meter. The measurement results showed that in one day, the maximum noise value in the entire comprehensive zone of the music hall did not exceed 55 dB, and remained below 40 dB, and the decibel value of the noise was below 30 dB during most of the time. According to the provisions of the environmental noise equivalent sound limit value in the GB3096-2008 Environmental Quality Standards for Noise [18], the noise level in the comprehensive zone of the music hall meets the requirements of the highest Category 0 functional area, which is one level higher than that of the ordinary library, and meets the setting of the noise range of music library.

3.4 Work Space Analysis

The work space of the music library is analyzed to find out whether it meets the relevant standards and work demands. If the work space is too wide, it will reduce the space utilization rate of the library; if the work space is too narrow, it will affect the work efficiency and may not be conducive to protecting the privacy of users. Therefore, it is significant to evaluate and analyze the work space of the music library.

As a music library, the composition of its work space includes not only the desks and chairs usually equipped in the ordinary libraries, but also equipment and systems such as audio, players, headphones and computers required for music appreciation.

The workbench, chairs and other facilities used in the comprehensive zone of the music hall are the same as other reading areas in the library. The computer screen is placed in the middle of the work surface. The combination of desk, chair and computer is more suitable. Except for the large seat surface of the chair, other data meets the requirements of Human Dimensions in Workspace GB/T 13547-1992 [19], which can bring better experience to users. A wide workbench can be provided to accommodate different sitting postures and appliances of users for activities such as reading, researching, using computers and so on while listening to music.

Generally speaking, in the music library, the spatial environment occupied by each person is relatively good, which allows people to appreciate music or read, research and work comfortably; in the aspect of functional division, certain partitions are also considered for avoiding interference, but there is still space for improving in terms of privacy.

4 Discussion

In this research, a preliminary evaluation of the acoustic, luminous, thermal and spatial environment of the music library was carried out through field measurements,

and the measured results basically met the relevant standards. In order to improve the man-machine-environment system of the music library, it is suggested to carry out the following further improvement.

- 1) Improvement of the thermal environment. When the indoor ambient humidity is low and too dry, it will cause discomfort to the human body. In the special environment of library, in order to keep the books dry, it has stricter requirements for ambient humidity. In a specific thermal environment, it is necessary to carry out further research on how to improve the humidity settings for meeting the demands of human comfort and preservation of books and image documents. The temperature caused by heating in winter is too high, which shall also be further controlled.
- 2) For the improvement of the acoustic environment. Evaluate the comfort of the speaker and headphone in the music library, optimize the equipment as needed, provide different types of facilities according to human factors, such as gender, age, hearing and actual demands, and provide use guidance to meet the personalized requirements of readers.
- 3) For the improvement of the luminous environment. Sound and light are two channels to realize man-machine interaction during the course of using the music library, and the two promote each other. Multimedia appreciation requires coordination between sound and light to achieve efficient and comfortable man-machine interaction. In order to improve the man-machine interaction effect, it can be taken into consideration to apply the virtual reality (VR) technology to the music library. VR technology converts planar vision into 3D images, which can enhance the visual effect. In this case, further design improvements should be carried out to maintain the privacy and prevent interference to others.

5 Conclusion

This research introduced the zones and functions of music library, and measured and evaluated the luminous environment, thermal environment and the most important acoustic environment. The results meet the relevant national standards, and some indicators were higher than the national regulations, which meets the orientation of music library of university. This construction model can be promoted in universities, so that more college teachers and students can experience the cultivation of high-quality music.

However, there is still space for further improvement in humidity control to meet the demands on material preservation and human comfort; improvements can also be considered in man-machine interaction equipment, such as adding VR equipment. For the optimization of the man-machine-environment system of music library, other auxiliary equipment can also be adopted to meet the demands of users with difficulties in listening, speaking, reading and writing. In addition, the increase of resource sharing between libraries can also be taken into consideration to meet the personalized requirements of more users.

References

1. Zhang, F.: Research on the application of ergonomics in libraries. *J. Beijing Forestry Univ. (Soc. Sci. Edn.)* **02**, 73–76 (2004)
2. Zhang, K., Yuan, Q.: Study of man–machine–environment system engineering on university library under internet condition. In: Long, S., Dhillon, B.S. (eds.) *MMESE 2017*. *LNEE*, vol. 456, pp. 841–849. Springer, Singapore (2018). https://doi.org/10.1007/978-981-10-6232-2_99
3. Zhang, K., Tan, L., Liu, Y.: Evaluation on the design of man-machine-environment system of interactive experience space in library. In: Long, S., Dhillon, B.S. (eds.) *MMESE 2018*. *LNEE*, vol. 527, pp. 693–702. Springer, Singapore (2019). https://doi.org/10.1007/978-981-13-2481-9_80
4. Zhang, K., Wei, X., Yuan, Q., Liu, J.: Evaluation on the man-machine-environment system of university library. In: Long, S., Dhillon, B.S. (eds.) *MMESE 2019*. *LNEE*, vol. 576, pp. 903–911. Springer, Singapore (2020). https://doi.org/10.1007/978-981-13-8779-1_102
5. Nie, W., Ma, H.: Acoustic design of music library of Tianjin library. *Art Technol.* **05**, 38–43 (2014)
6. Zhang, W.: Research on interior environment design of Music Library. Dalian University of Technology (2015)
7. Weigl, D.M., Lewis, D., Crawford, T., Knopke, I., Page, K.R.: On providing semantic alignment and unified access to music library metadata. *Int. J. Digit. Libr.* **20**(1), 25–47 (2017). <https://doi.org/10.1007/s00799-017-0223-9>
8. Luo, J.: Analysis on the function of music in promoting readings of Library. *Media Forum* **2020**(03) (2020)
9. Guan, J.: Description and thinking of system structure of digital music library based on KUKU. *Libr. J. Henan* (2020)
10. Wan, Q.: Application and practice of background music in libraries. *The Aurora Borealis* **2018**(06) (2018)
11. Zhao, B.: Multi-perspective analyses on the service of Library audio and video collection resources in the era of big data – taking “multimedia reading area music library” of Dalian Library as an example. *Libr. J.* **2018**(12) (2018)
12. Niu, S.: Discussion on the construction and management of professional music library. *Modern and Ancient Cultural Creation* (2020)
13. Fang, J.: Reading in the music—Investigation on the integration of reading and music. *Inside Outside Lantai* **23**, 40–42 (2020)
14. Liu, X., Liu, Z.: Overview of the current situation and future development trend of Academic Music Libraries in the United States. *Collections* **2018**(5) (2018)
15. Chen, Y.: Novel experience of characteristic service of public libraries—Taking the characteristic service of music library of Tianjin Library as an example. *Libr. Work Res.* **01**, 83–86 (2016)
16. GB 50034-2013 Standard for lighting design of buildings
17. GB/T 5701-2008 Thermal environmental conditions for human occupancy
18. GB 3096-2008 Environmental quality standard for noise
19. GB/T 13547-1992 Human dimensions in workspaces



Research on Man-Machine–Environment Design of Stratospheric Airships

Jing Lv^(✉), Yuanping Zhang, Qian Wang, and Heng Gao

Aerospace Information Research Institute, Chinese Academy of Sciences, Beijing 100094, China
stunner2006@126.com

Abstract. Stratospheric airship needs to consider the interaction of man-machine-environment due to the complexity of its design and the particularity of its working environment. Aiming at the deficiencies in the traditional stratospheric airship design, this paper proposes a comprehensive design method for the man-machine ring, and builds the design process. On this basis, the multi-disciplinary design concept is introduced, and it starts from the aspects of safety design, environmental adaptability design, splicing module design, system configuration design, visual accessibility and operability design of equipment layout, and flight control design, carried out the overall design of man-machine-environment integration. The research results show that this design method of human-machine-environment interaction is reasonable and feasible, and can make up for the shortcomings of traditional design to a certain extent, and improve the comprehensiveness of the design. We will consider using this method to further realize the unification of “man-machine-environment”, and provide more guidance and help for the design of stratospheric airships.

Keywords: Stratospheric airships · Man-machine-environment · Environmental adaptability · Flight control

1 Introduction

Near Space, which is generally defined as a space 18–100 km above the ground, is located in the stratosphere and middle layer of the earth atmosphere [1]. With the development of aerospace and microelectronics, especially the development of energy technology, high altitude power technology and material technology, it is possible for people to use in this field. Stratospheric airship is undoubtedly an important direction for the development of airship in near space, which has great strategic value and economic value in military field and civilian field. [2] Stratospheric airship is an aircraft that depends on its own buoyancy and power to lift off and control flight [3], with the working height of about 18–24 km.

Stratospheric airship mainly consists of hull, energy system, propelling system, navigation control system, load system and flight control system. Carry out man-machine-environment design research to ensure the operability, controllability and maintainability of stratospheric airship.

2 Characteristics of Airship Man-Machine-Environment Design

Man-machine-environment is an interdisciplinary applied discipline which researches the man-machine-environment interrelation. The obvious feature of the airship from other aircraft is that it is lifted by the buoyancy of gases lighter than air. Based on this feature, the airship man-machine-environment design has the following characteristics.

(1) Characteristics of work environment

Airship mainly depends on buoyancy to lift off, and the amount of buoyancy relies on the density and volume of gas displaced by the airship, so we pay special attention to the features of fluid. In this case, the buoyant gas used in airships shall be lighter than air [4]. Atmosphere properties also vary greatly even in the smaller area in which the airship flies, so safety shall be fully considered when selecting gas.

In the stratosphere, the temperature increases with height rising, the lower half varies less with height, and the temperature in the upper half increases rapidly. Temperature increasing with the height rising is caused by the concentration of ozone in the atmosphere at this layer and strong absorption of UV radiation from the sun.

(2) The capsule used in providing buoyancy is large

Stratospheric airship hovers or flies in the air by buoyancy and gravity balancing, and its power is mainly used to cruise and overcome aerodynamic resistance in the atmospheric circulation field to hold fixed points.

According to the simple principle of buoyancy, buoyancy and gravity balancing when the airship reaches hovering height, then:

$$W = V(\rho_a - \rho_g)g \quad (2.1)$$

If you use the atmosphere and helium as ideal gases, you can obtain the pressure of the airship from the following formula.

$$P = \frac{RT_a}{(\mu_a - \mu_g)g} \frac{W}{V} \quad (2.2)$$

Among them: W - Total weight of airship, ρ_a and ρ_g - Atmospheric density at the hovering height of balloon and the density of lifting gas (helium), μ - Gas gram molecular weight, P and T - Gas pressure and temperature, R - Universal gas constant.

Obviously, in order to make the pressure height P smaller, that is, the airship height is higher, the volume V of airship needs to be very large.

For the airship with a huge volume and size, the non-rigid airship with flexible structure is adopted to strictly control the weight. The design and construction of large non-rigid airship structure is a huge technical challenge, which requires solving specific scientific and engineering problems, manufacturing process and testing process problems of flexible membrane structures, such as flexible structure dynamics and fluid-structure interaction.

(3) Compact layout of equipment and load

In addition to flexible capsule, the stratospheric airship contains the equipment installed on the capsule, and mission payloads. The equipment mainly includes various rigid structural parts such as fan, valve, pod, hanging bracket. Among them, pod is used to install flight control, measurement and control, safety control, avionics, energy, propulsion and other equipment. In order to reduce the stress on the capsule and avoid unnecessary damage to the capsule, we reduce the size and weight of the pod as much as possible. When selecting equipment, it is necessary to select the equipment that is light and easy to install, so as to meet the functional requirements. Payload is the application system installed outside or inside the pod, which shall comply with the above principles. In addition, the layout of equipment and payloads shall be considered for easy installation and assembly, operability of subsequent maintenance, including visual, reachable and other requirements.

(4) High difficulty in flight control

The flight process of stratospheric airship includes “lift off”, “stay in the air” and “return” stages. Three stages have different requirements for control, resulting in the complexity and diversity of stratospheric airship control.

The flight control of stratospheric airship includes airship control, air line planning and control, fixed point control, etc. It involves many parameters such as attitude, position, course, wind direction and speed for the control of action controller, computer, control unit, etc. It is necessary to conduct the system design, dynamics modeling and analysis, and the research and determination of control law and control strategy.

The pressure control of airship is interacted with the flight control to carry out the coupling control, which increases the difficulty in the control of stratospheric airship.

3 Man-Machine-Environment Design Methods

3.1 Safety Design

(1) Design of blasting prevention

The airship generates static buoyancy through filling the air bag with the gas lighter than air. The gas lighter than air is called buoyant gas. There are three main requirements for buoyancy gas suitable for airships, namely, light, safety, cheap. Hydrogen is flammable, explosive and unsafe, while helium is an inert gas which isn't easy to bring out chemical changes with oxygen and is safe and stable, so helium instead of hydrogen is used to ensure safety and avoid explosion.

During the product development, follow reliable design procedures and design principles, determine the product definition and reliability index, carry out product design, establish reliability model, conduct the reliability analysis and pre-calculation, and then carry out reliability verification. During the capsule design, analyze the structural strength allowance of different capsules, and further verify that the structural strength is consistent with the analysis results through the extreme pressure resistance test of equal scale airship or reduced scale airship, so as to prevent affecting human safety due to airship fracture.

(2) Mechanical Safety Design of interface

The equipment, instrument board and bracket that touch the airship are chamfered to avoid the damage to human body due to sharp edges. If not, they shall be wrapped with soft materials to avoid mechanical damage.

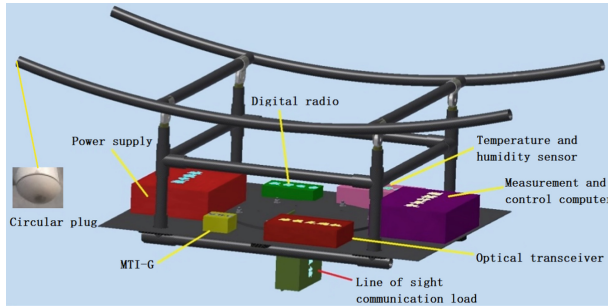


Fig. 1. Pod structure diagram

Aluminum alloy, titanium alloy and composite materials are the main materials of aerospace structures, which are also widely used in the structure of stratospheric airship. The structure of pod is made of carbon fiber composite materials with the high strength of carbon fiber, small specific gravity, excellent corrosion resistance and radiation resistance. A typical small pod structure is shown in Fig. 1, which adopts carbon fiber. Two ends of carbon fiber are sharp, two ends are sealed with light spherical plastic to avoid the possible damage of personnel during operation. See Fig. 1 on the left.

(3) Safety voltage supply design

Safety voltage less than 36 V are used in power supply. Meet the requirements of the power supply of airship equipment, and ensure that operators are in a safer working environment. The equipment on the stratospheric airship requires DC, so DC is used in power distribution. At the same time, emergency lithium battery pack is used as backup to prevent power failure. In case of failure, the lithium battery pack of main power supply is switched to emergency lithium battery to continue power supply. The solar battery on the top of airship can be used as a power source to charge the lithium battery pack, so as to ensure power supply of the stratospheric airship for long-time flight.

3.2 Environment Adaptability Design

Stratospheric environment may have high and low temperature alternation, low pressure, high irradiation environment, strong UV radiation, severe convective interference, etc.

Take the following measures to design:

- (1) Analyze hardware and software environmental impact for the environmental adaptability of the whole platform, formulate the requirements of complete and applicable environmental test, and make clear regulations according to different parts and components of platform.

- (2) Design for environmental adaptability, take measures of active and passive temperature control, and perform the environmental simulation test for verification to ensure reliability.
- (3) Do a good job in packaging and maintenance of product during transportation to adapt to the environment in the process of long-distance transportation.
- (4) Full coverage of environmental tests meet the requirements of environmental tests.

3.3 Splicing Module Design

(1) Splicing design

Splicing design is used to divide the huge capsule into many splicing modules so as to solve the manufacturing difficulty and reliability problems.

It is easy for maintenance. When a single module is damaged, it can be repaired or replaced in a short period of time.

According to the configuration of stratospheric airship, it is divided into main balloon, ballonet and tail, as shown in Fig. 2. According to specific design conditions, main balloon, ballonet and tail are divided into smaller splicing modules.

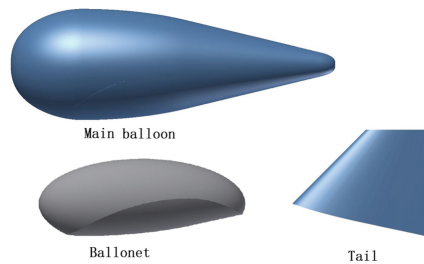


Fig. 2. Schematic diagram of the main splicing modules of the stratospheric airship

(2) Continuous welding improves efficiency

The traditional method of welding adopts high-frequency heat bonding machine or direct-heated type bonding machine, such welding machines are used to achieve the forming connection of capsule materials, as shown on the left side of Fig. 3. But its machining process isn't continuous, resulting in low efficiency, and a possibility of a small segment of solder skip.

The continuous bonding machine is used to process the capsule of airship in order to improve welding efficiency, which can be used for continuous rolling and continuous hot pressing welding with the capsule material to ensure the heat seal of heating area under the pressure of two rubber wheel. This connection method is mainly used in seal welding of membrane, which is characterized by high speed connection, uniform and reliable processing.

When splicing modules are welded and assembled, the traditional welding processing method can be used due to the complex shape and large volume, which is as the assembly and final sealing of structural components on the capsule.



Fig. 3. Conventional welding and continuous welding

3.4 System Configuration Layout

The stratospheric airship system includes the airship in the air and integrated control on the ground, and the airship consists of body, tail wing, pod, power propulsion, flight control and pressure control device, etc.; the integrated ground control mainly consists of airship, flight control and navigation hardware and software. The airship and ground navigation control are linked by a radio link protocol (Fig. 4).

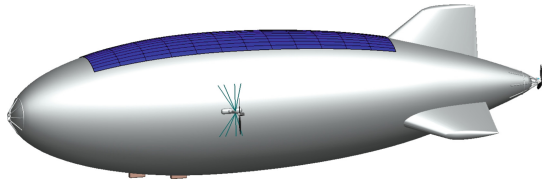


Fig. 4. Schematic diagram of a stratospheric airship

According to the basic composition of the stratospheric airship system, the stratospheric airship system is divided into 7 subsystems, including: airship body and structure, power and propulsion, flight and control, measurement and control and communication, energy and power supply, payload, ground support, so as to the subsequent maintenance. Each system adopts a certain modular design to test and debug relatively independently. The relative independence of subsystem can ensure the safety of stratospheric airship. If the power and propulsion subsystem has any failure, it can control the measurement and control and communication subsystem separately, and make the airship gradually fall down through pressure control.

3.5 Visual Accessibility and Operability of Equipment Layout

The Visual accessibility and operability design means that the maintenance personnel is easy access to the repair position in case of product failure. “Visual” - visual accessibility; “access” - physical accessibility, for example, a part of the body or a tool that can access the repair site, with enough space for maintenance. The reasonable layout of maintenance window and maintenance channel is an important way to solve the problem of “visual, access”.

In the design process of the hull subsystem, the maintainability requirements for equipment maintenance and replacement, equipment configuration and design simplifying, the operation convenience and simplicity and rapidity have been fully considered. The modular design for rapid disassembly and replacement has been adopted to achieve the rapid maintenance and restoration of the airship system and to effectively reduce system failures caused by misoperation.

3.6 Flight Control

Conventional aircraft flies on aerodynamic lift, while the lift of stratospheric airship is provided by buoyancy gas which is lighter than air. The stratospheric airship is characterized by large volume, slow flight and obvious flexible, which is greatly affected by the surrounding environment, such as wind speed, wind direction and temperature. Its system must be maintained after the airship flies in the stratosphere. Therefore, man-machine-environment relationship shall be fully considered in designing the flight control system.

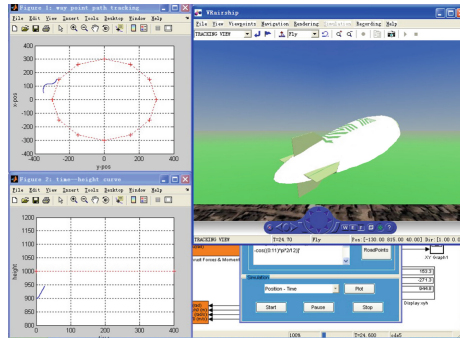


Fig. 5. Flight control simulation of stratospheric airship

In view of design independence and easy maintenance, the system is decomposed into each relatively independent and interrelated functional module according to the relationship between quantities in actual flight of airship. In the process of establishing the all-digital system model, each module is modeled to facilitate division of labor and cooperation; if a module has a more accurate model, it can be easily replaced without affecting the work of other components; if the related real-time semi-physical simulation is required, the relevant module can be a physical device according to requirements, which is easy to carry out the simulation clearly and conveniently.

The flight control module of stratospheric airship is decomposed into the following main functional modules, including airship dynamics module [6], wind field module, standard atmosphere module, navigation and control module, aerodynamic calculation module, buoyancy and gravity calculation module, steering engine servo module, propeller servo module [7] and pushing force calculation module.

As shown in Fig. 5, the airship completed the simulation process of altitude control, airspeed maintenance and way point tracking in the wind field with a fixed direction and

average value of 2 m/s of the first-order Markov Model. The simulation results showed the motion state and motion features of airship, and the effect of control law was tested to achieve the purpose of simulation.

4 Summary

In this paper, the design of stratospheric airship and the basic condition of work environment are analyzed, multidisciplinary design concepts are introduced, man-machine-environment integration is considered in the aspects of safety design, environmental adaptability design, splicing module design, system configuration design, visual and accessible and operable design of equipment layout, flight control design, etc. Finally, sort out the comprehensive design method of stratospheric airship man-machine-environment, establish the design process, and draw the following conclusions:

- (1) The stratospheric airship runs in the external environment of low temperature, low pressure and complex wind field. It is necessary to carry out multi-factor integrated man-machine-environment interaction design due to specific work environment, complex design and development;
- (2) It is of practical importance to introduce safety, environmental adaptability, modular splicing, operational accessibility and other design ideas into the design of stratospheric airship, and integrate more people's ideas into the design stratospheric airship to better service for man-machine interaction;
- (3) The man-machine-environment interaction design is reasonable and feasible, which can make up for the shortages of conventional design and improve design comprehensiveness. In the future, we'll use this method to further achieve the man-machine-environment integration and provide more guidance and help for the design of stratospheric airship.

Acknowledgement. This work is supported by the Strategic Priority Research Program of Chinese Academy of Sciences, No. XDA26010203.

References

1. Lindstrand, P.: ESA-HALE. Airship research and develop program. In: The Second International Conference on Stratosphere Platform, vol. 9, pp. 15–21 (2000)
2. Schäfer, I., Küke, R., Lindstrand, P.: Airships as unmanned platforms: challenge and chance. In: 1st UAV Conference, 20–23 May, Portsmouth, p. 3423 (2002)
3. Garg, A., Burnwal, S., Pallapothu, A., et al.: Impact of Helium permeability on endurance and altitude control of geostationary stratospheric airship-a mathematical model. In: 11th AIAA Aviation Technology, Integration, and Operations (ATIO) Conference, Including the AIAA Balloon Systems Conference and 19th AIAA Lighter-Than-Air Systems Technology Conference, 20–22 September, Virginia Beach, p. 6994 (2011)
4. Khoury, G.A., Gillett, J.D.: Airship Technology. Cambridge University Press, Cambridge (1999)

5. Cicerone, R.J.: Changes in stratospheric ozone. *Science* **237**(4810), 35–42 (1987)
6. Mueller, J.B., Paluszek, M.A.: Development of an aerodynamic model and control law design for a high altitude airship. In: *The 3rd AIAA Unmanned Unlimited Technical Conference*, Chicago (2004)
7. Lee, S.J., Kim, S.P., Kim, T.S., et al.: Development of autonomous flight control system for 50 m unmanned airship. In: *Intelligent Sensors, Sensor Networks and Information Processing Conference*, pp. 457–461. IEEE, USA (2004)



Hand Operation Ergonomics Study and Design of CCGA Grinding Process

Haoting Liu¹(✉), Jianyue Ge¹, Yuan Wang¹, Shengjie Wang², Pengrong Lin², Shaohua Yang³, and Duming Wang⁴

¹ Beijing Engineering Research Center of Industrial Spectrum Imaging, University of Science and Technology, Beijing 100083, China

liuhaoting@ustb.edu.cn

² Beijing Microelectronics Technology Institute, Beijing 100076, China

³ Northwest Institute of Nuclear Technology, Xi'an 710024, China

⁴ Department of Psychology, Zhejiang Sci-Tech University, Hangzhou 310018, China

Abstract. An ergonomics study and design of Ceramic Column Grid Array (CCGA) grinding using hand operation are performed. A systemic CCGA grinding process procedure is developed. First, the typical grasp method of CCGA chip is defined. Eleven points in chip are selected. Second, the operation order of grinding parts are designed and the grinding times is also proposed. The common grinding order is the front part, middle part, and back part of the CCGA chip; and the grinding time should be large than 3. Third, two indices are considered to evaluate the grinding operation effect, i.e., the grinding time and CCGA flatness degree. The CCGA flatness degree can also be used for grinding effect evaluation (rather than the grinding operation effect). Many experiment results have shown that the proposed grinding method can improve the grinding effect and quality stability of CCGA chip.

Keywords: Hand operation · CCGA · Grinding process · Aerospace manufacturing · Ergonomic design

1 Introduction

The Ceramic Column Grid Array (CCGA) package [1] is a newly developed process technique for chip manufacture in recently years. Figure 1 presents the sketch map of its side view. The CCGA mainly points to the leadout of a chip which is composed by thousands of solder columns. For example, its amount can be 31×31 or 41×41 for a typical chip whose size is $32.5 \text{ mm} \times 42.5 \text{ mm}$ or $42.5 \text{ mm} \times 42.5 \text{ mm}$, respectively. The reflow soldering technique is always used to connect the solder column with the chip main body. After the reflow soldering, the flatness of CCGA may be poor [2]. The improper flatness mainly comes from different arrange attitudes or the variable soldering depth of solder column. To control the flatness of CCGA end face, the grinding process is necessary. The grinding process uses a grinding table with certain rotation speed to process CCGA end face and the hand grinding is extensively used in engineering currently [3].

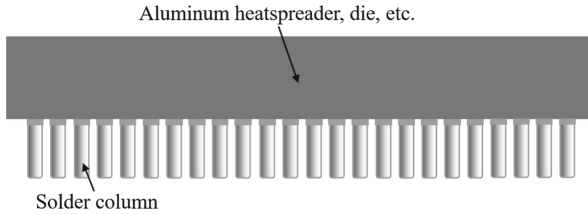


Fig. 1. Sketch map of CCGA hip

A hand operation ergonomics study and design of CCGA grinding process is proposed in this paper. First, the typical grasp positions when implementing grinding task are defined in the CCGA chip surface. Eleven grasping points are appointed in the chip surface. Second, the grinding order and times are proposed for the typical CCGA chip. The grinding order is from the chip front to the chip rear end; the proposed grinding times should be large than 3. The maximum grinding force is better less than 10.0 N. Third, two evaluation indices are utilized to assess the grinding operation effect. The indices include the grinding time and flatness degree which can reflect the integrated grinding efficiency and effect of CCGA chip. The main contribution of this paper is: a systemic grinding technique including the grasping method, grinding operation method, and grinding operation assessment method is proposed.

2 Ergonomics Study of Hand Operation

Many researches have been done regarding the hand operation. It is well known that the hand is a multi-joint system which has 27 bones. The familiar motions of hand bone include flexion and extension, adduction and abduction. In general, the hand has 31 free degrees in theory; while only 25 free degrees are commonly used in engineering. In general, three methods are used for the hand operation research. The first method uses the simulation [4], such as computer graphics, robotics to study the hand operation; the second technique adopts the physiological signal [5], such as the electromyography (EMG) or muscle force to describe hand operation quantitatively; and the third approach consider the experiment-based measurement [6], i.e., the ergonomics method to analyze the hand operation. Figure 2 present the examples of ordinary hand operation research methods. In Fig. 2, (a) is the sketch map of hand joint and bone; (b) is the photo of electromyography signal measurement of hand operation; and (c) is the ergonomics research of hand operation.

3 CCGA Grinding Process

3.1 Proposed Grinding Process

The descriptions of traditional CCGA grinding process are presented below.

- 1) The operator observes the surface of CCGA end port and sets the working speed of grinding table according to his or her experiences.

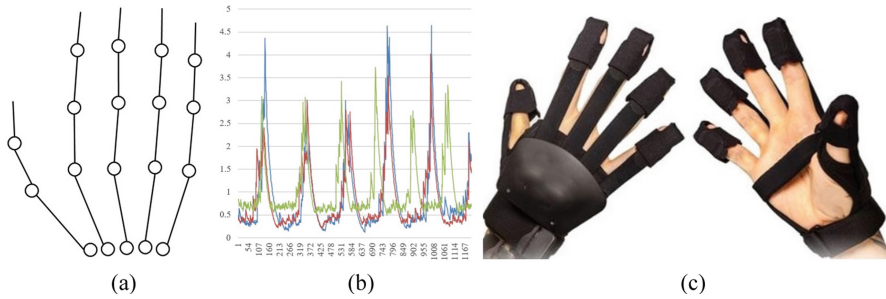


Fig. 2. Examples of hand operation research

- 2) The operator pinches the chip using his or her thumb and the other two or three fingers (index finger, middle finger, and ring finger). There is no strict pinch position requirement during that operation.
- 3) The operator presses the chip on the grinding table, the intensity of press force is decided by the grinding experience of operator. Then the chip grinding process will start.
- 4) After each grinding, the operator observes the grinding effect to evaluate the flatness degree of CCGA end port according to his or her experience to decide whether further grinding is necessary.
- 5) If the operator thinks the grinding quality is unqualified, i.e., the grinding cannot be stop, the step 3) will be performed again; otherwise the grinding is terminated.

Clearly, the traditional CCGA grinding process has lots of drawbacks. First, no strict operation regulations are made during the chip grinding procedure which will lead to an uncontrollable grinding effect. Different operators will use different grinding methods to process the CCGA end port. The chip direction, the chip strength point, and the grinding times is random. Second, the arbitrary grinding process will also create a low working efficiency. For example, if the one-time grinding operation is improper, more grinding processes will be needed. Third, the grinding experiences are also not accumulated which is a waste for chip manufacture. The proper grinding method of operator cannot be recorded and shared in a traditional grinding process.

To conquer these drawbacks above, a new CCGA grinding process is proposed. Its processing steps are illustrated below.

- 1) The initial flatness state of CCGA end port will be measured by camera, and the working speed of grinding table will be estimated by the machine learning tools. Then the operator can set the proper rotation speed of grinding table.
- 2) The operator pinches the chip in the positions illustrated in Fig. 3 and Table 1. Figure 3 and Table 1 also appoint the operation pattern of chip grinding.
- 3) The operator will wear a digital glove and presses the chip on the grinding table, the intensity of press force is decided by the grinding experience of operator (in general it should be less than 10.0 N). Then the chip grinding process will start. If the size of press force is large than a threshold, a vibration will be created by the digital glove to remain the operator the proper press force.

- 4) After each grinding, the operator will use a camera to observe the grinding effect to evaluate the flatness degree of CCGA end port to decide whether further grinding is necessary.
- 5) If the image analysis result of grinding quality is unqualified, i.e., the grinding cannot be stop, the step 3) will be performed again; otherwise the grinding can be terminated.

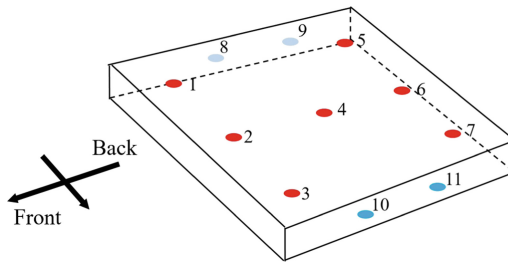


Fig. 3. Sketch map of CCGA chip

Table 1. Proposed CCGA hand grinding method (right hand)

Number	Grasping method					Grinding effect
	Thumb	Index finger	Middle finger	Ring finger	Little finger	
1	10	1	8	9	/	Region under point 1
2	10	2	8	9	/	Region under point 2
3	10	3	8	9	/	Region under point 3
4	10	4	8	9	/	Region under point 4
5	9	7	11	10	/	Region under point 7
6	9	6	11	10	/	Region under point 6
7	9	5	11	10	/	Region under point 5

3.2 Grinding Effect Evaluation Method

Many indices can be used to assess the grinding effect of CCGA chip including the mechanical indices, electrical indices, or integrated application effect indices, etc. For

the sake of simpleness, only the grinding time and grinding flatness degree are considered in this study. The grinding time is defined by the accumulated time span between the start time point when a new CCGA chip begins to be grinded and the end time point when the CCGA chip finishes grinding (the grinding quality is qualified). In many cases, the multiple times grinding is needed. The grinding flatness degree is an index which can characterize the planeness of multiple ceramic columns. The laser flatness measurement device is always used to assess that index. Some new methods use the imaging camera and its image processing method to solve the grinding flatness degree evaluation problem. According to the national standard, the flatness after CCGA grinding should be less than 0.15 mm.

4 Experiments and Discussions

Some preliminary experiments were performed to test the effectiveness of proposed grinding process. Figure 4 presents the actual photos of CCGA chip grinding. In Fig. 4, (a) and (b) show the traditional grinding method of CCGA; (c) illustrates one of the quality test steps after grinding: the operator wears the rubber anti-static finger sleeve to grind the end face of CCGA chip; if some detritus exist in the ceramic columns, the operator has to use the tweezers or needle to pick them out. From Fig. 4, the traditional method does not appoint the detailed operation order and method during grinding, the chip grinding efficiency and effect cannot be standardized. The familiar unqualified problems include: the extrusion deformation of ceramic columns, the creation of more detritus, or the production of surface burr, etc. Differently, if the grinding process is formulated, the possible quality problems can be foreseen regularly, then the effective measurements can be performed to avoid them.

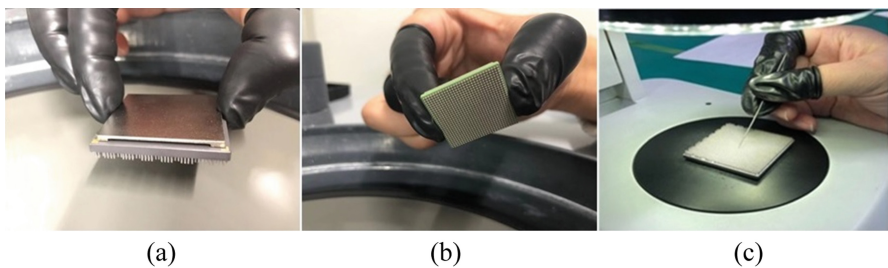


Fig. 4. Photos of CCGA chip grinding

The comparison experiments of CCGA grinding using the traditional and our proposed methods were implemented. Because we do not accumulate enough CCGA grinding data, currently, the results of image processing step and machine learning method are not reported in this paper. The results related the data glove will also presented in future. We use the grinding experiment of bare hand to test the effectiveness of proposed process. Considering the experiment cost, an alternative chip is used here. The alternative chip is an object which has the similar appearance parameters like the real

CCGA chip. Because the average diameter of finger of Chinese people is about 120 mm to 180 mm, all the points in Fig. 3 can be used for chip clamping. After preliminary test, our proposed method can shorten the grinding time dramatically while keep the same grinding flatness degree as well as the traditional method. Here the grinding time means all the accumulated grinding operation span including the multiple chip grindings, surface quality checks, and all kinds of quality problem fixings.

Although the manufacturing of high-end chip always represents the processing and assembly technology with ultra-high precision; however the human-involved surface grinding is still needed currently. Regarding the CCGA, no ergonomic analysis about the grinding process is performed in the past; the operator can implement the chip grinding according to their arbitrary experiences. As a result, the grinding efficiency may be slow and the grinding effect cannot be guaranteed. In this paper, after investigating the size of CCGA chip, the typical grasp and grinding methods of them are proposed. The proposed method regulates the operation method and flow of CCGA chip grinding, which can improve the grinding quality to a certain level. In this paper, the evaluation of machine learning method is not mentioned because we do not have enough data to carry out the training currently. The machine learning method can use the image after grinding to build a connection between the rotation speed of grinding table and the final grinding effect. With the accumulation of the CCGA grinding data, the machine learning tool will be used.

The proposed grinding method at least has three merits. First, the proposed method has a strong operability. In our method, the finger touch points, the operation times, and even the maximum operation force are all defined clearly [7]. The operator can understand how to implement the proposed grinding process clearly by using the proposed method. Second, the grinding effect is better than the traditional method. After the experiment test, the grinding time can be reduced while the flatness degree of ceramic columns can still be kept. These results are very important for the chip grinding task. Third, the technology popularization of proposed method is also good. Eleven finger touch points are defined in our method; however, less points can be considered if the size of chip is small. For example, the points 1, 2, 3 (or 5, 6, 7) which are always pushed by the index finger can be reduce from 3 points to 2 points. Clearly, our method still has some drawbacks. For example, when the size of chip is very small, e.g., the size of chip is too small that the index finger cannot be used, our proposed method cannot solve that case currently.

5 Conclusion

The ergonomic analysis and a new grinding process of CCGA are proposed in this paper. First, the grasp method of CCGA chip grinding is defined. The eleven typical finger touch points in the chip surface are designed carefully. Second, the operation method of CCGA grinding is proposed. The operation orders of different fingers are given; and both the grinding times and the finger touch force of chip upper surface are also presented. Third, two indices, i.e., the grinding operation time and the CCGA flatness degree after grinding, are also utilized to evaluate the grinding effect of proposed method. Compared with the traditional method, our proposed process can reduce the grinding time and keep a stable

grinding quality. In future, the digital glove will be used during the hand grinding; and some machine learning techniques will be used to assist operator to control speed of grinding table which will the grinding quality.

Acknowledgement. This work was supported by the National Natural Science Foundation of China under Grant No. 61975011, the Fund of State Key Laboratory of Intense Pulsed Radiation Simulation and Effect under Grant No. SKLIPR2024, and the Fundamental Research Fund for the China Central Universities of USTB under grant No. FRF-BD-19-002A.

References

1. Patel, S., Pandey, D.K., Patil, S.A., et al.: Solder immersion process of ceramic column grid array package assembly for space applications. *IEEE Trans. Compon. Packag. Manuf. Technol.* **10**, 717–722 (2020)
2. Park, S.B., Joshi, R.: Comparison of thermo-mechanical behaviour of lead-free copper and tin-lead column grid array packages. *Microelectron. Reliab.* **48**, 763–772 (2008)
3. Kang, M., Zhang, L., Tang, W.: Modeling of the distribution of undeformed chip thickness based on the real interference depth of the active abrasive grain. *IEEE Access* **8**, 101628–101647 (2020)
4. Gorce, M.D.L., Fleet, D.J., Paragios, N.: Model-based 3D hand pose estimation from monocular video. *IEEE Trans. Pattern Anal. Mach. Intell.* **33**, 1793–1805 (2011)
5. Kim, M., Kim, K., Chung, W.K.: Simple and fast compensation of sEMG interface rotation for robust hand motion recognition. *IEEE Trans. Neural Syst. Rehabil. Eng.* **26**, 2397–2406 (2018)
6. Lu, Z., Li, Y., He, H.: Research on hand grasping strategy for ergonomics simulation. In: *World Congress on Intelligent Control and Automation*, pp. 6117–6220 (2008)
7. Wu, X.: The application of ergonomic manual operation principle to the design of mouse. In: *IEEE International Conference on Computer-Aided Industrial Design & Conceptual*, pp. 1357–1360 (2009)



Correction to: Prediction Model of Accident Vehicle Speed Based on Artificial Intelligence Decision Tree Algorithm

Wei Ji, Tiantong Yang, Quan Yuan, Gang Cheng, and Shengnan Yu

Correction to:
Chapter “Prediction Model of Accident Vehicle Speed Based on Artificial Intelligence Decision Free Algorithm”
in: S. Long and B. S. Dhillon (Eds.):
***Man-Machine-Environment System Engineering*, LNEE 941,**
https://doi.org/10.1007/978-981-19-4786-5_44

In the original version of the book, the following correction has been made: The title of Chapter 44 has been changed from “Prediction Model of Accident Vehicle Speed Based on Artificial Intelligence Decision Free Algorithm” to “Prediction Model of Accident Vehicle Speed Based on Artificial Intelligence Decision Tree Algorithm”. The book and the chapter have been updated with the change.

The updated original version of this chapter can be found at
https://doi.org/10.1007/978-981-19-4786-5_44

© The Author(s), under exclusive license to Springer Nature Singapore Pte Ltd. 2023
S. Long and B. Dhillon (Eds.): MMESE 2022, LNEE 941, p. C1, 2023.
https://doi.org/10.1007/978-981-19-4786-5_101

Author Index

B

Bai, Yu, 24
Bi, Xiyu, 226

C

Cao, Jie, 37
Cao, Jieren, 272
Cao, Kun, 574, 579, 584, 590
Cao, Xiaodong, 397
Cao, Yi, 203, 370
Cao, Zhengtao, 24
Chen, Dongxue, 184
Chen, Jiaao, 279, 287
Chen, Jianwu, 99, 376, 411, 650
Chen, Shan, 115
Chen, Siyu, 3
Chen, Xia, 73
Chen, Xiaotong, 411
Chen, Yi, 509
Chen, Yonghong, 279
Chen, Yongsheng, 153
Chen, Yunfei, 427
Chen, Zhenfang, 99, 376, 411, 650
Chen, Zhenling, 146
Chen, Zihang, 250
Cheng, Gang, 317
Cheng, Tianxin, 60

D

Dai, Funan, 44
Dang, Sina, 3
Deng, Ye, 30
Di, Hanzheng, 218
Ding, Ding, 218

Ding, Kai, 418
Ding, Yanyan, 384, 552, 644
Dong, Bo, 457
Dong, Hanwen, 17
Dong, Haochen, 170
Du, Jian, 115, 159, 184
Du, Shan, 170
Du, Shuxin, 164, 302
Duan, Yu, 24

F

Fang, Yiao, 44
Feng, Duzhong, 195
Feng, Wei, 684, 691
Fu, Yan, 434

G

Gao, Haiyang, 54
Gao, Heng, 710
Gao, Jingqi, 99
Gao, Yan, 164
Ge, Jianyue, 719
Gong, Peng, 579, 584
Guan, Xin, 44
Guo, Junlong, 539
Guo, Li, 691
Guo, Liang, 479
Guo, Mingyang, 134
Guo, Sheng, 37
Guo, Xiaochao, 24

H

Han, Liangliang, 325
Hao, Danning, 234

Hao, Heyuan, 336, 527, 539
 Hao, Yan, 295, 697
 He, Xiangjun, 265
 He, Xinying, 234
 Hong, Xinye, 140
 Hou, Yongqing, 661
 Hu, Cancan, 37
 Hu, Haimin, 626, 644
 Hu, Yiwen, 177
 Huan, Shang, 325
 Huang, Baiqiao, 668, 675, 684, 691
 Huang, Shan, 418
 Huang, Xiaodan, 203
 Huang, Yanan, 164
 Huang, Zhouce, 309

J

Ji, Wei, 317
 Jiang, Hao, 638
 Jiang, Rufen, 567
 Jiang, Shu, 73
 Jiang, Wei, 146
 Jiang, Yin, 99
 Jiang, Zhengqing, 44, 77, 257
 Jiao, Zeliang, 384
 Jin, Jian, 661
 Jin, Miao, 177
 Jin, Weiyi, 287
 Jin, Xiaoping, 134

K

Kong, Lingpeng, 527, 533

L

Lai, Chaoan, 617
 Lee, Yuchi, 140
 Lei, Quxiao, 287
 Li, Chenming, 226, 485, 494
 Li, Feimin, 600
 Li, Hao, 73
 Li, Hongyi, 384
 Li, Jianfeng, 539
 Li, Ke, 272, 279, 287, 544
 Li, Lili, 146
 Li, Mengxi, 73
 Li, Mingze, 73
 Li, Qingkun, 126
 Li, Renping, 272
 Li, Tao, 539
 Li, Tong, 242
 Li, Wei, 170
 Li, Wen, 457, 464
 Li, Yajie, 343, 356
 Li, Yangguang, 195
 Li, Zengming, 115

Li, Zhihai, 265
 Liang, Dengchao, 195
 Liang, Zhi, 84
 Liao, Guangshan, 427, 434
 Liao, Yang, 159, 177, 184
 Lin, Pengrong, 719
 Lin, Rong, 184
 Liu, Chuang, 54
 Liu, Guiqing, 450
 Liu, Haitian, 242
 Liu, Hao, 626, 644
 Liu, Haoting, 343, 349, 356, 418, 719
 Liu, Huayan, 203
 Liu, Huichao, 558
 Liu, Jiantao, 384
 Liu, Junyao, 242
 Liu, Liang, 427
 Liu, Lin, 527
 Liu, Qian, 384, 632
 Liu, Qingfeng, 24
 Liu, Tiebing, 146
 Liu, Weijiang, 411
 Liu, Weixin, 384, 626, 632, 638, 644
 Liu, Xin, 177
 Liu, Xun, 302
 Liu, Yuan, 30
 Liu, Zaochen, 533
 Lu, Aiguo, 457
 Lu, Dongdong, 54
 Lu, Zhibo, 389
 Luo, Yu, 73
 Lv, Bao, 609
 Lv, Hui, 67
 Lv, Jing, 710

M

Ma, Tao, 609
 Ma, Xinyue, 195
 Mei, Zhengguo, 574, 579, 584, 590, 595
 Min, Zhiyong, 203
 Mo, Fengfeng, 164, 302, 404

N

Ni, Qianqian, 302
 Nie, Shuang, 302, 404
 Niu, Xuejun, 567

O

Ou, Hongyan, 384, 626, 632, 638, 644
 Ou, Yilin, 234

P

Pan, Xiangpeng, 107
 Pang, Li, 533
 Pang, Liping, 10, 17, 30, 397, 479

Q

Qi, Xiaogang, 418
 Qian, Bing, 336
 Qin, Lipeng, 67
 Qiu, Zezheng, 479
 Qu, Hongquan, 10, 17
 Qu, Jue, 3
 Qu, Min, 234
 Qu, Ying, 295

R

Ren, Huifeng, 24
 Rong, A., 397

S

She, Jiahong, 325
 Shen, Qian, 584, 595
 Shen, Yuhong, 226, 485, 494
 Shi, Feina, 503
 Shi, Jianguo, 558
 Shun, Yanqiu, 411
 Song, Yaxuan, 218
 Su, Hanqin, 675
 Sui, Haolin, 170
 Sun, Jiwen, 539
 Sun, Yanqiu, 99, 376

T

Tan, Lifeng, 434
 Tan, Xilian, 552
 Tang, Lei, 626
 Tian, Dawei, 115, 153, 404
 Tian, Yu, 60, 427, 434
 Tong, Xiaoye, 457

W

Wan, Xi, 464
 Wang, Chuan, 389, 509, 517
 Wang, Chunhui, 434
 Wang, Chunlai, 473
 Wang, Chunxin, 574
 Wang, Congyi, 92
 Wang, Duming, 60, 427, 719
 Wang, Hu, 73
 Wang, Jia, 99
 Wang, Juan, 389
 Wang, Junfei, 626, 632, 644
 Wang, Kunfu, 668, 684, 691
 Wang, Lian, 60
 Wang, Lie, 574
 Wang, Lijing, 272, 279, 287, 544
 Wang, Lizhi, 427
 Wang, Meixian, 544
 Wang, Mengmeng, 349
 Wang, Ning, 544

Wang, Qian, 710
 Wang, Qiufang, 503
 Wang, Runsen, 218
 Wang, Shengjie, 719
 Wang, Shuxin, 632, 638
 Wang, Ting, 509
 Wang, Wenjun, 126
 Wang, Xiaojun, 509, 517
 Wang, Xin, 30
 Wang, Yan, 650
 Wang, Yanjiao, 579
 Wang, Yanyan, 24
 Wang, Yaping, 37
 Wang, Yifeng, 287
 Wang, Ying, 210
 Wang, Yuan, 343, 356, 719
 Wang, Yujin, 552
 Wang, Zhenyuan, 126
 Wang, Zhongnan, 242
 Wang, Ziyang, 389, 509, 517
 Wei, Huilin, 226, 485, 494
 Wei, Zhongliang, 134, 503
 Wu, Bing, 661
 Wu, Di, 632
 Wu, He, 552
 Wu, Hongjiao, 600
 Wu, Weifei, 574, 579, 584, 590, 595
 Wu, Yuan, 434

X

Xia, Weifeng, 164
 Xiang, Qingsheng, 115
 Xiang, Siyi, 195
 Xiang, Xinyu, 272
 Xie, Fang, 134, 503
 Xie, Shaoli, 325
 Xing, Ruolin, 697
 Xing, Zhendeng, 210
 Xiong, Duanqin, 24, 184
 Xiong, Wei, 84, 92
 Xu, Chuang, 177
 Xu, Haishan, 146
 Xu, Ruoshi, 494
 Xu, Xianfa, 146
 Xue, Hongjun, 3
 Xue, Shuqi, 434
 Xue, Yanhui, 442

Y

Yang, Bin, 99, 376, 411
 Yang, Chenyuan, 30, 479
 Yang, Hanjun, 427
 Yang, Haoyu, 703
 Yang, Hong, 650
 Yang, Jian, 325

Yang, Liu, 159, 177, 184
 Yang, Shaohua, 349, 719
 Yang, Tiantong, 317
 Yang, Zheng, 450
 Yao, Handong, 302, 404
 Yao, Xuechen, 595
 Yu, Fei, 115
 Yu, Jiamin, 242
 Yu, Kang, 638
 Yu, Shengnan, 317
 Yu, Wei, 336
 Yu, Xiaoqing, 84, 92
 Yuan, Jilei, 442
 Yuan, Qiang, 272
 Yuan, Quan, 126, 309, 317, 703
 Yuan, Zhen, 60

Z

Zhan, Wenhao, 427
 Zhang, Ao, 99
 Zhang, Deli, 325
 Zhang, Guoyuan, 210
 Zhang, Huairui, 567
 Zhang, Jianyi, 170
 Zhang, Jiarong, 250
 Zhang, Jun, 54
 Zhang, Junhao, 397
 Zhang, Ke, 533
 Zhang, Kunzhu, 703
 Zhang, Lantao, 365
 Zhang, Mengyu, 10
 Zhang, Miao, 650
 Zhang, Peng, 668, 684, 691
 Zhang, Ping, 272
 Zhang, Qing, 376
 Zhang, Wei, 265, 661
 Zhang, Wobo, 558

Zhang, Xiaoyan, 3
 Zhang, Xiulin, 287
 Zhang, Xuhan, 203
 Zhang, YaFei, 295
 Zhang, Yafei, 697
 Zhang, Yan, 159, 177, 184
 Zhang, Yang, 544
 Zhang, Yijie, 77
 Zhang, Yishuang, 159, 177, 184
 Zhang, Yuanping, 710
 Zhang, Yuqi, 600, 609
 Zhang, Yuxiang, 279
 Zhang, Zhixian, 434
 Zhao, Bin, 544
 Zhao, Junyu, 279
 Zhao, Ruobing, 617
 Zhao, Xinyang, 170
 Zhen, Chong, 287
 Zhen, Jun, 295, 684, 697
 Zheng, Haiyun, 77
 Zheng, Qiaoyang, 73
 Zheng, Quanyi, 210
 Zheng, Shengyao, 195
 Zheng, Shoujun, 418
 Zheng, Sijuan, 134, 503
 Zhou, Dapeng, 544
 Zhou, Haocheng, 265
 Zhou, Qianxiang, 517
 Zhou, Qinglin, 115
 Zhu, Bo, 195
 Zhu, Chunjian, 272
 Zhu, Haoran, 336
 Zhu, Yaru, 257
 Zhu, Ying, 427
 Zhu, Yuyang, 177
 Zou, Ting, 485
 Zuo, Peiwen, 67